# ODESSA ASTRONOMICAL PUBLICATIONS

Volume 20, Part 1
(2007)

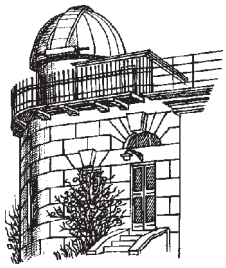

Odessa
«AstroPrint»

# FOREWORD

This issue of the "Odessa Astronomical Publications" (V.20, 2007) collects up the articles that were presented at the International jubilee scientific conference "Modern Problems of Astronomy" that has been devoted to the 100th anniversary of the outstanding astronomer Vladimir Platonovich Tsessevich (1907–1983). The conference was held in Odessa (Ukraine), in that city where V.P.Tsessevich lived in childhood and worked in 1944-1983. The conference was organized by I.I.Mechnikov Odessa National University on August 12-18, 2007. The Memorial part of the conference was held on August 13, 2007 and was devoted to the Tsessevich's life, his scientific, pedagogical and popularization activity.

Together with University the following organizations took part in the conference organization: Euro-Asian Astronomical Society (Moscow), Ukrainian Astronomical Association (Kiev), Odessa Astronomical Society, Department of Astronomy, Research Institute "Astronomical Observatory" of I.I.Mechnikov Odessa National University and Odessa Radioastronomical Observatory of Radioastronomical Institute of Ukrainian Academy of Sciences.

The scientific program included the following sections: 1. Memorial Meeting. 2. Physically Variable Stars. 3. Interacting Binary Stars. 4. Chemical Composition and Evolution of the Stars and Galaxies. 5. Variable Radiosources. 6. Cosmology. 7. Near-Earth Astronomy, Astrometry and Celestial Mechanics. 8. Meteoric Astronomy. 9. Telescopes, Registration and Processing of Images and Signals. 10. Astronomical Education, Popularization of Astronomy, New Society.

About 180 scientists from 15 countries of the America, Asia, Australia and Europe participated in the conference. On the Memorial part there were delivered 10 talks of his pupils and former staff astronomers. On sections more that 87 scientific talks were delivered (23 of them were the plenary talks). The total number of the poster presentations was about 45. In the conference resolution it was noted that the Tsessevich's conferences was very productive.

According to the SOC decision, the publication of the Tsessevich's conference proceeding was divided into two parts. The first part consists the talks in English and the second part consists the talks in Russian. The first part begins with report: "Vladimir Platonovich Tsessevich – Astronomer-Romantic". The next talks are given in the alphabetic order on a surname of the first author. The arrangement of the reports in the second part follows the same principle. The contents and abstracts of both parts are given in English. In summary, as the editor-in-chif of this journal, I bring deep gratitude to all participants of the conference "Modern Problems of Astronomy" for performances in memory about V.P.Tsessevich.

V. G. Karetnikov

# CONTENTS

Foreword
V.G.Karetnikov ..... 2
Contents ..... 3
VLADIMIR PLATONOVICH TSESSEVICH – ASTRONOMER-ROMANTIC
M.Yu.Volyanska, V.G.Karetnikov, O.E.Mandel ..... 6
ABOUT TREND IN ZINC STELLAR ABUNDANCES WITH METALLISITY
U.Sh.Bayazitov, F.Thevenin ..... 12
V.P. TSESSEVICH – PROMINENT RESEARCHER OF VARIABLE STARS
V.P.Bezdenezhnyi ..... 15
THE CLASSICAL CEPHEIDS' HISTOGRAMS OF PERIODS DISTRIBUTION
V.P.Bezdenezhnyi ..... 17
PERIOD ANALYSIS AND MODE IDENTIFICATIONS OF RRab LYRAE STAR X ARIETIS
V.P.Bezdenezhnyi ..... 20
ON THE LAW OF PLANETARY DISTANCES IN THE SOLAR SYSTEM
V.P.Bezdenezhnyi ..... 22
ON THE DETERMINATION OF GALAXY STRUCTURE ELLIPTICITY
M.Biernacka, P.Flin, T.Juszczyk, E.Panko ..... 26
ABOUT COMPILED CATALOGUE OF SPECTROSCOPICALLY DETERMINED α-ELEMENTS ABUNDANCES FOR STARS WITH ACCURATE PARALLAXES
T.V.Borkova, M.S.Katchieva, B.A.Marsakov, D.M.Pitkina ..... 30
PROGRAMS FOR DATA REDUCTION AND OPTIMIZATION OF THE SYSTEM WORK
V.V.Breus ..... 32
MODELING OF REGIONS OF ASTEROID POSSIBLE MOTION
A.M.Chernitsov, O.M.Dubas, V.A.Tamarov ..... 36
TSESEVICH AND KRAKOW'S ASTRONOMERS
P.Flin ..... 40
PHOTOMETRIC RESEARCHES OF ASTEROIDS ON 1.5-M RUSSIAN-TURKISH TELESCOPE
A.Galeev, R.Gumerov, I.Bikmaev, G.Pinigin, I.Khamitov, Z.Aslan ..... 43
ON THE STABLE SPHERICALLY-SYMMETRIC CHARGED DUST CONFIGURATIONS IN GENERAL RELATIVITY
V.D.Gladush ..... 47
THE RADIAL MOTIONS OF CHARGED PARTICLES IN THE FIELD OF THE CHARGED OBJECT IN GENERAL RELATIVITY AND THEIR CLASSIFICATION
V.D.Gladush, M.V.Galadgyi ..... 51
HIGH-RESOLUTION SPECTROSCOPY OF LONG-PERIODIC ECLIPSING BINARY ε AURIGAE
A.Golovin, Yu.Kuznyetsova, M.Andreev ..... 55
THORIUM LINES IN THE SPECTRA OF SEVERAL SMC SUPERGIANT STARS
V.F.Gopka, S.V.Vasil'eva, A.V.Yushchenko, S.M.Andrievsky ..... 58
ON THE POSSIBLE NATURE OF Bp-Ap STARS: AN APPLICATION TO HD101065 and HR465
V.F.Gopka, O.M.Ulyanov, S.M.Andrievsky ..... 62
SECULAR EVOLUTION OF THE GALAXY
E.Griv, M.Gedalin, C.Yuan ..... 66
GENETIC ALGORITM ECLIPSE MAPPING
A.V.Halevin ..... 70
NEW CONCEPT OF HUNGARIAN ROBOTIC TELESCOPES
T.Hegedüs, Z.Kiss, B.Bíró and Z.Jäger ..... 74
CESEB: A REPORT ON LATEST RESULTS
T.Hegedüs, O.Latkovic, H.Markov, I.Vince, A.Cséki, J.Nuspl, N.Markova, E.Rovithis-Livaniou, J.Vinkó ..... 76
OFFSET GUIDE OF THE ZEISS-2000 TELESCOPE
N.V.Karpov, V.Ya.Choliy ..... 78
PROBLEMS OF LOCAL PLUMB RECONSTRUCTION FROM LONG-TERM ASTROOPTICAL SETS
L.Ya.Khalyavina, T.Ye.Borisyuk ..... 82

THE INTERNATIONAL HELIOPHYSICAL YEAR 2007-2009 AND IMMEDIATE TASKS OF MODERN METEOR SCIENCE
S.V.Kolomiyets ..... 84
THE OBJECT MWC 137
L.N.Kondratyeva ..... 86
DE SITTER METRIC WITH MAGNETIC FIELD
M.P.Korkina, V.S.Kazemir ..... 88
COLOUR EXCESSES OF 74 SUPERGIANTS AND 30 CLASSICAL CEPHEIDS
V.V.Kovtyukh, C.Soubiran, S.I.Belik, M.P.Yasinskaya, F.A.Chehonadskih, V.Malyuto ..... 91
HD152786: A LITHIUM GIANT?
T.Krátká, V.Štefl ..... 95
AMATEUR ASTRONOMY MOVEMENT IN SLOVAKIA
I.Kudzej, P.A.Dubovsky ..... 97
ASTRONOMICAL OBSERVATORY AT KOLONICKÉ SEDLO AND ITS RESULTS IN VARIABLE STARS OBSERVING
I.Kudzej, V.G.Karetnikov, P.A.Dubovsky, L.S.Paulin, N.N.Fashchevskyi, A.V.Ryabov, T.N.Dorokhova, N.I.Dorokhov, N.I.Koshkin, M.Vadila, S.Parimucha ..... 100
SPECTROSCOPY AND PHOTOMETRY OF BE STAR MWC340
A.V.Kurchakov, F.K.Rspaev ..... 106
THE ROLE OF PHYSICAL EXPERIMENTS IN POPULARIZATION OF EXACT SCIENCES
S.Ledvinka, J.Pisala ..... 108
ASTRONOMICAL EDUCATION IN THE NICHOLAS COPERNICUS OBSERVATORY AND PLANETARIUM IN BRNO
S.Ledvinka, J.Pisala ..... 110
PHOTOMETRY OF THE ASYNCHRONOUS POLAR V1500 CYG AT VARIOUS PHASES OF THE SYNODICAL CYCLE IN 2005-2006 YRS
A.A.Litvinchova, E.P.Pavlenko, S.Yu.Shugarov ..... 112
EVALUATION OF OUTER CORE VISCOSITY INFLUENCE ON THE EARTH FORCED NUTATION
M.V.Lubkov ..... 114
ABOUT INFLUENCE OF LATERAL HETEROGENEITIES IN THE EARTH UPPER MANTLE ON THE LOVE NUMBERS FOR DIURNAL TIDES
M.V.Lubkov ..... 117
DUPLICITY AND EVOLUTION STATUS OF THE EARLY-TYPE Be STAR V622Per, THE MEMBER OF THE $\chi$ Per OPEN STAR CLUSTER
S.L.Malchenko, A.E.Tarasov, K.Yakut ..... 120
HOMOGENIZATION OF STELLAR CATALOGUES THROUGH DATA INTERCOMPARISON
V.Malyuto ..... 124
THE TALLINN PUBLIC OBSERVATORY IN CHANGING CONDITIONS
M.Mars, T.Aas, V.Harvig ..... 126
STAR FORMATION HISTORY IN THE GALACTIC THIN DISK
V.A.Marsakov, M.V.Shapovalov, T.V.Borkova ..... 128
STELLAR OBJECTS OF EXTRAGALACTIC ORIGIN IN THE GALACTIC HALO
V.A.Marsakov, T.V.Borkova ..... 134
THE BENEFITS OF THE ORTHOGONAL LSM MODELS
Z.Mikulášek ..... 138
THE STARS OF THE LOWER PART OF MAIN SEQUENCE
T.V.Mishenina, S.I.Belik, I.A.Usenko, O.Bienaymé, C.Soubiran, V.V.Kovtyukh, S.A.Korotin ..... 143
CHEMICAL COMPOSITION OF GALACTIC DISK STARS
T.V.Mishenina, N.Yu.Basak, T.I.Gorbaneva, C.Soubiran, V.V.Kovtyukh ..... 149
ABUNDANCES OF N – CAPTURE ELEMENTS IN STARS OF THIN AND THICK DISKS
T.V.Mishenina, T.I.Gorbaneva, N.Yu.Basak, C.Soubiran, V.V.Kovtyukh ..... 151
THREE-DIMENSIONAL HYDRODYNAMICAL MODELING OF MASS TRANSFER IN THE CLOSE BINARY SYSTEM $\beta$ LYR WITH AN ACCRETOR WIND.III
V.V.Nazarenko, L.V.Glazunova ..... 154
3C 390.3 – JET OR DISK
L.S.Nazarova, N.G.Bochkarev, C.M.Gaskell ..... 158

OPTICAL VARIABILITY OF NGC 4151 DURING 100 YEARS
V.L.Oknyanskij, V.M.Lyuty ..... 160
INFLUENCE OF SPIRAL PATTERNS ON DYNAMICAL EVOLUTION OF GALACTIC DISC
M.V.Paliienko ..... 161
OBSERVATIONS OF CATACLYSMIC VARIABLES AT KOLONICA OBSERVATORY
Š.Parimucha, P.Dubovský, I.Kudzej ..... 164
KOROAPS – SYSTEM FOR A LARGE SCALE MONITORING AND VARIABLE STARS SEARCHING
Š.Parimucha, D.Baludanský, M.Vadila ..... 166
WZ SGE STARS
E.P.Pavlenko ..... 168
V1504 CYG: OUTBURSTS
E.P.Pavlenko, E.Berezina ..... 174
EXTREMELY PECULIAR STARS
Ya.V.Pavlenko ..... 176
SPECTRAL VARIATION OF Be HERBIG STARS
L.A.Pavlova, L.N.Kondratyeva, R.R.Valiullin ..... 180
CIRCUMSTELLAR ACTIVITY OF THE HERBIG AE STAR HD163296
M.A.Pogodin, M.M.Guimaraes, S.H.P.Alencar, W.J.B.Corradi, S.L.A.Vieira ..... 182
ON QUASI–PERIODIC INTRINSIC LIGHT VARIABILITY IN A CLOSE SPECTROSCOPIC BINARY CX DRA
I.Pustylnik, P.Kalv, V.Harvig, T.Aas ..... 186
ON THE EVOLUTIONARY HISTORY OF PROGENITORS OF EHBS AND RELATED BINARY SYSTEMS BASED ON ANALYSIS OF THEIR OBSERVED PROPERTIES
V.-V.Pustynski, I.Pustylnik ..... 189
V.P.TSESEVICH AND MOSCOW VARIABLE-STAR ASTRONOMERS
N.N.Samus ..... 193
STUDIES OF GALACTIC CEPHEIDS: THE INASAN/SAI INTEGRATED PROGRAM
N.N.Samus, S.V.Antipin, L.N.Berdnikov, A.K.Dambis, N.A.Gorynya, A.S.Rastorguev ..... 197
THE OBSERVATION OF TOTAL SOLAR ECLIPSE ON MARCH 29, 2006 IN KAZAKHSTAN
L.I.Shestakova, F.K.Rspaev, G.S.Minasyants, A.I.Dubovitskiy, A.Chalabaev ..... 203
THE CBS SPECTRA INVESTIGATION AS METHOD OF THE PN CHEMICAL COMPOSITION ANALYSIS
N.N.Shimanskaya, V.V.Shimansky, I.F.Bikmaev, N.A.Sakhibullin, R.Ya.Zhuchkov ..... 205
SIMULATION OF COLOR VARIATIONS IN GRAVITATIONALLY LENSED QUASAR Q2237+0305 (THE EINSTEIN CROSS)
G.V.Smirnov, V.G.Vakulik, R.E.Schild, V.S.Tsvetkova ..... 208
THE DETERMINATION OF METEOROIDS' LIFE TIME UNDER ACTION OF PHOTONS AND PROTONS
E.N.Tikhomirova ..... 212
EXPANSION OF COCOONS AND PHYSICAL FEATURES OF THE FRI-FRII MORPHOLOGY OF EXTRAGALACTIC RADIO SOURCES
N.O.Tsvyk ..... 215
PHOTOMETRIC OBSERVATIONS AND PERIOD CHANGES FOR THE THREE RR LYRAE TYPE STARS: DM CYG, V341 AQL and AV PEG
S.N.Udovichenko ..... 217
POLARIS ($\alpha$ UMi) – MULTISTELLAR SYSTEM IN THE OPEN CLUSTER
I.A.Usenko, A.S.Miroshnichenko, V.G.Klochkova, V.E.Panchuk ..... 220
PULSATIONAL AND ORBITAL PERIODS OF SMALL-AMPLITUDE CEPHEID SU CAS
I.A.Usenko, V.G.Klochkova, N.S.Tavolzhanskaya ..... 225
THE DISTRIBUTION OF THE GALAXY NONTHERMAL RADIO EMISSION SPECTRAL INDEX AT DECAMETER WAVELENGTHS
N.M.Vasilenko ..... 229
SEARCH OF TRACES OF GEOPHYSICAL PHENOMENA IN SERIES OF LATITUDE DETERMINATIONS ON PRISMATIC ASTROLABE IN POLTAVA
N.M.Zalivadnyi, L.Ya.Khalyavina, T.Ye.Borisyuk ..... 233
OSCILLATIONS IN TW DRACONIS
M.Zejda, Z.Mikulášek ..... 235

# VLADIMIR PLATONOVICH TSESSEVICH – ASTRONOMER-ROMANTIC

M.Yu.Volyanska, V.G.Karetnikov, O.E.Mandel

Odessa Astronomical Observatory, Odessa National University
T.G. Shevchenko Park, Odessa 65014 Ukraine

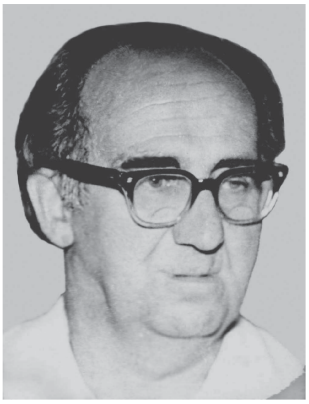

Figure 1: V.P.Tsessevich (1907-1983)

October 11, 2007 marks 100th anniversary of the birthday of the outstanding astronomer, the corresponding member of the Academy of Sciences of the USSR, Honored Scientist of the USSR, Doctor of physical and mathematical sciences, Professor Vladimir Platonovich Tsessevich. Since 1944 till the end of his days he was Head of the chair of astronomy of the I.I.Mechnikov Odessa State University and the Director of the University's Observatory.

Vladimir Platonovich was born on October 11, 1907 in Kiev (he was christened in the Cathedral of Saint Vladimir) in the family of actors: then already known opera singer Platon Tsessevich, later – the National actor of Russian Federation, and young opera actress Elizaveta Kuznetsova, who later worked as a teacher. Soon family broke up, the son remained with the mother, together with whom he lived all his life, taking gentle care of her. The mother imparted in the son the feeling of deep respect to the father – the man talented and not ordinary.

In his early years V.P.Tsessevich lived in Odessa and till 1914 studied at school. Having moved to Petrograd, he continued study in a Real school, then at Uniform labour school. At the end of 1920 he became astronomy amateur and a member of the youth section of the Russian Society of the amateurs "Mirovedenie" and began to observe heaven bodies. In 1922 V.P.Tsessevich, less than 15 years old, entered the Faculty of Physics and Mathematics of the Leningrad (then Petrograd) University. He was helped to overcome the age qualification by the known astronomer professor S.P.Glazenap (as Vladimir Platonovich himself recollected later). When 17 years old, he published his first scientific work in the best magazine of that time (Astronomische Nachrichten, B.221, No.14, S.230-232, 1924). He graduated from the University in 1927 and continued studying in post-graduate in Pulkovo observatory under supervision of G.A.Tikhov, become famous later for studies of the physical nature of Mars. The ways in science of the post-graduate student and his supervisor parted, V.P.Tsessevich conducted scientific researches independently; however, through all his life he talked with great respect about G.A.Tikhov.

After finishing post-graduate studies V.P.Tsessevich worked in the Leningrad University, taught astronomy and mathematics in a number of other high schools of the City on Neva. But his basic interests were connected to variable stars, studying which was the subject of the many of his scientific works. Even when a young man, he came several times in summer with a group of the young amateur astronomers to Odessa, "where the heavens are clear long". In that time the outstanding astronomer A.Ya.Orlov managed the Observatory. Strict and even severe from the outside, A.Ya.Orlov always patronized the young people, who were fond of science. He gave tools and accommodation to Leningrad's amateurs, was interested in their successes and gave to them advices and recommendations. More than once Vladimir Platonovich recollected the beneficial influence of A.Ya.Orlov's personality on the formation of him as a scientist.

V.P.Tsessevich was the actual founder of Astronomical Observatory in Stalinabad (nowadays, the Institute of Astrophysics of the Academy of Science of Tadzhikistan) and in 1933-1937 years – its director. In the same years he worked as a dean of the Physics and Mathematics Faculty of the Night Pedagogical Institute in Stalinabad. On returning to Leningrad in 1937-1942 years he was a scientific fellow of the Astronomical Institute of the Academy of Sciences of the

USSR and a professor of N.M. Pokrovsky Pedagogical Institute. Having begun observing variable stars in 1922, V.P.Tsessevich already made about 200 thousand only visual estimations of the brightness of the variable stars, published many scientific articles. And in 1937 he was given the scientific degree of the Candidate of Physical and Mathematical sciences and the scientific rank of the Professor.

The war of 1941-1945 years found V.P.Tsessevich in Leningrad, he was blockade-survivor, and in 1942 was moved to Stalinabad (nowadays, Dushanbe, Tadzhikistan). The blockade has left a deep trace in his life, in Leningrad his daughter Marina died (he dedicated to her memory the book "What and how to observe in the sky?" which sustained 6 lifetime editions). At the same time his two adopted sons died. Later he brought up adopted daughter Regina, who lives in Kiev, and the daughter of his own Anna (mother E.P. Gladun), who lives in Odessa. From words of the colleagues, who knew "the Professor" (he was called that name often by his students and colleagues) during the first postwar years, he within several years after war constantly carried in the voluminous bag a loaf of bread – the memory of a blockade-survivor did not give him rest.

In Dushanbe V.P.Tsessevich taught in the Odessa high schools, evacuated there, and together with them, in 1944, he came back to Odessa, to which he had grown fond of since young years. He was invited to the University, where he at first became a head of the Chair of the Astronomy, and then was appointed the Director of the University's Astronomical Observatory. (In the same year at the Kazan University he defended a dissertation for the scientific degree of a Doctor of physical and mathematical sciences). The hard job of fixing the work of the Chair and the Observatory in postwar years lay on the shoulders of V.P.Tsessevich. The publishing was renewed. For several years in 1950s V.P.Tsessevich was also a dean of physical and mathematical faculty of the University. Besides, he taught in the Odessa Institute of the Engineers of a Marine Sea Fleet (nowadays Odessa Marine University) and in the Institute of Refrigerating Industry (nowadays the Academy of Cold), was one of the founders of Chair of the Nautical Astronomy in the Odessa High Marine school (nowadays Odessa Marine academy). In 1948 he was selected the member-correspondent to the Academy of Sciences of Ukraine – at this time (1948-1950) combining jobs he worked also as the Director of the Main Astronomical Observatory of the Ukraine, where he established the scientific direction of studying of the variable stars.

In the second half of the 50s of the last century the period of rapid development of the Odessa Observatory begins. From July, 1957 till December, 1958 the International Geophysical Year (IGY) took place under the aegis of the international scientific organizations, which basic task was the all-round research of the influence of the solar activity on processes in the atmosphere of the Earth and circumterrestrial space. Participation in such forum, the process of preparation to it gave a strong push to the development of the Observatory, strengthened its scientific authority.

By this time the design of a meteoric patrol with shutter of the variable section was developed by the scientific employee of the Observatory E.N.Kramer (subsequently by doctor of physical and mathematical sciences, professor) for the research of the atmosphere at heights of 60-120 km by the methods of the meteor astronomy. This design allowed with great accuracy to record the time of the flight of a meteor, taken on a photo snapshot. Having photos from two spatially remote points, it is possible to calculate an orbit of a meteoric particle and characteristics of the atmosphere on a site of its flight. The design of the meteoric patrol received an approval of the scientific public, and it was decided to use such devices in the period of IGY.

It is necessary for the effective work of the patrol, as a minimum, two observation point. The Observatory in Odessa was hardly a choice as one of them because of the ambient light illumination of the sky by the city lights. The question of building the stations in the country aroused. And the organizational talent of Vladimir Platonovich showed itself in its full: his purposefulness, energy, the gift to persuade very different people – from Soviet and the Party officials to the workers, who were carrying out the orders on manufacturing the equipment. Already in 1956 the station in Kryzhanovka in the suburbs of Odessa begins to work, the observation point in the Botanical Garden of the University in "Small Fountain" area is organized. The building of the last and, probably, the most favorite child of V.P.Tsessevich starts – the observation station in the village Mayaki, 40 km from Odessa on the banks of the river Dnestr.

While preparing to IGY and during the implementation of its program it became possible to expand considerable the staff of the Observatory, increasing it by the graduates from the University. V.P.Tsessevich managed to unite the team around solving the tasks of construction and implementation of scientific programs, to pass to the employees his unquenchable enthusiasm. The systematic observations on meteor patrol and seven-camera astrograph began in 1957 on the Mayaki station. An ex-student of V.P.Tsessevich, the talented astronomer S.V. Rublev, was appointed the director of the station, later he was a Deputy Director of the Special Astrophysical Observatory (SAO) of the Academy of Sciences of the USSR in the Northern Caucasus (near stanitsa Zelenchukskaya).

The Professor was usually very attached to his exstudents, always was ready to support them, defend and, if necessary, help financially. Parting with them, especially their transfer to work in other organizations, the Professor took it close to heart painfully, often

the relationship stopped for some time. Unfortunately, there were some people, who played that string in the character of V.P.Tsessevich, deepening the pain from the parting. Although, the employees, who had left the Observatory, in their majority understood this feature in V.P.Tsessevich's nature and in time the relations, as a rule, mended.

Many employees of the Observatory, students of the Faculty of Physics and Mathematics of the University, let alone the students of the Astronomy specialization, took the direct part in the construction of the Mayaki station, and all this without and administrative pressure. The Professor together with everybody else took part in filling the foundations with concrete, building the walls of the pavilions, designing the garden, planting the trees and bushes. Vladimir Platonovich tried by all means to take his guests, often from abroad, to the Mayaki station, sometimes even violating the regime, because that area at the time was closed for the foreigners.

If Mayaki is the favorite child of V.P.Tsessevich, then seven-camera astrograph is his favorite device in Mayaki. The professor himself designed its project, carried out the control over the manufacturing of the device in the University workshops, patiently watched, that the device worked regularly and productively, that the images of the stellar sky, taken on the astrograph in two parts of spectrum, were used effectively in the scientific work, gave instructions on the modernization of the tool. It has to be mentioned, that before this tool V.P.Tsessevich built an astrograph in the Stalinabad Observatory, and in Odessa it was already his third astrograph. Earlier he created "2-camera" astrograph and then the astrograph "Hedgehog" that had 3 cameras. At all, before the 7-camera astrograph about 10000 of photo plates with the images of the stellar sky were collected in Odessa in 1945-1957.

V.P.Tsessevich was the organizer of introduction in Odessa of electro-photometric observations of variable stars, and in the Observatory was created second in the world Depositary of electro-photometric observations of variable stars. At him in the Observatory has arisen and the established new direction for Observatory on stellar spectroscopy, very wide themes on the base of economical agreements on creation spectrophotometric standards and positional and photometric observations of the artificial satellites of the Earth. The means received from performance of contractual works essentially have increased opportunities in updating park of devices and coming into being of new directions of researches.

To 1980s Mayaki turned into modern observatory, which allowed conducting scientific researches at a level, answering to international standards. On the basis of the Observatory in Mayaki a number of All-Soviet Union and international programs was carried out, as within IGY, International Year of Geophysical Cooperation (IGCY), International Quiet Sun Year (IQSY), as according to separate agreed plans (for example, the plan of cooperative observations of the flare stars together with British observatory Jodrell Bank).

Giving all himself to work, living for the long periods of time in his study (I'm the real "office" scientist, – joked he on this occasion), being unpretentious in meals and clothes (though, he knew sense in both), Vladimir Platonovich could not always understand the people, who had any household inconveniences. So, he quite sincerely spoke to the employees, complaining on constrained housing conditions in Mayaki: "But you see you have one more room, which is at your orders round- the- clock – your office. There it is possible to read and to work, and to study".

V.P.Tsessevich loved youth, cared of it, supported the scientific initiative, trusted. Everyone, whom the destiny reduced with him, will find in the life episodes confirming validity of these words. In 1956 there was a great opposition of Mars. There were not many scientific employees in observatory staff then and in interesting observations V.P.Tsessevich involved the students and even of the schoolboys. Sketches of a surface of Mars the young astronomers made, observing a planet in reflector, created by inhabitant of Odessa – known optic and designer of astronomical tools N.G.Ponomarev. Then under the insistence of V.P.Tsessevich these observations were processed and are published. It was joyful event for all participants.

By the same unforgettable event was the preparation for observations and then observations of the first artificial heavenly body – artificial Earth satellite (AES), October 4, 1957, started in the USSR. V.P.Tsessevich himself frequently participated in training employment of group of the observers, took a keen interest in results of the further observations. After start first AES was found out, that their brightness varies. V.P. first has executed photometric observations of AES, has stated the basic ideas on use of such observations and then has transferred the further development of a theme to the post-graduate student V.M.Grigorevsky. For last photometry of AES and the problems, connected to it, have made the basic direction of scientific activity, became a subject of his candidate and doctor's dissertations.

There are some more facts on memoirs of the authors describing the attitude V.P.Tsessevich to youth. Per student's years the group of three men, among them one of the authors of the present article (O.E.Mandel), carried out collective observations of variable stars with the help Zeiss binocular. At change of the observer at an eyepiece someone unintentionally has hooked on a support, binocular has fallen, on a pipe was formed the dent. We very much worried that happen. However V.P.Tsessevich, having established, that the incident took place during work, but not soiling, has not discharged anybody of observations, has disposed and in

the future to give out to us the tool. One of the authors (O.E.Mandel) in the period, when V.P.Tsessevich supervised over Chair of High mathematics in the Institute of the engineers of Marine fleet, conducted there on conditions of hourly payment practical employment. Unexpectedly V.P.Tsessevich is directed to long business trip in USA. "Will read instead of me course under the theory of functions complex variable and theory of a field", – the Professor speaks. "But I in general yet did not read rates of lectures"! "Anything, there is the abstract of a rate for you, you have some pedagogical experience, and training others, and yourself will learn something. So for the post-graduate student it only will be useful".

Distinctive feature V.P.Tsessevich was trust to the employees, belief that by them on forces the decision of the diversified tasks. This conviction was based that all material opportunities of observatory were given in the order to the students, employees. Democracy of Vladimir Platonovich, his almost constant stay in observatory provided an opportunity of advices practically at any time of day. At many astronomical conferences of a delegation from Odessa were one of most numerous and young on age.

In 1965 to V.P.Tsessevich there has arrived the deputy Director building S of Academy of Sciences of the USSR O.B.Vasiliev (director there was a corresponding member of AS USSR O.A.Mel'nikov). It was time already to make sectoring of the base for a six-meter telescope , and exact coordinates of an installation site of a telescope (in mountains, at height 2100 ) yet was not appointed. The geodetic organizations were loaded, and not so aspired to determine astro-point in difficult conditions of high-mountain, and the matter was urgent. V.P.Tsessevich has offered to execute work by forces of the Odessa astronomers. At this time in observatory still worked known astrometrist, possessing experience of definition of astropoints, Boris Vladimirovich Novopashenny. He has agreed to head expedition, however shortly before departure was found out, that on a condition of health seven-ten years' Boris Vladimirovich can not participate in expedition. Then Vladimir Platonovich charges performance of work to three young research fellows, and he becomes at the head of expedition. The astropoint was determined. The construction works have begun in time.

V.P.Tsessevich twice flied to town Mineralnye Vody, reached on mountain roads in stanitsa Zelenchukskaya, rose on impassability (road only was under construction) on a mountain. At signing the certificate of completion of works one of the participants has joked: "What you, astrophysicist, have trained for a new profession in astrometry"? "And I, by the way, professor of Astronomy also is obliged to have a wide outlook and skills of work in various areas of a science about the stellar sky", – has answered Vladimir Platonovich. And many witness validity of these words, whether the business of astronomical instrument making (creation "firm Zeissevich" on manufacturing telescopes), organization of a fireball network, radar-tracking observations of meteors, problems connected with AES, asteroids or wave mode at moorings of seaport in Illichevsk town near Odessa concerned.

By the way, on investigations of asteroids. The first work of Vladimir Platonovich on this subject has appeared in 1930 and was devoted to research variation of brightness asteroid Eros. Further, on an extent almost 50-y years V.P.Tsessevich studies of physics of small planets was published about ten scientific researches and this subjects was handed over his post-graduate student N.I.Koshkin, which subsequently has protected the candidate dissertation on a theme "Photometric method of definition of orientation of an axis of rotation and others kinematical and optical characteristics of asteroids with the large amplitudes of change of brightness". In this work were concentrated and the ideas V.P.Tsessevich on application of photometric observations of asteroids for their all-round research are advanced. It may confirm that the works of V.P.Tsessevich on early researches of photometric features of Eros and definition of the period of its rotation and direction of an axis of rotation became that basis, which has helped to apply these methods to definition of the same parameters of the first artificial Earth satellites advanced subsequently by V.M.Grigorevsky.

However, first of all V.P.Tsessevich was all the same astrophysicist- "peremenschik", that is, researcher of variable stars. Having begun observations somewhere in 1922, he remained faithful to this matter all life. Into an orbit of his interests all types of variable stars got practically. But, being "by the observer at a telescope", by virtue of the temperament he preferred that of them, where the change of brightness could be fixed directly by eye within night. This condition is answered by stars such as RR Lyrae- type, and also eclipsing variables. In understanding of a nature of such stars, the contribution V.P.Tsessevich is most significant. Per 30 years of the last century at active participation of the Professor in USSR the service of "antalgols" was adjusted, as then frequently named stars such as RR Lyrae variables. The tracking the periods of these stars and light curves was carried out. This service was renewed already at the international level under aegis of the International Astronomical Union per the sixtieth years. By the coordinator of the program was acted the Odessa observatory. The results of researches were published as the appendix to "Rochnik Astronomichny" of Krakow observatory (Poland). Results of the extensive researches of these stars V.P.Tsessevich has summed up in the monograph "Stars of RR Lyrae type", and also in the multivolume collective monograph "Non-stationary stars and methods of their research", where he represented himself as the editor and

author of a lot of the chapters. The especially important results are received by him in the description and interpretation of effect Blazhko from RR Lyrae variables.

In the field of study eclipsing variables V.P.Tsessevich was indisputable authority. He is the author of the several monographs concerning a nature of these stars and definition of their orbits, co-author known fundamental three-volume monograph "Variable stars". The tables, made by him for the resolve of light curve of eclipsing variables some generations of the astronomers used. They find application and now. As recognition of merits V.P.Tsessevich his election a Chairman of Commission 42 on eclipsing variables of the International Astronomical Union was.

Essential contribution of V.P.Tsessevich in study of other types of variable stars: Cepheid variables, RV Tauri stars, Mira Ceti stars, some unique objects. For the Professors the aspiration was characteristic to tie up among themselves different directions of astronomical researches. So, classical astrometric works he tried to sate with the astrophysical contents. Under his management in Odessa were executed meridian observations of the catalogues of positions and proper motions of red-giant stars (B.Novopashenny, M.Volyanska, I.Suprunets), Cepheid variables (E.Ludchenko), eclipsing binaries (M.Volyanska).

V.P.Tsessevich accumulated and in the majority processed huge numbers of visual observations of variable stars and estimations of brightness on photos of the stellar sky. As the observer, he amazed all virtuosity of process. He knew and remembered by decades the positions in the sky of tens, if not hundreds, variable stars and that allowed him to build optimum transition from one star to another during observations. He together with M.S.Kazanasmas issued the atlases of search cards of vicinities 4512 variable stars. Process of observations Professor usually finished "by walk on the sky", inducing a telescope on remarkable objects: ring nebula in Lyra, globular cluster in Hercules, nebula in Orion, nebula in Andromeda, galactic cluster in Perseus, many-coloured double and multiple stars. Thus he received the large pleasure, if someone was near and shared with him delight from seen.

At V.P.Tsessevich there were many pupils. Some of them from him have apprehended a virus of construction and organization of new astronomical establishments. We already mentioned S.V.Rublev. The Director of Pulkovo observatory became V.K.Abalakin. Reconstructed astronomy in Moldova and built there observatory V.M.Grigorevsky. The schoolboys of V.P. have organized observant stations of Odessa observatory on peak Terskol in Caucasus; on a mountain Dushak-Erekdag in Turkmenistan, on pass Bezimenny in Armenia, went for observation and creation of astrostation in Mondy by border with Mongolia, on Pamir (height 4000 ). The stations were equipped by tools and devices created in Odessa astronomical observatory. Under the initiative of the Professor were made 40- telescopes for V.I.Lenin's school in Ulyanovsk, for All-Union pioneer camp ""Orlenok" near Novorossiysk, for the Bolivian station of Astronomical Council USSR, for Sheged University in Hungary. By the way, last telescope became a basis for creation astronomical observatory of Sheged University fruitfully working and presently. The telescopes for many others observatory of Union were made. Almost in everyone observatory in territory former USSR will be the pupils of the Professor.

V.P.Tsessevich easily entered the confidential relations with the representatives of the different peoples, with deep respect concerned to their culture and language. Among his pupils and post-graduate students there were representatives of Azerbaijan, Georgia, Kirghizia, Tadzhikistan, Bulgaria and other countries. Many from them carried out the researches in Mayaky. Versatility of interests of V.P., his work, besides university, a head of a chair of High mathematics in different time in present Academy of a Cold, Marine Academy, Marine University promoted to that the Professor had very many pupils and among not of the astronomers. Many from them under his management became the candidates and doctors of sciences and successfully work in high schools, scientific institutions, at factories of Odessa both other cities and countries of the world.

The cooperation with High Marine School was especially fruitful, as then the Marine academy referred to as. On the basis of astrometry section of Odessa observatory on meridian circle, passage, universal tools carried out researches the post-graduate students and teachers of chairs of nautical astronomy, navigation, automation of navigation. At the same time employees of observatory had an opportunity to make use of the computer park of a school. On the basis of carried out in observatory observations by the employees of a school are defended of more ten candidate dissertations and one doctor's, tens scientific articles, star catalogues are published. And all V.P.Tsessevich has prepared about 40 candidates of sciences, and his many pupils have defended the doctor's dissertations. Remarkable feature of V.P.Tsessevich was his scientific generosity. Distributing scientific ideas, giving out results of the observations, he never applied for the co-authorship, and quite often he should be persuaded, that he should have put the signature under article, where the joint development, and frequently and primary results, received by him were used.

Some more words about the attitude of Vladimir Platonovich to the employees. In heavy times with habitation (these times in our country unfortunately do not stop) V.P.Tsessevich used all opportunities, available at his disposal, to facilitate a situation of the people. In observatory and observation stations long

time many employees, frequently together with families lived. The professor had to be engaged and pull the strings for reception of normal habitation for the employees. Eventually, many from living in observatory collaborators have found habitation in city, and he has helped some to find and summer residence in prestigious areas of city.

V.P.Tsessevich, as far as we know, was not specifically engaged in sports, was not a heated fan, but understood well the importance of sports, especially for youth. In the observatory in the city and in Mayaky there were volleyball fields (Professor himself sometimes stood in a team), there was a table for table tennis in Mayaky, billiard-table, a boat for rowing on river Dnestr, in the observatory in the city – cruising yacht, the competitions among the employees were carried out. The cultural initiatives of any sort were also supported. For cultural needs in Mayaky the tape recorder, TV set (rare in 1950s -1960s) were acquired, there were newspaper subscriptions, the quite good library of literature collected. Village children resorted ran to watch television programs – V.P.Tsessevich welcomed that very much. In general, he supposed, that the Observatory should become the center of culture in the village. Under his initiative in Mayaky the cycle of lectures on natural and humanitarian subjects was read for the villagers. The lecturers from the University were invited and the scientists from the Observatory took part also.

In general, the contribution of V.P.Tsessevich in the popularization of scientific knowledge deserves a special conversation (mention). The perfect lecturer, he was one of the founders of the Odessa regional organization of the society "Znanie" ("Knowledge"), the permanent Chairman of the Odessa branch of the All-Union Astronomy and Geodetic Society and the member of the Central Council of that. Due to persisting efforts of the Professor the Regional Planetarium was open in Odessa in 1963 and the first lecture "A Walk along the Stellar Sky" was read by V.P.Tsessevich. When any outstanding scientists came to Odessa, the Professor always tried, sometimes contrary to the personal predilections that they would talk in front of the astronomers, scientific public, city people. So, though his relation with the member – correspondent of the Academy of the Sciences of the USSR I.S.Shklovsky cannot be named cloudless, when this brilliant scientist came to Odessa together with R.S.Sagdeev and N.S.Kardashev, the meeting with them was held and in the Central lecture-hall of the society "Znanie", and in the Observatory. And when well-known American astrophysicist L.Goldberg was in Odessa, the meetings with him were organized both in the Observatory, and at the University, and in the Central lecture-hall, and part of the fee for the lecture V.P.Tsessevich paid from his personal savings. And how many of these personal savings he spent on different needs of the Observatory! It cannot be counted, but it is safe to tell, that it was a lot.

Despite his wide scientific interests and big achievement in many areas of astronomy, in last years of his life in conversations with the colleagues V.P.Tsessevich expressed sometimes some dissatisfaction with his activity. Probably, it was related to the restriction of mobility because of illness – that, certainly, had an effect on his moods, the man, who had got used to a very active lifestyle. With all his consuming interest to astronomy he also had a good knowledge of literature (especially, he loved Rabelais, Mark Twain), music, played on a piano, and in 1950 years, it happened, sang in the company of the employees. The colleagues certify, that he had quite good dramatic tenor, he loved romances, especially, "Ya vstretil vas" ("I met you"). At the end of his life way it always seemed to him, that something main in his life he had not yet made. It was necessary to dissuade him, to remind of the scientific merits, that now it is necessary to give more attention to health. But as soon as improvement came, the sad thoughts left the Professor, and he again developed energetic activity, so that many young people could envy his energy. Such active, cheerful he remained in the memory of people, who knew him. V.P.Tsessevich died on October 28, 1983 and is buried on the Second Christian cemetery of Odessa.

In the scientific baggage that V.P.Tsessevich left to us there is about 400 thousand estimations of the brightness of about 500 variable stars of different types; the list of his publications totals more than 730 scientific articles, notes and other publications, among which 22 monographs. And taking into account his editorial work, introductions, interviews and comments, this figure increases considerably. More than 80 publications are dedicated to V.P.Tsessevich and his biography.

The merits of V.P.Tsessevich were marked by the high governmental awards: by an order of Lenin, order of the Red Banner of Labor, many medals, and difficult to count number of honorable and gratitude letters from the governments of different republics of the USSR. In memory of the Professor on the main building of the Odessa Astronomical Observatory, where he lived and worked about 40 years, on October 11, 1990 there was established a memorial board with a bas-relief, and during the next years 6 scientific conferences dedicated to him were carried out. The memory about V.P.Tsessevich remained in centuries – in the depths of space there goes along its orbit the asteroid 2498 with a name "Tsessevich".

# ABOUT TREND IN ZINC STELLAR ABUNDANCES WITH METALLISITY

U.Sh. Bayazitov[1], F. Thevenin[2]

[1] Department of Physics, Magnitogorsk State Technical University
Lenin Str. 38, Magnitogorsk 455000 Russia, *bayazit@mail.ru*
[2] Department Cassini, Observatoire de la Cote d'Azur, Nice 06304 France

ABSTRACT. We have carried out investigation of zinc abundance behavior in wide range of stellar metallicities from 0 to -5. It has been determined zinc abundance using our Zn atom model and NonLTE calculation method. It has been shown that difference between LTE and NonLTE Zn abundances may reached up to 1.27$dex$.We have obtained the dependence of $[Zn/H]$ from $[Fe/H]$. The first value is greater as metallicity lower.

**Key words**: abundances - stars: fundamental parameters - stars.

## 1. Introduction

The well known metallicity index [Fe/H] is close connected with stellar age. The study of relationships of stellar chemical elements abundances with $[Fe/H]$ is the actual astrophysical task. Sneden et al. (1991) and Mishenina et al. (2002) conducted the determinations of zinc abundance for the wide range of stars (mainly for AGB type stars). Particularly, they investigated the correlation between $[Zn/H]$ and $[Fe/H]$ values. But this correlation were not been found in range of metallicities from 0 to -3. The Zn abundance determinations by previous authors was been carried out in LTE assumption for the stellar atmospheres.

This assumption may lead to great errors in the abundance estimations. Our study has been carried out without LTE assumption. For this purpose we have used MULTI code (Carlsson, 1998) and stellar atmosphere models of Kurucz (1993).

## 2. Zn atom model and test calculations

Our Zn atom model consists of 12 Zn I levels and one Zn II level. We have used 18 radiative transitions in detail.

The test calculations has been carried out using our Zn atom model and solar atmosphere model of Kurucz (1993). The zinc abundance equals to $\log(\epsilon_{\odot}) = 4.60$ has been taken from Anders and Grevesse (1989).

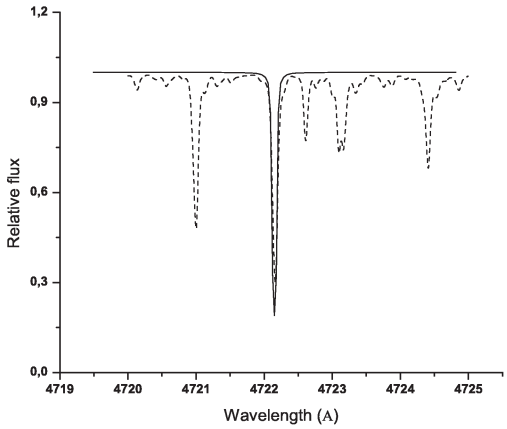


Figure 1: Calculated and observed (dot) profiles of $\lambda 4722 ZnI$ line.

We have used constant micro-turbulence velocity value equals to 1 km/s. The fig.1 shows observed (dot) and calculated profiles of $\lambda$4722 ZnI lines. As it follows from this figure the good agreement has been reached between observed and calculated profiles.

We also calculated equivalent widths of $\lambda\lambda 4722, 4810 ZnI$ lines for the solar disc center and for the whole disc. These values with observed ones (Moore et al. 1966) are given in table 1. Good agreement between calculated and observed values has been achieved again. This is means, that our atom model as well as Kurucz's atmosphere models are useful for the stellar zinc abundance determinations.

Table 1: The calculated and observed equivalent widths of $\lambda\lambda 4722, 4810 ZnI$ lines for the solar disc center and for the whole disc.

| $\lambda(\AA)$ | W(center) | W (disc) | W(center)Moore et al. |
|---|---|---|---|
| 4722.151 | 75.390 | 75.143 | 63 |
| 4810.527 | 86.102 | 85.504 | 84 |

### 3. Dependence of stellar $[Zn/H]$ values from metallicity

As it has been mentioned above, Sneden at al. (1991) and Mishenina et al. (2002) carried out study of [Zn/H] dependence from $[Fe/H]$ for the wide range of stellar metallicities. They not obtained this dependence. We have restudied this problem using NonLTE Zn abundance determination and stellar list from these works. The $\lambda\lambda 4722, 4810 ZnI$ lines equivalent widths, stellar effective temperatures, gravities and metallicities have been adopted according previously mentioned articles.

We have also included two extremely metal poor stars HR4045 and CS 22949-037. The Zn observed equivalent widths and stellar parameters for these stars have been taken from Takeda et al. (2002) and Depagne et al. (2002), respectively.

We have plotted Zn abundance differences versus stellar effective temperatures. The NonLTE effects in these abundances grow linearly with temperature rising. We have also investigated dependence of the NonLTE Zn abundance discrepancies from stellar gravity. These discrepancies have complicated character and we not discuss these ones now.

Fig.2 shows dependence of $[Zn/H]$ from $[Fe/H]$. According for our calculations the $[Zn/H]$ values grow linearly with metallicity decreasing. The slope of approximation line has value -0.084. This result contradicts for that one obtained by Sneden et al. (1991) and Mishenina et al. (2002). We remind, that according them the $[Zn/H]$ values are not changed in wide range of stellar metallicities. For the checking our conclusion we added two stars not from list of Snaden et al. (1991)and Mishenina et al. (2002). There are HR4045 (Takeda et al. (2002)) and CS 22949-037 ( Depagne et al. (2002) with extremely low metallicities -4.7 and - 3.9 respectively. As it is shown from fig.3 the investigated dependence has now exponential character. This dependence may be described by function $[Zn/H] = 0.064 + 0.0031 \exp(\frac{-[Fe/H]}{0.66})$.

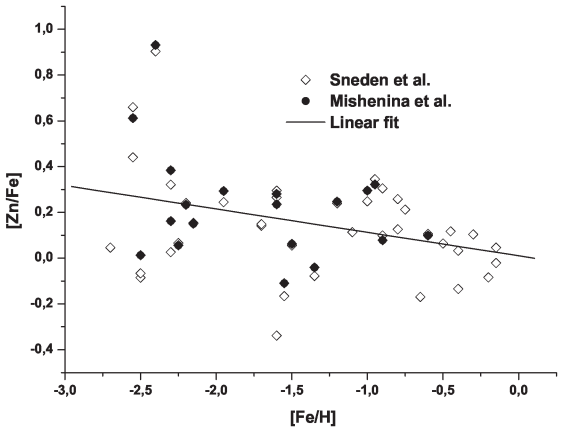


Figure 2: The dependence of $[Zn/H]$ from $[Fe/H]$ for the Sneden's et al. and Mishenina et al. stellar lists.

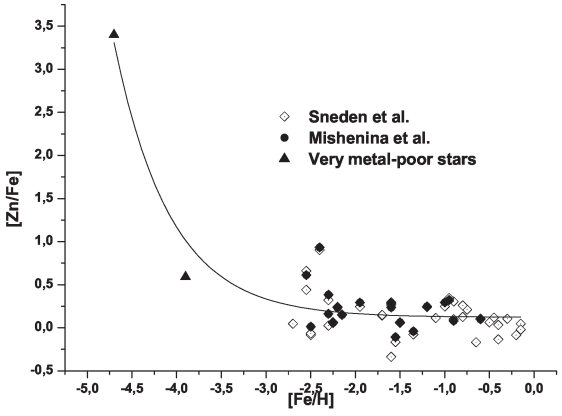


Figure 3: The dependence of $[Zn/H]$ from $[Fe/H]$ with two added metal-poor stars.

### 4. Conclusions

We have carried out investigation of zinc abundance behavior for wide range of stellar metallicities.

It has been determined zinc abundance using our Zn atom model and NonLTE calculation method (MULTI code (Carlsson 1998)). The list of investigated stars has been chosen from Sneden et al. (1991) and Mishenina et al. (2002). We have also included two extremely metal pure stars to used stellar list. It has been shown that difference between LTE and NonLTE Zn abundances may reached up to 1.27 dex (HR4045). NonLTE deviations grow by rising of stellar effective temperatures.

We have obtained the dependence of [Zn/H] from [Fe/H]. The first value is greater as metallicity lower. This result contradicts to that one was obtained by Sneden et al. (1991) and Mishenina et al. (2002).

If our conclusion is true, this is means that zinc abundance values was higher in earlier stages of stellar evolution than this ones in younger stars.

Because the [Zn/H] trend from metallicity is unlinear, we must include to further investigations wide set of stars with extremely low metallicities near -4, -5.

*Acknowledgements.* We wish thank Dr. T. Mishenina for giving us unpublished stellar Zn equivalent widths.

**References**

Sneden C., Gratton R.G., Crocker D.A.: 1991, *Astron.Astrophys.,* **246**, 354.

Mishenina T.V., Kovtyuukh V.V., Soubrian C., Travaglio C., Busso M.: 2002, *Astron.Astrophys.,* **396**, 189.

Carlsson M.: 1998, *Uppsala Spec. Rep.,* **126**.

Kurucz R.L.: 1993, *ASP.Conf.Ser.,* **44**, 87.

Anders E., Grevesse N.: 1989, *Geochem. et Cosmochim. Acta.,* **53**, 197.

Moore C.E., Minnaert M.G., Houtgast J.: 1966, *NBS Monog.,* **61**.

Takeda Y., Parthasarathy M., Aoki W. et al.: 2002, *Publ. Astron. Soc. Japan.,* **54**, 765.

Depagne E. Hill V., Spite M. et al.: 2002, *Astron.Astrophys.,* **390**, 187.

# V.P. TSESSEVICH - PROMINENT RESEARCHER OF VARIABLE STARS

Vladimir P. Bezdenezhnyi
Department of Astronomy, Odessa National University
T.G.Shevchenko Park Odessa 65014 Ukraine
*astro@paco.odessa.ua*

"I talk it to you as variabler about Variabler."

"Who is variabler?" - the nescient will ask, having heard this word on astronomic jargon. It is a researcher of variable stars, if to talk in normal language. But here is some fineness in understanding, a certain tint. Even in the "Department of researches of variable stars", that was organized by V.P. Tsessevich, being director of the Astronomical observatory of Odessa State University, and which he headed a few decades, he considered not all of employees (staff researchers, research fellows, research assistants) as variablers. Only those, who themselves observed variable stars in a telescope by eye or using an equipment (electrophotometer, spectorgraph or photocamera), who saw with the eye in the eyepiece of telescope or guide as a star changed the brightness, who knew its position on the sky in relation to other brighter stars, and could quickly point a telescope at a star. In fact quick changing of the brightness of short-period star, for example, RR Lyrae or delta Scuti type, will not wait for observer. A good time resolution needs for careful research of variable star, construction of its light curve and determination of some their specific features in its variations. Especially, as an observer can follow after a few, and even tens of variable stars one after another, as more frequent as possible pointing a telescope on each of them. And life of observer is not easy! It is often necessary to observe in stuffy summer night, sometimes in an uncomfortable pose, suffering the bites of mosquitoes, and in winter at 20 degrees of frost, such that observer stick to the telescope.

V.P. Tsessevich himself, as the saying goes, felt a star, knew that it "had gone" from a minimum of brightness to a maximum one or vice versa. He was in earnest about observations and their subsequent reduction as to the sainted action; had phenomenal memory and could very quickly find in the sky any of hundreds observed him variable stars, sometimes after a long time-break (even in tens of years) in observations of this star. It was sui generis art which many observers delighted in. V.P. Tsessevich remembered photometric and physical properties of many stars investigated by him. Possessing enormous erudition and diligence, he summarized the results of these long-term researches in a few monographs on different types of variable stars: RR Lyrae, RV Taurus, eclipsing variables et cetera. In these works V.P. Tsessevich proved as prominent systematizer of knowledge about variable stars. Some his books were translated into English and other languages and published in different countries of the world. He was an outstanding expert in the world on RR Lyrae type stars and eclipsing variables.

V.P. Tsessevich possessed good mathematical skills, holding two jobs in different years he was a professor and even manager by the department of higher mathematics in some institutes of Leningrad and Odessa. He improved the methods of mathematical reduction of eclipsing variables stars, calculated by hand (comhuters were absent at that time) the detailed tables for determination of elements of orbits of these stars from the analysis of their photometric light curves. However for fun, he named mathematical statistics, applied at reduction of observations, by the third type of lie. V.P. Tsessevich delivered some difficult theoretical lectures for students: "Relativistic astrophysics", "Celestial mechanics", "Theory of internal structure of stars" et cetera. But he admitted to us, the students and young employees then, that his "brain is arranged somehow not in theory". We thought then, looking at the top of his position and authority: "were evrybody had such brains!" He translated from English into Russian the future Nobel Prize Laureate S. Chandrasekar's fundamental theoretical book "Introduction into the studies of the structure of stars". But it is true, V.P. Tsessevich had no such purely theoretical works. Thirty years ago V.P. Tsessevich admitted to the author of this article: "P.P. Parenago had ideas in science, B.V. Kukarkin had ideas, P.N. Kholopov (which was not a person of the same age as V.P. Tsessevich, but fifteen years younger than him - remark by author) had ideas, too. But Tsessevich did not have ideas!" After this he struck his hand on the table. Certainly, he had in view great ideas, leaving substantial contribution in science. I tried to object something,

feeling that he was in a bad temper. V.P. Tsessevich only waved his hand on that. And another time, when we rode by microbus from the university, V.P. Tsessevich said (being in bad temper after a talk with the authorities): "How they dare to answer me so! I am the son of People's artist and honoured worker myself!" (V.P. Tsessevich's father - Platon Ivanovich was a prominent opera singer, People's artist of Russia, sang on the French stage together with F.I. Shalyapin; V.P. Tsessevich was a Corresponding Member of Academy of Sciences and Honoured worker of science of Ukraine).

Vladimir Platonovich had a good English, and not only read and translated the articles and books in English, but also spoke fluently. After a half-year stay in 60-th in Harvard observatory (USA), he was invited to give a lecture in English at the faculty of foreign languages of Odessa State University. Organizers appreciated his spoken language.

V.P. Tsessevich was the charming teller of different life's histories and anecdotes, he remembered enormous amount of them. He was acquainted with many famous people of the time. I remember how we, charmed students, listened to the professor's recital about his congratulation (Symposium of IAU in 1963) of living classic of science Eynar Herzsprung concerning his 90 years anniversary. V.P. Tsessevich presented to person whose anniversary was celebrated crystal wineglass. I remember other case, when we four together (V.P. Tsessevich, Yu.A. Medvedev, V.V. Dragomireckiy and me) made a business trip to Moldavia (Kodry), to help moldavian colleagues to arrange the recently organized observatory. Telescope in a dome was put in order for two or three days; then my colleagues left, and I stayed for a month to share experience of observations of variable stars and their reduction. Having arrived to Kodry, we sat in the small hours, speaking on different (not only astronomic) themes. With the great pleasure we listened to the stories which V.P. Tsessevich told including his witty anecdotes. There I tried to vie with him in the telling of anecdotes, on what V.P. Tsessevich answered that he would bequeath to me his two notebooks with anecdotes. But because there were political anecdotes too, he promised me these notebooks only after his death. (V.P. Tsessevich was very afraid of KGB - not for nothing!) Unfortunately, these notebooks from his archive disappeared somewhere. What a pity! There was a lot of historical and witty things.

And it must be said especially that V.P. Tsessevich possessed another remarkable talent - it was his activity as popularizer of science. He did much for propaganda of astronomic knowledge, delivering lectures for different audiences, including radio and television. And his popular scientific books on astronomy, such as "What and how to observe in the sky?", "Leading lights of the Universe" and "Variable stars and methods of their researches" were the table-books of astronomers-amateurs in the USSR. Due to them many enthusiasts fell in love with astronomy and devoted their lives to it, becoming astronomers - professionals.

The name of V.P. Tsessevich forever added a glorious page to history of astronomy. One of asteroids of the Solar system is named in his honour. And after 30 years many researchers cite his works on variable stars. Every five years the international anniversary scientific conferences of astronomers are held in Odessa in his honour. There were little such enthusiasts - researchers of variables stars as V.P. Tsessevich and another prominent German astronomer Kuno Hofmeister. They investigated enormous amount of variable stars and carried out hundreds and thousand observations! It is titanic labour of high artists - science devotees!

*Acknowledgement.* The author would like to thank S.M. Andrievsky for some help with English.

# THE CLASSICAL CEPHEIDS' HISTOGRAMS OF PERIODS DISTRIBUTION

Vladimir P. Bezdenezhnyi
Department of Astronomy, Odessa National University
T.G.Shevchenko Park Odessa 65014 Ukraine
*astro@paco.odessa.ua*

ABSTRACT. On the base of GCVS sampling has been carried out the analysis of periods of classical Cepheids. We have studied the histograms of periods distributions for the stars with small amplitudes (DCEPS) and large ones (DCEP) separately. These two histograms have different sight (amplitudes of the peaks), but their peaks follow to general sequence. We have given the modal interpretation of the histograms on the base of mode identifications.
**Key words:** Stars: classical Cepheids, histograms of periods distribution, mode identifications

On the base of the sampling (473 classical Cepheids with the known periods) taken from the fourth edition of the General Catalogue of Variable Stars (volumes 1-3, 1985 a, 1985 b, 1987, hereafter GCVS) we have constructed two preliminary histograms of periods distribution of these variable stars. The intervals of periods in these two histograms are 5 and 2 days respectively. It lets us to distinguish positions and realities of peaks. The most distinct peaks of periods distribution are at periods: 3.25, 4.25, 5.25, 7.25, 9.75, 12.75 and 15.5 days in these two histograms.

However we take into account that all classical Cepheids subdivide into two subclasses. And so, we have constructed two histograms (see Tab.1, Tab.2 and Fig.1, Fig.2) of periods distribution of these variable stars with small amplitudes (DCEPS) and large ones (DCEP) separately. The intervals of periods in these two histograms are 2 days. We have studied the histograms of periods distribution for two subclasses (435 and 38 stars respectively) of these variable stars with the purpose of detection their common characteristics and particular features.

Comparison of two histograms in Fig.1 and Fig.2 confirms that DCEP and DCEPS stars are different objects. As we can see (Tab.2 and Fig.2), the main peak of periods distribution for DCEPS stars is at the mean period about 3.3 days, and two more clear peaks are present at 4.4 and 5.5-5.6 days. Less reliable peaks with small amplitudes are also present at: 1.9, 2.7, 3.1, 6.5, 7.5, 8.4, 9.6, 13.7 and 17.1 days.

Experience shows, that identifications of periods

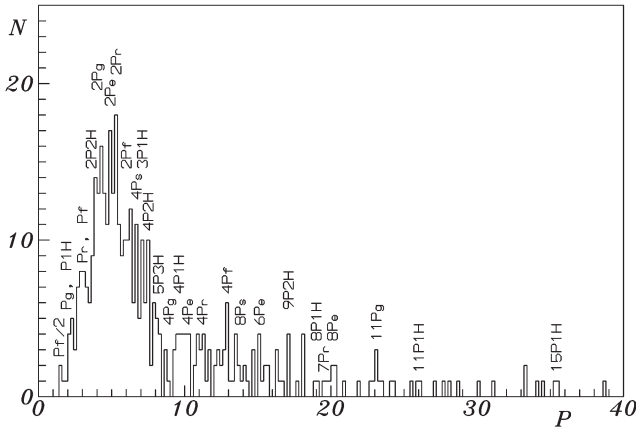


Figure 1: Periods distribution (dP=0.2 days) of large amplitude classical Cepheids (DCEP)

among possible alternatives are easier and more reliable, if we begin analysis with big periods, even they have peaks with small amplitudes. At that, a key to identification is an analysis of periods commensurability (or multiplicity) relations. We take as hypothesis, that period of 17.1 days is Pg-overtone and 13.7 days is period Ps. The latter has found by us in frequency analysis of bimodal Cepheids and RR Lyrae - type stars (Bezdenezhnyi, 1997a, 1997b). And a peak at 9.6 days is a half period $P_{1H}/2$. So we have periods relations 9.6/13.7=0.701 and 13.7/17.1=0.801, near to theoretical values 0.703 and 0.8. It allows to explain all the set of DCEPS stars' periods.

Then the rest of periods from the set of DCEPS stars' periods will be identified as: 1.9 days = $P_{2H}/4$, 5.6 days = $P_r/4$, 2.8 days = $P_r/8$, 8.4 days = $P_g/2$, 6.5 d = $P_s/2$, 3.3 d = $P_s/4$, 4.3 d = $P_g/4$, 7.5 d = $P_{2H}/2$, 3.1 d = $P_f/8$. Period 3.1 days with the largest amplitude is the basic one. We adopt it as fundamental period $P_f$, then new identification will be obtained from previous by means of multiplication by a factor of eight. 1.9 d = $2P_{2H}$, 2.8 d = $P_r$, 3.1 d = $P_f$, 3.3 d = $2P_s$, 4.3 d = $2P_g$, 5.6 d = $2P_r$, 6.5 d = $4P_s$, 7.5 d = $4P_{2H}$, 8.4 d = $4P_g$, 9.6 d = $4P_{1H}$, 13.7 d

Table 1: The histogram of large amplitude classical Cepheids' (DCEP) periods distribution (dP=0.2 days, n=435 stars)

| ΔP | N | ΔP | N | ΔP | N |
|---|---|---|---|---|---|
| 0.0 - 1.0 | 0 | 9.6 - 9.8 | 4 | 18.4 - 18.6 | 0 |
| 1.0 - 1.2 | 0 | 9.8 - 10.0 | 4 | 18.6 - 18.8 | 0 |
| 1.2 - 1.4 | 0 | 10.0 - 10.2 | 4 | 18.8 - 19.0 | 1 |
| 1.4 - 1.6 | 2 | 10.2 - 10.4 | 4 | 19.0 - 19.2 | 1 |
| 1.6 - 1.8 | 1 | 10.4 - 10.6 | 0 | 19.2 - 19.4 | 0 |
| 1.8 - 2.0 | 1 | 10.6 - 10.8 | 2 | 19.4 - 19.6 | 1 |
| 2.0 - 2.2 | 4 | 10.8 - 11.0 | 4 | 19.6 - 19.8 | 1 |
| 2.2 - 2.4 | 5 | 11.0 - 11.2 | 3 | 19.8 - 20.0 | 1 |
| 2.4 - 2.6 | 3 | 11.2 - 11.4 | 4 | 20.0 - 20.2 | 2 |
| 2.6 - 2.8 | 7 | 11.4 - 11.6 | 1 | 20.2 - 20.4 | 2 |
| 2.8 - 3.0 | 8 | 11.6 - 11.8 | 3 | 20.4 - 20.6 | 0 |
| 3.0 - 3.2 | 8 | 11.8 - 12.0 | 0 | 20.6 - 20.8 | 0 |
| 3.2 - 3.4 | 7 | 12.0 - 12.2 | 2 | 20.8 - 21.0 | 1 |
| 3.4 - 3.6 | 6 | 12.2 - 12.4 | 3 | 21.8 - 22.0 | 1 |
| 3.6 - 3.8 | 9 | 12.4 - 12.6 | 2 | 22.6 - 22.8 | 1 |
| 3.8 - 4.0 | 14 | 12.6 - 12.8 | 3 | 22.8 - 23.0 | 1 |
| 4.0 - 4.2 | 13 | 12.8 - 13.0 | 6 | 23.0 - 23.2 | 3 |
| 4.2 - 4.4 | 16 | 13.0 - 13.2 | 1 | 23.2 - 23.4 | 1 |
| 4.4 - 4.6 | 13 | 13.2 - 13.4 | 1 | 23.4 - 23.6 | 1 |
| 4.6 - 4.8 | 11 | 13.4 - 13.6 | 4 | 24.0 - 24.2 | 1 |
| 4.8 - 5.0 | 17 | 13.6 - 13.8 | 2 | 24.2 - 24.4 | 1 |
| 5.0 - 5.2 | 13 | 13.8 - 14.0 | 1 | 25.4 - 25.6 | 1 |
| 5.2 - 5.4 | 18 | 14.0 - 14.2 | 2 | 25.8 - 26.0 | 1 |
| 5.4 - 5.6 | 11 | 14.2 - 14.4 | 1 | 26.0 - 26.2 | 1 |
| 5.6 - 5.8 | 9 | 14.4 - 14.6 | 0 | 27.0 - 27.2 | 1 |
| 5.8 - 6.0 | 10 | 14.6 - 14.8 | 3 | 27.6 - 27.8 | 1 |
| 6.0 - 6.2 | 10 | 14.8 - 15.0 | 0 | 28.0 - 28.2 | 1 |
| 6.2 - 6.4 | 12 | 15.0 - 15.2 | 4 | 28.6 - 28.8 | 1 |
| 6.4 - 6.6 | 6 | 15.2 - 15.4 | 1 | 30.0 - 30.2 | 1 |
| 6.6 - 6.8 | 11 | 15.4 - 15.6 | 2 | 31.0 - 31.2 | 1 |
| 6.8 - 7.0 | 5 | 15.6 - 15.8 | 2 | 33.2 - 33.4 | 2 |
| 7.0 - 7.2 | 10 | 15.8 - 16.0 | 0 | 34.0 - 34.2 | 1 |
| 7.2 - 7.4 | 6 | 16.0 - 16.2 | 0 | 34.4 - 34.6 | 1 |
| 7.4 - 7.6 | 10 | 16.2 - 16.4 | 3 | 35.2 - 35.4 | 1 |
| 7.6 - 7.8 | 2 | 16.4 - 16.6 | 1 | 35.4 - 35.6 | 1 |
| 7.8 - 8.0 | 6 | 16.6 - 16.8 | 1 | 38.6 - 38.8 | 1 |
| 8.0 - 8.2 | 5 | 16.8 - 17.0 | 0 | 41.2 - 41.4 | 1 |
| 8.2 - 8.4 | 4 | 17.0 - 17.2 | 4 | 45.0 - 45.2 | 1 |
| 8.4 - 8.6 | 0 | 17.2 - 17.4 | 0 | 48.6 - 48.8 | 1 |
| 8.6 - 8.8 | 3 | 17.4 - 17.6 | 0 | 49.4 - 49.6 | 1 |
| 8.8 - 9.0 | 1 | 17.6 - 17.8 | 1 | 49.6 - 49.8 | 1 |
| 9.0 - 9.2 | 0 | 17.8 - 18.0 | 0 | 51.0 - 51.2 | 1 |
| 9.2 - 9.4 | 3 | 18.0 - 18.2 | 4 | 64.2 - 64.4 | 1 |
| 9.4 - 9.6 | 4 | 18.2 - 18.4 | 0 | 68.4 - 68.6 | 1 |

Table 2: The histogram of small amplitude classical Cepheids' (DCEPS) periods distribution (dP=0.2 days, n=38 stars)

| ΔP | N | ΔP | N | ΔP | N |
|---|---|---|---|---|---|
| 1.8 - 2.0 | 1 | 3.8 - 4.0 | 1 | 5.8 - 6.0 | 0 |
| 2.0 - 2.2 | 0 | 4.0 - 4.2 | 1 | 6.0 - 6.2 | 0 |
| 2.2 - 2.4 | 1 | 4.2 - 4.4 | 3 | 6.2 - 6.4 | 0 |
| 2.4 - 2.6 | 1 | 4.4 - 4.6 | 2 | 6.4 - 6.6 | 1 |
| 2.6 - 2.8 | 2 | 4.6 - 4.8 | 0 | 6.6 - 7.4 | 0 |
| 2.8 - 3.0 | 1 | 4.8 - 5.0 | 0 | 7.4 - 7.6 | 1 |
| 3.0 - 3.2 | 4 | 5.0 - 5.2 | 0 | 8.2 - 8.4 | 1 |
| 3.2 - 3.4 | 6 | 5.2 - 5.4 | 1 | 9.4 - 9.6 | 1 |
| 3.4 - 3.6 | 1 | 5.4 - 5.6 | 3 | 13.6 - 13.8 | 1 |
| 3.6 - 3.8 | 1 | 5.6 - 5.8 | 3 | 17.0 - 17.2 | 1 |

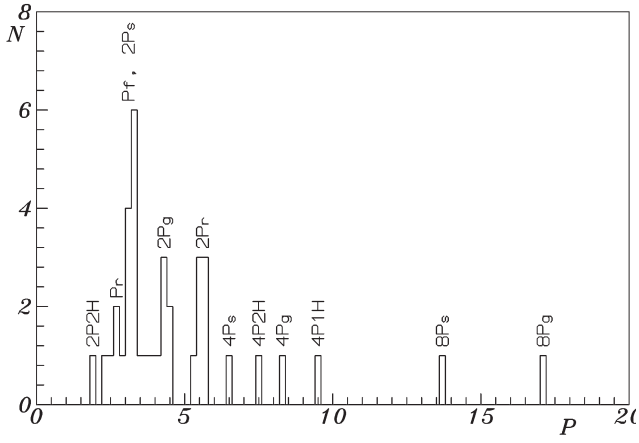


Figure 2: Periods distribution (dP=0.2 days) of small amplitude classical Cepheids (DCEPS)

= $8P_s$, 17.1 d = $8P_g$.

Period Pf specified from correlations of multipleness (equal 3.15 days) coincides with a value of 3.1528 = 28 $P_{fund}$, where $P_{fund}$ = 0.1126 d is a fundamental period of radial pulsations of the Sun. Though the sampling of DCEPS stars with the known periods in GCVS is not large, we can identify the primary peaks in the histogram of periods distribution. The ratios of periods show that periods are commensurable (often - multiple ones), as in the case of other types of pulsating stars.

Overtones $P_r$, $P_e$, $P_g$ and $P_s$ were introduced into practice by the author (Bezdeneznyi, 1994 a, 1994 b, 1997 a, 1997 b) for variable stars RR Lyrae, $\delta$ Scuti types and bimodal Cepheids. Overtones $P_s$ and $P_e$, $P_g$ and $P_f$, are related like $P_{3H}$ and $P_{1H}$: $P_{1H} = 3/2P_{3H}$, $P_f = 3/2P_g$, $P_e = 3/2P_s$. Similarly three pairs of overtones are related like $P_{1H}$ and $P_f$: $P_f = 4/3P_{1H}$, $P_r = 4/3P_g$, $P_e = 4/3P_{2H}$, $P_g = 4/3P_{3H}$. And by analogy with above we have the following

multiple relations: $P_{1H} = 5/4P_{2H}$, $P_f = 5/4P_e$, $P_g = 5/4P_s$. Hence two new multiple relations take place: $3P_r = 4P_g = 5P_s$, $4P_f = 5P_e = 6P_g$, besides relation known earlier: $3P_f = 4P_{1H} = 5P_{2H} = 6P_{3H}$. Two new relations may be combined into one: $8P_f = 9P_r = 10P_e = 12P_g = 15P_s$. This relation connects all new overtones with fundamental period $P_f$. And at last this relation may be combined with known earlier one into universal relation: $24P_f = 27P_r = 30P_e = 32P_{1H} = 36P_g = 40P_{2H} = 45P_s = 48P_{3H}$.

It appears that identification, made for DCEPS stars with small amplitudes, fits for large-amplitudes (DCEP) stars too. As we can see from Fig. 1 and Fig. 2, for every sub-group of variable stars we have its own distribution of periods, with different maxima of distribution and different main peaks. But all of these peaks follow to one general regularity (one general sequence, determined by $P_f = 3.15$ days). There is a distinct peak (see Fig. 1) in area of $P_f = 3.15$ day and a period $P_r = 2.8$ days in its left wing. To the left of these periods we find out the step with two periods coincident to the theoretical first overtone $P_{1H} = 2.36$ days and overtone $P_g = 2.1$ days. More to the right than these two peaks we have two main peaks, determining maxima of distribution: at 4.3 and 5.2 days. Each of these peaks consists of a few near periods: $2P_g = 4.2$ days, $2P_{2H} = 3.8$ days and $2P_e = 3P_s = 5.0$ days, $2P_r = 5.6$ days, $3P_{2H} = 5.7$ days.

Some more to the right is a peak $2P_f = 3P_g = 6.3$ days, a peak of a period $4P_s = 6.7$ days is next to this and two more peaks $3P_{1H} = 7.1$ days and $3P_e = 4P_{2H} = 7.6$ days are present. A wide peak is visible with a center about 9.8 days, formed by the periods $4P_{1H} = 5P_{2H} = 9.45$ days, $4P_e = 6P_s = 10.1$ days, $5P_g = 10.5$ days. Also a peak of periods $4P_r = 11.2$ days and $6P_{2H} = 11.3$ days is present. There are some peaks $6P_e = 9P_s = 15.1$ days, $9P_{2H} = 17.0$ days, $8P_e = 12P_s = 20.1$ days and $11P_g = 23.1$ days.

Thus, for two sub-groups of classical Cepheids different overtones and their harmonics of the same period Pf = 3.15 days, typical for all ensemble of these stars, are present. A period Pf is multiple to the fundamental period of radial oscillations of the Sun Pfund = 0.1126 days.

**References**

Bezdenezhnyi V.P.: 1994a, *Odessa Astron. Publ.,* **7, Part 1**, 55.

Bezdenezhnyi V.P.: 1994b, *Odessa Astron. Publ.,* **7, Part 1**, 57.

Bezdenezhnyi V.P.: 1997, *Odessa Astron. Publ.,* **10**, 89.

Bezdenezhnyi V.P.: 1997d, *Odessa Astron. Publ.,* **10**, 95.

Kholopov P.N. (ed.): 1985a, 1985b, 1987, General Catalogue of Variable Stars (Volumes 1-3, abbr. GCVS), Nauka, Moscow.

# PERIOD ANALYSIS AND MODE IDENTIFICATIONS OF RRab LYRAE STAR X ARIETIS

Vladimir P. Bezdenezhnyi
Department of Astronomy, Odessa National University
T.G.Shevchenko Park Odessa 65014 Ukraine
*astro@paco.odessa.ua*

ABSTRACT. On the base of Preston and Paczynski's (1964) simultaneous photoelectric (U, B, V) and spectroscopic observations (358 U-B and 61 Radial Velocities from Lick Single-Trail Spectrograms) has been carried out the analysis of periods of RRab Lyr star X Arietis. It has been given an interpretation of the periods of this star. All these periods were identified as radial overtones of fundamental period and their harmonics. It was proposed rhat this variable star is an multimodal one according to its mode identifications. The comparisons with the periods of AE Bootis, RW Ari, ST CVn, T Sex, BK Dra and V363 Cas are carried out.

**Key words:** Stars: RR Lyrae, mode identifications

X Arietis belongs to RRab Lyrae variables - radially pulsating stars of the galactic halo (Population II). Depending on their light curves and pulsation characteristics RR Lyrae stars are divided into two different subclasses (according to Bailey classification): RRab and RRc Lyrae stars. Suffixes "ab" or "c" indicate asymmetric or symmetric light curves. RRab stars (with large-amplitude non-sinusoidal light curves) display the fundamental (F) radial mode. They have periods from 0.3 to 1.2 days, and amplitudes from 0.5 to 2 mag in V. RRc Lyrae variables (with nearly symmetric, sometimes sinusoidal, light curves) have periods from 0.2 to 0.5 days and smaller amplitudes not greater than 0.8 mag in V. They display the radial first (1H) overtone. Then classical Bailey classification was extended with RRd or RR(B) - (bimodal or double - mode) - RR Lyrae variables showing two simultaneously operating pulsation modes (fundamental F and the first overtone 1H). And at last RRe Lyrae variables, which are the second (2H)-overtone radial pulsators, they are discussed recently. RR Lyrae variables stars often found in globular clusters. Some of RR Lyrae stars exhibit the Blazhko Effect - periodic variations in period and light curve.

The author in a series of works (Bezdeneznyi, 1994a, b; 1997a, b, c, d, e; 2001a, b; 2005a, b) has extended this classification by means of introducing four new radial overtones $P_r$, $P_e$, $P_g$ and $P_s$ for pulsating variable stars RR Lyrae, $\delta$ Scuti, $\beta$ Cep and bimodal Cepheids (see in detail the paper on classical Cepheids in this volume).

Earlier the author (Bezdeneznyi, 1988) had made an analysis of the behaviour of the mean fundamental pulsation period for X Arietis. The system of two linear elements (2 and 3) was determined by a least squares solution. One can see (in Figure 1 in that work) longtime periodicity (P=4000 days) with amplitude of 0.4 days. The same was detected by author (1985) for the star V363 Cas (P=1450 days). We considered this effect (Bezdenezhnyi, 1985) of the duplicity among RR Lyraes in detail for some stars.

Frolov (1976) during the analysis of metallic lines velocities has discovered that velocity amplitudes are extremely different on different JD. He suspected the existence of unusual Blazko-effect for X Ari which influences only U and U-B curves. He sepposed the existence of some high temperature processes (for example shortwave recombination radiation produced by a shock wave in higher layers of stellar atmosphere) whose effectiveness is modulated with the mean period of about 31 days. Prof. Kukarkin B.V. proposed to that idea that the coincidence of unusual Blazko-effect and the very low metal abundance of X Ari may not be casual.

In present work we analyzed periods of RRab Lyr star X Arietis on the base of Preston and Paczynski's (1964) simultaneous photoelectric (U, B, V) and spectroscopic observations (358 U-B and 61 Radial Velocities from Lick Single-Trail Spectrograms). We have been carried out the Fourier analysis of periods of X Arietis for searching for the regularities in its light curve and identifications of its periods.

The Fourier analysis of periods of X Arietis on the base of radial velocities give (after substructing of the fundamental frequency 1.5355 $\frac{c}{d}$ and its six harmonics) two new frequencies: $f_e$=1.920 $\frac{c}{d}$ and 5.761 $\frac{c}{d}$ (this we recognized as the double $f_s$-frequence). U-B data give the following frequencies: $4f_f$, $8f_f$, $f_f$ and $2f_{2H}$=5.1067 $\frac{c}{d}$. The theoretical ratios for periods $P_e$, $P_s$ and $P_{2H}$ to $P_f$ are 0.(8), 0.5(3) and

Table 1: Frequency content of multimode RR Lyrae stars

| Star | Tipe | Amplitude | Period | D | Frequencies |
|---|---|---|---|---|---|
| X Ari | RRab | 0.98 V | 0.6511426 | 13 | F, 2F, 3F, 4F, 5F, 6F, 7F, 8F, E, 2S, 2(2H) |
| BK Dra | RRab | 1.28 V | 0.5920815 | 12 | S, 2S, 3S, 4S, 2E, 2(1H), 2(2H) |
| RW Ari | RRc | 0.48 V | 0.354341 | 42 | S, S/3, (1H), |
| AE Boo | RRc | 0.44 V | 0.3148921 | 45 | (1H), F, G, (2H), E, 2R, 2E, 2(1H), 2(2H), S, 2S |
| T sex | RRc | 0.51 V | 0.3246980 | 42 | (1H), 2(1H), 3(1H), 4(1H), 5(1H), 3S, 9(1H) |
| ST CVn | RRc | 0.56 V | 0.329045 | 43 | (1H)/4, (1H), 2(1H) |

0.6, respectively.

Thus, individual values of periods of X Ari confirm their commensurability with the primary period $P_f$, its overtones $P_{2H}$, $P_e$ and $P_s$. This star may be consider as multimodal one.

Frequencies of oscillations, discovered by the author (Bezdenezhnyi, 1994a, 1997d, 2001b and this paper) for two RRab type stars (X Ari and BK Dra) and for four RRc type stars (RW Ari, AE Boo, T Sex, ST Cvn), are resulted in Table 1. Other information on these stars is taken from General Catalogue of Variable Stars (Kholopov et al., 1985a, b, 1987).

Three frequencies resulted by Penicke et al. (1989) for RRc type star ST Cvn were identified by the author (Bezdenezhnyi, 1994a): $f_{1H}/4$, $f_{1H}$ and $2f_{1H}$. Thus, the largest amplitude is at frequency $f_{1H}/4$. This star shows (1H)-frequency and its harmonics, but it isn't (1H)-pulsator speaking strictly.

The frequency $f_{1H}$ is the main one (with the largest amplitude) for RRc type star T Sex, a few its harmonics and the frequency $3f_s$ (with small amplitude) are present too. This star also can be considered as (1H)-pulsator.

The frequency $f_{1H}$ is also the main one for RRc type star AE Boo, fundamental frequency (F) goes after it (in the order of decreasing of amplitude). Taking into consideration only these two main frequencies of AE Boo it is possible to consider this star as bimodal one, pulsating in (1H) and F modes. But we have the frequency $f_{2H}$ and a set of all (!) introduced by us new overtones: $f_g$, $f_s$, $f_e$, $f_r$ (and some their harmonics) too. Hence, this star is a multimodal one. But the largest amplitude is at the overtone (1H) that allowed to add it to RRc stars.

And RRc type star RW Ari has S-mode as the main frequency, $f_S/3$ and $f_{1H}$-frequencies are present too. Although the frequency $f_{1H}$ is present, but the frequency $f_S$ and its harmonic $f_S/3$ (or period $3P_s$) prevail. Thereby, among RRc stars not all are (1H)-pulastors. RW Ari can be named rather as S-pulsator.

It brings together RW Ari with the RRab type star BK Dra, at which S-mode and its harmonics prevail, but the frequencies (with smaller amplitudes) $2f_E$, $2f_{1H}$, $2f_{2H}$ are present too. And X Ari is a pulsator of fundamental mode (F): except for F-mode and seven its harmonics three more frequencies (with small amplitudes) $f_E$, $2f_S$ and $2f_{2H}$ are present too.

Bailey classification requires substantial improvement, offered by the author, even if we take into consideration its extension with bimodal RRd-pulsators and pulsators of the second overtone (RRe).

**References**


Bezdenezhnyi V.P.: 1985, *Problems of Astronomy,* **No 2558, UA-85**

Bezdenezhnyi V.P.: 1988, *Variable Stars,* **22, No 6**, 909.

Bezdenezhnyi V.P.: 1994a, *Odessa Astron. Publ.,* **7, Part 1**, 55.

Bezdenezhnyi V.P.: 1994b, *Odessa Astron. Publ.,* **7, Part 2**, 91.

Bezdenezhnyi V.P.: 1997, *Odessa Astron. Publ.,* **10**, 89.

Bezdenezhnyi V.P.: 1997b, *Odessa Astron. Publ.,* **10**, 92.

Bezdenezhnyi V.P.: 1997c, *Odessa Astron. Publ.,* **10**, 93.

Bezdenezhnyi V.P.: 1997d, *Odessa Astron. Publ.,* **10**, 95.

Bezdenezhnyi V.P.: 1997e, *Odessa Astron. Publ.,* **10**, 96.

Bezdenezhnyi V.P.: 2001a, *Odessa Astron. Publ.,* **14**, 118.

Bezdenezhnyi V.P.: 2001b, *Odessa Astron. Publ.,* **14**, 122.

Bezdenezhnyi V.P.: 2005a, *Odessa Astron. Publ.,* **18**, 19.

Bezdenezhnyi V.P.: 2005b, *Odessa Astron. Publ.,* **18**, 21.

Kholopov P.N. (ed.): 1985a, 1985b, 1987, General Catalogue of Variable Stars (Volumes 1-3, abbr. GCVS), Nauka, Moscow.

Frolov M.S.: 1976, *IBVS,* **No 1097.**

Penicke R., Gomez T., Parrao I., Pena J.H.: 1989, *As.Ap.,* **209**, 59.

Preston G.V. and Paczynski B.: 1964, *Astrophys. J.,* **140**, 181.

# ON THE LAW OF PLANETARY DISTANCES IN THE SOLAR SYSTEM

Vladimir P. Bezdenezhnyi
Department of Astronomy, Odessa National University
T.G.Shevchenko Park Odessa 65014 Ukraine
*astro@paco.odessa.ua*

**ABSTRACT.** Representations of major semiaxes of planets and distances of nearby planets by means of degrees of two and prime numbers are made. We analyse different formulas for these representations and give new formulas (3)-(4) and a system of formulas (6)-(8) which by the best appearance presents all the planets of the Planetary system, including Neptune and Pluto. Recommendations are given for the search of the tenth planet (instead of Pluto) and eleventh one.

**Key words:** Solar system: Titius-Bode's Law, the Law of planetary distances, its modifications

## 1. Introduction

The Titius-Bode's Law is an approximative empirical relationship of the planets distances from the Sun. It is a simple numerical sequence that basically predicts the spacing of the planets.

A(AU)=0.4+0.3*$2^n$, (n=-$\infty$, 0, 1, 2, 3, 4, 5, 6) (1)

Chechel'nicky (1983) showed, that major semiaxes of planet orbits (A(i)) and their differences ($\Delta$A(i) = A(i+1) - A(i)) for nearby planets normalized on specially chosen value of A* = 0.0372193 AU (astronomical unit) are near to degrees of two. He gave the formula (2) as a modification of Titius-Bode's Law that reflects regularity of planetary distances of Solar system for planets (except for Neptune and Pluto) and for the Belt of asteroids.

A(n)=$A_0$+$2^n$, ($A_0$=10.4, n=-$\infty$, 3, 4, 5, 6, 7) (2)

($A_0$ = 0, n = 8, 9, 10).

Also it was pointed there that all differences of major semiaxes of nearby orbits (except for the second) are near to whole numbers.

## 2. Results

We give all datas from above paper in Table 1, adding information (Allen, 1964) for the Belt of asteroids and Pluto. There are representations of major semiaxes of planets by means of degrees of two and prime numbers there. Representations of distances of nearby planets by means of degrees of two and prime numbers are presented in Table 2.

We notice that the value of A* is equal to eight radiuses of the Sun. As we can see from Table 1, Anorm (normalized values) for Saturn and Uranium are near to the values of degrees of two (256 and 512, respectively). Differences $\Delta$=$A_{norm}$-$A_0$, where $A_0$ is the normalized major semiaxes of Mercury, are closed to the values of degrees of two for nearer to the Sun planets and for Belt of asteroids. However we don't see from the Table 2, that all differences of major semiaxes nearby planets are also near to the values $2^n$.

Table 2: Representation of distances of nearby planets by means of degrees of two and prime numbers

| planets | $\Delta$A | $2^n$ | n | prime number |
|---|---|---|---|---|
| Venus-Mercury | 9.034 | 8 | 3 | 7 |
| Earth-Venus | 7.434 | 8 | 3 | 7 |
| Mars -Earth | 14.072 | 16 | 4 | 13 |
| Belt of aster-Mars | 34.290 | 32 | 5 | 31 |
| Jupiter-Belt of aster | 64.554 | 64 | 6 | 67 |
| Saturn-Jupiter | 116.070 | 128 | 7 | 113 (127) |
| Uranium-Saturn | 259.033 | 256 | 8 | 257 |
| Neptune-Uranium | 292.999 | ? | ? | 293 |
| Pluto-Neptune | 249.996 | 256 | 8 | 251 |

For example, 116 and 293 are distant from the degrees of two: 128, 256. It is possible to notice, that both major semiaxes of planets and differences nearby ones are near to prime numbers: 7, 11, 13, 19, 29, 41, 73, 97, 113, 139, 257, 293, 509.

The normalized differences ($\Delta$) of the observed major semiaxes of planets and calculated ones from the formulas (2) are presented in the last column of the Table 1. Evidently, that the difference ($\Delta$) for Pluto (+33.882) is very large in comparison with differences for other planets. Thereby, the formula (2) badly represents the distance of Pluto. Pluto was excluded from the list of large planets by the decision of Congress of International Astronomical Union (IAU). So nothing frightful will happen, if we exclude it from the formula (2). Business is worse

Table 1: Representations of major semiaxes of planet's orbits by means of degrees of two and prime numbers

| planet | (AU) | $A_{norm}$ | $2^n$ | n | prime number | $\Delta$=$A_{norm}$-A(n) |
|---|---|---|---|---|---|---|
| Mercury | 0.387097676 | 10.400 | 0 | -$\infty$ | 11 | 0 |
| Venus | 0.723335194 | 19.434 | 8 | 3 | 19 | +1.034 |
| Earth | 1.000007872 | 26.868 | 16 | 4 | 29 | +0.468 |
| Mars | 1.523749457 | 40.940 | 32 | 5 | 41 | -1.460 |
| Belt-ast | 2.8 | 75.230 | 64 | 6 | 73 | +0.830 |
| Jupiter | 5.202655382 | 139.784 | 128 | 7 | 139 | +1.383 |
| Saturn | 9.522688738 | 255.854 | 256 | 8 | 257 | -0.146 |
| Uranium | 19.16371889 | 514.887 | 512 | 9 | 509 | +2.887 |
| Neptune | 30.06894040 | 807.886 | ? | ? | 809 | ? |
| Pluto | 39.37364135 | 1057.882 | 1024 | 10 | 1061 | +33.882 |

Table 3: Representation of major semiaxes of planets by means of formulas

| planet | $A_{norm}$ | A(1) | A(2) | A(2b) | A(2c) | A(3) | A(4) |
|---|---|---|---|---|---|---|---|
| Mercury | 10.400 | 10.747 | 10.4 | 10.400 | 10.4 | 10.40 | 10.400 |
| Venus | 19.434 | 18.807 | 18.4 | 18.460 | 18.4 | 18.25 | 18.352 |
| Earth | 26.868 | 26.868 | 26.4 | 26.521 | 26.4 | 26.10 | 26.272 |
| Mars | 40.940 | 42.988 | 42.4 | 42.641 | 42.4 | 41.80 | 42.081 |
| Belt of aster | 75.230 | 75.229 | 74.4 | 74.882 | 74.4 | 73.20 | 73.636 |
| Jupiter | 139.784 | 139.712 | 138.4 | 139.365 | 138.4 | 136.0 | 136.619 |
| Saturn | 255.854 | 268.677 | 256 | 268.330 | 266.4 | 261.6 | 262.333 |
| Uranium | 514.887 | 526.606 | 512 | 526.259 | 522.4 | 512.8 | 513.257 |
| Neptune | 807.886 | - | - | - | - | - | - |
| Pluto | 1057.882 | 1042.465 | 1024 | 1042.118 | 1034.4 | 1015.2 | 1014.103 |

with Neptune, as it is the major planet of the Solar system and is not represented with the formulas (1) and (2). When Titius-Bode's Law was laid down, Neptune was not discovered yet. Therefore there was no misunderstanding. When Neptune was discovered, its difference ($\Delta$) of the observed major semiaxes and calculated ones from Law of planetary distances was explained (the book of N'etto, 1976) by different hypotheses. That the orbit of Neptune was strongly distorted by gravity influence going by an unknown major planet, or that Neptune was captured by the Solar system from the planetary system other passing by star. Anyway, but Neptune is not described by the formula (2).

One more difficulty for this formula consists in the facts that orbits of Saturn (n=8) and Uranium (n=9) are not described by the same formula with a free member, equal major semiaxes of Mercury, and require a zero free member. The formula (2), written in two lines (i. e. with two free members), actually presents two formulas. That would reflect two different histories of planets forming of Solar system, internal (including Jupiter) and external (Saturn and Uranium). The sum of squares of differences of the major semiaxes for eight planets calculated on the formula (2), including Belt of asteroids, from the observed values is $\delta(2)$=$\sum \Delta(i)^2$=14.380 (without Neptune and Pluto).

The formula (1), normalized on the value of A* = 0.0372193 AU looks like the folliwing one (2a):

A*(n)=10.747+8.0603*$2^n$, (n=-$\infty$, 0,1,2,3,4, 5, 6) (2a)

If we replace free member on more exact meaning in this formula, 10.400, equal to the orbit of Mercury, we get the formula (2b).

A*(n)=10.400+8.0603*$2^n$, (n=-$\infty$, 0,1,2,3,4, 5, 6) (2b)

And replacing a coefficient 8.0603 before a degree of two on integer-valued 8 =$2^3$, we get the formula (2c):

A*(n)=10.400+8*$2^n$, (n=-$\infty$, 0, 1, 2, 3, 4, 5, 6) (2c)

or, uniting the degrees of two, we get an equivalent equation (2d):

A*(n)=10.400+$2^{n+3}$, (n=-$\infty$, 0, 1, 2, 3, 4, 5, 6) (2d)

Designating $n+3$ through m we get formula (2e).

It coincides with the formula (2), if we write down it with only one free member $A_0$=10.4. This formula is true for all planets, including m=8 and 9 (Saturn and Uranium):

A*(n)=10.400+$2^n$, (n=-$\infty$, 3, 4, 5, 6, 7, 8, 9) (2e)

Values of $\sum \Delta(i)^2$ sums of squares of discrepancies

for these formulas are the following: $\delta$(2a)=306.503, $\delta$(2b)=289.23, $\delta$(2c)=$\delta$(2d)= $\delta$(2e)=173.687.
The formula (2c) after varying of coefficient at $2^n$ (a minimum of parabolic function at a coefficient 7.85) gives the smallest $\delta$(3)=58.543. Thereby, there can be an alternative formula (3) to the formula (2):
A*(n)=10.400+7.85*$2^n$, (n=-$\infty$, 0, 1, 2, 3, 4, 5, 6) (3)
or the formula (4), which can be obtained from the formula (2) after varying of degree 2:
A*(n)=10.400+1.996$^n$, (n=-$\infty$, 3, 4, 5, 6, 7, 8, 9) (4)
$\delta$(4)=60.02 for it, i. e. rather more of the sum of squares of discrepancies $\delta$(3) for the formula (3).

We present representations of major semiaxes of planets by means of different formulas in Table 3.

So, the formulas (2) give the least sum of squares of discrepancies ($\delta(2)=\sum\Delta(i)^2$=14.38), but its imperfection is that it consists of two lines, i.e. actually from two formulas. The first line describs six internal planets, including Belt of asteroids and Jupiter, and second one - two external planets (Saturn and Uranium). Though the formulas (3) and (4), got by us, have four times greater values of the sum of squares of discrepancy as compared to the formulas (2), however they describe uniformly and exactly enough eight objects of Solar system, from Mercury to Uranium, including Belt of asteroids.

Squares of discrepancies for every the planets are parabolic functions and have the minimum at the different coefficients q (base of power) in the vicinity of two: Venus (at q=2.0827), Earth (2.0144), Mars (1.9814), Belt of asteroids (2.0043), Jupiter (2.0031), Saturn (1.9895), Uranium (1.9967), Neptune (1.9506), Pluto (2.0045). The formula (4) has a minimum value of sum of squares of discrepancies (60.02) at q=1.996 for n=3-9 (without Pluto), Saturn and Uranium have the largest discrepancies here. Without these two planets (n=3-7) the sum of squares of discrepancies will be far less than ($\delta$=15.386), taking on a minimum value at q=2.003 ($\delta$=4.092). That is why Saturn and Uranium have minima of discrepancies at the values of q equal 1.9895 and 1.9967, respectively. Including them in the formula (4) lowers q to the value of 1.996. Oddly enough, but addition of Pluto with its q=2.0045, again gives the minimum sum of squares of discrepancies ($\delta$=463.56) at the same value of q equal 2.003, i.e. Pluto compensates the contributions of Saturn and Uranium. Again the formula (5) is true with q=2.003:
A*(n)=10.400+2.003$^n$, (n=-$\infty$,3,4,5,6, 7, 8, 9, 10) (5)
It shows, why the Law of planetary distances has statistical nature. It is named not a law but a rule sometimes.

Did not hurry with Pluto, depriving its status of tenth planet? It has q equal 2.0045 near to the values of q for Belt of asteroids (2.0043) and Jupiter (2.0031). Values of this parameter greater than 2 have another two planets: Earth (2.0144) and Venus (2.0827).

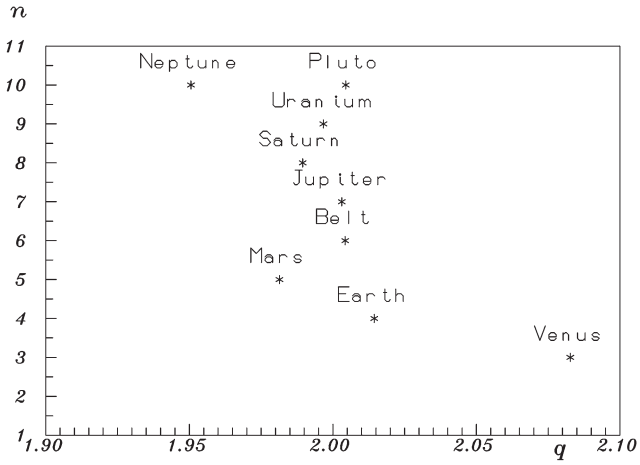


Figure 1: The dependence of a number of planet (n) from the parameter q

It gives an occasion to unite these five planets in one group, for which the formula (6) is true giving a strikingly small sum of squares of discrepancies $\delta$(6)=9.200:
A*(n)=10.400+2.004$^n$, (n=3, 4, 6, 7, 10) (6)
Remaining three planets with the parameter q less than two Mars (1.9814), Saturn (1.9895) and Uranium (1.9967) give a minimum of sum of squares of discrepancies at the parameter q equal 1.996, as well as in the formula (4):
A*(n)=10.400+1.996$^n$, (n=5, 8, 9) (7)
The sum of squares of discrepancies $\delta$(7) is equal 45.930 for them. Addition of another planets, except for Pluto, converts the formula (7) into the formula (4). It gives $\delta$(4)=60.020, but addition of Pluto gives the sum of squares of discrepancies $\delta$=1976.62! The same three planets (n= 5, 8, 9) at q equal 2.004 would increase the sum of squares of discrepancies $\delta$(6)=9.200 in relation to the formula (6) by about 500.748! If we take a double formula - system (6)-(7) by analogy with a double formula (2), then $\delta$(6-7)=9.200+45.930= 55.130 for eight planets (including Pluto). That is less than $\delta$(4)=60.020 at the same coefficient q equal 1.996 for all planets (except for Pluto) and considerably less than $\delta$(4)=1976.62, including Pluto. Value of $\delta$(6-7)=55.130 is also much less than $\delta$(2)=1162.37, including Pluto. Thereby, the system (6)-(7) presents all the planets of the Planetary system (except for Neptune) in the best way.

In Figure 1 we give the graph of dependence of number of planet n from the parameter q. One can see a clear peak, in the top of which is the point of Uranium (n=9). The point of Pluto (n=10, q=2.0045) is displaced to the right on 0.0045 from the integer-valued q=2. If the tenth planet (instead of eliminated Pluto) is discovered, the ideall value of q would be equal 2, to be a maximal point on the graphic. For Neptune q is equal 1.95, it differs by

about 0.05 from the integer-valued q equal 2. This difference is more than ones for other planets except for Venus, for which $\Delta$ q equal 0.08 is outstandingly large, but only towards the greater value of q equal 2.08 (see Fig. 1). However Neptune follows none the formulas resulted above. The formula (8) is true for it:

$A^*(n)=10.400+1.95^n$, (n= 3, 4, 5, 10) (8)

at n=10, as well as for Pluto in the formulas resulted above. The formula (8) presents the major semiaxes of another three planets, but with larger discrepancies than Titius - Bode's Law: Venus (n=3), Earth (n=4) and Mars (n=5). The discrepancies $\Delta$ for them are equal 1.61, 1.99 and 2.30, respectively. The sums of squares of discrepancies for the formula (8) and Titius - Bode's Law are as following: 11.84 and 4.60. We will notice that at the value of parameter q equal 2.10 and n=9 the calculated value of major semiax of Neptune (804.680) will be also near to the observed one (807.886). The formula (9) with this value of parameter q presents the major semiaxes not only for Neptune ($\Delta$=3.206) but also for Venus ($\Delta$=-0.227) and Earths ($\Delta$=-2.980). Mars follows ($\Delta$=0.099) to the same formula but without a free member. Venus and Neptune are two extreme representatives on the parameter q, they both surprisingly fit the formula (9) at this parameter q equal 2.10.

$A^*(n)=10.400+2.10^n$, (n=3, 4, 9) (9)

Following these reasonings, it is possible to suppose that the graph in the Fig. 1 is periodic with the period on $\Delta$q equal 0.05. The formula (10) corresponds to a supposed peak (not supported by points) at q equal 2.05:

$A^*(n)=10.400+2.05^n$, (n= 3, 4) (10)

This formula describes the major semiaxes of Venus ($\Delta$=0.4189) and Earths ($\Delta$=-1.193), without a free member it describes Mars ($\delta$=4.735) and Belt of asteroids ($\Delta$=1.01). We remind that the formula (2) also gives smaller discrepancies for Saturn and Uranium without the free member (10.4).

According to the formula (2e) we have at integer-valued q=2 for n=10: $A^*(10)$ =1034.4 (the normalized major semiax). Multiplying it by 0.0372193 AU, we get A(10)=38.5 AU. It is an ideal value of major semiax for tenth planet. We remind for comparison that the major semiaxes of Neptune and Pluto are equal 30.07 and 39.37, respectively. For eleventh planet following this law strictly, a major semiax would be equal 76.6 AU. The formula (6) gives the maximal values of major semiaxes for the prognosis of planets discovering: A(10)=39.37 AU (equal to the value for Pluto) and A(11)=78.3 AU. The formula (7) gives analogical minimum values: A(10)=37.7 AU and A(11)=75.0 AU. According to the formula (8) A(10)= 30.07 AU (naturally coincides with the value for Neptune) and A(11)=58.1 AU.

### 3. Conclusions

Thereby, in the Solar planetary system we can see three sequences of planets for which the major semiaxes of their orbits are described with three formulas (6), (7) and (8). System (6)-(7) presents all the planets by the best appearance, except for Neptune. For the last the formula (8) is true. These information can be used for the search of tenth and eleventh planets and at the calculations of hydrodynamic models of the planetary system forming.

### References

Chechel'nickiy A.M.: 1983, *Astronomic circular,* No. 1257, 5.

N'etto M.M.: 1976, *Titius - Bode's Law,* Moscow.

Allen C.W.: 1964, *Astrophysical Quantities,* London, 141.

# ON THE DETERMINATION OF GALAXY STRUCTURE ELLIPTICITY

M. Biernacka[1], P. Flin[1], T. Juszczyk[2], E. Panko[3]

[1] Institute of Physics, Pedagogical University,
ul.Swietokrzyska 15, 25-406 Kielce, Poland *sfflin@cyf-kr.edu.pl*
[2] Bednarski High School, ul. Czackiego 11, 30-501 Krakow, Poland
[3] Kalinenkov Astronomical Observatory of the Nikolaev State University,
Nikolskaya 24, Nikolaev 50030, Ukraine

ABSTRACT. We discuss factors influencing the determination of the observed shape of galaxy clusters when the covariance ellipse method is involved. The analysis of 377 Abell clusters show that at greater distances from the cluster center the ellipticity is rather smooth. There were no statistical differences among ellipticities when the cluster center was located at the brightest cluster member, the third brightest galaxy, the mean as well as the median values of galaxy coordinates. Moreover, we show that for rich galaxy clusters the distribution of ellipticities is the same for two totally different cluster samples.

**Key words**: galaxy clusters, properties;

## 1. Introduction

Galaxies form different structures, some are less, some are more numerous. The shape of the structure is an important parameter. Various scenarios of galaxy origin predict different shape of structures. One of the most popular method of finding the intrinsic, three dimensional shape of structure is based on the observed, projected, this is two dimensional shape of structure. Before going into the problems dealing with inversion of the distribution of the apparent shape of galaxy clusters we would like to concentrate on the first stage of investigation, this is on the determination of the observed shape of galaxy clusters. There are several methods of shape determination. The most popular is fitting the covariance ellipse; inertia tensor method and Minkowski functionals can be regarded as some other ones. Our paper is oganised in the following manner. Section two describes the applied method of analysis, this is standard covariance ellipse method, while section three presents our observational data. The main results of our work are given in section four, while conclusions ends the paper.

## 2. The covariance ellipse method

We used covariance ellipse method (Carter & Metcalfe, 1980) to obtain galaxy cluster ellipticity. The method is based on first five moments of the observed distribution:

$$M_{10} = \frac{1}{N}\sum_i x_i \tag{1}$$

$$M_{01} = \frac{1}{N}\sum_i y_i \tag{2}$$

$$M_{20} = \frac{1}{N}\sum_i x_i^2 - \left(\frac{1}{N}\sum_i x_i\right)^2 \tag{3}$$

$$M_{02} = \frac{1}{N}\sum_i y_i^2 - \left(\frac{1}{N}\sum_i y_i\right)^2 \tag{4}$$

$$M_{11} = \frac{1}{N}\sum_i x_i y_i - \frac{1}{N^2}\sum_i x_i \sum_i y_i \tag{5}$$

where $x_i$ and $y_i$ are galaxy coordinates. The centroid of the contour is: $x_0 = M_{10}$, $y_0 = M_{01}$. The semi - principal axes are the solution $\lambda_u$ and $\lambda_v$ of the quadratic equation:

$$(M_{20} - \lambda^2)(M_{02} - \lambda^2) - M_{11}^2 = 0, \tag{6}$$

the eigenvalues of the matrix of moments of the distribution. The cluster ellipticity is given by:

$$e = 1 - \sqrt{\frac{1-\epsilon}{1+\epsilon}} \tag{7}$$

where

$$\epsilon = \frac{\sqrt{(M_{20} - M_{02})^2 + 4M_{11}^2}}{M_{20} + M_{02}} \tag{8}$$

### 3. Observational data

We selected all Abell clusters with galactic latitude $|b| > 40^\circ$ and Richness Class$\geq$ 1. In such way we obtained 1238 clusters. We take all clusters with redshift $z < 0.2$ determined by Struble & Rood, (1999). In such manner our sample contains 377 Abell clusters. For each of these clusters the area covering 2x2 Mpc on the sky ($h = 0.75$, $q_0 = 0.5$) was extracted from DSS. A catalogue contains objects within the magnitude range $m_3$, $m_3 + 3$ where $m_3$ is the brightness of the third brightest galaxy in the investigated area. The catalogues were obtained applying FOCAS packages to DSS. Afterwards, the automatically obtained catalogues were visually corrected. Each catalogue contains information about right ascension, declination of galaxies, x and y galaxy positions on the photographic plate, instrumental magnitude, area of object, ellipticity and position angle.

The PF Catalogue (Panko & Flin, 2006) served as a second source of data. The catalogue contains 6188 structures having more than 10 members. These structures were extracted from Münster Red Sky Survey galaxy catalogue (MRSS hereafter). MRSS is the result of a large-scale galaxy survey in the red spectral region, covering an area of 5,000 square degrees, and forming one of the largest coherent data base for cosmological investigations in the southern hemisphere (Ungruhe et al., 2003).

We selected the Voronoi tessellation technique (VTT hereafter) for cluster detection (Panko and Flin, 2004), Icke and van de Weygaert (1987), Ramella et al. (1999, 2001). This technique is completely non-parametric, and therefore sensitive to both symmetric and elongated clusters, allowing correct studies of non-spherically symmetric structures with non-uniform galaxy background (Kim et al., 2002). The search of over dense region was made using the procedure *kiang*, the corn of the VGCF (Voronoi Galaxy Cluster Finder), an automatic package for the identification of galaxy clusters in photometric, two-dimensional galaxy catalogues (Ramella et al., 1999)

For each structure in our catalogue, further analysis was carried out individually. The structures with at least 10 galaxies in the considered area were included to our catalogue. For galaxies in brightness lying inside the magnitude limits $m_3$, $m_3 + 3^m$, calculations were carried out. For each structure, the covariance ellipse was inscribed, considering only galaxies above the mentioned magnitude limit. This allows us to determine the ellipticity and the position angle of the structure.

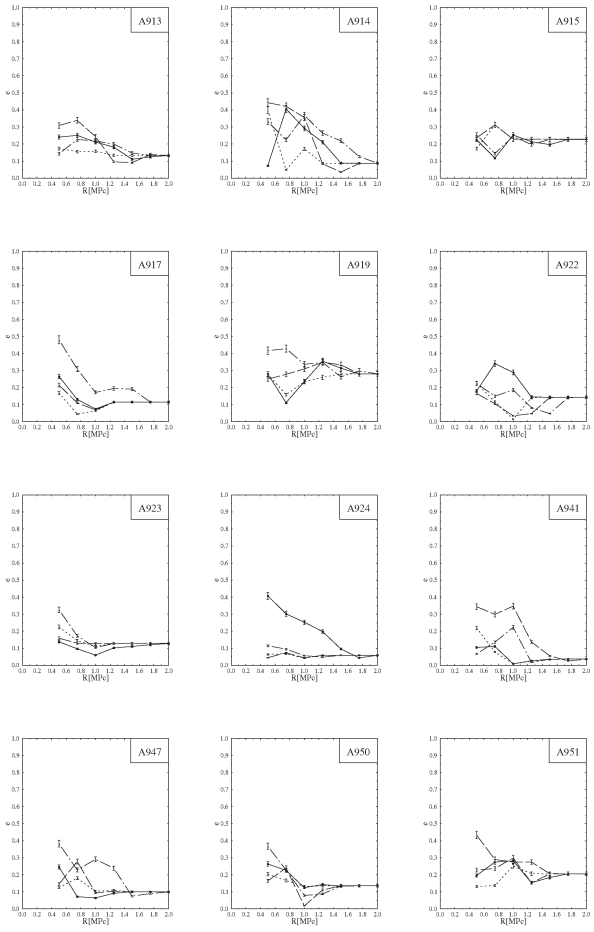


Figure 1: The change of the cluster ellipticity with the distance from the cluster center.

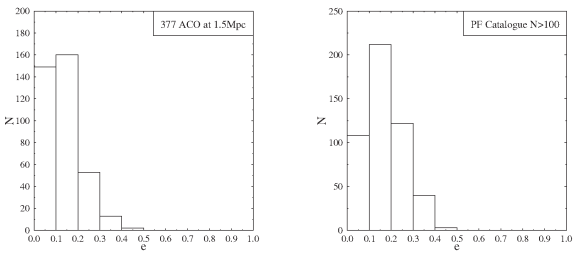


Figure 2: The ellipticity distribution for 377 ACO clusters ($R = 1.5Mpc$), the mean coordinates of galaxy positions accepted as cluster center and ellipticity distribution for structures having more than 100 members in the PF Catalogue.

Table 1: The statistics of cluster center influence

The $\lambda$ statistcs for K-S test for $R = 1.5$Mpc

| | The brightest galaxy | third brigtest | median | mean |
|---|---|---|---|---|
| The brightest galaxy | X | 0.137 | 0.780 | 0.876 |
| third brightest | 0.137 | X | 0.932 | 0.823 |
| median | 0.780 | 0.932 | X | 0.109 |
| meana | 0.876 | 0.823 | 0.109 | X |

The $\lambda$ statistcs for K-S test for $R = 1.75$Mpc

| | The brightest galaxy | third brigtest | median | mean |
|---|---|---|---|---|
| The brightest galaxy | X | 0.069 | 0.151 | 0.069 |
| third brigtest | 0.069 | X | 0.178 | 0.082 |
| median | 0.151 | 0.178 | X | 0.041 |
| mean | 0.069 | 0.082 | 0.041 | X |

The $\lambda$ statistcs for K-S test for $R = 2.0$Mpc

| | The brightest galaxy | third brigtest | median | mean |
|---|---|---|---|---|
| The brightest galaxy | X | 0.041 | 0.041 | 0.041 |
| third brigtest | 0.041 | X | 0.055 | 0.041 |
| median | 0.041 | 0.055 | X | 0.000 |
| mean | 0.041 | 0.041 | 0.000 | X |

## 4. Results

We used covariance ellipse method (Carter & Metcalfe, 1980) to obtain galaxy cluster ellipticity. It is well known that ellipticity depends also on the distance from the cluster center (e.g. Carter & Metcalfe (1980), Flin (1984), Trevese et al. (1992), Struble & Ftaclas (1994)). The influence of this fact was checked studying the cluster ellipticity at various distances from the cluster center. We calculated the ellipticity in circular rings for the distance range from 0.5 Mpc to 2 Mpc with the step 0.25 Mpc. We used four methods for cluster center determination: the mean position of all galaxies, the brightest galaxy in the cluster, the third brightest galaxy in the cluster and the median of galaxy coordinates. For these four galaxy cluster center determinations we calculated ellipticities at distances described above (Fig. 1). For the significance level $\alpha = 0.01$ (the critical value $\lambda_{0.01} = 1.627$) the Kolmogorov - Smirnow test confirmed the similarity of the distributions. The Table 1 present the values of the Kolmogorov - Smirnow test statistics for various centers at $r \geq 1.5 Mpc$.

The observed ellipticity distributions for structures with various number of members, as given in PF Catalogue are different. Using the Kolmogorov - Smirnow test we found that the distribution of cluster ellipticities in the case of 377 ACO clusters and very rich galaxy clusters, this is containing 100 and more members in the PF Catalogue are identical at the confidence level $\alpha = 0.01$.

## 5. Conclusions

The main goal of this work was to check the influence of different factors to the determined projected ellipticity of galaxy cluster. The ellipticity of projected galaxy clusters depends on the radial distance from the cluster center. In projection, close to the center, clusters are more elongated than at greater distances. Moreover, the changes of ellipticity nearby the center are great, the parameter is noisy. At greater distance from the center the run of ellipticity is usually quite smooth. Therefore, we decided to use in all analyses cluster ellipticity determined at 1.5 Mpc. We checked also the ellipticity distribution at greater radii (r=1.5 Mpc and 2 Mpc), but we do not find statistically significant differences. The influence of the adopted cluster center is negligible. This conclusion is based on the analysis of the ellipticity distributions at greater distances from the cluster center, when four different cluster centers were considered, namely: the brightest cluster galaxy, the third brightest member, the average and the median of galaxy coordinates. We checked the distribution of ellipticities for various structures in the PF Catalogue. These distributions strongly depend on the structure richness. For rich clusters, the distributions of ellipticities in both data set were identical.

**References**

Abell G., Corwin H., Olowin R.: 1989, *Astrophys. J. Suppl. Ser.*, **70**, 1-138.

Carter D., Metcalf N.: 1980, *Mon. Not. R. Astron. Soc.* **191**, 325-337.

Flin P.: 1984, in *Clusters and Groups of Galaxies. International Meeting held in Trieste, Italy, September 13-16, 1983 / Ed. F. Mardirossian, G. Giuricin, M. Mezzetti, D. Reidel, Dordrecht*, p. 163.

Icke V. and van de Weygaert R.: 1987, *Astron. Astrophys.*, **184**, 16-32.

Kim R.S.J., Kepner J.V., Postman M., Strauss M.A., Bahcall N.A., Gunn J.E., Lupton R.H., Annis J., Nichol R.C., Castander F.J., Brinkmann J., Brunner R.J., Connolly A., Csabai I., Hindsley R.B., Ivezić Ž., Vogeley M.S., York D.G.: 2002, *Astron. J.*, **123**, 20-36.

Panko E. and Flin P.: 2004, in: *Outskirts of Galaxy Clusters: Intense Life in the Suburbs, IAU Colloquium 195, ed. A. Diaferio (Cambridge University Press, Cambridge)*, p. 245.

Panko E. and Flin P.: 2006, *J. Astron. Data*, **12**, 1.

Ramella M., Nonino M., Boschin W., Fadda D.: 1999, in *Observational Cosmology: The Development of Galaxy Systems, ASP Conf. Ser.*, **176**, ed. G. Giuricin, M. Mezzetti and P. Salucci (Astron. Soc. of the Pacific, San Francisco, California), p. 108.

Ramella M., Boschin W., Fadda D., Nonino M.: 2001, *Astron. & Astrophys.*, **368**, 776-786.

Struble M.F., Ftaclas F.: 1994, *Astron. J.*, **108**, 1-23.

Struble M.F., Rood H.J.: 1999, *Astrophys. J. Suppl. Ser.*, **125**, 35-71.

The Digitized Sky Survey, Space Telescope Science Institute, Association of Universities for Research in Astronomy Inc., 1993, 1994.

Trèvese D., Flin P., Migliori L., Hickson P., Pittella G.: 1992, *Astron. Astrophys. Suppl. Ser.*, **94**, 327-357.

Ungruhe R., Seitter W.C., Duerbeck H. W.: 2003, *J. Astron. Data*, **9**, 1.

# ABOUT COMPILED CATALOGUE OF SPECTROSCOPICALLY DETERMINED $\alpha$-ELEMENTS ABUNDANCES FOR STARS WITH ACCURATE PARALLAXES

T.V. Borkova, M.S. Katchieva, B.A. Marsakov, D.M. Pitkina

Southern Federal University
Rostov-on-Don 344090 Russia,
*borkova@ip.rsu.ru*

ABSTRACT. We present a new version of the compiled catalogue of nearby stars for which was published the spectoscopically determined effective temperatures, surface gravities, and abundances of iron, magnesium, calcium, silicon, and titanium. Distances, velocity components, galactic orbital elements, and ages was calculated for all stars. The atmospheric parameters and iron abundances were found from 4700 values in 136 publications, while relative abundances of alpha-elements were found from 2800 values in 81 publications for $\approx 2000$ dwarfs and giants using a three-step iteration averaging procedure, with weights assigned to each source of data as well as to each individual determination and taking into account systematic deviations of each scale relative to the reduced mean scale. The estimated assumed completeness for data sources containing more than five stars, up to late April 2007, exceeds 90 %. For the vast majority of stars in the catalogue, the spatial-velocity components were derived from modern high-precision astrometric observations, and their Galactic orbit elements were computed using a three-component model of the Galaxy, consisting of a disk, a bulge, and a massive extended halo. Ages was determined for dwarfs and subgiants using Yale isochrones 2004. For this purpose the original codes was developed, based on interpolation with the 3D-spline functions of theoretical isochrones, and with subsequent interpolation in metallicity and abundances of $\alpha$-elements.

**Key words:** Galaxy (Milky Way), stellar chemical composition, thin disk, Galactic evolution.

The various published abundances of an element for a given star often differ quite appreciably, even when the spectra reduced by different authors are of similarly high quality. If several abundance values are available for the same star, they can simply be averaged. However, when an abundance is presented in only one paper, the possibility of systematic differences must be considered. We collected all available lists (with $\geq 5$ stars) of relative abundance estimates of four $\alpha$-elements ([Mg/Fe], [Ca/Fe], [Si/Fe], [Ti/Fe]) for field stars from high-resolution spectra with high signal-to-noise ratios published after 1989. We estimate the completeness of the abundances published for solar-vicinity stars up through April 2007 to be better than 90 %. The raw material for this study were 81 publications containing 2800 $\alpha$-element-abundance determinations for $\approx 2000$ stars.

To derive reliable atmospheric parameters and abundances, we applied three-step iterative technique for compiling data, which in detail described in the paper (Borkova, Marsakov, 2005), with awarding of weight both to each source and to each determination of the averaged value. Stellar effective temperatures, metallicities, and relative abundances of $\alpha$-elements were leaded to scales of Edvardsson et al. (1993). The surface gravities was leaded to scale of Gratton et al. (2003), where they was determined on the basis of trigonometric parallaxes. We found it necessary to differentiate between the two metallicity groups because the uncertainties in all the parameters are considerably larger for the metal-poor stars.

The first step of averaging procedure was a simple mean. Our analysis shows that the scatter of the deviations and the systematic offset of individual atmospheric parameters and abundance determinations relative to the calculated mean values vary from list to list and also depend on metallicity. To take these small but systematic trends into account, we divided each list into two metallicity ranges at $[\mathrm{Fe/H}] = -1.0$ and calculated the mean deviations for these ranges. We then corrected all the individual determinations of each parameter for these biases. These corrections leave the determined parameter for stars present in several lists virtually unchanged. However, if a star's parameter was determined in a single study only, the correction will strongly affect the final determined parameter.

The next step after correcting for systematic biases was to determine weights for the data sources and cal-

Table 1: Internal accuracy of final atmospheric parameters and relative abundances of $\alpha$-elements for catalogue stars

| [Fe/H] range | $T_{eff}$ K° | $\log g$ | $\varepsilon$[Fe/H] dex | $\varepsilon$[Mg/Fe] dex | $\varepsilon$[Ca/Fe] dex | $\varepsilon$[Si/Fe] dex | $\varepsilon$[Ti/Fe] dex |
|---|---|---|---|---|---|---|---|
| $> -1.0$ | 58 | 0.12 | 0.06 | 0.07 | 0.07 | 0.05 | 0.15 |
| $< -1.0$ | 137 | 0.24 | 0.09 | 0.09 | 0.09 | 0.11 | 0.15 |

culate new weighted means. Each source was assigned a weight that was inversely proportional to the corresponding dispersion for the deviations in each of the metallicity ranges. In this case one and the same source could obtain different weight for each determined parameter. The lowest scatter for the higher metallicity range was found for the lists of Mashonkina et al. (2003), Edvardsson et al. (1993), and Jehin et al. (1999), and they were assigned unit weights. At lower metallicity range, the lowest scatter was shown by the lists of Nissen & Schuster (1997), Mashonkina et al. (2003) and Jehin et al. (1999). The lowest weights assigned to some of the lists were $\approx 0.2$. We then calculated a new weighted mean each parameter for each star taking into account the biases and weights assigned to the lists.

The next step was also a weight-assigning procedure, this time for individual parameter determinations. This procedure was intended to assign lower weights to initial values showing larger deviations. Clearly, such a procedure can work only if there are three or more values for the same star. When assigning the weights, we considered the mean absolute value of the deviations for all stars in the list containing the given value. As a result, this procedure assigns the lowest weights to the least-reliable determinations and enables us to obtain final values that are close to those given for most of the sources, with no single measurement rejected.

For all parameters, we estimated the uncertainties of the averages based on the scatter of the individual values about the final average for each star; i. e., from the agreement of the values obtained by the various authors. The corresponding uncertainties are presented in Table 1. All these estimates are close to the lower limits of the uncertainties for these parameters claimed by the authors.

We determined the distances to the stars using trigonometric parallaxes with uncertainties below 20 %. In their absence we adopted the photometric distances, derived using uvby$\beta$ photometric data. The uncertainty in photometric distances is usually claimed to be $\pm 13$ %.

We took the proper motions from the catalogs Hipparcos (1997), in their absence we adopted other background catalogs. spatial velocities and galactic orbital elements we computed the $U$, $V$, and $W$ components of the total spatial velocity relative to the Sun for stars with distances, proper motions, and radial velocities. The main contribution to the uncertainties in the spatial velocities comes from the uncertainties in the distances, rather than the uncertainties in the tangential and radial velocities. For mean distance uncertainties of 15 % and the mean distance from the Sun of the sample stars, $\approx 60$ pc, the mean uncertainty in the spatial velocity components is $\approx \pm 2$ km/s.

We calculated the Galactic orbital elements by modeling 30 orbits of each star around the Galactic center using the multi-component model for the Galaxy of Allen & Santillan (1991), which consists of a disk, bulge, and extended massive halo.

Ages were determined on the basis of Yale isochrones (2004) approximately for 1000 dwarfs and subgiants. For this purpose was developed the original procedure of 3D-spline interpolation of published theoretical isochrones. Procedure considers not only the metallicity of star, but also the content of $\alpha$-elements in it.

The complete describing of the catalog will be published latter in Astronomical Repots.

*Acknowledgements.* This work was supported in part by the Federal Agency for Education (projects RNP 2.1.1.3483 and RNP 2.2.3.1.3950) and by the Southern Federal University (project K07T – 125).

**References**

Allen C., Santillan A.: 1991, *Rev. Mex. Astron. y Astrofis.*, **22**, 255.

Borkova T.V., Marsakov V.A.: 2005, *Astron. Zh.*, **82**, 453; it Astron. Rep., **49**, 405.

Edvardsson B., Andersen J., Gustafsson B., *et al.*: 1993, *Astron. and Astrophys.*, **275**, 101.

Gratton R.G., Carretta E., Desidera S., *et al.*: 2003, *Astron. and Astrophys.*, **406**, 131.

Jehin E., Magain P., Neuforge C., *et.al.*: 1999, *Astron. and Astrophys.*, **341**, 241.

Mashonkina L., Gehren T., Travaglio C., Borkova T.: 2003, *Astron. and Astrophys.*, **397**, 275.

Nissen P.E., Schuster W.J.: 1997, *Astron. and Astrophys.*, **326**, 751.

# PROGRAMS FOR DATA REDUCTION AND OPTIMIZATION OF THE SYSTEM WORK

V.V. Breus

Department of Astronomy, Odessa National University
T.G.Shevchenko Park, Odessa 65014 Ukraine, *bvv_2003@pisem.net*, *bvv_2004@ua.fm*

ABSTRACT. During last years, some new computer programs were developed. In this article, will be described three of them.

The "Variable Stars Calculator" was developed for processing photometrical observations of variable stars. It helps the observer at each step from converting estimates of brightness into stellar magnitudes to searching a period of changing brightness, PCA analysis, searching extremums by the polynomial approximation etc. The program has Ukrainian, Russian an English interface languages and it is possible to add new ones.

The "PolarObs" was developed for processing polarimetrical observations, obtained at the 2.6 Shain telescope in the Crimean astrophysical observatory. It was used either for processing observations of cataclysmic variable stars, or for comets.

"TrayDog" is a system tool for Windows with more than 50 functions. Enhanced Task manager, that can view and edit properties of process, windows, libraries, threads, network ports and opened files. Other functions are: switching between desktops by hot-key, minimize any window to the system tray area, system information, blocking pop-ups of any kind, view and connect network shared resources, alarm clock and many other functions. The interface of the current version is only in Russian.

These and some other programs can be downloaded from the pages http://uavso.org.ua/breus, http://uavso.org.ua/breus

**Key words**: Software; data reduction; photometric, polarimetric observations; system tools; BY Cam.

## 1. Variable Stars Calculator

The program "Variable Stars Calculator v3 PROFI" is intended for automatic processing of the observations of variable stars and other processes. It has the great set of new functions, useful not only for processing of the observations of variable stars but also for any other processes. It is possible by this program:

- to translate estimates of brightness using the Niyland - Blazhko method into stellar magnitudes,
- to transform the numbers of plates of plate's collection in the Julian dates,
- to calculate the barycentric correction,
- to calculate a phase curve,
- to calculate the period of change of brightness,
- to determine ekstrema of brightness of any star,
- to calculate differences between the value of signal and the fitting polynomial,
- to perform the Principal component analysis,
- to compute partial restoration of signal (filtration),
- to build any graph,
- to look over double-channel diagrams.
- the program works as with single channel, as with multicolumn datafiles (five-colour photometry and other).

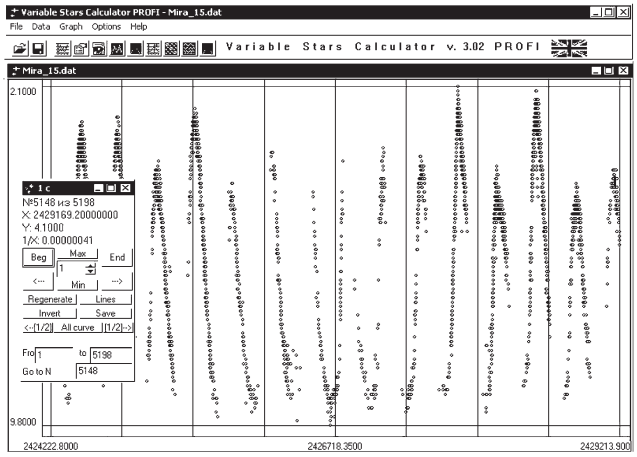


Figure 1: "Variable Stars Calulator": one column mode. A part of the light curve of the Mira (omicron) Ceti from the AFOEV database.

The program is multilingual, 3 languages of interface are currently supported: Ukrainian, Russian and English. Addition of other languages is possible (see chapter "Languages"). The program is published at my Internet page at the site of the Ukrainian association of variable stars observers (UAVSO) http://uavso.org.ua/breus and in the internet - catalogues softodrom.ru, softbox.ru, softnew.ru etc. The program works under the OS Windows. However, it may also run under Linux using Wine

(http://www.wine.org), e.g. under the Slax Linux (http://slax.linux-live.org).

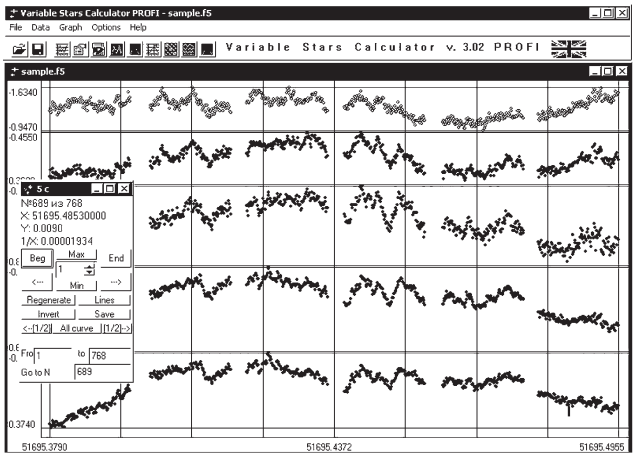


Figure 2: Variable Stars Calulator: UBVRI photometry.

*1.1. Transformation of estimates of brightness to the stellar magnitudes.*

The function is used for reducing visual observations. The Niyland - Blazhko method is optimal for determination of stellar magnitudes of variable stars. It's description is presented e.g. in the monograph by Tsessevich (1980). Using the program, it is possible to convert estimates to stellar magnitudes either from the paper "journal of observations", or from a file. User should enter estimates and magnitudes of comparison stars into the wizard-like dialog box. As a result of these actions, Julian dates (JD) and stellar magnitudes will be added into a data file.

*1.2. Transformation of numbers of plates of plate's collection into JD.*

The function was made for the observations on photo-plates of 7-camera astrograph of the Odessa astronomical observatory. Using the astrograph database (compiled by A.I.Pikhun), the program reads the file that contains numbers of plates and stellar magnitudes and outputs the file that contents Julian dates and magnitudes.

*1.3. Calculation of barycentric correction.*

The method is described by Soma et al. (1988). This algorithm was translated into the Delphi programming language. The user can enter the coordinates of the star and the program will apply barycentric correction to the Julian dates in the datafile.

*1.4. Calculation of phase curve.*

While processing observations of periodic variable star, the user can use the option of calculating the phase curve (dependence of stellar magnitude on a phase), which are much more "dense" than the individual curves, if the interval of observations is much larger than the period (e.g. Tsessevich 1980). The phase curve can be viewed either in the Variable Stars Calculator, or in another viewer that works with ANSI text files.

*1.5. Calculation of period of change of brightness*

In this program, the periodogram analysis of variable signal is realized using the Lafler-Kinman method. The detailed description of the method and its basic modifications and comparison of their statistical properties, is presented by Andronov and Chinarova (1997).

The periodogram can be viewed either in the Variable Stars Calculator, or in another viewer. Then the user can calculate the phase curves using the periods that correspond to the minimal values of the test-function.

*1.6. Viewing of the graphs*

The program has one big module for graph drawing that consists of the graph window and panel of navigation, that can be moved. User can set many options. Among them - line connection, viewing some selected columns of the datafile, range files, data reduction, exporting graph as a picture of different format and colors (from black and white to 24bit), viewing double-channel diagrams and many other functions.

*1.7. Determination of moments of extremums of brightness using the polynomial approximation*

The light curve is approximated by a polynomial (up to degree 10) and the program calculates extremums of the polynomial. All moments of extremums (corresponding to different degrees) are listed in the dialog box and the user can select them and view corresponding polynomial, moment and accuracy estimate.

*1.8. The PCA analysis and signal filtering.*

This function can be used for multicolumn files. The detailed description of method and it's basic

modifications are described by Andronov (2003). By choosing the corresponding menu item, the user can see on the graph the principal components instead of the light curve. After it, the function of signal filtering will be allowed. In the dialog box, the user can unselect that components, which are suggested as "noise" and then make partial restoration of the signal.

## 2. PolarObs

Cataclysmic variables are observed, particularly, in the Crimean Astrophysical observatory using the 2.6 meter Shain telescope with a new polarimeter constructed by N.M.Shakhovskoy and D.N.Shakhovskoy. It contains of the rotating $\lambda/4$ phase plate and an immobile analyzer. Data are saved in a file as 8 columns of counts. Processing of observations requires a software which would automatize it. A review on polarimetry is presented in this volume by Kolesnikov (2007). Because of new 2-channel polarimeter with the $\lambda/4$ phase plate, the use of old software is impossible. Besides, the possibilities of the old program (Shakhovskoy et al. 1998) under MS DOS was limited, as compared with programs under MS Windows. The new program "PolarObs" was developed (Breus et al. 2007).

All data files consist of series of observations. Any series (observations of star, background, comparison star, standard star) have properties - filter and exposure time. When opening the data file, the program automatically determines the type of series, at the same time enabling the user to apply or change it. This style minimizes the number of keys to be pressed.

After opening a data file, the program shows 2 curves - the light curve of object at the top, measurings of background at the bottom of the workspace (for 1 from 8 channels). After smoothing the values of background by a polynomial, the background values are subtracted from the signal separately for all channels. User can smooth the values of the comparison star to determine the stellar brightness of object.

After it, the program calculates linear combinations of counts in channels, hereafter named the "vectors" S1-S4. The first and second vectors determine the circular polarization, and the third and fourth - the linear polarization. After this step, it is possible to save the "P-file", containing as photometry as these vectors.

User can save the "C-file" instead, that contains no photometry. This function was developed for processing polarimetric observations of comets. This file can be viewed later. The next step will be to analyze the diagram of the vectors S2 on S1 and S4 on S3. Under the graphs, there are the values of polarization, position angle and other information.

If user is processing observations of standart of zero or nonzero polarization, these values are a final result.

While processing the star (object), it is possible to

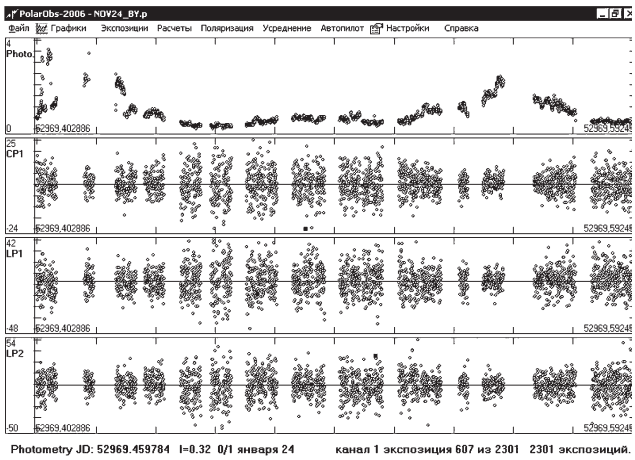


Figure 3: PolarObs: P-file mode (potometry, circular polarization, linear polarization). The observed star - BY Cam.

turn the diagram of circular polarization for adduction of axis connecting 0 and center of distribution to the OX direction and linear polarization to an angle determined for the standard of nonzero linear polarization. It is possible to approximate vectors by a polynomial

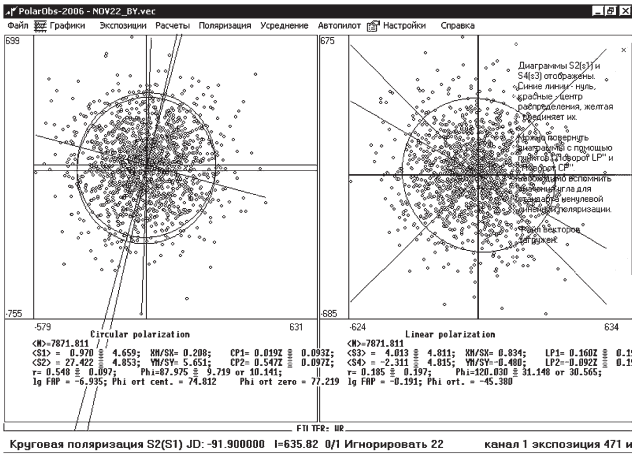


Figure 4: PolarObs: vector diagrams. Observations of BY Cam.

or to determine mean points and their accuracy estimate. To determine the statistically optimal number of points, we use 3 test functions, which are listed in a listbox.

Some modules, like approximation by a polynomial and component for drawing the graphs, which where developed earlier for our program "Variable Stars Calculator", were used in "PolarObs".

Many processes, including search of data files on the user's disk are automated, that make the work easier. The program settings allow to change an interface and some parameters. While processing observations, the user can save files of different format, that can be used

by other software as well. The help is made like a popup transparent window, which also contains all tips and messages.

The program passed the practical tests. Using PolarObs, there were processed observations of different cataclysmic variable stars - AM Her, BY Cam, V1432 Aql, QQ Vul and comets.

## 3. TrayDog

TrayDog is a system tool for OS Windows. It has more than 50 functions. Some brief description of the main functions of the program (full description can be viewed on my web-sites (Breus 2007)).

### *3.1. Enchanced Task manager*

With it user can view all launched processes, change it's priority, kill process etc. It is possible to view the windows of the process, threads, used libraries (dll), the "parent process" (process that launched current one). The network and disk activity of the process can be also viewed. User can see which files and ports are opened by some program. Sometimes it helps to kill wrong-working processes, find computer viruses and for programming purposes like find the classname or handle of some window.

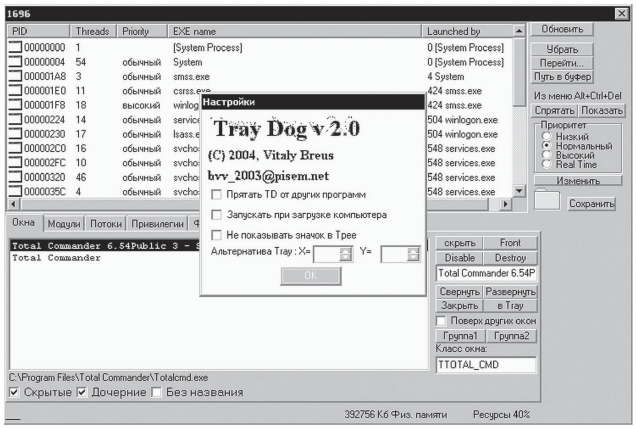


Figure 5: TrayDog: Task manager and options dialog.

### *3.2. System information*

TrayDog doesn't show more system information than a famous products but some functions are rare and it can easy save all information for further comparing. The program shows version and serial number of the operating system, bios version and date, real frequency of the CPU, drive list and file systems, find virtual drives among them, show all dial-up connections with logins, passwords and phone numbers, environment variables etc.

### *3.3. Other functions*

Switching between desktops by hot-key
Minimize any window to system tray area
Blocking pop-ups of any kind, listed in a text file
Setting folder or drive icons
Creating virtual drives from any folder
Disabling system shutdown (used for some installations that can't ask should computer be restarted now or later)
View and connect network shared resources
Alarm clock with user specified music file
Launch up to 20 programs from list by one click, "launch in the past" (for shareware software).
Hiding any process from other software
Hiding all desktop icons, some Start-menu items, clock, Start button etc.
Saving desktop icons positions for further restoring after changing screen resolution or system faillure.
Clearing last documents, URLs, searched files and other history lists
Changing mouse cursor icons
Quick launch of Control-Panel applications
Blocking ANY network access
Quick IP - Name and Name - IP resolving
Blocking and opening any CD Drive
Turning off the monitor
Turning off the system speaker (Win9x)
Quick (2-seconds) shutdown (Win9x)
View kernel driver list (Win9x)
and many other functions. Current version is available only in Russian. Now we develop a new version TrayDog-2007.

A complete list of my programs is available from the WEB site (Breus, 2007).

*Acknowledgements.* Author is thankful to Ivan L. Andronov, Sergey V. Kolesnikov, Nikolay M. Shakhovskoy for fruitful discussions.

## References

Andronov I.L., 2003, *ASP Conf Ser.*, **292**, 391.
Andronov I.L., Chinarova L.L., 1997, *Kinematics and Physics of Celestial Bodies*, **13**, N6, 67.
Breus V.V., 2007, *http://uavso.pochta.ru/breus, http://uavso.org.ua/breus.*
Breus V.V., Andronov I.L., Kolesnikov S.V., Shakhovskoy N.M.: 2007, *As.Ap.Trans.*, **26**, N4.
Kolesnikov S.V, 2007, *Odessa Astron. Publ.,* **20**.
Shakhovskoy N.M., Andronov I.L., Kolesnikov S.V., Halevin A.V., 1998, *Kinematics and Physics of Celestial Bodies*, **14**, 468.
Soma M., Hirayama Th., Kinoshita H.: 1988, *Celestial Mechanics.* **41**, 389.
Tsessevich V.P.: 1980, *"Variable stars and observations of them".* (in Russian), Moscow, "Nauka".

# MODELING OF REGIONS OF ASTEROID POSSIBLE MOTION

A.M. Chernitsov, O.M. Dubas, V.A. Tamarov

Tomsk State University,
Lenin pr., 36, Tomsk 634050 Russia, *astrodep@niipmm.tsu.ru*

ABSTRACT. Peculiar properties of construction of initial regions of asteroids' possible motion from observational data in the form of probabilistic ellipsoids are investigated. For the objects which observed only in one appearance, this problem may be essentially nonlinear, and the usual method for their construction with the help of linear estimations of covariance matrices may became unacceptable. In order to make possible application of the linear estimation methods which has been developing in mathematical statistics the problem of decreasing nonlinearity is discussed. The solution of this problem with the help of appropriate system of initial parameters of asteroid orbits choice, as well as initial time and weighting matrices of observational errors is proposed. Efficiency of such technique had justified by numerical experiments with the usage of model and real observations.

**Key words**: asteroid, probabilistic motion, initial region, weighting matrix, nonlinearity.

The number of asteroids known today (e.g. from Bowell catalogue) is about 375000. About a quarter of them is observed only at one appearance, and the sixth part is observed on small measured intervals (less than 40 days). For such objects, the regions of possible motion defined with traditional methods of linear estimation, may be inauthentic. Determination of asteroid's probabilistic motion contained two basic stages: the forming of the initial region $C_q^0$ in space of the motion parameters $q = (q_1, ..., q_m)$ and its reflection $C_q^0 \to C_p^t$ to space of the parameters $p = (p_1, ..., p_s)$, on any given time $t$ (Chernitsov et al., 1998). The display statement is differential equation system of the asteroid motion, as well as equations joined with each other spaces $\{q\}_t$ and $\{p\}_t$. The reflection is realized by means compact ensemble of trajectories from the whole of initial region or from its boundary surface. The methods of solution this problem is well developed and so basic our efforts were turned to the problem of construction of initial region.

The problem of determination of the initial region is reduced to finding estimations initial parameters $\hat{q}$ and their covariance error matrix $\hat{D}$ for construction of probabilistic ellipsoids which enveloped the regions of possible motion of investigated asteroid. For objects, which were observed only in one appearance, this problem may be essentially nonlinear, and usage of covariance matrices become impossible. But, if in some way or other one reduces initial nonlinearity to permissible level, the application of well-known technique of linear estimation on basis of using covariance matrices becomes rightful (Chernitsov et al., 2006). With that end in view we fulfilled great number of numerical experiments based on real and model observations. Simulation has been realized in the following way:

1. The initial parameters of the asteroid orbit are taken as "true";
2. On basis of these parameters the "true" values of measured parameters have been determined on given times of observations;
3. In these "true" values one introduced errors so that model observations were not uniformly precise. For that random number generators and given weighting matrices of observation errors have been used;
4. After that nonlinear least squares problem have been applied for finding estimations of initial parameters and their covariance error matrix.

For construction of error ellipsoids in nonlinear problems one use covariance matrices, although that is, strictly speaking, acceptable only within the framework of the theory of linear estimation.

The least squares problem is reduced to minimization of target function

$$\Phi(q) = [d - d^*]^T P [d - d^*] = min,$$

where $d$ is $N$ - dimensional vector function measured parameters, $d^*$ is $N$ - dimensional vector measurements, $P$ is the weighting matrix. In linear formulation $d = Aq$, where $q$ is $m$-dimensional vector defined parameters, and solution evaluated by relations

$$\hat{q} = \left(A^T P A\right)^{-1} A^T P d^*,$$

$$\hat{D} = \sigma_0^2 \left(A^T P A\right)^{-1}.$$

Here $\sigma_0 = \sqrt{\Phi(\hat{q})/(N-m)}$ is root-mean-square error of unit weight. In nonlinear case connection between measured and defined parameters is nonlinear, $d = d(q)$, hence the problem may be solved only by numerical iterative methods (e.g. by method of differential correction data)

$$q^{n+1} = q^n - \left\{ \left[R^T(q) P R(q)\right]^{-1} R^T(q) \left[d(q) - d^*\right] \right\}_{q=q^n}.$$

Here $R(q) = (\partial d/\partial q)$ is the matrix of $(N \times m)$ - dimension; $n = 0, 1, ...$ is the number of iteration. Covariance matrix one calculated by means of the same relation as in linear case

$$\hat{D} = \sigma_0^2 \left(R^T P R\right)^{-1}_{q=\hat{q}}.$$

These solutions defined probabilistic regions for error's dispersion. In linear case their isosurfaces will be ellipsoidal, while in nonlinear case they will be non ellipsoidal. Distinction of the level surface from ellipsoidal ones is given by remainder term $\Delta\Phi$ in expansion of target function of nonlinear least-squares problem

$$\Phi(q) = \Phi(\hat{q}) + \Delta q^T \left(R^T R\right) \Delta q + \Delta\Phi.$$

Subject to value of that term the initial region may be found either weakly or strongly nonlinear. The degree of nonlinearity is depended on size of the region probabilistic spread of estimations for initial parameters and on degree of nonlinearity functional connection between measured and defined parameters. In many problems of estimation the influence of the last factor on legitimacy for application of the linear methods is negligible because of relatively small-sized regions of probabilistic solution spread (e.g. the problem of positioning with the help of the satellite system NAVSTAR). In the case of asteroids, which have been observed at one appearance, regions of probabilistic solution spread will be large, and degree of nonlinearity of the functional connection between measured and defined parameters will produce the strongly nonlinear initial region.

To obtain how often the strong nonlinearity of estimation problem occurred for such objects, we investigated a few hundred asteroids which were observed in one appearance. As parameter of nonlinearity we have used the quantity

$$\chi = \frac{\sigma_{max} - \sigma_{min}}{\sigma_{min} - \sigma_0},$$

where $\sigma_{max}$ and $\sigma_{min}$ is maximal and minimal root-mean-square residuals in vertices of an error ellipsoid. This quantity gives deviation of the level surface of probabilistic solution dispersion from ellipsoidal ones. We have considered the influence of some factors on value of this parameter. These factors were the space of used phase variables, disposition of initial time with respect to measuring interval, the insertion of suitable weighting matrices in estimation algorithms and possibility of decreasing nonlinearity with the help of screening observations.

In the table 1 are given asteroids of some hundred ones, for which the estimations of nonlinearity factor were obtained by construction of initial domain in spaces of Cartesian and Keplerian variables. About one third part of these asteroids has low nonlinearity in Cartesian variables, whereas in Keplerian variables the nonlinearity is strong for all objects. In this case that due to the fact that functional connection between rectangular coordinates and measured parameters $\alpha, \delta$ is less nonlinear than connection with them Keplerian elements.

Table 1: The nonlinearity coefficients in spaces of Cartesian ($\chi_{dec}$) and Keplerian ($\chi_{kep}$) variables. $\Delta T$ is the measured interval (in days), $N$ is the number of observations.

| Object | $\Delta T$ | $N$ | $\chi_{dec}$ | $\chi_{kep}$ |
|---|---|---|---|---|
| 2001XN254 | 48 | 47 | 0.000 | 0.690 |
| 2001XN254 | 48 | 47 | 0.000 | 0.690 |
| 2004GE2 | 12 | 94 | 0.000 | 245.7 |
| 2003WN188 | 24 | 75 | 0.009 | 1805.9 |
| 2004RZ164 | 22 | 15 | 0.580 | 17.13 |
| 1998QA62 | 21 | 44 | 3.584 | 7097.9 |
| 2003WV172 | 25 | 09 | 12.56 | 25995.3 |
| 2003UN284 | 31 | 06 | 62.97 | 44194.3 |
| 2003XB22 | 09 | 16 | 168.84 | 20369.0 |
| 2003QZ30 | 49 | 55 | 441.5 | 44288.1 |
| 2002PQ142 | 14 | 18 | 822.0 | 70990.0 |

The estimations of nonlinearity factor for some asteroids from Bowell catalogue, whose initial moments lie outside of measured observations interval are given in table 2. One can see that by choice of initial moments from Bowell catalogue the problem of construction initial probabilistic regions of motion is strongly nonlinear. Displacement of initial moment to inside of measured interval essentially decreases nonlinearity for all objects and make estimation problem weakly nonlinear for four asteroids.

In the table 3 and figure 1 we presented experimental results of decreasing nonlinearity of least-squares problem with the help of appropriate screening observations. Here $n = 0$ corresponds to initial sample of observations and $n = 1, 2, 3$ corresponds to samples of observations after first, second and third screening.

The insertion of suitable weighting matrix in algorithm of construction of initial domain may significantly decrease it, but we do not know for the time

Table 2: The nonlinearity of initial region by various choice of initial time. Here $\chi$ is nonlinearity factor where initial moment lie outside of measured interval, $\chi^{'}$ is nonlinearity factor where initial moment is arithmetical mean of observational moments, $\Delta t$ is the value of initial moment shift (in day).

| Object | $\Delta t$ | $\chi$ | $\chi^{'}$ |
|---|---|---|---|
| 2003WC168 | +11 | 69.93 | 7.03 |
| 2003WU172 | +04 | 12.56 | 12.52 |
| 2003WX153 | +09 | 44.55 | 3.94 |
| 2003XB22 | +09 | 168.8 | 13.79 |
| 2003XG | +02 | 5.07 | 1.56 |
| 2003YQ94 | +15 | 515.1 | 4.61 |
| 2004XO63 | -44 | 1.42 | 0.05 |
| 2004XM130 | +14 | 344.4 | 24.45 |
| 2004YA | -44 | 158.1 | 0.71 |
| 2004YC | -43 | 8.28 | 0.05 |
| 2004YD | -43 | 35.83 | 0.24 |
| 2004YD5 | -40 | 12.52 | 0.01 |
| 2004YE | -43 | 30.95 | 0.63 |
| 2004YG1 | +17 | 13.50 | 2.52 |
| 2004YR | +17 | 371.7 | 15.21 |
| 2004YZ23 | +02 | 50.51 | 45.53 |
| 2005AB | +11 | 68.96 | 17.80 |
| 2005AC | +11 | 94.31 | 29.80 |

present how made that in real case. However, in case of modeling unequal precise observations we specified weighting matrix for observational errors, which may be used later on as exact weighting matrix for solution of the least-squares problem. Numerical experiments have showed that exact weighting coefficients distinctly decreases nonlinearity of least-squares problem and probabilistic region, if there are more than one group of observations with the same numbers, the mean accuracy of which differed from each other more than three times. Such result was received both for observability of asteroid in one appearance and in several ones. The last result is especially important, since for many asteroids which were observed in several appearances in 80 – 90-th of the past century take place just such distinction in mean accuracy of observations in different appearances. For example, observational accuracy of asteroid Geographos has been increased from 2" up to 0.5", i.e. about in 4 times. For such cases of observability of asteroids sufficiently simple method of weighting matrices construction is realizable. We named such matrices "averages". They represent diagonal matrices, whose elements are constant for observations of single appearance, and they are defined by the rule

$$p_i = \frac{\sigma^2}{\sigma_{0i}^2},$$

Table 3: The estimations of nonlinearity factors by screening observations of asteroid 2004XM130. Here $n$ is the sample number, $N$ is the number of observations, $\Delta T$ is the measured interval (in days), $\chi$ is the nonlinearity factor.

| $n$ | $N$ | $\Delta T$ | $\chi$ |
|---|---|---|---|
| 0 | 36 | 5 | 20.06 |
| 1 | 33 | 5 | 18.42 |
| 2 | 30 | 5 | 15.95 |
| 3 | 28 | 5 | 13.42 |

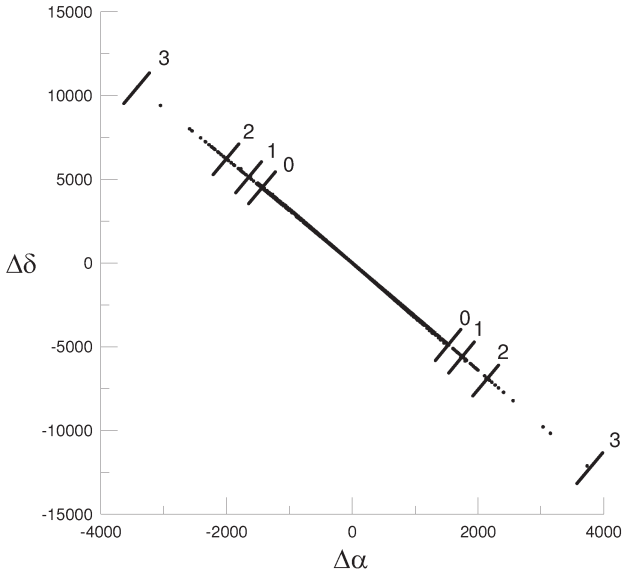


Figure 1: The regions of probabilistic motion of asteroid 2004XM130 obtained by successive screening observations.

where $\sigma_{0i}^2$ is the mean-square error for representation of observations of $i$-th appearance.

In the figure 2 we presented the probabilistic dispersion of estimations, which were obtained by using "exact", "average" and identity weighting matrices. One can see that utilization of "average" weighting coefficient in the least-squares problem allows us to reduce essentially the region of probabilistic displacements of initial parameter estimations in comparison with generally accepted variant, when weighting matrix is considered as identity. Similar picture is for probabilistic regions defined by means of covariance matrices of initial parameter estimations (figure 3).

The comparison of domain size supplements the numerical estimations of their volumes (table 4). These estimations represent the ratio of volumes of probabilistic error ellipsoids, defined with usage of "average" ($V_{p\sigma}$) and "exact" ($V_{pt}$) weighting coefficients, to vol-

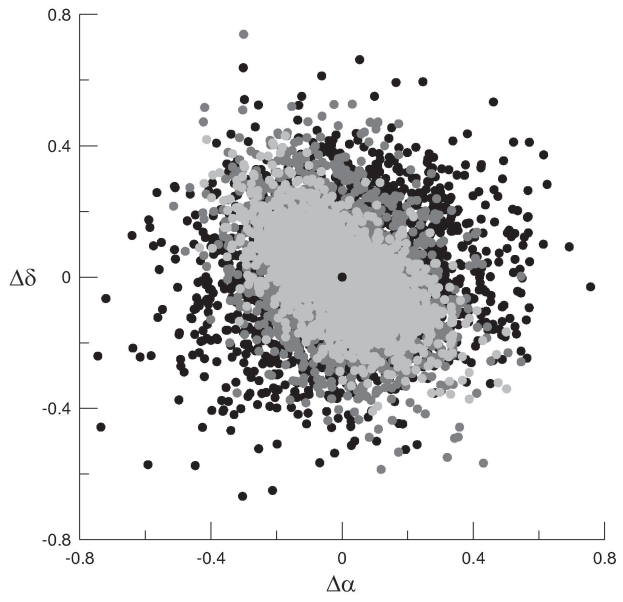


Figure 2: The probabilistic dispersion of estimations, which were obtained with usage of "exact" (light-grey colour), "average" (dark-grey colour) and identity (black colour) weighting matrices. $\Delta\alpha$ and $\Delta\delta$ are given in second of arc, and represented the deviation of estimation from the "true" solution.

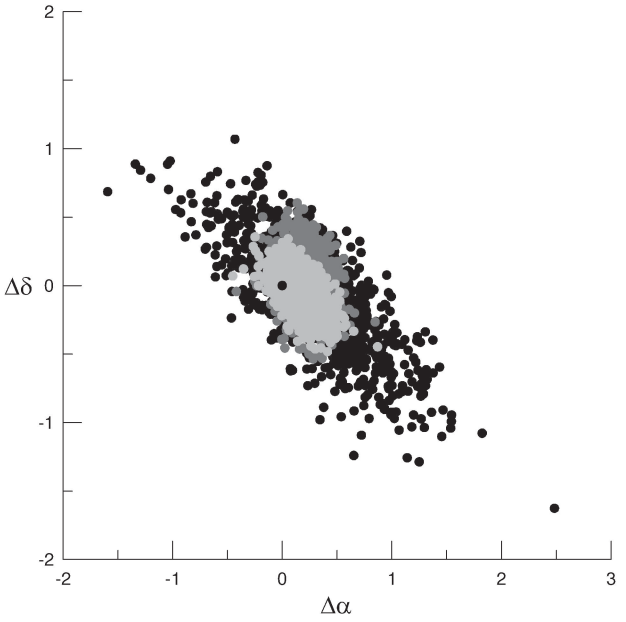


Figure 3: The probabilistic regions defined by means of covariance matrices of initial parameter estimations with different weighting matrices.

ume of error ellipsoid obtained under the assumption of equal precision for all observations ($V_I$). One can see that usage of "average" weighting coefficients in case of observability of asteroid in two appearances with different accuracy, distinguished on average in 4 times, allows us noticeably to decrease both regions of probabilistic dispersion of initial parameter estimations itself and computational probabilistic error regions of these estimations, which are defined by their covariance matrices.

Table 4: The ratio of volumes of probabilistic error ellipsoids, defined with different weighting coefficients.

| | min | max | average | dispersion |
|---|---|---|---|---|
| $V_{p\sigma}/V_I$ | 0.0023 | 0.197 | 0.0377 | 0.0279 |
| $V_{pt}/V_I$ | 0.0007 | 0.044 | 0.0055 | 0.0049 |

So, the computations carried out allows us to make conclusions as follow:

1. Utilization of rectangular coordinate system makes the problem of construction of initial probabilistic region practically linear on numerous occasions. Properties of differential correction method in space of Cartesian coordinates (convergence domain and rate of convergence) are also better than in spaces of other variables.

2. The estimation problem has the least nonlinearity, if initial moment is equal to arithmetical mean of observational moments.

3. In some cases the nonlinearity of problem may be decreased by means of screening of observations.

4. Insertion of suitable weighting matrix in estimation algorithms also decreases nonlinearity of problem and size of probabilistic regions. If observations of asteroid cover more than one appearance, in a number of cases there may be an easy method of construction of such weighting matrices.

*Acknowledgements.* This work was supported by RFBR grant N 05-02-17043.

**References**

Chernitsov A.M., Baturin A.P., Tamarov V.A.: 1998, *Solar System Research*, **5**, 32, pp. 405-412. *Translated from Astronomicheskii Vestnik*, **5**, 32, pp. 459-467.

Chernitsov A.M., Dubas O.M., Tamarov V.A.: 2006, *"Izvestiya Vysshikh Uchebnykh Zavedenii. Fizika"*, **2**, 49, pp. 44-51. (In Russian)

# TSESEVICH AND KRAKOW'S ASTRONOMERS

P. Flin

Pedagogical University, Institute of Physics
ul. Swietokrzyska 15, 25-406 Kielce, *sfflin@cyf-kr.edu.pl*

ABSTRACT. In the paper I present some aspects of collaboration between Prof. Vladimir Platonovich Tsessevich and Cracow's astronomers working in the field of variables stars.

## 1. Introduction

Contrary to many papers presented by collaborators and disciples of Prof. Tsessevich this is the remembrance of person who never met him personally. According to my best knowledge he never visited Cracow. Probably the oldest personal relations were between Prof. Eugeniusz Rybka (1898 - 1988) and Prof. Tsessevich. (After living Lvov in 1945, where he was a professor (1932-1945) Eugeniusz Rybka have been in Wroclaw till 1958 and later on became the Director of the Astronomical Observatory of the Jagiellonian University in Cracow until retirement in 1968). Prof. Kazimierz Kordylewski (1903 -1981) working in the field of eclipsing variable visited him in Odessa, as well as in the middle seventies of the previous century Dr ( in those days) Jerzy M. Kreiner paid a visit in Odessa.

While the personal contacts were rather scarce, the scientific ones were numerous. My paper is divided into two sections. In the first I refer to Cracow Yearbook, in the second one I am giving my personal recollections referring to Tsessevich's works.

## 2. Tsessevich and SAC

Starting from the year 1923 the Director of the Cracow Observatory Prof. Tadeusz Banachiewicz (1882 - 1954) published Rocznik Astronomiczny Obserwatorium Krakowskiego, Dodatek Midzynarodowy (Astronomical Yearbook of the Cracow Observatory, International Supplement). The Yearbook itself disappeared rather quickly, but the Supplement lived his own life, well known as SAC (Supplemento Internationale de Anuario Cracoviense).

In each Yearbook the list of eclipsing binaries and bases of the ephemerides were presented.

The first time the name of Zessewitsch appeared in SAC No 4 (ephemerides of eclipsing variables for the year 1926) published in 1925. Observations of

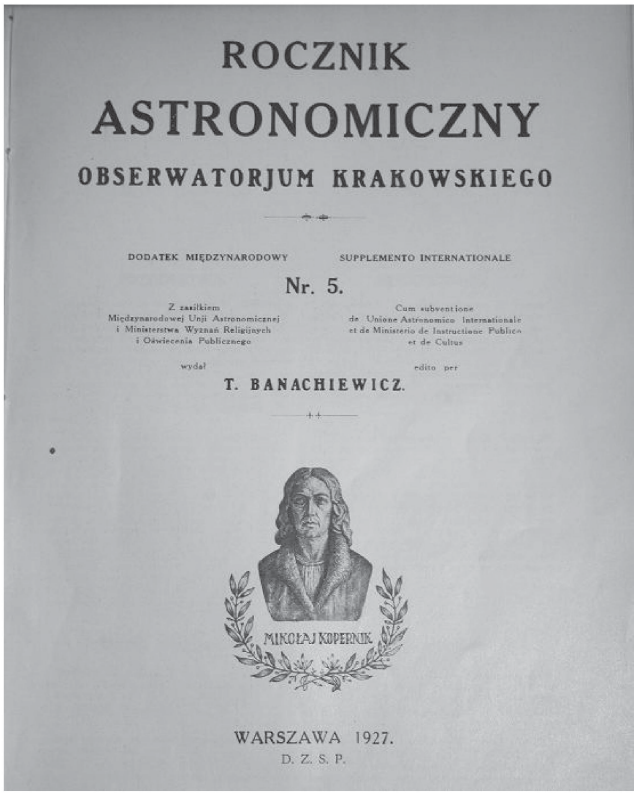
ROCZNIK
ASTRONOMICZNY
OBSERWATORJUM KRAKOWSKIEGO
DODATEK MIĘDZYNARODOWY SUPPLEMENTO INTERNATIONALE
Nr. 5.
T. BANACHIEWICZ.
MIKOŁAJ KOPERNIK
WARSZAWA 1927.
D. Z. S. P.

Figure 1: The front page of Supplemento Internationale de Anuario Cracoviense No 5.

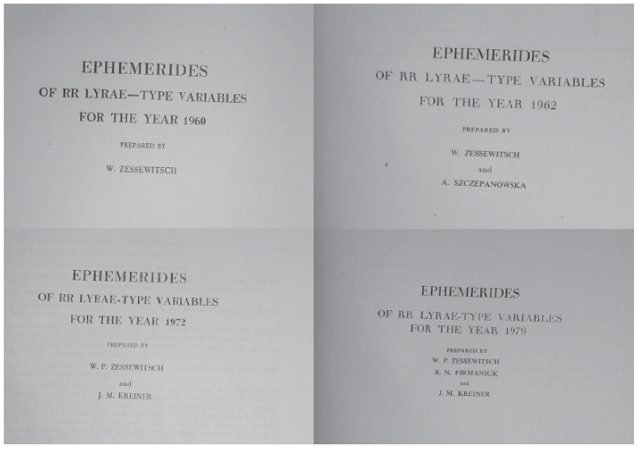
EPHEMERIDES
OF RR LYRAE—TYPE VARIABLES
FOR THE YEAR 1960
W. ZESSEWITSCH
EPHEMERIDES
OF RR LYRAE—TYPE VARIABLES
FOR THE YEAR 1962
W. ZESSEWITSCH
A. SZCZEPANOWSKA
EPHEMERIDES
OF RR LYRAE-TYPE VARIABLES
FOR THE YEAR 1972
W. P. ZESSEWITSCH
J. M. KREINER
EPHEMERIDES
OF RR LYRAE-TYPE VARIABLES
FOR THE YEAR 1979
W. P. ZESSEWITSCH
B. N. FIRMANIUK
J. M. KREINER

Figure 2: Front pages of RR Lyrae variable stars ephemerides.

S Equ published in Astronomische Nachrichten 5332 were quoted.

In SAC No 5 (published in 1926) his name appeared several times in connection with published in AN and BZ data dealing with following stars: WZ And, ZZ Cas, S Equ, TW Lac, AQ Peg, WX Sgr, XY Sgr, EG Sgr and T Sex.

Next year, the editor Thadeus Banachiewicz in introduction wrote that some data reported by letters from Cessewich (Leningrad) were used. Of course, the previous results incorporated in SAC and quoted in the list were preserved.

Starting from 1926 till the end of publication of SAC in the middle of nineties of the previous century the results obtained by Tsessevich were used.

In SAC No 31 for the Year 1960 (published in 1959) the following sentence, written by the editor, Prof. Rybka appeared:

"It is the first time that according to the resolution of Commission 27 of the International Astronomical Union - ephemerides for RR Lyrae type variables calculated from the data supplied by Prof. V. Tsesevich of Odessa have been included in the Yearbook."

Probably calculations of the ephemerides were performed by Dr Aldona Szczepanowska using data supplied by Prof. W. Tsessevich.

This had been explicitly written starting from SAC No 33 for the Year 1962 till Ephemerides for 1971 (SAC No 42). After that ephemerides of RR Lyrae stars were prepared by W.P. Zessewitsch and J.M. Kreiner and ephemerides from1979 till 1985 were arranged by W.P. Zessewitsch, B.N. Firmaniuk and J.M. Kreiner. In order to complete this story I have to add that after the death of Prof. Zessewitsch the ephemerides were procured by B.N. Firmaniuk and J.M. Kreiner.

### 3. Observations of Eclipsing Variables

In sixties of the XX century Krakow's observers of eclipsing binaries were very active. They were amateur astronomers. Well known observer of eclipsing variables Dr Rozalia Szafraniec (1910 - 2001) mentioned this activity together with Sky and Telescope, Brno and BAV observers.

They observed visually a lot, mainly in summer. The main goal was timing minima and they were forced to prepared the finding charts for stars. This was done copying on the tracing paper the appearance of sky till 5 or 6 magnitude. After that usually from BD the appropriate region containing the variable star vicinity was copied. The last element must be the vicinity of the variable star itself. The maps published by Tsessevich among others in Izvestya Odesskoy Observatoryi vol. IV were very popular. I have been involved in preparation of maps and in that time my first acquaintance with works of Prof. Vladimir Platonovich

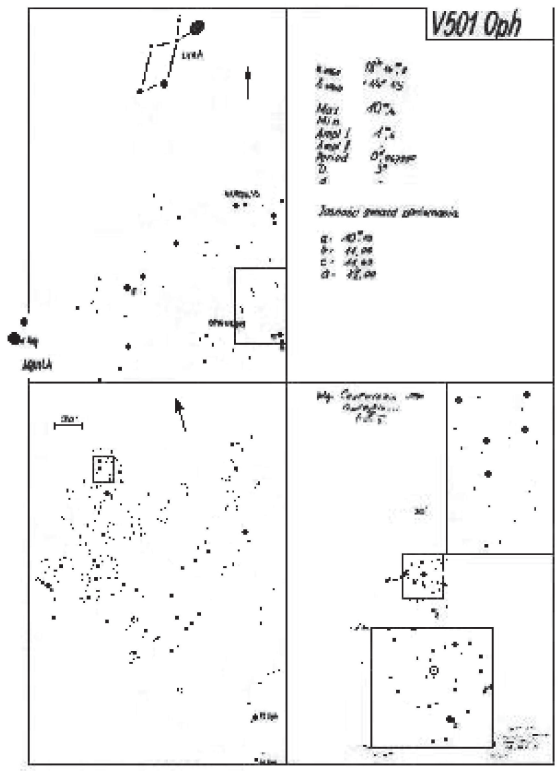


Figure 3: The map of V501 Oph.

Tsessevich took place.

This type of work was continued later on too. In Cracow Astronomical Observatory preparing maps of variable stars quite often we used above mentioned source, as well as Atlas of the vicinity of variable stars and other maps placed in various books and publications of Prof. Tsessevich.

### 3. Conclusions

Prof. Tsessevich observations of eclipsing variable stars gave him the worldwide reputation. It is obvious that these observations were incorporated in SAC and his name was frequently placed among authorities. The first reference in SAC to his observation published in leading astronomical journal was when he was under twenty years old in 1925. His name among authorities can be found in last issue of SAC in 1996. This means that the results of his observations appeared in SAC during the period of seventy years. The publication of maps of vicinities of variable stars helped several observers. This influence is quite often not seen easily, but it is important and cannot be forgot. My last thoughts are connected with the transcription of Vladimir Platonovicz name. In Polish is quit simple: Cesewicz. Sometime it is written Cessewicz, which is

probably the influence of German transcription. Following the German transcription in SAC quite often it is written Zessewitsch. But even in the same issue of SAC there are several different transcriptions! Officially, the memorial conference was dedicated to Prof. Tsessevich, which is English transcription. I dare to recall your attention to Prof. Rybka statement. He wrote Prof. Tsesevich, which probably is the most correct English transcription.

**References**

Supplemento Internationale de Anuario Cracoviense (from 1925 till 1996).

Szafraniec R.: 1970, *Vistas in Astronomy*, **12**, 7.

# PHOTOMETRIC RESEARCHES OF ASTEROIDS ON 1.5-M RUSSIAN-TURKISH TELESCOPE

A. Galeev[1,2,3], R. Gumerov.[1,2], I. Bikmaev[1,2], G. Pinigin[4], I. Khamitov[5], Z. Aslan[5]

[1] Department of Astronomy, Kazan State University, Kremlevskaya Str. 18, Kazan, 420008, Russia, *almaz@ksu.ru*
[2] Tatarstan Academy of Science, Bauman Str. 20, 420111, Kazan, Russia
[3] Department of Physics, Tatar State University of Humanitarian and Pedagogical Sciences, Tatarstan Str. 2, Kazan, 420021, Russia
[4] Nikolaev Astronomical Observatory, Observatornaya Str, Mykolayiv, 54030, Ukraine
[5] TÜBITAK National Observatory, Akdeniz Universitesi Yerleskesi, Antalya, 07058, Turkey

ABSTRACT. This work describes some research results based on the photometric studies on Russian-Turkish telescope during last five years. During 2004-2006 observations of minor planets were carried out within the international collaboration between Kazan State University, TÜBITAK National Observatory and Nikolaev Astronomical Observatory for studying the physical parameters and kinematics of asteroids. As a result the photometric characteristics of these objects have been obtained; the lightcurves frequently demonstrating changes of brightness of these objects caused by their rotation around an axis are constructed. The variability periods and amplitudes for asteroids (762) Pulcova, 2000PN9, (6006) Anaximandros have been found.

**Key words**: Asteroids: photometry: rotation; asteroids: individual: (762) Pulcova, 2000PN9, (6006) Anaximandros.

## 1. Introduction

During the last decade in connection with the opening of tens of thousands of new objects, detection of the large transneptunians bodies and discovery of some asteroids binarity the tasks of studying Solar system's minor planets were widely extended. The basic tasks of complex astrometric and photometric asteroids researches are a specification of the characteristics of orbits and a definition of the basic physical parameters (mass, rotation period). These researches are very important from the point of view of determinations of the sizes, forms and densities of asteroids, establishment of correlations between rotation and size, specifying taxonomic class of a minor planet (Britt et al., 2002). The significant information about the asteroids characteristics can be obtained with the help of results of multi-color photometric observations of these objects on 1-2 meter telescopes.

Now the rotation characteristics of about 3000 numbered asteroids are known (see the Center of Minor planets of NASA – NASA, 2006). The rotational periods of asteroids are rather various: from the hundredth shares of an hour (2001 WV1, 2004 BV18), up to tens of days (1997 AE12, (288) Glauke), and the amplitudes of brightness changes reach $1.5^m - 2.0^m$, but usually they are about five tenths of a magnitude in R band. In spite of the fact that many minor planets near opposition appear rather bright ($10^m - 15^m$), this precision photometric observations can be possible only on large telescopes. The characteristics of this telescope and its receiver equipment enable us to get the images of asteroids with magnitudes up to 22.

## 2. Observations

The systematic observations and researches of asteroids in the main belt, and near-Earth, and Kuiper-belt objects have being conducted since 2002 on the 1.5-m Russian-Turkish telescope (RTT150), at the TÜBITAK National observatory (TÜBITAK Ulusal Guzlemevi - TUG) near Antalya (South Turkey), on the Bakirlitepe mountain, on the altitude of 2500 m (Aslan et al., 2001). Now the observatory has Minor Planet Center code A84. At the time of observations the thermoelectrically cooled CCD camera ANDOR (model DW436, 2048 × 2048 with 13.5 × 13.5 m pixels) with an operating temperature of -60 C installed at the Cassegrain focus was used. Observations in $1 \times 1$ and $2 \times 2$ binned mode of CCD were executed. Most of observations were carried out in the BVR photometric system. The SDSS system filters have been used since December 2006. These equipments of the

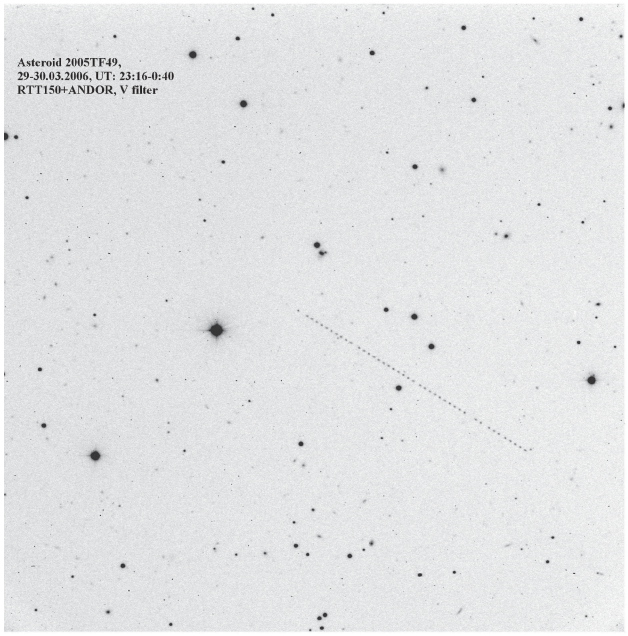


Figure 1: The track image of the asteroid 2005TF49, observed on RTT150.

RTT150 allow to conduct the photometric studies with an accuracy of about $0.01^m$ at 17 magnitude and about $0.05^m$ at 20 mag in the Cousins Rc-band and fit the lightcurves of objects with minimal uncertainty (as an example see results researches of asteroid 2002NY40 in Uluc et al., 2007). We execute also an absolute photometry of some observed minor planets. Figure 1 shows the combined image of positions of asteroid 2005TF49, which was observed on RTT150 with CCD Andor in March, 2006 (field of view $8.2' \times 8.2'$).

During 2004-2007 observations of minor planets were carried out within the international project on studying the physical parameters and kinematics of asteroids. This project includes the decision of the following tasks. 1) Definition of orbits of asteroids, which are brighter than $20^m$; 2) Specification of the position of the Solar system baricenter; 3) Search for binarity and estimation of masses of some main belt asteroids; 4) Determination of the rotation periods, form and density of the fast-rotating asteroids; 5) Observations of Near-Earth asteroids and definition of their main parameters. At present more than 20000 observations for about 100 various asteroids have been obtained, including chiefly main belt asteroids (for example, (60) Echo, (133) Syrene, (673) Edda etc.), also more than 10 near-Earth objects (1998OX4, 2004XL14, (4179) Toutatis) and the most interesting transneptunian objects (Pluto, 2003UB313 – Erida). Some observing information about several asteroids studied on RTT150 is shown in Table 1. The columns of this table include date of observation, name (number) of the asteroid, exposure times and number of images for filters indicated in the last column of the table. The authors have full table with observational data.

Table 1: The journal of observations of asteroids on RTT150 in 2004-2007 (fragments).

| Date of obs. | Number of aster. | Exp. times, s | Quantity of exp. | Filters |
|---|---|---|---|---|
| ... | ... | ... | ... | ... |
| 23.09.04 | 846 | 20 | 25 | R |
| 23.09.04 | 416 | 5 | 50 | R |
| 24.09.04 | 133 | 20 | 25 | R |
| 24.09.04 | 718 | 20 | 23 | R |
| ... | ... | ... | ... | ... |
| 03.07.05 | 381 | 20 | 9,8 | V,R |
| 03.07.05 | 34 | 10 | 3,3 | V,R |
| 19.08.05 | Erida | 30-60 | 3,3,3,3 | B,V,R,I |
| 20.08.05 | Erida | 60-120 | 3,3,3,3 | B,V,R,I |
| ... | ... | ... | ... | ... |
| 05.11.06 | 6006 | 30-40 | 45,45 | V,R |
| 10.11.06 | 253 | 30 | 1,3,3 | B,V,R |
| 13.12.06 | 965 | 20-30 | 55,50,50 | r,g,u |
| 15.12.06 | 6006 | 30 | 66,63 | g,r |
| ... | ... | ... | ... | ... |
| 23.07.07 | 5303 | 60-120 | 3,6,6 | B,V,R |
| 23.07.07 | 110 | 30-90 | 3,6,6 | B,V,R |
| 24.07.07 | 673 | 30 | 6,12,12 | B,V,R |
| 25.07.07 | 209 | 60-120 | 3,6,6 | B,V,R |
| ... | ... | ... | ... | ... |

## 3. Photometry of (762) Pulcova

During September 16, 20-23, 2003 in unfiltered light and in filters B, V, R observations of the main belt binary asteroid (762) Pulcova were carried out. Each night observations cover a full 5.8 h variation period. The differential photometry was made with the help of nearby stars, among which asteroid was moving during the observational night. The accuracy of photometrical measurements is in the range 0.01-0.02 magnitude, which agrees with observational accuracy of other authors. The data of each night were plotted as differential instrumental magnitude vs UT, and they show two maxima and two minima. The main minimum is more sharper than the secondary. Perhaps, peculiarities of lightcurves for various filters in the phase of growth after the main minimum and near secondary minimum can be explained by different albidos of the corresponding areas of Pulcova surface. The minima and maxima of lightcurves in different filters coincided. The time interval between maxima after a secondary minimum was used for estimating the rotational period of the asteroid. This have led to values of 5.88 hours in filter

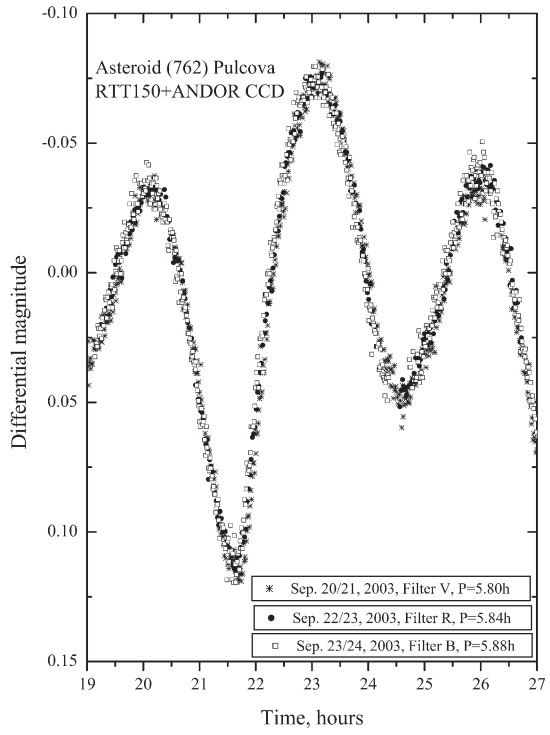


Figure 2: The lightcurves for (762) Pulcova in three filters.

B, 5.80 h in V and 5.84 h in red light (see penultimate column in Table 2), which give the mean period, which equals $5.839 \pm 0024$ hours. This result confirm the recent observations of Davis (2001). But amplitude of brightness variations for Pulcova from our lightcurves is less than in cited work. It was 0.20 magnitudes (Figure 2).

The deviation between values of main and secondary minima detected here equal $0.06^m$. Similar discrepancy was obtained by Devis in February the 9th, 2000. It is accounted for by the vicinity of phase angles of asteroid (then it was 5.83 degree). Distinct from this is that in our lightcurves the intensity of the main maximum is 0.04 magnitudes more than that of the secondary. Thus maximal amplitude of variability of (762) Pulcova in this observational set attains 0.2 magnitudes, and the difference in magnitude between second maximum and second minimum for this session was $0.1^m$. These data for three filters were presented in table 2.

Table 2: Photometrical data from lightcurves of (762) Pulcova.

| Filter | Maximal amplitude | Minimal amplitude | Phase angle | Period, hours |
|---|---|---|---|---|
| B | 0.199 | 0.100 | 6.2 | 5.876 |
| V(20.09) | 0.201 | 0.097 | 6.8 | 5.827 |
| V(21.09) | 0.196 | 0.089 | 6.6 | 5.812 |
| R | 0.192 | 0.093 | 6.4 | 5.841 |

## 4. Observations for international project

Last three years positional and photometric observations for large group of asteroids were carried out in the international collaboration between Astronomy department of Kazan State University, TÜBITAK National Observatory and Nikolaev Astronomical Observatory. Almost all the internal observational errors for the observed objects up to 17 magnitude are within 0.1", with a mean value less than 0.05" in both coordinates (Aslan et al., 2007). Accuracy of asteroid positions from the observations at RTT150 is good enough for use in mass determinations by the dynamical method, based on the analysis of the perturbations of small asteroids by big ones (Ivantsov, 2007). The papers of Aslan et al. (2006, 2007) present the preliminary calculations of mass determinations for 21 asteroids.

As we can see in Table 1 first observations were made only with one filter (R). Later, the availability of the filter wheel at the Cassegrain focus provided us with the opportunity for multi-color observations. For photometric researches we used long-time (more than 10 images) observations of asteroids. Besides some objects (for example, (121) Hermione, (253) Mathilde, (673) Edda, (1042) Amazone etc.) during these three years were observed scores of times. Also on RTT150 we can observe asteroids with possible short rotation periods ($P_{rot} < 3$ hours). This permits us to determine and specify the rotation periods of these objects.

In March 29-30, 2006 on RTT150 long-time observations in V-filter for asteroids (846) Lipperta, 2000PN9, 2005TF49 and (673) Edda were carried out. The asteroid 2000PN9 demonstrated brightness variations with amplitude of $0.11^m$ and period of 1.77 hours. These observations show similar results to the ones got earlier by Pravec (2003), who obtained $P_{rot} = 2.5325$ h and amplitude $0.15^m$. At the end of 2006 the basis of two-color observations in November, 2006 a minimum in the lightcurve of mail belt asteroid (6006) Anaximandros was discovered. The special observations of this asteroid during 2.5 hours in December, 2006 have confirmed this result. The lightcurves in SDSS filters g and r for this object with respect to a standard star are shown in Figure 3. Thus (6006) Anaximandros has the variability with a rotation period of 1.37 hr and amplitudes of 0.32 and 0.30 mag in g and r

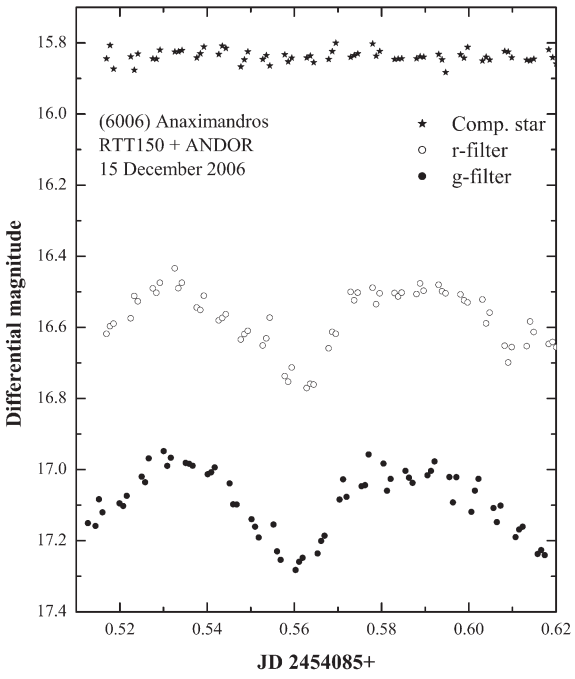


Figure 3: The lightcurves for (6006) Anaximandros in two filters.

bands, respectively. The lightcurves of this object in different filters demonstrate obvious asymmetry and distinctions, which are explained by the features of the nonspheric form and mineral structure of the asteroid surface.

## 5. Results

Last five years the international project for determination of physical characteristics of asteroids is realized on 1.5-m Russian-Turkish Telescope in TÜBITAK National Observatory. More than 100 different asteroids have been observed and the photometric characteristics of these objects have been derived. The lightcurves frequently demonstrating changes of brightness of these objects caused by their rotation around an axis are constructed with an accuracy of $0.01^m - 0.05^m$. The variability periods for two asteroids (2000PN9 - 1.77 hours and (6006) Anaximandros - 1.37 hours) have been found.

*Acknowledgements.* This work is done as a partial support of the Russian fund of fundamental researches (grant RFBR 05-02-17637) and Russian state science programm NSh-784.2006.2. Also this work was supported by TÜBITAK National Observatory, Turkey (project TUG-RTT150.04.013-07.31). A.G. is very grateful for Kazan University to financial support in travelling to Odessa.

## References

Aslan Z., Bikmaev I.F., Vitrichenko E.A. et al.: 2001, *Astron. Lett.*, **27**, 398.

Aslan Z., Gumerov R.I., Hudkova L.A. et al.: 2006, *26th meeting of the IAU, 22-23 August 2006, Prague, Czech Republic,* **16**, 67.

Aslan Z., Khamitov I., Gumerov R. et al.: 2007, *in: Study near-Earth objects and small bodies of Solar system, Ed. G. I. Pinigin, Mykolayiv,* 33.

Aslan Z., Gumerov R., Hudkova L. et al.: 2007, *in: Solar and Stellar Physics Through Eclipses, eds. Demircan O., Selam S.O., Albayrak B., ASP Conf. Ser.,* **370**, 52.

Britt D. T.,YeomansD., Housen K., Consolmagno G.: 2002, *Asteroids III, W. F. Bottke Jr., A. Cellino, P. Paolicchi, and R. P. Binzel (eds), University of Arizona Press, Tucson,* 485.

Devis R. G.: 2001, *Minor Planet Bull.*, **28**, 10.

Ivantsov A.: 2007, *Kinem. and Phys. of Celest. Bodies*, **23**, 95 (in Russian).

NASA: 2006, *http://cfa-www.harvard.edu/cfa/ps /mpc.html.*

Pravec P.: 2003, *http://www.asu.cas.cz/ ppravec/neo.htm.*

Uluc K., Khamitov I., Ozisik T. et al.: 2007 *in Solar and Stellar Physics Through Eclipses, Eds. O. Demircan, S.O. Selam, and B. Albayrak, ASP Conf. Ser.,* **370**, 358.

# ON THE STABLE SPHERICALLY-SYMMETRIC CHARGED DUST CONFIGURATIONS IN GENERAL RELATIVITY

V.D. Gladysh

Department of Physics, Dnepropetrovsk National University
Naurkova Str., 13 , Dnepropetrovsk 49050 Ukraine,
*vgladush@ff.dsu.dp.ua*

ABSTRACT. The radial motion of a self-graviting charged dust and stability condition of the static charged dust spheres are considered. The stability is possible for the bound states of the weakly charged layer with abnormal charge with respect to the active mass.

**Key words**: charged dust; classification of motions; stability conditions.

## 1. Introduction

The collapse of a spherically-symmetric charged dust cloud is the important problem of a General Relativity. In the papers of Vickers P.A. (1973), Markov M.A. and Frolov V.P., (1970,1972), Bailyn M. and Eimerl D. (1972), Ivanenko D.D., Krechet V.G. and Lapchinski V.G. (1973) the solution of the Einstein-Maxwell equations is reduced to the first integrals. The exact solutions for charged dust spheres are obtained in the works of Hamoui A. (1969), Bekenstein J.D. (1971), Bailyn M., Eimerl D. (1972), Shikin I.S. (1974), Khlestkov Yu.A.(1975), Pavlov N.V. (1976), Ori A. (1990). The main goal for researches is to find the conditions under which the gravitational collapse of the charged mediums is impossible. Let us note the problem of shell crossing, which arises here. In works of Ori A. (1991) and Goncalves S.M. (2001) it is shown that shell crossing is inevitable in the gravitational collapse of weakly charged dust spheres. The important problem is also to find stability conditions of charged dust spheres. The equilibrium of a charged dust sphere with extremal charge distribution was considered by Bonnor W.B (1965). The similar problem was considered by Bonnor W.B (1993), Gladush V.D. and Galadgyi M.V. (2007) for charged particles in the Reissner-Nordström field. In this paper we introduce the classification of charged spherically-symmetric configurations, and further we find the stability conditions for them.

## 2. The equations of motion for spherical layers of the charged dust

The space-time metric has the form

$$ds^2 = \gamma_{ab}dx^a dx^b - R^2 d\sigma^2\,, \qquad (1)$$

where $d\sigma^2 = d\theta^2 + \sin^2\theta d\alpha^2$, $\gamma_{ab} = \gamma_{ab}(x^a)$ and $R = R(x^a)$, $x^a$ - time-radial coordinates $(a, b = 0, 1)$.

For dynamics description of a charged dust sphere we shall consider small region without not shell crossing. The evolution of a spherical layers of Lagrangian radius $r$ $(dr/ds = 0)$, which bounds of the sphere of the total mass $M_{tot}(r)$ and charge $Q(r)$, can be described by the equation (see, for example, Ori A. (1991)).

$$\left(\rho c^2\frac{dR}{ds}\right)^2 = -U \equiv \varepsilon_{tot}^2 - \rho^2c^4 + \\ + (\kappa\rho^2c^2M_{tot} - \rho_e\varepsilon_{tot}Q)\frac{2}{R} - (\kappa\rho^2 - \rho_e^2)\frac{Q^2}{R^2}\,. \qquad (2)$$

Here $U = U(R, M_{tot}, Q)$ is an "effective velocity potential", $\rho$ and $\rho_e$ are the dust and charge densities, $\varepsilon_{tot}$ is the energy density. In this case the following relations take place:

$$\alpha(r) = \frac{\rho_e}{\rho c^2} = \frac{dQ(r)}{c^2 d\mathcal{M}(r)}\,, \quad \mathcal{H}(r) = \frac{\varepsilon_{tot}}{\rho c^2} = \frac{dM_{tot}(r)}{d\mathcal{M}(r)}\,,$$
$$\varepsilon_u = \frac{\varepsilon_{tot}}{\rho c^2} - \frac{\rho_e}{\rho c^2}\frac{Q(r)}{R} = \mathcal{H}(r) - \alpha(r)\frac{Q(r)}{R}\,,$$

where $\mathcal{M}(r)$ is a total rest-mass of a dust.

## 3. Classification of charged dust spherically-symmetric configurations

The character of evolution of spheres is determined by the motion of layers

The regions of the admissible motions of the layers are defined by the inequality $U(R) \le 0$, the equality $U = 0$ gives turning points $R_m$. The object of our classification is a sphere with its boundary layer. The potential $U$ here is not suitable, as it depends on parameter of classification – the total energy of the sphere $\mathcal{E}_{tot} = M_{tot}\,c^2$. From the equation (2) it follows that $M_{tot} \ge U_M$. We shall accept this condition as a basis of classification. Here

$$U_M = \frac{1}{2\kappa\rho^2c^2}\left((\rho^2c^4 - \varepsilon_{tot}^2)R + \right. \\ \left. + 2\rho_e\varepsilon_{tot}Q + \left(\kappa\rho^2 - \rho_e^2\right)\frac{Q^2}{R}\right) \qquad (3)$$

is the "effective mass potential". This potential depends both on global magnitudes – the charge $Q$ and radius $R$ of the sphere, and on local ones — the densities $\rho\,, \rho_e$ and $\varepsilon_{tot}$. Solutions of the equation $M_{tot} = U_M$ define the turning points $R_m$ of the layer. The asymptotics of the mass potential define the character of the layers motions. Under $R \to 0$ we have the following cases:

**1.1.** $U_M \to +\infty, \quad \kappa\rho^2 > \rho_e^2$ – the case for weakly charged layer;

**1.2.** $U_M \to \rho_e\varepsilon_{tot}Q/\kappa\rho^2, \kappa\rho^2 = \rho_e^2$ – the case for the layer with an extremal density of charge;

**1.3.** $U_M \to -\infty, \kappa\rho^2 < \rho_e^2$ – the case for the layer with an abnormal density of charge. These conditions define the type of behaviour of a layer depending on its local electrical characteristics. On the other hand, under $R \to \infty$ we have:

**2.1.** $U_M \to +\infty,$ if $\rho^2c^4 > \varepsilon_{tot}^2$ – the case for the bound states of a dust;

**2.2.** $U_M \to \rho_e\varepsilon_{tot}Q/\kappa\rho^2,$ if$\rho^2c^4 = \varepsilon_{tot}^2$ – the case for the critical density of a dust;

**2.3.** $U_M \to -\infty,$ if $\rho^2c^4 < \varepsilon_{tot}^2$ – the case for the unbound states of a dust. These conditions define the type of behaviour of a layer depending on its local energy characteristics. Thus there are nine basic types of behaviour of the mass potential $U_M$ which are determined by local characteristics of a sphere. Besides, the sphere of Lagrangian radius is characterized by integral magnitudes – $M_{tot}(r)$ and $Q(r)$. For the given total charge $Q(r)$ the value of a total mass $M_{tot}(r)$ determines three types of the sphere:

**3.1.** $M_{tot}\sqrt{\kappa} > |Q|$ – the weakly charged sphere;

**3.2.** $M_{tot}\sqrt{\kappa} = |Q|$ – the sphere with an extremal charge;

**3.3** $M_{tot}\sqrt{\kappa} < |Q|$ – the sphere with an abnormal charge.

As a result the charged layers have 27 variants of motion. In the dimensionless coordinates $\{V_M = U_M\sqrt{\kappa}/Q,\ x = c^2R/Q\sqrt{\kappa}\}$, these cases are illustrated at Fig. 1-9. The regions of the admissible motions are determined by segments of an axis $x$, for which the line $V_M = M_Q$ lays above the curve $V_M = V_M(x)$. The turning points $x_m$ $(R_m)$ can be found as abscissae of intersection points of the curve $V_M = V_M(x)$ and of the line $V_M = M_Q$. The segment of the dashed line $V_M = 1$ corresponds to the motion of a layer in the field of the sphere with the extremal charge. The segments of the dotted lines with $V_M > 1$ and $V_M < 1$ correspond to the motions of the layers in a field of the weakly and abnormally charged spheres, accordingly.

### 4. The stability conditions for spherically-symmetric configurations of the charged dust

The stable static state of the layer is possible for bound states of the weakly charged layer (fig. 3), when $\kappa\rho^2 > \rho_e^2\,,\ \rho^2c^4 > \varepsilon_{tot}^2$. If the layer is at the bottom of the potential well the conditions of the stationarity

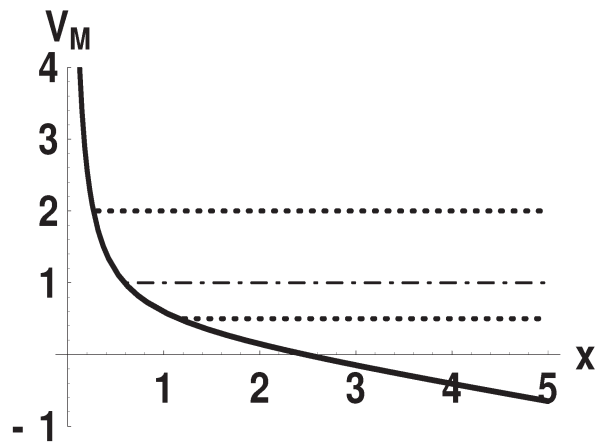


Figure 1: The unbound states of the weakly charged layer: $\kappa\rho^2 > \rho_e^2\,,\ \rho^2c^4 < \varepsilon_{tot}^2$.

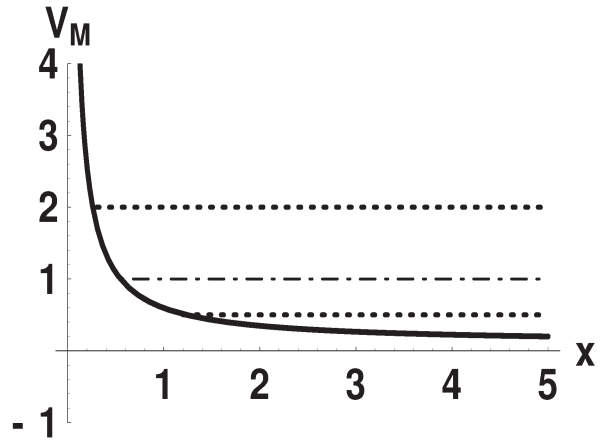


Figure 2: The weakly charged layer with the critical density of the dust: $\kappa\rho^2 > \rho_e^2\,,\ \rho^2c^4 = \varepsilon_{tot}^2$.

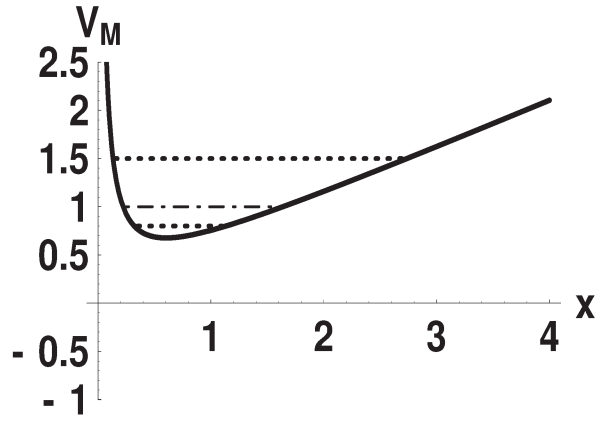


Figure 3: The bound states of the weakly charged layer: $\kappa\rho^2 > \rho_e^2\,,\ \rho^2c^4 > \varepsilon_{tot}^2$.

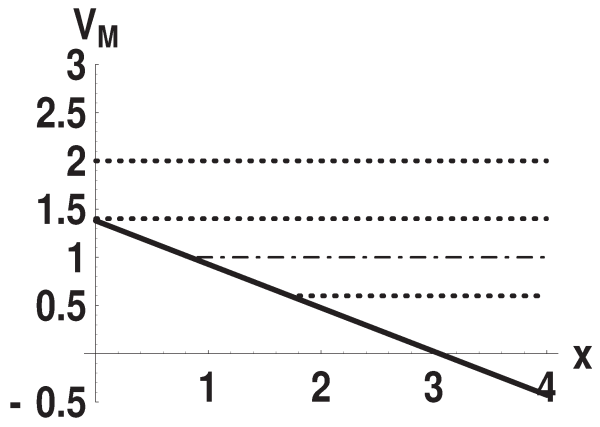


Figure 4: The unbound states of the layer with extremal density of the charge: $\kappa\rho^2 = \rho_e^2\,,\ \rho^2c^4 < \varepsilon_{tot}^2$.

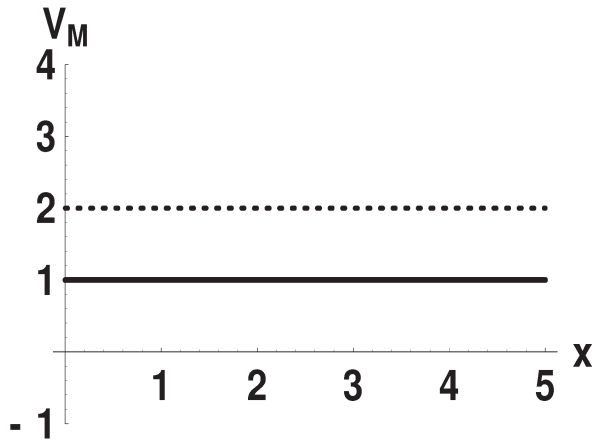


Figure 5: The layer with extremal density of the charge and critical density of the dust: $\kappa\rho^2 = \rho_e^2\,,\ \rho^2c^4 = \varepsilon_{tot}^2$.

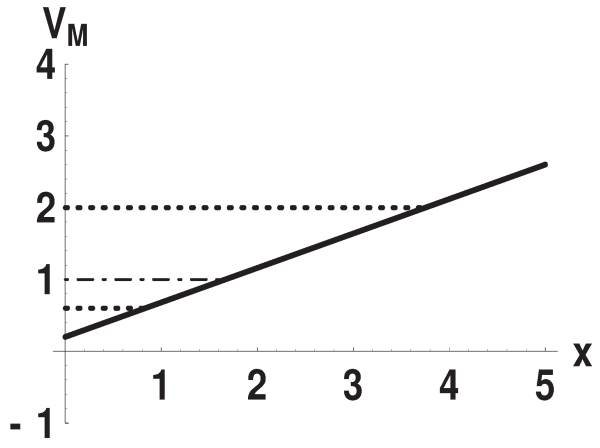


Figure 6: The bound states of the layer with extremal charge density: $\kappa\rho^2 = \rho_e^2\,,\ \rho^2c^4 > \varepsilon_{tot}^2$.

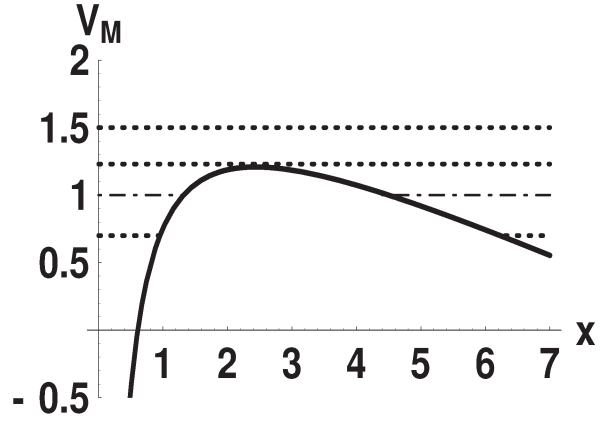


Figure 7: The unbound states of the layer with the abnormal density of charge: $\kappa\rho^2 < \rho_e^2\,,\ \rho^2c^4 < \varepsilon_{tot}^2$.

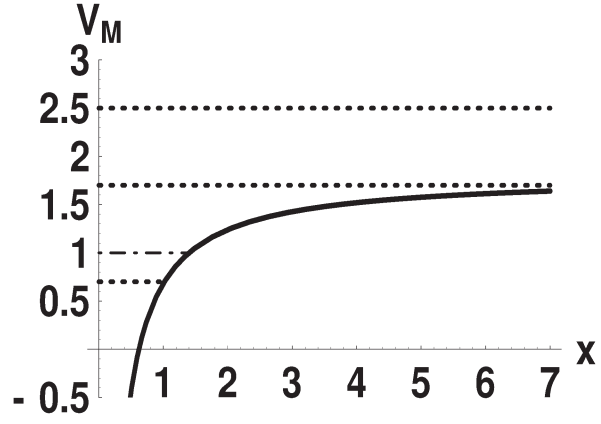


Figure 8: The layer with the abnormal density of the charge and critical density of the dust: $\kappa\rho^2 < \rho_e^2$, $\rho^2c^4 = \varepsilon_{tot}^2$.

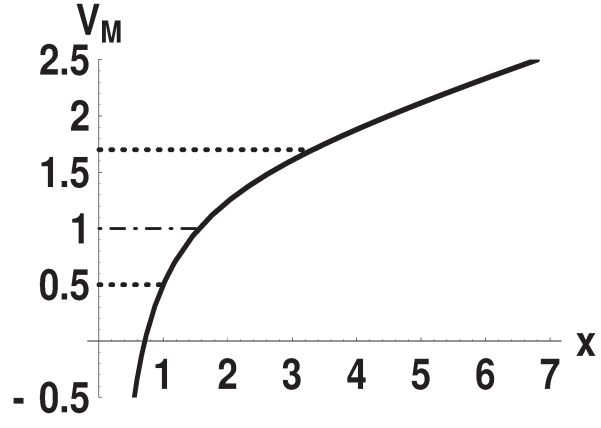


Figure 9: The bound states of the layer with the abnormal charge density: $\kappa\rho^2 < \rho_e^2\,,\ \rho^2c^4 > \varepsilon_{tot}^2$.

and equilibrium are satisfied:

$$\left(\frac{dR}{ds}\right)^2 = \left(\mathcal{H}(r) - \alpha(r)\frac{Q(r)}{R}\right)^2 - \\ - 1 + \frac{2\kappa M_{tot}(r)}{c^2 R} - \frac{\kappa Q^2(r)}{c^4 R^2} = 0, \tag{4}$$

$$\frac{d^2R}{ds^2} = \left(\mathcal{H}(r) - \frac{\alpha(r)Q(r)}{R}\right)\frac{\alpha(r)Q(r)}{R^2} - \\ - \frac{\kappa M_{tot}(r)}{c^2 R^2} + \frac{\kappa Q^2(r)}{c^4 R^3} = 0. \tag{5}$$

Hence we obtain the following equilibrium condition for the layers

$$\left(\frac{\kappa M_{tot}(r)}{Q(r)} - \alpha c^2 \mathcal{H}(r)\right)^2 = \\ = \left(1 - \mathcal{H}^2(r)\right)\left(\kappa - \alpha^2 c^4\right). \tag{6}$$

Thus for radius of an equilibrium layer we have

$$R = \frac{\kappa M_{tot}(d\mathcal{M})^2 - QdQdM_{tot}}{c^2((d\mathcal{M})^2 - (dM_{tot})^2)}, \tag{7}$$

that corresponds to the minimum of potential $M_{tot}$. Using integral magnitudes we obtain necessary and sufficient conditions of a stable equilibrium of the charged dust configuration:

$$|d\mathcal{M}| > |dM_{tot}|, \quad \sqrt{\kappa}|d\mathcal{M}| > |dQ|, \tag{8}$$

$$\kappa\Phi(dM_{tot}, dQ) \equiv \kappa Q^2(dM_{tot})^2 - \\ - 2\kappa Q M_{tot} dQ dM_{tot} + Q^2(dQ)^2 = \\ = \kappa\left(Q^2 - \kappa M_{tot}^2\right)(d\mathcal{M})^2. \tag{9}$$

Than it follows that

$$\kappa\left(QdM_{tot} - M_{tot}dQ\right)^2 = \\ = \left(Q^2 - \kappa M_{tot}^2\right)\left(\kappa(d\mathcal{M})^2 - (dQ)^2\right) > 0. \tag{10}$$

In virtue of (8) one can formulate the following theorem: the stable static states are possible only for the bound states of the weakly charged layer with the abnormal charge $Q$ with respect to the active mass $M_{tot}$:

$$|d\mathcal{M}| > |dM_{tot}|, \ \sqrt{\kappa}|d\mathcal{M}| > |dQ|, \ Q^2 > \kappa M_{tot}^2. \tag{11}$$

It follows from here, that for the stable static sphere of the charged dust the quadratic form $\Phi(dM_{tot}, dQ)$ in (10) is positively defined $\Phi(dM_{tot}, dQ) > 0$.

From (10) we obtain one more relation for stable static states of the charged dust sphere:

$$\frac{\sqrt{\kappa}\, dM_{tot}}{dQ} = \frac{\sqrt{\kappa}\, M_{tot}}{Q} \pm \\ \pm \sqrt{1 - \frac{\kappa M_{tot}^2}{Q^2}}\ \sqrt{\frac{\kappa(d\mathcal{M})^2}{(dQ)^2} - 1}. \tag{12}$$

This equation is invariant with respect to scale transformation

$$M_{tot}(r) = aM'_{tot}(r), \ Q(r) = aQ'(r), \ \mathcal{M}(r) = a\mathcal{M}'(r).$$

Here $R = aR'$. Thus we have a scaling law. If we multiply the distribution functions of the charge, total and proper mass by factor of $a$ the new configuration remains stable, and its radius will grow by the same factor $a$.

As an example, let us consider the particle-like configuration with parameters of an electron (mass $m_e = 9,109 \cdot 10^{-28}\,\mathbf{g}$, charge $e = 4,803 \cdot 10^{-10}\,\mathbf{cm}^{3/2}\,\mathbf{g}^{1/2}\,\mathbf{s}^{-1}$) and with the geometrodynamical charge $q_{m_e} = \sqrt{\kappa}m_e = 23,53 \cdot 10^{-32}\mathbf{cm}^{3/2}\mathbf{g}^{1/2}\mathbf{s}^{-1}$. Since $e/q_{me} = 2 \cdot 10^{21} \gg 1$, we deal here with the abnormally charge object. Let us consider now point object with parameters of an electron and the exterior gravitational field of the Reissner-Nordström. In virtue of inequality $e > \sqrt{\kappa}m_e$ a naked singularity takes place. It contradicts to the cosmic censorship hypothesis of Penrose (1969), according to which the singularity should be hidden by horizon. Thus it follows, that the electron can not be the point object. If we neglect an intrinsic moment, the simplest classical model of such object can be particle-like spherical configuration of the charged dust with the total mass $M_{tot} = m_e$ and charge $Q = e$, which satisfies the indicated stability conditions.

**References**


Vickers P.A.: 1973, *Ann. Inst. H. Poincare,* **18**, 137.

Markov M.A., Frolov V.P.: 1970, *Theor and Math. Phys.,* **3**, 3.

Markov M.A., Frolov V.P.: 1972, *Theor and Math. Phys.,* **13**, 41.

Bailyn M., Eimerl D.: 1972, *Phys. Rev. D,* **5**, 1897.

Ivanenko D.D., Krechet V.G., Lapchinskiy V.G.: 1973, *Izv. Vyssh. Uchebn. Zaved. SSSR Fiz,* **12**, 63.

Hamoui A.: 1969, *Ann. Inst. H. Poincare,* **10**, 195.

Bekenstein J.D.: 1971, *Phys. Rev. D,* **4**, 2185.

Bailyn M., Eimerl D.: 1972, *Phys. Rev. D,* **5**, 1897.

Shikin I.S.1: 1974, *JETP,* **67**, 433.

Khlestkov Yu.A.: 1975, *JETP,* **68**, 387

Pavlov N.V.: 1976, *Izv. Vyssh. Uchebn. Zaved. SSSR Fiz,* **4**, 107.

Ori A.: 1990, *Class. Quantum Grav.,* **7**, 985.

Ori A.: 1991, *Phys. Rev. D,* **44**, 2278.

Goncalves S.M.: (2001), *Phys. Rev. D,* **63**, 124017.

Bonnor W.B.: (1993), *Class. Quantum Grav.,* **10**, 2077.

Bonnor W.B.: (1965), *Mon. Not. Roy. Astron. Soc.***129**, 443.

Gladush V.D., Galadgyi M.V.: 2007, *Odessa Astron. Publ.,* **20**, (in press).

Penrose R.: 1969, *Riv. Nuouo Cimento,* **1**, 252.

# THE RADIAL MOTIONS OF CHARGED PARTICLES IN THE FIELD OF THE CHARGED OBJECT IN GENERAL RELATIVITY AND THEIR CLASSIFICATION

V.D. Gladush[1], M.V. Galadgyi[2]

Department of Physics, Dnipropetrovsk National University
Naurkova Str., 13, Dnipropetrovsk 49050 Ukraine,
[1]*vgladush@ff.dsu.dp.ua,* [2]*galadgyi@gmail.com*

ABSTRACT. The radial motions of the charged test particles in the field of a spherically symmetric charged object in general relativity are considered and their classification is built. The conditions of equilibrium for these particles are studied and equilibrium stability conditions are received. It is shown, that stable states are only possible for the bound states of the weakly charged particle in the field of the abnormally charged central source.

**Key words**: classification of motions, effective potential; stability conditions.

## 1. Introduction

The consideration of motion of the charged particles is an important part of the general research of the behavior for the charged configurations in general relativity. The motion of the charged test particles in Reissner-Nordström field was considered by Cohen (1979), the radial motions was studied by Finley (1974). One of the main reasons of the researches is the receiving of the conditions under which the falling on the center takes no place, and the finding of the stability conditions for the charged particles in the field of the charged object. Thus, the paper Bonnor (1993) was dedicated the study of the equilibrium stability conditions for the charged particles. Note that in his paper this problem was considered without taking into account the conservation law and has been solved incompletely.

In this paper we carry out the classification of the radial motions for the charged particles in the spherically symmetric gravitational and electrical fields of the central source by using the energy conservation law. The research of this problem leads to the equilibrium conditions of stable states of the charged particles in the Reissner-Nordström field.

## 2. The equation of motion for the charged particle

The gravitational field of a spherically symmetric source with mass $M$ and charge $Q$ is described by Reissner-Notdström metric

$$ds^2 = Fc^2dT^2 - F^{-1}dR^2 - R^2(d\theta^2 + \sin^2\theta d\varphi^2)\,, \quad (1)$$

where

$$F = 1 - \frac{2\gamma M}{c^2 R} + \frac{\gamma Q^2}{c^4 R^2}\,, \quad (2)$$

$\gamma$ and $c$ — are the gravitation constant and velocity of light respectively. In dependence on the relation between mass and charge it is possible to separate following types of the charged relativistic objects: the charged black hole ($\sqrt{\gamma}M > |Q|$), the extremely charged black hole ($\sqrt{\gamma}M = |Q|$), the abnormally charged object ($\sqrt{\gamma}M < |Q|$).

Lagrangian of a test particle with mass $m$ and charge $q$ is given by:

$$L(R, \dot{R}) = -mc\sqrt{Fc^2 - F^{-1}\dot{R}^2} - qQ/R\,, \quad (3)$$

where a dot denotes differentiation with respect to $T$. It is easy to see, that the total energy of the charged particle is conserved and equals to

$$E = \frac{qQ}{R} + \frac{mc^2 F}{\sqrt{F - F^{-1}\dot{R}^2/c^2}}\,. \quad (4)$$

From here we have the equation of radial motion:

$$\left(mc^2\frac{dR}{ds}\right)^2 = \left(E - \frac{qQ}{R}\right)^2 - m^2c^4\left(1 - \frac{2\gamma M}{c^2 R} + \frac{\gamma Q^2}{c^4 R^2}\right)\,. \quad (5)$$

The similar equation for Reissner-Nordström-de Sitter metric has been received by Gonçalves (2001) by using Killing vector. Further, for the particle acceleration we find:

$$\frac{d^2R}{ds^2} = \frac{1}{m^2c^4}\left[\left(EqQ - m^2c^2\gamma M\right)\frac{1}{R^2} + \left(\gamma m^2 - q^2\right)\frac{Q^2}{R^3}\right]\,. \quad (6)$$

### 3. Classification of the radial motions

The standard method of the qualitative analysis of the particle trajectories is based on the study of effective "velocity potential" behaviour $\left(mc^2 dR/ds\right)^2 \equiv -U$ (see, for example, Wilkins (1972), Cohen and Gautreau (1979), Dymnikova (1986), Gonçalves (2001)). Let us rewrite the potential (5) in the form

$$U(Q,M,R) = m^2c^4 - E^2 - \left(\gamma M m^2 c^2 - EqQ\right)\frac{2}{R} + \\ + \left(\gamma m^2 - q^2\right)\frac{Q^2}{R^2}\,.$$

The admissible motions are defined by an inequality $U(Q,M,R) \le 0$ where equality specifies the turning points. The presence of parameter of classification $M$ in the potential $U$ is not suitable for particles dynamics analysis. Therefore, let us introduce the "mass potential" $U_m$ which is the solution of the equation $U = 0$ with respect to $M$

$$U_m(Q,R) = \frac{1}{2\gamma m^2 c^2}\left[(m^2c^4 - E^2)R + 2EqQ + \right. \\ \left. + \left(\gamma m^2 - q^2\right)\frac{Q^2}{R}\right]\,. \qquad (7)$$

In this case the regions of admissible motions are specified by an inequality $U_m(Q,R) \le M$. Besides the potential $U_m$ let us introduce one more function $U_g$ which can be find from the equation $F = 0$ defining horizons

$$M = \frac{1}{2}\left(\frac{Rc^2}{\gamma} + \frac{Q^2}{Rc^2}\right) \equiv U_g(Q,R)\,. \qquad (8)$$

The function $U_g$ determines a value of the mass of black hole having charge $Q$ and radius of horizon $R$.

The behavior of function $U_m(Q,R)$ depends on the relation between particle parameters defining its asymptotics. As a result we obtain the following cases:

**1.** when $R \to 0$ we have
- **1.a** if $\gamma m^2 > q^2$, then $U_m(Q,R) \to +\infty$, for the weakly charged particle;
- **1.b** if $\gamma m^2 = q^2$ then $U_m(Q,R) \to EqQ/\gamma m^2 c^2$, for the extremely charged particle;
- **1.c** if $\gamma m^2 < q^2$ then $U_m(Q,R) \to -\infty$, for the abnormally charged particle.

**2.** when $R \to \infty$ we have
- **2.a** if $E^2 < m^2c^4$ then $U_m(Q,R) \to +\infty$, for the bound states of the particle;
- **2.b** if $E^2 = m^2c^4$ then $U_m(Q,R) \to EqQ/\gamma m^2 c^2$, for the particle with a critical mass;
- **2.c** if $E^2 > m^2c^4$ then $U_m(Q,R) \to -\infty$, for the unbound states of the particle.

For certainty we suppose $Q > 0$ and $M > 0$. Thus, the introduced conditions define 9 types of behavior for potential $U_m$. Taking into account the sign of a charge $q$ and type of the central object we obtain 54 types of behavior.

To plot and analysis functions $U_m$ and $U_g$ suitable to use the dimensionless variables

$$\widetilde{\mathcal{U}}_m(\varepsilon,\beta,x) = \frac{1}{2}\left[(1-\varepsilon^2)x + 2\varepsilon\beta + \left(1-\beta^2\right)\frac{1}{x}\right]\,, \\ \widetilde{\mathcal{U}}_m(\varepsilon,\beta,x) \le \mathcal{M}\,, \qquad (9)$$

$$\widetilde{\mathcal{U}}_g(x) = \frac{1}{2}\left(x + \frac{1}{x}\right)\,, \qquad (10)$$

where $\widetilde{\mathcal{U}}_m = \sqrt{\gamma}U_m/Q$, $\widetilde{\mathcal{U}}_g = \sqrt{\gamma}U_g/Q$, $x = Rc^2/\sqrt{\gamma}Q$, $\varepsilon = E/mc^2$, $\beta = q/\sqrt{\gamma}m$, $\mathcal{M} = \sqrt{\gamma}M/Q$.

Comparing $\widetilde{\mathcal{U}}_m$ and $\widetilde{\mathcal{U}}_g$, we come to the relation

$$\widetilde{\mathcal{U}}_g(x) = \widetilde{\mathcal{U}}_m(\varepsilon,\beta,x) + \left(\varepsilon\sqrt{x} - \frac{\beta}{\sqrt{x}}\right)^2 \qquad (11)$$

from which it follows that $\widetilde{\mathcal{U}}_g(x) \ge \widetilde{\mathcal{U}}_m(\varepsilon,\beta,x)$. From this it follows that the curve $\widetilde{\mathcal{U}}_g(x)$ lies always below then the "mass potential" curve. The reason is that the turning radiuses do not exist in T-region where the radial coordinate becomes time-like. The equality $\widetilde{\mathcal{U}}_g(x) = \widetilde{\mathcal{U}}_m(\varepsilon,\beta,x)$ defines a point of a contact for these curves $x_{tang} = \beta/\varepsilon$ whence it follows that $R_{tang} = qQ/E$. Let us note, that a particle with the energy $E = qQ/R_+$, where $R_+ = \left(\gamma M + \sqrt{\gamma(\gamma M^2 - Q^2)}\right)$ — is the exterior horizon, has a turning point on the events horizon exactly (Chandrasekhar, 1986).

The plots for potentials $\widetilde{\mathcal{U}}_m(\varepsilon,\beta,x)$ and $\widetilde{\mathcal{U}}_g(x)$ for all cases of classification are represented at fig. 1-9.

As an example let us consider fig.1 which corresponds to the bound states of the weakly charged particles. The curves $a$ and $b$ correspond to the mass potentials $\widetilde{\mathcal{U}}{+}_m$ and $\widetilde{\mathcal{U}}{-}_m$ for the cases $q > 0$ and $q < 0$ respectively. The curve $\widetilde{\mathcal{U}}_g(x)$ describes a line of horizon. The segments of horizontal lines define the trajectories of the motions of particles. The intersections of curves $\widetilde{\mathcal{U}}{+}_m$ and $\widetilde{\mathcal{U}}{-}_m$ with a line $\widetilde{\mathcal{U}}_m(\varepsilon,\beta,x) = \mathcal{M}$ give the turning points. The line 1 describes the motion of a particle in the field of the weakly charged black hole, the line 2 — is for the case in the field of the extremely charged black hole, and the lines 3 and 4 — are for the motion of the particles with charges $q > 0$ (a curve $a$) and $q < 0$ (a curve $b$) in the field of the abnormally charged object. The character of motion of the particles for other cases can be consider in a similar way.

### 3. The stability conditions

The stationary positions $R_{extr}$ of a particle are defined by conditions $dR/ds = 0$ and $d^2R/ds^2 = 0$. Moreover if $d^2R/ds^2 > 0$ when $R < R_{extr}$, and $d^2R/ds^2 < 0$ when $R > R_{extr}$ then the position $R_{extr}$ will be steady. From definitions for the "velocity" and "mass" potentials it follows

$$U_m(Q,R) = \frac{R}{2\gamma m^2 c^2}\,U(Q,M,R) + M\,. \qquad (12)$$

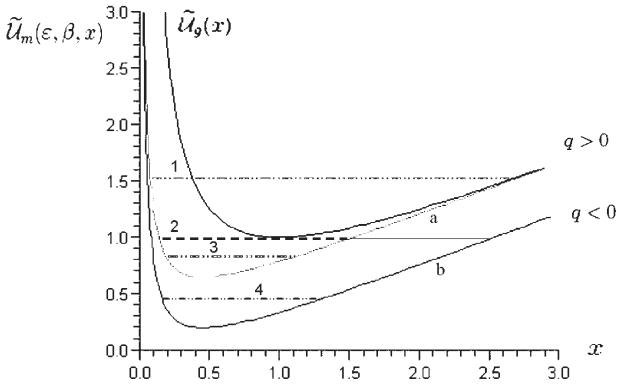


Figure 1: The bound states ($E^2 < m^2c^4$) of the weakly charged particle ($\gamma m^2 > q^2$).

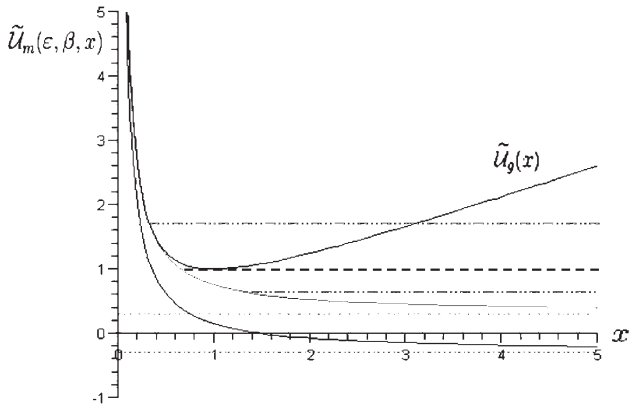


Figure 2: The weakly charged particle ($\gamma m^2 > q^2$) with a critical mass ($E^2 = m^2c^4$).

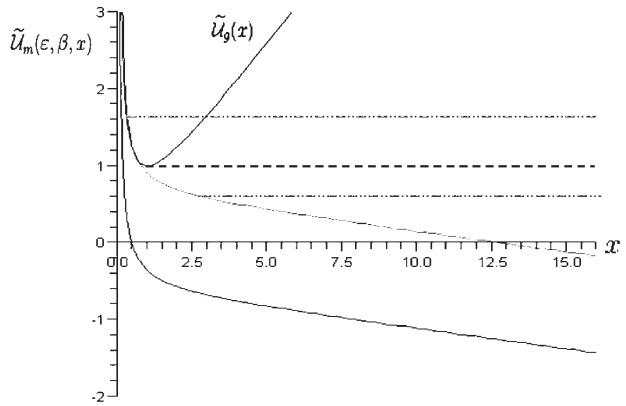


Figure 3: The unbound states ($E^2 > m^2c^4$) of the weakly charged particle ($\gamma m^2 > q^2$).

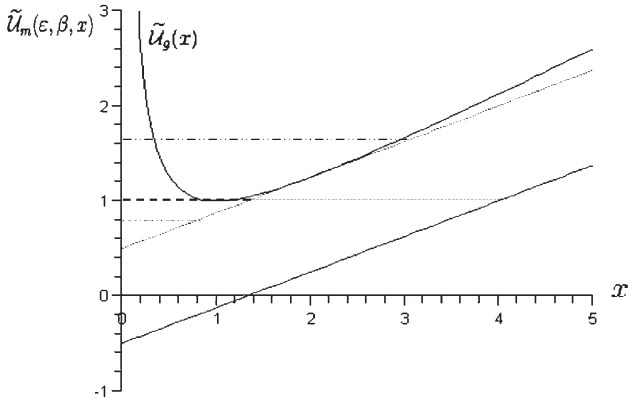


Figure 4: The bound states ($E^2 < m^2c^4$) of the extremely charged particle ($\gamma m^2 = q^2$).

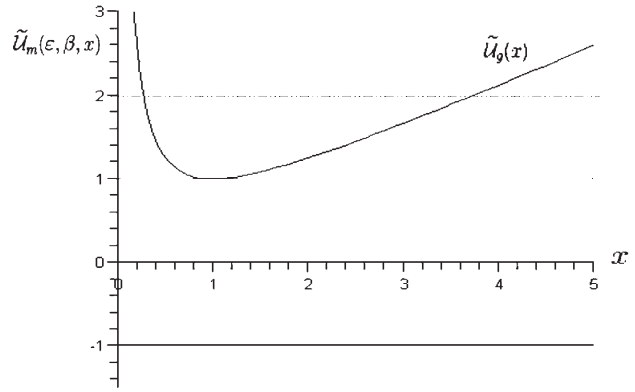


Figure 5: The extremely charged particle ($\gamma m^2 = q^2$) with a critical mass ($E^2 = m^2c^4$).

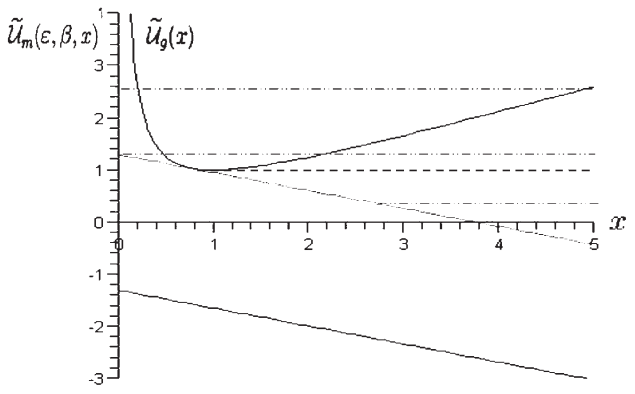


Figure 6: The unbound states ($E^2 > m^2c^4$) of the extremely charged particle ($\gamma m^2 = q^2$).

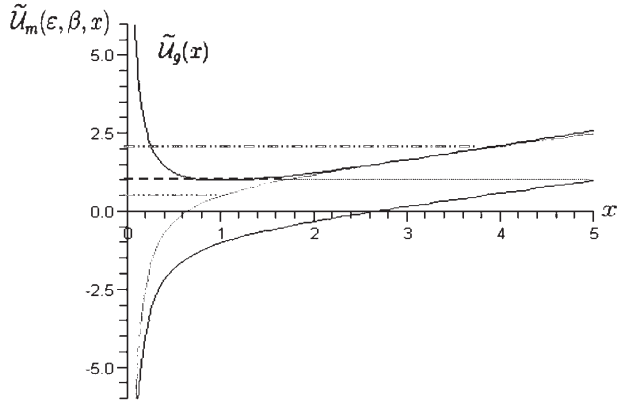


Figure 7: The bound states ($E^2 < m^2c^4$) of the the abnormally charged particle ($\gamma m^2 < q^2$).

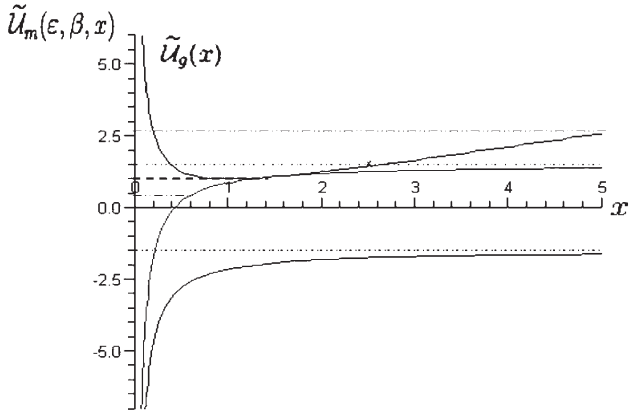


Figure 8: The abnormally charged particle ($\gamma m^2 < q^2$) with a critical mass ($E^2 = m^2c^4$).

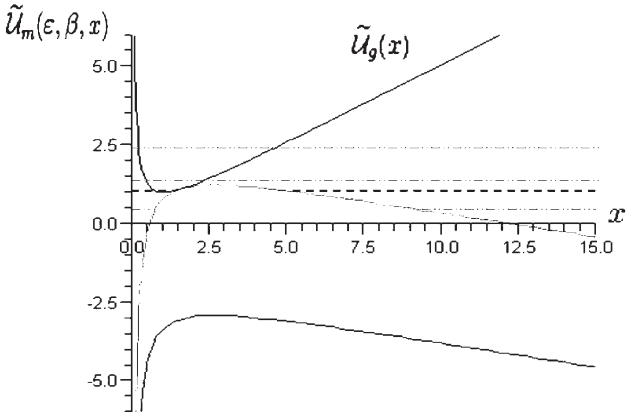


Figure 9: The unbound states ($E^2 > m^2c^4$) of the abnormaly charged particle ($\gamma m^2 < q^2$).

In a stable point $R_{extr}$, where $U(R_{extr}) = 0$ or $U_m(R_{extr}) = M$, the conditions $(\partial U/\partial R)|_{R_{extr}} = 0$ and $(\partial U_m/\partial R)|_{R_{extr}} = 0$ coincide and give

$$R_{extr} = Q\sqrt{\frac{\gamma m^2 - q^2}{m^2c^4 - E^2}}\,. \tag{13}$$

Excluding variable $R$ from $dR/ds = 0$ and $d^2R/ds^2 = 0$ we receive the relation

$$(m^2c^4 - E^2)(\gamma m^2 - q^2)Q^2 = (m^2c^2\gamma M - EqQ)^2 \tag{14}$$

from which we find two systems of inequalities

$$\begin{aligned} &|q| < m\sqrt{\gamma}, \quad |E| < mc^2\,, \\ &|q| > m\sqrt{\gamma}, \quad |E| > mc^2\,. \end{aligned} \tag{15}$$

Rewriting (16) in the form

$$(Q^2 - \gamma M^2)(\gamma m^2 - q^2) = \gamma\left(\frac{EQ}{c^2} - qM\right)^2 \tag{16}$$

in a similar way we obtain

$$\begin{aligned} &|q| < m\sqrt{\gamma}, \quad |Q| > M\sqrt{\gamma}\,, \\ &|q| > m\sqrt{\gamma}, \quad |Q| < M\sqrt{\gamma}\,. \end{aligned} \tag{17}$$

From classification of motions and relations (15) and (17) we find the following conditions: $|E| < mc^2$, $|q| < m\sqrt{\gamma}, |Q| > M\sqrt{\gamma}$ is for stable equilibrium of the bound states of weakly charged particle in the field of the abnormally charged object; $|E| > mc^2$, $|q| > m\sqrt{\gamma}$, $|Q| < M\sqrt{\gamma}$ is for instable equilibrium of the unbound states of the abnormally charged particle in the field of the charged black hole. The stability conditions (17) were received by Bonnor (1993) without use of the conservation laws. However he did not indicate, which of the conditions of equilibrium is stably and did not receive stable point of a particle. Note that in the work of Markov and Frolov (1972) it is stated that in case of the abnormally charged object $|Q| > M\sqrt{\gamma}$ the stable system is impossible.

Thus, the stable stationary positions are only possible for the bound states of weakly charged particle in the field of the abnormally charged central object.

**References**

Wilkins D.: 1972, *Phys. Rev. D,* **5**, 814.
Dymnikova I.G.: 1986, *Usp. Phys. Nauk,* **148**, 393.
Bonnor W.B.: 1993, *Class. Quantum Grav.,* **10**, 2077.
Chandrasekhar S.: 1983, *The mathematical theory of black holes,* Oxford.
Cohen J.M., Gautreau R.: 1979, *Phys. Rev. D,* **19**, 2273.
Gonçalves S.M.: 2001, *Phys. Rev. D,* **63**, 124017.
Markov M.A., Frolov V.P.: 1972, *J. Theor. and Math. Phys.,* **13**, 41.
Finley J.D.: 1974, *J. of Mat. Phys.,* **15**, 1698.

# HIGH-RESOLUTION SPECTROSCOPY OF LONG-PERIODIC ECLIPSING BINARY $\varepsilon$ AURIGAE

Golovin Alex[1,2], Kuznyetsova Yuliana[2,3], Andreev Maxim[2,3]

[1] Kyiv National Taras Shevchneko Univeristy, Kyiv, Ukraine
*golovin.alex@gmail.com, astron@mao.kiev.ua*
[2] Main Astronomical Observatory of National Academy of Science of Ukraine, Kyiv, Ukraine
[3] Terskol Branch of Institute of Astronomy RAS, Russia

ABSTRACT. The results of spectroscopic observations of long-periodic eclipsing binary $\varepsilon$ Aur are reported. The observations were carried out during 2 nights in 2007 at 2-meter telescope located at the peak Terskol, Northern Caucasus (Russia). Here we present series of $\varepsilon$ Aur spectra together with EW measurements of the most prominent absorption lines.

**Key words**: Stars: binary: eclipsing; stars: individual: $\varepsilon$ Aur.

## 1. Introduction

$\varepsilon$ Aur is well-observed long-periodic eclipsing binary, but still one of the most puzzling star. It is the eclipsing binary with longest known orbital period – 27.1 year. The main enigma is considered in the eclipsing object (it is supposed that the eclipsing body is of gigantic proportions, on the order of 2,000 solar radii). Its nature discussed for a long time, but still no reasonable explanation was given.

The eclipsing nature of $\varepsilon$ Aur was first mentioned by Fritsch (1824), where he discussed first ever-observed minimum in 1821. Since that $\varepsilon$ Aur' eclipses were observed each 27.1 years (Ludendorff, 1904) (in 1848, 1875, 1902, 1929, 1956, 1983), the next is expected in 2010 (first contact – Aug, 06, 2009; mid-eclipse – Jul, 09, 2010).

Recently (Carroll et al., 1991) $\varepsilon$ Aur ***secondary*** was interpreted as a protoplanetary system. So, spectroscopic monitoring before and during the eclipse is of great interest.

## 2. Observations

Spectroscopic observations were done at the Terskol Observatory (Russia, Northern Caucasus) during two nights, particularly at March, 30-31 and March, 31-April, 1 in 2007. 2-meter Zeiss telescope and coude-echelle spectrometer was used. The wavelength range covers from 3660 to 9500 Åin 80 orders. The reciprocal dispersion ranges from 0.038 to 0.09 Å/pixel. The spectral resolution was R=45000.

## 3. Discussion

Our research was focused on searching for the short-time variations of $H\alpha$ line profile. $H\alpha$ line was detected in absorption together with prominent blue and red emission wings symmetrical one to another, which is quite exciting (see Fig. 1 for the plot of $H\alpha$ region of $\varepsilon$ Aur spectrum).

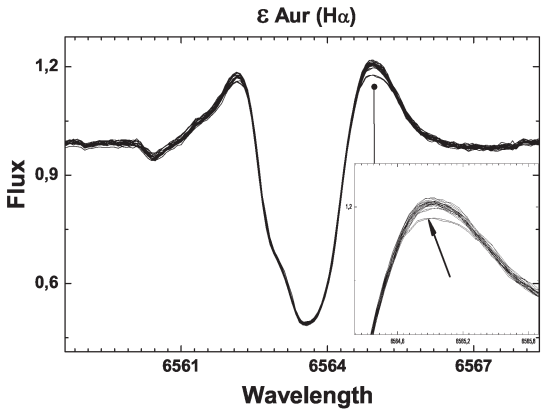


Figure 1: $H\alpha$ region of $\varepsilon$ Aur spectrum during March, 30-31, 2007 observations

The value variations of equivalent widths (EW) of the blue wing, the red wing and the absorption core of the $H\alpha$ line profiles were calculated ($F/Fc > 1$ – emission, $F/Fc < 1$ – absorption) and given in Table 1.

EW was calculated by direct numerical integration over the area under the line profile.

As could be seen from Fig. 1, the blue wing of $H\alpha$ line underwent a changes during the course of observa-

Table 1: List of spectra and equivalent widths of components of $\varepsilon$ Aur $H\alpha$ line.

| No. | Exp. time, min | S/N | EW of blue wing, Å | EW of central absorption, Å | EW of red wing, Å |
|---|---|---|---|---|---|
| | 30.03.-31.03.2007 | | | | |
| 1 | 6 | 170 | -0.145 | 0.647 | -0.204 |
| 2 | 6 | 200 | -0.154 | 0.645 | -0.209 |
| 3 | 6 | 220 | -0.155 | 0.642 | -0.212 |
| 4 | 6 | 250 | -0.155 | 0.644 | -0.211 |
| 5 | 6 | 250 | -0.151 | 0.645 | -0.207 |
| 6 | 6 | 220 | -0.155 | 0.643 | -0.210 |
| 7 | 6 | 250 | -0.158 | 0.640 | -0.213 |
| 8 | 6 | 220 | -0.156 | 0.641 | -0.208 |
| 9 | 6 | 200 | -0.157 | 0.64 | -0.214 |
| 10 | 6 | 230 | -0.155 | 0.642 | -0.213 |
| 11 | 6 | 220 | -0.155 | 0.644 | -0.211 |
| 12 | 6 | 200 | -0.154 | 0.642 | -0.212 |
| 13 | 6 | 200 | -0.156 | 0.642 | -0.211 |
| 14 | 6 | 220 | -0.154 | 0.642 | -0.214 |
| 15 | 6 | 200 | -0.151 | 0.644 | -0.209 |
| 16 | 6 | 200 | -0.153 | 0.645 | -0.211 |
| 17 | 6 | 220 | -0.148 | 0.646 | -0.210 |
| 18 | 6 | 200 | -0.154 | 0.644 | -0.214 |
| 19 | 6 | 200 | -0.152 | 0.645 | -0.211 |
| 20 | 6 | 200 | -0.145 | 0.645 | -0.193 |
| 21 | 6 | 200 | -0.147 | 0.645 | -0.194 |
| | 31.03.-01.04.2007 | | | | |
| 1 | 5 | 200 | -0.157 | 0.648 | -0.212 |
| 2 | 5 | 200 | -0.156 | 0.645 | -0.208 |
| 3 | 5 | 200 | -0.155 | 0.649 | -0.206 |
| 4 | 5 | 200 | -0.157 | 0.647 | -0.207 |
| 5 | 5 | 200 | -0.154 | 0.645 | -0.207 |
| 6 | 5 | 220 | -0.155 | 0.648 | -0.206 |
| 7 | 5 | 220 | -0.155 | 0.647 | -0.208 |
| 8 | 5 | 200 | -0.156 | 0.646 | -0.205 |
| 9 | 5 | 200 | -0.155 | 0.645 | -0.210 |
| 10 | 6 | 180 | -0.156 | 0.646 | -0.208 |
| 11 | 6 | 170 | -0.155 | 0.648 | -0.206 |
| 12 | 6 | 180 | -0.153 | 0.649 | -0.200 |
| 13 | 6 | 200 | -0.160 | 0.643 | -0.214 |
| 14 | 5 | 200 | -0.155 | 0.650 | -0.201 |
| 15 | 6 | 200 | -0.152 | 0.653 | -0.205 |
| 16 | 6 | 220 | -0.157 | 0.650 | -0.212 |
| 17 | 7 | 220 | -0.152 | 0.654 | -0.206 |
| 18 | 7 | 200 | -0.149 | 0.655 | -0.204 |

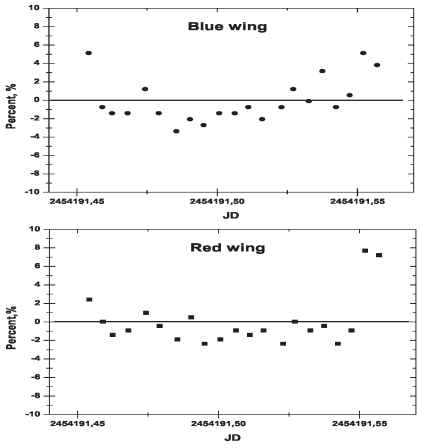


Figure 2: EW variability of $H\alpha$ during March, 30-31, 2007 observations

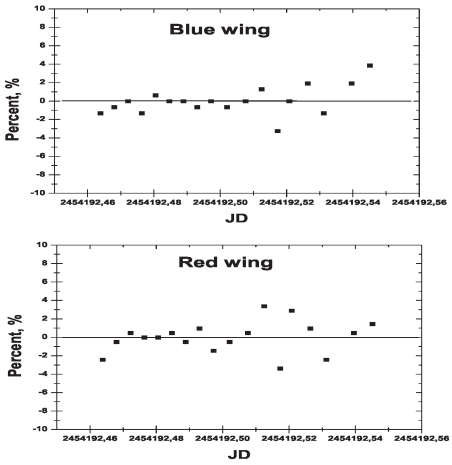


Figure 3: EW variability of $H\alpha$ during March, 31 – April, 1 in 2007 observations

tions at March, 30-31, 2007. This changes reach up to 8%, that could be considered to be significant. During the next night no changes were detected, reaching 5% limit (see fig. 2 and 3 for plot of EW changes in % during both nights).

Schanne, L. (2007) interpreted emission components of $H\alpha$ as evidence of gas behind the star (for red-shifted component) and radial outward flows, attributed to instabilities in the star (blue-shifted component).

Cha et al. (1994), Cha et al. (1995) attributed blue wing emission source to region region which contains an HII cloud with a short time scale variation.

Also EW of the following absorption lines all of which exhibit long-term variability (Thompson et al. 1987) were mesured: Fe I (3922.9 Å), Ti II (4028.0 Å), Ti II (4443.85 Å), Ti II (4468.48 Å), $H\beta$ (4861.5 Å), Na DI (5889.953 Å), Na DII (5895.923 Å), O I (7772 Å). No short-time variability, reaching 5% limit, were detected.

Fig. 4 illustrates several portions of $\varepsilon$ Aur average spectra, with the most prominent lines being identified and denoted.

Further photometrical and spectroscopical monitoring of this object is critically important for understanding $\varepsilon$ Aur – the most puzzling eclipsing binary.

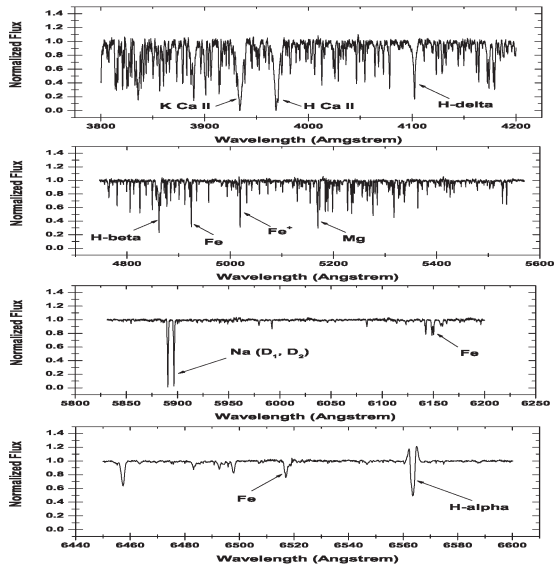


Figure 4: Portions of $\varepsilon$ Aur average spectra, with the most prominent absorption lines being marked

**References**

Cha G. et al.: 1994, *A&A*, **284**, 874-882.
Cha G. et al.: 1995, *IBVS*, No. 4149.
Fritsch J.M.: 1824, *Berl. Jahrb.*, p. 252.
Schanne L.: 2007, *IBVS*, No. 5747.
Thompson D.T. et al.: 1987, *ApJ*, **321**, 450-458.

# THORIUM LINES IN THE SPECTRA OF SEVERAL SMC SUPERGIANT STARS

V.F. Gopka[1], S.V. Vasil'eva[1], A.V. Yushchenko[2], S.M. Andrievsky[1]

[1]Astronomical observatory, Odessa National University
T.G. Shevchenko Park, Odessa, 65014, Ukraine,
*gopkavera@mail.ru, cerera_sveta@rambler.ru*

[2]Astrophysical Research Center for the Structure and Evolution of the Cosmos, Sejong University, Seoul, 143-747, Korea
*yua@sejong.ac.kr*

ABSTRACT. We present the results of identifications of the Th II lines in the spectra of four stars in the Small Magellanic Cloud: PMMR 23, PMMR 39, PMMR144, and PMMR 145. We report about detection of the lines of Th II in the visible part of spectra of K-supergiants. Thorium lines in the spectra of these stars are stronger than the thorium lines in the spectra of HD221170 and Arcturus. The thorium abundances in the atmospheres of four SMC stars are scattered from +0.05 to -0.69 in the scale where logN(H)=12.

**Key words**: stars: abundances; stars: individual (PMMR23, PMMR39, PMMR144, PMMR145); nucleosynthesis; galaxies: stellar content; galaxies: individual (Small Magellanic Cloud).

## 1. Introduction

Investigation of the thorium abundance in the atmospheres of different stars in our Galaxy has a long history. Only strongest line of Th II $\lambda$ 4019.129 Å was used before. But new values of oscillator strength of the thorium lines (Nilsson et al, 2002.) permit us to increase significantly the list of measurable thorium lines in stellar spectra. For example, thorium halo star HD 221170 has the thorium lines in the visible part of its spectrum (Yushchenko et al. 2005).

Determination of the elemental abundances in SMC stars is very usefull for construction of the theory of evolution of this galaxy. It is very important to investigate the heavy elements. Surveys of the heavy element abundances were made by Russell and Bessel (1989) and Spite et al. (1991). It was shown that the heavy neutron-capture elements in the Magellanic Clouds were formed similarly to the formation of these elements in the Galactic halo, but not in the Sun (Russell, 1991).

The apparent overabundances of the neutron-capture elements heavier than Ba in the atmospheres of supergiants, that was found earlier in several investigations, permits us to suppose that the search for thorium lines in these stars can be fruitful.

We used high-resolution CCD-spectra of SMC red K-supergiants, obtained by V. Hill from 1989 to 1993 at ESO (La Silla, Chile), using the New Technology Telescope equipped with the ESO Multi-Mode Image EMMI and the 3.6 meter telescope with the CASPEC spectrograph. (Hill, 1997).

## 2. Investigation of thorium lines

The underabundance of elements heavier than barium was found in F-supergiants of both Magellanic Clouds by Russel and Bessell (1989). Russell (1991) outlined that one of the important areas of futher researches can be the acquiring the data about spectral lines of heavy neutron-capture elements in these stars.

The distribution of the abundances of these elements indicates that they were produced by the r-process (Russell, 1991). Hill (1997) and Hill et al., (1997) analysed the chemical compositions of K-supergiants in Magellanic Clouds and found that in all investigated stars, except PMMR144, s- and r-process elements heavier than Ba are enhanced by +0.4 dex. The abundances of 35 and 20 chemical elements in the atmospheres of PMMR23 and PMMR39 were obtained by Gopka et al. (2005).

For elements with atomic numbers less than 56 we found the underabundances with respect to the Sun near -0.7 dex. The abundances of elements heavier than barium are similar to the solar abundances of these elements.

The main goal of this investigation is the identification of all lines of ionized thorium in visible part of the spectra of K-supergiant stars in the Small Magellanic Cloud: PMMR23, PMMR39, PMMR144, and PMMR145.

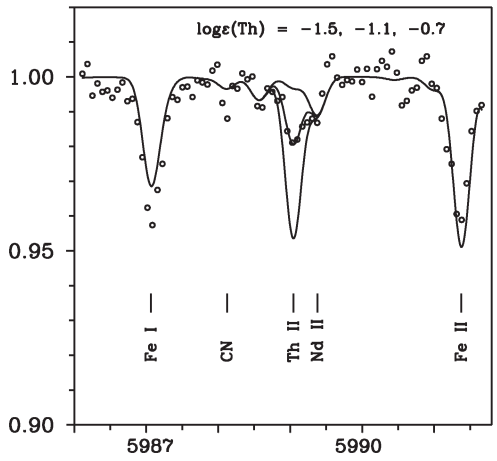


Figure 1: Spectrum of HD221170 near $\lambda$ 5989.045 Å. Circles - observed spectrum, lines - synthetic spectra calculated with different thorium abundances.

We compared the lines of Th II in the spectra of SMC stars with these lines in the spectra of halo star of our Galaxy HD221170 and Arcturus. Observed spectra were taken from Yushchenko et all. (2005) and from Hinkle et al. (2000) for HD221170 and for Arcturus respectively. Thorium line $\lambda$ 5898.045 Å in the spectra of HD221170, Arcturus and SMC supergiant stars is shown in Figures 1-3. Thorium line $\lambda$ 6044.433 Å in the spectra of PMMR23, PMMR39, and PMMR144 can be found in Fig. 4.

We can see that thorium lines in the spectra of SMC supergiants (Fig. 3) are stronger that the lines in the spectra HD221170 and Arcturus (Fig. 1-2). It should be noted that line $\lambda$ 5898.045 Å is blended by Nd II line. In the case of PMMR144 the blending is not significant since the Nd is underabundant with respect to the Sun approximately by -1 dex.

Other thorium lines are not so strong in the spectra of SMC stars, but they are still strong in comparison with the spectra of HD221170 and Arcturus. It seems reasonable to search for thorium lines in the spectra of K-supergiants of our Galaxy with similar to SMC stars temperatures and gravities.

The equivalent widths of thorium lines were estimated by fitting their profiles with a Gaussian function. The thorium abundance was calculated using the model atmosphere method on the basis of the Kurucz (1995) WIDTH9 program. Parameters of atmosphere models were taken from prevoius investigations of these stars. The results for individual lines can be found in Table 1, where for all used lines we pointed the wavelength, the oscillator strength, and the pairs (equivalent width – abundance) for four program stars.

The mean abundances of thorium in the atmospheres of PMMR23, PMMR39, PMRR144, and PMMR145 are found to be equal to $\approx -0.10 \pm 0.13, -0.63 \pm 0.13, -0.69 \pm 0.09$, and $+0.05$ dex (in the scale logN(H)=12), using 6, 2, 4, and 1 thorium lines respectively.

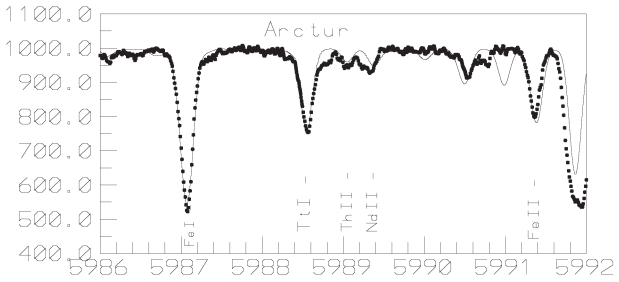


Figure 2: Spectrum of Arcturus near $\lambda$ 5989.045 Å. Thin line is synthetic spectrum, filled circles - observed one.

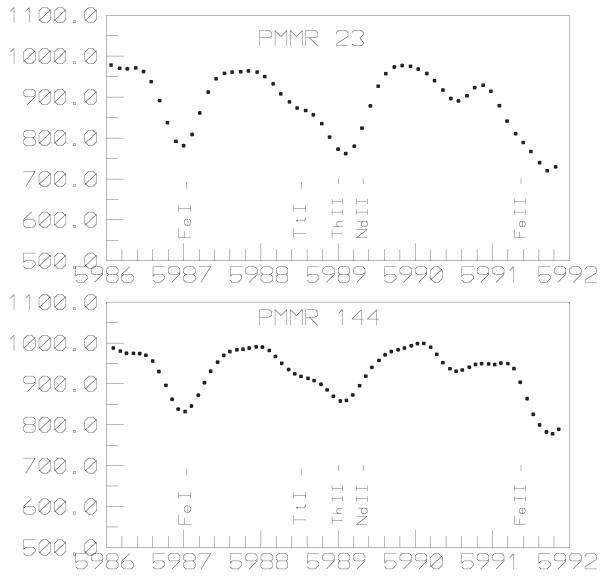


Figure 3: Spectra of PMMR23, and PMMR144 in vicinity of $\lambda$ 5989.045 Å.

Table 1: Thorium lines and the abundances of thorium in the atmospheres of PMMR23, PMMR39, PMMR144, and PMMR145.

| $\lambda$ | *loggf* | Equivalent widths and abundances | | | | | | | |
|---|---|---|---|---|---|---|---|---|---|
| | | 23 | | 39 | | 144 | | 145 | |
| 5488.630 | -2.61 | 18 | -0.16 | | | 12 | -0.80 | | |
| 5989.045 | -1.41 | 130 | 0.07 | | | 102 | -0.56 | | |
| 6044.433 | -1.87 | 16 | -0.30 | 16 | -0.76 | 20 | -0.76 | | |
| 6112.837 | -1.83 | 50 | -0.15 | 30 | -0.50 | | | 49 | 0.05 |
| 6619.944 | -1.81 | 29 | -0.10 | | | 11 | -0.65 | | |
| 6993.037 | -1.57 | 26 | 0.06 | | | | | | |

The blend of $\lambda$ 5989.045 of Th II line with line of Nd II at $\lambda$ 5989.378 Å has equivalent width which exceeds 100 mÅ in the spectra of SMC K-supergiants. It is better to use synthetic spectra method to find the precise abundances of thorium (Gopka et al. 2005). The weaker thorium lines shows similar values of abundances, the scattering is smaller than 0.2.

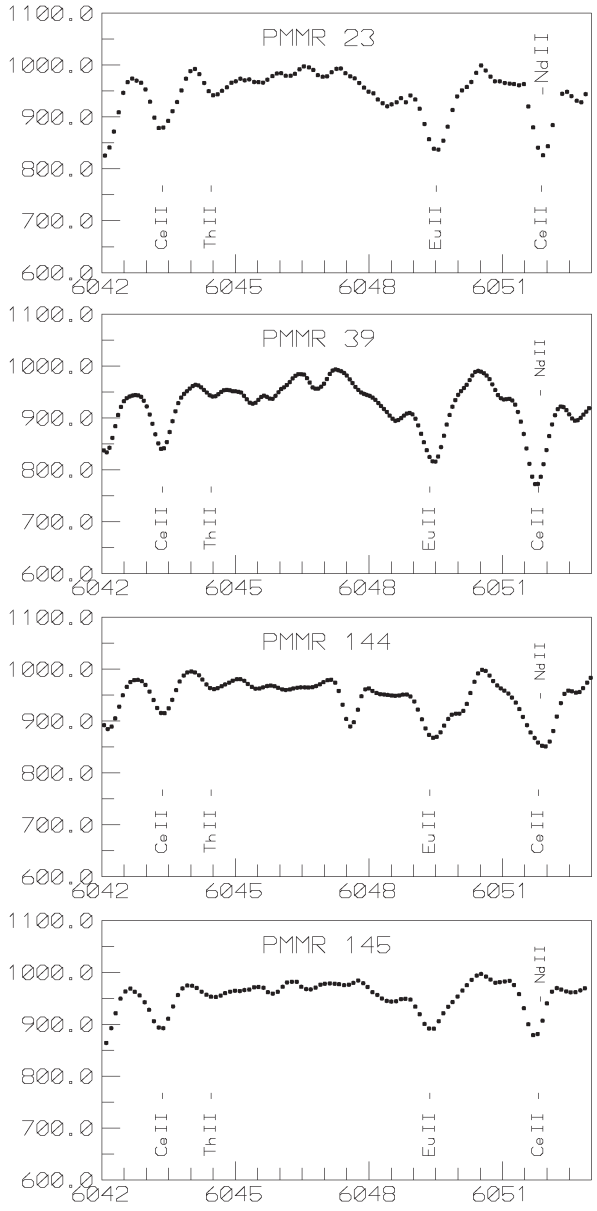


Figure 4: Spectra of PMMR23, PMMR39, and PMMR144 in vicinity of $\lambda$ 6044.433 Å.

### 3. Discussion

We hope that the discovery of strong thorim lines in the visible part of the spectrum permits to investigate the abundance of thorium in supergiant stars of our Galaxy, Magellanic Clouds and dwarf satellites of the Galaxy. As it was pointed here before, only the strongest line of ionized thorium $\lambda$ 4019.129 Å was used in numerous investigations of thorium abundance in galactic stars. It was the base of all important results concerned the evolution of the Galaxy, ecspesially its halo stars.

The brief overview of the best investigations of halo stars was made by Yushchenko et al. (2005). It was pointed out that only five galactic $r-$process-rich halo stars (GS31082-001, GS22892-052, HD115444, BD+17$^o$3248, and HD221170) have detailed abundance patterns that permit to have some imagination about the history of formation of the heavy elements in these stars.

The ratio of thorium and europium abundances in three of these stars is close to -0.6, while in two stars (GS31082-001 and HD221170) it is near -0.2. Later, Ivans et al. (2006) using the spectra of HD221170 obtained at KECK telescope reanalysed the abundance pattern of HD221170. It was found that the mean difference between the abundances of chemical elements found by Yushchenko et al. (2005) using 2-m Terskol Observatory telescope and Ivans et al. (2006) using 10-m KECK telescope and 2.7-m Mc-Donald Observatory telescope is as small as +0.04±0.19 dex, but the difference in Th/Eu ratio is significant, and this ratio is close to -0.6 for HD221170.

It permitted Ivans et al. (2006) to claim that the production of $r-$process elements in different supernova explosions is similar. The only exception is GS31082-001. Ivans et al. (2006) proposed that anomalous Th/Eu ratio for this star can be explained by a contamination from a nearby SN II event, sufficiently nearby, like in the binary system.

In accordance with Ivans et al. (2006) there are 5 $r-$process-rich halo stars with detailed abundance patters, and the peculiarity of one of these stars should be explined by close supernova event.This explanations was first proposed by Qian & Wasseburg (2001) to explain the chemical composition of GS 31082-001 only.

But can we expect that 20 percents of this type of stars have been influenced by the nearby explosions? Is it really possible that all the stars with a non-standard Th/Eu ratio suffered close SNe event?

Honda et al. (2004) investigated 22 very metal-poor stars with [Fe/H]<-2.5 and found that Th/Eu abundance ratios log(Th/Eu) are distributed over the range $-0.10$ to $-0.59$ with typical error of 0.10 to 0.15 dex. It seems that this result indicates real star-to-star

scatter, not contamination by close SN event. We hope that thorium lines in the red part of spectrum will be useful to resolve this and other problems of stellar evolution.

## 4. Conclusion

The main results of our investigation are:

1. The lines of Th II in the spectra of PMMR23, PMMR39, PMRR144, and PMMR145 are stronger than thorium lines in the spectra of other stars that were investigated earlier. We obtained, that the intensity of Th II line $\lambda$ 5898.045 Å in the spectra of these stars are also stronger than in the spectra of halo star HD221170 and Arcturus (Fig. 1-6).

2. The abundances of thorium in the atmospheres of PMMR23, PMMR39, PMMR144, and PMMR145 are scattered from +0.05 to –0.69 in the scale where logN(H)=12.

3. Six thorium lines were identified in the spectrum of PMMR23. Equivalent widths of these lines are in the range from 16 to 130 mÅ.

4. Detection of of thorium lines in the visible part of the spectrum is very important for the future investigations of $r-$, $s-$process elements and for the cosmochronology. These identifications can give a possibility to investigate the thorium abundances in other stars of Magellanic Clouds, our Galaxy, dwarf satellites of the Galaxy.

## References

Nilsson H., Zang Z.G., Lundberg H., Johansson S., and Nordstrom B.: 2002, *A&A*, **382**, 368.

Russell S. and Bessel M.: 1989, *ApJ Suppl. Ser.*, **70**, 865.

Spite F., Spite M., Francois P.: 1989, *A&A*, **210**, 25.

Russell S.: 1991, *Irish Astron. J.*, **20**, 42.

Hill V.: 1997, *A&A*, **324**, 435.

Hill V., Barbuy B., Spite M.: 1997, *A&A*, **323**, 461.

Hinkle K., Wallace L., Valenti J., Harmer D.: 2000, Visible and Near Infrared Atlas of the Arcturus Spectrum 3727-9300 Å, *Astron. Soc. Pacific*

Honda S., Aoki W., Kajino T., Ando H., Beers T.C., Izumiura H., Sadakane K., Takada-Hidai M.: 2004, *ApJ*, **607**, 474

Gopka V.F., Yushchenko A.V., Goriely S., Vasil'eva S.V., Kang H.: 2005, *IAU Symp. No 228.*, **228**, 535.

Ivans I.I., Simmerer J., Sneden C., Lawler J.E., Cowan J.J., Gallino R., Bisterzo S.: 2006, *ApJ*, **645**, 613.

Qian Y.-Z., Wasseburg G.J.: 2001, *ApJ*, **552**, L55.

Yushchenko A., Gopka V., Goriely S., Musaev F., Shavrina A., Kim C., Kang Y. Woon, Kuznietsova J., Yushchenko V.: 2005, *A&A*, **430**, 255.

# ON THE POSSIBLE NATURE OF Bp-Ap STARS: AN APPLICATION TO HD101065 and HR465

V.F. Gopka[1], O.M. Ulyanov[2], S.M. Andrievsky[1]

[1] Department of Astronomy, Odessa National University
T.G. Shevchenko Park, Odessa 65014 Ukraine, *gopka.vera@mail.rus; scan@deneb1.odessa.ua*

[2] Institute of Radio Astronomy of National Academy of Sciences of Ukraine
4 Chervonoprapona str., Kharkov 61002, Ukraine, *oulyanov@rian.kharkov.ua*

ABSTRACT. We have proposed the new explanation of some magnetic chemically peculiar (MCP) stars anomalies, which is based on assumption that such stars can be the close binary systems with a secondary component being neutron star. Within this hypothesis one can naturally explain the main anomalous features of MCP stars: first of all, an existence of the short-lived radioactive isotopes detected in some stars (like Przybylski's star and HR465), and some others peculiarities (e.g. the behavior of CU Vir in radio range, the phenomenon of the roAp stars).

**Key words**: Przybylski's star, HR465, close binary system, roAp star, neutron star, pulsar, magnetar.

## 1. Introduction

It is known that about 10-15% of upper main sequence stars have atmospheres with anomalies in elemental abundance (Bagnulo, 2002). These stars are often classified as magnetic chemically peculiar stars (MCP, or Bp-Ap stars) and nonmagnetic (Hg-Mn and Am-Fm) stars. Hg-Mn stars have a higher temperature than MCP stars and overlap with MCP stars in the region of the higher temperatures, while Am-Fm stars have the lower temperatures than MCP stars.

Among the MCP stars one can select the following subclasses (Kurtz & Martinez, 2000):

1. SrCrEu stars (spectral classes A3-F0).
2. Si stars(B8-A2).
3. He-weak, Si, SrTi stars (B3-B7).
4. He-strong stars (B1-B2).

Some of the peculiarities seen in the chemically peculiar stars can be explained by considering different non-nuclear processes first proposed by Michaud (1970) and then elaborated in a series of the subsequent papers (Turcotte et al., 1998; Turcotte et al., 2000; Richard et al., 2002).

## 2. MCP stars: the main features

The main characteristics of MCP stars are the following:

1. MCP stars show periodic variations of the light, spectrum and magnetic field. It is believed that these variations are due to the rotation of the star. MCP stars has been regarded as rigid magnetic dipoles with respect to the rotation axis (Babcock, 1949; Stibss, 1950). In the later works it was obtained that MCP stars can be stars with a multi-pole magnetic field (Landstreet, 1990; Mathys, 1991).

2. Some MCP stars are the source of radio emission (Drake et al., 1987). The flat spectra and variability of radio emission on time scales as short as a few hours, as well as the well known strong magnetic field indicate a nontermal gyrosynchrotron emission process (Lynsky et al., 1989). Later Lynsky (Lynsky et al., 1992) remarked, that all observed properties of radio emission from these stars may be understood as optically thick gyrosynchrotron emission from a nonthermal distribution of electron emitters. The radio luminosities of MCP stars are correlated with effective temperature and magnetic field strength (Drake et al., 1994).

3. Some MCP stars are detected as X-ray sources (Drake et al., 1994). They have been investigated during the ROSAT All-Sky Survey. Drake (1998) emphasized that only 10 X-ray sources detected at the positions of 100 magnetic Bp-Ap stars.

4. Shore & Brown (1990) showed that MCP are characterized by an anisotropic stellar wind. MCP stars have been known to have moderate circular polarization (Drake et al., 2002). Trigilio et al. (2000) showed that only CU Vir (Si-star) have a strong 1.4 GHz flux enhancement around phases 0.4 and 0.8, with a right circular polarization of almost 100%. Leto et al., (2007) remarked that only MCP star with a high photospheric temperature develop a radiative-driven stellar wind, which is the cause of the radio emission.

5. Among MCP stars there is known the phenomenon of roAp-stars. roAp stars are the main sequence SrCrEu chemically peculiar stars from mid-A to early-F, which pulsate with periods in the range of 5-16 min and amplitudes $< 0.016$ mag (Kurtz & Martinez, 2000). The mechanisms responsible for an existent of the roAp star pulsations remain unknown. HD101065 is the first Ap star where pulsations were detected. Kurtz & Wegner (1979) detected the well-defined pulsations with a peak-to-peak amplitude of 0.012 mag and a period of 12.14 min (Kurtz & Wegner, 1979).

6. The most unusual feature is the chemical composition of MCP stars. The first studies of the abundance anomalies in magnetic stars $\alpha 2$ CVn, HD133029, HD151199 showed that there can be the certain nuclear reactions in the star (Burbidge et al., 1958). Now it is accepted that detected over- and/or under-abundance of some elements do not reflect the chemical composition of the entire star, but only its photosphere. There are the most extremal cases among the MCP stars. For example HD101065 with its chemical composition is the most unusual roAp star. The star HD101065 in fact is the unique astrophysical laboratory for understanding and exploring the extreme phenomena of the stellar evolution. This stars shows the high lithium abundance, as well as unusual isotopic lithium ratio (Shavrina et all., 2000). The presence of the short-lived lanthanide promethium $Z = 61$ was noted by Wagner & Petford (1973), Cowley et al. (2004), Fivet et al. (2007). The lines of some short-lived transbismuth isotopes were detected by Gopka et al. (2004), Gopka et al. (2005), Bidelman (2005), Quinet et al. (2007). Cowley & Hubrig (2002), Cowley et al. (2007) found anomalous isotopic ratio of Ca in the HD101065 atmosphere.

## 3. About nucleosynthesis on the stellar atmosphere

The idea about the possibility of the nucleosynthesis in the stellar atmosphere is not new. In the mid of past century the first papers concerning the chemical composition of Ap stars showed that overabundance of heavy elements really exist. In some cases overabundance of some elements can reach 6 dex and more comparing to the solar abundance. E.M. Burbidge and G.R. Burbidge wrote: "The list of elements with the increased content led us to the thought, that in this case we deal with the nuclear, not with atomic processes and that somewhere and somehow the neutrons take part in them." (Burbidge & Burbidge, 1996).

Nevertheless, the mechanism responsible for such uncommon processes was not identified at that time. Recently, Goriely (2007) showed that nucleosynthesis of heavy (including radioactive) elements can occur in the star's atmosphere due to the high-energy particles entering the atmosphere of the star. At the same time, the origin of such particles was not clearly specified. This idea was also discussed in Arnold et al. (2007).

The r-process has been frequently mentioned in relation to the abundance anomalies observed in Ap stars (Cowley et al., 1973). In particular, Burbidge (1965) indicates the fact that the explosion remnants of a more massive star can be possible explanation of the origin of the peculiarity. For instance, a supernova explosion in the binary system and following contamination of its companion star with freshly synthesized material could, in principle, explain the peculiarity, observed in HD101065. The only problem is that in this case one has to suppose that such an event should have happened not very long ago, since we are observing now the signs of the short-lived isotopes in atmosphere of this star.

## 4. Possible origin of roAp stars HD101065 and HR465

In order to explain several anomalous features of some MCP stars, and especially their extremely peculiar chemical composition (an existence in atmosphere the short-lived radioactive elements) we propose the following hypothesis. Let us consider an example of HD101065 (Przybylski's star, PS), and assume that PS is a close binary system with a non-seen companion being the neutron star (NS). For this system an orbital plane is near perpendicular to the line of sight (Fig. 1). The rapid wind, generated by NS, which consists of the electron-positron plasma, is accelerated almost to the speed of light and hit the PS atmosphere. The electron-positron plasma falling on the PS must be ultrarelativistic, so that their kinetic energy $E > m_e c^2$. The estimations show that the gamma-factor of the "fast" electrons/positrons, which is necessary for starting the photonuclear reactions, must exceed 20. This estimation is completely realistic, since gamma-factors of the electron-positron plasma in the upper magnetosphere of a radio pulsar can be within 10-10000 (Ruderman & Sutherland, 1975). In the spectrum of one of the most studied pulsar PSR B0531+21 (Crab Nebula pulsar) there really exist the gamma quanta within the required range of energies (Fig. 2).

The high-energy electrons from electron-positron plasma can also generate free neutrons via the direct interaction with hydrogen nuclei in the PS atmosphere ($p + e^- \rightarrow n + \nu$). Such free neutrons are necessary for the r-process to occur in the considered medium.

Thus, the nuclei of heavy elements (including the radioactive isotopes) in the PS atmosphere can be synthesized as a result of two processes: the photonuclear reaction and neutron capture by the seed nuclei of the lighter element. In both cases the source of the en-

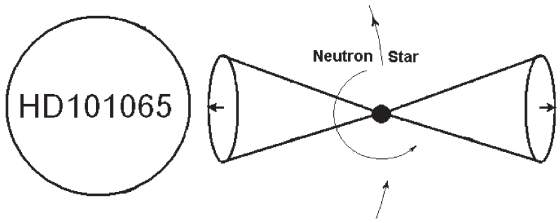


Figure 1: Geometry of the binary system containing Przybylsky's star and neutron star.

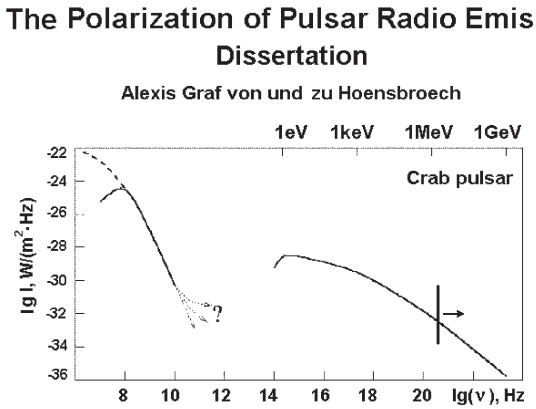


Figure 2: Spectrum of the Crab pulsar.

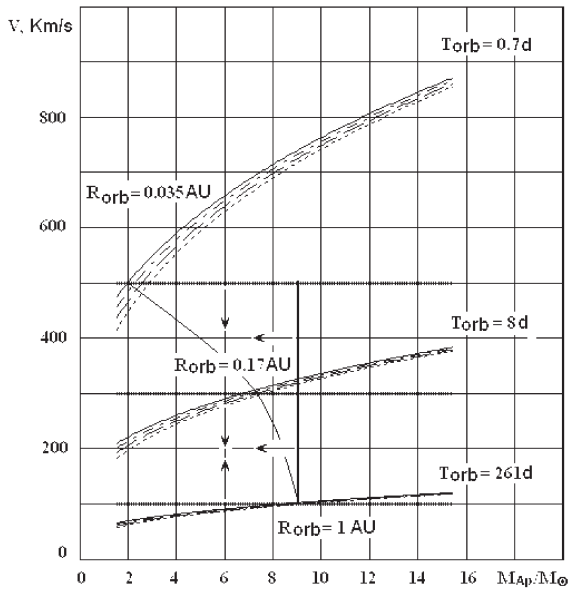


Figure 3: Parameters of a close binary system Ap star - neutron star.

ergetic particles, that trigger the nuclear reactions in the PS atmosphere, is associated with the NS magnetosphere.

Let us show why the binary system PS-NS must be the close one. At present there exist a large uncertainty in the mass estimations of the PS. Thus, if we take one extreme estimate of its effective temperature as 6600° K, and consider another one (spectral class B5, Perryman et al., 1997), then from the spectral class-luminosity relation we obtain that mass of this star falls in the range $M_{PS} \approx 1.5 - 8 \cdot M_{\odot}$. For the further estimates we assume that masses of the PS and NS are $M_{PS} = (1.5 - 8)M_{\odot}$ and $M_{NS} = (0.7 - 1.4)M_{\odot}$ respectively.

It is possible to estimate the parabolic velocity for this system from the main integral of energy: $V_{PAR} = \sqrt{\frac{2G(M_{PS}+M_{NS})}{R}}$ (were $R$ is the distance from the center of mass to the NS). Taking into account that the range of characteristic tangential velocities for the known radio-pulsars is $V_{PSRs} \in \{100 - 500\}$ km/s, and the fact that these velocities must not exceed the parabolic velocity of the considered system, we obtain the range of the most probable parameters (distance, the center of mass of the PS-NS system, the orbital period, the corresponding masses of components). This range is show in Fig. 3. It can be seen that the distances, estimated in that way, ranges from 0.035 AU for a minimum mass $M_{PS}$ to 1.0 AU (for maximum mass). Knowing the parallax of PS $\pi \approx 7.95 \pm 1.07$ mas (Perryman et al., 1997), one can estimate its distance ($D = 125.8 \pm 15.7$) pc and angular size (0.17 mas for minimum mass and 14 mas for maximum mass).

With parameters listed above, the orbital period of PS ranges from 261 days up to 0.7 days. Note that HR465, which has invisible companion (but orbital plane is parallel to the line of sight) has rotation period of 273 days (Scholz, 1978; Fig. 4). At the same time, the spectroscopic, photometrical data and magnetic field measurements could be well represented with a period of 22-23 years (Fuhrhmann, 1989).

Such a long-term variation can be caused by some active region on the stellar surface that changes its position because of the weak precession. In 1996 the magnetic field of this star was 5000 Gs, and the lines of CrII were extremely strong. In 2004 the strong lines of lanthanides and actinides (ThIII, UIII) were seen in the visible part of spectra (Gopka et al., 2007). Magnetic field at that time was 1300-1500 Gs (the estimate of Shavrina). Chromium abundance changed by about 0.7 dex during the period of 8 years. Within our model (MCP star + NS) active region (i.e. local increase of the temperature, in particular) can be formed on the surface of MCP stars as a result of a localized interaction of atmosphere gas with relativistic plasma ejected by NS. To estimate the local temperature increase one can use the value of

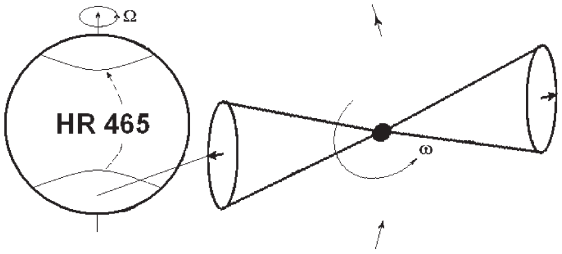


Figure 4: Geometry of HR465 binary system. The position of active area changes with period of 23 years.

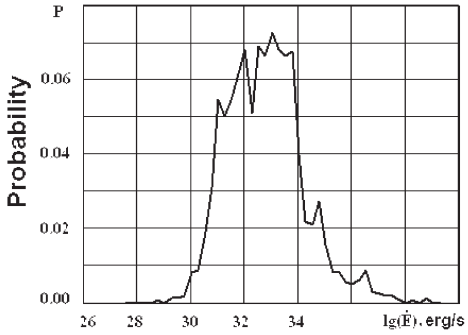


Figure 5: The energy distribution of kinematic losses of 1627 pulsars.

kinematic losses for known pulsars (Fig. 5) Resulting value is close to 3000°- 6000° K. The short-term light variation (roAp phenomenon) can be also explained by such kind of interactions.

## 5. Conclusions

The proposed hypothesis, which consists in the supposition that some MCP stars can be the binary stellar systems containing as a secondary component neutron star, can be capable in natural explaining of some peculiarities associated with these stars. Among them: anomalous chemical composition, an existence of the short-lived radioactive isotopes, short-time and long-period variations of the light and magnetic field, X-ray and radio-emission detected for some MCP stars.

*Acknowledgements.* The authors thank V.V.Ilyushin and V.V.Zakharenko, who helped with useful discussion and remarks concerning this article. Gopka V.F. was (partially) supported by research fund of Ghonbuk National University, Korea.

## References

Arnold M., Goriely S., Takashi K.: 2007, *Astrophysic*, **5**, 1.
Babcock H.W.: 1949, *Observatory*, **69**, 191.
Bagnulo S.: 2003, *IAU Symp. No 210.*, **210**, 9.
Bidelman A.: 2005, *ASP Conf. series*, **336**, 309.
Burbidge E.M., Burbidge G.R., Fowler W.A.: 1958, *IAU Suppl. Cambrudge Universyty press*, **6**, 222.
Burbidge G.R.: 1965, *Proc. of the IUA, Symp.*, **22**, 418.
Burbidge E.M., Burbidge G.R.: 1986, *Nucl. Astrophys.*, 22.
Cowley C., Hatoog M.R. et al.: 1973, *Ap. J.*, **183**, 127.
Cowley C. & Hubrig S.: 2005, *A. A.*, **196**, 21.
Cowley C., Hubrig S., Castelli F.: 2007, *Contrib. Astron. Obs. Scalnete Pleso*, **35**, 1.
Cowley R.C., Bidelman W.P. et al.: 2004, *A. A.*, **419**, 1087.
Drake S.A.: 1998, *CoSka.*, **27**, 382.
Drake S.A., Abbot D.C. et al.: 1987, *Ap. J.*, **322**, 902.
Drake S.A., Lynsky J.L. et al.: 1994, *Ap. J.*, **420**, 387.
Drake S.A., Linsky J.L., Wade G.A.: 2002, *AAS, Bull. of American Astron. Soc.*, **34**, 1156.
Fivet V., Quinet P. et al.: 2007, *MNRAS*, **380**, 771.
Fuhrmann K.: 1989, *A. A. Suppl. Ser.*, **80**, 399.
Gopka V.F., Shavrina A.V.: Izv. KrAO, **104**, accepted.
Gopka V., Yushchenko A. et al.: 2005, *AIP Conf. Proc., Tokio, Japan*, **843**, 389.
Gopka V., Yushchenko A. et al.: 2004, *IAU Symp. Poprad, Slovakia*, **224**, 119.
Goriely S.: 2007, *A. A.*, **466**, 619.
Kurtz D.W. and Martines P.: 2002, *Baltic Astron.*, **9**, 253.
Kurtz & Wegner: 1979, *Ap. J.*, **196**, 51.
Landstreet J.D.: 1990, *Ap. J.*, **352**, 5.
Leto P., Trigilio C. et al.: 2007, *A. A.*, **102**, 272.
Lynsky J.L., Drake S.A., Bastian T.S.: 1989, *BAAS*, **21**, 742.
Lynsky J.L., Drake S.A. et al.: 1992, *Ap. J.*, **393**, 341.
Mathys G.: 1991, *A. A. Suppl. Ser.*, **89**, 121.
Michaud G.: 1970, *Ap.J.*, **160**, 641.
Perryman M.A.C., Lindegren L. et al.: 1997, *Astron. and Astrophys.*, **323**, L49.
Richard O, Michaud G. & Richard J.: 2002, *Ap. J.*, **580**, 1100.
Ruderman M.A., Sutherland P.G.: 1975, *Ap. J.*, **196**, N 1, 51.
Scholz G.: 1978, *Astron. Nachr.*, **299**, 81.
Shavrina A.V., Polosukhina N.S. et al.: 2003, *Astron. and Astrophys.*, **400**, N2, 707.
Shore & Brown: 1990, *Ap. J.*, **196**, 51.
Stibbs D.W.N.: 1950, *MNRAS*, **110**, 395.
Trigilio C.: 2000, *Ap. J.*, **196**, 51.
Turcotte S., Richard O, Michaud G.: 1998, *Ap. J.*, **504**, 559.
Turcotte S., Richard O. et al.: 2000, *A. A.*, **272**, 559.
Quinet P., Argante C. et al.: 2007, *A. A.*, **474**, 307.
Wegner G., Petford A.D.: 1974, *MNRAS*, **168**, 575.

# SECULAR EVOLUTION OF THE GALAXY

E. Griv[1], M. Gedalin[1], and C. Yuan[2]

[1] Department of Physics, Ben-Gurion University of the Negev
Beer-Sheva 84105 Israel, *griv@bgu.ac.il, gedalin@bgu.ac.il*
[2] Institute of Astronomy and Astrophysics, Academia Sinica
POB 23-141, Taipei 106 Taiwan, *yuan@asiaa.sinica.edu.tw*

ABSTRACT. The theory of spiral structure of rotationally supported disk-shaped galaxies has a long history, but is not yet complete. Even though no definitive answer can be given at the present time, the majority of experts in the field is yielded to opinion that the study of the stability of gravity perturbations (e.g., those produced by spontaneous disturbances) in disk galaxies of stars is the first step towards an understanding of the phenomenon. We analyse the reaction between almost aperiodically growing Jeans-unstable gravity perturbations and stars of a rotating and spatially inhomogeneous disk of highly flattened galaxies. A mathematical formalism in the approximation of weak turbulence (a quasi-linearization of the Boltzmann collisionless kinetic equation) is developed, which is a direct analogy with the plasma quasi-linear (weakly nonlinear) formalism. A diffusion equation in configuration space is derived which describes the change in the main body of equilibrium distribution of stars. The distortion in phase space resulting from such a wave-star interaction is studied. The theory, applied to the Solar neighborhood, accounts for the increase in the random stellar velocities with age and the essential radial spread of the Galaxy's disk. We argue that the Sun has migrated from its birth-place at the galactocentric radius $r = 6 - 7$ kpc in the inner part of the Galaxy outwards by $\Delta R_\odot = 2 - 3$ kpc during its lifetime of $t \approx 4.5 \times 10^9$ yr. This $\Delta R_\odot$ is in fair agreement with the estimate of Wielen et al. (1996) $\Delta R_\odot \approx 1.9$ kpc based on a radial galactic gradient in metallicity.

**Key words**: Galaxies: spiral; stars: individual: Sun.

## 1. Introduction

The bulk of the total optical mass in the Milky Way and other flat galaxies is in stars. In the spirit of Lin et al. (1969) and Shu (1970), we regard spiral structure in most galaxies of stars as a wave pattern, which does not remain stationary in a frame of reference rotating around the center of the galaxy at a proper speed, excited as a result of the gravitational Jeans-type instability. The instability is set in when the destabilizing effect of the self-gravity in the disk exceeds the combined restoring action of the pressure and Coriolis forces. The wave propagation is a process of rotation as a solid about the center of the galaxy at a fixed phase velocity, despite the general differential rotation of the system. The instability is driven by a strong nonresonant interaction of the gravity fluctuations with the bulk of the particle population, and the dynamics of Jeans perturbations can be characterized as a fluidlike wave-particle interaction. The instability represents the ability of a self-gravitating disk to relax from a nonthermal (or an almost nonthermal) state by collective collisionless processes in much less time than the binary collision time. It is our purpose to extend the investigation by studying the natural nonlinear effects. The problem is formulated in the same way as in plasma kinetic theory (Krall & Trivelpiece 1986).

## 2. Basic Equations

A thin rotating disk is taken as a model of the flat galaxy in many papers for analysis of the gravity perturbations. Following Morozov (1981), Griv & Peter (1996), and Griv et al. (2000, 2001, 2002), we solve the system of the collisionless Boltzmann equation and the Poisson equation describing the motion of a self-gravitating ensemble of stars in such a system within an accuracy of up two orders of magnitude with respect to small parameters $1/|k_r|r$ and $c_r/r\Omega$ for the radial wavenumber $k_r$, the dispersion of radial peculiar velocities $c_r$, and the angular velocity $\Omega$, looking for waves which propagate in a two-dimensional galactic disk. This approximation of an infinitesimally thin disk is a valid approximation if one considers perturbations with a radial wavelength $\lambda = 2\pi/k_r$ that is greater than the typical disk thickness.

In configuration space we introduce cylindrical coordinates $r$, $\varphi$, $z$, and $0z$ axis directed along the axis of rotation. The projections of the peculiar velocity of a

star on the coordinate axis is designated by $v_r$, $v_\varphi$, $v_z$, respectively. Let us assume that the stars move in the disk plane so that $v_z = 0$. This allows us to use the two-dimensional distribution function $f(r, \varphi, v_r, v_\varphi, t)$ such that $\tilde{f} = f\delta(z)\delta(v_z)$, $f = \int \tilde{f} \mathrm{d}z\mathrm{d}v_z$, and $\int f \mathrm{d}v_r \mathrm{d}v_\varphi = \sigma$, where $\sigma(\mathbf{r}, t)$ is the surface density. In galaxies the function $f(\mathbf{r}, \mathbf{v}, t)$ must satisfy the Boltzmann collisionless equation of continuity

$$\frac{\partial f}{\partial t} + \mathbf{v} \cdot \frac{\partial f}{\partial \mathbf{r}} - \frac{\partial \Phi}{\partial \mathbf{r}} \cdot \frac{\partial f}{\partial \mathbf{v}} = 0 \,. \tag{1}$$

In Eq. (1), $\Phi(\mathbf{r}, t)$ is the total gravitational potential (including a dark matter, if it exists at all) determined self-consistently from the Poisson equation

$$\frac{\partial^2 \Phi}{\partial r^2} + \frac{1}{r}\frac{\partial \Phi}{\partial r} + \frac{1}{r^2}\frac{\partial^2 \Phi}{\partial \varphi^2} + \frac{\partial^2 \Phi}{\partial z^2} = 4\pi G \sigma \delta(z) \,, \tag{2}$$

where $\delta(z)$ is the Dirac delta-function with respect to the spatial coordinate $z$. The Boltzmann and Poisson equations with appropriate boundary conditions give a complete description of the problem for disk modes of collective oscillations. The relationship between the frequency of the oscillations and the wave vector is found by equating the solutions of Eqs. (1) and (2).

Suppose that up to the time $t = 0$ the disk remains in a stationary state, i.e., for $t < 0$

$$f = f_\mathrm{e} \quad \text{and} \quad \Phi = \Phi_\mathrm{e} \,,$$

where $f_\mathrm{e}$ and $\Phi_\mathrm{e}$ are the equilibrium distribution function and the equilibrium gravitation potential, respectively. At $t = 0$ the disk is perturbed in some manner, so that for $t > 0$

$$f = f_\mathrm{e} + f_1 \quad \text{and} \quad \Phi = \Phi_\mathrm{e} + \Phi_1 \,.$$

The quantities $f_1$ and $\Phi_1$ characterize the deviations, or perturbations, of the distribution function and the field from the corresponding equilibrium values. We are interested in the time dependence of the perturbations, which we will assume are small.

We proceed by applying the procedure of the quasi-linear approach. In the quasi-linear theory, one may follow the standard procedure of linearization by writing $f = f_0(r, \mathbf{v}, \mu t) + f_1(\mathbf{r}, \mathbf{v}, t)$ and $\Phi = \Phi_0(r, \mu t) + \Phi_1(\mathbf{r}, t)$ with $|f_1/f_0| \ll 1$ and $|\Phi_1/\Phi_0| \ll 1$ for all $\mathbf{r}$ and $t$. The functions $f_1$ and $\Phi_1$ are functions oscillating rapidly in space and time, while the functions $f_0$ and $\Phi_0$ describe the slowly developing "background" against which small perturbations develop; $\mu \ll 1$; $f_0(t = 0) \equiv f_\mathrm{e}$ and $\Phi_0(t = 0) \equiv \Phi_\mathrm{e}$. The distribution $f_0$ continues to distort as long as the distribution is unstable. Linearizing Eq. (1) and separating fast and slow varying variables one obtains the equation for the fast developing distribution function

$$\frac{\mathrm{d}f_1}{\mathrm{d}t} = \frac{\partial \Phi_1}{\partial r}\frac{\partial f_0}{\partial v_r} + \frac{1}{r}\frac{\partial \Phi_1}{\partial \varphi}\frac{\partial f_0}{\partial v_\varphi} \,, \tag{3}$$

where $\mathrm{d}/\mathrm{d}t$ means total derivative along the star orbit and $f_0$ is a given equilibrium distribution function determined from the following equation (see Eq. (1)):

$$\mathbf{v} \cdot \frac{\partial f_0}{\partial \mathbf{r}} - \frac{\partial \Phi_0}{\partial \mathbf{r}} \cdot \frac{\partial f_0}{\partial \mathbf{v}} = 0 \,.$$

The equation for the slow part of the distribution function is

$$\frac{\partial f_0}{\partial \mu t} = \left\langle \frac{\partial \Phi_1}{\partial r}\frac{\partial f_1}{\partial v_r} + \frac{1}{r}\frac{\partial \Phi_1}{\partial \varphi}\frac{\partial f_1}{\partial v_\varphi} \right\rangle , \tag{4}$$

where $\langle \ldots \rangle$ denotes a time average over the fast oscillations,

$$f_0 = \langle f \rangle = \frac{1}{\mathcal{T}} \int_0^{\mathcal{T}} f \mathrm{d}t \quad \text{and} \quad \langle f_1 \rangle = \langle \Phi_1 \rangle = 0 \,,$$

and $\mathcal{T}$ is the characteristic time of the quasi-linear relaxation, i.e., the time during which the oscillations influence the equilibrium state.

It is useful to define a generalized entropy function (Krall & Trivelpiece 1986, p. 364)

$$S_\mathrm{gen} = -\int f_0 \ln f_0 \mathrm{d}\mathbf{r}\mathrm{d}\mathbf{v} \,. \tag{5}$$

Contrary to the case of the true entropy $S_\mathrm{true} = -\int f \ln f \mathrm{d}\mathbf{r}\mathrm{d}\mathbf{v}$, which is constant in the absence of collisions, with this definition the "entropy" is not constant, and can be used to measure the increase of disorder (e.g., temperature) of the system. It is, incidentally, just such a *coarse-grained* single-particle distribution function $f_0$ that is determined in practice, particularly in stellar dynamics, where it is determined in a fairly large region of phase space.

## 3. Perturbation

In the familiar Wentzel-Kramers-Brillouin (WKB) approximation in Eqs. (3) and (4), assuming the weakly inhomogeneous disk, each perturbation of equilibrium parameters is selected in the form of a plane wave (in the circular rotating frame)

$$X_1(\mathbf{r}, \mathbf{v}, t) = \sum_{\mathbf{k}} X_\mathbf{k} e^{ik_r r + im\varphi - i\omega_{*,\mathbf{k}} t} + \text{c.c.} \,, \tag{6}$$

In Eq. (6), $X_\mathbf{k}$ is an amplitude that is a constant in space and time, $m$ is the nonnegative azimuthal mode number (= number of spiral arms), $\omega_{*,\mathbf{k}} = \omega_\mathbf{k} - m\Omega$ is the Doppler-shifted wavefrequency, $r \sim R$, $|k_r| r \gg 1$, $|\mathrm{d}\ln k_r / \mathrm{d}\ln r| \ll 1$, suffixes $\mathbf{k}$ denote the $\mathbf{k}$th Fourier component, and "c.c." means the complex conjugate. Evidently, in Eq. (6) $X_1$ is a periodic function of $\varphi$, and hence $m$ must be an integer. The criteria for stability differ for each $m$, and must be determined by a detailed analysis. The assumption that $X_\mathbf{k}$ has a

weak spatial dependence corresponds to the quasiclassical approximation in quantum mechanics and to the approximation of geometrical optics in the propagation of light in an inhomogeneous medium. It is convenient to write the eigenfrequency $\omega_{*,\mathbf{k}}$ in a form of the sum of the real part $\Re\omega_{*,\mathbf{k}}$ and the imaginary part $i\Im\omega_{*,\mathbf{k}}$. The imaginary part of $\omega_{*,\mathbf{k}}$ corresponds to a growth ($\Im\omega_{*,\mathbf{k}} > 0$) or decay ($\Im\omega_{*,\mathbf{k}} < 0$) of the components in time, $f_1, \Phi_1 \propto \exp(\Im\omega_{*,\mathbf{k}}t)$, and the real part to a rotation with angular velocity

$$\Omega_\mathrm{p} = \frac{\Re\omega_{*,\mathbf{k}}}{m}\,. \tag{7}$$

Thus, when $\Im\omega_{*,\mathbf{k}} > 0$, the medium transfers its energy to the growing wave and oscillation buildup occurs. A galaxy is considered as a superposition of different oscillation modes. A disturbance in the disk will grow until it is limited by some nonlinear effect.

In the linear theory, one can select one of the Fourier harmonics:

$$X_1(\mathbf{r},\mathbf{v},t) = X_\mathbf{k} e^{ik_r r + im\varphi - i\omega_* t} + \text{c.c.}\,. \tag{8}$$

The solution in such a form represents a spiral wave with $m$ arms (or a ring, $m = 0$) whose shape $\Phi_1$ in the plane is determined by the relation

$$k_r(r - r_0) = -m(\varphi - \varphi_0)\,.$$

With $\varphi$ increasing in the rotation direction, we have $k_r > 0$ for trailing spiral patters, which are the most frequently observed among spiral galaxies. A change of the sign of $k_r$ corresponds to changing the sense of winding of the spirals, i.e., leading ones. With $m = 0$, we have the density waves in the form of concentric rings that propagate away from the center when $k_r > 0$ or toward the center when $k_r < 0$.

Paralleling the analysis leading to Eq. (13) of Griv & Peter (1996), from Eqs. (3) and (8) it is straightforward to show that the perturbed distribution function is

$$f_1 = -\Phi_1 \sum_{l=-\infty}^{\infty}\sum_{n=-\infty}^{\infty} \frac{\exp[i(n-l)(\phi-\zeta)]}{\omega_* - l\kappa} \times J_l(\chi)J_n(\chi)\left[l\kappa\frac{\partial f_0}{\partial(v_\perp^2/2)} + \frac{2m\Omega}{r\kappa^2}\frac{\partial f_0}{\partial r}\right], \tag{9}$$

where $J_l(\chi)$ is the Bessel function of the first kind of order $l$ with its argument $\chi = k_* v_\perp/\kappa$, $k_*$ is the effective wavenumber, $v_\perp^2 = v_r^2 + (2\Omega/\kappa)^2 v_\varphi^2$, and $\kappa \sim \Omega$ is the epicyclic frequency. In Eq. (9) the denominators vanish when $\omega_* - l\kappa = 0$. This occurs near corotation and other resonances. The above resonances take place where the frequency with which a star crosses the peaks and dips of the wave potential, $|\omega - m\Omega|$, is either zero (i.e., the star is always in phase with the wave) or equal to the oscillation frequency of the star about a circular orbit. The corotation resonance occurs at a radius where $l = 0$ in Eq. (9). The Lindblad resonances occur at radii where the field $(\partial/\partial\mathbf{r})\Phi_1$ resonates approximately with the harmonics $l = -1$ (inner resonance) and $l = 1$ (outer resonance) of the epicyclic (radial) frequency of equilibrium oscillations of stars $\kappa(r)$. Clearly, the location of these most important resonances depends on the rotation curve and the spiral pattern speed $\Omega_\mathrm{p}$; the higher the $m$ value, the closer in radius the resonances are located (Lin et al. 1969). Resonances are places where linearized equations describing the motion of particles do not apply. In the vicinity of the resonances it is necessary to use nonlinear equations, or to include terms of higher orders into the approximate form of the equations (Griv et al. 2000). In this work only the main part of the disk is considered, which lies sufficiently far from the resonances: in all equations $\Re\omega_* - l\kappa \neq 0$ (Lin et al. 1969; Griv et al. 2002). The distortion of the wave packet due to the disk inhomogeneity is included through the second term in the brackets on the right-hand side in Eq. (9).

## 4. Diffusion Equations

We anticipate that the fluidlike Jeans-unstable oscillations must influence the distribution function of the main part of stars in such a way as to hinder the wave excitation, i.e., to increase the peculiar velocity spread ultimately at the expense of circular motion and gravitational energy. This is because the Jeans instability, being essentially a gravitational one, tends to be stabilized by chaotic motions of stars. Simultaneously, unstable perturbations effectively transfer angular momentum outward to the outer parts of the system, as mass flows both inward to the growing center mass concentration and outward to the outer regions through gravitational torques. Eventually the disk evolves toward a quasi-stationary Jeans-stable distribution.

Let us suppose that the nonlinear effects in galactic disks are small, so that the linear theory is a good first approximation. Next, we substitute the solution (9) into Eq. (4) and average the latter over time. After averaging over $\phi = \arctan(2\Omega/\kappa)v_\varphi/v_r$, the equation for the slow part of the distribution function is obtained:

$$\frac{\partial f_0}{\partial\mu t} \approx \sum_\mathbf{k}\mathcal{E}_\mathbf{k}\frac{\partial}{\partial v_\perp}\frac{k_*\kappa}{v_\perp\chi}\frac{J_1^2(\chi)}{\kappa^2}\Im\omega_*\frac{\partial f_0}{\partial v_\perp} + \sum_\mathbf{k}\mathcal{E}_\mathbf{k}\frac{k_*\kappa}{v_\perp^2\chi}\frac{J_1^2(\chi)}{\kappa^2}\Im\omega_*\frac{\partial f_0}{\partial v_\perp} + \sum_\mathbf{k}\mathcal{E}_\mathbf{k}\frac{2\Omega}{\kappa^2}\frac{m}{r}\frac{\partial}{\partial r}\frac{2\Omega}{\kappa^2}\frac{m}{r}\frac{J_1^2(\chi)}{\kappa^2}\Im\omega_*\frac{\partial f_0}{\partial r}\,, \tag{10}$$

where $\mathcal{E}_\mathbf{k} = 8\pi|\Phi_\mathbf{k}|^2\exp(2\Im\omega_* t)$, and we considered both $\omega_* = \Re\omega_* + i\Im\omega_*$ and the complex conjugate frequency of excited waves $\omega_*^* = \Re\omega_* - i\Im\omega_*$.

As usual in the quasi-linear theory, in order to close the system one must engage an equation for $\mathcal{E}_{\mathbf{k}}$. Averaging over the fast oscillations, we obtain

$$(\partial/\partial t)\mathcal{E}_{\mathbf{k}} = 2\Im\omega_*\mathcal{E}_{\mathbf{k}}\,. \qquad (11)$$

Equations (10) and (11) form the closed system of quasi-linear equations for Jeans oscillations of the rotating inhomogeneous disk of stars, and describe a *diffusion* in both velocity and coordinate space.

### *4.1 Velocity Diffusion*

Growing density waves (spiral arms) excite random motions parallel to the equatorial plane. According to Eq. (10), the heating efficiency of unstable density wave features depends on their spatial and temporal form. Let us evaluate the law for the age-velocity dispersion rate $\langle v_\perp^2\rangle(t)$ and the heating $\Delta v_\perp$ for a realistic model of the disk of the Galaxy in the Solar neighborhood ($\langle v_\perp^2\rangle$ is the averaged squared velocity dispersion in the $z = 0$ equatorial plane). In accordance with the theory as developed above, we consider the fastest growing mode with $\Im\omega_* \approx \Omega$. According observations, in the Solar vicinity $\mathcal{E}_{\mathbf{k}}/\Phi_0^2 \approx 10^{-2}$ (Lin et al. 1969), $\Phi_0 \approx 0.5 r_\odot^2\Omega^2$, $r_\odot \approx 8.5$ kpc, $c_r(t=0) \approx 10$ km s$^{-1}$, and $\kappa \approx 1.5\Omega$. From Eq. (10), one easily obtains

$$\langle v_\perp^2\rangle \propto t\,, \qquad (12)$$

and $\Delta v_\perp = 20 - 30$ km s$^{-1}$, where $t = 10^9$ yr (Griv et al. 2001, 2002). These values of $\langle v_\perp^2\rangle$ and $\Delta v_\perp$ are in agreement with both estimates based on the observed stellar velocities (Wielen 1977; Grivnev & Fridman 1990; Dehnen & Binney 1998) and $N$-body simulations (e.g., Liverts et al. 2003). Thus already in the first 3-4 galactic revolutions, in say about $10^9$ yr, the stellar populations see their epicyclic energy vary by a factor of ten. de Souza & Teixeira (2007) have detected such a velocity variation in $10^9$ yr by considering the kinematic segregation of nearby disk stars.

### *4.2 Migration of the Sun's Guiding Center*

As we have mentioned above, the amplification of spiral gravitational instabilities produces not only heating but also redistribution of matter in the disk. In this connection, there is considerable scatter in the metallicities of stars that have a common guiding center and age (Edvardsson et al. 1993). On the other hand, it is widely believed that all interstellar material at a given time and radius has a common metallicity. The paradox can be resolved if one assumes that these stars were born at different radii and then migrated to its present locations as a result of a series of uncorrelated scattering events (Wielen et al. 1996).

The migration may be explained naturally by "collisions" of stars with the Jeans-unstable density waves. Let us estimate the scale of radial migration $\Delta R_\odot$ of the Sun's guiding center. According to observations, we adopt the ratio $\mathcal{E}_{\mathbf{k}}/\Phi_0^2 \approx 10^{-2}$, $m \approx 1$, $r_\odot = 8.5$ kpc, and $\Im\omega_* \approx \Omega$. Then from Eq. (10) we obtain $\Delta R_\odot = 2 - 3$ kpc (Griv et al. 2002). This $\Delta R_\odot$ is in fair agreement with the estimate of Wielen et al. (1996) $\Delta R_\odot \approx 1.9$ kpc based on a radial galactic gradient in metallicity. We conclude that the Sun has migrated from its birth-place at $r \approx 7$ kpc in the inner part of the Galaxy outwards by approximately 2 kpc during its lifetime of $t \approx 4.5\times10^9$ yr.

## 5. Summary

With passage of time as the perturbation energy increases, the initial distribution spreads ($f_0(v_\perp^2)$ becomes less peaked) and the temperature grows (Eq. (12)). In other words, the relaxation of the stars takes place. Formally, the relaxation corresponds to the presence of the collision integral on the right-hand side of Eq. (10). In addition, the radial spread of the disk is increased. The diffusion in configuration space is due entirely to the growth of the Jeans-unstable modes ($\Im\omega_* > 0$) in a self-gravitating collisionless system subject to a time-dependent potential.

*Acknowledgements.* The authors were supported in part by the Israel Science Foundation and the Israeli Ministry of Immigrant Absorption.

## References

Edvardsson B., Andersen B., Gustafsson B., D.L. Lambert et al.: 1993, *A&A,* **275**, 101.
Dehnen W., Binney J.: 1998, *MNRAS,* **298**, 387.
Griv E., Gedalin M., Eichler D.: 2001, *ApJ,* **555**, L29.
Griv E., Gedalin M., Eichler D., Yuan C.: 2000, *Phys. Rev. Lett.,* **84**, 4280.
Griv E., Gedalin M., Yuan C.: 2002, *A&A,* **383**, 338.
Griv E., Peter W.: 1996, *ApJ,* **469**, 84.
Grivnev E., Fridman A.: 1990, *Soviet Astr.,* **34**, 10.
Krall N.A., Trivelpiece A.W.: 1986, *Principles of Plasma Physics.* San Francisco Press.
Lin C.C., Yuan C., Shu F.H.: 1969, *ApJ,* **155**, 721.
Liverts E., Griv E., Gedalin M., Eichler D.: 2003, in *Galaxies and Chaos,* ed. G. Contopoulos, N. Voglis. Berlin, Springer, p. 340.
Morozov A.G.: 1981, *Soviet Astr.,* **25**, 421.
de Souza R.E., Teixeira R.: 2007, *A&A,* **471**, 475.
Shu F.H.: 1970, *ApJ,* **160**, 99.
Wielen R.: 1977, *A&A,* **60**, 263.
Wielen R., Fuchs B., Dettbarn C.: 1996, *A&A,* **314**, 438.

# GENETIC ALGORITM ECLIPSE MAPPING

A.V. Halevin

Department of Astronomy, Odessa National University
T.G.Shevchenko Park, Odessa 65014 Ukraine, *halevin@odessa-astronomy.org*

ABSTRACT. In this paper we analyse capabilities of eclipse mapping technique, based on genetic algorithm optimization. To model of accretion disk we used the "fire-flies" conception. This model allows us to reconstruct the distribution of radiating medium in the disk using less number of free parameters than in other methods. Test models show that we can achieve good approximation without optimizing techniques.

**Key words**: methods: numerical - stars: novae, cataclysmic variables - accretion, accretion disks

## 1. Introduction

Eclipse mapping (EM) techniques are used for reconstruction of accretion disks structure in cataclysmic variables. Eclipse mapping was developed by Horne (1985). One of the most important possibilities of EM is reconstruction of the radial temperature distribution inside accretion disk. It allows to test the different accretion disk models. EM has now many modifications, such as flickering mapping (Bortoletto & Baptista 2004), 3D eclipse mapping (Rutten 1998), stream eclipse mapping with "fire-flies" (Hakala 2002), genetic algorithm EM (Bobinger 1999) and Physical Parameters Mapping by Vrielmann (1997).

In this paper we propose extension of the EM with fire-flies for reconstruction of radiating medium in the systems with flat and optically thin accretion disks.

## 2. The fire-flies conception and the algorithm.

The idea of fire-flies mapping was developed by Hakala (2002) to reconstruct the structure of accretion flows in eclipsing polars. In this method radiation is modeled by a set of points with angle-dependent emission. Using genetic algorithm techniques it is possible to evolve of fire-flies spatial distribution to fit eclipse light curve by summing the brightness of the fire-flies visible at each phase. The distribution of fire-flies gives us an emission volume. The mostly luminous parts of accretion stream are visible as a larger number of fire-flies placed in a smaller volume.

To model of accretion disk we used the fire-flies with isotropic emission, which reduce the number of variables, associated with single fire-fly to only two plane coordinates. So, in the frame of this conception, we can calculate of emission of accretion disk with formula

$$F_{disk} = \frac{F_0}{n_p} \sum_{j=1}^{n_p} E(\phi), \qquad (1)$$

Here $F_0$ is uncovered total accretion disk flux, $n_p$ is a number of fire-flies, $E(\phi)$ is an eclipse function, which equal to 0 if fire-fly is eclipsed and equal to 1 if fire-fly is visible (Fig.1).

As a fitting-function we used $\chi^2$ model parameter with some extension:

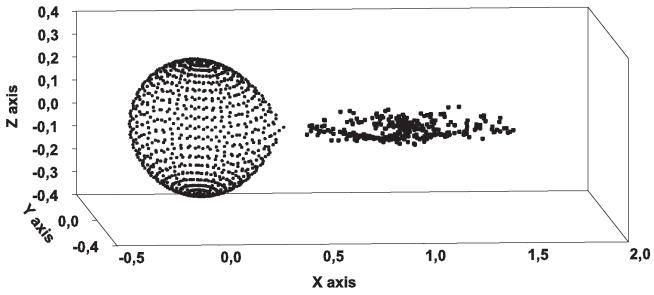


Figure 1: Model scheme.

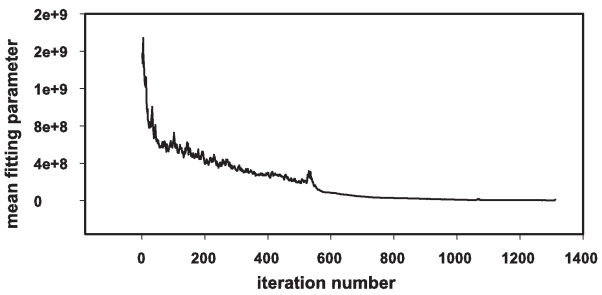


Figure 2: Mean fitting parameter evolution.

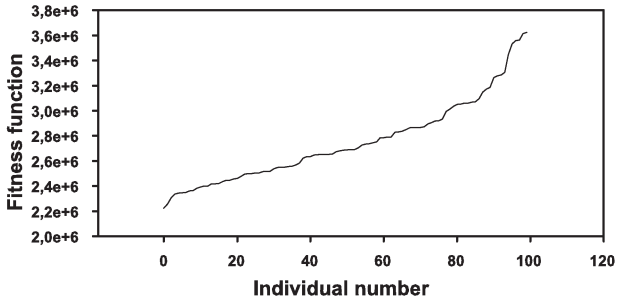


Figure 3: Distribution of individuals in offspring by the fitting parameter.

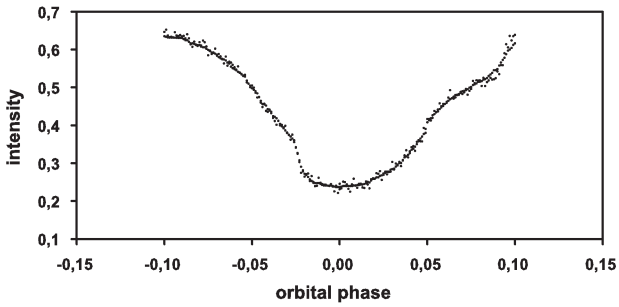


Figure 5: Artificial light curve and fit for hot spot model.

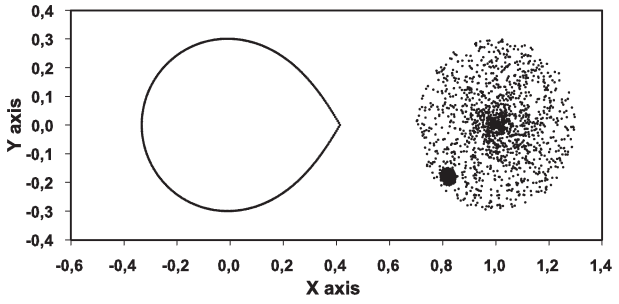


Figure 4: Initial model of accretion disk with hot spot.

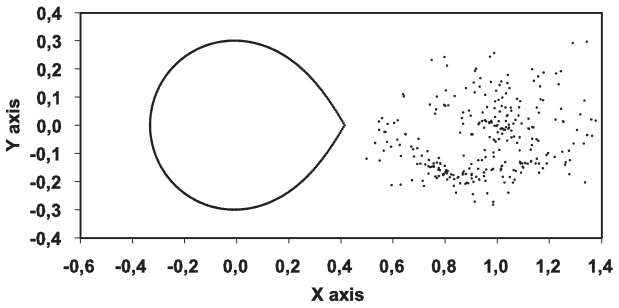


Figure 6: Distribution of fire-flies for hot spot model.

$$f_i = \frac{1}{\chi_i^2 + \lambda e_i} \tag{2}$$

where $e_i$ is an entropy parameter, which we calculate as a mean value of first 100 minimal distances between pairs of particles. $\lambda$ is some constant which controls the importance of the smoothness for the quality determination.

As a fitting algorithm we have used a Genetic algorithm (Charbonneau 1995) with 100 genes, crossover operations and variable mutation rate. Also we used such additional modes as conservation of the fittest individuals (so-called elitism) and catastrophic and Black Sheep regimes (Bobinger 2000). It takes about 1000÷2000 generations to achieve a good result (Fig.2). During calculations we control the fitting distribution of different individuals (Fig.3), to avoid degeneracy in the offspring.

As a free parameters in our models are used the total disk flux $F_0$, constant non-eclipsed component and $n \times 2$ parameters of fire-flies coordinates. As usually, in our models we have used $n = 300 \div 400$ to achieve reasonable computational time. Each unknown variable has 6-digits precision. Initial population is generated as a set of points, randomly distributed inside Roche lobe of the compact star. Actually, we have two heterogeneous sets of parameters: main constants which describe system luminosity and coordinates of the points. To achieve a faster convergence, during first iterations we used increased mutation rate for the first set of parameters.

## 3. Test models

To test of our method we have made several artificial configurations of accretion disks. The most typical situation for low luminosity states is the presence of three main radiation sources: the accretion disk, hot spot where accretion stream couples with disk and filled its Roche lobe secondary star (Fig.4). In the Fig.5 one can see resulted light curve with added noise and the best fit (Fig.6) represents eclipse map, which have found with eclipse mapping method. One can see that main radiation sources are traced very well. Distortions of the image are typical for eclipse mapping techniques (see Horne 1985). So this method allows resolve compact sources in accretion disk.

Several cataclysmic variables show significant asymmetry of their disks which arise due to tidal effects.

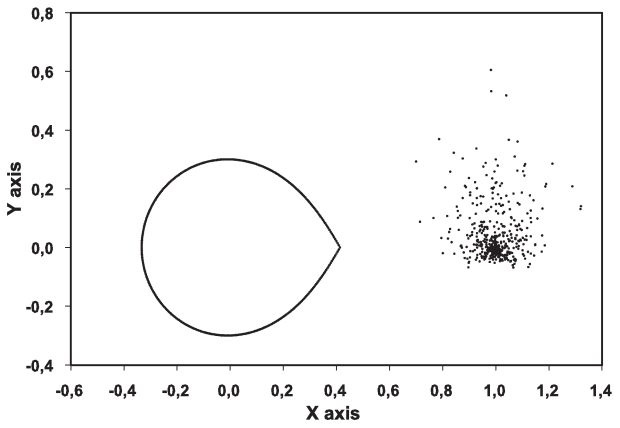


Figure 7: Model of elliptical accretion disk.

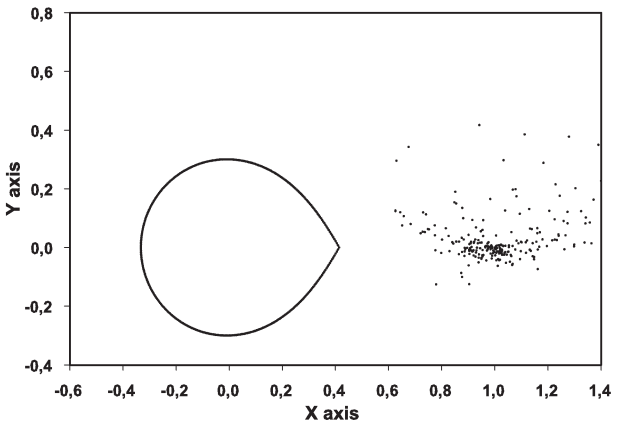


Figure 9: Reconstructed fire-flies distribution for elliptical accretion disk model.

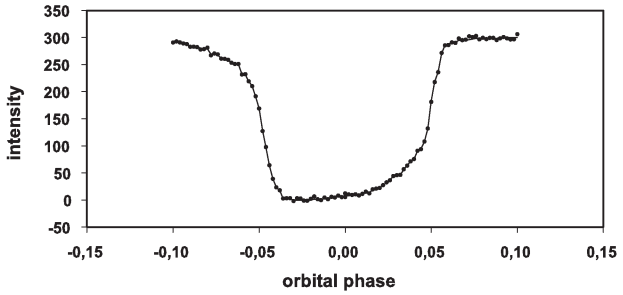


Figure 8: Artificial light curve and fit for elliptical accretion disk model.

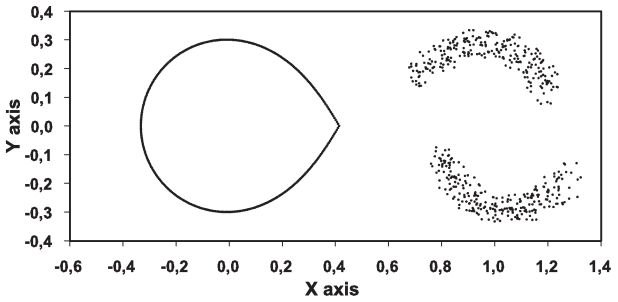


Figure 10: Model of spiral arms structure in accretion disk.

This feature is shown as so called superhumps on light curves. To test such situation we modeled elliptical accretion disk with radiation concentrated near white dwarf (Fig.7). Eclipsing profile and model fit for such configuration one can see in the Fig.8. Resulted distribution of fire-flies in the Fig.9 shows very close to initial distribution picture. There is also some distortion along x-axis.

Sometimes in accretion disk we can observe spiral arms, which are also product of tidal forces. This feature is traced only by emission lines. We tried to test reconstruction of such configuration using our modification of eclipse mapping. Light curve with fit and initial emission distribution are in Fig.10 and Fig.11. Fig.12 shows that we can determine the presence of this feature.

## 4. Discussion

Here we see that the fire-flies based eclipse mapping allows reconstruct of accretion disk structure with some x-axis distortions, which are typical for this class of methods. It is interesting that we do not used any regularization techniques to achieve appropriate result. We must say that our method has good convergence because several consecutive calculations for the same light curve gave the same results. The only one important restriction for such approach is demand to accretion disk to be optically thin. Significant opacity in accretion disk is observed as non-eclipse mid-time scale variability because short time scale variability, so called flickering, is the consequence of unstable processes in active regions of accretion disk. Previous investigators in their works used de-trending of eclipsing part of light curve to avoid an influence of covering effects in the disk. So, we can reconstruct only visible directly before and after the eclipse parts of accretion disk. It is obvious that we can see source which are mainly close to the secondary star due to opacity effect.

So the most adequate model could be the combination of radiating fire-flies with some opaque medium.

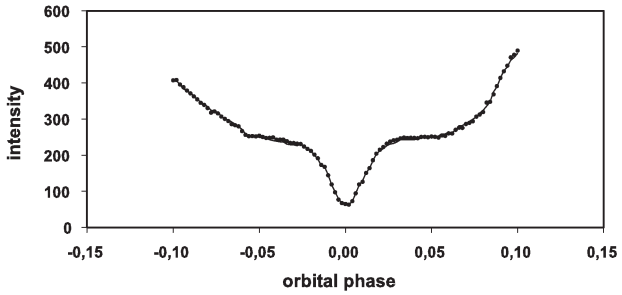


Figure 11: Artificial light curve and fit for model of spiral arms in accretion disk.

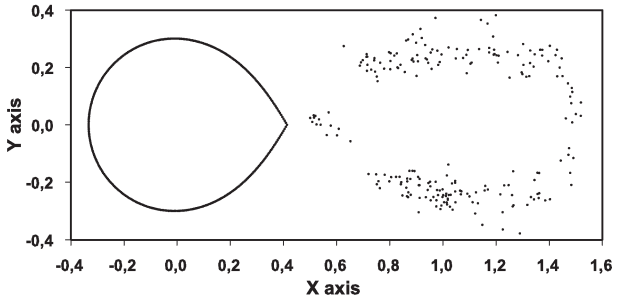


Figure 12: Reconstruction of spiral arms in accretion disk.

The main problem is how we must model of this opaque medium. If we use it distribution as a free parameter the model will be poorly conditioned. If we use some predetermined configuration of an opaque medium it dramatically simplifies the model. In our next papers we are going to use some models for opaque medium to fit also non-eclipsing parts of light curves.

## 5. Conclusions

Using several artificial configurations typical for accretion disks of cataclysmic variables we tested fire-flies conception based eclipse mapping technique. Our results show that we can use it successfully to reconstruct of radiating medium distribution in optically thin flat accretion disks.

*Acknowledgements.* The author is thankful to S.V.Kolesnikov for helpful discussions during development of this method.

## References

Bobinger A.: 2000, *A&A*, **357**, 1170.
Bortoletto A., Baptista R.: 2004, *RevMexAA Conf.Ser.*, **20**, 247.
Charbonneau P.: 1995, *Ap.J. Suppl. ser.*, **101**, 309.
Hakala P., Cropper M., Ramsay G.: 2002, *A&A*, **334**, 990.
Horne K.: 1985, *MNRAS*, **213**, 129.
Horne K.: Stiening R., 1985, *MNRAS*, **216**, 933.
Rutten R.G.M.: 1998, *A&ASupl*, **127**, 581.
Vrielmann S.: 1997, *PhD Theses.*

# NEW CONCEPT OF HUNGARIAN ROBOTIC TELESCOPES

Hegedüs T., Kiss Z., Bíró B. and Jäger Z.

Baja Astronomical Observatory of the Bács-Kiskun County,
H-6500 Baja, Szegedi út, KT.766. Hungary
*hege@electra.bajaobs.hu*

ABSTRACT. As the result of a longer innovation of a few Hungarian opto-mechanical and electronic small companies, a concept of fully robotic mounts has been formed some years ago. There are lots of Hungarian Automated Telescopes over the world (in Arizona, South Korea, Izrael and atop Mauna Kea, just below the famous Keck domes). These are cited as HAT telescopes (Bakos et al. 2002), and served thousands of large-frame time-series CCD images since 2004, and the working team found already 6 exoplanets, and a number of new variable stars, etc... The newest idea was to build a more robust robotic mount, hosting larger optics (D > 50 cm) for achieving much fainter celestial objects, than the HAT series (they are operating with Nikon teleobjective lenses) on a still relatively wide celestial area. The very first sample model is the BART-1, a 50cm f/6 telescope.

**The Baja Observatory and the Robotic Telescope System:**

The observatory is located in south of Hungary, close to the Serbian-Croatian common border, at the Danube. Geographical coordinates are: N 46 10 48.6 E 19 00 39 (in WGS-84 system). We operated here a 40 cm Classical Cassegrain Telescope made in the Odessa Astronomical Observatory, between 1985-1991. Since 1995, the main telescope was a 50 cm f/8.4 Ritchey-Chrétien type equatorial fork mount telescope (made by OGS, US). The latest development was the design and built of a fully robotized 50 cm f/6 modified-Cassegrain type telescope (made by Fornax 2002 Ltd. and theirs collaborators in 2004-2005, Hungary). This project has been supported by the Hungarian National Fund of Development, grant no.: MFC-03 0501 04. The full cost of the project were about 74,400 EUR, including some important sub-systems (an all-sky night camera, an automatic meteorological station, and the main CCD detector) as well as all the necessary bricklayer works at the site. The development of the telescope is partly underlying the existing scientific-technology cooperation between our observatory and the Sternberg Astronomical Institute of Moscow State University. The main technical details of the mount:

- The control system is running under Real-Time Linux on an industrial PC (there were not any frozening during the continuous operation in the last 1 year!)
- Drivers and the graphical environment and the official web site are written in Hungary (by Mr. Lázár, J. in C++, Mr. Kiss, Z. in IDL, and Jäger, Z. respectively)
- The robust mount is driven by 3-phases stepper motors
- The resolution of the motors are $0.25''$/step
- The maximum speed of the telescope (in GOTO mode): about $3^\circ$/sec
- The periodical error of the RA axe: about $\pm 5''$ (valid for the base model)
- An existing optional upgrade: closed-loop PEC - with this $< \pm 1''$ (!)

Figure 1: BART.

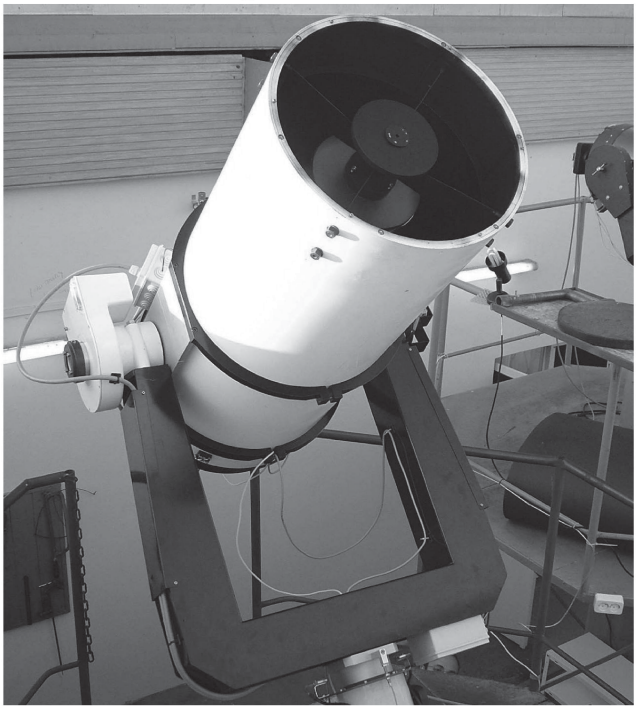

- The focusing of the optical tube is not done by the movement of any of the optical elements (as usually worldwide), but by a stepper-motor controlled special-design modified Crayford-type focuser
- The optical system is re-modelled by Dr. Bíró (Baja Observatory) by OSLO software
- There were a subsequent refinements in the original design (calculated and built by Baja staff and of the Physical Institute of Pécs University).
- The automated large-format filter selector system is also Hungarian-made

**The imaging capabilities of BART-1:**

The relatively large (flat-corrected) field of view, together with a large-scale CCD chip are the inseparable parts of the "BART" series concept. The present optical system is an 50 cm f/6 modified Cassegrainian. The main CCD detector is an Alta U 16 (made by Apogee Inc., US) uses Grade 2 KAF16801E front-illuminated chip (4096x4096 $9\mu$ x $9\mu$ format pixels). This combination yields an about 42x42′ wide field of view. This is presently the largest in Hungary, and also in CESE region (see the example single shot on Fig. 2).

*The main technical details of the camera:*

- imaging area: 36.86 x 36.86 mm (typical)
- digitization rate: 5 MHz (in 12 bit mode) 1 MHz (in 16 bit mode)
- Quantum Efficiency at the peak: 66% (at 580 nm)
- Linear Full Well capacity: about 100,000 $e^-$
- nominal dark current: 1 $e^-$ /pixel / sec (at -20°C)
- cooling: Peltier, max. 40°C below ambient (water circulating is an option)
- read-out noise: about 15 $e^-$ RMS typical (at 1 MHz)
- control: USB 2 interface (average download time of 1x1 bin: 11 secretary)
- programmable on-chip binning: from 1x1 to 10x4096

**The present plans, scientific and educational programs:**

BART robotic telescope system is specially designed for small observatories and universities of Central-East-South Europe, since it is a low cost, widely utilizable complete instrument. It can be started from as low as 37,200 EUR, which has no competing telescope at this range and at this level of automatization (of course, this lowest level of price is valid without any extras, CCD detector, etc., i.e. simply the base model, complete with the optical tube and of the control system, too).

Figure 2: h and $\chi$ Persei.

**Science with BART-1:**

- supernova search (in cooperation with Szeged Universitiy team)
- systematic crowded-field long-time-series photometry of selected fields (in cooperation with Konkoly Observatory)
- minor planets and comets (cooperation with Szeged & Modra Observatories)

**Education with BART-1:**

- the "deep sky in the classroom" initiative (remote observation by students)

**References**

Bakos et al.: 2002, *PASP*, **114**, 974.

# CESEB: A REPORT ON LATEST RESULTS

T. Hegedüs[1], O. Latkovic[2], H. Markov[3],
I. Vince[2], A. Cséki[2], J. Nuspl[4], N. Markova[3],
E. Rovithis-Livaniou[5], J. Vinkó[6]

[1] Baja Astronomical Observatory of the Bács-Kiskun County H-6500 Baja, Szegedi út, KT.766. Hungary
[2] Astronomical Observatory Volgina 7, 11160 Belgrade, Serbia
[3] Institute of Astronomy, National Astronomical Observatory p.o. box 136, 4700 Smolyan, Bulgaria
[4] Konkoly Observatory H-1525 Budapest, PF.67, Hungary
[5] Astronomical Institute, National Observatory of Athens Zografos, Athens, Greece
[6] Department of Optics & Quantum Electronics, University of Szeged POB 406, Szeged H-6701, Hungary

ABSTRACT. Central-East-South European Binary star study group - CESEB - is an international research team focused on the study of binary stars through combined spectral and photometric observations that can be made using the Bulgarian NAO 2m telescope and several smaller telescopes located at various places in the Central East South European region. This paper is a report on our activities and results.

**Key words**: Stars: binaries: eclipsing - stars: binaries: spectroscopic - stars: radial velocity curve - stars: individual: HS Her, EP And

## 1. Introduction

Several eclipsing binary systems have been selected for combined spectral and photometric observations using the Bulgarian NAO 2m telescope and several smaller telescopes located at various places in the Cental-East-South European (hereafter CESE) region. A pilot study were started in 2001, about radial velocity and light curve variations of the active W UMa system LS Del, which has been presented in 2005 (Hegeds et al., 2006). After that, the continuous photometry and simultaneous spectroscopy has been started for the selected list of targets. The present paper is a temporary status report of our international working group.

## 2. CESEB Spectroscopy

Spectroscopic observations in the frame of CESEB collaboration have been made at National Astronomical Observatory Rozhen, Bulgaria, in the period form 2002 to 2007, with the 2-m Ritchey-Chretien telescope and the Coude horizontal spectrograph, with wavelenght range of approximately 200 Å centered on two areas of interest: around Na I D1/D2 (5889.95/5895.92 Å) lines, and around Mg II (4481.15 Å) line.

Data reduction for all the observations has been done at Astronomical Observatory of Belgrade, Serbia, using standard IRAF packages for CCD reduction; images were bias and flatfield corrected, cleaned from cosmic rays, and wavelength calibrated using reference spectra of a ThAr lamp. The extracted spectra were continuum-normalized, and image headers were supplemented by the calculated corrections for radial velocity of Earth's motion. The reduction process was carefully standardized in the hope of future automatization.

So far radial velocities have been measured from Doppler shifts of spectral lines; this method is suitable for single-lined binaries and systems with relatively few lines in the selected spectral regions, but fails, for instance, in the case of V994 Her (which is a suspected hierarchical 4-body system) although this object hase the best phase coverage, or in the case of RX Her which, on the other side, prooved to have too few prominent lines. However, preparations are underway to measure radial velocities of all objects using the more advanced cross-correlation and spectral disentangling techniques.

In the following section we present the preliminary results of radial velocity measurements for HS Her.

### *2.1. HS Her*

HS Herculis is a bright ($m_v = 8.61$) detached binary system with a blue giant primary (Sp. B6III + A4); it has been a target of many photometric measurements due to the its apsidal motion and a suspected third body in the system (Wolf & al. 2002). However, the only previos spectroscopic measurements were made by Cesco & Sahade (1945).

We have obtained a single-lined radial velocity curve

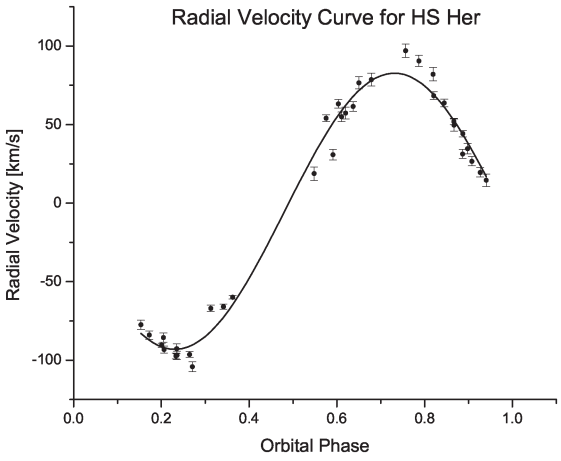


Figure 1: Radial velocity curve for HS Her.

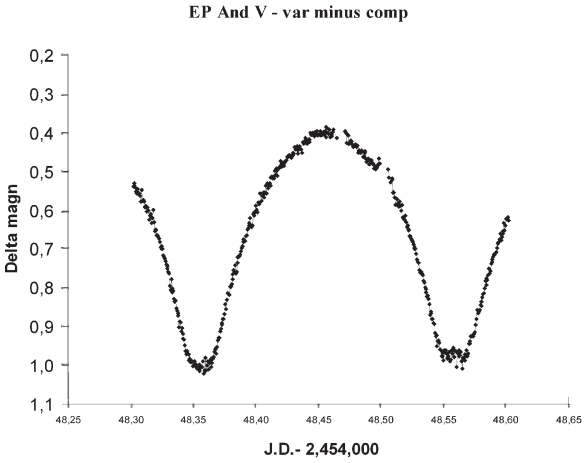


Figure 2: Figure 2. The sample photometric data from BART-1

for HS Her (Figure 1) from 35 observations. We used lines of neutral helium and ionized magnesium (He I at 5875.62, 4387.93 and 4471.48 Å and Mg II at 4481.23 Å) to calculate Doppler shifts of observed spectra, in which we measured the central wavelengths by fitting Gaussians to the lines.

Fitting the radial velocity curve to the data was done using PHOEBE (Prsa & Zwitter 2005), a modelling facility based on Wilson-Devinney code. The free parameters of the fit were the system's semi-major axis, center of mass radial velocity, mass ratio, eccentricity, and the argument of perriastron, while we fixed the values of period to $P = 1.63743125$ days (from Wolf & al. 2002) and the inclination to $i = 88°.5$ (Martynov et al. 1988). The results are given in Table 2.

Table 1: Results of radial velocity curve fitting for HS Her.

| Parameter | Value |
|---|---|
| $K_1[\frac{km}{s}]$ | $90 \pm 5$ |
| $S.m.a[R_\odot]$ | $7 \pm 1$ |
| $\gamma[\frac{km}{s}]$ | $-7 \pm 2$ |
| $\omega[deg]$ | $25 \pm 20$ |
| $q = \frac{m_2}{m_1}$ | $0.6 \pm 0.2$ |
| $e$ | $0.08 \pm 0.03$ |

## 3. CESEB Photometry

We made numerous BVR measurements of the target systems of CESEB cooperation during 2001-2007 at the Baja Observatory, using the Apogee AP7 CCD of the 50 cm f/8.4 RC telescope, and V measurements using the new 4k2 Apogee Alta U16 CCD on the brand-new 50cm f/6 MC robotic telescope. Large part of these data are mainly served as exact timing of one or both minima of the target systems for having good phases for construction of the RV curves. Some complete light curves were also obtained, good enough for light curve analysis - see e.g. Figure 2. The analysis of these data sets are under way.

*Acknowledgements.* The authors wish to acknowledge the support of Ministry of Science of Republic of Serbia, that supports this research through project no. 146003.

### References

Cesco, C. & Sahade, J. 1945, *ApJ,* 101, 114
Hegedüs et al. 2006, *ApSpSci,* 304, 51
Martynov, D. J., Voloshina, I. B., Khaliullina, A. I., 1988, *Astron. Zhurnal,* **65**, 1225.
Prsa, A., Zwitter, T.: 2005, *Astrophys. J.,* **628**, 426.
Wilson, R. W., Devinney, E. J.: 1971, *Astrophys. J.,* **166**, 605.
Wolf, M., Harmanec, P., Diethelm, R., Hornoch, K., Eenens, P.: 2002, *A&A,* **383**, 533.

# OFFSET GUIDE OF THE ZEISS-2000 TELESCOPE

N.V. Karpov[1], V.Ya. Choliy[1,2]

[1] International Center for Astronomical, Medical and Ecological Research, Terskol, Russia
*karpov@terskol.com*

[2] Kiev Schevchenko University, Kiev, Ukraine
*charlie@mail.univ.kiev.ua*

ABSTRACT. We present offset guide of 2-m-Zeiss-RCC telescope of the Terskol observatory. The main goal of the device is to help in the observations of the faint or moving objects and made the process as much as possible automatic. The device is equiped with the optical system, CCD cameras and controller to connect the device to the computer. Hardware is controlled with the software written in our team. That software is working unger Windows operation system and is based upon the system level hooks which allow us to catch the messages from the mouse and keyboard and react accordingly. Second part of the software manages the messages sent to and received from the stepping motors microprocessor controller which are used to manipulate with the position of the optical system of the device.

There are two different setup mode of the offset guide: guiding of the inmovable objects and guiding of the moving objects like comet or asteroid. The management of the optical subsystem and CCD cameras is doing in both cases by software only.

First results of the observations with the new offset guide show us that the device is quite usefull in the automatization of the observation on 2-meter-RCC telescope.

**Key words**: Observations: telescopes: appliances; guiding: automatic systems: offset guide.

## 1. Introduction

During the observations of the faint objects, long time exposures and guiding of the objects with the apparent motions it is necessary to guide the telescope with high precision. Offset guiding allows us make quality observations as offset guide works in the same conditions as the other receivers on the telescope does, and take the light beams from the main telescope mirror. It means that geometry of the offset guide is very close to the geometry of any other receivers.

Offset guide doesn't use any of personal features. Equipped with the CCD camera it cancels a possible personal errors and helps us to save the observation time. Wasting the time during the observation caused with the list of the reasons. These are:

- slow movement of the platform with the observer; very often it is impossibe to place the platform in the position where the observer can reach the current position of the eyepieces of the guide and finder;
- long time for the selection of the appropriate guidance star;
- in the observation of the moving objects it is necessary to extrapolate the direction and possible cruising rate of the guide until its physical limits; the situations when the exposure still continues but there is no place to move should be totally avoided;
- sometimes the guide may move to the unreacheable position and it will cause the observer to finish the guidance, somehow in the middle of the exposure;
- we should be really carefull when manipulate the platform with the observer in the vicinity of the telescope or attached devices.

## 2. Hardware

Offet guide is placed in the telescope mounting zone behind the main mirror and the image is build with the optical system which may undergo some movements with the help of micrometer screws in the Cassegrain focal plane.

Focusing features of the offset guide itself allows additional focusing in the range of 12 mm. General field of view is 125 × 125 mm. Output part of the offset guide have the possibility to switch the viewfield and to set up different light filters.

General internal view of the offset guide is shown on the Figure 1. Numbers on the picture mean 1 - Y-coordinate carriage, 2 - collimator, 3 - mirrors, 4 - X-coordinate carriage, 5 - final switches.

Figure 2 shows the viewfields of CCD cameras installed with the offset guide. Field of view of the telescope $1^o10'$ occupied with two central cameras 1,2 (red and blue channels), wide field camera 3, special purpose camera 4 and offset guide camera 5. Part of the field of view (11') is directed to the CCD5 with the system of mirrors, shown as part 3 on the fig.1.

Overall architecture of the offset guide and its connections shown on the next Figure 3.

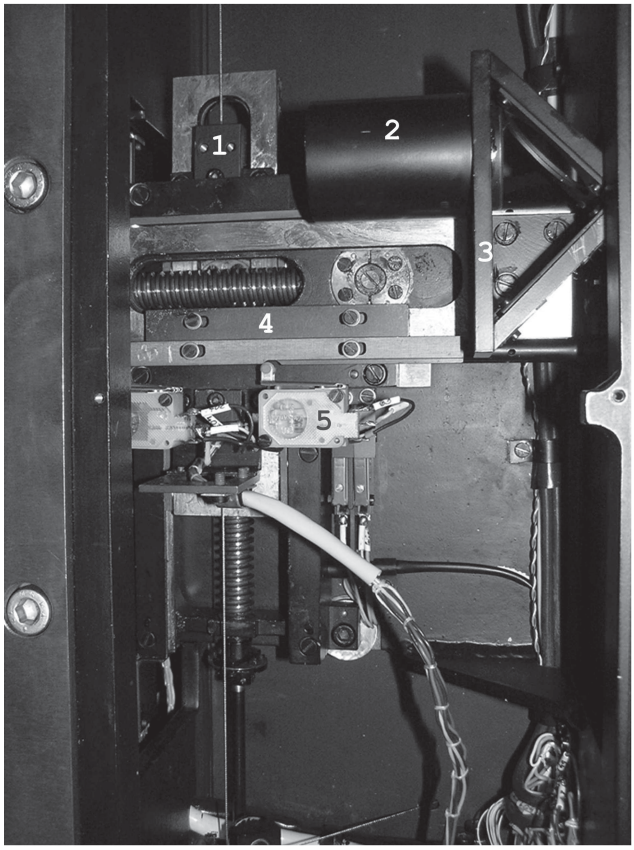


Figure 1: Offset guide internals.

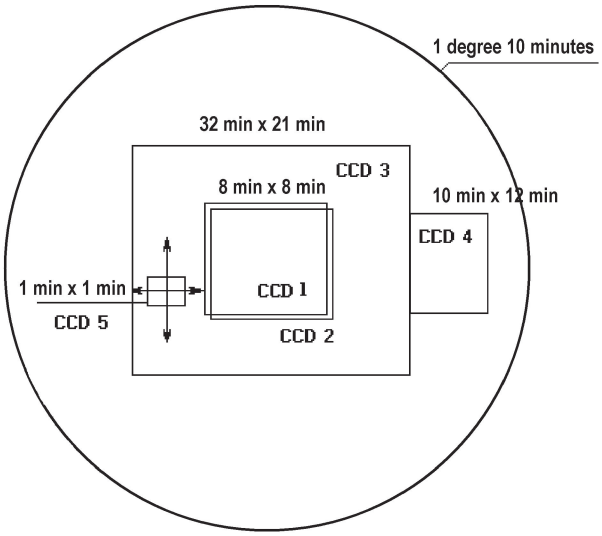


Figure 2: Viewfields of CCD cameras.

Table 1: CCD cameras used in the offset guide.

| camera | pixels | seconds |
|---|---|---|
| ST-4 | $192 \times 165$ | $32 \times 28$ |
| ST-7 | $768 \times 510$ | $76 \times 51$ |
| SAO | $600 \times 400$ | $75 \times 41$ |

One of the main parts of the offset guide is stepping motor controller C10, produced in Germany by the ISEL. The named controller has build in programmable memory to store programs. With the RC-232 interface it may be connected to the PC and programmed with the special set of the commands. It may manage up to three stepping motors with the different speeds up to 10000 steps per second.

We use only two motors to presicely move the prism of the CCD camera. Precision of the movement is nearly 0.0005 mm/step. Movement of the prism is possible in the square $125 \times 125$ mm. In-field testing of the mechanics set upper limit for the speed of movement in 4000 steps/second. Controller automatically interpolate the movements so the movement in any suitable direction is possible simultaneously in two directions.

The last point allows steering movement of the prism with the wide range of speeds and directions. In the real world it means the possibility to follow the most of the astronomical objects in the sky, excluding, possibly, only the fastest comets and asteroids.

Movement of the prism is doing quite pecisely. The scale factors in the hour angle and declination are near 154.10 and 153.00 steps per second of arc. Used CCD camera have 0.11"/pixel, so 15 steps move the mirror for the one second in coordinate.

ST-4 Star Tracker Imaging Camera was assigned for the guiding the telescopes. It has outlets to attach to the hand control device of the telescope. By the way, Zeiss-2000 is guided with the controlling unit through the sequence of the codes via wires and/or infrared channels. The controlling unit don't allow two or more movement commands in the same time.

The ciphering chip SAA1050 was added to the camera controller to resolve this difficulty. Afterwards the list of testing observations with automatic guiding was done and that observations showed us that continuous guiding with such the unit is quite difficult task.

There are near 15 parameters which should be estimated for every observation night and for the object coordinates. These are: allowed errors in the coordinates, sizes and rates of the object center recalculation, rate of the corrections, mechanical histeresises in the telescope systems e.g.

That is why without offset guide we still use visual guiding with the help of the operator.

### 3. Software

The guiding process is controlled with the software. First of all we use Guide 8.0 as a source of the object coordinates and an overall view of the eyefield. Operator can select the stars on the screen by inserting the preliminary coordinates into Guide search fields. The

most interesting for the guiding process is that Guide 8.0 presents all necessary information in the legend, when requested. In standard case that legend is placed in the left bottom corner of the screen (See figure 4).

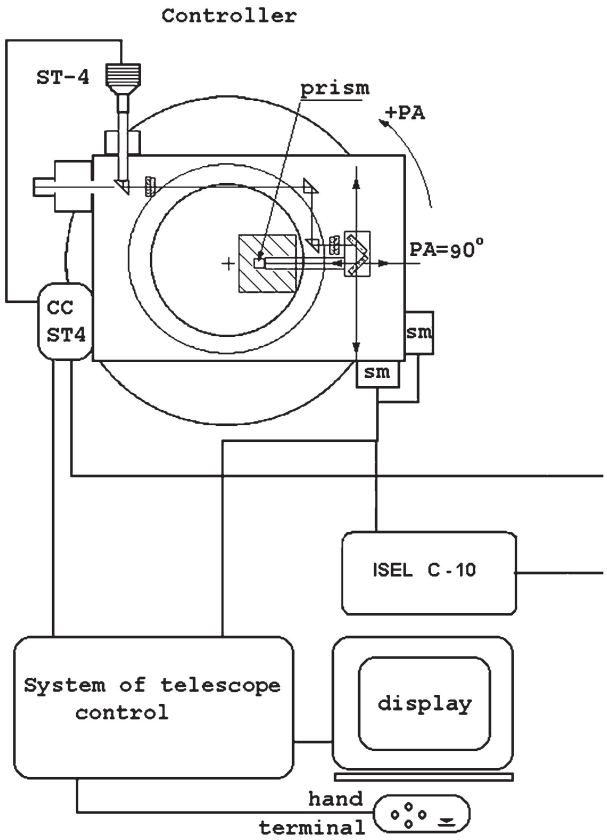


Figure 3: Schematic view of the system in general.

The Guide 8.0 is used as a binary module (unfortunately, the source code is not accessible). Taking the information from the screen of another program was our first problem. We wrote system level hook library (Hooker) which analyses any movements of the mouse pointer and pressings of the keyboard keys of Guide 8.0. This software component has only very little icon in the lower right screen corner and absolutely don't disturbs the process. Then our logic was added to the message passing process in the system.

After selection of the object operator must set up the appropriate coordinates in Guide and move the telescope to the final position. Then operator should press A button on the keyboad and click left mouse button on Guide screen in the vicinity of the telescope field center. Now the A button must be relesed. The operator repeat the explained procedure for the guiding star keeping D button pressed.

After releasing key (A or D) the Hooker reads the part of the screen with the legend and recognize the coordinates of the mouse (in this case that coordinates will be spherical right ascension and declination). The two pair of the coordinates (center of the field and guiding star) are packed and sent to Stepper component to manipulate with the offset guide mechanics.


Figure 4: Legend field of Guide 8.0.

Hooker is universal component which may be used in any case when one want to read some numbers or text from the window of another program. Hooker uses only low-level Windows API functions and may work on any existing Windows versions, even on 3.1. To make the recognition it uses neural network approach. At current moment it can recognize numbers and some subset of the latin alphabet. When used in the situation, showed in figure 4, Hooker produce 811551, 310857 and J as an result. That last symbol J give the information about coordinate system epoch. Be sent to the Stepper component these three strings cause Stepper to recalculate all necessary numbers and generate the commands to the stepping motors controller.

The Stepper component of the software is used to analyse the data from Hooker and to prepare the commands for the stepping motors. Main window of the Stepper presented on the Figure 5.

Standard ISEL controller attached to the COM port. But in most of the modern computers COM port absent or exists as an addidtional part. Most of the modern devices are controlled via USB ports. On the fig.5 one can see COM15 which is unbelievably huge number of the COM port. That is why it is really not a COM but emulation of the COM on USB. This is done with special COM to USB converter. Stepper, as we can see now may work on COM port or USB.

Before we start the observation we must first of all open the port. The buttons become to be "live" and we may manipulate with the software. Next step - homing the motors (Home button) and reloading (if necessary) the previous session parameters. (On the fig.5 we have the example with the port closed).

The white square, which occupied the most of the

window is allowed field to move the guidance mirror. Clean red and blue lines with the little square near the intersection point shows us the future position of the carriage with the guidance prism. Another little square shows current position of the prism. There are many possibilities to manipulate of the prism position: by pressing the buttons, surrounded the white square, by using the mouse pointer inside the white square, by inserting the numbers into "Future pos" or "Difference" fields. All that numbers are steps.

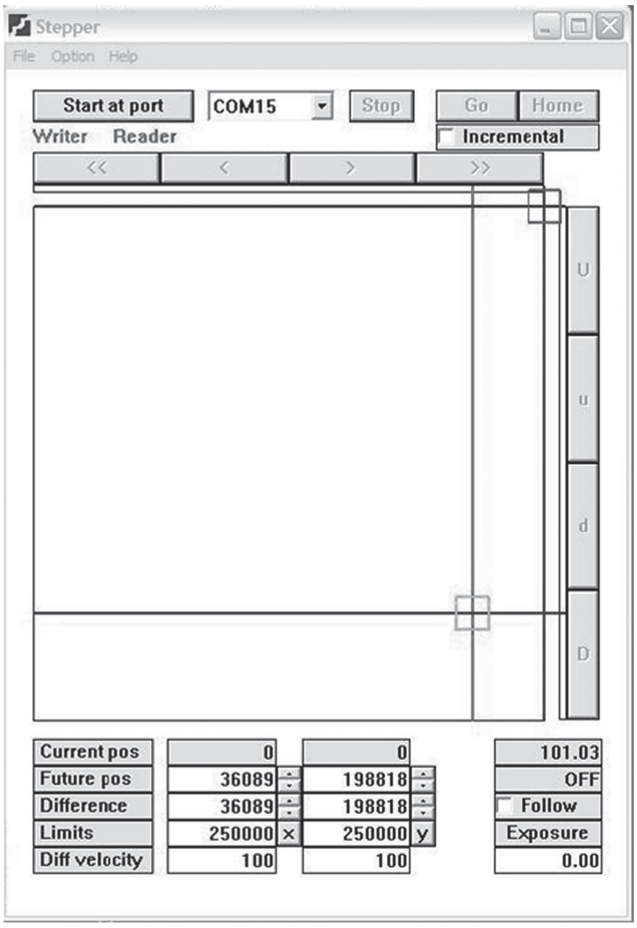


Figure 5: Overall view of the Stepper window.

There are two main setup modes of the Stepper: absolute and incremental movements. In the first case the movements are calculated from the home position of the motors. In the second - from its current position.

Another interesting possibility of the Stepper - automatic guidance with the given velocities. In this case we must insert proper numbers in the "Diff velocity" fields, setup exposure time and check "Follow" box. Stepper is quite intelligent and it allows movement of the carriage only within the specified limits (250000 steps in our case). Exposure time will be changed accordingly if with the given exposure that limits may be overcomed.

The Guide-Hooker-Stepper-Controller software works in very straightforward way - run Guide and Stepper, open port and home the motors, run Hooker. Hooker searches for that two software and if Guide and Stepper already run, the software system become ready.

All offset field is accessible with changing the angle of the telescope rotator. Stepper automatically takes the rotator angle into account. Stepper may correct the star positions for the precession and nutation if necessary. Refraction is taking into account by the telescope controller.

Review them and if all things are Ok, just press Go in Stepper window. Estimated time for carriage movement is shown in the toppest window in the rightmost window stack of the Stepper. All commands are controlled with the ISL answer. The answers are sent back to the Stepper after the finishing of the command. Until the answer is not received, the interface of the Stepper are "dead".

The Stepper is quite robust. It means that most of the operator errors are treated and the inserted numbers are just rejected. There is no possibility to move the carriage out of the physical limits. In the worst case, intermediate Home and then Go will repair the situation.

The Stepper options are managed with the special Option dialog. The information about home velocities and different shifts of the coordinate systems are presented and edithed there.

*Acknowledgements.* This job was partly supported with the UNTC grant 4134. Authors are thankful to the Head of the Terskol observatory of the International Center for Astronomical, Medical and Ecological Research, Taradiy V.K., Dr.Sci., who helped in understanding and supporting the job.

**References**

Petzold Ch.: 1997, *BVH, Saint-Petersburg,* Windows-95 programming, 876 p.

Hart J.: 2005, *Wrox Publishing, Kiev,* System Windows programming, 592 p.

# PROBLEMS OF LOCAL PLUMB RECONSTRUCTION FROM LONG-TERM ASTROOPTICAL SETS

L.Ya. Khalyavina, T.Ye. Borisyuk

Poltava Gravimetrical Observatory NAS of Ukraine
27/29 Myasoedova Str, Poltava 36029 Ukraine, *pgohal@mail.ru*

ABSTRACT. Problems of reconstruction of a local plumb variations from long sets of astrooptical observations are considered. The attempt of its practical realization on the data of latitude observations in Poltava with 3 astrometrical instruments is undertaken.

**Key words**: Astrometry: latitude variation, zenith-telescope, astrolabe; geodynamic: local plumb, the Earth figure evolution.

## 1. Introduction

Long-term sets of astrometrical observations of coordinates of station contain diverse information about processes in all geo-stratums. Most important for geodynamic is information about variations of local plumb (Gozhy, Tyshchuk,1995). Available data about local plumb are contained in slow zenith variations which are caused by many factors. There are the reasons to solve this problem now. The pure local vertical variations may be obtained after excluding such factors from zenith variations. 1) Polar component, by using C04 solution for EOP. 2) Errors of coordinates and proper motions of stars, by using new catalogues (HC, ARIHIP, FK6, Thycho-2). 3)Inexactitude of Earth rotation model, by using IAU2000 precession-nutation model. 4) Influences of tectonics of lithosphere plates, by basing on NUVEL-1 NNR model. 5) Local shifts of Earth crust, by geodetic monitoring. 6) Long-term instability of instrumental system should be researched specially. 7) Possible long-term influences of atmospheric states. The last two items are problematic. The use of the observations results obtained with several instruments at the same station gives opportunity to avoid the problems. There is the opportunity in Poltava gravimetrical observatory (PGO) where the regular observations of latitude have been conducted with 3 instruments (2 zenith-telescopes (Z-t) and prismatic astrolabe) during 30-40 years.

## 2. Initial data

For preliminary attempt to obtain local plumb variations, 3 latitude sets had been used. There is short information about them in Table 1.

Table 1: Set characteristics.

| Instrument | Observational method | Duration | Short marking |
|---|---|---|---|
| Astrolabe | equal height | 1962-2007 | FA |
| Z-t Zeiss | Talkot pairs | 1949-1987 | FZ |
| Z-t Zeiss | zenith stars | 1939-1967 | FB |
| Z-t ZTL-180 | zenith stars | 1968-2007 | FB |

The set FA and fragment of FZ (1962-1987) are reprocessed in reference to the ICRS catalogues (HC, ARIHIP, Thycho-2) and with use of the IAU2000 precession-nutation model. The combined series of bright zenithal stars observations FB were kindly given to us for analysis by colleagues A.Gozhy and M.Tyshchuk. The common analysis for three series is conducted beginning with 1962.0. The sets were reduced to single origin, which coincides with astrolabe point, by using the geodetic determining (Popov, Budz'ko,1980; Samoilenko *et al.*,1999). The geodetic measurements do't show relative displacements of instruments during twenty years. GPS observations, that began in PGO in 2001, also reveal the absence of horizontal moving. The change of latitude due to move of Eurasian plate is taken into account. Non-polar components of latitude are obtained by excluding of the polar ones, by using C04 EOP solution. Long-term instrumental instability are determined most carefully for astrolabe (Khalyavina *et al.*, 2001). So the resulting series are refined from factors 1-6.We mark them as ZA,ZZ,ZB, respectively. Due to some uncertainty of instrumental errors for FZ set the common analysis of three series have shortened up to 1981.0.

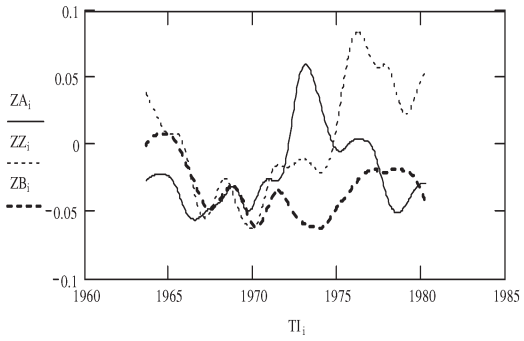


Figure 1: Slow zenithal variations in meridian observations with 3 instruments.

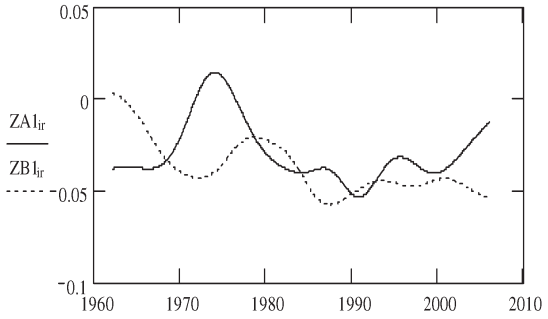


Figure 2: Slow zenithal variations from observations with astrolabe and zenith-telescope ZTL-180.

### 3. The reconstruction variances

In order to obtain slow zenith variations the series ZA,ZZ,ZB was smoothed by movin method with Gauss window with 1,5 year w high-frequency variations of zenith in meric cut down. The smoothed curves are presente

During of 1964-1972y. all curves were locat ridor with width less then 0,05″ and correlati cients between them approached to 0,9. Thi may be one of the basic segments for recon of local plumb. Since 1972 the curves div bly up to 0,12″. Similar results had been in the earlier analysis (Popova *et al.*,1983). T ble reason of the divergences may be due to of non-modeling refraction on diverse observ stars (zenithal, meridional, at equal heights). that discrepancies of real conditions of at from its standard model differ considerable case. Indirectly it is confirmed by degree of c between the short-periodic components for ZB sets: corr($ZA^s$,$ZZ^s$)=0,11; corr($ZA^s$,ZI corr($ZZ^s$,$ZB^s$)=0,37. The components depen on refractions.

Obviously, refractional and plumb effect be separated for the middle-term variations $(1.5 < T < 6.0)$. As the atmospheric influ more instable comparing the slow variations we have increased the smoothing window to So refractional influences on resulting curves diminished considerably. In Fig.2 new versio ations of meridional component of zenith fo and ZB is presented on 44-year interval (196

The divergences between two curves do n 0.055″ now. For long-term intervals they in bounds of 0.01″. These segments are ones, which are cleaned from refractional i to a marked degree. We suppose that they the supported data for local plumb recons The average meanings of ZA and ZB dat corresponding intervals can be seen as a first

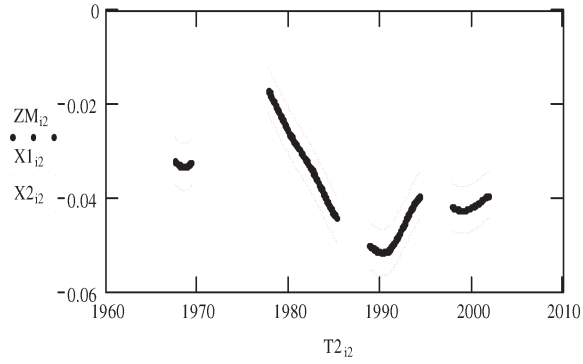


Figure 3: Fragments of reconstructed plumb variations in Poltava.

Derived fragments of curve ZM show: 1)non-linear character of changes; 2)the negative trend with rate about -0.0006"/y. on interval 1962-2006y. The results should be thoroughly checked and compared with data of other geophysical sciences.

*Acknowledgements.* The authors are thankful to our colleagues A.Gozhy and M.Tyshchuk for giving of the new version of data of zenith bright stars observations.

### References

Gozhy A., Tyschuk M.: 1995, *Journees, Warsaw,* 170.

Budz'ko V.K., Popov N.A.: 1980, *Vrashchenie i prylivnye deformatsii Zemli.,***12**, 84.

Samoilenko O.M., Zayets'V.V., Markitan O.V.: 1999, *Report of research work,* 23p.

Khalyavina L.Ya., Kislitsa Ye.N., Borisyuk T.Ye. *et al.*: 2001, *Kinemat. and Physik of celest. bodies,* **17**, 372.

Popova R.I., Podschipkova Ye.I., Otkidach L.S.: 1983, *Vrashchenie i prylivnye deformatsii Zemli.,* **15**, 60.

# THE INTERNATIONAL HELIOPHYSICAL YEAR 2007-2009 AND IMMEDIATE TASKS OF MODERN METEOR SCIENCE

S.V.Kolomiyets

Kharkiv National University of Radioelectronics,
14 Lenin ave., Kharkiv, 61166, Ukraine
*s.kolomiyets@gmail.com*

The IGY had given impetus to the development of meteor research all over the world and first of all in the republics of the former Soviet Union in Russian language. Meteors have appeared extremely important in numerous aspects for IGY1957 taking into account the incoming space era and revolutionary implementation of radar methods in scientific researches. Meteor particles in the terrestrial atmosphere together with the Sun influence on the conditions in the ionosphere. Geophysical aspects (turbulence, composition, etc.) and meteor activity were in the ranks of meteor research tasks of the IGY. Meteor researches were included into the section V "The Ionosphere. Meteors" in the IGY 1957 Program (Fig. 1, 2).

The IHY Conveners had included the meteor researches into the IHY program under the title "Meteors, Meteoroids and an Interplanetary Dust". This title emphasizes the widening of area of meteor research in new Heliophysical year http://ihy2007.org. During the Geophysical year 1957 the phenomena caused by meteor particles (the meteors) were studied directly in the terrestrial atmosphere (Kolomiyets & Sidorov, 2007). During the incoming Heliophysical year meteor particles (meteoroids) will be an object of study on all an extent from the Sun up to borders of Solar system will be studied, actually on all an extent of a heliosphere (Kolomiyets & Slipchenko, 2007). Using meteor monitoring in the frame of the International Year Planet Earth (IYPE) together with preserving orbital data in the frame of the Electronics Geophysic Year (eGY) is discussed. The coordinated investigation program CIP at number 65 "Meteors in the Earth atmosphere and Meteoroids in the Solar system" in the list of the IHY is presented http://www.ukssdc.ac.uk/cgi-bin/ihy/cip-filter.pl.

**References**

Kolomiyets S.V., Sidorov V.V.: 2007, *In Proc. IAU Special Session 5*, eds. J.B. Hearnshaw, P. Martinez, Cambridge University Press, Cambridge, U.K., **4**, 189.

Kolomiyets S.V., Slipchenko M.I.: 2007, *in Proc. Meteoroids 2007, Springer: Moon, Earth and Planets*, eds. Trigo-Rodriguez J.M., Rietmeijer F.J.M., Llorca J., Dordrecht, the Netherlands, **No 9209**, **60**, 2.

**Tabl. 1. Participants of program IGY 1957 on meteor research in the USSR**

R - radar, Ph - photographic, V - visual

| N | City | $\varphi$ | $\lambda$ | $H$ m | Scientific institutes / Country / Chairs | Program, N igy |
|---|---|---|---|---|---|---|
| 1 | ***Ashkhabad*** | 37 ° 56 ' | 58 ° 24 ' | 200 | Astrophysical Laboratory of the Institute of Physics and Geophysics AS **Turkmen SSR** I.A. Astapovich, Ya.F. Sadykov. | R, Ph, V N696 (C126) |
| 2 | ***Kazan*** | 55 ° 47 ' | 49° 07 ' | 80 | Astronomical observatory named Engelgardt of the Kazan University **Russian SFSR** K.V. Kostylyov. | R N233 |
| 3 | Kiev | **50 ° 27 '** | 30° 30 ' | 185 | Astronomical observatory of the Kiev University **Ukrainian SSR** A.F.Bogorodskiy, | R, Ph, N320 |
| 4 | Odessa | **46 ° 29 '** | 30° 46 ' | 50 | Astronomical observatory of the Odessa University **Ukrainian SSR** V.P.Tsesevich, E.N. Kramer | R, Ph, V N621 |
| 5 | Stalinabad ***Dushanbe*** | 38 ° 34 ' | 68° 46 ' | 820 | Institute of Astrophysics AS **Tajik SSR** L.A. Katasev, P.B. Babadzhanov, A.M. Bakharev. | R, Ph, V N680 (C115) |
| 6 | ***Tomsk*** | 56 ° 29 ' | 84° 59 ' | 120 | Tomsk Polytechnical Institute( *faculty of Radiophysics)* **Russian SFSR** Ye.F.Fialko. | R N224 |
| 7 | Kharkov | 50 ° 00 ' | 36° 14 ' | 140 | Kharkov Polytechnical Institute *(faculty of Radioengineering)* **Ukrainian SSR** B.L. Kashcheyev | R N358(B141) |

Figure 1:

**Addresses of the organizations coordinating meteor researches in the USSR during time IGY (as of 1957):**

**1) Moscow, B. Gruzinskaja 10, Astronomical Council AS of the USSR, the Commission on Comets and Meteors.**

**2) Odessa, Park named Shevchenko, Astronomical observatory of the Odessa University (parent organization of meteor service of the USSR during period IGY).**

**On organizational questions also:**
**3) Moscow, the Kaluga highway 71, Interdepartmental Committee on carrying out IGY at Presidium AS of the USSR, working group on studying meteors.**

**Materials should be sent to the address:**
**4) the Moscow area, post Vatutenki, the Scientific research Institute of Terrestrial Magnetism, an Ionosphere and Distribution of Radiowaves (now IZMIRAN)**


Figure 2:

# THE OBJECT MWC 137

L.N. Kondratyeva

Fessenkov Astrophysical Institute,
Almaty 050020 Kazakhstan, *kondr@aphi.kz lu_kondr@mail.ru*

ABSTRACT. The main results of the long-term spectral observations of MWC 137 are presented. Variability of the profiles and equivalent widths of H$\alpha$, H$\beta$ and HeI, 5876 is shown and discussed.

**Key words**: Stars: Ae/Be Herbig stars: individual: MWC 137

## 1. Introduction

MWC 137 is the central star of the extended HII region Sh2-266. An active study of MWC 137 began at the end of 80th years, and it has been included in the various programs of Be, B[e] and Ae/Be Herbig stars researching. In the Fessenkov Astrophysical Institute the first spectrograms of Sh2-266 and MWC 137 have been received in 1971. Some low-excitation emission lines: HI, [NII], [OI] and [SII] have been revealed in the spectrum of the nebula. The spectrum of the central star showed the faint emissions of FeII, HeI and the broad emission lines of HI: FWHM(H$\alpha$)=5.6$\pm$ 0.3$\AA$ (Kondratyeva, 1975). Here we present the main spectral results, obtained in 1971–2007.

## 2. Observations

Observations were carried out with the slit spectrograph mounted at the 70 cm telescope AZT-8. A three-cascade image tube was used as a detector until 1998, and ST-8 CCD since 1999. Spectrograms with a dispersion 70–150 Åmm$^{-1}$ (or 0.5–1.0 Å pixel$^{-1}$) covered a spectral range about 1000–2000Å. In addition spectrograms with a dispersion 0.18Å pixel$^{-1}$ were received for study of emission line profiles.All spectrograms were reduced following the standard procedure consisting of bias subtraction and flat-field normalization and then all counts were corrected from atmospheric extinction and calibrated from instrumental chromatic response through observations of standard stars from the Catalogue of Kharitonov et al. (1988). Wavelength calibration was done using a laboratory source of HeI, NeI and ArI emission lines.

## 3. Results

Our values of equivalent widths EW(H$\alpha$) and EW(H$\beta$) are compiled in the Table 1 together with the results of the other authors. As a rule, values EW were determined by measure of 2 or 3 spectrograms. We estimate the errors to be about 10%, the less precision (20–30%) arose because of overexposed H$\alpha$ images (when the image-tube was used) or if a level of measured continuum was too low (with CCD matrix). Observable variations of EW (H$\alpha$) (from 130 up to 550 Å) considerably exceed a range of possible errors and probably reflect the real changes of ionized mass in the circumstellar envelope.The emission profile of H$\alpha$, presented in Fig. 1, consists of a red shifted single peak. The values of FWHM(H$\alpha$) and $V_r$ – heliocentric radial velocities are listed in the Table 2.

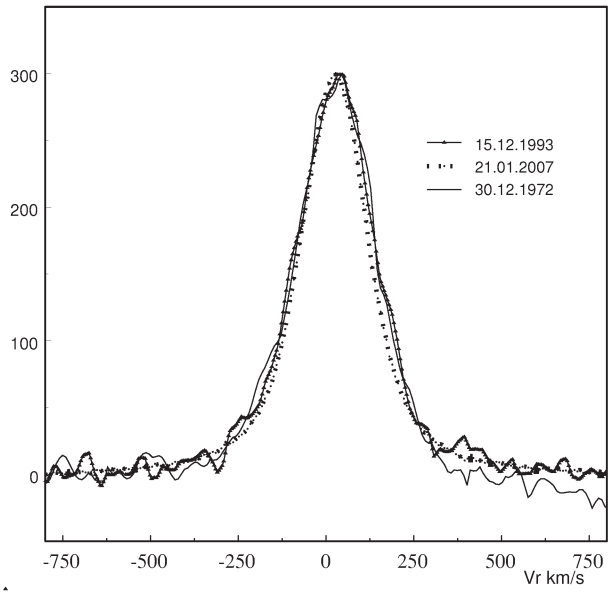


Figure 1: The profile of H$\alpha$ line for different dates. The Y axes is expressed in the relative intensities.

Our earlier measurements of $V_r$ are in agreement with the data from the other sources (Table 2), However in 2007 $V_r$ (H$\alpha$) has considerably decreased,

Table 1: Equivalent widths of the hydrogen lines in the spectrum of MWC 137

| Date | EW(H$\beta$)(Å) | EW(H$\alpha$)(Å) |
|---|---|---|
| 21.02.1971 | | 362±35 |
| 10.02.1972 | | 288±48 |
| 29.12.1972 | | 180±40 |
| 21.02.1974 | 44.6±4.2 | 205±15 |
| 02.03.1978 | 32.4±3.2 | |
| 31.03.1978 | 34.5±6.0 | |
| 03.04.1978 | | 210±11 |
| 04.04.1978 | | 203±29 |
| 06.04.1978 | 49.6±2.4 | |
| 07.03.1981 | | 316±23 |
| 09.1981 | | 133 (Finkenzeller, 1984) |
| 09.1987 | | 395 (Zickgraf, 2006) |
| 15.02.1988 | 53.5 | |
| 07.11.1988 | 44±18 | |
| 10.11.1988 | 45±8 | |
| 30.01.1989 | 37±7 | |
| 14.01.1991 | | 330±40 |
| 27.02.1993 | 48.1 | 318±11 |
| 15.12.1993 | | 360±40 |
| 10.1994 | | 254±17(Esteban, 1998) |
| 31.12.1996 | | 550 (Oudmaijer, 1999) |
| 26.02.1998 | | 213±16 |
| 20.12.1999 | | 404 (Vink, 2002) |
| 01.2000 | 54.4 | 394(Hernandez, 2004) |
| 02.2002 | | 464 (Zickgraf, 2006) |
| 21.01.2007 | | 530±70 |

and became closer to $V_r$ (5876) = +29.7±8.0 km s$^{-1}$ and $V_r$(6678)= +27 ±9.0 km s$^{-1}$ for the same date. By the way, almost the same value $V_r$ (5876) = 32 km s$^{-1}$, has been received in 2002 (Zickgraf, 2006). It is appreciably, that profiles of H$\alpha$, presented in Fig. 1, are not absolutely similar, the most "smooth" and narrow profile was received in 2007. Emission lines HeI,5876, 6678 and 7065 *Å* are presented on all our spectrograms of MWC 137. In the paper of Zickgraf, (2006) the author mentioned, that in September, 1987 the line HeI, 5876 was observed in absorption. Probably, this phenomenon was short-term as on our spectrograms, received in February 1988, this line was again in emission. A modern profile of this line is given in Fig. 2. Its form is asymmetric, probably, a "blue" wing is disturbed by a weak absorption. The value of FWHM (5876) = 234±15 km s$^{-1}$ is more than FWHM (H$\alpha$)= 222±12km s$^{-1}$. In other words the widths of lines increase with potential of ionization and decrease with the distance from the star. Thus we confirm a conclusion of Zickgraf, (2006), that the main mechanism of line broadening is rotation. From the other hand, decreasing of FWHM (H$\alpha$) and an asymmetry of HeI profile observed in 2007, testify probably, that outflow mechanism is being activated.

Table 2: Characteristics of H$\alpha$ profile

| Date | FWHM(H$\alpha$) km sec$^{-1}$ | Vr (H$\alpha$) km sec$^{-1}$ |
|---|---|---|
| 29.12.1972 | 255±18 | +43.7±9.0 |
| 21.02.1974 | | +47.4±10 |
| 15.12.1993 | 258±18 | +42.3±9.0 |
| 21.01.2007 | 222±12 | +28.6±8.0 |
| 09.1987(Zickgraf, 2006) | 197 | +42 |
| 10.1994(Esteban, 1998) | 210 | |
| 02.2002(Zickgraf, 2006) | 196 | +43 |

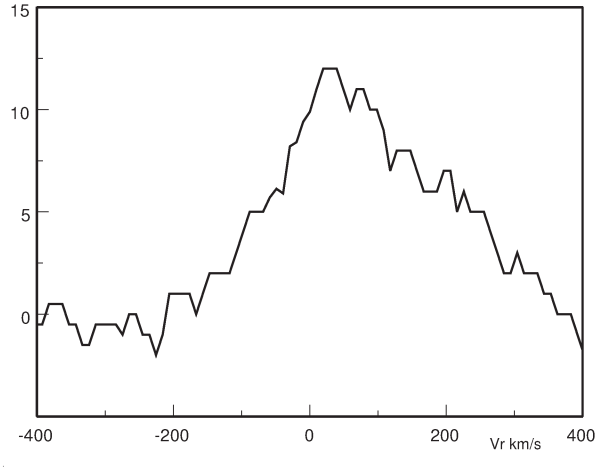


Figure 2: The profile of HeI,5876 line, obtained on January,21 2007. The Y axes is expressed in the relative intensities.

**References**

Esteban C., Fernandez M.: 1998, *MNRAS,* **298**, 185.
Finkenzeller U., Mundt R.: 1984, *AASS,* **55**, 109.
Hernandez J., Calvet N.: 2004, *AJ,* **127**, 1682.
Kharitonov A.V., Tereshchenko V., Knyazeva L.: 1988, *Spectrophotometric Catalogue of stars*, Nauka, Kazakhstan.
Kondratyeva L.N.: 1975, *Trudy of AFIF,* **25**, 23.
Oudmaijer R., Drew J.: 1999, *MNRAS,* **305**, 166.
Vink J., Drew J.: 2002, *MNRAS,* **337**, 356.
Zickgraf R.: 2006, *A&A, in print.*

# DE SITTER METRIC WITH MAGNETIC FIELD

M.P. Korkina, V.S. Kazemir

Department of Physic, Dniepropetrovsk National University,
Naukova str, 13, Dniepropetrovsk, 49050, Ukraine, *korkina@ff.dsu.dp.ua, kazemirws@ukr.net*

ABSTRACT. De Sitter model with magnetic field was considered. The exact solution was obtained. The properties of the model in comparison with empty de Sitter model were analyzed.

**Key words**: de Sitter, model; vacuum; magnetic, field; anisotropic, Universe.

## 1. Introduction

There is the considerable interest arose in cosmological models describing magnetic field in the Universe (Шикин, 1966; Vajk and Eltgroth, 1970; Banerjee and Sanyal, 1986; Giovannini, 2000). At the initial stage of evolution of the Universe such magnetic field was much strong and played the important role in expansion of the Universe. According to the present observations (Riess, 2004; Virey J.-M., 2005) the Universe expands with acceleration. Accelerated expansion of the Universe now is explained by presence of cosmological vacuum with a state equation:

$$\varepsilon_\Lambda + p_\Lambda = 0, \tag{1}$$

where $\varepsilon_\Lambda = const$. The vacuum energy density dominates over energy densities of all other matter (Perlmutter S., 1998). De Sitter model describes the Universe with matter with the state equation (1). From Einstein equations we obtain de Sitter metric in the form:

$$ds^2 = (1 - \frac{r^2}{a_\Lambda})dt^2 - \frac{dr^2}{(1 - \frac{r^2}{a_\Lambda})} - r^2 d\sigma^2, \tag{2}$$

where $d\sigma^2 = d\theta^2 + \sin^2\theta d\varphi^2$, $a_\Lambda^2 = \frac{3c4}{8\pi G\varepsilon_\Lambda}$. Let us take for simplicity system of units in which Newton gravitational constant $G = 1$ and light velocity $c = 1$. This metric contains R and T-regions. There is T-solution under $r < a_\Lambda$. Under $r > a_\Lambda$ this solution describes R-region of the manifold. Recently many original papers and reviews have been devoted to the cosmological vacuum (Sahni and Starobinsky, 1999; Carrol M., 2000; Чернин, 2001; Sahni, 2004). In this article we propose to consider de Sitter model with a frozed magnetic field for the early Universe.

## 2. Solution

Let's consider the homogeneous but anisotropic magnetic field which depends on time only and choose an axis along magnetic field. In synchronous coordinate system we consider the spherically symmetric metric in the form:

$$ds^2 = dt^2 - e^{\lambda(t)}dR^2 - r^2(t)d\sigma^2. \tag{3}$$

The nonzero components of Maxwell tensor for the frozed magnetic field are $F_{23} = -F_{32} = H_1$ where $H_1$ is magnetic field strength. Than from Maxwell equations it follows that $\frac{\partial H_1}{\partial t} = 0$ (Коркина, Мартыненко, 1977). Therefore stress-energy tensor of magnetic field can be written in the following form:

$$T^0_{0mag} = T^1_{1mag} = -T^2_{2mag} = T^3_{3mag} = \frac{H_1^2(\theta)}{4\pi r^2 sin^2\theta}. \tag{4}$$

Cosmological vacuum has constant energy density and pressure. For the chosen metric nonzero components of stress-energy tensor are:

$$T^0_0 = \varepsilon_\Lambda, T^1_1 = T^2_2 = T^3_3 = p_\Lambda. \tag{5}$$

We assume the independence of the dust and magnetic field. Then from conservation equation

$$T^\mu_{\nu;\mu} = 0 \tag{6}$$

for magnetic field it follows that:

$$H_1 = qsin\theta, \tag{7}$$

where $q = const$. Than we take the stress-energy tensor as a sum of stress-energy tensors of vacuum and magnetic field.

$$8\pi T^0_0 = 8\pi T^1_1 = \frac{q^2}{r^4} + \frac{3}{a_\Lambda} \; and \; 8\pi T^2_2 = -\frac{q^2}{r^4} + \frac{3}{a_\Lambda}. \tag{8}$$

Then taking (8) into account we obtain Einstein field equations in the form:

$$\frac{\dot\lambda\dot r}{r} + \frac{\dot r^2}{r^2} + \frac{1}{r^2} = \frac{q^2}{r^4} + \frac{3}{a_\Lambda}, \tag{9}$$

$$\frac{2\ddot{r}}{r} + \frac{\dot{r}^2}{r^2} + \frac{1}{r^2} = \frac{q^2}{r^4} + \frac{3}{a_\Lambda}, \qquad (10)$$

$$\frac{\dot{\lambda}\dot{r}}{2r} + \frac{\ddot{\lambda}}{2} + \frac{\dot{\lambda}^2}{4} + \frac{\ddot{r}}{r} = -\frac{q^2}{r^4} + \frac{3}{a_\Lambda}, \qquad (11)$$

where a dot $\dot{}$ denotes differentiation with respect to $t$. Integrating the equation (9) on time, we obtain:

$$\dot{r}^2 = \frac{r^2}{a_\Lambda^2} - 1 - \frac{q^2}{r^2} + C. \qquad (12)$$

Without a magnetic field we must obtain de Sitter solution. We take an integration constant $C = 0$. Than integrating (12) under $q = 0$ we obtain $r = a_\Lambda ch(t/a_\Lambda)$. The metric coefficient $e^\lambda$ we find from (9):

$$e^\lambda = sh^2(t/a_\Lambda). \qquad (13)$$

The obtained metric is the de Sitter solution in synchronous coordinates:

$$ds^2 = dt^2 - sh^2(t/a_\Lambda)dx^2 - a_\Lambda^2 ch^2(t/a_\Lambda)d\sigma^2. \qquad (14)$$

Integrating the equation (12) for case $q \neq 0$ we obtain:

$$\frac{r^2}{a_\Lambda^2} - \frac{1}{2} + \sqrt{\left(\frac{r^2}{a_\Lambda^2}\right) - \frac{1}{4} - \frac{q^2}{a_\Lambda^2}} = C_1 e^{2t/a_\Lambda}, \qquad (15)$$

where $C_1$ is an integration constant. As far as the obtained solution (15) must turn into de Sitter one, thus $C_1 = \frac{1}{2}$. Finally we have for $r^2(t)$:

$$r^2(t) = a_\Lambda^2 ch^2(t/a_\Lambda) + q^2 e^{-2t/a_\Lambda}. \qquad (16)$$

After integration of (9) we obtain the metric coefficient $e^{\lambda(t)}$ in the form:

$$e^\lambda = \frac{r^2}{a_\Lambda^2} - 1 - \frac{q^2}{r^2}, \qquad (17)$$

E ti (16) d (17) d t i d Sitt l ti with magnetic field. In expression (16) the magnetic field contribution gives an item $q^2 e^{-2t/a_\Lambda}$ therefore influence of a magnetic field on expansion in a radial direction weakens exponentially Dependences $r(t)$ and $e^{\lambda(t)}$ in comparison with de Sitter metric are shown at figures 1 2 Under $t \to \infty$ the obtained solution turns into de Sitter solution.

As for as $\dot{r} = 0$ corresponds to a minimum $r(t)$ than metric coefficient $e^\lambda = \dot{r}^2$ turn into zero under $r = r_{min} = a_\Lambda \sqrt{\frac{1}{2} + \frac{1}{2}\sqrt{1 + \frac{4q^2}{a_\Lambda^2}}}$ . However energy densities of a magnetic field and vacuum are finite, the obtained critical point is not the space-time singularity.

In curvature coordinates obtained metric have the form:

$$ds^2 = e^\nu dt^2 - e^\lambda dR^2 - e^\mu d\sigma^2, \qquad (18)$$

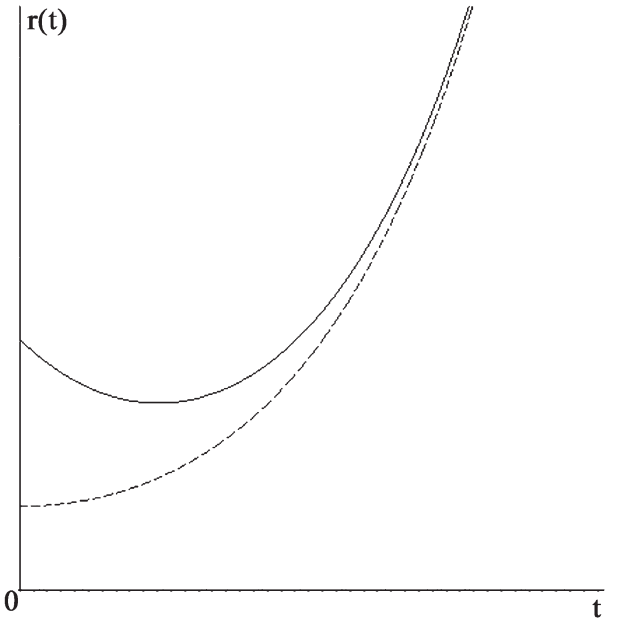


Рис. 1: Dependence $r^2(t)$. Dash curve is for $r^2(t)$ for de Sutter metric, Solid curve is for de Sitter metric with magnetic field.

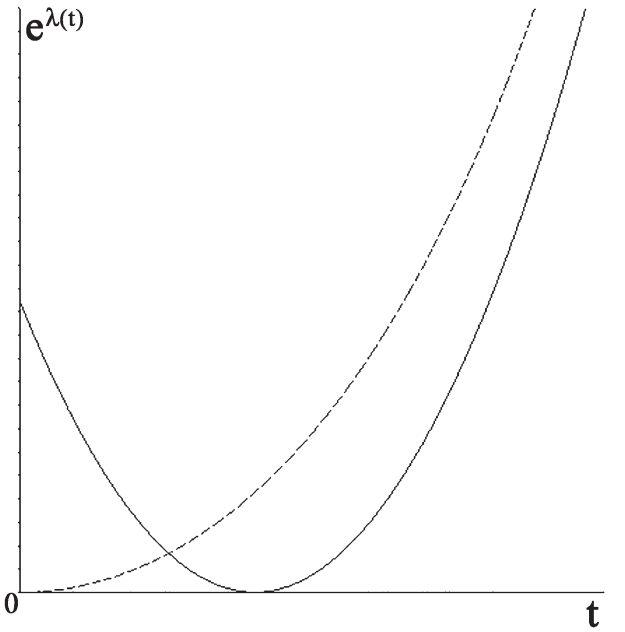


Рис. 2: Dependence $e^\lambda(t)$. Dash curve is for $e^\lambda(t)$ for de Sutter metric, Solid curve is for de Sitter metric with magnetic field.

where $e^{\nu} = 1 - \frac{x^2}{a_\Lambda^2} + \frac{q^2}{x^2}$, $e^{\lambda} = e^{-\nu}$, $e^{\mu} = x^2$. The event horizon between R- and T-regions is determined by expression:

$$e^{\lambda}\acute{\mu}^2 = e^{\nu}\acute{\mu}^2, \tag{19}$$

where an $\acute{\mu}$ denotes differentiation with respect to $x$. For the obtained solution from (19) we have an equation:

$$1 - \frac{x^2}{a_\Lambda^2} + \frac{q^2}{x^2} = 0. \tag{20}$$

This equation has one positive solution:

$$x_1 = a_\Lambda \sqrt{\frac{1}{2} + \frac{1}{2}\sqrt{1 + \frac{4q^2}{a_\Lambda^2}}}. \tag{21}$$

Under $x > x_1$ there is T-solution, under $x < x_1$ there is R-solution. As far as constant $q$ characterizes a magnetic field, than the presence of a magnetic field changes boundary between R- and T-regions of de Sitter metric

### 3. Conclusion

magnetic field has been obtained and the properties of the model have been analysed. R- and T-region of the model have been considered. It was shown, that the influence of magnetic field decreases with time and when $t \to \infty$ de Sitter solution take place.

### References


Коркина М.П., Мартыненко В.Г.: 1977, *УФЖ,* **22,** 853.

Новиков И.Д.: 1962, *Сообщения ГАИШ*, **120**.

Чернин А.Д.: 2001 *УФН,*, **11**, 1155.

Шикин И.С.: 1966, *ДАН СССР,* **171**, 73.

Banerjee A., Sanyal A.K.: 1986, *Gen. Relat. and Grav.,* **18,** 1251.

Carrol M.: 2000, *arXiv:astro-ph/0004075.*

Giovannini M.: 2000, *arXiv:gr-qc/0003112*

Perlmutter S. et al.: 1998, *arXiv:astro-ph/9812133.*

Riess A.G. et al.: 2004, *arXiv:astro-ph/0402512*

Sahni V.: 2004, *arXiv:astro-ph/0403324.*

Sahni V., Starobinsky A.: 1999, *arXiv:astro-ph/9904398.*

Vajk J.P., Eltgroth P.G.: 1970, *J. Math. Phys.,* **11,** 2212.

Virey J.-M.: 2005, *arXiv:astro-ph/0502163.*

# COLOUR EXCESSES OF 74 SUPERGIANTS AND 30 CLASSICAL CEPHEIDS

V.V. Kovtyukh[1], C. Soubiran[2], S. I. Belik[1], M. P. Yasinskaya[1], F. A. Chehonadskih[1], V. Malyuto[3]

[1] Odessa Astronomical Observatory, Odessa National University T.G. Shevchenko Park, Odessa 65014 Ukraine, *val@deneb1.odessa.ua*

[2] Observatoire Aquitain des sciences de l'univers, UMR 5804, BP 89, 33270 Floirac, France

[3] Tartu Observatory, EE2444 Tartumaa, Tõravere, Estonia

ABSTRACT. We derive accurate, homogeneous atmospheric parameters ($T_{\rm eff}$, log g, $V_t$, [Fe/H]) for 74 FGK non-variable supergiants and for 30 classical cepheids in 302 pulsation phases based on the high-resolution, high signal-to-noise echelle spectra. The extremely high precision of the effective temperature determination (10–30 K) is achieved by using the line-depth ratio method. These parameters are correlated with unreddened B–V colour index compiled from the literature for investigated stars to obtain an empirical relationship of the form

$$(B-V)_0 = 57.984 - 10.3587(logT_{\rm eff})^2 +$$
$$+1.67572(logT_{\rm eff})^3 - 3.356logg + 0.0321V_t +$$
$$+0.2615[Fe/H] + 0.8833(logg)(logT_{\rm eff})$$

This expression have been used for the estimation of the colour excesses E(B–V) of individual supergiants and classical cepheids with an error 0.05 mag, which matches precision of the most sophisticated photometric techniques. The application range is F0–K0, luminosity classes I and II. Considering the large distances of supergiants, this method opens up a possibility for the large-scale extinction mapping of the Galaxy, with sensitivity down to 0.1–0.2 mag.

**Key words**: Stars: fundamental parameters; stars: colour excesses; stars: supergiants; stars: classical cepheids.

## 1. Introduction

The Cepheid period-luminosity (P–L) relation has played a key role in the determination of distances within Local Group and to nearby galaxies. The absolute calibration of the P–L relation requires not only accurate distance measurements but also appropriate accounting for the effects of interstellar extinction and reddening because Galactic Cepheids are heavily obscured with an average E(B–V) of order 0.5 mag. We propose a new method of an accurate E(B–V) determination which relies on the spectroscopically determined stellar parameters.

## 2. Observations

The spectra of the supergiants were obtained using facilities of the 1.93 m telescope of the Haute-Provence Observatoire (France) equipped with échelle-spectrograph ELODIE (Soubiran et al. 1998). The resolving power was $R$ =42 000, wavelengths range 4400–6800 ÅÅ, and S/N>100 (at 5500 Å). The initial processing of the spectra (image extraction, cosmic ray removal, flatfielding, etc) was carried out as described in Katz et al. (1998).

In addition we employed spectra obtained with UVES at the VLT unit Kueyen (Bagnulo et al. 2003). All supergiants were observed with two instrumental modes *Dichroic*1 and *Dichroic*2, in order to cover almost completely the wavelength interval from 3000 to 10 000 Å. The spectral resolution is about 80 000, and for most of the spectra, the typical S/N ratio is 300–500 in the V band.

For Classical Cepheids we have used our published results (Andrievsky, Luck & Kovtyukh 2005, Kovtyukh et al. 2005).

The further processing of spectra (continuum level location, measuring of line depths and equivalent widths) was carried out by us using the DECH20 software (Galazutdinov 1992). Line depths $R_\lambda$ were measured by means of a Gaussian fitting.

## 3. Atmosphere parameters of supergiants and Classical Cepheids

We used Kurucz's WIDTH9 code with an atmospheric model for each star interpolated from a grid

Table 1: The computed colour excesses for Classical Cepheids

| Name | P, day | E(B–V) | error | N | E(B–V)$_{LC}$ | Name | P, day | E(B–V) | error | N | E(B–V)$_{LC}$ |
|---|---|---|---|---|---|---|---|---|---|---|---|
| $\eta$ Aql | 7.177 | 0.103 | 0.010 | 13 | 0.138 | SV Mon | 15.233 | 0.203 | 0.036 | 11 | 0.214 |
| SZ Aql | 17.141 | 0.590 | 0.024 | 9 | 0.531 | Y Oph | 17.127 | 0.694 | 0.011 | 14 | 0.668 |
| TT Aql | 13.755 | 0.473 | 0.025 | 7 | 0.432 | VX Per | 10.889 | 0.503 | 0.030 | 8 | 0.477 |
| YZ Aur | 18.193 | 0.648 | 0.030 | 3 | – | X Pup | 25.961 | 0.463 | 0.015 | 6 | 0.399 |
| RW Cam | 16.415 | 0.449 | 0.083 | 14 | 0.659 | S Sge | 8.382 | 0.111 | 0.014 | 9 | 0.099 |
| RX Cam | 7.912 | 0.545 | 0.034 | 9 | 0.553 | U Sgr | 6.745 | 0.402 | 0.020 | 9 | 0.421 |
| SU Cas | 1.949 | 0.299 | 0.019 | 12 | 0.282 | W Sgr | 7.595 | 0.087 | 0.017 | 8 | 0.108 |
| DL Cas | 8.001 | 0.500 | 0.024 | 14 | 0.499 | Y Sgr | 5.773 | 0.192 | 0.020 | 12 | 0.195 |
| $\delta$ Cep | 5.366 | 0.046 | 0.015 | 16 | 0.087 | WZ Sgr | 21.850 | 0.435 | 0.023 | 10 | 0.467 |
| X Cyg | 16.386 | 0.242 | 0.027 | 24 | 0.208 | YZ Sgr | 9.554 | 0.288 | 0.014 | 8 | 0.298 |
| SU Cyg | 3.845 | 0.085 | 0.020 | 12 | 0.091 | S Vul | 68.464 | 0.972 | 0.054 | 6 | 0.674 |
| CD Cyg | 17.074 | 0.454 | 0.024 | 14 | 0.513 | T Vul | 4.435 | 0.076 | 0.014 | 20 | 0.054 |
| Y Lac | 4.324 | 0.152 | 0.012 | 9 | 0.195 | U Vul | 7.991 | 0.665 | 0.016 | 7 | 0.640 |
| Z Lac | 10.886 | 0.426 | 0.032 | 7 | 0.368 | X Vul | 6.320 | 0.800 | 0.021 | 6 | 0.702 |
| T Mon | 27.025 | 0.175 | 0.023 | 18 | 0.188 | SV Vul | 44.995 | 0.528 | 0.020 | 23 | 0.412 |

Remark: E(B–V)$_{LC}$ values are from Laney & Caldwell (2007, BELRED values).

of models calculated with microturbulent velocity of 4 $\mathrm{km\,s^{-1}}$. At some phases Cepheids can have microturbulent velocities significantly deviating from this model value; however, our previous test calculations showed that changes in the model microturbulence over a range of several kilometers per second have an insignificant impact on the resulting elemental abundances.

The effective temperature for each Cepheid at each pulsational phase and for supergiants has been determined using the calibrating relations from Kovtyukh (2007). These relations combine the effective temperature with a set of spectral line depth ratios. The internal accuracy of the effective temperature determined in this way is rather high in the temperature range 5000 K to 6500 K: typically 150 K or less (standard deviation or 10 to 20 K for the standard error). Another very important advantage of this method (or any spectroscopic method) is that it produces the reddening-free $T_{\rm eff}$estimates. The effective temperature obtained from this new technique gives currently one of the most precisely determined fundamental stellar parameters – the relative precision is of the order of 0.1 percent.

The method used for gravity and microturbulent velocity determination in a supergiant star such as these Cepheids is described in detail by Kovtyukh & Andrievsky (1999). This method determines the microturbulent velocity using Fe II lines: the dominant ionization species of iron and hence less susceptible to any NLTE effects which might be in play in supergiant atmospheres. The gravity value is found by enforcing the ionization balance condition (the mean iron abundance from Fe II lines equals the iron abundance which results from the Fe I – EW relation extrapolated to zero equivalent width). This method resolves some previous problems within the abundance analysis of supergiant stars. Note that in these analyses we have used no lines stronger than 175 mÅ.

The uncertainty in the microturbulent velocity and the gravity is more difficult to assess. For the microturbulence a variation of 0.5 $\mathrm{km\,s^{-1}}$ from the adopted velocity causes a significant slope in the relation between Fe II line abundance and equivalent width. We therefore adopt 0.5 $\mathrm{km\,s^{-1}}$ as the uncertainty in the microturbulence. For $\log$ gwe adopt 0.1 dex as the formal uncertainty based on the numerical result that a change in gravity at that level will result in a difference of 0.05 dex between the total iron abundance as computed from the Fe I and Fe II lines. Since we have forced an ionization balance we do not allow a spread larger than 0.05 dex in the total abundance of iron as derived from the two ions and thus our uncertainty estimate (Andrievsky, Luck & Kovtyukh 2005, Kovtyukh et al. 2005).

The final results of the determinations of $T_{\rm eff}$, $\log$ g, $\mathrm{V_t}$ and [Fe/H] for supergiants are given in Table 2.

## 4. Colours excesses

The $T_{\rm eff}$, $\log$ g, $\mathrm{V_t}$ and [Fe/H] obtained in the manner described above can be used for determining the intrinsic colours of the target Cepheids and FGK supergiants. From Bersier (1996) and from Laney & Caldwell (2007) we take the unreddened B–V colour index for these stars. With the lack of simultaneous photometry, the instantaneous "observed" B–V color index is determined from Berdnikov's (2007) extensive data set of Cepheids. The latter contains multicolour photoelectric observations for all of our 30 Cepheids. The light curves were subjected to Fourier analysis and the coefficients determined up to the third to fifth order. Thus a pair of reddened and unreddened B–V values

Table 2: The computed colour excesses for supergiants. The negative E(B–V) have been set to zero.

| HD | $T_{\rm eff}$ | log $g$ | $V_t$ | [Fe/H] | E(B–V) | HD/BD | $T_{\rm eff}$ | log $g$ | $V_t$ | [Fe/H] | E(B–V) |
|---|---|---|---|---|---|---|---|---|---|---|---|
| 000725 | 7053 | 2.1 | 6.3 | –0.04 | 0.271 | 171635 | 6151 | 2.15 | 5.2 | –0.04 | 0.051 |
| 001457 | 7636 | 2.3 | 4.8 | –0.04 | 0.394 | 172365 | 6196 | 2.5 | 7.5 | –0.07 | 0.180 |
| 004362 | 5301 | 1.6 | 4.4 | –0.15 | 0.219 | 173638 | 7444 | 2.4 | 4.7 | 0.11 | 0.302 |
| 007927 | 7341 | 1.0 | 8.7 | –0.24 | 0.425 | 174104 | 5657 | 3.1 | 4.8 | –0.02 | 0.045 |
| 008890 | 6008 | 2.2 | 4.35 | 0.07 | –0.007 | 179784 | 4956 | 2.0 | 2.5 | 0.08 | 0.394 |
| 008906 | 6710 | 2.2 | 4.8 | –0.07 | 0.350 | 180028 | 6307 | 1.9 | 4.0 | 0.10 | 0.320 |
| 009900 | 4529 | 1.7: | 2.7 | 0.10 | 0.073 | 182296 | 5072 | 2.1 | 3.6 | 0.17 | 0.321 |
| 009973 | 6654 | 2.0 | 5.7 | –0.05 | 0.434 | 182835 | 6969 | 1.6 | 4.9 | 0.00 | 0.268 |
| 010494 | 6672 | 1.25 | 7.5 | –0.20 | 0.813 | 183864 | 5323 | 1.8 | 3.5 | –0.02 | 0.425 |
| 011544 | 5126 | 1.4 | 3.5 | 0.01 | 0.174 | 185758 | 5367 | 2.4 | 2.1 | –0.03 | 0.037 |
| 016901 | 5505 | 1.7 | 4.3 | –0.03 | 0.110 | 187203 | 5710 | 2.2 | 5.1 | 0.05 | 0.222 |
| 017971 | 6822 | 1.3 | 8.7 | –0.20 | 0.644 | 187299 | 4566 | 1.2 | 3.5 | 0.03 | 0.257 |
| 018391 | 5756 | 1.2 | 11.5 | 0.02 | 0.991 | 187428 | 5892 | 2.4: | 2.9 | 0.02 | 0.177 |
| 020902 | 6541 | 2.0 | 4.8 | –0.01 | 0.039 | 190113 | 4784 | 1.9 | 3.5 | 0.05 | 0.360 |
| 025056 | 5752 | 2.1 | 5.6 | 0.15 | 0.437 | 190403 | 4894 | 2.0 | 2.5 | 0.09 | 0.133 |
| 025291 | 7497 | 2.65 | 4.1 | 0.00 | 0.241 | 191010 | 5253 | 2.1: | 1.9 | 0.05 | 0.171 |
| 026630 | 5309 | 1.8 | 3.7 | 0.02 | 0.085 | 194093 | 6244 | 1.7 | 6.1 | 0.05 | 0.087 |
| 032655 | 6755 | 2.7 | 5.0 | –0.12 | 0.059 | 195295 | 6572 | 2.4 | 3.5 | 0.01 | 0.001 |
| 032655 | 6653 | 2.5 | 5.0 | –0.13 | 0.044 | 200102 | 5364 | 1.6 | 3.3 | –0.13 | 0.250 |
| 036673 | 7500 | 2.3 | 4.4 | 0.07 | –0.046 | 200805 | 6865 | 2.2 | 4.6 | –0.03 | 0.455 |
| 036891 | 5089 | 1.7 | 3.3 | –0.06 | 0.081 | 202314 | 5004 | 2.1 | 3.2 | 0.12 | 0.082 |
| 039949 | 5239 | 2.0: | 3.3 | –0.05 | 0.233 | 202618 | 6541 | 2.8 | 4.0 | –0.16 | 0.053 |
| 044391 | 4599 | 1.6 | 3.4 | 0.03 | 0.119 | 204022 | 5337 | 1.5: | 3.9 | 0.01 | 0.602 |
| 045348 | 7557 | 2.2 | 2.7 | –0.10 | 0.016 | 204075 | 5262 | 2.0 | 2.6 | –0.08 | 0.186 |
| 047731 | 4989 | 2.0 | 3.2 | 0.02 | 0.092 | 204867 | 5431 | 1.6 | 4.15 | –0.04 | 0.006 |
| 048329 | 4583 | 1.2 | 3.7 | 0.16 | 0.021 | 206859 | 4912 | 1.2 | 2.5 | 0.04 | 0.065 |
| 052497 | 5090 | 2.45 | 3.6 | –0.02 | 0.033 | 207489 | 6350 | 2.85 | 5.6 | 0.13 | 0.119 |
| 054605 | 6364 | 1.5 | 10.2 | –0.03 | 0.085 | 208606 | 4702 | 1.4 | 4.0 | 0.11 | 0.323 |
| 057146 | 5126 | 1.9 | 3.6 | 0.17 | –0.019 | 209750 | 5199 | 1.4 | 3.55 | 0.02 | 0.022 |
| 061227 | 7433 | 2.5 | 5.5 | –0.16 | 0.284 | 210848 | 6238 | 3.0 | 3.2 | 0.08 | 0.001 |
| 074395 | 5247 | 1.8 | 3.0 | –0.01 | –0.028 | 216206 | 5003 | 2.1 | 3.2 | 0.02 | 0.158 |
| 077912 | 4975 | 2.0 | 2.4 | 0.01 | 0.061 | 218600 | 7458 | 2.4: | 4.8 | –0.07 | 0.653 |
| 084441 | 5281 | 2.15 | 2.15 | –0.01 | 0.006 | 219135 | 5430 | 1.75 | 3.6 | –0.01 | 0.296 |
| 092125 | 5336 | 2.4 | 2.7 | 0.05 | 0.020 | 220102 | 6832 | 2.5 | 5.8 | –0.23 | 0.262 |
| 159181 | 5214 | 2.2 | 3.4 | 0.04 | 0.087 | 223047 | 4864 | 1.7 | 3.4 | 0.07 | –0.005 |
| 164136 | 6483 | 3.1 | 4.5 | –0.37 | 0.018 | 224165 | 4804 | 1.9 | 2.5 | 0.08 | 0.064 |
| 171237 | 6792 | 2.6 | 4.4 | –0.09 | 0.175 | +60 2532 | 6268 | 1.8 | 5.2 | –0.01 | 0.597 |

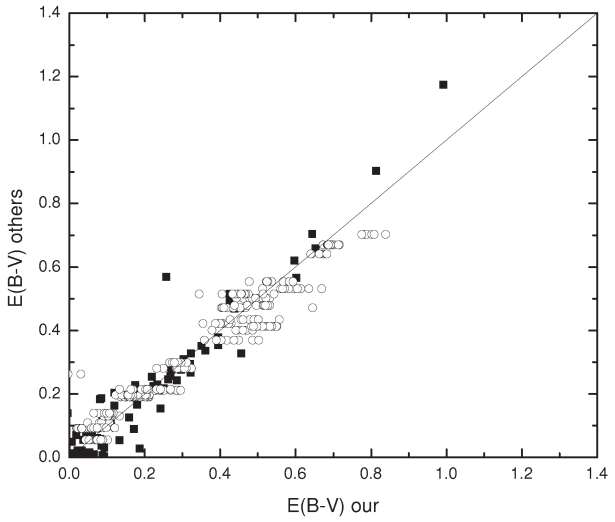


Figure 1: Comparison of our colour excesses with estimates from the literature: filled squares – Bersier (1996) for supergiants; open circles – Laney & Caldwell (2007) for Classical Cepheids (showed are the individual phases for each cepheid).

was generated for each moment of spectral observation. The colour excess should not vary during a pulsational cycle. Using the least-square method we have obtained the following relation (based on 376 individual equations between $(B-V)_0$ and $T_{\rm eff}$, log g, $V_t$, and [Fe/H]):

$$(B-V)_0 = 57.984 - 10.3587(logT_{\rm eff})^2 +$$
$$+1.67572(logT_{\rm eff})^3 - 3.356logg + 0.0321V_t +$$
$$+0.2615[Fe/H] + 0.8833(logg)(logT_{\rm eff})$$

Using this relation the colour excesses E(B–V)=(B–V)–(B–V)$_0$ for 30 Classical Cepheids and 74 supergiants are determined in Tables 1, 2. The final precision of $(B-V)_0$ is 0.05 mag (1 sigma), for the spectra of R=42000, S/N=100–150. This can be further improved with higher resolution and larger S/N. We note that this error budget does not include the possible uncertainties that arise from the individual properties of stars, like rotation, chemical composition, binarity, etc.

## 5. Results and summary

Tables 1 and 2 list the results for Classical Cepheids and supergiants, respectively. For Cepheids the name and P (period) are given in columns (1) and (2) respectively; the average color excess determined as described above is in column (3); the standard error of the mean is in column (4); the number of determinations used to calculate the mean is in column (5). The average E(B–V) was obtained by averaging the values of E(B–V) over the pulsational cycle. Individual reddenings estimates from Laney & Caldwell (2007) are also listed in Table 1, and comparisons with our estimates are shown in Figure 1.

In Table 2 we report colour excesses for 74 supergiants derived from our calibration. Each entry includes the name of the star, mean $T_{\rm eff}$, log g, $V_t$, [Fe/H] and E(B-V).

Fig. 1 compares for 104 objects our colour excesses with estimates from the literature.

Summarizing, supergiant colour excesses determined in this work using our expression, have been demonstrated to be of extremally high internal precision and agree well with the most accurate estimates from the literature.

*Acknowledgements.* This work is based on spectra collected with the 1.93-m telescope of the OHP (France) and the ESO Telescopes at the Paranal Observatory under programme ID266.D-5655. One of us (V.M.) gratefully acknowledges a support from the Estonian Science Foundation (Grant No. 6106).

### References

Andrievsky S.M., Luck R.E., Kovtyukh V.V.: 2005, *AJ*, **130**, 1880.
Bagnulo S., Jehin E., Ledoux C. et al.: 2003, *ESOMessenger*, **114**, 10.
Berdnikov L.N.: 2007, *http://www.sai.msu.ru/groups/cluster/cep/phe.*
Bersier D.: 1996, *A&A*, **308**, 514.
Galazutdinov G.A.: 1992, *Prepr.SAORAS*, **92**, 28.
Katz D., Soubiran C., Cayrel R., Adda M., Cautain R.: 1998, *A&A*, **338**, 151.
Kovtyukh V.V.: 2007, *Mon.Notic.RAS*, **378**, 617.
Kovtyukh V.V., Andrievsky S.M.: 1999, *A&A*, **351**, 597.
Kovtyukh V.V., Andrievsky S.M., Belik S.I., Luck R.E.: 2005, *AJ*, **129**, 433.
Kurucz R.L.: 1992, *IAUSymp.N*149, Dordrecht: Kluwer, 225.
Laney C.D., Caldwell J.A.R.: 2007, *Mon.Notic.RAS*, **377**, 147.
Luck R.E. & Andrievsky S.M.: 2004, *AJ*, **128**, 343.
Soubiran C., Katz D., Cayrel R.: 1998, *A&ASS*, 133, 221.

# HD 152786: A LITHIUM GIANT?

T. Krátká, V. Štefl

Department of Theoretical Physics and Astrophysics, Faculty of Science, Masaryk University
Kotlářská 2, CZ-611-37 Brno, Czech Republic, *terka@physics.muni.cz*

ABSTRACT. We were presented poster about interpretation of spectrum of the late-type lithium star HD 152786 acquired within UVES Paranal Observatory Project. Using the Synspec code for synthetic spectrum calculations we obtained some physical characteristics of the star and chemical abundances of some elements including Fe and Li.

We concluded that HD 152786 appears to be supergiant of spectral class K3 II or K3 Ib with effective temperature $T_{\rm eff} = 4500$ K, surface gravity $\log g = 0.5$, metallicity of [Fe/H] $= -0.41$ and lithium abundance of $A_{\rm Li} = 1.15$. From H-R diagram with evolutionary tracks we estimated mass of the star of (6–9) $M_\odot$.

**Key words**: star HD 152786, luminosity class, chemical composition, lithium

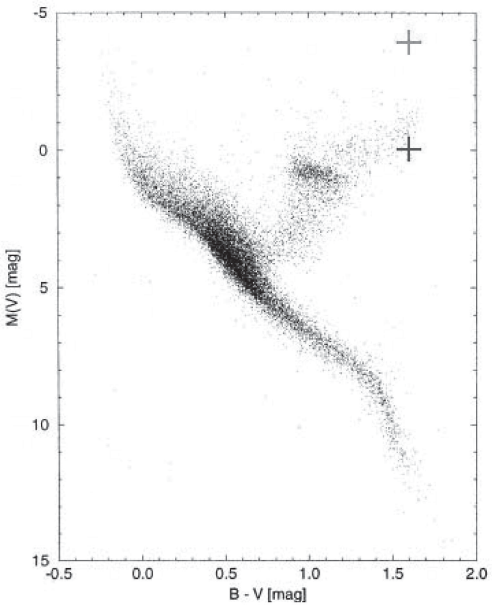


Figure 1: The position of the star in the H-R diagram (figure from Perryman et al., 1997) has been dramatically changed after the Hipparcos measurements were done (*blue* and *red crosses* denote the position prior and after the Hipparcos, respectively).

## 1. HD 152786 in present publications

The star lies near the Galactic plane and it is classified as young star of population I. In Astronomical Database Simbad are presented some basic data of the star: beside others parallax $(5.68 \pm 0.91)$ mas, magnitude in filter V: 3.13 mag, colour index $B - V = +1.60$ mag and $U - B = +1.96$ mag and spectral type of K3 III.

A parallax of the star obtained by Hipparcos astrometric satellite is nearly an order of magnitude smaller then its earlier values. Therefore, the luminosity of the star as well as the luminosity class determined before Hipparcos are not in agreement with the Hipparcos measurement. According to the Hipparcos mission, a distance of the star is 176 pc and absolute magnitude in filter V is $-3.95$ mag. The luminosity of HD 152786 can be estimated as about $6310\,L_\odot$. As you can see in Fig. 1, position of the star in the H-R diagram is different.

Based on the new measurements, the star should be classified as a bright giant or a supergiant, with the luminosity class of II or Ib.

## 2. Spectral analysis

Using the Synspec code we calculated synthetic spectra for several parameters of star atmosphere. The parameters of the star atmosphere can be considered to be the same as that of the calculated spectrum with the best fit to normalized measured data. Four different regions of the matching spectra are presented in Fig. 2.

## 3. Results

By means of comparing synthetic and measured spectra we determined the effective temperature as $T_{\rm eff} = 4500$ K, surface gravity $\log g = 0.5$ and abundances of some chemical elements for the star listed in Tab. 1.

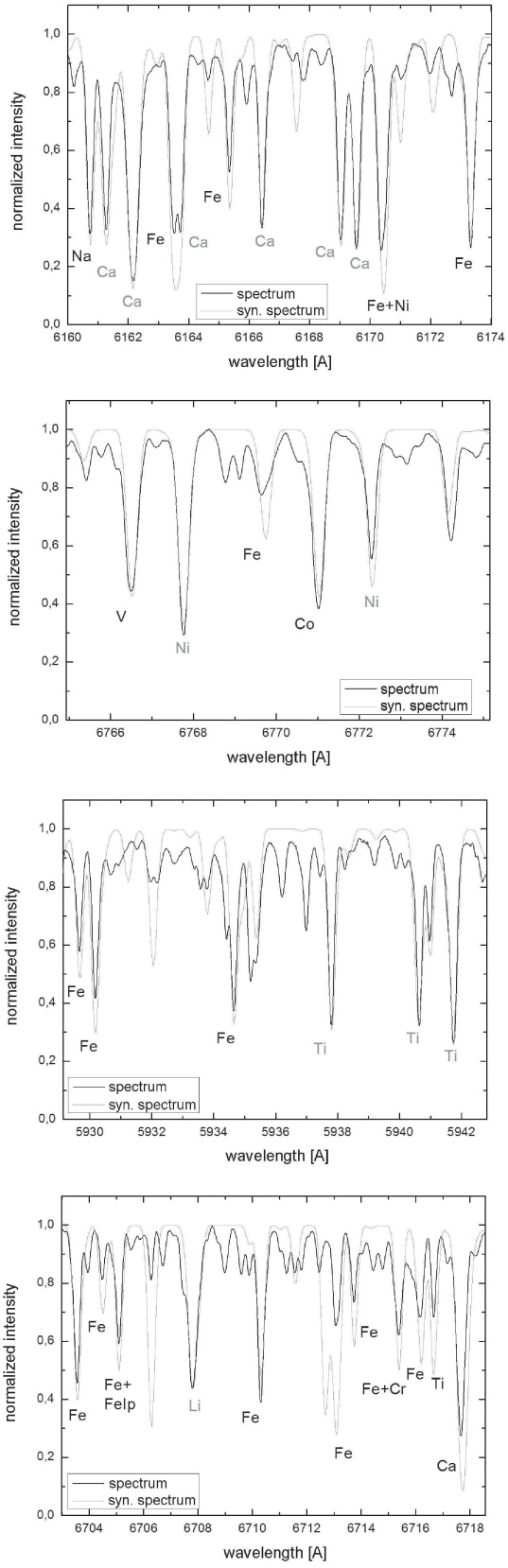


gure 2: Different regions of the matching spectra (*red e* – calculated spectrum, *black line* – measured spectrum).

Table 1: Obtained abundances of some elements.

| A (element) | $A_{\rm A}$ | [A/H] |
|---|---|---|
| Li | 1.15 | +0.10 |
| Al | 5.60 | −0.77 |
| Ca | 5.90 | −0.41 |
| Ti | 5.90 | +1.00 |
| V | 4.95 | +0.95 |
| Fe | 7.04 | −0.41 |
| Co | 4.78 | −0.14 |
| Ni | 5.30 | −0.93 |

The value of surface gravity confirms assigning the star to the supergiants class.

From the physical parameters the star can be placed into the H-R diagram with evolutionary tracks and than its mass and approximate evolutionary state could be estimated (see Conclusion).

## 4. Conclusion

According to the research HD 152786 appears to be supergiant of spectral class K3 II or K3 Ib with effective temperature $T_{\rm eff}$ = 4500 K, surface gravity $\log g$ = 0.5 and metallicity of [Fe/H] = −0.41, which confirms that HD 152786 is a metal-rich population I star. Obtained lithium abundance $A_{\rm Li}$ = 1.15 does not correspond to values of lithium stars. The mass estimated from H-R diagram is (6–9) $M_\odot$. Therefore, the evolutionary state must be close to the point where the energy source in the star's interior is changing. As consistent with current theories, the measured value of lithium abundance is in a good agreement with the guessed state of the star.

## References

Astronomical Database Simbad, *http://simbad.u-strasbg.fr/simbad/*

Perryman M. C., Lindegren L. and Kovalsky J.: 1997, *A&A*, **323**, L49

Johnson H. L., Iriarte B., Mitchell R. I., et al.: 1966, *Comm. Lunar Plan. Lab.*, **4**, 99

Houk N. and Cowley A. P.: 1975, *Michigan Spectral Survey, Ann Arbour, Dep Astron., Univ. Michigan*

Synspec code, *http://nova.astro.umd.edu/Synspec43/synspec.html*

# AMATEUR ASTRONOMY MOVEMENT IN SLOVAKIA

I. Kudzej, P.A. Dubovsky

Vihorlat Observatory Mierová 4, 06601 Humenné Slovakia,
*vihorlatobs1@stonline.sk*

ABSTRACT. We present brief history of astronomical education in Slovakia. The actual state of public observatories network is described as well. We also give an example of educational project supported by state agency "Slovak Research and Development Agency".

**Key words**: History of astronomy; Telescopes.

## 1. History

Popularization of astronomy has an old tradition in Slovakia. The first information has appeared in the l5th century and is bind with ACADEMIA-ISTROPOLITANA (1467). Two famous astronomers also worked there: JOHANNES MÜLLER-REGIOMONTANUS and MARTIN BYLICA. In the 16th century JAKUB PRIBICER, rector of CATINA school in Banská Bystrica wrote a very interesting publication about the comet TRACTATUS de COMETA qui sub anni and also CHRISTO 1577, which is the first book about the astronomy subject on the area of contemporary Slovakia.

In the 17th century, in 1661 the first astronomical observatory has been established in Slovak town Prešov, thanks to IZRAEL HIEBNER. In 1680 MARTIN SZENTIVÁNYI established the observing place in Trnava, which was reconstructed by plan of Slovak astronomer MAXIMILIÁN HELL in 1756 to astronomical observatory of TRNAVA university. The Observatory served for pedagogical and educational purposes. FRANTIŠEK KERY, ANTON REVICKÝ, ONDREJ JASLINSKÝ, JÁN BAPTISTA HORVÁTH, are representatives of heliocentrism lectured there.

In the 19th century together with the peoples movement for national renascence increases also the renascence of science and popularization of astronomy information. Astronomy observatory of The 1st Slovak Grammar school in Banská Bystrica also performed an important role, which had been established by VÁCLAV KAROL ZENGER and later JOZEF SZAKMÁRY continued in that work. In 1871 in Hurbanovo, dr. MIKULÁŠ KONKOLY THEGE established a new astronomical observatory in the end of the 19th century. At the beginning of the 20th century this observatory belonged to the most famous astro-physical observatories in the Central Europe. In addition to expert activity in the field of spectral analysis, photometry and photography, the important place in observatory activity has the popularization.

The period before the world war the first is connected with dr. MILAN RASTISLAV ŠTEFÁNIK and his astronomy activity. He is the first world famous Slovak astronomer. He worked in Paris observatory in MEUDONE, he was the director of mountain observatory on MONT BLANC and he made several expeditions for eclipses of sun. He was also a famous statesman, general of France army and the founder of the Czechoslovak state in 1918 together with another important statesmen.

Amateur astronomy movement was formed very slowly. Astronomical circles, unions, and astronomical societies helped it very much. The total result of these activities in the period between two world wars was the rise of the private observatory, which belonged to dr. ALEXANDER DUCHOŇ in PREŠOV (1932) and astronomical observatory in Bratislava (1936). Closely to the world war the second the private observatory of ANTONÍN BEČVÁŘ was also established in ŠTRBSKÉ PLESO (1937) and in SKALNATÉ PLESO the astronomical observatory was established in 1943.

Development of amateur astronomy after the world war the second on the Slovak territory we can divide into the two stages:
The 1-st: from 1945 to 1969 it is a stage of astronomical amateur institutions and social organizations network formation.
The 2-nd: 1969 up to these days it is a stage from the 1-st Slovak Conference regarded to amateur astronomy and the stage of constructing national observatories, astronomical cabinets and planetariums.

At the first stage activities of astronomical societies culminated by a developing of national observatories in Prešov (1948), in Humenné (1952), in Levice (1956), in Hlohovec (1958). In 1961 activity of observatory in Hurbanovo was renovated, and another observatories in Banská Bystrica, Žilina, Žiar nad Hronom, Rožňava and Bratislava were established.

In 1969-1970 Slovak Amateur Astronomy Central Office was founded in Hurbanovo and it started to coordinate a growth of astronomical amateur move-

Table 1: Public observatories East Slovakia

| ***Name*** | ***Locality*** | ***Main instrument*** | ***Main scientific program (if any)*** |
|---|---|---|---|
| Observatory and Planetarium | Prešov | Planetarium ZKP 2, 10 m, 68 seats | |
| Observatory | Roztoky | 40 cm Cassegrain | Variable stars |
| Vihorlat Observatory | Humenné | 25 cm Cassegrain | Sun |
| AO Kolonické sedlo | Kolonica | **100 cm VNT** | Variable stars |
| Observatory | Michalovce | 20 cm Cassegrain | |
| STM | Košice | Planetarium ZKP 2, 8 m, 41 seats | |
| CVČ | Košice | Planetarium ZKP 2, 10 m, 78 seats | |

Table 2: Public observatories Middle Slovakia

| ***Name*** | ***Locality*** | ***Main instrument*** | ***Main scientific program (if any)*** |
|---|---|---|---|
| Observatory and Planetarium M. Hell | Žiar nad Hronom | Planetarium ZKP 2P, 10 m, 54 seats | |
| Gemer Observatory | Rimavská Sobota | 35,5 cm Cassegrain | Occultations |
| Observatory Vartovka | B. Bystrica | 35 cm Cassegrain | Meteor showers |
| Observatory Malý diel | Žilina | 25 cm Newton | Occultations |
| Observatory Kysuce | Kysucké n. mesto | 20 cm refractor | Sun, occultations |

Table 3: Public observatories West Slovakia

| ***Name*** | ***Locality*** | ***Main instrument*** | ***Main scientific program (if any)*** |
|---|---|---|---|
| Slovak National Observatory | Hurbanovo | Solar spectrograph | Sun |
| Observatory and Planetarium | Hlohovec | 60 cm Cassegrain, Planetarium ZKP 2, 10 m, 64 seats | Variable stars |
| Hornonitrianska Observatory | Partizánske | 15 cm Coudé refractor | |
| Astronomical Observatory | Sobotište | 40 cm Newton - Dobson | Variable stars |

Table 4: Scientific observatories

| ***Name*** | ***Locality*** | ***Main instrument*** | ***Main scientific program*** |
|---|---|---|---|
| Astronomical Institute of Slovak Academy of Science | Lomnický peak (2632 m a.s.l.) | 20 cm coronograph 2x | Solar corona |
| | Skalnaté Pleso (1786 m a.s.l.) | 61 cm Newton, 60 cm Cassegrain | Asteroids, Variable stars |
| | Stará Lesná (785 m a.s.l.) | 60 cm Cassegrain, 50 cm Newton, Solar spectrograph | Variable stars, Sun |
| Faculty of mathematics, physics and informatics UK Bratislava | Modra (531 m a. s. l.) | 60 cm Newton | Asteroids |

ment. Simultaneous network of national observatories was connected with the Ministry of Culture of SR, which supported them. In 1970 Slovak Union of Amateur Astronomers as a social organization coordinated amateur astronomy was founded. Today it has 312 members in 24 local societies.

In the second stage new observatories were built in R. Sobota, Svidník, Michalovce, Kysuce, Trebišov, Partizánske.

Today there are in Slovakia 15 public observatories, 3 planetaries, 6 astronomical cabinets and various individual observers stations.

### 2. List of public observatories in Slovakia

Astronomical institutions dedicated to amateur astronomers in Slovakia we presents in three tables divided geographically. For comparison in Table 4 we presets scientific observatories of Slovak academy of Sciences and Comenius University.

### 3. Educational project Universe Live

Nice example of educational activity in Slovakia is our project Universe Live supported by the Slovak Research and Development Agency. Main goal of the project is to mediate the most modern astronomical research methods to talented students from secondary schools. We want to achieve this goal during 3 years of realization of the project. The main activity of the project is **Practical astronomical exercise**. It is weekend movement for twenty people, organized at Astronomical Observatory in Kolonica Saddle. It lasts from Friday evening to Sunday morning. Participants are chosen by the school coordinator. The program is organized by the project manager in cooperation with a responsible organizer. One lecturer attends the exercise and analyzes chosen topic its theoretical and practical aspects. During the project there will be implemented three series of practical astronomical exercises concentrated on variable stars, interplanetary matter and the occultations. Practical astronomical exercises are the foundation stone of the project. Groups of students are created here and these groups will participate in the next activities. Another activities are: Expeditions, Astronomical research fellowships, The KOLOS course, The KOLOFOTA course and Informational days at regional high schools.

**Expected outcomes and results of the project:**

Forty-two activities are going to be realized in the Astronomical Observatory in the Kolonica Saddle during the project (total participant number about 800).

About hundred and fifty students from the secondary schools are going to participate at least in one activity.

Directly during the project activities the participants will obtain observational data: photoelectric photometry (˜ 10000 integrations), CCD photometry (˜ 10000 measurements), meteors (˜ 5000 records), lunar occultations (˜ 10 timings).

During the project we are going to address about 1500 students (during twelve informational days)

We expect there will be at least three new regular amateur observers of variable stars who will produce at least 3000 photometric measurements during the project.

At least one of the participants will break into the national round of physics or mathematic olympiad and at least three into county rounds.

### 4. Conlcusions

We believe, structural changes in our society wouldn't break favorable conditions for the development of amateur astronomy in Slovakia. We hope, that a flow of information, exchange of experiences and knowledge will enrich our observatories. You can regard this walk throw the history of Slovak amateur astronomical movement like an invitation for visiting territory of Slovakia, where you can find beautiful nature, historical sightseeing, but also a lot of people connected by love with sky and stars.

*Acknowledgements.* Grant of Slovak Research and Development Agency LPP-0049-06.

# ASTRONOMICAL OBSERVATORY AT KOLONICKÉ SEDLO AND ITS RESULTS IN VARIABLE STARS OBSERVING

I. Kudzej[1], V.G. Karetnikov[2], P.A. Dubovsky[1], L.S. Paulin[2], N.N. Fashchevskyi[2], A.V. Ryabov[2], T.N. Dorokhova[2], N.I. Dorokhov[2], N.I. Koshkin[2], M. Vadila[1], S. Parimucha[3]

[1] Vihorlat Astronomical Observatory
Mierová 4, Humenné 06601 Slovakia, *vihorlatobs1@stonline.sk*

[2] Department of Astronomy, Odessa National University
T.G.Shevchenko Park, Odessa 65014 Ukraine, *astro@paco.odessa.ua*

[3] Institute of Physics, University of P.J.Šafárik
Košice, Slovakia,, *parimuch@ta3.sk*

ABSTRACT. There is presented a brief report of the actual equipments in the Astronomical Observatory at the Kolonické Sedlo. Description of Vihorlat National Telescope of 1 meter diameter equipped with the two-star high-speed photoelectric photometer and autoguiding system as well as various small telescopes capabilities are included. The results of CCD and PMT observations are presented. The future observational programs are presented as well.

**Key words**: Instrumentation: PMT photometer, CCD cameras; site testing; telescopes.

## 1. Introduction

Astronomical Observatory of Odessa National University (AO ONU, Ukraine) and Vihorlat Astronomical Observatory (VAO, Humenne, Slovakia) are cooperatively developing the new Observatory at the Kolonické Sedlo (VAO KS), which is located at northeast of Slovakia, in Vyhorlat mountains, in 40 km from Humenne: latitude=$48^o$ 57'N, longitude=$22^o$ 16'E, alt=465m. Atmospheric conditions are relatively good for the central Europe, in spite of low altitude. About 100 nights per a year are usable for a photometry. The average seeing is about 2.5 arcsec in the best nights.

The observing station at Kolonické Sedlo was launched in **1987**. The observations were done during observing stages and expeditions.

A very important step in the development of the observatory was done in **1999** when the main building of new observatory was finished. During the opening ceremony the Treaty between AO ONU and VAO on the technical assistance and collaboration was signed. According to this treaty the 1 meter telescope manufactured in AO ONU should be installed at the Kolonické Sedlo. Installation has been done in six stages and the telescope was officially inaugurated in **2002**. Thereby, the VAO KS have acquired on the cooperative basis the telescope of the primary mirror 1 m diameter, named the Vihorlat National Telescope (VNT). At present the VNT is the biggest astronomical instrument in Slovakia.

Some small telescopes, Newton 11 inch, Newton 14 inch, etc., were also installed at the observatory and are used for a visual and CCD observations. The experts of AO ONU assisted actively in the adjustment of all instruments.

This set of instruments allow carrying out a wide spectrum of astronomical researches for several observers at once. The VAO KS became a featured astronomical complex having a complete infrastructure with the working rooms and accommodation in its area for about 20-30 persons.

The Observatory is adapted in the high level for educational purposes covering numerous excursions for pupils and students, winter and summer schools for young astronomers from local region and practical exercises for astronomy students of the AO ONU and of the Šafárik University Košice. The principal observing program of the VAO KS is pointed to variable stars researches.

## 2. Instrumentation

The VNT is placed in 5 m dome (see Fig.2, which motion is synchronized with the motion of the telescope tube. The optical layout of the VNT is shown in Fig. 1 and main characteristics are given in Table 1.

Observational instruments could be installed in two focuses, Cassegrain and Nasmyth. For the work in the Cassegrain focus the optical system of the VNT is corrected by two lenses situated in front of the secondary mirror.

In 2005 the Cassegrain focus of the telescope was equipped by the high speed two-star photometer, which

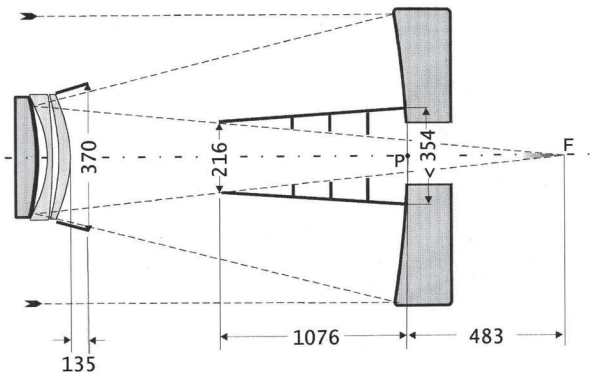


Figure 1: The optical layout of VNT

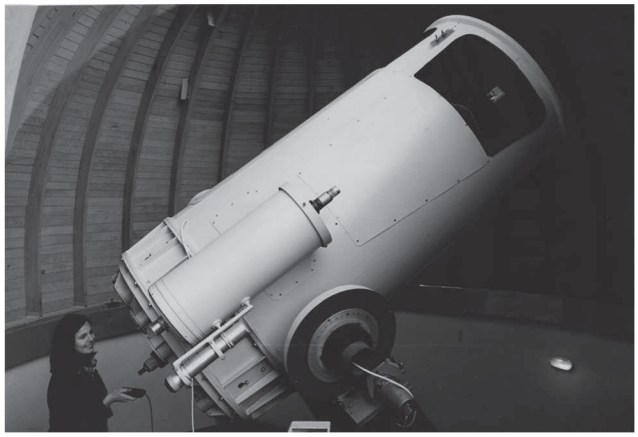

Figure 2: The VNT in the dome

Table 1: Main characteristics of VNT

| | |
|---|---|
| Optical system | Modified Argunov-Fashchevskyi |
| Main mirror shape | spherical |
| Diameter of the main mirror | 1 m |
| Diameter of the secondary mirror | 0.3 m |
| Effective focal length | 9 m |
| Length from the main mirror to secondary | 2.03 m |
| Field of view FOV | 0.5 arcmin |
| FOV diameter in focal plane | 78 mm |
| Scale of FOV | 0.043 mm/arcsec |

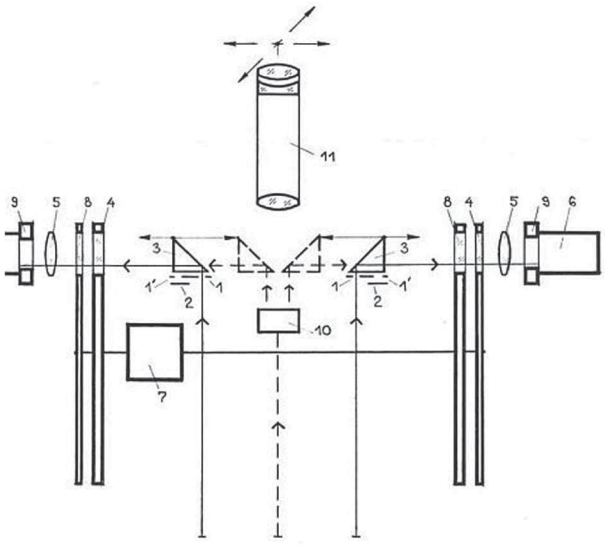


Figure 3: The optical scheme of the PMT two-star photometer

was constructed in AO ONU. The design and observing performance are similar to the previous photometer, which was applied with the Odessa 0.8 m telescope at the Mt. Dushak-Erekdag Observatory in Turkmenistan (Dorokhov & Dorokhova, 1994).
Some improvements were brought into the optical scheme (Fig. 3):
1 - diaphragm (5 different diameters), 1'- diaphragm for sky measurement, 2 - cover automatically uncover diaphragm 1 and 1', 3 - mirrors reflecting the light to the photomultiplier, 4 - filter wheel, 5 - Fabry lens, 6 - photomultiplier, 7 - simultaneous turning of filter wheels, 8 - neutral filter, 9 - photomultiplier cooling, 10- mechanical displacement of mirrors 3, 11- microscope.

The main problem for the multichannel PMT-photometers is the accurate verification of the channels' sensitivity (Breger & Handler, 1993). For this reason there are provided calibrations with using the artificial emission sources (Dorokhov, 1999).

The Nasmyth focus is preparing now for CCD multicolor photometry and/or for spectroscopy. The switching from the Cassegrain focus detector to the Nasmyth focus one could be done by insertion of the flat mirror located inside the telescope tube.

Since the telescope and photometer were manufactured recently they both required the detail investigations and improvements. Specially, there were many telescope's problems: a right installation, an optic alignment, an adjustment of the hourly motion, etc. Particularly important for the time series of observations there is clearing the telescope hourly motion from the periodic components which are arisen due to an irregular rotation of the driving gears. There was not succeed completely removing this problem. Thus the telescope is needed in the automatic guiding.

The automatic guiding of the telescope was developed by Martin Myslivec by using Mintron CCD camera CCD initially through the 30 cm Ritchey-Chretien pointer.

### 3. The test of two-stars photoelectric photometer

Initially, the photometer was used for the VNT testing. At first we selected the pairs of constant stars of the same magnitudes and colors frequently in open clusters. On such observations we revealed that the pointer changed a little its direction in respect to the main telescopes as a result of bents during the movement of the VNT. Then the stars left the diaphragms sometimes during a night. The problem was removed when CCD-autoguide was directly installed on the photometer's eyepiece.

After that we examined the dual-channel advantages in a windy cloudy night. In Fig. 4 there are shown the simultaneous observations of pair of the stars:
HD161677 ( V: 7.14, B-V:-0.02, sp:B6V);
HD161603 (V: 7.34, B-V:-0.00, sp:B5V)
in Johnson's B filter with 10 sec integration time. It is seen that even when accounts in each channel are decreased on about 100% the average line on the bottom panel have deviations less than 3%.

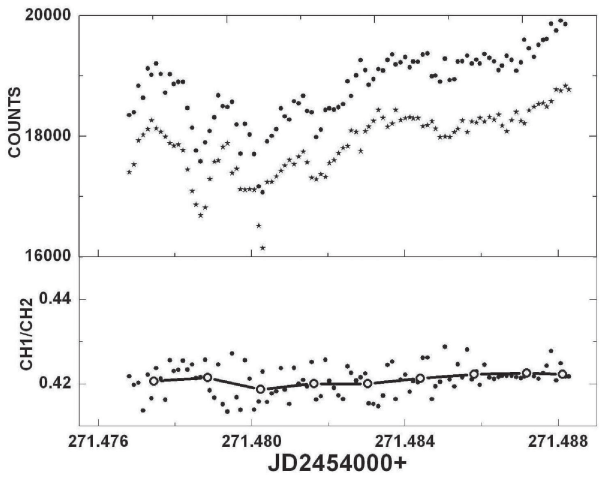


Figure 4: Simultaneous measurements of constant stars HD161677 and HD161603 with the two-star photometer in the windy cloudy night. There are presented: the data of each channel in the top panel and the ratio of these data in the bottom panel. The solid line with empty circles indicates the 2 min. averages of the data.

For achieving a high photometric quality we followed the standards and techniques of the global asteroseismology networks: DSN, Delta Scuti Network (see, e.g., Breger & Handler, 1993) and WET, Whole Earth Telescope((Nather et al., 1990; Kalytis et al., 1993). For accounting an atmospheric influence we focused on the

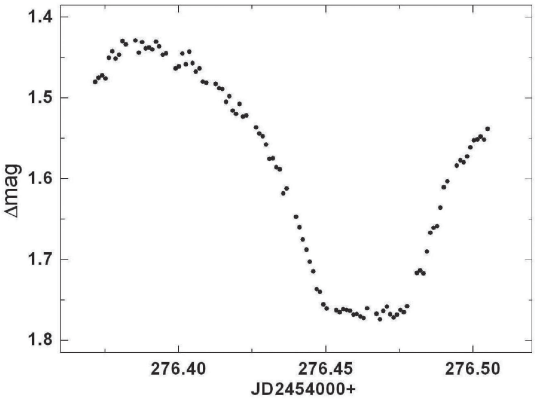


Figure 5: Light curve of EW/KW star TZ Boo obtained with the VNT + PMT photometer + V filter in 24.06.2007

Figure 6: One of the small telescope, "Pupava" of 280 mm mirror diameter.

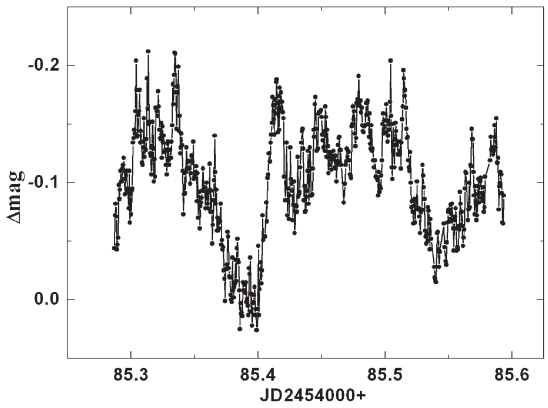


Figure 7: The flickering and irregular variations of the brightness at the minutes' time scale of cataclysmic variable star GK Per obtained in 15.12.2006 with Pointer + SBIG ST-9XE camera.

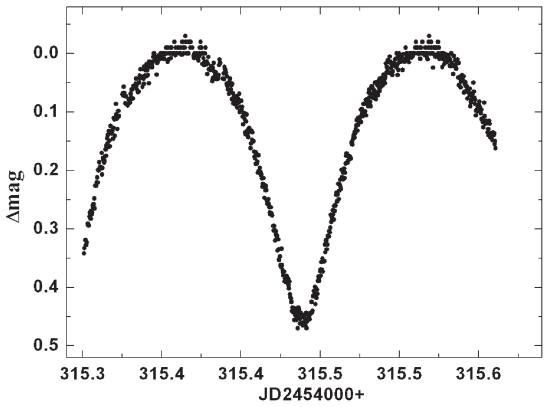


Figure 8: The minimun of W UMa type star CW Cas observed with Hugo+ Meade DSI Pro+V filter in 02.08.2007

factors described in the paper of Pakstiene & Solheim (2003).

In June-July 2007 we tested the system of VNT-photometer on the recently discovered low amplitudes Lambda Boo star V2314 Oph (Kim et al., 2007) in the frames of the multi-site campaign. These observations showed the accuracy of the continuous photometry sometimes more then $0.^m01$. Nevertheless, the VAO KS data are coincident in a phase with the light curve obtained in the Sierra-Nevada Observatory (Martin Ruiz, 2007).

We detected that the photomultiplier of the channel 2 has a low sensitivity and we replaced it by another FEU79. After that the the accuracy was improved till $0.^m002$-$0.^m003$ under the good atmospheric transparency.

Now the instrument is regularly observing the program stars. The eclipse of well known EW/KW binary TZ Boo (V= 10.41, Sp G2V) is presented in Fig. 5.

## 4. CCD photometry at VAO KS

The CCD photometry was also helpful as for an examination of the VNT as well the PMT two-star photometer. We registered the deflections of the images at both coordinates, thus cleared the reasons of the periodic deflections of the VNT tube. We also tested the photometer's sensitivity when the target star pass through the diaphragm. Simultaneous observations of the same object with the VNT+PMT photometer and with some of other telescopes+CCD camera gave an opportunity excluding the possible bugs in programmes and/or construction.

As it was mentioned already, some small telescopes work in the Observatory. Every of them has own task and own name, in according with its character. One is shown in Fig. 6. It was supplied by the name "Pupava" ("dandelion") to for the cheerful yellow colour. The Meade DSI Pro cameras with Sony ExView HAD Monochrome CCD Sensor with 510 x 492 pixels are usually used with these telescopes.

In Table 2 we give descriptions of these telescopes including the pointer of the VNT.

CCD observations were started after arrival of the permanent observer (PAD) to the VAO KS in March 2006. First CCD measurement was made on 07 April 2006 with the camera Meade DSI Pro mounted on Lichtenckencker telescope of 150 mm. Actually, 3 CCD cameras worked with Hugo, Púpava telescopes and 400 mm telephoto lense. The observations were acquired mainly during the summer campaigns and astronomical practical exercises for young astronomers. During 197 observational nights from 07 April to 31 July 2007 we have obtained 338 light curves of 87 stars. We have collected 141 times of minima in 53 eclipsing binaries. Totally, we have acquired 101737 images.

A large data base of 2581 measurements in 10 nights of 2006-07 was acquired with SBIG ST-9XE for GK Per, symbiotic binary: sdBE + K2IVp, the nova of 1901.

This very interesting cataclismic variable has varies types of activity: rapid irregular variations $\Delta$m $0^m.1$ in several minutes), irregular fluctuations from night to night $\Delta$m $0^m.3$), slow irregular variations and bursts. Flickering and variations of the brightness at the minutes' time scale are presented in Fig.7.

## 5. Observing program of VAO KS

So, the main observational program is focused on the researches of pulsating stars, eclipsing binaries, specially, cataclysmic and symbiotic stars.

Table 2: Characteristics of some small telescopes in the VAO KS

| | ***Pointer*** | ***Chermelin*** | ***Hugo*** | ***Pupava*** |
|---|---|---|---|---|
| Optical system | Ritchey-Chretien | Newton | Newton | Newton / Cassegrain |
| Diameter [mm] | 300 | 300 | 265 | 280 |
| Focal lenghth [mm] | 2400 | 1500 | 1360 | 1500/3500 |
| Mount | Fork equatorial | Alt/Az | German equatorial | German equatorial |
| Constructor (telescope/mount) | AO Odessa | AO Odessa / CVUT Prague | AO Odessa / Uniwersal Poland | Uniwersal Poland / AO Odessa |
| Exploitation | Autoguiding of VNT | Automated monitoring of cataclysmic variable stars (future) | CCD photometry times of minima of eclipsing variable stars | Time series color CCD photometry of cataclysmic variable stars |

Table 3: Observing program of the VAO KS

| ***Observed objects*** | ***Equipment*** | ***Actual situation*** |
|---|---|---|
| Astroseismology, Flickering in Cvs, fine effects on light curves of EBs | 1 meter VNT + photometer | Testing observations with photometer |
| Four color photometry of CVs (Polars) | 100 cm VNT + CCD | Nasmyth focus of VNT (in preparation) |
| Monitoring of faint CVs | 30 cm Chermelin + CCD | In preparation of alt-azimuthal mount |
| High speed photometry of CVs | 28 cm Púpava + CCD | Observing |
| Times of minima of EBs with strange O-C | 26,5 cm Hugo + CCD | Observing |
| Times of minima of bright EBs | 400 mm telephoto lens + CCD | Observing |
| Monitoring of bright CVs | Visually with Newton 30 cm | Until now using 30 cm Chermelin telescope |
| Semi regular variables, Be stars, Symbiotic variables, EBs without known elements | Newton 30cm visually, Somet and DB binocular | Observing |

Table 4: Observing program for the VNT, according the KOLOS-2006

| ***Object type*** | ***Observational purposes*** | ***Targets*** | ***Researchers*** |
|---|---|---|---|
| Interacting binaries | Flickering in symbiotic binaries | V694 Mon, T CrB, RS Oph, V404 Cyg, V627 Cas | Hric, Parimucha, Dobrotka |
| Interacting binaries | Pulsations of cold components | IU Per, TW Dra | Hric, Zejda |
| Chemically peculiar stars | Multicolor photometry | AR Aur, V624 Her, HD 37776 | Zverko, Žižňovský, Mikulášek |
| Algol type EB | Rotation velocity | BW Boo | Glazunova |
| Pulsating variables | Asteroseismology | V2314 Oph, VW Ari | Dorokhova |
| Be stars, Novalike, X ray | Outbursts, rapid variations | V725 Tau, X Per, V831 Cas, V635 Cas, TT Ari | Dorokhova, Dorokhov |
| Eclipsing binaries | The shape of light curve, fine effects | AK Her, RV Oph, V729 Cyg, EE Peg, BM Ori, AW UMa, BH UMa, V577 Oph, KP And, FF Cnc | Kudzej |

Initially, there were visual estimates of the minima times of eclipsing binaries. Afterwards, this directions were transformed to the CCD photometry of contact systems of the W UMa type, with ellipsoidal components of F0-K spectral type. Before mentioned CW Cas and TZ Boo are related to this type of variability. For these systems is typical that depths of minima are vary significantly from year to year, sometimes Min II become deeper than Min I. The light curves' shape and parameters are also usually variable. We are seeking to acquire such amount of light curves which make possible the unambiguous theoretical conclusions concerning the processes in these key objects.

We also take part in the campaigns of global photometry on Nova-like stars V603 Aql and V Sge. The basic work was made for superoutbursts' observations of SU UMa type stars IY UMa, MR UMa, V419 Lyr, CI UMa, RXSJ053234, VY Aqr, V844 Her. Till present time by using these CCD-observations two papers have published in OEJV (Parimucha& Dubovsky, 2006), one in IBVS (Parimucha et al. 2007) and a few papers are in preparation.

Later, with adoption of the PMT photometry, the pulsating variables were attached and are dynamically investigated.

The observational activity is mainly done according to the international cooperation of four institutions:

Vihorlat Astronomical Observatory, Humenné

Astronomical Observatory of Odessa National University, Odessa

Astronomical Institute of Slovak Academy of Science, T. Lomnica

Institute of Physics, Šafárik University, Košice.

The future development of observing activities is scheduled in the Table 3.

## 6. Conclusion

Observing strategy (see Table 4) is arranged within the international seminar KOLOS, which is regularly holds in early December from 2003. The experts of different institutions and different directions of the science, engineers, amateurs and students have an opportunity for a discussion, uniting their efforts for a development of astronomy in Slovakia and, particularly, for an enhancement of the research scope in the VAO KS .

More detailed description of the VAO KS, as well as the astronomical tools are available at the Observatory website:

http://www.astrokolonica.sk.

*Acknowledgements:* The work was supported by the Ukrainian MON grant No M/153-2006 and the Bilatelar APVV grant SK-UK-01006, as also the Grant of the Slovak Research and Development Agency LPP-0049-06, VEGA grant 7011 and grant of the Šafárik University VVGS 9/07-08 and The National Scholarship Programme of the Slovak Republic.

## References

Breger M., Handler G.: 1993, *Communications in Asteroseismology*, **58**, 1.

Dorokhov N.I.: 1999, *Kinematika Fiz. Nebesn. Tel*, **15**, 189.

Dorokhov N.I. & Dorokhova T.N.: 1994, *Odessa Astronomical Publ.*, **7**, 168.

Fashchevskij N., Paulin L., Ryabov A.: Sozdanie 100 cm teleskopa v Odesse, 2002, *Odesskyi Astronomicheskyi Kalendar*, 180.

Kim Chulhee, Yushchenko A.V., Gopka V.F., Dorokhova T.N., Musaev F.A., Kim S.-L., Jeon Y.-B., Ibrahimov M., Tarasov A.E.: 2007, *AJ*, **134**, 926.

Kalytis R., Skipitis R., Karaliunas A., Dzindzeleta B.: 1993, *Baltic Astronomy*, **2**, 504.

Kudzej I., Dorokhova T., Dubovsky P., Ryabov A., Vadila M., Dorokhov N., Koshkin N.: *Communications in Astroseismology*, **150**, 319.

Martin Ruiz S.: 2007, private communications

Nather R.E., Winget D.E., Clemens J.C. et al.: 1990, *ApJ*, **361**, 309.

Pakstiene E., Solheim J.-E.: 2003, *Baltic Astronomy*, **12**, 221.

Parimucha S., Dubovsky P.: 2006, *Open Europ. J. Var. Stars*, **50**.

Parimucha S., Dubovsky P.: 2006, *Open Europ. J. Var. Stars*, **52**.

Parimucha S., et al.: 2007, *Inf. Bull. Var. Stars*, **5777**.

# SPECTROSCOPY AND PHOTOMETRY OF BE STAR MWC340

A.V. Kurchakov, F.K. Rspaev

Fesenkov Astrophysical Institute
Almaty 050020 Kazakhstan *anatol@aphi.kz*

ABSTRACT. The spectroscopic and photometric observations of Be star MWC 340 made at Fesenkov Astrophysical institute during 2001-2006 are presented.

**Key words**: HAEBE stars: spectroscopy, photometry.

## 1. Introduction

Investigated by us MWC 340 (BD+40$^o$4124 = V1685 Cyg) star is embedded into diffuse gas nebula of inhomogeneous structure. At distance of 2 arc minutes from star in south-east direction is extended the thin rim (length near 7 arc minutes), passed in south-west direction into diffuse envelope, separated from star by dark most likely absorbed envelope. The molecular coma-like cloud (Hillebrand, Meyer, Strom et al. 1995), extended from south to north, is overlapped on all that. Firstly about small aggregate of stars with emission lines, connected with MWC 340, was reported by Herbig G.H. (1960). The MWC 340 region consist of few tens very young stars attributed to HAEBE stars. The data about 33 stars of isolated association of stars up to main consequence, related with two HAEBE stars MWC 340 and V1686 Cyg, are given in (Hillenbrand at al, 1995). Only eleven of them are seen in visual. Our observations includes the spectral and photometric data for MWC 340 and photometric ones in V band for N2, N3 and N6 (V1686 Cyg = LkHa 224) stars from Table 1 of Hillenbrand, Meyer, Strom et al (1995). The spectroscopic and photometric observations were carried out at the Assy-Turgen highmountain observatory 1-m telescope of the Fesenkov Astrophysical Institute of National Academy of sciences of Kazakhstan Republic during 2001 September - 2006 September.

## 2. Observations

The spectral observations were made with the spectrograph UAGS and CCD camera ST-8 with 1530 1020 pixels. The inverse dispersion was 0.5 Å on pixel. The spectral investigations of MWC 340 were mainly carried out in the regions of H$\alpha$ and H$\beta$ lines. The flat field for spectrophotometry was received from dome, illuminated by usual tungsten lamp. The reductions for instrumental contour were not made. The equivalent width of H$\alpha$ line was defined without taking into account the blending them by absorption lines. All spectra have the resolution R=6000. The S/N ratio reaches about 25 and 12 in region of H$\alpha$ and H$\beta$ lines, respectively. The photometric BVRI data were received with CCD camera ST-7 and filters of SBIG firm. In spite of that the R and I filters most likely gives the magnitudes in Johnson-Cousiens system, we reduced the our observations to the standard Johnson system. All photometric observations were corrected for flat field, received from twilight sky. The variety of H$\alpha$ lines intensity relatively to continuum (from 13 to 21) is observed. For this time the H$\alpha$ line equivalent width EW is changed in the limits 110 - 160 Å, the brightness in range V= $10.^m70$ - $10.^m85$; (B-V)= $0.^m84$ - $0.^m94$; (V-R)= $0.^m95$ - $1.^m02$. Herewith it should be noted that the measuring error of equivalent width determining at different taking into account of continuum is near 2%. The photometric measuring error of magnitude determining is less than $0.^m01$.

## 3. Results and discussion

The optical spectrum of MWC 340 shows the strong emission of H$\alpha$ and H$\beta$ lines, the forbidden oxygen [OI] $\lambda\lambda$ 6300; 6363 and numerous FeII emission lines. H$\alpha$ and H$\beta$ lines have the clear cut double-peaked profiles with practically non-shifted central absorption, and the ratio of red and blue intensities is changed with time. H$\alpha$ profiles received in different observational dates are shown as example on Fig.1. H$\alpha$ profile with minimum value for blue component (received 2005 October 1) is given off by thick solid line. The nonsymmetrical profile of H$\alpha$ line may be explained by three models:
-a model, in which the shape of gas envelope is deviate from spherical one;
-a model of rotating and extending envelope;
-a model with relatively small inclination of circumstellar discs to the observer, so that a disc material is closed the line of sight.

However, the third model will always provide for $I_{blue} \succ I_{red}$, what is inconsistent with our observations.

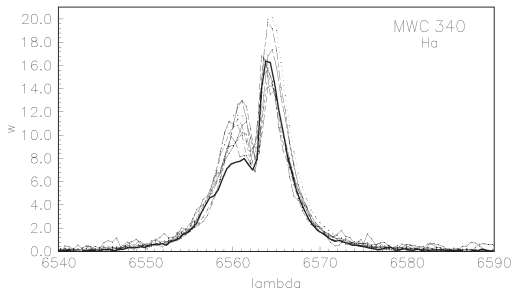


Figure 1: The observed profiles of H$\alpha$ lines.

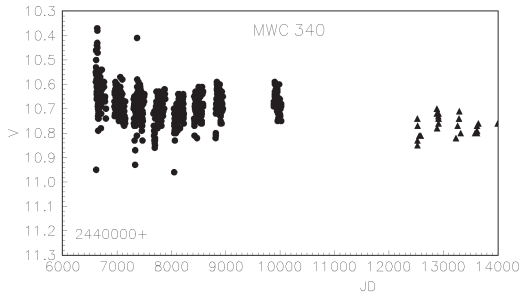


Figure 2: The light curve of MWC340

The first and second models best satisfy to our observations. But in case of third model we must have the some displacement of emission line in spectrum violent region. And if the displacement is little, this is difficult to observe on our spectrograms, taking into account the low resolution (R=6000). The problem may be only solved after theoretical calculations with provision for value $I_{blue}$ / $I_{red}$. On our observations the MWC 340 star has the practically symmetric and non-shifted [OI] $\lambda$ 6300.31 emission relatively the laboratory wavelength. Herewith there are observed the variations both the equivalent width (from 0.8 to 1.7 Å - on our observations; 1.10 - the work (Corcoran and Ray 1997); 1.5 - the work (Finkenzeller 1985)) and the maximum intensity of line relatively to the continuum. In generally, as it assumes, the stars having such profile structure of forbidden lines may be regarded as more evolved than stars, in which the emission are shifted in blue region of spectrum (Finkenzeller, 1985). Any distinct correlation's of H$\alpha$ line equal width EW with brightness V and color indexes of star were not observed on our observations. Herewith it should be marked that in observed period the amplitude of changing both the brightness V and color indexes of MWC 340 was lower (Fig.2, where filled circles - the Maidanak's data in V band (Herbst and Shevchenko 1999), filled triangles - our measurements), than on data of Maidanak observatory (V=$10^m$.37-$10^m$.96, (B-V)=$0^m$.68-$0^m$.93, (V-R)=$0^m$.91-$1^m$.27). Our photometric measurements in V band for N2, N3 and N6 stars from Table 1 of Hillenbrand, Meyer, Strom et al (1995) showed the variability of N2 (V=$13^m$.64-$14^m$.01) and N6 (V=$14^m$.21-$15^m$.31) stars and practically brightness constancy of N3 ( $12^m$.08) star, what most likely give evidence about no belonging of this star to the association, but about its projection on given region. The stars in MWC 340 region are significantly younger than those in the surrounded OB associations with the low- and the high-mass stars having formed nearly simultaneously, what lead some authors to the assumption that star formation in this association might have been induced by the propagation of external shock wave into the cloud core.

**References**

Hillebrand L.A., Meyer M.R., Strom S.E., Strutskie M.F.: 1995, *Astron. J.,* **109**, 280.

Herbig G.H.: 1960, *Astrophys. J. Suppl.,* **4**, 337.

Corcoran M., Ray T.P.: 1997, *Astron. Astrophys.,* **321**, 189.

Finkenzeller U.: 1985, *Astron. Astrophys.,* **151**, 340.

Herbst W., Shevchenko V.S.: 1999, *Astrophys. J.*, **118**, 1043.

# THE ROLE OF PHYSICAL EXPERIMENTS IN POPULARIZATION OF EXACT SCIENCES

S.Ledvinka[1,2], J.Pisala[1]

[1]The Nicholas Copernicus Observatory and Planetarium, Kravi hora 2, 61600 Brno, Czech Republic

[2]Department of Theoretical Physics and Astrophysics, Masaryk University, Kotlarska 2, 611 37 Brno, Czech Republic

ABSTRACT. Physical experiments play crucial role in exact sciences. We test our theories which we try give account of the world by experiments. On the one hand, themselves are an inexorable judge which one judge our conceptions about function of the world and on the other side physical experiments can demonstrate a beauty of laws of nature. The Nicholas Copernicus Observatory and Planetarium in Brno (the Czech Republic – EU) has a longtime experience with it.

**Key words**: education: popularization

## 1. Introduction

Education plays important role in our civilisation, therefore we need to pay attention to it. In addition to formal school education an informal education take place outside the system, where knowledge gained can be put in a use in entertaining way.

## 2. The Nicholas Copernicus Observatory and Planetarium

The Nicholas Copernicus Observatory and Planetarium is in Brno in the southeast of the Czech Republic. It is almost inn the centre of the city, which makes it easily accesible for tourists, school trips and members of the public.

Our main focus is on educating and informing the public about astronomy. We stage astronomical observations, audiovisual performance for schools and general public, exhibitions and give lectures on optics for elementary and high schools. I was deputed originate a new conception of lessons on optics.

On the list of the multi-visual performances for the public you will find programmes aimed at a modern survey of the solar system structure and a study of remote areas of the universe at the observation satellites, the ancient history of Brno, etc. We must not forget to mention our foreign language programmes, productions and performances for people with visual impairment. The pleasant environment of the main planetarium, which includes top audio-visual technologies, is also very convenient for various commercial presentations, seminars and formal events.

At the Brno observatory we have several types of telescopes on disposal, beginning with portable apparatuses up to lenses of 15 or 20 centimetres in diameter. The attractions of the evening sky can be examined with assistance from staff at the observatory. Our visitors will be able to see the moon, some of the planets and, naturally, also distant objects in the universe, such as double stars, star clusters, nebulae and galaxies. One can also observe the actual Sun in detail by means of a projection of the Sun onto a large screen by specially adapted telescopes. For foreign visitors we have prepared an audiovisual performance called 'People and Stars'. On the photographic shots, the audience will be shown all the attractive parts of Brno. They will also see the star sky the brightest stars and distinctive constellations and for a finale, they will hear a dramatic story about the explosion of a supernova, which occurred in 1987. The presentation, which is a commentary with slides combined with a projection on the sky dome, lasts approximately one hour. Visitors can also take a look at the exhibition in the planetarium foyer and can buy astronomy books. More about us (*www.hvezdarna.cz*).

We have not made only audio-visual performances, observation of sky and exhibitions but we have organized professional as well as popular lectures too.

## 3. The Adventure Science

We have a long time and rich experience in astronomical education, see (Pokorny, 2001; Mikulasek, 2001). For general public we have prepared special series The Advanture Science. The series Adventure Science includes two special shows: *The Adventure Physics* (Tyc, 2006) and *The Adventure Chemistry* (Pisala, 2006) for general public. *The Adventure Optics* is third part of series The Adventure Science, this once for students

of elementary and middle schools. These shows show Physics and Chemistry as attractive natuaral sciences for everyone.

*3.1.1 The Adventure Physics*

The Adventure Physics is a special show. The lecturer is showman with excellent knowledge of physics and other natural sciences. The lecturer shows some amusing experiments from mechanics, thermodynamics, acoustics, optics and electromagnetism.

For example:

- mechanics: squeak of door, law of conservation angular momentum with revolving chair, Archimedes' cannon, swimming of picayune on water level
- acoustics: Lissajous figures, blow out of the candle
- thermodynamics: hot-flue balloon, liquid nitrogen
- optics: reflection, diffraction and scattering of light
- electromagnetism: eddy currents, experiments with microwave oven and CD disc

*3.1.2 The Adventure Chemistry*

The Adventure Chemistry is second part of the series The Adventure Science. The lecturer demonstrates nontraditional chemical experiments (e.g. colored acido-basics reactions, explosives reactions with hydrogen and oxygen, fast crystallization) and explains fundamentals of chemistry, which we can watch every day around us in common life.

*3.1.3 The Adventure Optics*

Structure of lectures:

- *Trailer*: Advertising trailer (it is manly for the teachers and students to have some idea what the (optics) lecture is about). We have prepared two trailers, for geometrical optics 'Autopsy of the eye' and for wave optics 'Blue sky – Scattering of the light'.)
- *Lecture*
  1. An introduction into the basic terms and jargon used in the field of physics (it can serve to refresh memory of those who has some previous knowledge and introduce new words and concepts to fresh students)
  2. Application, explanation about the use of the optics in the arts, technology and military use, also in the nature. We show them applications of laws of optics in everyday life.
  3. Reinforcing the gained theoretical knowledge by short but spectacular experiments, underline the use of the optics in everyday life events. For example, to show the boundary of geometrical optics an experiment with the use of two polarised filters and optically active substance (in this case my glasses with the hardened plastic lenses and cellophane, which has mysterious influence on students because they could not understand yet the laws and phenomenon of the optics and they are lost to explain the observed experiment. Similarly, in the wave optics, the observation of fluorescence in the glass with the tonic illuminated by UV LED diode and comparison with the same glass filled only with the water (Ledvinka, 2007).
- *After lecture.* The printed materials will remind student of the experiments they witnessed and in addition, it will point into everyday application of the optics. Those printed materials follow the structure of the lecture, using the appropriate and correct terms and jargons, then the application and evaluation. However, those materials do not attempt to replace any textbooks or lessons. I am preparing the file of all experiments for my co-workers which ones are used.

## 4. Conclusion

Our experience evince interest of general public about natural sciences. School children can be capture by science too but they need an attractive form of natural sciences.

This text did not pass stylistic revision and grammar check.

*Acknowledgements.* The authors are thankful to anybody who has read this contribution to the end.

## References

Pokorny Zd.: 2001, *Astronomicke vzdelavani (Astronomical Education), inaugural dissertation.*

Mikulasek Zd.: 2001, *Course of Astrophysics, inaugural dissetation.*

Ledvinka S.: 2007, *Dobrodruzna optika na brnenske hvezdarne (The Adventure Optics in The N.C.O.P in Brno). In Modern trends 3. Plzen*, 1 p.

Ledvinka S.: 2005a, *Phys. Ed., Bristol, UK: IOP Publ.*, **40**, 305-305, *ISSN 0031-9120.*

Ledvinka S.: 2005b, *In Proc. 37th Conf. On Variable Stars Research. pub. Brno*, 2 p.

Tyc T.: 2006, *Dobrodruzna fyzika (The Adventure Physics), The Nicholas Copernicus Observatory and Planetarium in Brno.*

Pisala J.: 2006, *Dobrodruzna chemie (The Adventure Chemistry), The Nicholas Copernicus Observatory and Planetarium in Brno.*

# ASTRONOMICAL EDUCATION IN THE NICHOLAS COPERNICUS OBSERVATORY AND PLANETARIUM IN BRNO

S. Ledvinka[1,2], J. Pisala[1]

[1] The Nicholas Copernicus Observatory and Planetarium, Kravi hora 2, 61600 Brno, Czech Republic

[2] Department of Theoretical Physics and Astrophysics, Masaryk University, Kotlarska 2, 611 37 Brno, Czech Republic

ABSTRACT. The astronomy can be an ideal vehicle for extending the informal education. The planetariums can be the appropriate choice for an extended education. The science of astronomy has a great advantage over other disciplines and all those attributes can be fully utilised in creation of an educational programs for students and general public. The following article will describe how The Nicholas Copernicus Observatory and Planetarium in Brno dealt with some aspects of the astronomical education.

**Key words**: Physics: experiments: education: popularization;

## 1. Introduction

Welcome to the world of dreams, of stars, of planets – welcome to The Nicholas Copernicus Observatory and Planetarium in Brno, Czech Republic – European Union.

## 2. Astronomy as Instrument of Popularization

The astronomy can be an ideal vehicle for extending the informal education. The planetariums or museums can be the appropriate choice for an extended education. The science of astronomy has a great advantage over other disciplines; the starry sky is familiar to every human. Even blinds can see stars in our institution because we have got a haptic planetarium. As humans, we are deeply moved by sunrise and sunset or the dark heavens with twinkling stars. Sun and Moon eclipses, despite our education can have a profound effect on us humans as it has on the builders of the Stonehenge. Therefore, the astronomy combines the poetic emotional side with the natural science. In addition, astronomy is a good example of the interdisciplinary science. All those attributes can be fully utilised in creation of an educational programs for student and public at large. The following article will describe how The Nicholas Copernicus Observatory and Planetarium in Brno dealt with some aspects of the popularization of science. Most of our activities are not only about creating programs about astronomy or observations, but also, for example, additional educational programs about the experiments in the field of optics. Where else can students find a better practical application about the optics, then here, at the planetarium! Astronomy can be, in this case, an instrumental tool helping to explain the laws of the optics (generally physics) to the students (Ledvinka, 2005a).

The Nicholas Copernicus Observatory and Planetarium is in Brno in the southeast of the Czech Republic. It is almost inn the centre of the city, which makes it easily accesible for tourists, school trips and members of the public.

Our main focus is on educating and informing the public about astronomy. We stage astronomical observations, audiovisual performance for schools and general public, exhibitions and give lectures on optics for elementary and high schools.

On the list of the multi-visual performances for the public you will find programmes aimed at a modern survey of the solar system structure and a study of remote areas of the universe at the observation satellites, the ancient history of Brno, etc. We must not forget to mention our foreign language programmes, productions and performances for people with visual impairment. The pleasant environment of the main planetarium, which includes top audio-visual technologies, is also very convenient for various commercial presentations, seminars and formal events.

At the Brno observatory we have several types of telescopes on disposal, beginning with portable apparatuses up to lenses of 15 or 20 centimetres in diameter. The attractions of the evening sky can be examined with assistance from staff at the

observatory. Our visitors will be able to see the moon, some of the planets and, naturally, also distant objects in the universe, such as double stars, star clusters, nebulae and galaxies. One can also observe the actual sun in detail by means of a projection of the sun onto a large screen by specially adapted telescopes.

### *2.1. Astronomical Education*

We offer a lot of astronomical shows for general public in planetarium dome. People can see the sky at day and at night. Visitors can come along observe Sun at day and they can see planet, nebulas, stars and constellations in the evening. The Advanture Science is a special serie of science show. The lecturer is showman with excellent knowledge of physics and other natural sciences. These shows show Physics and Chemistry as attractive natuaral sciences for everyone.

- The Adventure Physics (Tyc, 2006) is first part of the series The Adventure Science. The lecturer shows some amusing experiments from mechanics, thermodynamics, acoustics, optics and electromagnetism.
- The Adventure Chemistry (Pisala, 2006) is second part of the series. The lecturer shows some amusing experiments from chemistry.

  We had a great success with those programs (The Adventure Physics and The Adventure Chemistry), which during its fourteen performances were visited by 3000 visitors (Pokorny, 2001; Ledvinka, 2005a).

#### *2.1.1 Astronomical Education For the Schoolable Public*

For pupils we have prepared a lot of audio-visual performaces with astromomical themes (*www.hvezdarna.cz*) (e.g. Sun forgotten star, Rare Earth, Moon hoax, etc).

The Adventure Optics is special lecture for students of elementary and high schools. This physical show demonstrate elementary laws of optics in amusing way. This show the great response from the schoolabele public. The Adventure Optics was visited by 3400 pupils in last year (Ledvinka, 2007).

#### *2.1.2 E-learning For Everyone*

Astronomical courses was prepared for a long time but the attendance became fall down recently. Hence we have prepared Internet astronomical course for everyone (Pokorny, 2006). Name of this course is *Vademecum – The Guide of the Universe.* Participants of the course graduate ten lessons from astronomy. Their knowledge are test. The participants can use consult of our staffers.

## 3. Conclusion

- Our experience evince interest of general public about natural sciences especially astronomy.
- School children can be capture by science too but they want an attractive form of natural sciences.
- And this is our duty.

## Reference

*www.hvezdarna.cz*

Pokorny Zd.: 2001, *Astronomicke vzdelavani (Astronomical Education), inaugural dissertation.*

Pokorny Zd.: 2006, *http://vademecum.hvezdarna.cz.*

Mikulasek Zd.: 2001, *Course of Astrophysics, inaugural dissetation.*

Ledvinka S.: 2007, *Dobrodruzna optika na brnenske hvezdarne (The Adventure Optics in The N.C.O.P in Brno). In Modern trends 3. Plzen*, 1 p.

Ledvinka S.: 2005a, *Phys. Ed., Bristol, UK: IOP Publ.*, **40**, 305-305, *ISSN 0031-9120.*

Ledvinka S.: 2005b, *In Proc. 37th Conf. On Variable Stars Research. pub. Brno*, 2 p.

Tyc T.: 2006, *Dobrodruzna fyzika (The Adventure Physics), The Nicholas Copernicus Observatory and Planetarium in Brno.*

Pisala J.: 2006, *Dobrodruzna chemie (The Adventure Chemistry), The Nicholas Copernicus Observatory and Planetarium in Brno.*

# PHOTOMETRY OF THE ASYNCHRONOUS POLAR V1500 CYG AT VARIOUS PHASES OF THE SYNODICAL CYCLE IN 2005-2006 YRS

A.A. Litvinchova[1], E.P. Pavlenko[1,2], S.Yu. Shugarov[3,4]

[1,2] Crimean Astrophysical ObservatoryNauchny 98409 Crimea, Ukraine, *litanya@ukr.net*
[3] Sternberg Astronomical Institute, Moscow, Russia
[4] Astron. Inst. of the Slovak Academy of Sciences, 05960, Tatranska Lomnica, Slovakia

ABSTRACT. We present photometry of the asynchronous polar Nova Cygni 1975 = V1500 Cyg in 2005-2006. The brightness of star in R in the 2006 was increased on $0.53^m$ in comparison with 2005. We constructed and analyzed the light curves of V1500 Cyg in the all intervals of phases of the cynodical cycle. Based on the photometric observations during 2005-2006 yrs, we confirmed that a modulation with the beat period is present (amplitude = $0.3^m$). The orbital O-C shown of dependence from phases of beat period in minima and maxima, that point to existence of additional asymmetric irradiation. At the beat phase 0.73 we found that the profile of the "orbital" light curve of V1500 Cyg differs from the ordinary profile of orbital light curve caused by the reflection effect.

**Key words**: Stars: binary: cataclysmic; stars: individual: V1500Cyg.

## 1. Introduction

Nova Cygni 1975 (V1500 Cyg) is the fast nova. V1500 Cyg is the only recognized Nova and asynchronous polar. In its post-nova state (R = $17.5^m$ - $20^m$) V1500 Cyg displays two prominent photometrical periods: the orbital period P1 = 0.1396129 day (Semeniuk et al., 1995) and the beat (synodical) period P2 = 8.4 day (Pavlenko et al, 2002). The orbital light modulation is caused by the strong reflection effect from the heated side of secondary arising as a result of the irradiation by the hot white dwarf. The early investigations of the asynchronous polar V1500Cyg (Pavlenko, 2003) shown that amplitude of the beat modulation has been changed from $0,5^m$ to vanishing small in 2000 - 2002. The beat profile also varied from one-humped to the two-humped shape for different years, pointing to the one-pole or two-pole accretion onto the white dwarf. We considered the pequliarities of V1500 Cyg behavior in 2005-2006 yrs in different beat phases.

## 2. Observations

The present CCD R observations of V1500 Cyg have been carried out in the Crimean astrophysical observatory in the primary focus of the 2.6-m Shajn telescope and with the 1.25 meter ZTE telescope of the Crimean Laboratory of the Sternberg Astronomical Institute in 2005 - 2006.

## 3. Results

### *3.1. Beat period*

For all data we calculated the phases of beat period using ephemeris: HJD=2452370.30+8.438E. The original data folded on the beat period are presented in Fig.1 (upper panel). The scattering is caused by the orbital light modulation. Some of the nightly observations of 2005 are on the identical beat phases with data of 2006 but are systematically brighter on $0.53^m$, possibly caused by the mean brightness increase. It is clearly seen in the middle panel of Fig.1, where the averaged data are given. Suggesting this, we shifted data of 2006 on the $0.53^m$. The all data normalized to the mean for 2005 year level are shown in Fig.1 (the lower panel). Despite the some scattering we have seen that the beat modulations is present but with respectively small amplitude $0.3^m$ similarly to the beat amplitude detected in 2002. The observations are in the agreement with one-hump model.

### *3.2. Atypical orbital light curve*

The typical orbital light curves of V1500 Cyg resemble the curves caused by reflection effect. However the times of maxima and minima could be slightly shifted. Sometimes the deviation from the typical profile could be observed. In Fig.2 we show the example of the orbital light curve (21 October 2006) with a $0.4^m$ - bump in the vicinity of minimum. This light curve we observed at the beat phase 0.73.

*3.3. O-C*

We calculated the times of minima and maxima of the V1500 Cyg brightness variations in R using the Pogson's method of chords. They age given in Table 1. The O-C was calculated using the ephemeris:

HJD (min) = 2453534.430+0.139613∗E

HJD (max) = 2453534.369+0.139613∗E

The dependence of orbital O-C on the phase of beat period is presented in Fig.3. One could see that O-C display the same sine-like dependence on the beat phase. The times of maxima are of the better accuracy.

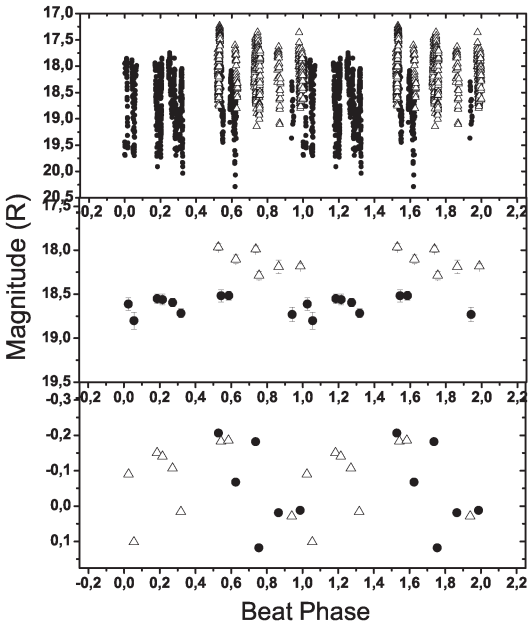


Figure 1: The 2005-2006 R-band data folded on the current 8.438 day beat period. Data of 2005 are marked by black squares and data of 2006 - open triangles. Upper panel: original data; middle panel: averaged data; lower panel: normalized averaged data.

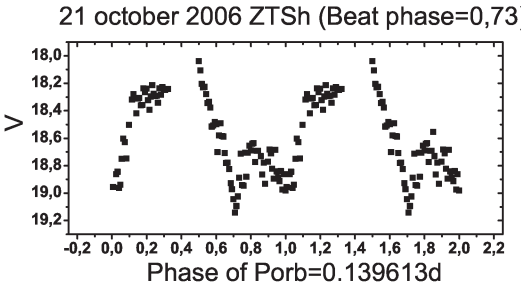


Figure 2: The orbital light curve showing strong discrepancy with reflection effect.

## 3. Conclusion

We have shown that the orbital light curve sometimes appears in the form differ from the pure reflection effect. The O-C residuals display the dependence on the beat phase.

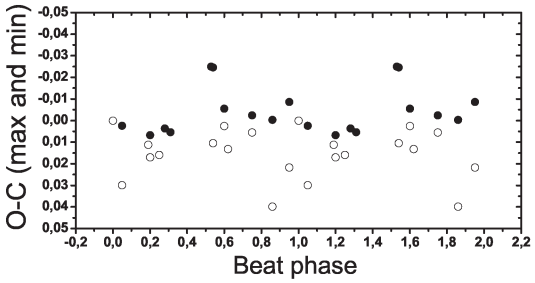


Figure 3: The dependence of orbital O-C on the phase of beat period. Minima are marked by open circles and maxima - by filled.

Table 1: Timings of Maxima and Minima for V1500 Cyg in 2005-2006

| JDHel(max) | JDHel(min) |
|---|---|
| 53534,369 | 53534,430 |
| 53560,479 | 53560,428 |
| 53562,438 | 53585,400 |
| 53585,471 | 53587,500 |
| 53612,418 | 53612,350 |
| 53613,365 | 53654,368 |
| 53615,320 | 53683,260 |
| 53683,191 | 54062,320 |
| 54062,383 | 54063,150 |
| 54064,200 | 54064,720 |
| 54065,169 | 54065,400 |

There could be two reasons, which promote appearance of the O-C variations:

1. The asymmetric and beat pase-depending heating of the red dwarf by the asynchronously rotating source of irradiation (accretion columns)

2. The "orbiting debris" around white dwarf may absorb an ultra-violet radiation of the white dwarf and reduces its heating effect on the secondary.

*Acknowledgements.* This work was partially supported by the grant of the Ukrainian Fund of Fundamental Research F 25.2/139.

### References

Kaluzny Ja., Semeniuk I.: 1987, *AcA.,* **37**, 349.

Pavlenko E.P. et al: 2002, *ASP Conf. Ser.,* **261**, 651.

Pavlenko E.P.: 2003, *Odessa Astron. Publ.,* **16**, 41.

Semeniuk I., Olech A., Nalezyty M.: 1995, *AcA.,* **45**, 747.

Schmidt G.D., Liebert J., Stockman H.S.: 1995, *ApJ,* **441**, 414.

Litvinchova A.A., Pavlenko E.P: 2006, *Abstract Book of the XXVIth General Assembly,* 225.

# EVALUATION OF OUTER CORE VISCOSITY INFLUENCE ON THE EARTH FORCED NUTATION

M.V. Lubkov
Poltava Gravimetrical Observatory of NASU, Poltava 36029 Ukraine, *pgo@poltava.ukrtel.net*

ABSTRACT. On the base of the combined method, consisting of the Sasao, Okubo, Saito (1980) approach with the iteration procedure, allowing couple finite element method with the solution of the Laplace equation, it have evaluated the influence of outer core viscosity on the components of the earth forced nutation. It was derived, that outer core viscosity actually doesn't have influence on the in phase nutation components, but this influence can reach some percents for out of phase nutation components, if we suggest the average value of the outer liquid core viscosity is the order of $10^{10}$ Pas.

**Key words**: Nutation: viscosity of outer core: finite element method.

## 1. Introduction

Still, it is absent certain opinion about the value of outer core viscosity and it's distribution. The evaluations of the average outer core dynamic viscosity, detected by different methods: astro-geodesic, seismic, geomagnetic, methods of melting metals, have scattering from $10^{-1}$ to $10^{14}$ Pas. Probably, this scattering have place due to different approaches. But analysis of the approaches permits pick out the order of the most coordinated average viscosity value about $10^{10}$ Pas. As for law of outer core viscosity distribution, in present time dominates conception: outer core consists on melting metal of the high-viscosity from $10^4$ near mantle boundary to $10^{14}$ Pas into inner core boundary layer of 100 km width [1]. In the Sasao, Okubo, Saito (1980) [2] generalization the tidal variations of the moments of inertia of the elastic mantle and of the fluid core are accounted being parameterized with the help of so called compliances $\kappa_c, \gamma_c, \beta_c$. This compliances may be expressed in terms of the static and dynamic Love numbers k of the second order for the earth and the outer core respectively. Such parametrization also permits to calculate the dissipative effects of the outer core by using imaginary parts of the compliances [3]. In this paper on the base of the combined method [4-6] we have detected the forced nutation of the rotating, self gravitating earth, which consists on elastic mantle, viscosity outer core and solid inner, without calculation of the ocean and atmosphere loadings.

## 2. Formulation of the problem

In the common case, the molecular liquid viscosity be quit of the shear viscosity $\eta_s$ and volume viscosity $\eta_v$. Because the shear viscosity $\eta_s$ plays the main role in the dissipative processes in the case of the toroidal oscillations of the liquid core due to precession-nutation movements of the earth, so we shall consider only this viscosity component. As the influences of the inner core dynamics on the Love number k of the second order are vanishing small, so using of the SOS (1980) approach for detecting of the nutation parameters is enough. Following this approach, we shall define the complex compliances of the earth, consisting on elastic mantle, viscous liquid outer core and inner solid core in the spherical quasi-statical approximation. In this case we have two quasi-statical equations for elastic mantle and viscous liquid core, presented in the Tisserand reference system (X, Y, Z):

$$0 = grad(V_c + \phi_n + V_1 u_R g(R)) - \\ -div\vec{u}gradW + \frac{1}{\rho} divP_1;$$

$$0 = grad(V_e + \phi_n + \phi_c + V_1) + \frac{1}{\rho} divP_2. \qquad (1)$$

Where $\vec{u}$ - displacement vector; $V_e = \gamma\Omega^2(xzcos\sigma t + yzsin\sigma t)$ - tesseral part of tidal wave potential, $\gamma$ - it's amplitude; $\phi_n = -\epsilon\Omega^2(xzcos\sigma t + yzsin\sigma t)$ - changing of centrifugal potential due to nutation; $\epsilon$ - polar motion radius of tidal wave; $V_1 = \gamma_1\Omega^2(xzcos\sigma t + yzsin\sigma t)$ - changing of gravitation potential due to earth deforming, $\gamma_1$ - it's amplitude; $\phi_c = -\beta\Omega^2(xzcos\sigma t + yzsin\sigma t)$ - changing of centrifugal potential due to earth core rotation; $\beta$ - polar motion radius of core rotation; $\Omega$ - angle earth velocity; $W$ - self gravitation potential; $\rho$ - density; $\sigma$ - frequency of the tidal wave; $R$ - earth point radius; $u_R$ - radial displacement; $g(R)$ - gravity acceleration; $P_1, P_2$ - changing of stress tensors in the elastic mantle and viscous liquid core respectively. Let

us suggest, that oscillations into the liquid core are going with the tidal wave frequency $\sigma$, also suggest the absence of the earth surface loads, make up Lagrange functionals. Those functionals express the full energy of the elastic mantle and liquid core in the cylindric coordinate system (z, r, $\varphi$), here axis r coincide with the Tisserand axis Z:

$$E_1 = \pi \int_{F_s} [C_1(\varepsilon_{zz}^2 + \varepsilon_{rr}^2 + \varepsilon_{\varphi\varphi}^2) + 4C_2\varepsilon_{zr}^2 + 2C_3(\varepsilon_{zz}\varepsilon_{rr} + \varepsilon_{zz}\varepsilon_{\varphi\varphi} + \varepsilon_{rr}\varepsilon_{\varphi\varphi})]rdzdr - \pi \int_{F_s} [2(\gamma - \epsilon + \gamma_1)\Omega^2 rw + w(\frac{\partial w}{\partial z}cos\alpha + 2\frac{\partial u}{\partial z}sin\alpha)g(R) + 2w(wcos\alpha + 2usin\alpha)g_R' cos\alpha - 2w(\frac{\partial w}{\partial z} + 2(\frac{\partial u}{\partial r}))g(R)cos\alpha + 2(\gamma - \epsilon + \gamma_1)\Omega^2 zu + u(2\frac{\partial w}{\partial r}cos\alpha + \frac{\partial u}{\partial r}sin\alpha)g(R) + 2u(2wcos\alpha + usin\alpha)g_R' sin\alpha - 2u(2\frac{\partial w}{\partial z} + \frac{\partial u}{\partial r} + \frac{u}{r})g(R)sin\alpha]\rho rdzdr; \quad (2)$$

$$E_2 = \pi \int_{F_s} [C_4(\varepsilon_{zz}^2 + \varepsilon_{rr}^2 + \varepsilon_{\varphi\varphi}^2) + 4C_5\varepsilon_{zr}^2 + 2C_6(\varepsilon_{zz}\varepsilon_{rr} + \varepsilon_{zz}\varepsilon_{\varphi\varphi} + \varepsilon_{rr}\varepsilon_{\varphi\varphi})]rdzdr - \pi \int_{F_s} [2(\gamma - \epsilon - \beta + \gamma_1)\Omega^2 rw + 2(\gamma - \epsilon - \beta + \gamma_1)\Omega^2 zu]\rho rdzdr. \quad (3)$$

Here $C_1 = K + \frac{4\mu}{3}, C_2 = \mu, C_3 = K - \frac{2\mu}{3}$ - real coefficients; $C_4 = K_f + \frac{4i\sigma\eta_s}{3}, C_5 = i\sigma\eta_s, C_6 = K_f - \frac{2i\sigma\eta_s}{3}$ - complex coefficients; $\mu, K$ - shear and compress modules of the elastic mantle; $K_f$ - compressibility of the liquid core; $\eta_s$ - shear dynamic viscosity of the liquid core; $i$ - imaginary unit; $\varepsilon_{ij}$ - deformation components; $w, u$ - displacement components along $z, r$ respectively; $F_s$ - meridional cross section area of the earth; $cos\alpha = \frac{z}{R}, sin\alpha = \frac{r}{R}$. For resolving the system equations (1), without calculation of the surface loads, the finite element method is using. This method is based on the variational Lagrange principal, expressing the minimum of the full system energy, tends to resolving system of variational equations, such as:

$$\delta E_1 = 0; \delta E_2 = 0. \quad (4)$$

The detailed description of the finite element resolving problem is presented in the publications [4,5]. But the finite element only, doesn't permit to calculate the earth gravity field relaxation due to it's deforming. For resolving this problem we will use Wu (2004) approach [7]. As earth deforming potential $V_1$ is harmonic function, so it must satisfy to Laplace equation. Another hand, exactly resolving of the Laplace equation can be defined from the radial displacements $u_r$ on the heterogeneity layer boundaries of the earth. The radial displacements can be detected by the finite element method [4]. The combined resolving of the problem is realizing during for iteration process:

1)firstly, the finite element problem is realizing for $V_1 = 0$, as a result, the radial displacements $u_r$ are defined;

2)the meanings of the earth deforming potential $V_1$ are defining from the detected radial displacements $u_r$ on the base of the Wu formalism [7];

3)then, presented here procedure repeats with the calculation of the defined meanings of the potential $V_1$;

4)the iteration process is continuing till of the convergence of the results of the resolving problem; as calculation shows, the convergence have been gained after 4 - 6 iterations.

### 3. The definition of the earth forced nutation with the calculation of the outer core viscosity

The retrograde and prograde circular nutation components in phase and out-of-phase are detected by formulas [8]:

$$\eta^+ = -\frac{1}{2}(\epsilon_r + \Psi_r sin\epsilon_0)(\frac{\eta^+}{\eta_r^+}) = B_R^+ - iB_I^+; \quad (5)$$

$$\eta^- = -\frac{1}{2}(\epsilon_r - \Psi_r sin\epsilon_0)(\frac{\eta^-}{\eta_r^-}) = B_R^- - iB_I^-. \quad (6)$$

Where $\epsilon_0$ - ecliptic obliquity; $B_R^+, B_R^-$ and $B_I^+, B_I^-$ - are retrograde and prograde circular nutation components in phase and out-of-phase respectively; the meanings of nutation for rigid earth in the obliquity $\epsilon_r$ and in the longitude $\Psi_r$ were took from Kinoshita (1977) theory [9]. The relative amplitudes of the retrograde $\frac{\eta^+}{\eta_r^+}$ and prograde $\frac{\eta^-}{\eta_r^-}$ circular nutation components were defined on the base of the combined method [4-6] with the calculation of the crossing from polar motion to nutation coordinates:

$$\eta(\sigma) = \frac{A_f}{A_m}\frac{e\Omega^2}{\sigma(\sigma - \sigma_0)}[1 - \frac{\gamma_c}{e} + \frac{\gamma_c - \kappa_c}{e}\frac{\sigma + \Omega}{\Omega}]\gamma + [\frac{e\Omega^2}{\sigma(\sigma + \Omega)} - \frac{\kappa_c\Omega}{\sigma}]\gamma; \quad (7)$$

$$\sigma_0 = -\frac{A}{A_m}(e_f - \beta_c)\Omega - \Omega; \quad (8)$$

$$\kappa_c = \frac{k_o R_e^5 \Omega^2}{3GA}; \gamma_c = \frac{k_0^f R_f^5 \Omega^2}{3GA_f}; \beta_c = \frac{k_1^f R_f^5 \Omega^2}{3GA_f}. \quad (9)$$

Here $e, e_f$ - ellipticities of the earth and outer core respectively; $A, A_m, A_f$ - the main moments of inertia of the earth, mantle and outer liquid core; $\sigma_0$ - the near diurnal resonance of the liquid core frequency; $R_e, R_f$ - radiuses of the earth and liquid core respectively; $G$ - gravitation constant. The complex, due to liquid core viscosity, static Love numbers of the second order for the earth and liquid core: $k_0, k_o^f$ were defined on the base of above presented iteration procedure under static conditions: $\gamma - \epsilon = 1, \beta = 0$, from the formulas: $k_0 = \gamma_1(R_e), k_0^f = \gamma_1(R_f)$. There $\gamma_1(R_e), \gamma_1(R_f)$ - are complex amplitudes of the gravitating potential $V_1$ on the earth and liquid core surfaces respectively. The complex dynamic Love numbers: $k_1, k_1^f$ were defined analogically under dynamic conditions: $\gamma - \epsilon = 0, \beta = 1$. Then complex compliances: $\kappa_c, \gamma_c, \beta_c$ were detected by the formulas (9). As for typical liquid core viscosity values the imaginary part of the $\beta_c$ parameter become vanishing small, so we have neglected by one and have considered only real part of the liquid core resonance frequency $\sigma_0$ (8). At the detection iteration process ten layer earth model, obtaining on the base of the standard earth "PREM" - model, was used. The obliquity and longitude nutation components in phase and out-of-phase can be defined by the formulas:

$$\epsilon_R = -B_R^- - B_R^+; \Psi_R sin\epsilon_0 = B_R^- - B_R^+;$$
$$\epsilon_I = B_I^- - B_I^+; \Psi_I sin\epsilon_0 = B_I^- + B_I^+. \qquad (10)$$

The meanings of the retrograde and prograde circle nutation components in phase and out-of-phase for: 18.6 - year, annual, semiannual and fortnightly terms in milliseconds are presented in the Table 1. The meanings were obtained by combined method for rotating, self gravitating earth, consisting on the elastic mantle, viscosity outer liquid core and rigid inner core, without calculation of the ocean and atmosphere loadings. It was considered 2 variants:

a)the variant of the homogeneous viscosity liquid core with the characteristic shear dynamic viscosity equaled $10^{10}$ Pas;

b)the variant, which calculates the outer-inner core boundary layer of 100 km width, with the viscosity value of the order $10^{14}$ Pas, in the rest part of the liquid core we choose the average viscosity value of the $10^8$ Pas.

For comparison, there are respective meanings of the nutation components, presented by modern nutation theory - MHB (2000) [10], at this table. The comparison shows, that viscosity effect of the liquid core actually doesn't have influence on the in phase nutation components, another hand this influence may reach some percents for the out-of-phase nutation components if we suggest the average liquid core viscosity value is equal $10^{10}$ Pas. Also the comparison of the results, obtaining on the base of two above considering variants (a) and (b), tends to suggestion, that value of the order $10^{10}$ Pas is the top boundary of the average liquid core viscosity.

Table 1: The retrograde and prograde circular nutations in phase and out-of-phase, presented for main nutation terms in milliseconds.

| Parameters | (a) | (b) | MHB-2000 |
|---|---|---|---|
| phase | in | in | in |
| | out of | out of | out of |
| 18.6-year | | | |
| $\eta^+$ | -1181.1903 | -1181.1903 | -1180.3727 |
| | -0.0028 | -0.0005 | -0.1035 |
| $\eta^-$ | -8021.8201 | -8021.8201 | -8024.8023 |
| | 0.0223 | 0.0037 | 1.4295 |
| annual | | | |
| $\eta^+$ | -31.3005 | -31.3005 | -33.0475 |
| | 0.0047 | 0.0008 | 0.3395 |
| $\eta^-$ | 25.6561 | 25.6561 | 25.6475 |
| | 0.0005 | 0.0001 | 0.1365 |
| semiannual | | | |
| $\eta^+$ | -24.5802 | -24.5802 | -24.5590 |
| | -0.0014 | -0.0002 | -0.0453 |
| $\eta^-$ | -549.0812 | -549.0812 | -548.5020 |
| | -0.0151 | -0.0025 | -0.5043 |
| fortnightly | | | |
| $\eta^+$ | -3.6401 | -3.6401 | -3.6417 |
| | -0.0001 | -0.0000 | -0.0153 |
| $\eta^-$ | -94.0103 | -94.0103 | -94.1722 |
| | 0.0047 | 0.0008 | 0.1477 |

## References


Zharov V.E., Pasynok S.L.: 2001, *Astron. J.,* **11**, 78.

Sasao T., Okubo S., Saito M.: 1980, *Proc. IAU Symp.*, 78.

Krasinsky G.A.: 2003, *Commn. IAA RAS.,* **157.**

Lubkov M.V.: 2004, *Geophys. J.,* **6**, 26.

Lubkov M.V.: 2005, *Kinem. phys. cel. bd.,* **5**, 21.

Lubkov M.V.: 2007, *Geohhys. J.,* **5**, 29.

Wu P.: 2004, *Gtophys. J. Int.,* **2**, 158.

Wahr J., Bergen Z.: 1986, *Geophys. J. R. Astr. Soc.,* **2**, 87.

Kinoshita H.: 1977, *Celest. Mech.,* 15.

Mathews P.M., Herring T.A., Buffet B.A.: 2000, *Washington: DC USA*

# ABOUT INFLUENCE OF LATERAL HETEROGENEITIES IN THE EARTH UPPER MANTLE ON THE LOVE NUMBERS FOR DIURNAL TIDES

M.V. Lubkov

Poltava Gravimetrical Observatory of NASU, Poltava 36029 Ukraine, *pgo@poltava.ukrtel.net*

ABSTRACT. On the base of the combined method, consisting of the Sasao, Okubo, Saito approach with the iteration procedure, allowing the coupling of the finite element method with the solution of the Laplace equation, it was defined the influence of the horizontal heterogeneities in the upper mantle on the diurnal Love and Shida numbers of the second order. It was determined, that maximum deviations due to such heterogeneities can reach 0.5 percent for Love numbers k and h, for Shida number - l the deviations don't depend from the tidal wave frequency and approximately make up 0.2 percent. For evaluation of the accuracy of the suggested method it was carried out the comparison of the Love numbers k for the main diurnal tides, obtained on the base of the PREM - earth model, with respective results of Mathews, Buffet, Shapiro (1995) and Dehant (1987).

**Key words**: Diurnal Love numbers : lateral heterogeneities of the upper mantle: finite element method.

## 1. Introduction

It is known about availability of the lateral heterogeneities in the earth upper mantle for a long time. The investigations of the earth surface wave propagation, started at the beginning of the last century, had permitted to discover horizontal heterogeneities of the upper mantle. The existence of this heterogeneities is the main factor, which makes difficulty on the detailed study of the upper part of the earth structure by the surface wave methods. So it's not wonder, that so far quantitative investigations of the horizontal heterogeneities of the earth upper part, so it's rest part, are on the initial state. The grave seismic investigation of horizontal heterogeneities of the upper mantle in the Tibet plate region was made by Woodward, Molnar (1995) [1]. The authors went to conclusion, that Tibet plate is the most significant by the depth and stretch of the horizontal heterogeneities of the upper mantle. At this region the width of continental lithosphere approximately two ones large then normal continental lithosphere width, stretches out more then 2000 km. It tends to the forming of the lateral heterogeneities with depth from 250 to 300 km in the upper mantle. It's arise the question, how much similar anomalies influence on the such earth global characteristics, as the Love and Shida numbers. Because it's very difficult to give strict answer on this question, so we have modeled the influence of horizontal upper mantle heterogeneities similar that, described in the work [1], on the diurnal Love and Shida numbers of the second order. For the evaluation of the accuracy of the suggested method it was carried out the comparison of the Love numbers k for the main diurnal waves, obtained on the base of spherical symmetric earth model PREM, with respective results of Mathews, Buffet, Shapiro (1995) [2] and Dehant (1987) [3].

## 2. Combined method resolving of the problem

As in further we shall consider the Love and Shida numbers of the second order in the diurnal range of tidal waves, so we can neglect by influences of the inner core dynamics [2] and use the approximate Saso, Okubo, Saito (1980) approach [4]. Following this approach, we shall define the complex compliances of the earth, consisting on the elastic lateral heterogeneity upper mantle, liquid outer core and inner solid core in the spherical quasi-statical approximation. In this case, we have two quasi-statical equations for elastic mantle and liquid core, presented in the Tisserand reference system (X, Y, Z):

$$0 = grad(V_c + \phi_n + V_1 u_R g(R)) - \\ -div\vec{u}gradW_g + \frac{1}{\rho} div\hat{P}_1;$$

$$0 = grad(V_e + \phi_n + \phi_c + V_1) + \frac{1}{\rho} div\hat{P}_2. \qquad (1)$$

Here $\vec{u}$ - displacement vector; $V_e = \gamma\Omega^2(xzcos\sigma t + yzsin\sigma t)$ - tesseral part of tidal wave potential, $\gamma$ - it's amplitude; $\phi_n = -\epsilon\Omega^2(xzcos\sigma t + yzsin\sigma t)$ - changing

of centrifugal potential due to nutation; $\epsilon$ - polar motion radius of tidal wave; $V_1 = \gamma_1\Omega^2(xzcos\sigma t + yzsin\sigma t)$ - changing of gravitation potential due to earth deforming, $\gamma_1$ - it's amplitude; $\phi_c = -\beta\Omega^2(xzcos\sigma t + yzsin\sigma t)$ - changing of centrifugal potential due to earth core rotation; $\beta$ - polar motion radius of core rotation; $\Omega$ - angle earth velocity; $W_g$ - self gravitation potential; $\rho$ - density; $\sigma$ - frequency of the tidal wave; $R$ - earth point radius; $u_R$ - radial displacement; $g(R)$ - gravity acceleration; $\hat{P}_1, \hat{P}_2$ - changing of stress tensors in the elastic mantle and liquid core respectively. Suggesting, that oscillations into the liquid core are happening with the tidal wave frequency $\sigma$, also suggesting the absence of the earth surface loads, make up Lagrange functionals. The functionals express the full energy of the elastic mantle and liquid core in the cylindric coordinate system (z, r, $\varphi$), here axis r coincide with the Tisserand axis Z:

$$\begin{aligned} E_m = \pi \int_{F_s} [B_1(\varepsilon_{zz}^2 + \varepsilon_{rr}^2 + \varepsilon_{\varphi\varphi}^2) + 4B_2\varepsilon_{zr}^2 + \\ + 2B_3(\varepsilon_{zz}\varepsilon_{rr} + \varepsilon_{zz}\varepsilon_{\varphi\varphi} + \varepsilon_{rr}\varepsilon_{\varphi\varphi})]rdzdr - \\ - \pi \int_{F_s} [2(\gamma - \epsilon + \gamma_1)\Omega^2 rw + w(\frac{\partial w}{\partial z}cos\alpha + \\ + 2\frac{\partial u}{\partial z}sin\alpha)g(R) + 2w(wcos\alpha + \\ + 2usin\alpha)g_R' cos\alpha - 2w(\frac{\partial w}{\partial z} + \\ + 2(\frac{\partial u}{\partial r}))g(R)cos\alpha + 2(\gamma - \epsilon + \gamma_1)\Omega^2 zu + \\ + u(2\frac{\partial w}{\partial r}cos\alpha + \frac{\partial u}{\partial r}sin\alpha)g(R) + 2u(2wcos\alpha + \\ + usin\alpha)g_R' sin\alpha - 2u(2\frac{\partial w}{\partial z} + \\ + \frac{\partial u}{\partial r} + \frac{u}{r})g(R)sin\alpha]\rho rdzdr; \quad (2) \end{aligned}$$

$$\begin{aligned} E_f = \pi \int_{F_s} [B_4(\varepsilon_{zz}^2 + \varepsilon_{rr}^2 + \varepsilon_{\varphi\varphi}^2) + 2B_4(\varepsilon_{zz}\varepsilon_{rr} + \\ + \varepsilon_{zz}\varepsilon_{\varphi\varphi} + \varepsilon_{rr}\varepsilon_{\varphi\varphi})]rdzdr - \\ - \pi \int_{F_s} [2(\gamma - \epsilon - \beta + \gamma_1)\Omega^2 rw + \\ + 2(\gamma - \epsilon - \beta + \gamma_1)\Omega^2 zu]\rho rdzdr. \quad (3) \end{aligned}$$

Where $B_1 = K + \frac{4\mu}{3}$; $B_2 = \mu$; $B_3 = K - \frac{2\mu}{3}$; $B_4 = K_f$; $\mu, K$ - shear and compress modules of the elastic mantle; $K_f$ - compressibility of the liquid core; $\varepsilon_{ij}$ - deformation components; $w, u$ - displacement components along $z, r$ respectively; $F_s$ - meridional cross section area of the earth; $cos\alpha = \frac{z}{R}, sin\alpha = \frac{r}{R}$. For resolving the system equations (1), without calculation of the surface loads, the finite element method is using. This method is based on the variational Lagrange principal, expressing the minimum of the full system energy, tends to resolving system of the variational equations:

$$\delta E_m = 0; \delta E_f = 0. \quad (4)$$

The detailed description of the finite element resolving problem is presented in the publications [5,6]. Another hand, the finite element only, doesn't allow to calculate the earth gravity field relaxation due to tidal earth deformations. For resolving this problem we will use Wu (2004) approach [7]. As earth deforming potential $V_1$ is harmonic function, so it must satisfy to Laplace equation. Another hand, exactly resolving of the Laplace equation can be derived from the radial displacements $u_r$ on the heterogeneity layer boundaries of the earth. The radial displacements can be detected by the finite element method [5]. The combined resolving of the problem is realizing during for iteration process:

1)firstly, the finite element problem is realizing for $V_1 = 0$, as a result, the radial displacements $u_r$ are defined;

2)the meanings of the earth deforming potential $V_1$ are defining from the detected radial displacements $u_r$ by the Wu formalism [7];

3)then, presented here procedure repeats with the calculation of the derived meanings of the potential $V_1$;

4)the iteration process is going on till of the convergence of the results of the resolving problem; as calculation shows, the convergence have been reached after 4 - 6 iterations.

## 3. The detection of the diurnal Love and Shida numbers with the calculation of the upper mantle heterogeneities

The diurnal Love and Shida numbers of the second order, following to the SOS (1980) approach [4], were detected by formulas:

$$k = k_0 + \frac{k_1\beta}{\gamma - \epsilon}; h = h_0 + \frac{h_1\beta}{\gamma - \epsilon}; l = l_0 + \frac{l_1\beta}{\gamma - \epsilon}; \quad (5)$$

$$\begin{aligned} \epsilon = (1 - \frac{\kappa_c}{e}\frac{n}{\Omega})\epsilon_r + \frac{A}{A_f}\frac{n}{\Omega - n}\beta; \\ \beta = \frac{A}{A_m}\frac{\Omega - n}{n - n_0}(1 - \frac{\gamma_c}{e} + \frac{\gamma_c - \kappa_c}{e}\frac{n}{\Omega})\epsilon_r; \\ \epsilon_r = \frac{e\Omega}{\Omega - n}\gamma; n_0 = -\frac{A}{A_m}(e_f - \beta_c)\Omega; \quad (6) \end{aligned}$$

$$\begin{aligned} \kappa_c = \frac{k_o R_e^5 \Omega^2}{3GA}; \gamma_c = \frac{k_0^f R_f^5 \Omega^2}{3GA_f}; \\ \zeta_c = \frac{k_1 R_e^5 \Omega^2}{3GA}; \beta_c = \frac{k_1^f R_f^5 \Omega^2}{3GA_f}. \quad (7) \end{aligned}$$

Where $G$ - gravitation constant; $\epsilon_r$ - polar motion radius for rigid earth; $e, e_f$ - ellipticities of the earth and outer core respectively; $A, A_m, A_f$ - the main

moments of inertia of the earth, mantle and outer liquid core; $n$, $n_o$ - the circle nutation frequency and resonance of the liquid core frequency; $R_e, R_f$ - radiuses of the earth and liquid core respectively. The static parameters: $k_0$, $k_o^f$, $h_0$, $l_0$ - were defined on the base of above presented iteration procedure under the static conditions: $\gamma - \epsilon = 1, \beta = 0$, from the formulas: $k_0 = \tilde{\gamma}_1(R_e), k_0^f = \tilde{\gamma}_1(R_f), h_0 = \tilde{u}_R(R_e), l_0 = \tilde{u}_\tau(R_e)$. There $\tilde{\gamma}_1(R_e), \tilde{\gamma}_1(R_f)$ - are undimensioned amplitudes of the gravitating potential $V_1$ on the earth and liquid core surfaces respectively; $\tilde{u}_R(R_e), \tilde{u}_\tau(R_e)$ - are undimensioned amplitudes of the radial and tangential displacement on the earth surface respectively. The dynamic parameters: $k_1, k_1^f, h_1, l_1$ - were defined analogically under dynamic conditions: $\gamma - \epsilon = 0, \beta = 1$. Then compliances: $\kappa_c, \gamma_c, \zeta_c, \beta_c$ were detected by the formulas (7). At the detection iteration process ten layer earth model was used. For the counting out of modeling of the lateral upper mantle heterogeneities the spherical symmetric earth model PREM was chose. Following to conclusions of the work [1], it was made suggestion, that power of the continental lithosphere in the region of the horizontal anomaly reaches 250 km. As horizontal dimensions of the upper mantle anomaly, the values: 1000 and 3000 km were took. In the Table 2. the meanings of the Love and Shida numbers of the second order for the main diurnal tidal waves, obtained on the base of the PREM model and with calculation of considering above horizontal anomalies, are presented. The comparison of the table data shows, that maximum deviations of such upper mantle heterogeneities for the Love number k change from 0.07 percent for the waves, distant from the liquid core resonance frequency $n_0$, to 0.5 percent for the tidal wave $\Psi_1$, for the Love number h from 0.03 to 0.5 percent. For the Shida number l - the deviations don't depend from the tidal wave frequency and approximately equal 0.2 percent. For the evaluation of the accuracy of suggested above combined method, the comparison of the Love numbers k of the second order for the main tidal waves, obtained by this method on the base of PREM model, with respective results of Mathews, Buffet, Shapiro (1995) [2] and Dehant (1987) [3] are presented in the Table 1.

Table 1: The Love numbers k of the second order for main tidal waves, obtained by the combined method for the PREM model, also analogical results of Mathews, Buffet, Shapiro (1995) and Dehant (1987).

| Tidal waves | Comb. method | MBS | Dehant |
|---|---|---|---|
| $O_1$ | 0.2951 | 0.2962 | 0.2958 |
| $M_1$ | 0.2940 | 0.2950 | 0.2945 |
| $P_1$ | 0.2841 | 0.2848 | 0.2850 |
| $S_1$ | 0.2773 | 0.2766 | 0.2783 |
| $K_1$ | 0.2535 | 0.2537 | 0.2547 |
| $\Psi_1$ | 0.4667 | 0.4662 | 0.4667 |
| $OO_1$ | 0.2977 | 0.2989 | 0.2985 |

Table 2: The Love and Shida numbers of the second order for main tidal waves, obtained by the combined method on the base of the spherical symmetric earth model PREM, also with calculation of the upper mantle heterogeneities of the order 1000 and 3000 km respectively.

| Tidal waves | PREM | 1000 km | 3000 km |
|---|---|---|---|
| $O_1$ | | | |
| k | 0.295093 | 0.295160 | 0.295293 |
| h | 0.597420 | 0.597486 | 0.597619 |
| l | 0.0837803 | 0.0838468 | 0.0839797 |
| $P_1$ | | | |
| k | 0.284098 | 0.284167 | 0.284305 |
| h | 0.575715 | 0.575783 | 0.575919 |
| l | 0.0844556 | 0.0845203 | 0.0846498 |
| $S_1$ | | | |
| k | 0.277294 | 0.277367 | 0.277513 |
| h | 0.562282 | 0.562357 | 0.562507 |
| l | 0.0848735 | 0.0849370 | 0.0850640 |
| 165.545 | | | |
| k | 0.256157 | 0.256257 | 0.256457 |
| h | 0.520556 | 0.520679 | 0.520926 |
| l | 0.0861716 | 0.0862304 | 0.0863481 |
| $K_1$ | | | |
| k | 0.253455 | 0.253560 | 0.253770 |
| h | 0.515221 | 0.515354 | 0.515619 |
| l | 0.0863376 | 0.0863957 | 0.0865120 |
| 165.565 | | | |
| k | 0.250363 | 0.250474 | 0.250696 |
| h | 0.509117 | 0.509261 | 0.509549 |
| l | 0.0865275 | 0.865848 | 0.0866995 |
| $\Psi_1$ | | | |
| k | 0.466626 | 0.467409 | 0.468975 |
| h | 0.936045 | 0.937565 | 0.940606 |
| l | 0.0732452 | 0.0732927 | 0.0733877 |
| $\Phi_1$ | | | |
| k | 0.324854 | 0.324943 | 0.325122 |
| h | 0.656171 | 0.656289 | 0.656525 |
| l | 0.0819524 | 0.0820218 | 0.0821606 |
| $OO_1$ | | | |
| k | 0.297658 | 0.297725 | 0.297859 |
| h | 0.602483 | 0.602550 | 0.602685 |
| l | 0.0836228 | 0.0836896 | 0.0838232 |

**References**


Woodward R.L., Molnar P.: 1995, *Earth. planet. sci. lett.*, 135.

Mathews P.M., Buffet B.A., Shapiro I.I.: 1995, J. Geophys. Res., B7, 100.

Dehant V.: 1987, *Phys. earth. planet. inter.*, 49.

Sasao T., Okubo S., Saito M.: 1980, *Proc. IAU Symp.*, 78.

Lubkov M.V.: 2004, *Geophys. J.,* **6**, 26.

Lubkov M.V.: 2007, *Geohhys. J.,* **5**, 29.

Wu P.: 2004, *Geophys. J. Int.,* **2**, 158.

# DUPLICITY AND EVOLUTION STATUS OF THE EARLY-TYPE Be STAR V622 Per, THE MEMBER OF THE $\chi$ Per OPEN STAR CLUSTER

S.L. Malchenko[1], A.E. Tarasov[2,1], K. Yakut[3,4]

[1] Tavrida National University
95007 Vernadskogo avenue 4, Simferopol, Crimea, Ukraine, *svetlana_mal@ukr.net*
[2] Crimean Astrophysical Observatory
98409, Naychny, Crimea, Ukraine, *tarasov@cra.crimea.ua, aetarasov@mail.ru*
[3] University of Ege, Faculty of Science, Department of Astronomy and Space Science
35100, Bornova, Izmir, Turkey
[4] Institut voor Sterrenkunde, Katholieke Universiteit Leuven,
Leuven, Belgium

ABSTRACT. On high-resolution spectra, obtained in the H$\alpha$ region and medium resolution spectra obtained in the region 4420-4960Å together with radial velocities, which was taken from other published sources we analyzed the radial velocities and calculate orbital parameters of the massive binary system V622 Per. It is shown that the system has an orbital period 5.2 days and is a post mass transfer binary. Temperature of components and an inclination angle of the system were obtained from light curve analysis of the ellipsoidal variability. Luminosity ration of components was found of about 4:1. $T_{eff}$ and $log\, g$ for each of components was estimated. It is shown that primary, less massive but brighter star is an evolved object that has lost a large part of the mass during its evolution. Estimations of the primary chemical composition showed a noticeable enrichment of products of the CNO cycles such as He/H reach 0.18, the nitrogen is in excess of about 0.5 dex, the carbon has lower abundances (by 2-3 dex lower) and the oxygen has 1 dex lower than solar abundance. The possible evolution of the binary with the known age 17 Myear is discussed.

**Key words**: Stars: binaries: spectroscopic - stars: individual: V622 Per; Galaxy: cluster: $\chi$ Per.

## 1. Introduction

Presence of massive interacting binaries in open stellar clusters is the useful tool for understanding short-lived phases of their evolution. Such stars are rare and each of them requires detail analyses.

Close binaries are powerful tools for testing the stellar structure and evolution models, since the fundamental properties of the components (e.g masses, radii, luminosities) can be accurately determined from the observation. These systems in young open clusters provide a way of finding the age, distance, accurate masses, radii and chemical composition, and show the way of making a good discriminating test of the physical ingredients of theoretical models.

During the studying of the hot B stars in young open clusters h/$\chi$ Per we found and analyzed the binary system V622 Per/ BD +56°578/ Oo 2371 (Oosterhoff, 1937). The star may be a good indicator of verifying the theory of the evolution.

Early spectral type of the star B2III Strom et al. 2005, relatively short orbital period $\sim 5.2^d$ (Krzesinski & Pigulski 1997), presence of emission details in the spectrum and unusual chemical composition of the atmosphere (Vranken et al. 2000) mean that the star is an interacting binary with unknown evolutional status, but locate in the open stellar cluster $\chi$ Per of the known age.

## 2. Observations and data reduction

Spectroscopic observations of V622 Per took place over four years from 1997 to 2000 as a part of studying emission spectrum of the Be stars in the young double open cluster h and $\chi$ Per (NGC 869 and NGC 884). We used the Coudé focus of the 2.6-m telescope of the Crimean Astrophysical Observatory. The spectral resolution was about 30000. The signal-to-noise ratio was $\sim$100. A total of 8 spectra was obtained in the H$\alpha$ line and one in the region of the HeI $\lambda$ 6678 Å line.

Additionally, as a part of program of studying B and

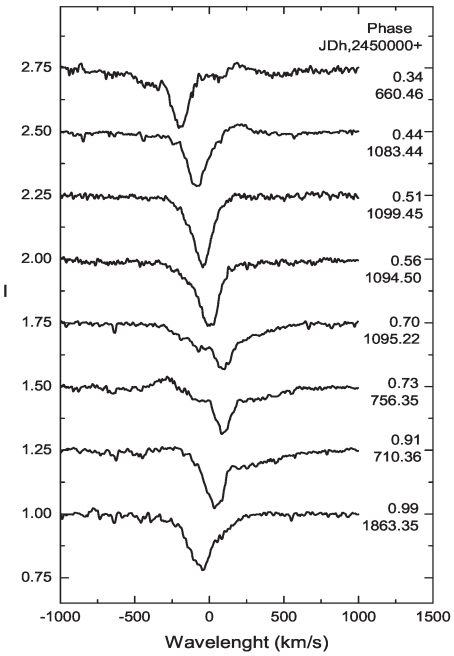


Figure 1: H$\alpha$ line profiles of V622 Per. On the left side of each spectrum JD and phase of the orbital period is presented. Intensities of each next spectrum are shifted by 0.25.

Be stars in the open stellar clusters, two medium 2.5Å resolutions of spectra were obtained in the Nesmith focus of the same telescope. They cover spectral region between 4420-4960 Å. The signal-to-noise ratio of these spectra was about 100.

The H$\alpha$ line has complex and it is variable in the time domain (Fig.1). The most pronounced component is a sharp absorption line with large amplitude of RV variation. Signatures of the broad absorption component are also seen on the most part of our spectra. Additionally, some faint emission line is presented in the red or blue wings of the line, but some spectra have no noticeable emission or they are hidden inside of the absorption profile. Gaussian fitting by three functions were used to deblend the H$\alpha$ line profile.

The He I $\lambda$ 6678 Å line profile can be seen in Fig.2. It has a single-component line profile without noticeable emission and some faint signatures of the additional absorption component in the blue wing of the line. Radial velocity was measured by fitting of two Gaussian functions with r.m.s. errors 1 and 5 km s$^{-1}$respectively for strong and hidden components of the line.

The observed blue region of the spectra is presented in Fig.4. The H$\beta$ line profile has no signs of the emission component on the both of our spectra. The weak absorption from the secondary is seen in the blue wing of the line. Radial velocities for the primary component, obtained by individual lines deblending and by cross-correlation methods, have the same radial velocities.

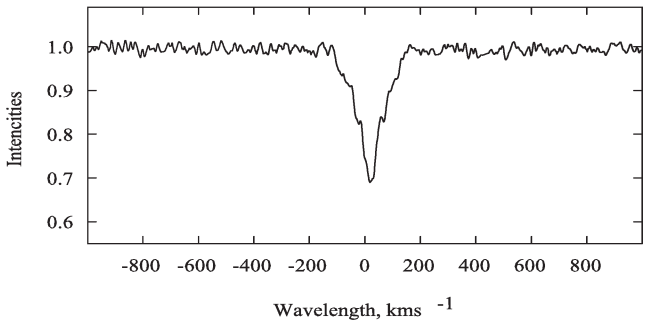


Figure 2: Line profile of the He I $\lambda$ 6678 Å line, obtained at JDh = 2451094.577

As it shows at Fig.4, the red wing of the H$\beta$ line has broad depression. It was found on all the spectra of other members of h/$\chi$ Per cluster, but absent in the spectra of the standard stars from the list Lybimkov et al. (2000). It is associated with the interstellar absorption band with unknown identification (Herbig 1975) and it has a very broad, asymmetric feature. According to Herbig (1975) wings of the line extend shortward edge to at least 4870 Å and longward to 4909 Å . The deepest point is about 4882 Å .

## 3. Radial velocities analysis and orbital solution

According to the rich BV photometry from Krzesinski & Pigulski (1997), V622 Per is an ellipsoidal double system with the orbital period $P_{orb}$ = 5.2132±0.003$^d$. The large fraction of our RV measurements were obtained from the emission H$\alpha$ line. Practically the same velocities of the He I and sharp component of the H$\alpha$ lines, is obtained in the same night, and "in phase" variability of the radial velocities, which is obtained from the Nesmith spectra, allow us to conclude that the sharp component of the H$\alpha$ line mostly appears in the photosphere of the bright star and can be used with some caution in solving orbit of V622 Per.

To confirm the value of orbital period derived from Krzesinski & Pigulski (1997), we used our RV measurements together with the data, which was obtained by Liu et al. (1989, 1991). Periodogram analyses based on nonparametric statistics were used for searching possible orbital period from radial velocities observations. Only one significant period, close to the value proposed in the work Krzesinski & Pigulski (1997), was found.

In order to solve spectroscopic orbit we used the FOTEL code (Hadrava 1990). Obtained orbit solution is presented in the Table 1 and its graphical equivalent is present in Fig.3. As it seen from orbital solution, V622 Per is an evolved massive system with the less

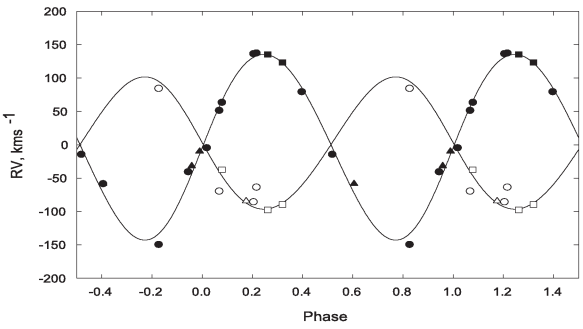


Figure 3: Radial velocity variability with the phase of orbital period. The filled symbols – orbital velocities of the primary component, open symbols – RVs of the secondary component. Filled circles – sharp component of the H$\alpha$ and the He I $\lambda$ 6678 Å lines. Circles – RVs derived from the H$\alpha$ line profile; squares – RVs, obtained from the two Nesmith spectra and the He I $\lambda$ 6678 Å line; triangles – RVs estimations from Liu et al. (1989, 1991) open triangle – ommited observation Liu et al. (1991)

Table 1: Orbital parameters of V622 Per based on radial velocity variability

| Element | Orbital solution |
|---|---|
| $P$ (days) | 5.21429±0.00008 |
| $T_{conj.1}$ | 2450661.4±0.2 |
| $K_1$ (km s$^{-1}$) | 139±6 |
| $K_2$ (km s$^{-1}$) | 99±11 |
| $q$ | 1.40±0.13 |
| $e$ | 0.05±0.04 |
| $\omega^\circ$ | 236±36 |
| $\gamma_1$ (km s$^{-1}$) | -44±3 |
| $\gamma_2$ (km s$^{-1}$) | 12±11 |
| $f_M$ (M$_\odot$) | 1.46 |
| $M_1 sin^3 i$ (M$_\odot$) | 3.0 |
| $M_2 sin^3 i$ (M$_\odot$) | 4.3 |
| $a_1 sin\, i$ ($R_\odot$) | 14.3 |
| $a_2 sin\, i$ ($R_\odot$) | 10.2 |
| No. of spectra | 11 spectrograms and 3 velocities by Liu (1989, 1990) |

massive, but more bright primary component. It has near circular orbit and low value of mass exchange.

We also used the rich BV photometry from Krzesinsḱi & Pigulski (1997) to perform light curve analysis. According to the light curve analysis V622 Per is an ellipsoidal double system, with colder primary component ($T_1$=21000K) and hotter secondary ($T_2$=24000K). The inclination angle of the system i=43.7$^0$ ± 2.9.

## 4. Physical parameters and chemical composition of the components

Radial velocities and photometrical variability due to ellipsoidality of the components allowed us to obtain most of the main physical parameters of the double system with exception of the radius of the components. The next step of our analysis was to constrain a model of atmosphere of the components with the goal to estimate chemical composition at least more luminous star.

Temperatures $T_{eff}$ of the components were found from the light curve analysis. Next pair of parameters $log\, g_1$ and $log\, g_2$ of the components can be found from the equivalent width of the H$\beta$ line, but only in assumption that gravity one of the components is taken elsewhere. We should accept that the less luminous component is still an undeveloped star which position on H-R diagram is close to the main sequence with $log\, g$=4.0. Then, using luminosity ratio of the components 4:1 and photometry index [c1] and $\beta$ (took from Fabregat et al. (1996) and Capilla and Fabregat (2002)), we found that observed EW of the H$\beta$ line satisfied approximation with $log\, g_1$=3.0 ± 0.5 .

Since we had only one high resolution observation of the photosphere line He I $\lambda$ 6678 Å this line of the secondary was heavy blended with the primary one, we were only able to estimate their rotational velocities. We obtained $V_1 sin\, i$=60±10km s$^{-1}$ and $V_2 sin\, i$=80±20km s$^{-1}$ for the primary and secondary components respectively. Rotation velocity of the secondary seems to be close to synchronization with the orbital velocity that is in agreement with the relatively short, less than 1 Myear, time of synchronization after an active mass transfer (Langer et al.2003)

The last step of our analyses was to determine the abundance of the elements of CNO cycle. We used the LTE line blanketing model Kurucz (1993) for solar abundances with the line formation problem solved by Tsymbal (1996) in the program SynthV for finding the basic parameters of the atmosphere of the cold component of V622 Per and the estimation of the chemical composition.

The synthetic spectra were calculate with the parameters of atmosphere each of the component taken from our data ($T_1$ = 21000K, $log\, g_1$=3.0, $T_2$ = 24000K $log\, g_2$=4.0, $V sin\, i$=60km s$^{-1}$, $V_{turb}$=10km s$^{-1}$ ). From analysis of synthetic spectrum we have found that CNO abundances of V622Per are far from solar. Nitrogen lines demonstrate overabundance in comparing to the normal solar abundance. The oxygen abundance is noticeable lower to compare to solar. And even on height-resolution spectra in the H$\alpha$ region we can not see the presence of the C II doublet at the $\lambda$6578 Å and $\lambda$6582 Å . The deficiency of the carbon is presented in the atmosphere of the both of components and should be et least 2-3 dex.

The quality of our data allowed us to obtain only estimations of the chemical composition. Abundance of helium He/H is 0.18, excess of the nitrogen is near

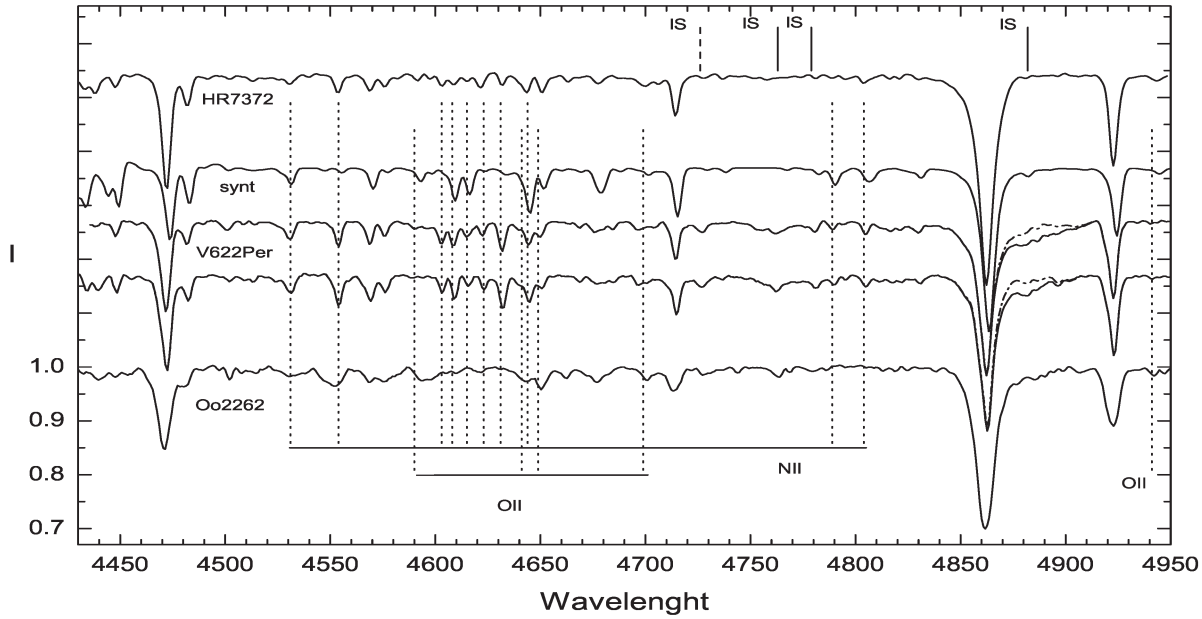


Figure 4: Medium resolution spectra of V622 Per, obtained in the spectral region 4420-4960 Å together with the spectra of two comparison stars HR6787 from list Lybimkov (2000) and member of h/$\chi$ Per cluster Oo2262. The calculated synthetic spectrum is also shown. Positions of stellar spectral lines with estimated abundances is present together with interstellar lines (IS). The dashed lines in the region of the blue wing of the H$\beta$ line are removed interstellar band.

0.5 dex and deficiency of the oxygen is about 1 dex in comparison to solar abundances.

## 5. Evolution status of the system

From our data we can conclude that the less massive component is evolved, it has left the TAMS which is in good agreement with those reported in literature, the more massive one is located between the ZAMS and TAMS. As it seen from our analysis, V622 Per is Algol type massive interacting binary with the masses of the component $M_1$= 9.0M$_\odot$ and $M_2$= 12.8M$_\odot$. The less massive evolved the primary leave of main sequence and it is on the way to the red gianr stars. Presence product of the CNO cycle in the atmosphere of the primary means that it has lost noticeable part of its outer layers and the part of its possible seen on surface of the secondary component.

The chemical composition of V622Per is similar with the composition of $\beta$ Lyr - is well know massive interacting binary with $P_{orb}$= 12.9 days. Balachandran et al. (1986) obtained large He enrichment, extreme nitrogen overabundant and very under abundant the oxygen and the carbon. Carbon lines are the same as in case of V622 Per were not found in the atmosphere of the primary component.

## References

Balachandran S., Lambert D.l., Tomkin J., Parthasarathy M.: 1986, *MNRAS*, **219,** 479.
Calilla, Fabregat J.: 2002, *A&A,* **394,** 394.
Hadrava P.: 1990, *Cont. Astron. Obs. Scalnaté Pleso*, **20**, 23.
Herbig G.H.: 1975, *Ap.J,* **V. 196**, 129.
Fabregat J., Torrejon J.M., Reig. P. et. al.: 1996, *A&AS,* **119,** 271.
Krzesiński J., Pigulski A.: 1997, *As&Ap,* **325**, 987.
Kurucz R.L.: 1993, *Atlas9 Stellar Atmosphere Program and 2km s$^{-1}$ grid. Kurutcz No. CD-ROM 13.*
Cambrige, Mass.: Simithsonian Astrophys. Obs., 13.
Langer N., Yoon S.-C. and Petrovic J.: 2003, in *Stellar Rotation, Proc. IAU Symp. No. 215*, ed A. Maeder anf P. Eenens.
Liu T., Janes K.A. & Bania T.M.: 1989, *AJ,* **98,** 626.
Liu T., Janes K.A. & Bania T.M.: 1991, *AJ,* **102,** 1103.
Lyubimkov L.S., Lambert D.L., Rachkovskaya T.M. et. al.: 2000, *MNRAS,* **316**, 19.
Oosterhoff P.T.: 1937, *Ann. Sterrewacht Leiden,* **17**,1.
Strom S.E., Wolff S.C., Dror D.H.A.: 2005, *AJ,* **129**, 809.
Vrancken M., Lennon D.J. Duffon P.L.: 2000, *As&Ap,* **358**, 639.
Tsymbal V.V.: 1996, *ASP Conf. Ser.*, **108**, 198.

# HOMOGENIZATION OF STELLAR CATALOGUES THROUGH DATA INTERCOMPARISON

V. Malyuto

Tartu Observatory
61602 Tartumaa, Tõravere, Estonia, *valeri@aai.ee*

ABSTRACT. The accuracies of some selected stellar catalogues of $T_{\rm eff}$ values have been estimated through data intercomparison. The technique of such estimating developed earlier for triples of catalogues has been adapted to a set of catalogues. A homogenized catalogue of $T_{\rm eff}$ values has been produced by weighted data averaging and compared with some available data.

**Key words**: Catalogues; stars: fundamental parameters.

## 1. Introduction

Catalogues of astrophysical parameters (APs: $T_{\rm eff}, \log g$, [Fe/H], etc.) provide important information about the detailed physical properties of each star observed, which encode the structure, star formation and chemical enrichment history of the Galaxy. To make the appropriate stellar samples more representative, different classification methods are used where the APs from some selected catalogues are involved to calibrate spectral or photometric data in large scale surveys. However the available catalogues are rather heterogeneous: there are systematical differences between the data, the estimates of accuracies of catalogues are differing and may be uncertain. The rapidly growing number of catalogues has imposed a need for refining procedures of merging catalogues of a kind of stellar data (APs, photometry etc.) into a respective mean data homogenized catalogue. A problem is being considered how to homogenize available stellar catalogues of APs published by different authors. Underlying procedures of merging catalogues should be a statistical weighting of data according to their statistical accuracies. For homogenization we use the published internal errors as well as the external errors of catalogues (the later values may be determined from data intercomparison). We treat only $T_{\rm eff}$ values in the present paper.

## 2. General principles

We try the following approach: to take one chosen catalogue (both extensive and precise) as a basic catalogue, to combine some selected catalogues into one scale and to average all data with the weights inversely proportional to the external errors of catalogues, their published internal errors are weighted too. The external errors of catalogues are determined from data intercomparison for triples of catalogues. If there are independent catalogues 1, 2, 3 having the stars in common (the systematical differences are removed), we may calculate the variances of data differences $\delta^2_{12}$, $\delta^2_{13}$, $\delta^2_{23}$ and determine the errors of catalogues $\sigma_1, \sigma_2, \sigma_3$ from the variances.

In the present approach we treat the published rms errors of $T_{\rm eff}$ values from different catalogues as internal errors ($\sigma_{int}$), the errors of $T_{\rm eff}$ obtained from data intercomparision are treated as external errors ($\sigma_{ext}$). To obtain the final $T_{\rm eff}$ for every star (where $n$ catalogues are available) we calculate

$$\sigma_i^2 = \sigma_{ext,i}^2 + \sigma_{int,i}^2\ ,\ \ T_{{\rm eff},final} = \frac{\sum_{i=1}^{n}(1/\sigma_i)^2(T_{{\rm eff},i})}{\sum_{i=1}^{n}(1/\sigma_i)^2}. \quad (1)$$

With these data a homogenized catalogue of $T_{\rm eff}$ values may be created.

## 3. Selected catalogues and data analysis

Short description of the selected catalogues used in the present analysis is given in Table 1. The $\sigma T_{\rm eff}$ values are the published errors which characterize the catalogues; their means (with their standard deviations) or the presentative $\sigma T_{\rm eff}$ values are given for every catalogue. To deal with more homogeneous $\sigma T_{\rm eff}$, we introduce some appropriate subsamples of the catalogues whose published $\sigma T_{\rm eff}$ are within certain intervals of these estimates (given in the first column of Table 1), the means of $\sigma T_{\rm eff}$ for the catalogues and for their appropriate subsamples are about the same.

All possible comparisons of the $T_{\rm eff}$ values in these catalogues by pairs for the stars in common have been

Table 1: Catalogues of the $T_{\rm eff}$ values with their subsamples used in the present analysis

| Reference*/Subsample | $N$ | Type of data | Method | mean $\sigma T_{\rm eff}$(K) |
|---|---|---|---|---|
| 1. | 10999 | $V$+2MASS photometry | SEDF Method | $64 \pm 14$ |
| $70 \geq \sigma T_{\rm eff} \geq 50$ | 6486 | - | - | $61 \pm 6$ |
| 2. | 754 | 17 photometric colors | IRFM | $67 \pm 19$ |
| $80 \geq \sigma T_{\rm eff} \geq 60$ | 421 | - | - | $70 \pm 4$ |
| 3. | 420 | $JHKL$ photometry | IRFM | $50 \pm 16$ |
| $60 \geq \sigma T_{\rm eff} \geq 40$ | 235 | - | - | $47 \pm 5$ |
| 4. | 189 | $uvby-\beta$ photometry | synthetic photometry | 25 |
| 5. | 950 | $R, I, K$ photometry | calibration | $46 \pm 23$ |
| $70 \geq \sigma T_{\rm eff} \geq 30$ | 498 | - | - | $54 \pm 8$ |
| 6. | 1039 | spectroscopy, Keck+Lick | synthetic spectra | 44 |
| 7. | 465 | spectroscopy, H.-Provence | line-depth ratios | $7 \pm 3$ |
| $10 \geq \sigma T_{\rm eff} \geq 4$ | 407 | - | - | $6 \pm 2$ |

* 1. Masana et al. (2006); 2. Ramirez, Melendez (2005); 3. Blackwell, Lynas-Gray (1997); 4. Edvardsson et al. (1993); 5. Taylor (2003a); 6. Valenti, Fisher (2005); 7. Kovtyukh et al. (2004, 2006).

Table 2: External errors of $T_{\rm eff}$ with their deviations for 7 referenced catalogues (their description is given in Table 1). The last line contains the mean published internal $\sigma T_{\rm eff}$ for the subsamples (or catalogues) taken from the last column of Table 1.

| | Cat. 1 | Cat. 2 | Cat. 3 | Cat. 4 | Cat. 5 | Cat. 6 | Cat. 7 |
|---|---|---|---|---|---|---|---|
| external error | 59±6 | 73±5 | 54±9 | 45±12 | 52±9 | 62±10 | 36±10 |
| internal error | 61 | 70 | 47 | 25 | 54 | 44 | 6 |

performed; we have found that the mean differences are significant in some cases but the dependences of differences on $T_{\rm eff}$ are not significant. We have calculated the sample mean differences and the standard deviations for every pair of the catalogues (and/or subsamples) from Table 1. We use the subsamples instead of the catalogues when necessary and their data are treated to calculate the variances of data differences for each pair of subsamples (or catalogues) for the stars in common.

With the use of these variances and the technique presented in Malyuto (1993) we obtain three appropriate external errors of $T_{\rm eff}$ for every triple of catalogues (all possible triples are analysed). We average the errors obtained with the different riples to obtain the mean values. The results (the averaged errors with their deviations) are presented in the first line of Table 2 for all analysed catalogues.

It is interesting to confront the external errors for stars for the catalogues and the published internal errors (given in the last line of Table 2). These data do not differ significantly for the photometric data (catalogues 1, 2, 3 and 5) but they are rather different in the cases where we deal with synthetic photometry and spectral data (catalogues 4, 6 and 7). We underline the importance to use the external errors in combination with the published internal errors as some weights in averaging the $T_{\rm eff}$ values compiled from different catalogues.

To produce a homogenized catalogue of the $T_{\rm eff}$ values, we consider the Masana et al. (2006) data as one basic catalogue, the averaged data are calculated with the formulae (1) for the stars which are in common at least with one other catalogue of Table 1. The results will be treated in a separate paper.

*Acknowledgements.* Financial support of this investigation by a Grant No. 6106 of the Estonian Science Foundation is acknowledged.

**References**

Blackwell D.E., Lynas-Gray A.E.: 1997, *Astron. Astroph. Suppl.*, **129**, 505.

Edvardsson B., Andersen J., Gustafsson B., Lambert D.L., Nissen P.E., Tomkin J.: 1993, *Astron. Astrophys.*, **275**, 101.

Kovtyukh V.V., Soubiran C., Belik S.I.: 2004, *Astron. Astroph.*, **427**, 933.

Kovtyukh V.V., Soubiran C., Bienayme O., Mishenina T.V.: 2006, *Monthly Notices*, **371**, 879.

Malyuto V.: 1993, *Astron. Astrophys.*, **278**, 73.

Masana E., Jordi C., Ribas, I.: 2006, *Astron. Astroph.*, **450**, 735.

Ramirez I., Melendez J.: 2005, *Ap. J.*, **626**, 446.

Taylor B.J.: 2003, *Astron. Astroph.*, **398**, 721.

Valenti J.A., Fisher D.A.: 2005, *Ap. J. Suppl.*, **159**, 141.

# THE TALLINN PUBLIC OBSERVATORY IN CHANGING CONDITIONS

M. Mars[1], T. Aas[1], V. Harvig[1,2]

[1]Tallinn Observatory, Tallinn University of Technology
*mars@staff.ttu.ee*
[2]Tartu Observatory, Estonia

ABSTRACT. The history of development of the Tallinn Public Observatory is described.

**Key words**: Observatoryes : Public Observatory.

In Estonia, as well as in whole Europe, after the World War II devastation, few amateur astronomical data have saved. Since Estonia has lost in this war 10-20 per cent of its population, the amateur astronomy needed rebirth. The period just after 1953 may be considered beeing a time of renascence. Life conditions improved, and the ÜAGÜ Tartu Branch (All Union Astronomical and Geodetical Society) was established. Later on its base the Estonian Branch was created (Estonian Branch of the All Union Astronomical and Geodetical Society).

The triumph of astronomy began at the times when the first human–mades satellite was launched. Being a really remarkable achievement, it caused space-related euphory, so the popularity of astronomy also increased. A building at Estonia pst 15 (ealier a private observatory) was conferred to amateurs in 1954, and in 1959 (Villmann(1961)) the desicion was made to establish a new Tallinn Observatory in Hiiu suburb. As strange as it may seem, the best period in the history of the Observatory was in 1970-1980. At that time, five research associate positions were available, the time suitable for observations was used effectively, and a sufficient number of publications was provided. Amateur astronomy was also quite popular, and amateurs were participating actively in research work (Aas and Harvig(2006)).

After desintegration of the Soviet Union and reestablishement of the Estonian Republic, financial support of fundamental studies decreased, as well as the personnel of the Observatory. At the same time the value system in the society changed, especially among the younger people, who's interests shifted away from natural sciences. At present moment situation has become more stable and the interest towards astronomy revives. It is mostly noticeable by organization of public astronomical events. Simultaneously, due to economical successes of the country, the possibilities to acquire new equipement are much better now.

Since the need for qualified personnel in exact sciences increases rapidly, the situation in the public observatory of Tallinn (which is the Educational Observatory of the Tallinn University of Technology) has significantly improved. For example this year (2007) the university budget for the repair of the building of the observatory is 300 000 €.

Figure 1: Former Edgar Höppener's private observtory as the public observatory in 1955

Figure 2: Ch. Villmann's lecture on space exploration in 1959

Figure 3: Observatory in 2007

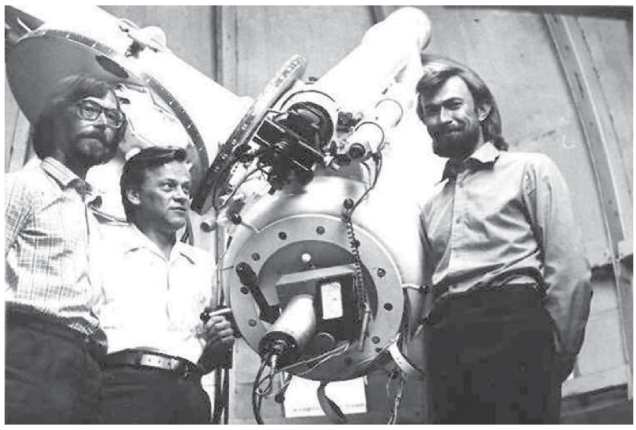

Figure 4: Observers in 1980

Figure 5: The last picture before reduction of the staff 1992

Figure 6: Public demonstration of Mars 2004


Figure 7: Educational observation 2007

**References**

Villmann Ch: 1961, *Tallinna tähetorni tänapäevast ja tulevikust, Tartu tähetorni kalender*,**41-52**

Aas T., Harvig V.: 2006, *Kui vana on Tallinna tähetorn, Tallinna tähetorni kalender*, **51-90**

# STAR FORMATION HISTORY IN THE GALACTIC THIN DISK

V.A. Marsakov, M.V. Shapovalov, T.V. Borkova

Southern Federal University
Rostov-on-Don 344090 Russia,
*marsakov@ip.rsu.ru*

ABSTRACT. We analyze the relations between the relative magnesium abundances in stars, [Mg/Fe], and their metallicities, Galactic orbital elements, and ages. The relative magnesium abundances in metal-poor thin-disk stars have been found to systematically decrease with increasing stellar orbital radii. This behavior suggests that, first, the star formation rate decreases with increasing Galactocentric distance and, second, there was no star formation for some time outside the solar circle while this process was continuous within the solar circle. The decrease in the star formation rate with increasing Galactocentric distance is responsible for the existence of a negative radial metallicity gradient ($\mathrm{grad}_R$[Fe/H]=$(-0.05 \pm 0.01)$ kpc$^{-1}$) in the disk. At the same time the relative magnesium abundance exhibits no radial gradient. We discovered that in the thin disk there is not only the connection between age and metallicity, but between age and relative magnesium abundance also. It is in detail considered the influence of selective effects on the form of both age – metallicity and age – relative magnesium abundance diagrams. It is shown that the first several billion years of the formation of the thin disk interstellar medium in it was on the average sufficiently rich in heavy elements. At the same time the relative magnesium abundance exhibits no radial gradient. We discovered that in the thin disk there is not only the connection between age and metallicity, but between age and relative magnesium abundance also. It is in detail considered the influence of selective effects on the form of both age – metallicity and age – relative magnesium abundance diagrams. It is shown that the first several billion years of the formation of the thin disk interstellar medium in it was on average sufficiently rich in heavy elements ($\langle$[Fe/H]$\rangle \approx -0.22$), badly mixed ($\sigma_{\mathrm{[Fe/H]}} \approx 0.21$), and the average relative magnesium abundance was comparatively high ($\langle$[Mg/Fe]$\rangle \approx 0.10$). Approximately 5 billion years ago average metallicity began to systematically increase, and its dispersion and the average relative magnesium abundance – to decrease. These properties may be explained by an increase in star formation rate with the simultaneous intensification of the processes of mixing the interstellar medium in the thin disk, provoke possible by interaction the Galaxy with the completely massive galaxy-satellite.

**Key words:** Galaxy (Milky Way), stellar chemical composition, thin disk, Galactic evolution.

The chemical composition of low-mass main-sequence stars can be used to estimate the star formation rate and as the time scale of a chemically evolving closed system. Thus, for example, the $\alpha$-elements (O, Mg, Si, S, Ca and Ti) together with a small number of iron atoms are currently believed to be synthesized in the high-mass ($M > 10M_\odot$) asymptotic-giant-branch progenitors of type II supernovae, while the bulk of the iron-group elements are produced during type Ia supernova explosions. Beginning from the paper by Tinsley (1979), the negative trend in the [$\alpha$/Fe] ratio as a function of metallicity observed in the Galaxy has been assumed to be due to a difference in the evolution times of these stars. Indeed, the evolution time scale for type II supernovae is only $\approx 30$ Myr while low massive SNe Ia explosions begin only in $\approx (0.5 \div 1.5)$ Gyr. The higher the star formation rate in the system, the larger the metallicity at which the knee attributable to the onset of SNe Ia explosions which result in an enrichment of the interstellar medium with iron-group elements, will be observed in the [$\alpha$/Fe]–[Fe/H] relation. The lower the star formation rate in the system, the steeper the further decrease in the [$\alpha$/Fe] ratio with increasing total metallicity. If star formation in the system is halted altogether then the source of $\alpha$-elements (i. e., SNe II) will vanish and only SNe Ia will enrich the interstellar medium with iron-group elements; therefore the [$\alpha$/Fe] ratio will decrease suddenly.

Since more than 90 % of the stars in the immediate solar neighborhood belong to the youngest (in the Galaxy) thin-disk subsystem, the chemical composition of this subsystem has been studied in greatest detail. However the sizes of the original samples in all works were very limited; this is probably the reason why the results and conclusions are occasionally in conflict with one another.

Since the published results disagree, analyzing the relations between the relative abundances of $\alpha$-elements and metallicity and other parameters of thin-

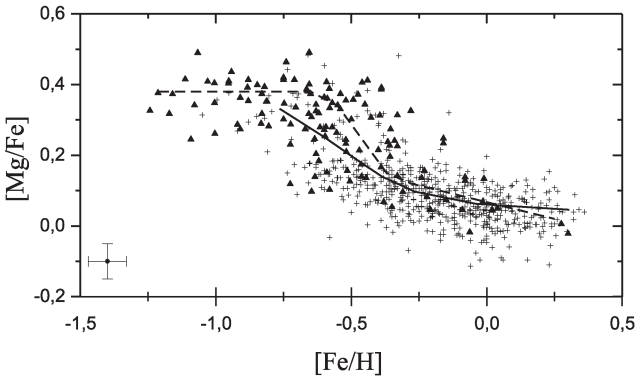


Figure 1: Relation between metallicity and relative magnesium abundance for the stars of both disk subsystems: the crosses and triangles indicate the thin-disk and thick-disk stars, respectively. The broken curves represent the median lines of the relations for the thin (solid line) and thick (dotted line) disks drawn by eye halfway between the upper and lower envelopes. The error bars are shown

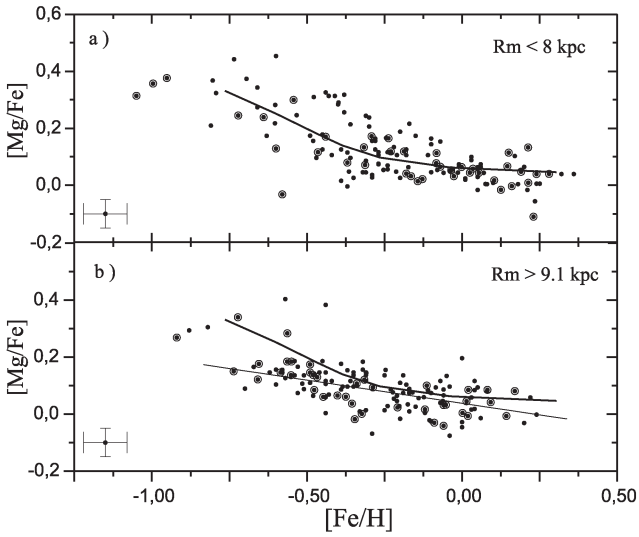


Figure 2: Relation between metallicity and relative magnesium abundance for the thin-disk stars in two ranges in mean orbital radii $R_m < 8$, and $> 9.1$ kpc. The broken curves in all panels represent the median curve for the thin disk. Thin line in panel (b) – straight regression for stars with $[Mg/Fe] < 0.2$. Is evident the decrease of the relative abundance of magnesium in the metal poor ($[Fe/H] < -0.4$) stars with an increase in the radii of the orbits.

disk stars based on a much larger statistical material seems very topical. At the beginning of this work we analyze the chemical properties of thin-disk stars using data from our compiled catalog of spectroscopically determined magnesium abundances (Borkova and Marsakov 2005). Almost all of the published magnesium abundances in dwarfs and subgiants in the solar neighborhood determined by synthetic modeling of high-dispersion spectra as of December 2003 were gathered in our catalog. This catalog is several times larger than any homogeneous sample that has been used until now to analyze the chemical evolution of the Galaxy.

The relative magnesium abundances in the catalog were derived for 867 stars using a three-pass iterative averaging procedure with a weight assigned to each primary source and each individual determination.

Since our main goal is to analyze the relations between the chemical composition and other parameters of thin-disk stars, we identified the latter solely according to kinematical criteria. The technique for identified the stars for which the probabilities of belonging to the thin disk is higher than the probability of belonging to the thick disk based on the dispersions of the space velocity components and the mean rotational velocity of both subsystem at the solar Galactocentric distance was taken from Bensby et al. (2003).

Figure 1 shows the [Fe/H]–[Mg/Fe] diagram where the thin-disk and thick-disk stars are denoted by different symbols. We see that the sequence for the thin disk in the metallicity range ($-1.0 < [Fe/H] < -0.4$) lies systematically lower than that for the thick disk. This suggests that the bulk of the thick-disk stars formed long before the onset of massive star formation in the thin disk. The [Mg/Fe] ratio begins to decrease with increasing metallicity in the thin disk immediately after the formation of the first stars in it, i. e., from $[Fe/H] \approx -1.0$. This is considerably farther to the left in the diagram than in the thick disk where the point of a sharp decrease is observed at $[Fe/H] \approx 0.5$. Hence, in the metal-poor interstellar matter from which the first thin-disk stars subsequently began to form, the enrichment with SNe II ejecta was less intense before this. It is quite probable that such metal-poor matter with a high relative magnesium abundance came into the thin disk as a result of accretion from regions with a different history of chemical evolution. The fast decrease in the relative magnesium abundance in the thin disk as the metallicity increases from $\approx -1.0$ dex to $\approx -0.7$ suggests that the star formation rate in it was initially low but it then suddenly increased, which subsequently led to a attending of the [Fe/H]–[Mg/Fe] relation. Subsequently when passing to stars with metallicities higher than the solar value, the slope of the [Mg/Fe]–[Fe/H] relation virtually vanishes, which is indicative of a new increase in the star formation rate and stabilization of the ratio of the contributions from supernovae (SN II/SN Ia) to the enrichment of the interstellar medium in the thin disk since then.

Let us now verify whether the positions of the thin-disk stars in [Mg/Fe] the [Fe/H]–[Mg/Fe] diagram depend on their mean orbital radii? Figure 2 shows two diagrams for the thin-disk stars with low ($R_m < 8$ kpc) and large ($R_m > 9.1$ kpc) orbits. Our median se-

quence is plotted in both diagrams. We see from the figure that only the stars with smallest mean orbital radii in Fig. 2 a closely follow our median curve at $[Fe/H] < -0.4$ dex. However at the largest distances, the [Mg/Fe]–[Fe/H] relation is almost linear (see the dashed line in Fig. 2 b). In this case, only a small number of stars with sharply enhanced magnesium abundances are observed above the curve. At the same time, it can be noticed that the metallicity range for the bulk of the stars with $[Mg/Fe] < 0.2$ is displaced from $(0.5 < [Fe/H] < +0.3)$ for the nearest stars to $(-0.7 < [Fe/H] < +0.2)$ for the farthest stars. The change in the behavior of the [Mg/Fe]–[Fe/H] relation with stellar orbital radius shows that the star formation rate closer to the Galactic center is higher than that on the periphery. Moreover it seems that star formation within the solar circle of the Galaxy has never been interrupted, but only slowed down before the massive formation of thin-disk stars. In contrast, the first thin-disk stars at great Galactocentric distances appeared only after the long phase of star formation delay. This follows from the presence of a distinct jump in the [Mg/Fe] ratio at metallicities $[Fe/H] < -0.4$ dex for stars with large orbital radii. The larger [Mg/Fe] ratios at high metallicities in the stars within the solar circle suggest that the star formation rate remains there higher even at present. The clear deficit of stars with metallicities higher than the solar value there is also indicative of a lower star formation rate at great Galactocentric distances.

Our interpretation was constructed on the suggestions that metallicity is good statistical age indicator in the thin disk. Indeed, lifetime of the thin disk is compared with the Galactic age, therefore the continuous process of the synthesis of chemical elements must lead during this period to a noticeable increase in the general abundance of heavy elements in the younger stars of subsystem. As a result in the thin disk the well expressed trend of metallicity from the age must be observed. However, in spite of the large history of the study of this question, in regard to this there is no unanimous opinion. Twarog (1980) was the first to derive the age–metallicity relation in the Galactic disk from F2–G2-stars and argued that it was unambiguous. However it was subsequently proven that the relation was by no means unambiguous and there was a significant spread in metallicity among the stars of any ages. This gave reason to suggest that there was no age–metallicity relation in the thin disk. The purpose of this work is the thorough analysis of possible selective effects on the age–metallicity diagram with the attraction together with photometric data of the spectroscopic determinations of the iron and magnesium abundances for the main sequence stars over a wide range of spectral classes. For investigation we used Geneva-Copenhagen Surveu (Nordstrëm et al. 2004), where on the data uvby$\beta$ photometry, and Hipparcos parallaxes

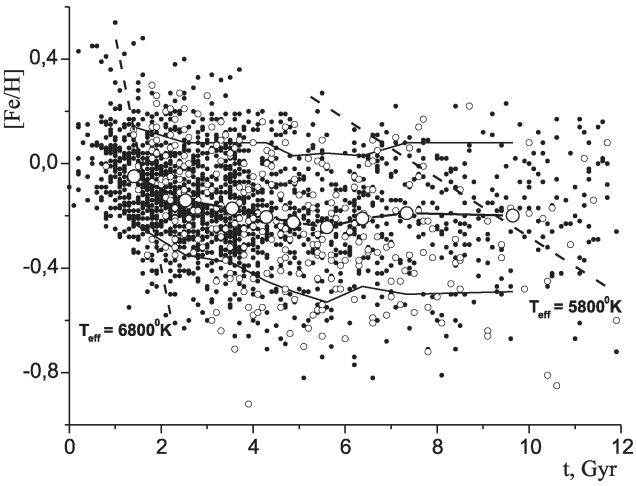


Figure 3: Age – metallicity diagram for the thin-disk stars from the catalog (Nordstrëm et al. 2004) with ($\varepsilon t > \pm 3$ Gyr), which lie nearer than 70 pc of the Sun. Large open circles connected by linear segments are the average values of the metallicity of stars in the narrow age ranges; broken lines - upper and lower ten-percent envelopes; inclined broken lines – theoretical isotherms for $T_{\rm eff} = 6800$ and 5800 K; the small open circles – star with the spectroscopic determinations [Fe/H] from the catalog (Borkova, Marsakov, 2005).

were determined temperature, metallicity, distance, absolute magnitude, and ages for about 14000 nearest F-G-K stars. The most probable ages was calculated on the base of Padova theoretical isochrones, using the sophisticated interpolation method, and Baysian computational techniques. After removing of the binary stars, marked in the catalog, far evolving stars ($\delta M_V > 3^m$), and stars with uncertainly determined ages ($\varepsilon t > \pm 3$ Gyr), in the sample remained 5540 supposedly single stars of thin disk. (Total average error in determination of age for the stars of the received sample comprised $\langle \varepsilon t \rangle = \pm 1.0$ Gyr.) In order to get rid of the selective effects, connected with a difference in the depth of survey for the stars of different metallicity and temperature, we limited sample with the distance from the Sun equal to 70 pc, within limits of which our sample can be considered complete for temperature range $(5400 - 7200)\,\mathrm{K}^\circ$. In finally formed thus sample remained 1890 stars of the thin disk.

Figure 3 gives age – metallicity diagram for the thin-disk stars of our sample. The large opened circles in the figure put average values of the metallicity of stars in nine narrow ranges on age. Upper and lower ten-percent envelopes are also constructed. From the figure one can see that among the old stars of Galactic disk is observed large spread in values [Fe/H], whereas among the young stars the explicit scarcity of metal poor stars (empty left-hand lower corner on the diagram) is observed. (Nordstrëm et al. 2004) explained

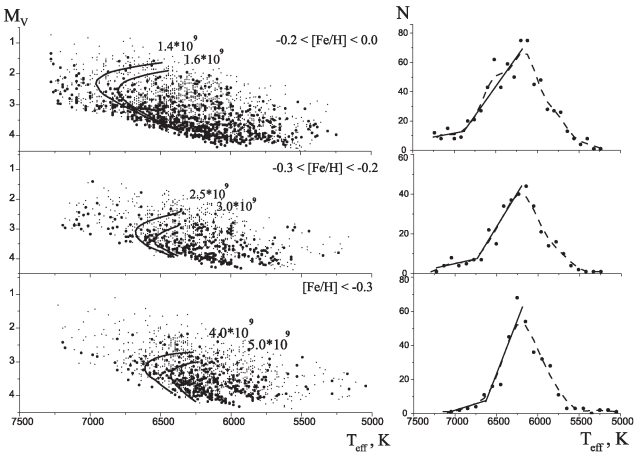


Figure 4: $T_{\rm eff} - M_V$ diagrams for the metal-poor stars lying within 70 pc from the Sun into narrow ranges on the metallicity (to the left) and distribution the number of stars depending on temperature for the same diagrams (to the right). Broken dotted lines on the histograms - smoothed on three points trends with the sliding averages, linear segments emphasize the positions of sharp fractures on the left boundaries of distributions. On left panels are substituted theoretical isochrones from works (Demarque et al., 2004), which correspond to the positions of fractures on the histograms (for comparison the isochrone of larger age are substituted more to the right them). The ages of isochrones are indicated.

this by the effect of the limitation of their catalog from the high-temperature side on the index $(b-y)$. In this case, in their opinion, the difference at the ages of the metal rich and metal poor stars of the same temperature just also provides observed inclination of lower envelope on the diagram. Let us verify this statement.

In Fig. 4 at the left the $T_{\rm eff} - M_V$ diagrams for the stars lying within 70 pc from the Sun into three narrow ranges on the metallicity are given. On the right for the same diagrams the distributions of number of stars depending on temperature are constructed. Broken lines on the right panels represent trends, smoothed on three points, and linear segments schematically designate the behavior of the left boundaries of distributions. It is seen that all metal poor groups ($[Fe/H] < 0.0$) demonstrate the sharp inflection envelope, when more to the right "inflection points" the number of stars abruptly increases. It is interesting that the temperature value of these points for all metal poor groups are far from the left edge of the diagrams. This means that the sharp scarcity of hotter (so also younger) stars in the metal poor groups is connected not to high-temperature limitation of sample but with existence of minimum age for the majority of the stars of given metallicity in the thin disk, i. e., with existence of "turnoff points" in the metal poor stars of field. On the left panels of figure the theoretical isochrones, passing through those isolated on the right panels "inflection points", are carried out according to the data of work (Demarkque et al., 2004). For the comparison are more to the right are everywhere substituted the isochrones of larger age

The effect of the limitation of sample from the high-temperature side, which it is discussed in the work ( Nordstrëm et al. 2004), also somewhat distorts real age – metallicity diagram. In figure 3 the dash inclined line is conducted on the basis of the theoretical isochrones for $_{\rm eff} = 5800$ K. This line corresponds to boundary, more to the right of which stars, hotter this temperature, cannot be – they have left from the main sequence already. (Let us note that precisely the limitation of sample from the low-temperature side with approximately Solar value of temperature (see the dash inclined line in the upper right-hand corner in the diagram) led to the exception of the oldest metal rich stars from the sample (Twarog, 1980), which caused his conclusion about a monotonic increase of the metallicity with the age in the thin disk.)

However, as can be seen from the diagrams, not this line, which intercepts an entirely small quantity of very young metal poor stars, but relative numbers of stars of different metallicity with the identical age determine the variation of average metallicity on the age. Note that lower envelope in Fig. 3 in the range $(1 < t < 4)$ Gyr practically coincides with left envelope of diagram. This means, that lower envelope reflects the variation of the "turnoff points" position of the stars of this metallicity on the age. As a result we see that "turnoff points" of metal poor stars are located in the middle of the temperature range, occupied by the stars of the sample, i. e., they are not connected with the action boundary selective effect.

To the distortion of the ages of stars can lead also the effect of their unresolved binary. Actually, the luminosities of the unresolved close binaries, calculated from the trigonometric parallaxes, are more than true (Suchkov, 2000). As a result the ages of stars not yet reached their turnoff point will be overestimated, whereas higher than it are located ever younger stars at an identical temperature. We isolated in our sample candidates into the dual according to the criterion, proposed in latter work. Such proved to be about 20 %, but constructed for the remained single stars age – metallicity diagram demonstrated that its form practically did not change.

Despite the fact that the position of a sufficiently large quantity of stars with the solar metallicity on the Hertzsprung - Russel diagram indicates their large ages, in the work (Pont, Eyer, 2004) existence of old metallic stars undergoes doubt.

Therefore let us verify, actually whether some metal rich stars are actually old? It is possible to do on the independent statistical indicator of age – kinematics.

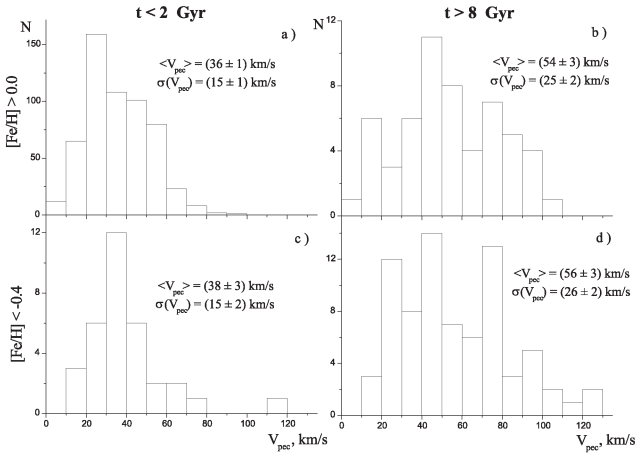


Figure 5: Distributions on peculiar velocities of metal-rich and metal-poor stars of different age. The corresponding values of average velocities and their dispersions are indicated on the panels. It is seen the coincidence of histogram of similar age.

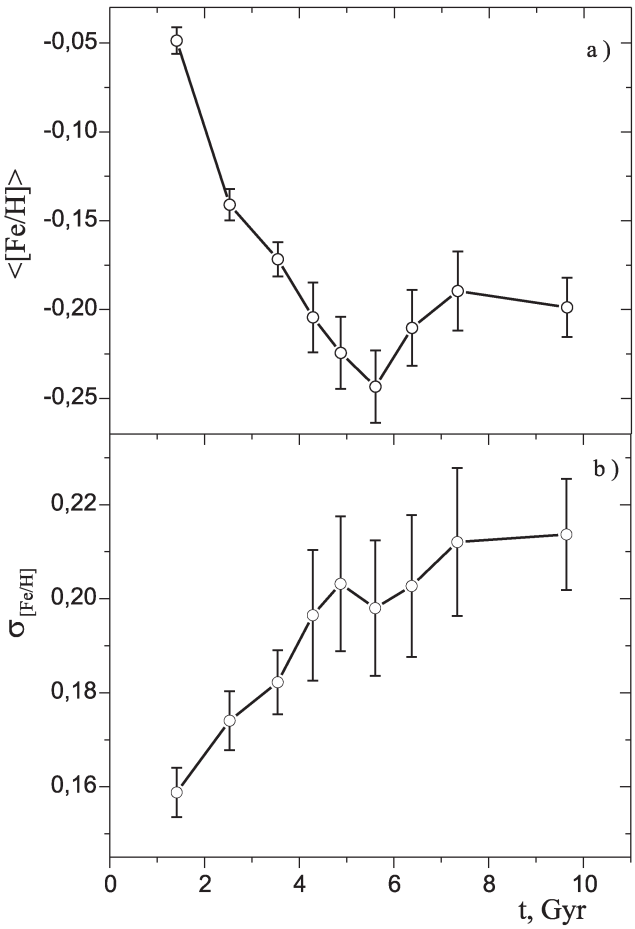


Figure 6: Dependences of average value (a) and dispersion of metallicity (b) from the age for the stars of thin disk in the 70 pc of the Sun from the catalog (Nordstrëm et al. 2004). Bars are error in determination of the corresponding values.

For this let us compare peculiar velocities distributions of metal rich ($[Fe/H] > 0.0$) and metal poor ($[Fe/H] < -0.4$) thin-disk stars, preliminarily isolate among them very young ($t < 2$ Gyr) and very old ($t > 8$ Gyr) star. The indicated histograms are given in Fig. 5. Comparison shows that the distributions of the stellar velocity of identical age, but different metallicity, are very similar. In this case old stars demonstrate one and a half times higher in both the average values and dispersions of peculiar velocities than young stars (see inscription on the appropriate panels). This behavior makes it possible to assert that the some metal rich stars have actually very large age.

We assume that none of the selective effects the known to us cannot substantially distort the common form of age – metallicity diagram in Fig. 3 for the sample of F-G stars in the 70 pc of the Sun. Therefore let us trace the behavior of the dependences of average value and dispersion of metallicity from age, constructed on the basis of these data. From Fig. 6 a, where the corresponding values were calculated in 9 narrow bins from the age, can be seen that at first average metallicity noticeably decreases with an increase in the age, and after $\approx 5$ Gyr it remains practically constant and equal to $\langle [Fe/H] \rangle = -0.22$. (Local minimum in the environment of 5 Gyr is most likely connected with the special features of the age determination procedure in the work (Nordstrëm et al. 2004).) Dispersion of metallicity, as can be seen from Fig. 6 b, always monotonically increases from 0.16 to 0.21; however, after $\approx 5$ Gyr this increase significantly slows down.

Photometric metallicity in some stars can be distorted by the disregarded systematic effects; therefore it is necessary to investigate age – metallicity dependence, also on the stars of our catalogue with the spectroscopic determinations of [Fe/H] (see the small open circles in Fig. 3). Let us note that in this sample the unresolved binaries deliberately be absent – otherwise they with the great probability would be known as spectrally binaries. Let us recall that since the number of stars here is not very great, we left all stars of thin disk in the sample. It is seen that on this diagram be absent very metal rich ($[Fe/H] > 0.3$) star – the apparently photometric "super-metallicity" of these stars actually is explained as an artifact of the deredding procedure for distant stars as this predicted in the work (Nordstrëm et al. 2004). In other respects the form of diagram practically did not change. From Fig. 7 a we see that age – metallicity relation, constracted on the stars of catalog with the spectroscopic determinations of [Fe/H], demonstrates the same behavior.

For understanding of the reason for such complex behavior of age – metallicity dependence it is important to trace the dependence of the relative content of magnesium on the age among the disk stars. Age –

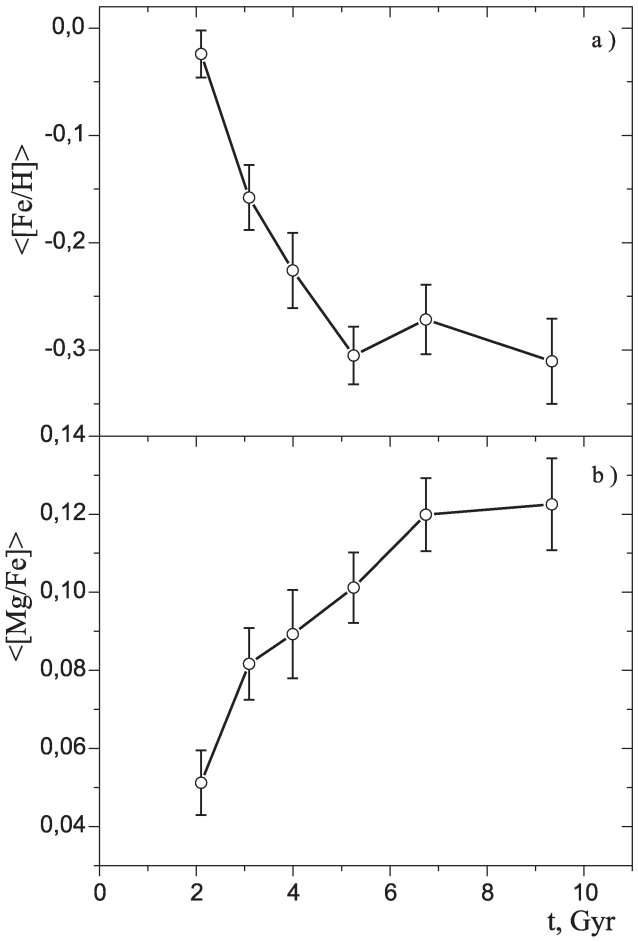


Figure 7: Dependences of average values $\langle[Fe/H]\rangle$ (a) and $\langle[Mg/Fe]\rangle$ (b) from the age for the thin-disk stars with the spectroscopically specific abundances of iron and magnesium from (Borkova, Marsakov, 2005). Bars are error in determination of the corresponding values.

magnesium abundance diagram itself according to the data of our catalog is given in Fig. **??** [b] in the work (Marsakov, Borkova, 2006), here in Fig. 7 b is represented only the variation of the relation $\langle[Mg/Fe]\rangle$ from the age. From the Fig. 7 b one can also see that, as in the case the connection between the age and the metallicity, bend is observed in the middle of the dependence between relative magnesium abundance and age. Bend evidences that the relative magnesium abundance in the thin-disk stars of being in the subsystem formation initial stages was sufficiently high ($\langle[Mg/Fe]\rangle \approx 0.10$). About 5 billion years ago it began to sharply decrease with the approximation to the present time. Thus, taking into account the uncertainty of the estimations of average values, we can assert that an increase in the average metallicity and the decrease of the average relative magnesium abundance in the stars of thin disk began simultaneously.

Thus components, confidently revealing on both $t-[Fe/H]$ and $t-[Mg/Fe]$ diagrams, testify that into the first several billion years of the formation of the thin-disk subsystem interstellar medium in it was, on average, sufficiently rich in heavy elements ($\langle[Fe/H]\rangle \approx -0.20$) and is badly mixed ($\sigma_{[Fe/H]} \approx 0.21$), and the average relative abundance of magnesium was comparatively high ($\langle[Mg/Fe]\rangle \approx 0.10$). Approximately 5 billion years ago the average metallicity began to increase, and the dispersion of metallicity and the relative magnesium abundance – to decrease. This occurred as a result sharply increased rate of star formation and making more active of the processes of mixing to the interstellar medium. By the possible reason for this could be interaction of the Galaxy with the completely massive satellite galaxy.

Thus, not all stars of the thin disk, which are at present located in the Solar neighborhood, were formed from the matter, which experienced united chemical evolution. We suppose that the difference in the star formation rate at the different galactocentric distances and sporadic fall out to the disk of gas from the exteriors of the Galaxy led to the ambiguity of dependence between the age and the metallicity in the so long-life subsystem.

The complete description of the first part of this work was published in (Marsakov, Borkova, 2006), but the second part will be published latter.

*Acknowledgements.* This work was supported in part by the Federal Agency for Education (projects RNP 2.1.1.3483 and RNP 2.2.3.1.3950) and by the Southern Federal University (project K07T – 125).

**References**

Bensby T., Feldsing S. and Lundstrem I.: 2003, *Astron. Astrophys.*, **410**, 527.

Borkova T.V. and Marsakov V.A.: 2005, *Astron. Zh.*, **82**, 453; *Astron. Rep.*, **49**, 405.

Demarque P., Woo J-H., Kim Y-C., Yi S.K.: 2004, *Astron. Astrophys. Suppl. Ser.*, **155**, 667.

Nordstrëm B., Mayor M., Andersen J. et al.: 2004, *Astron. Astrophys.*, **418**, 989.

Marsakov V.A. and Borkova T.V.: 2006, *Pis'ma Astron. Zh.*, **32**, 419.

Pont F., Eyer L.: 2004, *Mon. Not. Roy. Astron. Soc.*, **351**, 487.

Suchkov A.A.: *Astroph. J.*, **535**, L 107.

Tinsley B.M.: 1979, *Astrophys. J.*, **229**, 1046.

Twarog B.A.: 1980, *Astrophys. J.*, **242**, 242.

# STELLAR OBJECTS OF EXTRAGALACTIC ORIGIN IN THE GALACTIC HALO

V.A. Marsakov, T.V. Borkova

Southern Federal University
Rostov-on-Don 344090 Russia,
*marsakov@ip.rsu.ru, borkova@ip.rsu.ru*

ABSTRACT. We identified globular clusters and field stars of extragalactic origin and investigated their chemical, physical, and kinematical properties. This objects as supposed was captured by the Galaxy at different times from debris of the dwarf satellite galaxies disrupted by its tidal forces. The results are follows. (1) The majorities of metal-poor stellar objects in the Galaxy have an extragalactic origin. (2) The masses of the accreted globular clusters decrease with the removal from the center and the plane of the Galaxy. (3) The relative abundances of chemical elements in the accreted and genetically connected stars are essentially distinguished. (4) The accreted field stars demonstrate the decrease of the relative magnesium abundanses with an increase in sizes and inclinations of their orbits. (5) The stars of the Centaurus moving group were born from the matter, in which star formation rate was considerably lower than in the early Galaxy. On the base of these properties was made a conclusion that with the decrease of the masses of the dwarf galaxies in them simultaneously decrease the average masses of globular clusters and the maximum masses of supernova SNe II. Namely latter fact leads to the decrease of the relative abundances of $\alpha$-elements in their metal-poor stars.

**Key words:** Galaxy (Milky Way), stellar chemical composition, accreted stellar objects, halo, Galactic evolution.

Still very recently they assumed that our Galaxy was formed from the united proto-galactic cloud, and all its objects are genetically connected together. However, the numerous observations of the last years demonstrate to us compelling evidence that the Galaxy closely interacts with the less massive satellite galaxies and gradually destroying them, captured their interstellar matter, separate stars and globular clusters. In particular, we are currently observing the disruption of dwarf galaxy Sagittarius by tidal forces from the Galaxy. About ten globular clusters are associated with this galaxy. The massive globular cluster M 54 is generally believed to be the nucleus of the system. The galactic orbital elements of same else clusters also suggest that they were captured from various satellite galaxies. There are convincing proofs that even $\omega$ Cen, the largest known globular cluster of the Galaxy, which is close to the Galactic center and has retrograde orbit, was the nucleus of a dwarf galaxy in the past. The theory of dynamical evolution predicts the inevitable dissipation of clusters through the combined actions of two-body relaxation, tidal destruction, and collisional interactions with the Galactic disk and bulge. Indeed, traces of the tidal interaction with the Galaxy in the shape of extended deformations (tidal tails) have been found in all the clusters for which high-quality optical images were obtained. It is even established for $\omega$ Cen that, after the last passage through the plane of the disk, this cluster lost slightly less than one percent of its mass in the form of stars. Thus, even in the nearest solar neighborhood, we may attempt to identify stars of extragalactic origin. It is interesting to investigate the distinctive properties of stellar objects of extragalactic origin and to estimate their relative number.

It turned out that metal rich ($[Fe/H] > -1.0$) objects form the rapidly revolving and completely flattened subsystem of the thick disk. But metal-poor objects are divided into two types of populations also. Is relied that the metal-poor stars of field with the peculiar velocities are less than the critical value and globulars with the extremely blue horizontal branches form the genetically connected with the thick disk spherical, slowly rotating subsystem of their own halo with the insignificant, but the different from zero radial and vertical metallicity gradients. The high velocity field stars and globulars with the horizontal branches of intermediate color form the spherical subsystem of external accreted halo, approximately into two and one-half of times of larger size than two previous. In this case the absence in it of the metallicity gradients, the predominantly elongated orbits, the large number of stars with retrograde galactic rotation, and often small ages confirm hypothesis about their extragalactic origin.

Very important for understanding of nature of accreted globulars is one of their properties. They

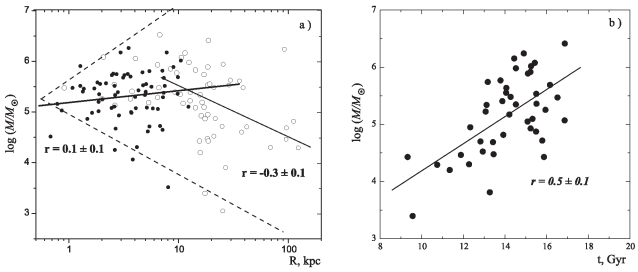


Figure 1: The relationships between the mass and the observed galactocentric distance (a), and between the mass and the age (b). The solid circles denote the genetically connected globular clusters, and open circles – the accreted ones. The solid lines are least square fits for genetically connected and accreted globulars. The dotted line in diagram (a) restrict the region of slow evolution of the globular clasters. The corresponding correlation coefficients are indicated. It is seen the good correlation for accreted clusters in both diagrams.

demonstrate the dependence of mass on the galactocentric distance (Borkova, Masakov, 2000). Solid lines in the diagram $R_a$ – mass (Fig. 1 a) are the regression straight lines for genetically connected and accreted globulars. As we see almost all accreted clusters are into the region of the slow evolution of globular clusters the existence of which is theoretically grounded. Therefore they did not undergo the significant action of dissipation and dynamic friction; i. e., in external halo their initial mass distribution was preserved almost without the change. It is evident that the genetically connected clusters do not reveal a change in the average mass with an increase in the distance from the Galactic center. While for the accreted clusters the observed anticorrelation is different from zero far beyond ranges of errors. Simultaneously accreted clusters demonstrate the decrease of average mass, also, with the decrease of age (Fig. 1 b). The genetically connected globulars of this effect do not reveal. It seems that the globulars with small masses frequently are formed beyond the limits of the Galaxy. Moreover, the greater the dimensions of their present galactic orbit, the less their mass and the ages in average. Hence the conclusion: the globular clusters with anomalously small mass and age are formed predominantly in the such low massive satellite galaxy, which even being located at sufficiently great distances from the Galactic center, lose their globulars under the action of its tidal forces.

It is unlikely that the interstellar matter from which the stars of own and accreted halo were formed has experienced an exactly coincident chemical evolution. Therefore, it would be interesting to search for subtle differences between them that could shed light on the histories of star formation inside and outside the single proto-galactic cloud. Owing to the position of the Sun in the Galactic plane, we have an opportunity to observe the stars of all its subsystems in the immediate vicinity of the Sun and to analyze in detail their chemical composition.

According to current conception the evolution time of close binary stars that subsequently explode as SNe Ia is short, $\approx$ 1 Gyr. Exclusively higher-mass ($M > 8M_{\odot}$) stars exploding as type II supernovae (SNe II) are currently believed to have enriched the interstellar medium with heavy elements at earlier stages. Their characteristic evolution time is only $\approx$ 30 Myr. Almost all of the nuclei of $\alpha$-elements are formed in SNe II while the bulk of iron-peak elements is ejected into the interstellar space during SN Ia explosions. Calculations show that the yield of the $\alpha$-elements depends strongly on the stellar mass. Therefore, the relative abundances of $\alpha$-elements ([$\alpha$/Fe]) in the ejecta of SNe II with different mass can differ markedly. Hence, the variations in the upper boundary of the initial mass function for stars that exploded inside and outside the Galaxy can be estimated from the relative abundances of various elements in genetically related and accreted stars. Concurrently because of the difference between the evolution times of SNe II and SNe I we can try to trace the star formation rate for this stellar ensemble by the coordinates of the characteristic knee in its [$\alpha$/Fe]–[Fe/H] diagram toward the sharp decrease in the relative abundance of the $\alpha$-elements with increasing total heavy-element abundance at the onset of SNe Ia explosions, i. e., $\sim$ 1 Gyr later.

The best-studied $\alpha$-element is magnesium because they exhibit several absorption lines in the visible spectral range. For the analysis, we took data from our compiled catalog of spectroscopically determined magnesium abundances (Borkova and Marsakov 2005). Almost all of the magnesium abundances in nearest stars determined by synthetic modeling of high-dispersion spectra and published before January 2004 were gathered in this catalog. The relative magnesium abundances in the catalog were derived from 1412 spectroscopic determinations in 31 publications for 867 dwarfs and subgiants using a three-pass iterative averaging procedure with a weight assigned to each primary source and each individual determination. The internal accuracy of the relative magnesium abundances for metal-poor ([Fe/H]$< -1.0$) stars is $\varepsilon$[Mg/Fe]=$\pm$0.07.

We justified the choice of the peculiar stellar velocity relative to the local standard of rest $V_{res} = 175$ km s$^{-1}$ as a criterion for separating the nearest thick-disk and halo stars. In identifying the stars of an extragalactic origin (which were called here accreted stars), we assumed that the stars born in a monotonically collapsing single proto-galactic cloud could not be in retrograde orbits. We included all of the stars with high orbit energy, i. e. of high peculiar velocities $V_{res} > 240$ km s$^{-1}$, as have all stars with retrograde orbits, in the group of presumably accreted stars.

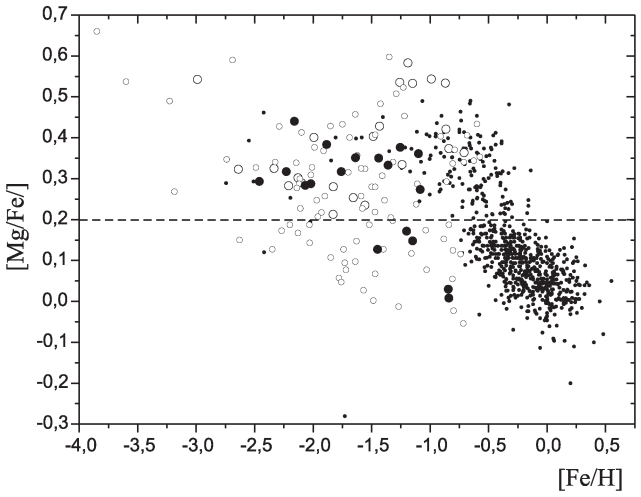


Figure 2: Metallicity vs. relative magnesium abundance for all of the stars in the catalog. The crosses, asterisks, and circles indicate thin- and thick-disk stars, own halo stars, and presumably accreted stars. The filled circles highlight the members of the Centaurus moving group among the accreted stars. The dashed line was drawn through $[Mg/Fe] = 0.2$.

Figure 2 shows the metallicity – relative magnesium abundance diagram for our catalog. It is seen that the accreted objects subsequently formed the bulk of the Galactic halo. (By this term we mean all of the objects that were born outside the single proto-galactic cloud, i. e., in the nearest satellite galaxies or in isolated proto-galactic fragments, and that subsequently escaped from them under the Galactic tidal forces.) We see also from the Figure 2 that the relative magnesium abundances in the own-halo stars are virtually independent of metallicity and that all stars of own halo lie above the dashed line drawn through $[Mg/Fe] = 0.2$. This behavior of own-halo stars suggests that, at least in the initial stage of its formation the interstellar matter in the early Galaxy either was well mixed or SNe II of the same mass exploded in all local volumes. In contrast, the presumably accreted stars exhibit a large spread in relative magnesium abundances in Fig. 2 that extends to negative [Mg/Fe]. The anomalously low relative magnesium abundances in some of the accreted stars are usually explained by an extremely low star formation rate in the dwarf satellite galaxies where these stars were born. However our analysis of the relative magnesium and europium abundances in a small sample of nearby field stars showed that large portion of the presumably accreted stars exhibited an [Eu/Mg] ratio that differed sharply from its Galactic value (Borkova and Marsakov 2004). Since the relative yield of these elements depends solely on the masses of the SN II progenitor stars where they are synthesized, we believe that a more likely mechanism of the magnesium abundance variations in accreted stars is the difference between the initial mass functions in their parent dwarf satellite galaxies. Therefore, it is interesting to try to identify genetically related stars in the accreted halo.

We identified from our catalog of the stars of moving group, which was supposedly lost by the dwarf galaxy, whose center as supposed was the cluster $\omega$ Cen. In the [Mg/Fe]–[Fe/H] diagram (see Fig. 2), all of them lie along a narrow strip. This behavior resembles the expected [Mg/Fe]–[Fe/H] relation derived in a closed model of chemical evolution, which is independent evidences for the genetic relationship between the identified stars. Hence, the low relative magnesium abundances in the metal-richest stars of this group resulted from the SN Ia explosions that began in their parent proto-galactic cloud and that ejected a large number of iron atoms into the interstellar medium and reduced the [Mg/Fe] ratio. The considerably lower metallicity of the knee point in this diagram than that in the Galaxy suggests that the stars of the Centaurus moving group were formed from matter in which the star formation rate was considerably lower than that in the early Galaxy. The high initial relations [Mg/Fe] evidences that, at least in this, presumably initially massive ($M \approx 10^9 M_\odot$) disrupted satellite galaxy (Tshuchiya, et al., 2003) the mean masses of the SN II progenitor stars were the same as those in our Galaxy. It is known that according to numerical simulations of dynamical processes during the interaction of galaxies (Abadi et al. 2003) the satellite galaxies are disrupted and lose their stars only after dynamical friction reduces significantly the sizes of their orbits and drags them into the Galactic plane. Less massive satellite galaxies are disrupted even before their orbits change appreciably under tidal forces. Therefore lost by them stars as a rule must be in higher and more distant orbit. Let us verify this theoretical assumption.

From Fig. 3 it is evident that only slowly rotating around the Galactic center stars with the small relations $[Mg/Fe] < 0.2$ are observed with $[Fe/H] > -1.0$. (Centaurus moving group also have the angular momentum close to zero with retrograde rotation.) Consequently we may to assume that all slow stars were born in the sufficiently massive satellite galaxies. Moreover the star formation rate in them was actually lowered, in comparison with the Galaxy, since the stars of them demonstrate less metal rich "knee point". While the overwhelming majority magnesium-poor and simultaneously metal-poor accreted stars fell within the range $|\Theta| < 50$ km s$^{-1}$.

From the Fig. 4 a, b, where are substituted only accreted stars, one can see well, that (1) stars with the low azimuthal velocities and the small orbital inclinations are majority. (This is understandable, because comparatively massive satellite galaxies lose many stars.) (2) Only star with small ($|\Theta| < 50$ km s$^{-1}$) and

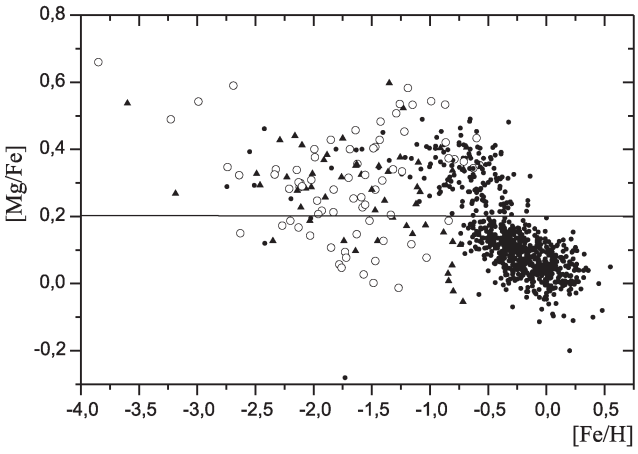


Figure 3: Relative magnesium abundances vs. metallicity. The crosses and circles indicate the genetically related stars and presumably accreted stars. The filled circles represent presumably accreted stars with azimuthal velocities in the ranges $\Theta > 50$ km s$^{-1}$.

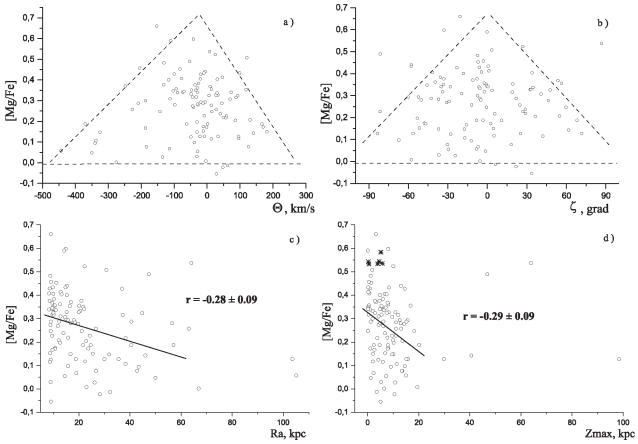


Figure 4: Relative magnesium abundances in accreted stars vs. their azimuthal velocities (a), Galactic orbital inclinations (b), maximum distances of the orbital points from the Galactic center (c) and plane (d). The dashed lines represent the envelopes of the points in the diagrams drawn by eye (upper row). The solid lines represent the regression lines for accreted halo stars (lower row).

with small orbit inclinations can have the high relative abundance of magnesium. (3) In contrast to them, the stars rapidly rotating around the Galactic center and stars with the large orbit inclinations, demonstrate in essence the low relations [Mg/Fe], uncharacteristic for such metal-poor stars. Further, (Fig 4 c, d) the negative radial and vertical gradients of the relative magnesium abundance also indicate the small relations [Mg/Fe] in the accreted stars with the extensive orbits. (These gradients reflect the sizes of the orbits, being located on which satellite galaxies lose their stars.)

Thus, sizes and inclinations of orbits in the accreted stars (and hence in their destroyed parent galaxies) increase with the decrease of the relative abundances of magnesium in them. The extensive and inclined orbits, according to the numerical simulation of the hierarchical formation of the galactic halo, as it was already said, one should expect in the debris of the low massive satellite galaxies, which are destroyed earlier than their orbit noticeably will change under the action of the tidal forces of the Galaxy. Apparently, low massive galaxies, intersecting galactic plane, lose not only stars, but also interstellar gas while crossing the Galactic plane. Star formation in them ends fairly rapidly because of the loss of interstellar matter. Therefore in them we barely see any metal rich stars. In view of this the anomalously low [Mg/Fe] ratios in the lost by them metal-poor stars are caused by the not so much low star formation rate in their parental dwarf galaxies, as the fact that in the less massive dwarf galaxies the initial stellar mass function is just truncated at the high masses. As a result, SNe II eject into the interstellar medium a smaller amount of light $\alpha$-elements into the interstellar medium and the [Mg/Fe] ratios for the stars become anomalously low compared the stars of the same metallicity that are genetically related to the Galaxy.

Thus, the properties of globular clusters and field stars discovered in the work are organically fit within the framework of a single hypothesis. According to it metal-poor stars with anomalously low $\alpha$-element abundances come into our Galaxy from debris of low-mass satellite galaxies in which the chemical evolution proceeded not only slowly but also with the absence of massive SNe II.

So, the results of comprehensive statistic studies testify that a significant quantity mainly of metal-poor objects, which belong at present to our Galaxy, were formed beyond its limits.

*Acknowledgements.* This work was supported in part by the Federal Agency for Education (projects RNP 2.1.1.3483 and RNP 2.2.3.1.3950) and by the Southern Federal University (K07T – 125)

### References

Abadi M.G., Navarro M.G., Steinmetzand M., Eke V.R.: 2003, *Astrophys. J.*, **591**, 499.

Borkova T.V., Marsakov V.A.: 2002, *Bull. Spec. Astrophys. Obs.*, **54**, 61.

Borkova T.V., Marsakov V.A.: 2004, *Pis'ma Astron. Zh.*, **30**, 173; *Astron. Lett.*, **30**, 148.

Marsakov V.A., Borkova T.V.: 2006, *Pis'ma Astron. Zh.*, **32**, 545; *Astron. Lett.*, **32**, 376.

Tshuchiya T., Dinescu D., Korchagin V.I.: 2003, *Astrophys. J.*, **589**, L29.

# THE BENEFITS OF THE ORTHOGONAL LSM MODELS

Z. Mikulášek[1,2]

[1] Institute for Theoretical Physics and Astrophysics, Masaryk University
Kotlářská 2, CZ-611 37 Brno, Czech Republic, *mikulas@physics.muni.cz*
[2] Observatory and Planetarium of J. Palisa, VŠB-Technical University
Ostrava, Czech Republic

ABSTRACT. In the last few decades both the volume of high-quality observing data on variable stars and common access to them have boomed; however the standard used methods of data processing and interpretation have lagged behind this progress. The most popular method of data treatment remains for many decades Linear Regression (LR) based on the principles of Least Squares Method (LSM) or linearized LSM. Unfortunately, we have to state that the method of linear regression is not as a rule used accordingly namely in the evaluation of uncertainties of the LR parameters and estimates of the uncertainty of the LR predictions.

We present the matrix version of basic relations of LR and the true estimate of the uncertainty of the LR predictions. We define properties of the orthogonal LR models and show how to transform general LR models into orthogonal ones. We give relations for orthogonal models for common polynomial series.

**Key words**: variable stars, observation, data processing, LSM, linear regression, orthogonal LSM models

## 1. Introduction

The development in the field of variable stars research from Tsessevichs times is enormous. The number of known variable stars has arisen by at least two orders, as well as the number of their observers and interpreters. It has arisen both the volume and common access to high-quality variable stars observing data and computational techniques. The number of new efficient statistical techniques and methods that are available for everybody thanks to wide spread personal computers have been developed and published. Nevertheless, the methods used for processing of variable stars data mostly have remained the same as those used in Vladimir Platonovichs era.

Every astrophysicist likes large quantities and better quality of modern observational data, new methods of processing are not so popular. Majority of them needs a good knowledge of matrix calculus, what is in discordance with a frequent syndrome of variable stars observers, which could be named *Matrixphobia*. Very rarely we are encountering with the opposite syndrome of *Matrixphilia* which invades mathematically erudite theoreticians loving new methods and matrices so much that they do not use them for real observational data. Both extremes in the data processing are bad and we should find our golden mean.

The contemporary statistics shares inexhaustible quantity of methods. It is necessary to select several of the most versatile and diverse methods, master them and to learn to combine them. The method of processing must not be unique, but always must be made-to-measure of the set problem.

The majority of variable stars data processing tasks are solved using least square method, strictly speaking linear regression, where as models serve the most frequently common polynomials or sine/cosine series. It should be noted that there exist several other methods which are able to give the same or better results. One of them is for example the Advanced Principal Component Analysis, which is the combination of LSM and standard Principal Component Analysis (see Mikulášek, 2007). The method is optimal for solving of a lot astrophysics problems as a realistic fitting of multicolour light curves, the determination of the moments of extrema of multicolour light curves, modeling of light multicolour curves which is necessary for the process of improvement of ephemerides, diagnostics of light curve (LC) secular changes, and the classification of LCs. Other methods of modern data treatment are also mentioned in Andronov, I., these Proceedings.

In the following section we will pay attention to some details of linear regression procedure which is very likely the most frequently used tool of variable stars data processing.

## 2. The Least Squares Method

The very frequent astrophysical task is to fit a curve through a series of $N$ observed points described by a triad $\{x_i, y_i, w_i\}$, where $x_i$ is an independent (well measured) quantity like time or a phase, related to the $i$-th measurement $y_i$ is the dependent, measured quantity

like magnitude, O−C, and $w_i$ is the weight of the measurement, as a rule inversely proportional to the square of the expected uncertainty of the value $y_i$. Hereafter we will use normalized weights $w_i$ the mean value $\bar{w}$ of which is equal to 1.

$F(x, \vec{\beta})$ is so called *model function* of $x$ described by the $k$ free parameters $\beta_1, \beta_2, \ldots, \beta_k$ arranged into the vector $\vec{\beta}$. We define a function of this vector $S(\vec{\beta})$:

$$S(\vec{\beta}) = \sum_{i=1}^{N} \Big[ y_i - F(x_i, \vec{\beta}) \Big]^2 w_i. \tag{1}$$

The solution of the LSM minimalization procedure, is finding of the vector of parameters $\vec{\beta} = \mathbf{b}$, for which is the quantity $S(\vec{\beta})$ minimal. The success of the method in the given situation depends above all on our skill in the creating of the mathematical model expressed by the function $F(x, \vec{\beta})$. Then the finding of the best fit in the range of functions admissible by the pre-selected model is relatively simple and straightforward. In principle it is solution of $k$ equations of $k$ unknown parameters arranged in the vector $\mathbf{b}$:

$$\left.\frac{\partial S}{\partial \vec{\beta}}\right|_{\vec{\beta}=\mathbf{b}} = \mathbf{grad}\Big[S(\vec{\beta} = \mathbf{b})\Big] = \vec{0}. \;\Rightarrow \tag{2}$$

$$\sum_{i=1}^{N} y_i \frac{\partial F(x_i, \mathbf{b})}{\partial \beta_j} w_i = \sum_{i=1}^{N} F(x_i, \mathbf{b}) \frac{\partial F(x_i, \mathbf{b})}{\partial \beta_j} w_i, \tag{3}$$

for $j = 1, 2, \ldots, k$.

### *2.1. Linear regression*

The LSM procedure of the determination of the solution will be considerably simplified if we use the linear model of the found function $F(x, \vec{\beta})$, assuming:

$$F(x, \vec{\beta}) = \sum_{j=1}^{k} \beta_j \, f_j(x), \tag{4}$$

where $f_j(x)$ are arbitrary functions of $x$. Eq. 1 then can be rewritten in the form:

$$S(\vec{\beta}) = \sum_{i=1}^{N} \left[ y_i - \sum_{j=1}^{k} \beta_j \, f_j(x_i) \right]^2 w_i. \tag{5}$$

Eq. 3 then switches to:

$$\sum_{i=1}^{N} y_i \, f_j(x_i) \, w_i = \sum_{i=1}^{N} \left[ \sum_{p=1}^{k} b_p \, f_p(x_i) \right] f_j(x_i) \, w_i, \tag{6}$$

It is advantageous to express all operations in matrix form. Then

$$\mathbf{X} = \begin{pmatrix} f_1(x_1) & f_2(x_1) & \cdots & f_k(x_1) \\ f_1(x_2) & f_2(x_2) & \cdots & f_k(x_2) \\ \vdots & \vdots & \ddots & \vdots \\ f_1(x_N) & f_2(x_N) & \cdots & f_k(x_N) \end{pmatrix}, \tag{7}$$

$$\mathbf{Y} = (y_1 \, y_2 \, \cdots \, y_N)^{\mathrm{T}} \,; \; \mathbf{W} = \mathbf{diag}\,(w_1 \, w_2 \, \cdots \, w_N)\,, \tag{8}$$

$$\mathbf{H} = \big(\mathbf{X^T W \, X}\big)^{-\mathbf{1}}, \; \mathbf{b} = \mathbf{H \, X^T W \, Y}, \; \mathbf{Y_p} = \mathbf{X \, b}, \tag{9}$$

$$R = \mathbf{Y^T W \, Y} - \mathbf{b^T X^T W \, Y}, \; s = \sqrt{\frac{R}{(N-k)}}, \tag{10}$$

where $\mathbf{Y}_{\mathrm{p}}$ is the vector of the predictions, $\overline{w}$ is the mean value of weights $w_i$, $R$ is the weighted sum of square deflections, $s$ is the weighted standard deviation of the fit.

The procedure of linear regression with the explicit linear model is quick and its solution is unique. In the general case we may find several solutions although some of them could be physically unreal. The most common method of finding of local minima on the $S(\beta)$ plane is an iterative gradient method, where we use the above mentioned apparatus of linear regression applied on the linearized model function.

### *2.2. Linearized regression*

The linearization of the general model function $F(x, \vec{\beta})$ consists in substitution of it by its Taylor expansion in respect of $\vec{\beta}$. We need to know as good as possible estimate $\mathbf{b_e}$ of the solution of LSM equations $\mathbf{b}$, $\mathbf{b_e} \to \mathbf{b}$. Then we can write:

$$F(x_i, \vec{\beta}) \cong F(x_i, \mathbf{b_e}) + \sum_{j=1}^{k} \frac{\partial F(x_i, \mathbf{b_e})}{\partial \beta_j} (\beta_j - b_{ej}). \tag{11}$$

$$S(\vec{\beta}) = \sum_{i=1}^{N} \left[ \Delta y_i - \sum_{j=1}^{k} f_j(x_i) \, \Delta\beta_j \right]^2 w_i, \tag{12}$$

where

$$\Delta y_i = y_i - F(x_i, \mathbf{b_e}), \quad f_j(x) = \frac{\partial F(x, \mathbf{b_e})}{\partial \beta_j},$$
$$\Delta\vec{\beta} = \vec{\beta} - \mathbf{b_e}. \tag{13}$$

The equations Eq. 5 and Eq. 12 are formally identical, despite the meanings of particular terms in them are different. We define column vector $\Delta\mathbf{Y} = [\Delta y_1 \, \Delta y_2 \, \cdots \, y_N]$, and the column vector of the correction of the solution estimate $\mathbf{b_e}$, $\Delta\mathbf{b}$.

$$\mathbf{H} = \big(\mathbf{X}^{\mathrm{T}}\mathbf{W \, X}\big)^{-1}, \; \Delta\mathbf{b} = \mathbf{H \, X}^{\mathrm{T}}\mathbf{W}\Delta\mathbf{Y},$$
$$R = \Delta\mathbf{Y}^{\mathrm{T}}\mathbf{W}\Delta\mathbf{Y}, \quad s = \sqrt{\frac{R}{(N-k)}}. \tag{14}$$

Correcting $\mathbf{b_e}$ by $\Delta\mathbf{b}$ we get the next solution estimate $\mathbf{b_e}$ and we can repeat the whole procedure several times. The convergence of accordingly selected LSM model function is as a rule very swift: after a few steps we state that $\Delta\mathbf{b} \to \mathbf{0}$, hence $\mathbf{b} = \mathbf{b_e}$.

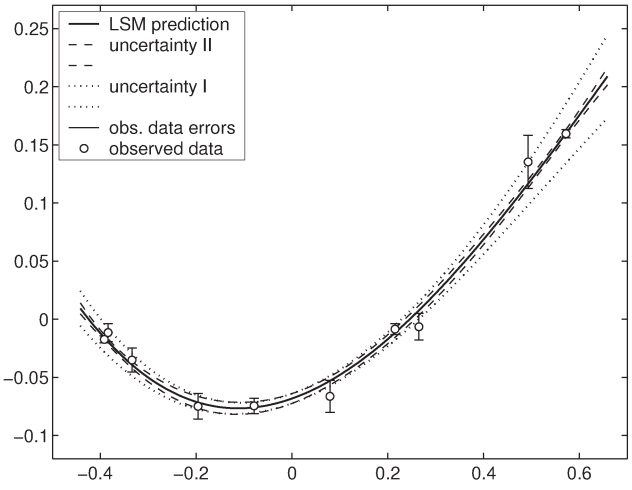


Figure 1: The illustrative figure displays the time dependence of an observed quantity measured with the accuracy denoted by the abscissa. The continuous line represents LSM fit by the polynomial of the 3-rd order (cubic parabola). Expected uncertainties of this prediction calculated by the formula Eq. 16 are denoted by dotted lines, true uncertainties given by Eq. 17 are signed by dashed lines.

### *2.3. Uncertainties of parameters and prediction*

There are at least three reasons why we should estimate the measure of uncertainty of the found parameters. Firstly, errors of parameters tell us a lot about the reliability of our results, secondly uncertainties of parameters would enable to calculate the uncertainty of the prediction done on the basis of our LSM analysis, and last but not least above mentioned errors are strictly demanded by teachers, scientific editors and referees. All LSM instructions and codes congruently get for uncertainty of the $j$-the parameter $\delta b_j$ the following relation:

$$\delta b_j = s\sqrt{H_{jj}}, \tag{15}$$

where $H_{jj}$ is the $j$-th element in the diagonal of the matrix $\mathbf{H}$.

It is a question whether $\delta b_j$ really expresses the uncertainty in the common sense. The response is no, strictly speaking sometimes yes, but very rarely. It can be demonstrated on the error of the absolute term in the LSM fit by straight line, which evidently depends on the choice of the origin of $x$ coordinate.

The suspicion that there is something incorrect in our comprehension of the true meaning of the quantity $\delta b_j$ defined by Eq. 15 will be supported by our attempt use these errors for the evaluating of the expected uncertainty of the prediction by the model function for the arbitrarily selected value of $x$:

$$\delta y_p(x) = \sqrt{\sum_{j=1}^{k} \delta^2 b_j \, f_j^2(x)} = \sqrt{\mathbf{g}(x)\, \mathbf{H}_{\rm dg}\, \mathbf{g}^{\rm T}(x)}, \tag{16}$$

where $\mathbf{H}_{\rm dg}$ equals to the matrix $\mathbf{H}$, whose all non-diagonal elements has been put zero. $\mathbf{g}(x)$ is the row vector of the gradient of the solution model function $\mathbf{F}(x, \mathbf{b})$, $\mathbf{g}(x) = [f_1(x)\, f_2(x)\, \ldots\, f_k(x)]$

The instructive picture Fig. 1 will show you that this intuitive relation gives quite inadequate results. Nevertheless, it can be shown that it is valid formally rather similar relation:

$$\delta y_p(x) = \sqrt{\mathbf{g}(x)\, \mathbf{H}\, \mathbf{g}^{\rm T}(x)}. \tag{17}$$

The matrix $\mathbf{H}$ is by the definition (see Eq. 9 and 14) a symmetric square $k \times k$ matrix with $k(k+1)/2$ independent elements. If we want to enable to anybody to compute the uncertainty of the prediction, we should publish either the whole matrix $\mathbf{H}$ or its non-trivial part at least. Nevertheless, there is another (more illustrative) possibility: to transform the model function into the orthogonal one. Then the matrix $\mathbf{H}$ will change in the diagonal one and the uncertainties of parameters will acquire its standard meaning. It will help you among other things expertly examine importance of individual terms.

## 3. Orthogonal LSM models

Let us assume that the functional dependence of observed quantities $y$ on $x$ is well described by the model function which can be expressed in the form of the linear combination of $k$ basic functions of $f_j(x)$ with coefficients $b_j$. The found solution does not change if we use another set of $k$ functions $\vartheta_j(x)$, which are created as linear combinations of the basic functions $f_j(x)$. Let us combine them so that the new set of basic functions $\vartheta_j(x)$ is orthogonal. It means we find the set of coefficients $\{a_{pj}\}$:

$$\vartheta_p(x) = \sum_{j=1}^{k} a_{pj}\, f_j(x), \quad \text{so that,} \tag{18}$$

$$\overline{\vartheta_p\, \vartheta_q} = \sum_{i=1}^{N} \vartheta_p(x_i)\, \vartheta_q(x_i)\, w_i = 0 \quad \text{if } p \neq q \tag{19}$$

The calculation of linear regression parameters and their uncertainties is then very simple:

$$b_j = \frac{\sum_{i=1}^{N} y_i\, \vartheta_j(x_i)\, w_i}{\sum_{i=1}^{N} \vartheta_j^2(x_i)\, w_i}; \quad \delta b_j = \frac{s}{\sqrt{\sum_{i=1}^{N} \vartheta_j^2(x_i)\, w_i}};$$

$$\delta y_p(x) = \sqrt{\sum_{j=1}^{k} \delta^2 b_j\, \vartheta_j^2(x)}. \tag{20}$$

The set of coefficients $\{a_{pj}\}$ fulfilling constraints Eq. 19 is not unique as well as the procedures of its finding. We recommend to use the following procedure which seems to us the simplest one:

$$\vartheta_1 = f_1; \quad \vartheta_2 = f_2 - a_{21}\vartheta_1;$$
$$\vartheta_3 = f_3 - a_{32}\vartheta_2 - a_{31}\vartheta_1;$$
$$\vartheta_p(x) = f_p(x) - \sum_{q=1}^{p-1} a_{pq}\,\vartheta_q(x), \tag{21}$$

where

$$a_{pq} = \frac{\overline{f_p\,\vartheta_q}}{\overline{\vartheta_q^2}} = \frac{\sum_{i=1}^{N} f_p(x_i)\,\vartheta_q(x_i)\,w_i}{\sum_{i=1}^{N} \vartheta_q^2(x_i)\,w_i}. \tag{22}$$

The first three orthogonalized terms will be:

$$\vartheta_1(x) = f_1(x); \quad \vartheta_2(x) = f_2(x) - \frac{\overline{f_2 f_1}}{\overline{f_1^2}};$$
$$\vartheta_3(x) = f_3(x) - \frac{\overline{f_3 f_2} - \overline{f_3}\;\overline{f_2}}{\overline{f_2^2} - \overline{f_2}^2}\,f_2(x) -$$
$$- \left[\frac{\overline{f_3 f_1}}{\overline{f_1^2}} - \frac{\overline{f_2 f_1}\,(\overline{f_3 f_2} - \overline{f_3}\;\overline{f_2})}{\overline{f_1^2}\left(\overline{f_2^2} - \overline{f_2}^2\right)}\right] f_1(x). \tag{23}$$

The explicit expression of successive terms of a set of the orthogonalized functions is more and more complex, however it is not very complicated to write an iterative PC code enabling to compute the formulae for arbitrary number of parameters.

### *3.1. Orthogonal polynomial model*

The most popular linear regression model (not only in astrophysics) $F(x, \vec{\beta})$ is:

$$F(x, \vec{\beta}) = \sum_{j=1}^{k} \beta_j\, x^{j-1}. \tag{24}$$

The model is known to have a lot uncomfortable properties which complicate both the calculation and the interpretation of found results. We should never used it without orthogonalization.

We recommend to put the origin of $x$-coordinates into the center of gravity of observations: $x \rightarrow x - \bar{x}$ before the application of the orthogonalization procedure. It will result in the considerable simplification in the form of regression model. Assuming now $\bar{x} = 0$ the first four orthogonal polynomials are as follows:

$$\vartheta_1(x) = 1;\ \vartheta_2(x) = x;\ \vartheta_3(x) = x^2 - \frac{\overline{x^3}}{\overline{x^2}}\,x - \overline{x^2},$$
$$\vartheta_4(x) = x^3 - \frac{\overline{x^2}^2\overline{x^3} + \overline{x^3}\;\overline{x^4} - \overline{x^2}\;\overline{x^5}}{\overline{x^2}^3 + \overline{x^3}^2 - \overline{x^2}\;\overline{x^4}}\,x^2 -$$
$$\frac{\overline{x^3}\;\overline{x^5} + \overline{x^2}^2\overline{x^4} - \overline{x^4}^2 - \overline{x^3}^2\overline{x^2}}{\overline{x^2}^3 + \overline{x^3}^2 - \overline{x^2}\;\overline{x^4}}\,x - \frac{\overline{x^2}^2\overline{x^5} + \overline{x^3}^3 - 2\overline{x^3}\;\overline{x^4}}{\overline{x^2}^3 + \overline{x^3}^2 - \overline{x^2}\;\overline{x^4}},$$

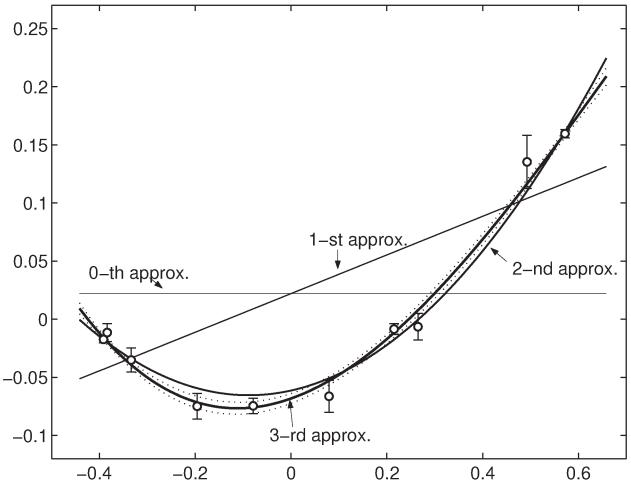


Figure 2: The subsequent approximations of the fit of observed data by orthogonal polynomial regression.

where,

$$\overline{x^p} = \frac{\sum_{i=1}^{N} x_i^p\,w_i}{\sum_{i=1}^{N} w_i}. \tag{25}$$

Fig. 2 displays the results of subsequent fitting of the model situation by constant, linear, quadratic and cubic orthogonal polynomials.

If the data are distributed uniformly in the interval $x_i \in \langle -\Delta;\, \Delta\rangle$, we can use the transformed Legendre polynomials (orthogonal on the interval $\langle -1;\, 1\rangle$) as the orthogonal (or quasiorthogonal) LSM model:

$$\vartheta_1 = 1;\ \vartheta_2 = x;\ \vartheta_3 = x^2 - \frac{\Delta^2}{3};\ \vartheta_4 = x^3 - \frac{3\,\Delta^2}{5}\,x;$$
$$\vartheta_5 = x^4 - \frac{6\,\Delta^2}{7}\,x^2 + \frac{3\,\Delta^4}{35};\ \cdots \tag{26}$$

### *3.2. Orthogonal sine, cosine model*

The basic tool for the analysis of cyclic and periodic processes in astrophysics is the linear regression with the model consisting of simple periodic functions, the most commonly:

$$F(\varphi, \vec{\beta}) = \beta_1 + \sum_{j=1}^{q} \beta_{2j}\cos(2\pi j\varphi) + \beta_{2j+1}\sin(2\pi j\varphi), \tag{27}$$

where $\varphi$ is the phase as an independent variable, $q$ is the order of set of harmonic functions. The model need not contain all of functions, it might be limited e.g. only to even functions etc.

In the case that the observations are spread over the whole cycle more or less uniformly, it is not needed to do any orthogonalization, because all functions are orthogonal itself. In the opposite case we should do

orthogonalization e.g. by the procedure described by Eq. 21 and Eq. 22.

## 4. Conclusions

We displayed the benefits of consequential usage of orthogonal LSM model functions with the emphasis on the polynomial regression as the chief tool of astrophysical data processing. Orthogonal models enable to give the true sense to errors of found parameters and easily compute estimates for uncertainties of the prediction. The orthogonality of the models removes the bad conditioning of the solved systems of equations and help us to obtain results not affected by computational errors. We recommend to use them always, compulsorily in the case of polynomial regression.

It is demanding to use new methods of variable stars data processing which enable us better exploit information hidden in observations. Endeavor connected with mastering of them will return in new subtle discoveries and revealing.

Matrix calculus, true using of weights, advanced principal component analysis, factor analysis, robust regression, creation and usage of orthogonal models and several other processing techniques should appertain to compulsory outfit of each variable stars observer of the 21st century.

*Acknowledgements.* This work was supported by grants GA ČR 205/06/0217, and MVTS ČRSR 10/15. The author is indebted to prof. Izold Pustylnik and Dr. Miloslav Zejda for careful and critical reading of the manuscript and suggestions which considerable improved the article.

## References

Mikulášek Z.: 2007, *Astron. Astrophys. Trans.,* **26**, 63.

# THE STARS OF THE LOWER PART OF MAIN SEQUENCE

T.V. Mishenina[1], S.I. Belik[1], I.A. Usenko[1], O. Bienaymé[2], C. Soubiran[3], V.V. Kovtyukh[1], S.A. Korotin[1]

[1]Astronomical Observatory, Odessa National University
T.G.Shevchenko Park, Odessa 65014 Ukraine, *astro@paco.odessa.ua*
[2]Observatoire Astronomique de l'Universitté Louis Pasteur
11 rue de l'université, Strasbourg, France
[3]Observatoire Aquitain des Sciences de l'Univers
CNRS UMR 5804, BP 89, 33270 Floirac, France

ABSTRACT. Atmospheric parameters ($T_{eff}$, $\log g$, [Fe/H], $V_t$), Li, and volatile (O, Na, Al, Zn) and refractory (Si, Ti, V, Cr, Co and Ni) element abundances in 133 stars belonging to the low part of MS have been determined. Among them about 30 stars are the variable stars of BY Dra type, for which the determination of the chemical composition was made for the first time. The effective temperatures $T_{eff}$ were estimated by the line depth ratio method. The surface gravities $\log g$ were determined by two methods (ionization balance of iron and using parallaxes). The abundances of lithium and oxygen were determined by the calculation of synthetic spectrum. The comparison of volatile and refractory element abundances in variable stars and other stars was made. We have found that the behaviour of the abundances of the majority of elements in MS stars and spotted stars does not differ. The Li is detected in 65 % BY Dra stars and in 26 % of MS stars. The Li abundance in variable stars is higher than in MS dwarfs.

**Key words**: Stars: fundamental parameters; stars: abundances; stars: main -sequence; stars: BY Dra type.

## 1. Introduction

In the cadre of the program of determination by a uniform technique of parameters and a chemical composition for the extensive sample of stars we represent the investigation of 133 stars of the low part of the Main Sequence (MS). Among the stars selected by us for this work more than 30 ones are variable stars belonging to a class of flashing stars, and, basically, to a subclass of BY Dra type stars. Till now any detailed spectral investigation of the chemical composition of this type stars has not been made. As a rule, spectral researches of these stars were spent for the analysis of spots on their surface. Thus, there is the unique opportunity to analyse chemical peculiarities of these stars for the first time. As all stars studied by us in the given work belong to solar type, and many researchers classify the Sun as a star of BY Dra type, it would be obviously important to investigate: 1) the general behaviour of various element abundances with metallicity [Fe/H] , 2) dependences (trends) of volatile and refractory element abundance with [Fe/H] which can testify in favour of presence of planetary systems in dwarfs and variable stars, 3) the lithium abundance as the indicator of activity and age of stars. The goals of our work are the determination of the atmospheric parameters for stars of the low part of MS, the analysis of the spectral peculiarities and the chemical composition (abundances of Li and volatile and refractory elements).

## 2. Observations and spectral processing

Our target stars were selected upon photometric criterion $M_V$, (B-V) as stars belonging to low part of MS, where $M_V = V + 5 + 2.5\log \pi$. The spectral classes Sp, magnitudes V, color index (B-V) and type of variability were taken from SIMBAD database, the parallaxes $\pi$ from Hipparcos catalogue (ESA 1997).

The spectra of 133 stars (F-G-K V) were obtained using the 1.93 m telescope of the Haute-Provence Observatoire (France) equiped with échelle-spectrograph ELODIE. The resolving power was 42000, the region of the wavelengths was 4400 - 6800 ÅÅ, the signal-to-noise ratio was about 130-230 (at 5500 Å). The primary processing of spectra (the image extraction, cosmic particles removal, flatfielding etc.) was carried out by following Kats et al. (1998). The further processing of spectra (continuum level location, measurement of the equivalent widths etc.) was performed using the software package DECH20 (Galazutdinov, 1992).

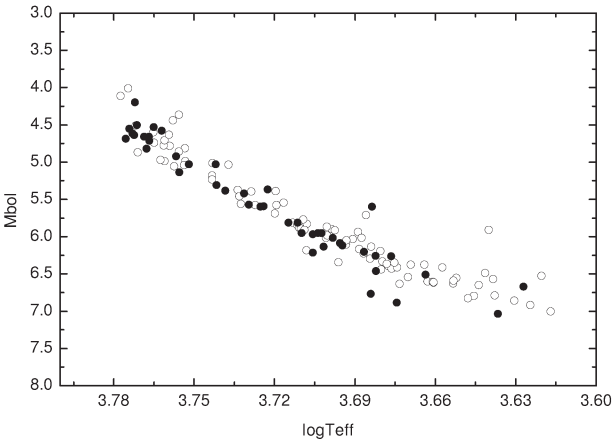


Figure 1: Location in the H-R diagram of MS (open circles) and variable (black circles) stars studied in this work.

The equivalent width are measured by gaussian fitting.

### 3. Peculiarities of spectra

The position of our target stars in the H-R diagram is given in Fig.1.

Bolometric magnitude $M_{bol}$ was determined upon the dependence: $M_{bol} = M_V + BC$, where the bolometric corrections BC were taken from Flower (1996). Among our studied stars there are more than 30 variable flashing or active stars. The big class of flashing (Fl) stars (generally UV Cet type) is divided into subclasses, including, the spotted short-amplitude stars of BY Dra type (Chugainov, 1966) having the spectral types F – M V and vsini $< 20$ km s$^{-1}$, and RS CVn type stars that are the detached or semi-detached systems with components which have Sp: F-G V-IV and G-K IV. The masses of flashing stars are within the limits of 1.5 to 0.05 $M_\odot$, they have age from $10^6$ to $10^9$ years, and the period of axial rotation is from about 10 hours to about 10 days. For BY Dra type stars the differential rotation of a solar type (equator rotates faster than poles) and cycles of activity (similar to solar 11 years) were found (Gershbrg, 2002).

Previous photometric and spectral researches of flashing stars have been directed on study of temperatures and areas of spots. Application of photometric methods and modelling has allowed to construct the zonal spottedness model by Alekseev (2006), that was applied to the Sun, to BY Dra (Alekseev & Gershberg, 1996), to RS CVn (Alekseev & Kozhevnikova, 2005). Polarization methods show that the magnetic fields are located on the same active longitudes, as most spotarea. Some successes have been reached by the usine of the doppler imaging + zeeman spectroscopy of the high resolution spectra. Estimations of spots temperature have been made, basing on calibrations of the ratios of line intensity. There are in our list some known stars of BY Dra type: V439 And, V435 And, V538 Aur, OU Gem, DX Lyn, HP Boo, V1654 Aql, V1803 Cyg, HN Peg, V453 And, V833 Tau; and of RS CVn type – SV LMi, V368 Cep, V774 Her (Fl) and V775 Her. We found that four stars of our list show $H_\alpha$ emission. Unfortunately, spectra do not contain the region of H and K Ca II lines that are more reliable indicator of stars chromosphere and spotted activity. Absence of the obvious attributes of activity has allowed us to assume, that the spectra have been received in a quiet stars condition and we can apply to them standard methods of investigation.

### 4. Parameter determination

Stars of BY Dra type have, basically, the insignificant fluctuations in (B-V), that is not exceeding $0.^m1$. There are only some stars with changes of (B-V) up to 0.4. Nevertheless, using of the photometric calibrations to determine $T_{eff}$ leads to significant errors in the temperature values. For example, d(B-V) = 0.02 gives the error in $T_{eff}$ is equal to ±40 K and d(B-V) = 0.10 gives one about ±170 K. In our work the effective temperatures $T_{eff}$ were estimated by the line depth ratio method which provides accuracy $\Delta\ T_{eff} = \pm 5 - 10$ K. Thus the received temperature characterizes the given current condition of an atmosphere that is very important in case of variable stars researching. To analyse the obtained $T_{eff}$ we have looked on Figs.2,3, where dependences of $\sigma\ T_{eff}$ for obtained $T_{eff}$ and stellar magnitude V are given. As can see the scatter does not exceed ±10 K on the average and is increasing up to 30 K at low temperatures ($T_{eff} < 4400$ K) and for faint stars ($V < 9^m$), i.e. it is due to lines blending and the low values of a signal to noise ratio (S/N) in the spectra of cool and faint stars, but MS stars and variable stars do not show any distinctions.

The surface gravities log g were determined by two methods (ionisation balance of iron and using the parallaxes), the average difference between two values obtained by these methods is $<$ log $g_{IE}$ – log $g_\pi$ $>$ = -0.06 ±0.16 (for $T_{eff} > 5000$ K, 80 stars). The results of these two methods of applications are in the good agreement. The microturbulent velocity $V_t$ was determined on the independence of the iron abundance log A(Fe) obtained from given Fe I line from equivalent width EW of this line. With the purpose of estimation of the parameters reliability and opportunities of their use in the analysis of variable stars, we have constructed also the dependence of turbulent velocity $V_t$ on temperature $T_{eff}$ (Fig.4).

As can see from the Fig.4, five stars show $V_t$ values above 1.6 km s$^{-1}$, four of them are variables. However, for other stars, we do not observe distinctions for MS dwarfs and variable stars. The [Fe/H] metallicity is

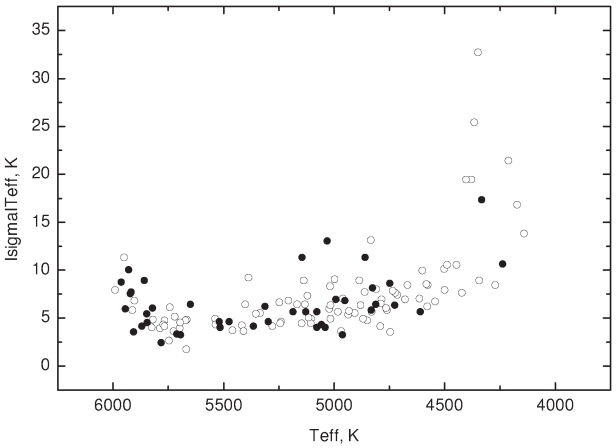


Figure 2: The dependences of $\sigma$ $T_{eff}$ on obtained $T_{eff}$ for our studied stars, the notation is the same as in Fig.1.

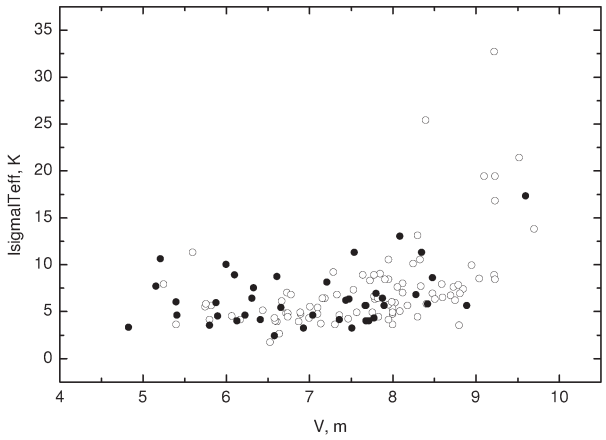


Figure 3: The dependenes of $\sigma$ $T_{eff}$ on stellar magnitude V for our studied stars, the notation is the same as in Fig.1.

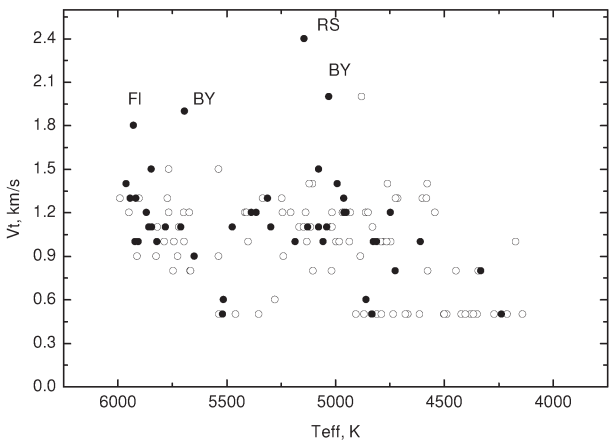


Figure 4: The dependences of $V_t$ on obtained $T_{eff}$ for our studied stars, the notation is the same as in Fig.1.

obtained as the iron abundance determined from Fe I lines. The accuracies of the parameter determination are: $\Delta$ $T_{eff}$ = $\pm$30 K, $\Delta$ log $g$ = $\pm$0.3 dex, $\Delta$ $V_t$ =0.2 $\pm$ km $s^{-1}$.

## 5. Determination of chemical composition

We employ the grid of stellar atmospheres from Kurucz (1993) to compute abundances of Li, volatile (O, Zn, Na, Al) and refractory (Si, Ca, Sc, Ti, V, Cr, Co and Ni) elements. The choice of the model was made using the standard interpolation on $T_{eff}$, and log $g$. The abundance analysis of Na, Al, Si, Ti, V, Cr, Co, Ni, and Zn has been done in the LTE approximation (Kurucz's WIDTH9 code) using the measured equivalent widths of these elements' lines and the solar oscillator strengths (Kovtyukh & Andrievsky, 1999). The Li abundances in program stars were obtained by fitting synthetic spectra to the observational profiles. We used STARSP LTE spectral synthesis code developed by Tsymbal (1996). Considering a wide range of temperatures and metallicities of our sample stars, the special effort was put into a compilation of a full list of atomic and molecular lines close to the $^7$Li 6707 Å line (Mishenina & Tsymbal, 1997). The O abundances by the synyhetic spectrum method were determined on [OI] 6300.3 Å line, the Ni I line and the CN lines were included in the final line list. For example, the total uncertainty due to parameters and EW errors for Fe I, Fe II, Si I and Ni I lines is 0.10, 0.12, 0.05, 0.09. correspondly.

## 6. Results and discussion

As we have not greater number of spectral observation for each spotted star, received during one period of a star, we cannot investigate temperature and an area of spots. But it is not the purpose of our work. Our target stars have given to us as an opportunity to consider behaviour of the elements' abundances with metallicity of the MS and spotted stars. As well as the Sun also belongs to BY Dra type stars it seems interesting to consider separately the behaviour of refractory and volatile elements. The behaviour of these elements is the key in testing one of hypotheses for detection of stars with planetary systems. There are two hypotheses which are based on the study of the chemical composition: 1) primordial scenario, reflects of the high metal content of the protoplanetary cloud from which stars and planets were formed (Santos et al., 2000), 2) different behavior of refractory (Si, Ca, Ti, Sc, V, Cr, Mn, Co, Ni) and volatile (C, S, Zn, N, O, Na, Al, Mg) elements derives from the accretion of a large amount of rocky planetesimal material on to the stars (Gonzales, 1997). Let's note, that in the paper

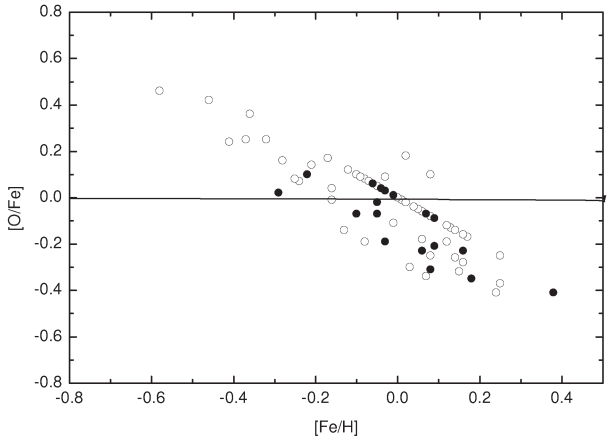


Figure 5: The trend of oxygen with [Fe/H], the notation is the same as in Fig.1.

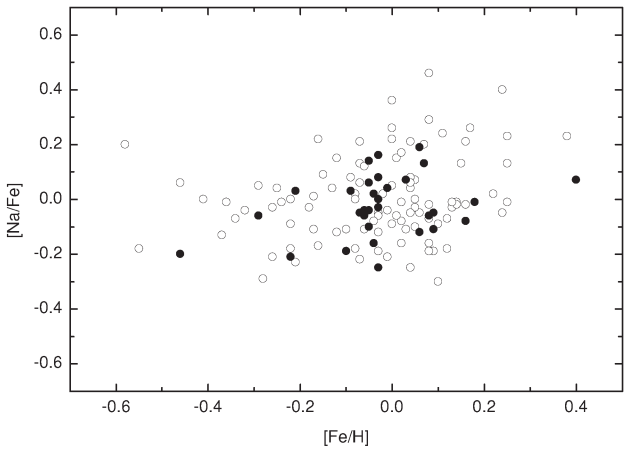


Figure 6: The trend of sodium with [Fe/H], the notation is the same as in Fig.1.

on studying the refractory elements' abundances (Gilli et al., 2006) for single stars and the stars with extrasolar planets the similar trends for these two groups were found. Also in the paper on the oxygen determination (it is one of volatile elements) (Ecuvillon et al., 2006) the appreciable trends distinction for these two groups of stars is not revealed. To analyse behaviour of the elemental abundances we have considered dependences of various element abundances on metallicity. Trends of the studied elements with [Fe/H] presented in Figs.5-13 , where MS stars are marked by open circles, and variable stars are designated by black circles.

We have calculated also the mean abundance values of different elements in the MS and spotty stars (Tabl.1).

As can see from Figs. 5-13 the abundance behaviour of the majority of elemental abundances in MS and spotted stars does not differ. Trend of the elemental abundance corresponds to the received earlier results

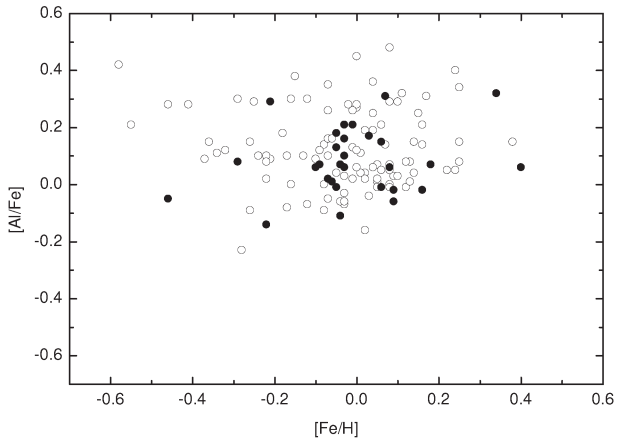


Figure 7: The trend of aluminium with [Fe/H], the notation is the same as in Fig.1.

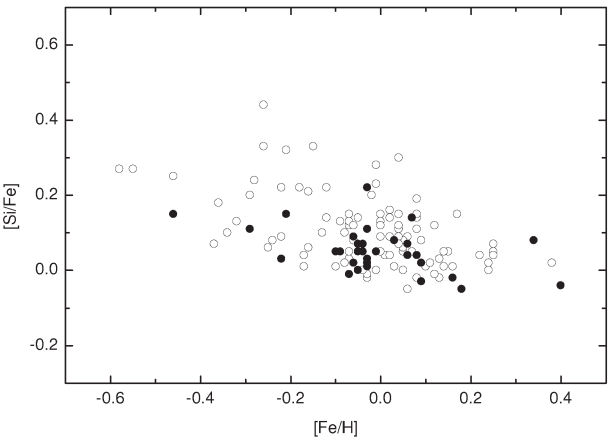


Figure 8: The trend of silicon with [Fe/H], the notation is the same as in Fig.1.

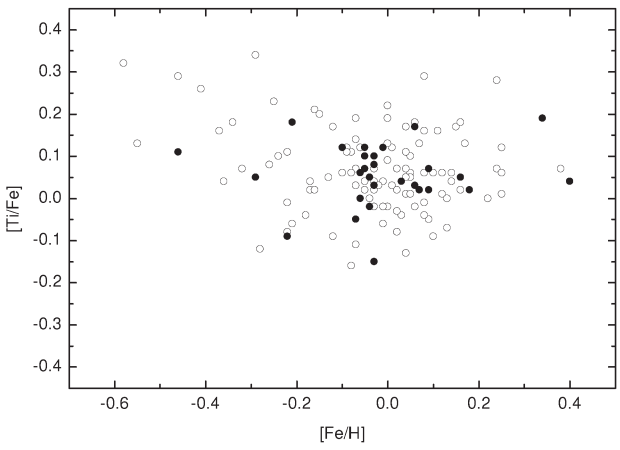


Figure 9: The trend of titan with [Fe/H], the notation is the same as in Fig.1.

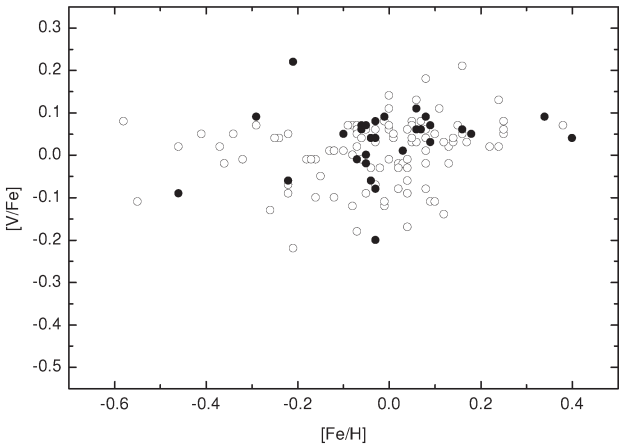


Figure 10: The trend of vanadium with [Fe/H], the notation is the same as in Fig.1.

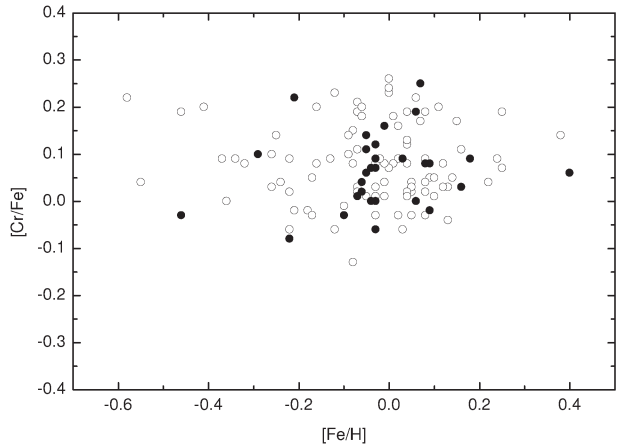


Figure 11: The trend of chromium with [Fe/H], the notation is the same as in Fig.1.

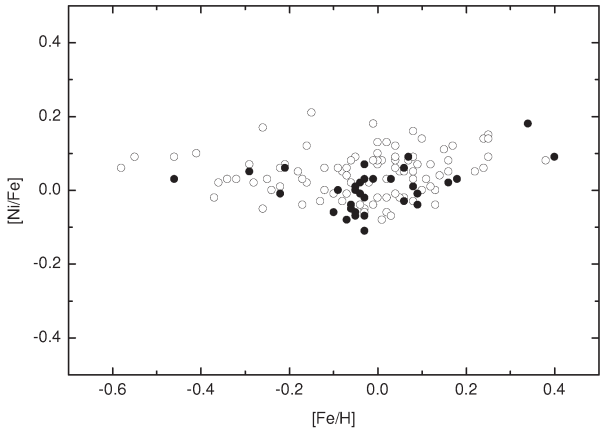


Figure 12: The trend of nikel with [Fe/H], the notation is the same as in Fig.1.

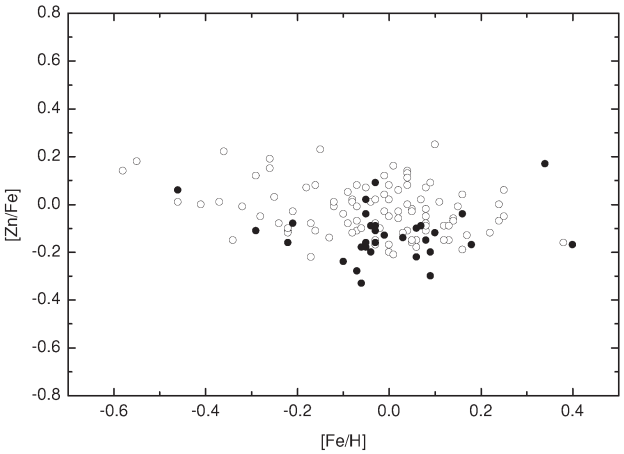


Figure 13: The trend of zinc with [Fe/H], the notation is the same as in Fig.1.

Table 1: The mean values of the elemetal abundance in MS stars [EL/Fe] and in variable stars $[El/Fe]_V$.

| Element | $< [El/Fe] >$ | $\sigma$ | N |
|---|---|---|---|
| $< [O/Fe] >$ | -0.01 | 0.18 | 71 |
| $< [O/Fe]_V >$ | -0.11 | 0.15 | 18 |
| $< [Na/Fe] >$ | 0.002 | 0.15 | 101 |
| $< [Na/Fe]_V >$ | -0.025 | 0.11 | 32 |
| $< [Al/Fe] >$ | 0.12 | 0.14 | 101 |
| $< [Al/Fe]_V >$ | 0.076 | 0.11 | 32 |
| $< [Si/Fe] >$ | 0.102 | 0.09 | 101 |
| $< [Si/Fe]_V >$ | 0.05 | 0.06 | 32 |
| $< [Ti/Fe] >$ | 0.07 | 0.10 | 101 |
| $< [Ti/Fe]_V >$ | 0.05 | 0.07 | 32 |
| $< [V/Fe] >$ | 0.01 | 0.08 | 99 |
| $< [V/Fe]_V >$ | 0.03 | 0.08 | 31 |
| $< [Cr/Fe]_V >$ | 0.06 | 0.08 | 31 |
| $< [Cr/Fe] >$ | 0.07 | 0.08 | 99 |
| $< [Ni/Fe] >$ | 0.04 | 0.06 | 101 |
| $< [Ni/Fe]_V >$ | 0.00 | 0.06 | 32 |
| $< [Zn/Fe] >$ | –0.025 | 0.10 | 99 |
| $< [Zn/Fe]_V >$ | –0.12 | 0.11 | 31 |

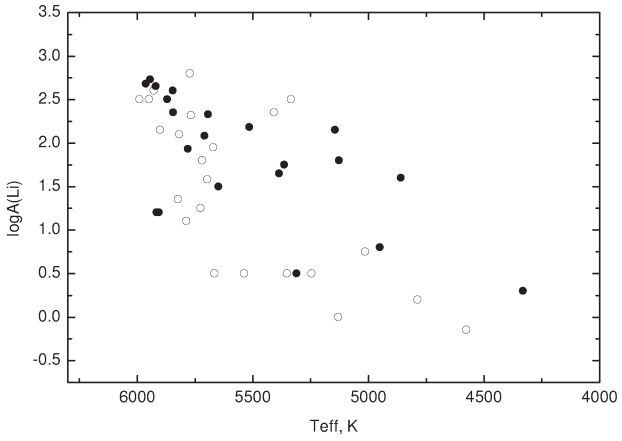


Figure 14: The dependence of Li abundance on $T_{eff}$, the notation is the same as in Fig.1.

and it is in consent with the galactic chemical evolution. The mean abundance values for MS dwarfs and spotted stars are differ within the limits of definition errors (Tabl.1).

And now we shall consider the lithium abundances in investigated stars. Tracing Li in different types of stellar and sub-stellar objects helps to study physical conditions and nuclear processes in their interia. Li is a very fragile element, destroyed at the temperatures hotter than 2.5 $10^6$ K, and this process begins already in the pre-main sequence stage. In most general case, the surface abundance of Li should in principle be a function of stellar mass, age, metallicity and to of somewhat poorly explored physical processes like rotation,convection, stellar wind, etc. Stars of BY Dra type belong to young stars, their age is about $10^8$ years by estimations of Chugainov (1990). In their spectra the lines of lithium which is the indicator of activity and age of stars are often observed. However these lines have different intensity, sometimes they are absent at all, and their intensity are not always correlates with other indicators of stellar activity. The obtained lithium abundances log A(Li) for investigated stars in functions of effective temperature $T_{eff}$ are presented in Fig.14 where MS stars are marked by black circles, and variable stars are marked by the open circles.

The mean value of Li abundance in the BY Dra type stars is equal to 1.82 ±0.81 and is higher than one (1.42 ±0.91) for MS dwarfs. Lithium is detected in 26 stars from 100 MS dwarfs and in 22 from 33 stars of BY Dra type that there correspond 26 % and 65 %, respectively. Our detailed spectroscopic research of the stars belonging to the low part of MS has shown that the lithium is detected more often in the BY Dra type stars and its average abundance in these stars is higher than in other MS stars.

## 7. Conclusion

For the first time the chemical composition of about 30 BY Dra type stars was found and the comparison of the lithium abundance in MS stars and of BY Dra type stars was made. There are obtained:

1. Trend of the elemental abundance corresponds to the received earlier results and it is in consent with the galactic chemical evolution.
2. The behaviour of the abundance of the majority elements in MS stars and spotted does not differ.
3. The Li abundance in variable stars is higher than in MS dwarfs and Li is detected in 65 % BY Dra stars and in 26 % of other ones.

## References

Alekseev I.Yu.: 2006, *Astrofizika*, **49**, 303.
Alekseev I.Yu., Gershberg R.E.: 1996, *Astrofizika*, **39** 67.
Alekseev I.Yu., Kozhevnikova A.V.: 2005, *Astrofizika*, **48**, 535.
Chugainov P.F.: 1966, *Inform. Bull. Var. Stars.*, 122.
Chugainov P.F.: 1990, Angular Momentum Evolution of Young Stars. Proceedings of the NATO Workshop,Sicily, Italy, Sept. 17-21, 1990. Editors, S. Catalano, J.R. Stauffer: 1991, P.175
Ecuvillon A., Israelian G., Santos N.C. et al.: 2006, *A&A*,**445**, 663.
ESA, 1997, The HIPPARCOS and TYCHO catalogues. Noordwijk, Netherlands: ESA Publications Division, 1997
Galazutdinov G.A.: 1992, Preprint SAO RAS, N 92
Gershberg R.E., Solar type activity of Main Sequence stars: 2002, Astroprint, Odessa.
Gilli G., Israelian G., Ecuvillon A. et al.: 2006, *A&A*,**449**, 723.
Gonzales G.: 1997, *MNRAS*, **285**, 403.
Flower P.J.: 1996, *ApJ*, **469**, 355.
Katz, D., Soubiran, C., Cayrel, R., Adda, M. & Cautain, R.: 1998, *A&A*, **338**, 151.
Kovtyukh V.V., Andrievsky S.M.: 1999, *A&A*, **351**, 597.
Kurucz R.L.: 1993, CD ROM n13
Mishenina T.V., Tsymbal V.V.: 1997, *Pis'ma v Astron. Zhurn.*, **23**, 693.
Santos N.C., Israelian G., Mayor M.: 2000, *A&A*,**363**, 228.
Tsymbal V.V.: 1996 *ASP Conf. Ser.*, **108**, 198.

# CHEMICAL COMPOSITION OF GALACTIC DISK STARS

T.V. Mishenina[1], N.Yu. Basak[1],T.I. Gorbaneva[1],C. Soubiran[2], V.V. Kovtyukh[1]

[1] Astronomical Observatory, Odessa National University
T.G.Shevchenko Park, Odessa 65014 Ukraine, *astro@paco.odessa.ua*
[2] Observatoire Aquitain des Sciences de l'Univers
CNRS UMR 5804, BP 89, 33270 Floirac, France

ABSTRACT. Abundances of Na, Al, Ca, in the stars of galactic disks are obtained. The separation of thin and stars on cinematic criterion was made early. The behavior of chemical element abundances with metallicity for studied stars was presented.

**Key words**: Stars: fundamental parameters; stars: abundances

## 1. Introduction

The trend of the elemental abundance [El/Fe] with metallicity [Fe/H] in the galactic disk is clue to understand the evolution of the disk and the Galaxy. The different trend (slope) of [El/Fe] vs. [Fe/H] in the thin and thick disks of the Galaxy evidences about different temps and origins of enrichment of the thin and thick disks, i.e. about different chemical and dynamical evolution of two galactic substructures.In this work we show the determination of Na, Al, and Ca abundances in 55 stars belonging to thin and thick disks. Two subsamples have been determined early on the basis of kinematics Mishenina et al. (2004).

## 2. Observations and parameters

The spectra of studied stars were obtained on 1.93 m telescope of the Observatoire Haute Provence (France) equiped with echelle-spectrograph ELODIE. A resolving power is 42000, the wavelength range is 3850-6800 ÅÅ. Spectrum extraction, wavelength calibration and radial velocity measurement have been performed at the telescope with the on-line data reduction software while straightening of the orders, removing of cosmic ray hits, bad pixels and telluric lines were performed as described in Kats et al. (1998). The continuum level drawing and equivalent width measurements were carried out by us using DECH20 code Galazutdinov, (1992). Equivalent widths of lines were measured by Gaussian function fitting.The

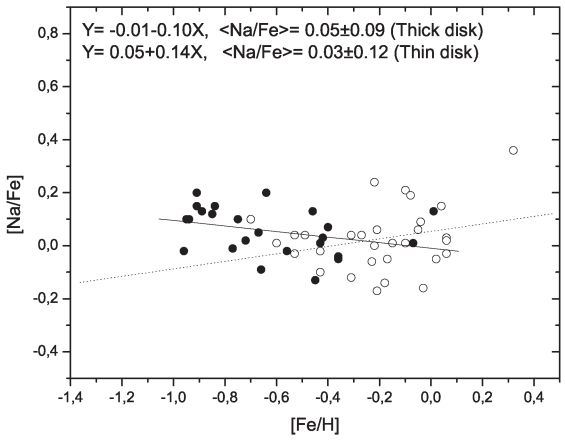


Figure 1: The run of [Na/Fe] with [Fe/H]. Thick disk stars are marked as filled circles, and thin disk stars as open circles.

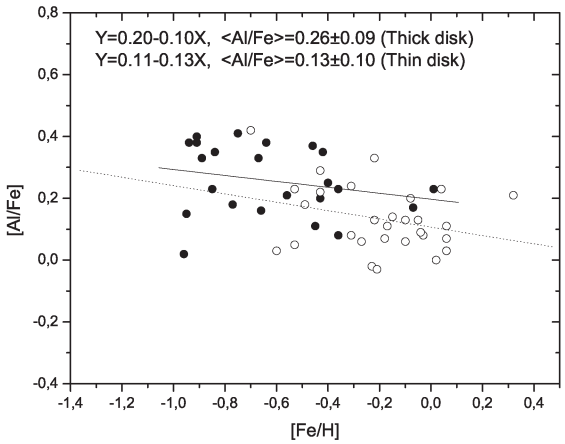


Figure 2: The run of [Al/Fe] with [Fe/H].The notation is the same as in Fig.1.

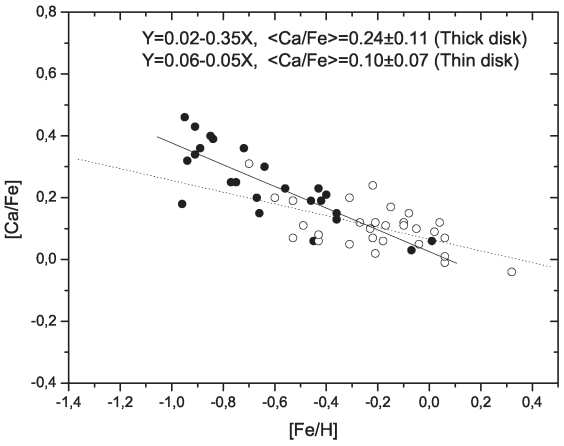


Figure 3: The run of [Ca/Fe] with [Fe/H].The notation is the same as in Fig.1.

temperatures were determined with the very high level of accuracy using the line depth ratios method. The surface gravity log g was determined using the iron ionization equilibrium assumption, where the average iron abundance determined from FeI lines and Fe II lines must be identical. Microturbulent velocities Vt were determined by forcing the abundances determined from individual FeI lines to be independent of equivalent width. The parameters are presented in Mishenina et al. (2004).

## 3. Elemental abundances

Using the derived stellar parameters and the atmosphere models of Kurucz (1993) we determined the elemental abundances Na, Al, and Ca from an LTE analysis of equivalent widths using the WIDTH9 code. Oscillator strengths for lines have been taken from Kovtyukh & Andrievsky (1999).

## 4. Results and conclusions

The dependences of [El/Fe] vs. [Fe/H] were presented on figures 1-3. Thick disk stars are marked as filled circles, and thin disk stars as open circles. Linear least-squares fits to both samples, the equations and mean values of Na, Al and Ca abundances are given in the same place. In thick disk stars the mean values of Al and Ca abundances are higher than those in thin disk stars. The thin and thick disk stars clearly show similar abundance trends for Al and Ca. The small inclination is observed for these elements. The inclination for Ca is typical for the $\alpha$l - elements and it is according with results on the magnesium obtained by Mishenina et al. (2004). For Na we observed the reverse inclination.

## References

Galazutdinov G.A.: 1992, *Preprint SAO RAS*, **92**.
Katz D., Soubiran C., Cayrel R. et al.: 1998, *A&A*, **338**, 151.
Kovtyukh V.V., Andrievsky S.M.: 1999, *A&A*, **351**, 597.
Kovtyukh V.V., Soubiran C. et. al: 2003, *A&A*, **411**, 559.
Kurucz R.L.: 1993, *CD ROM*, **13**.
Mishenina T.V., Soubiran C., Kovtyukh V.V.: 2004, *A&A*, **418**, 551.
Tsymbal V.V.: 1996, *ASP Conf. Ser.*, **108**, 198.

# ABUNDANCES OF N - CAPTURE ELEMENTS IN STARS OF THIN AND THICK DISKS.

T.V. Mishenina[1], T.I. Gorbaneva[1], N.Yu. Basak[1],C. Soubiran[2], V.V. Kovtyukh[1]

[1] Astronomical Observatory, Odessa National University
T.G.Shevchenko Park, Odessa 65014 Ukraine, *astro@paco.odessa.ua*
[2] Observatoire Aquitain des Sciences de l'Univers
CNRS UMR 5804, BP 89, 33270 Floirac, France

ABSTRACT. Abundances of neutron-capture (n-capture) elements in the stars belonging to thin and thick disks are obtained. The separation of thin and thick stars on kinematic criterion was made early. The spectra were obtained with the ELODIE spectrograph at the 1.93-m telescope of the Observatoire de Haute Provence (France). The determination of elemental abundances was carried out in LTE assumption by model atmosphere method, for Ba and Eu taken into account the hyperfine structure. The dependences of n-capture element abundances on metallicity for thin and thick disks are presented.

**Key words**: Stars: fundamental parameters; stars: abundances abundances:n-capture elements, r-, s-process

## 1. Introduction

The behavior of n-capture elemental abundances in the thin and thick is very important for the investigation of the galactic disks evolution. The different sources of r-, s- process brings the different contribution in enrichment of ISM by these elements. The change of the slope of [El/Fe] vs. [Fe/H] in the thin relatively TO thick disk may characterize the change of contribution (in %, for example) from different sources to the two substructures. In this paper we present the abundance determination of Y, Zr, Ba, La, Ce, Nd, Sm, and Eu and the analysis of abundance trends.

## 2. Observations and parameters.

The spectra of studied stars were obtained on 1.93 m telescope of the Observatoire Haute Provence (France) equiped with echelle-spectrograph ELODIE. A resolving power is 42000, the wavelength range is 3850-6800 ÅÅ. Spectrum extraction, wavelength calibration and radial velocity measurement have been performed at the telescope with the on-line data reduction software while straightening of the orders, removing of cosmic ray hits, bad pixels and telluric lines were performed as described in Kats et al. (1998). The continuum level drawing and equivalent width measurements were carried out by us using DECH20 code Galazutdinov (1992). Equivalent widths of lines were measured by Gaussian function fitting. The temperatures were determined with the very high level of accuracy using the line depth ratios. The surface gravity log g was determined using the iron ionization equilibrium assumption, where the average iron abundance determined from FeI lines and Fe II lines must be identical. Microturbulent velocities $V_t$were determined by forcing the abundances determined from individual FeI lines to be independent of equivalent width. The parameters determination and the separation of thin and thick stars on kinematic criterion was made early (Mishenina, 2004).

## 3. Elemental abundances

Using the derived stellar parameters and the atmosphere models of Kurucz (1993) we determined the elemental abundances of Y, Zr, La, Ce, Nd, and Sm from an LTE analysis of equivalent widths using the WIDTH9 code. Oscillator strengths for lines have been taken from Kovtyukh & Andrievsky (1999). Ba and Eu abundances are determined from the BaII resonance line 4555 Å, and from the EuII subordinate line 6645 Å, by line profile fitting of the stellar spectra calculated spectra by the STARSP code (Tsymbal, 1996). BaII and EuII ions considered here have the lines that show appreciable hyperfine structure (hfs). The atomic data for these lines were taken from Mashonkina & Gehren (2000). Recent NLTE calculation for BaII and EuII have been carried out by Mashonkina & Gehren (2000) and Mashonkina et al (1999). They have shown that for the line Ba

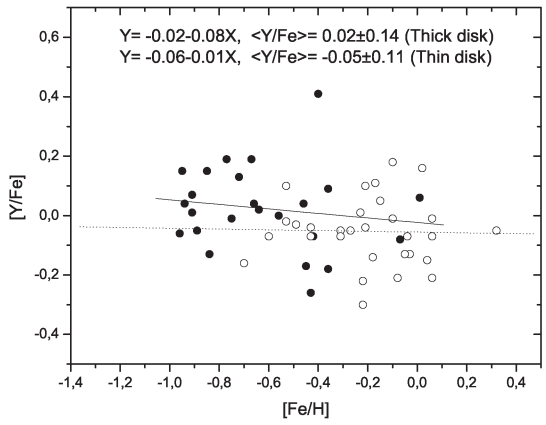


Figure 1: The run of [Y/Fe] with [Fe/H]. Thick disk stars are marked as filled circles, and thin disk stars as open circles.

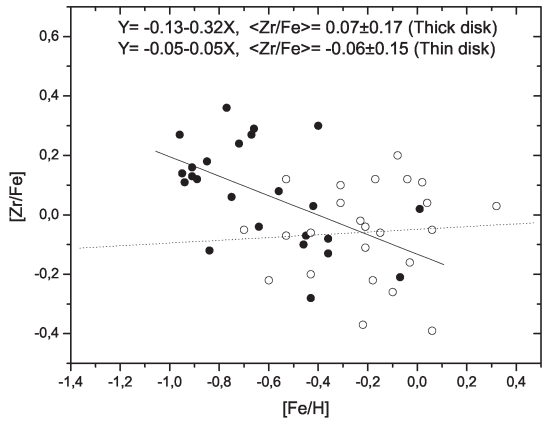


Figure 2: The run of [Zr/Fe] with [Fe/H].The notation is the same as in Fig.1.

II 4555 Å, which we used in our calculations, NLTE effects are small for [Fe/H] > -1.9. For Eu 6645 Å, the correction NLTE ranges from 0.04 dex to 0.06 dex. The dependences of n-capture elements abundances on metalliciti are presented in Fig. 1.

## 4. Results and conclusions

The dependences of [El/Fe] vs. [Fe/H] were presented on figures 1-8. Thick disk stars are marked as filled circles, and thin disk stars as open circles. Linear least-squares fits to both samples, the equations and mean values of Y, Zr, Ba, La, Ce, Nd, Sm and Eu abundances are given in the same place.

The abundance behavior of different elements for the two disks is different. The average Y, Zr, La, Nd, Sm

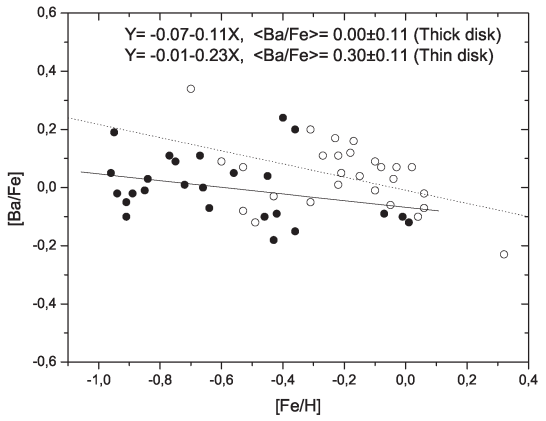


Figure 3: The run of [Ba/Fe] with [Fe/H].The notation is the same as in Fig.1.

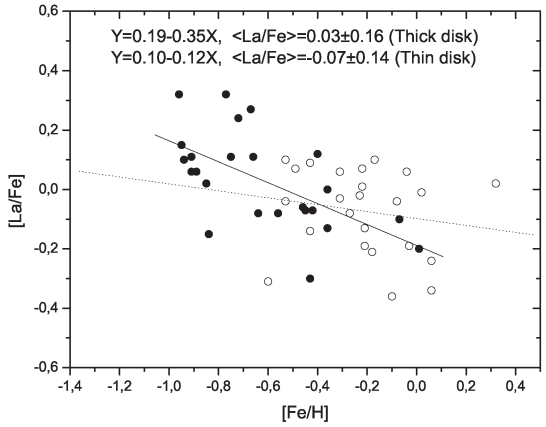


Figure 4: The run of [La/Fe] with [Fe/H]. Thick disk stars are marked as filled circles, and thin disk stars as open circles.

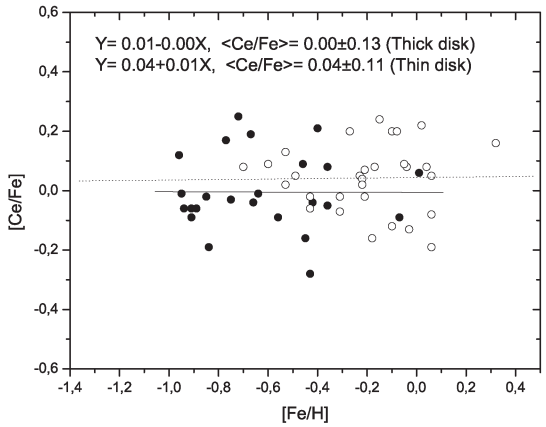


Figure 5: The run of [Ce/Fe] with [Fe/H].The notation is the same as in Fig.1.

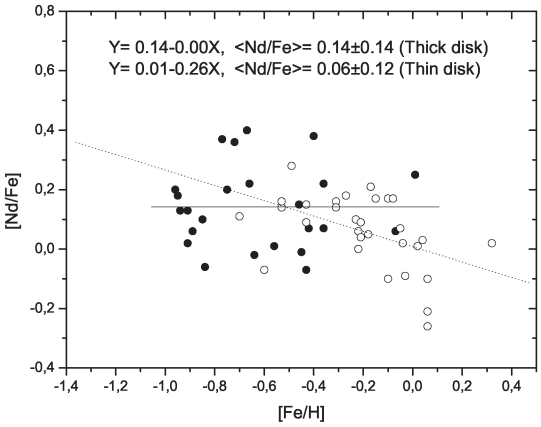


Figure 6: The run of [Nd/Fe] with [Fe/H].The notation is the same as in Fig.1.

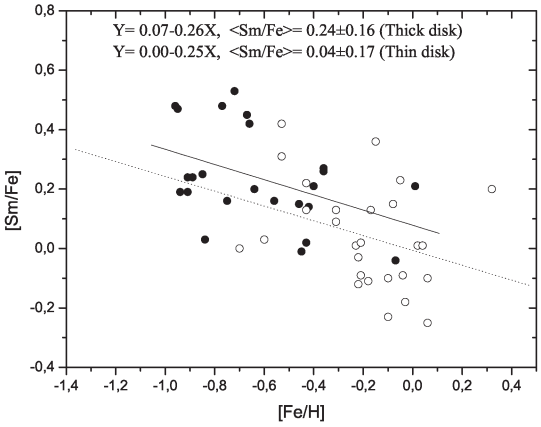


Figure 7: The run of [Sm/Fe] with [Fe/H].The notation is the same as in Fig.1.

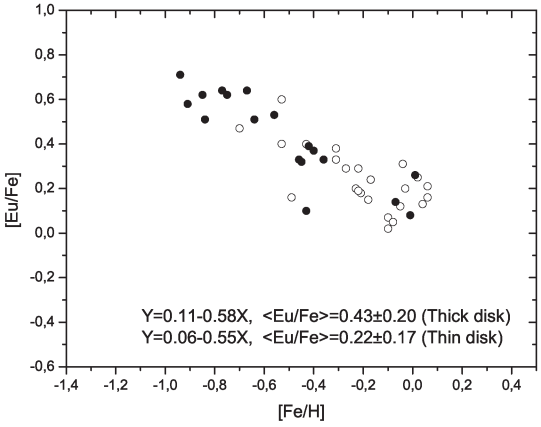


Figure 8: The run of [Eu/Fe] with [Fe/H].The notation is the same as in Fig.1.

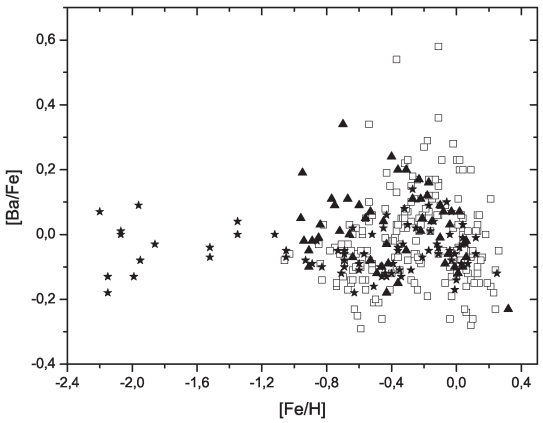


Figure 9: The run of [Ba/Fe] with [Fe/H].

and Eu abundances are higher in the thick disk stars than those of thin disk; the mean values of Ce abundance for two subsamples are similar within determination errors. The thin and thick disk stars clearly show similar abundance trends for Y, Ba, La, Ce, Sm, Eu. However, the Eu abundance shows remarkable declination, the La, Sm show some declination, the Nd shows one only for thin disk stars, and Zr shows one for thick disk stars. The Ce abundance do not show any declination. Break on metallicity close to -0,4 is observed for Ba, the increase of the Ba abundances for thin disk stars is observed.

We observe in our sample of stars the trend of [Ba/Fe] and [Eu/Fe] vs. [Fe/H] similar to the those for disk stars studied in the works Edvardsson (1993) and Mashonkina (2000) (see, Fig.9).

## References

Edvardsson B.J., Andersen B., Gustafsson et al.: 1993, *A&A*,**275**, 101.

Galazutdinov G.A.: 1992, *Prepr.SAORAS*, **92**, 28.

Katz D., Soubiran C., Cayrel R. et al.: 1998, *A&A*, **338**, 151.

Kovtyukh V.V., Andrievsky S.M.: 1999, *A&A*, **351**, 597.

Mashonkina L., Gehren T.: 2000, *A&A*, **364**, 249.

Mashonkina L., Gehren T., Bikmaev I.: 1999, *A&A*, **343**, 519.

Kurucz R.L.: 1993, *CD ROM*, **13**.

Mishenina T.V., Soubiran C., Kovtyukh V.V. et al.: 2004, *A&A*, **418**, 551.

Tsymbal, V.V., 1996, *ASP Conf. Ser.*, **108**, 198.

# THREE-DIMENSIONAL HYDRODYNAMICAL MODELING OF MASS TRANSFER IN THE CLOSE BINARY SYSTEM $\beta$ LYR WITH AN ACCRETOR WIND.III

V.V. Nazarenko, L.V. Glazunova

Department of Astronomy, Odessa National University
T.G.Shevchenko Park, Odessa 65014 Ukraine, *astro@paco.odessa.ua*

ABSTRACT. The present paper continues our work on numerical modelling of formation of the accretion disc in CBS $\beta$ Lyrae taking into account the stellar wind of the accretor. On having used methods of additional reduction of numerical viscosity, as well as different variants of the stellar wind and terms of its displacement out of the orbital plane while forming a disc, we defined the disc parameters close to the observational ones, and also jet like structures, where gas velocity equals to the velocity of the accretor's stellar wind.

**Key words**: Stars: binary: hydrodynamical modeling: individual: $\beta$ Lyr.

## 1. Introduction

$\beta$ Lyrae is a well investigated binary system at stage of rapid mass transfer with complex structure of gas envelope. Many parameters of this binary are received quite precisely and presented in the summarizing article of Harmanec et al. (1996): P=12.9d, Sp=B6-8II+B0-3V, $\dot{P}$ =19/year, $\dot{M} = 3 \times 10^{-5} M_\odot$/year, A $= 58 R_\odot$ $M_a = 12 M_\odot, R_a = 6 R_\odot, T = 30000 K$, $M_{don} = 2.9 M_\odot, T_{don} = 13000 K$, $vsini_{don} = 55 km/s$, where index $a$ means the accretor, and index $don$ is the donor.

But parameters of the donor were defined not so accurately as it is closed for observing with a thick accretion disc. The complex structure of gas envelope was specified on the results of observations for different waves length ranges. Modelling of light curve of this binary for the waves of length from 3000 to 10000 $\mathring{A}$, Linnell (2000) received parameters of optically and geometrically thick cylindrical accretion disc with $R_d = 30 R_\odot$, $h_d = 8 \div 12 R_\odot$, $T_d = 9000 K$, $M_d = 3.6 \times 10^{-6} \div 3.4 \times 10^{-4} M_\odot$, $vsini_d = 180 km/s$, where the index $d$ means a disk. To explain a Balmer jump in the observing energy distribution in the spectrum of this binary Linnell (2000, 2003) assumed that there was a dispersing envelope (corona) above the disc with particles concentration $N_e = 10^{11} cm^{-3}$ in height $h = 14 R_\odot$ and temperature 30000 K. As assumption of Harmanec et al (1996) the basic part of emission in lines $H_\alpha$ and HeI $\lambda 6678 \mathring{A}$ the given system is formed in the bipolar jet-like structures, moving perpendicularly to the orbital plane; moreover, it is possible that envelope absorption lines are also generated there. Gas velocity at such structures at the angle of orbit slope to the vision ray $83^o$ is about 700-1000 km/sec. shells absorption lines are formed in the same place too. The observation in a radio range have allowed to find out the extended environment surrounding this system and reaching to distance near 40 AU with temperature of 11000 K. The given environment is connected to a stellar wind of the donor that is estimated to be equal $\dot{M} = 6 \times 10^{-7} M_\odot$/year.

The main goal of our first work on three-dimensional hydro dynamical modelling of forming an accretion disc in CBS $\beta$ Lyrae with the regard for the accretor's stellar wind Nazarenko, Glazunova (2006) was to simulate an accretor's stellar wind with the velocity profile close to the model by Castor et al. (1975), to compute a disc model with different velocities of the stellar wind (700 and 1200 km/sec) and to determine the disc's parameters and possible jet like structures. In the mentioned paper the term of wind displacement by the stream was a linear decrease of the wind velocity to zero in the set field of computation at co-ordinate z $\pm 0.04$. The following results were received: while interacting the stream displace the wind out of the space fields, near to the orbital plane, where the disc with $R_d = 25 R\odot$ $h_d = 6 R_\odot$ $T_d = 15000 \div 20000$ K $N_e = 10^{12} \div 10^{14} cm^{-3}$ is formed; interaction of the stellar wind from the accretor's polar areas with the envelope above the disc results in generating jet like structures, where gas moves from the accretor with the velocities close to the accretor's stellar wind velocity. The densest part of the structure locates at co-ordinate y=-0.15 with the particles concentration $10^{12} \div 10^{14} cm^{-3}$ and

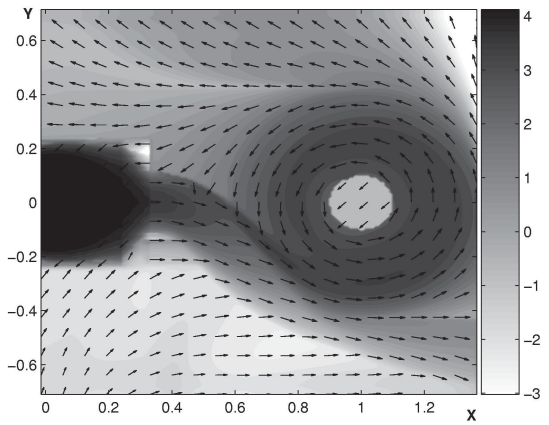


Fig.1a Isolines of equal density and current lines at the orbital plane (variant 1-1).

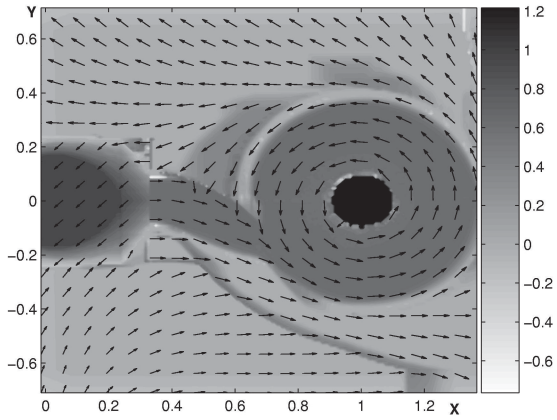


Fig.1b Isolines of equal temperature at the orbital plane (variant 1-1).

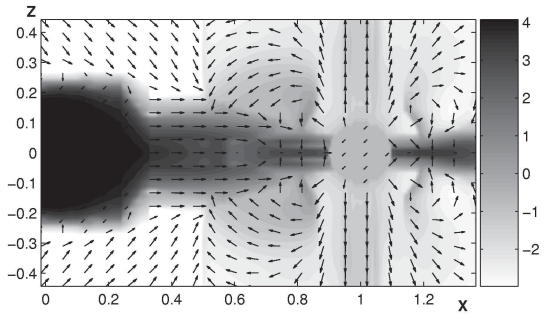


Fig.2a Isolines of equal density and velocity field at area z-x (variant 1-1).

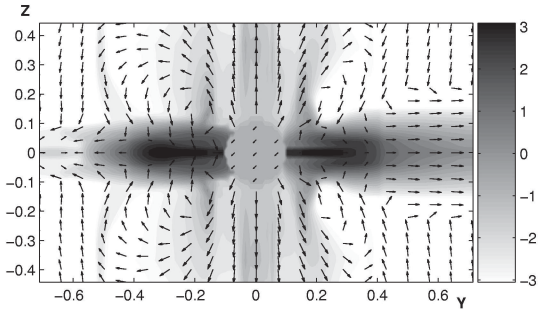


Fig.2b Isolines of equal density and velocity field at area z-y (variant 1-1).

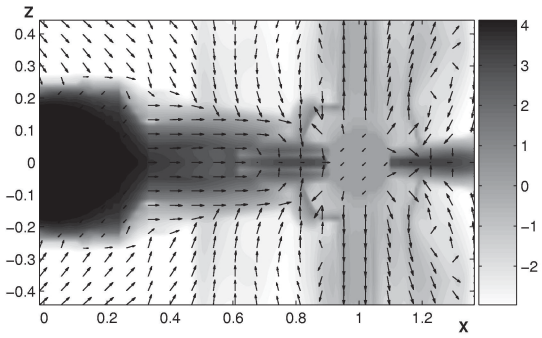


Fig.3a Isolines of equal density and velocity field at area z-x (variant 1-10).

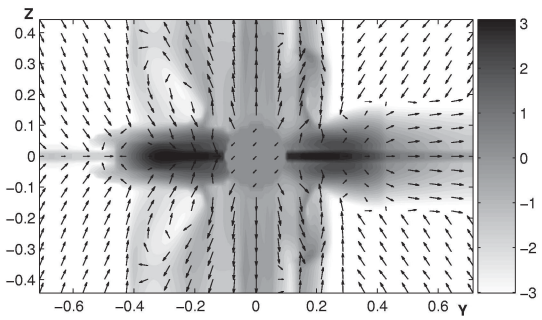


Fig.3b Isolines of equal density and velocity field at area z-y (variant 1-10).

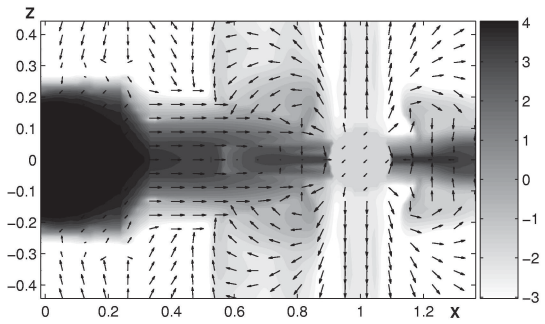


Fig.4a Isolines of equal density and velocity field at area z-x (variant 1-0.1).

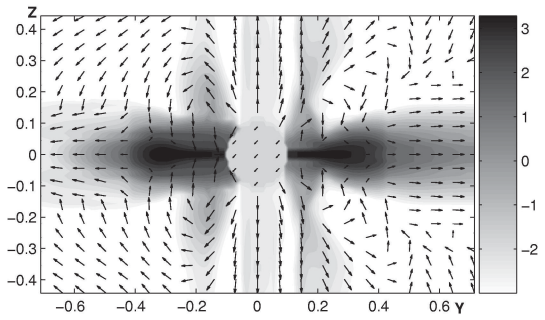


Fig.4b Isolines of equal density and velocity field at area z-y (variant 1-0.1).

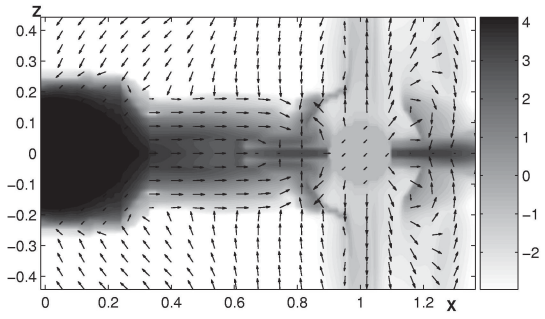


Fig.5a Isolines of equal density and velocity field at area z-x (variant 10-0.1)

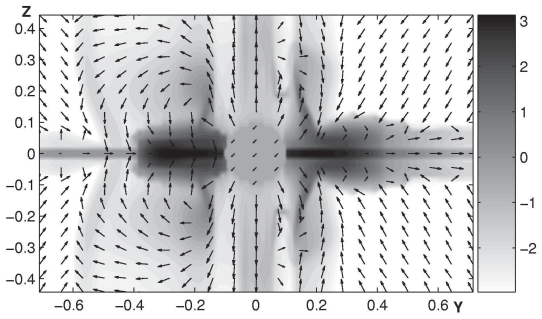


Fig.5b Isolines of equal density and velocity field at area z-x (variant 10-0.1)

temperature of $35000 \div 45000$ K; interaction of jet like structure and the disc evokes a strong shock wave, in which observation emission lines of the system can be generated; the mass transfer in the binary becomes non conservative - $50L_1$ ($\dot{M}_{L1}$) out of the system. Thus, in the present model we succeeded in getting the observing jet like structures with gas velocity about 700 km/sec; however, such disc parameters as $R_d$ and $h_d$ turned to be much less than the observing ones.

## 2. Features of three-dimensional hydrodynamical modelling of of mass transfer with an accretor wind.

Our approach to calculation of mass transfer in system $\beta$ Lyrae, both initial boundary conditions and model of binary system are similar to the first part of article (Nazarenko, Glazunova 2006 I). The parameters of binary system and a degree of the overflow by the donor of its Roche-lobe is the same to the article I. We also resolve the nonstationary Euler hydrodynamics equations using the same version of the large-particle method by Belotserkovskii and Davydov 1982 in the same variant, as in the first article.

The area of calculations in the given work is limited accretors Poche-lobe with the sizes of a numerical grid 160*160*70. In the present work to reduce numerical viscosity we apply the method of regularization of the velocity field, using the procedure of division on physical processes, admissible for the numerical method of large particles (Nazarenko 2007). The viscosity for our computations equals to 0.01 in units of a standard *alpha*-disc viscosity. The model of the accretor's radiating wind, used in this paper, was built as follows. To simulate the stellar wind from the accretor initially we build the accretor's atmosphere, which is to be steady for the whole computation period. Then we

Table 1:

| $\rho_w/\rho_{aw}$ Par gas str | 1-1 | 1-10 | 1-0.1 | 10-1 | 0.1-1 | 10-0.1 | Observ par |
|---|---|---|---|---|---|---|---|
| $R_d(R_\odot)$ | 30 | 23 | 26 | 23 | 25 | 15-17 | 30 |
| $H_d(R_\odot)$ | 6-8 | 4-6 | 3-5 | 4-6 | 4-6 | 3-4 | 8-12 |
| $\rho_{jet}1^{11}sm^{-3}$ | 0.1-1 | 1 | 0.01 | 0.1 | 0.01-0.1 | 0.01 | 1 |
| form | tor | cyli | tor | cylin | cylin | cylin | cylin |
| $h_{shell}1011sm^{-3}$ | 18 | 18 | 12 | 15 | 10 | 18 | 14 |
| $\rho_{shell}10^{11}sm{-}3$ | 0.1-1 | 0.1-1 | 0.1 | 1-10 | 0.1 | 1-10 | 1 |
| $v_{zsh}$ km/c (0.8,0.3) | 75 | -250 | -19 | -310 | 240 | 78 | 700 |

define its radiating pressure in approximation of optically thin layer ($P_r = \alpha\sigma T^4$/c ,where $\alpha$ is the Thompson scattering coefficient,$\sigma$ is the constant of Stephan-Boltsmann, and $c$ is the speed of light) and of optically thick layer ($P_r = 4\pi\sigma T^4$ /c ). On practice we select the smaller radiating pressure of two to make the calculations steadier for the whole computation period. To avoid unreal high accelerations for low densities we equate radiating acceleration to zero for the density less than $4 \times 10^8 cm^{-3}$.

Gas acceleration in the upper layer of the accretor's atmosphere is determined by the forces balance: gravitational force, Coriolis force, radiant pressure in continuous spectrum and in the lines of Layman series. Gas acceleration is given for the field between 1 and 2 star's radii. As a result we obtain the velocity profile close to the profile of the stellar wind model by Castor et al. (1975). To make the mechanism of wind displacement by the stream out of the orbital plane more correct and to select such parameters, which ensure the disc's form to be similar to its observational characteristics, when jet like structures are generating, we input two free parameters $\rho_w$: if the density in the set cell is higher than that signature, the wind velocity linearly falls to zero, and $\rho_{aw}$ is initial density of the stellar wind.

As it is shown in our previous calculations (Nazarenko, Glazunova 2006 II) to form jet like structures with observational velocity 700 km/sec, we must set the same signature of accretor's stellar wind velocity. That is why in the present paper the wind velocity at infinity is to be equal 700 km/sec, although such velocity is a bit low for the stellar wind of the dwarf of B0 spectral class, which might be the accretor.

### 3. Results of calculations.

The general results of computations are presented on Fig. 1-5 and Table 1. Main differences of those computations from the results of article I are the following: a round disc with low numerical viscosity, as well as correct calculation of the stellar wind displacement out of the orbital plane let us receive a cylindrical thicker disc. Such disc is more common to the disc, obtained by analysis of the light curves (Linnell 2000).

Fig. 1 shows density and temperature division in the orbital plane for the signatures of parameters $\rho_w$ and $\rho_{aw}$ 1-1. The radius of a disk is 25 $R_\odot$, density is of $10^{12} \div 10^{14} sm^{-3}$, temperature is 20000-40000 K. Density and temperature signatures for the disc remain the same for all variants of our computations, but radius and heights of the disc vary. Fig. 2-5 presents density division at areas z-x and z-y for different signatures of parameters $\rho_w$ and $\rho_{aw}$. Table 1 show signatures of the main parameters of the disc and different types of envelopes for all variants $\rho_w$ and $\rho_{aw}$. From all figures and table it is clear that signatures 1-1 and 0.1-1 are the closest to the observational parameters of the disc. For displacement density $10^{11} cm^{-3}$ and initial density of a star wind of $10^{10} sm^{-3}$ (the variant 1-1) the sizes and height of a disk are maximal and are close to observable, however, the disc form is close to torus and the envelope expands $18R_\odot$ high, that contradicts the observations. Among all variants with the disc form close to cylindrical variant 0.1-1 is the closest to the observational disc parameters.

### References


Harmanec P, Morand F., Bonneua D., Jiang Y., Yang S., Guinan E.F., Hall D.S., Mourrd D., Hadrava D., Bozie H., Sterken C., Tallon-Bose I., Walker G.AH., McCook G.P., Vakili F., Stee Ph., Le Contel J.M.: 1996,*Astron. and Astrophys.,* **312**, 877.

Linnell A.: 2000, *MNRAS,* **319**, 255.

Linnell A.: 2003, *MNRAS,* **332**, 21.

Nazarenko V.V., Glazunava L.V.: I 2006, *Astron. Rep.,* **50**, 380.

Castor J., Abbott D., Klein R.: 1975, *Astrophys. J.,* **195**, 157.

Belotserkoskii O.M., Davydov Yu.M.: 1982, *The big particles code in gas dynamics*, Moskaw, Scientist.

Nazarenko V.V., Glazunava L.V.: II 2006, *Astron. Rep.,* **50**, 369.

Nazarenko V.V.: 2007, *in print.*

# 3C 390.3 – JET OR DISK

L.S. Nazarova[1], N.G. Bochkarev[2] and C.M. Gaskell[3]

[1] Euro-Asian Astronomical Society, University Pr. 13, Moscow, 119899, Russia
[2] GAISH, Univemrsity Pr. 13, Moscow, 119899, Russia
[3] Departament Physics & Astronomy, Univessity of Nebraska, Lincoln, NE68588-0111

ABSTRACT. Analysis of the UV and optic spectra of the active galaxy 3C 390.3 shows that the observed line ratios for the broad components of lines: CIV/L$\alpha$, L$\alpha$/H$\beta$ and H$\alpha$/H$\beta$ can be accounted by two system of clouds. One corresponds to the region with an electron density $10^{8-10}$cm $^{-3}$, located above an accretion disk - probably in jets. This region emits the high ionization lines L$\alpha$ and CIV at the distance $\approx$ 40-60 days and low ionization lines H$\beta$ and H$\alpha$ at the distance $\approx$ 80 days. The other system corresponds to the zone which is probably part of an accretion disk and has a higher electron density $10^{12-13}$cm$^{-3}$.

## 1. Introduction

3C390.3 is the prototype of the class of AGN showing complex broad-line profiles with displaced distributions and/or an anisotropic illumination of the broad-line region (BLR). The double-peaked emission lines often used as a strong indication of the disk presence (Chen et al.1989;Eracleous and Halpern2003).The outflowing biconical gas stream (Veilleux et al. 1991; Zheng et al. 1991:Gaskell (1996) as a mechanism producing the double-peaked structure of emission line. More complex disk models such as : a localized hot spot in accretion disk (Zheng et al. 1991: two-armed spiral waves in accretion disk (Eracleous at al.1995) or disklike configuration of clouds (Sergeev et al. 2000) have been developed for expending the variable flux ratio of the profile wings. However the double-peaked profiles in optic differ from single-peaked profiles in some galaxies.

## 2. Analysis of Line Profiles

The UV and optical spectra of 3C390.3 were taken from the AGN Watch database for the period January 1995 – January 1996.. We took the UV and optic spetra at times of maximum and minimum luminosity during the taken period. The profiles of the CIV, L$\alpha$, H$\beta$ and H$\alpha$ lines have been divided into seven parts, the width of each part being equal to 2000 km s$^{-1}$. The core of the lines is measured between -1000 and +1000 km s$^{-1}$. The blue in the low-ionization lines Ha and Hb is stronger than in the high ionization lines CIV and La at the maximum of nuclear activity. However the blue peak in the high ionization lines is more prominent at maximum of nuclear activity. The C IV/Ly$\alpha$ ratio is low in the low-velocity regions of the line profile, but becomes higher in the blue wing, particularly when 3C 390.3 is more active. The asymmetry in the line ratios between the blue and red wings could be real, since the blue peak was stronger at this time, but it could also be an artifact of the extreme difficulty in removing NV $\lambda$1240 emission from the wing of Ly$\alpha$ in an object with line profiles as complex as 3C 390.3. The observed Ly$\alpha$/H$\beta$ ratio is high at low velocity and decreases in the wings for both high and low states of the nuclear activity. This velocity dependence is the opposite of what is seen for most AGNs (see Snedden & Gaskell 2004), where Ly$\alpha$ is usually broader than the Balmer lines.

## 3. Photoionization Models

The modeling of the observed line ratios CIV/L$\alpha$, L$\alpha$/H$\beta$ and H$\alpha$/H$\beta$ has been done with the photoionization code CLOUDY, in its plan parallel version, and assuming solar abundances. The computed line ratios of CIV/La, La/Hb and Ha/Hb for a given luminosities (at maximum and minimum states) were calculated for different distances from the center- (20, 40, 60 and 80) days.

The comparison of the observed and the computed line ratios show that the ratios varies along the line profiles. The ratio CIV/L$\alpha$ varies in range (0.2-1.8). According to the UV study, the lag of CIV and L$\alpha$ are equal to 37$\pm$14 days and 60$\pm$24 days respectively (O'Brien 1998). Therefore the theoretical line ratio at the distance from the center may corresponds $10^7$cm$^{-3}$ in the center to $10^{10}$cm$^{-3}$ in the wings or $10^{12}$ cm$^{-3}$ in the center of line ratio to the $10^{10}$cm$-3$ in the wings. However the electron density in the wings usually higher than in the center because the center of lines get the contribution from low density narrow line regions. The observed line ratio L$\alpha$ corresponds to the electron density $10^{10}$cm$^{-3}$ in

the center of line and $10^{13}$ cm$^{-3}$ in the wings for the distance from the center 60-80 days. Similar electron density corresponds to the observed line ratio H$\alpha$/H$\beta$ for the distance from the center 60-80 days.

## 4. Discussion

The study of the optical spectra of 3C390.3 for period 1992-2000 (Sergeev et al. 2002) found the lag between continuum and H$\beta$ emission line variation to be 89±11 days. The difference with time lag obtained by Deitrich et al. (1998) and equals 20±8 days is probably due to sampling effects. Sapovalova et al.(2001) give a double value: 100 and 35 days. Arshakian et al. (2006) found that there is the observational evidance for the link between variability of the radio emission of the relativistic jet and optical continium emission in 3C390.3. It indicates that the source of varibility non-thermal continium radiation is located in the innermost part of the relativistic jet. This emission from jet forming the conocal region whith broad emission lines. Therefore it seems resonable to suggest that there are two broad regions: one is localized at the disk and another is forming by the jet with the electron density $10^{8-10}$ cm $^{-3}$ and localized at the distance from the center about 60-80 days.

*Acknowledgements.* LN and NB acknowledge support under RFBR (grant 06-02-16843).

### References

Arshakian T.G. et al.: 2007, astro-ph 0602016.
Chen K. et al.: 1989,*ApJ*, **39**, 742.
Deitrich M. et al.:, 1998, *ApJS*, **115**, 185D.
Eracleous M. et al.: 1994, *ApJS*, **90**, 1.
Eracleous M. et al.: 2003, *ApJ*, **582**, 633.
Gaskell C.M.: 1996, *ApJ*, L107.
O'Brien P. et al.: 1998, *ApJ*, **509**, 1630.
Sergeev S. et al.: *ApJ*, **576**, 660.
Shapovalova A. et al.: 2001, *A&A*, **376**, 775.
Snedden S.A., Gaskell C.M.: 2004, astro-ph/0402508.
Zheng et al.: 1991, *ApJ*, **381**, 411.

# OPTICAL VARIABILITY OF NGC 4151 DURING 100 YEARS

V.L. Oknyanskij[1], V.M. Lyuty[2]

[1] Sternberg Astronomical Institute,
Universitetskij Prospect 13, 119992 Moscow, Russia *oknyan@sai.msu.ru*
[2] Sternberg Astronomical Institute, 98409, Naychny, Crimea, Ukraine

ABSTRACT. We present historical light curve of NGC 4151 (Fig.1.) for 1906-2007. The light curve include mostly our published photoelectric (taken during the years 1968-2007 $\sim$ 1040 mean per night measurements) and photographic (mostly Odessa's and Moscow's plates taken during the years 1906-1982, $\sim$ 352 measurements) points. Additionally we include all published by other authors data obtained before 1968 (de Vaucouleurs and de Vaucouleurs, 1968; Sandage, 1966; Wisniewski and Kleinmann 1967; Fitch et al.1967; Barness 1967) (19 measurements taken during the years 1958-1967) as well as photographic data of Pacholczyc et al.(1983) (Harward's and Steward's patrol plates taken during the years 1910-1968, $\sim$ 209 measurements). Look the references about the used data at Luytyi and Oknyanskii (1987) and see also Lyuty (2005,2006). All this data are reduced to the one photometrical system. Applying Fourier (CLEAN algorithm) we have found periodic component 15.4 years in the 100 years light curve. 30 years ago about the same "period" was firstly reviled from Odessa's photometrical data (Oknyanskij, 1977, 1978). There is strong correlation between spectral type and brightness. 14-16 years circles seen in the light curve probably correspond to some accretion dynamic time.

**Key words**: AGNs: individual: NGC 4151

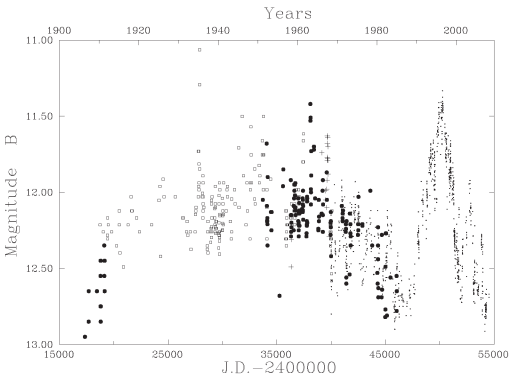


Figure 1: Observed light curve of the nucleus of NGC 4151 over 1906-2007. Points – Lyuty's photoelectric data, + – photoelectric measurements before 1968, circles – Oknyasnkij's photographic data, boxes – Pacholczyk's et al. photographic data

*Acknowledgements.* We are thank Dr. O.E. Madel for help in photographic data measuremts.

## References

Barnes T.G.: 1968, *Ap. Let.*, **1**, 171.
de Vaucouleurs G., de Vauculeurs A.G.: 1968, *Publications University of Texas, Series II, Austin*, **N 7**, 1.
Fitch W.S., Pacholczyk A.G., Waymann R.J.: 1967, *Ap.J.*, **150**, L67.
Lyutyi V.M., Oknyanskij V.L.: 1987, *Sov. Astron.*, **31**, 249.
Lyuty V.M.: 2005, *Astron. Lett.*, **31**, 645.
Lyuty V.M.: 2006, *ASP Conf. Ser.*, **360**, 3.
Oknyanskij V.L.: 1977, *Astron. Tsirkulyar*, **N944**, 2.
Oknyanskij V.L.: 1978, *Peremenye Zvezdy*, **21**, 71.
Sandage A.: 1967, *ApJ.*, **150**, L177.
Pacholczyk A.G., Penning W.R., Ferguson D.H., Lubart N.D., Turnshek D.: 1983, *Ap. Let.*, **23**, 225.
Wisniewski W.Z., Kleinmann D.E.: 1968, *AJ*, **73**, 866.

# INFLUENCE OF SPIRAL PATTERNS ON DYNAMICAL EVOLUTION OF GALACTIC DISC

M.V. Paliienko
Department of Astronomy, Odessa National University
T.G.Shevchenko Park, Odessa 65014 Ukraine, *astro@paco.odessa.ua*

ABSTRACT. This paper reports on the theoretical investigation of evolution of the Galactic disc, taking in account the influence of spiral patterns. The spiral patterns can be considered as some kind of indicators of the dynamical processes in the disc. We investigate influence of spiral patterns on the surface density of gas, stars and metallicity in time at the solar neighbourhood. We consider the models in the approximation of instantaneous recycling of material. Results of models are compared with observational data, that give possibility to predict correct model for evolution of the Galactic disc. The results of the model predictions differ significantly comparing to the case of the standard Galactic evolutionary model.

**Key words**: Galaxy:dynamics:spiral pattern.

## 1. Introduction

At present the very important problem is an investigation of the gas, stars distributions and metallicity in the Galactic disc with an account of the spiral arms. These arms can be considered as some kind of indicators of the dynamical processes in the disc. The dynamics of stars affected by perturbations from both spiral structure and the Milky Way bar (*Quillen*, 2002). The main criteria of the model reliability is a comparison with some observational data (*Boulares*, 1989; *Gilmoreet.al.*, 1990 and others). It is known that spiral arm affect significant the star formation processes. The star formation rate is proportional to parameter $k$, it is adopted 1 and 1.4 at the solar neighbourhood (see, for example, *Kennicut*, 1998). As a rule, for the angular velocity of the arm rotation is adopted to be 20 km $s^{-1}$ $kpc^{-1}$ (sometimes the value 27 km $s^{-1}$ $kpc^{-1}$ is used, or 21 km $s^{-1}$ $kpc^{-1}$ is used (see *Vorobyov*, 2006)), while corotation radius is 9 *kpc*. There are also two specific regions of the *Lindblad* resonances in the disc at 2.8 and 12.8 *kpc* (*Andrievskyetal.*2004; *Amaral&Lepine*, 1997).

## 2. Spiral patterns

Spiral patterns – are prominent feature of spiral galaxies, to which our Galaxy is belonged also.

Occurrence of a wave can be connected either with external indignation or with instability of the disc. Besides waves can be generated by a bar, and also emissions of weights of gas from the central area of the Galaxy.

In difference from stars, braking of gas on the internal party of a pattern occurs not gradually, and jump. Gas of a disk runs to more dense gas in the pattern, stops almost and compressed. If speed of the gas concerning the pattern was more, than full speed of a sound in the gas and amplitude of the spiral wave of density is not too small, there is a shock wave.

The amplitude of the shock wave depends from speed from which gas catches up with the spiral pattern. With removal from the center angular speed of rotation of the Galaxy falls, and for spiral patterns it remains constant. Therefore with removal from the center of the Galaxy relative speed of the gas and a pattern decrease, the amplitude of the wave decreases, on some distance it ceases to be shock. When speed of rotation becomes nearer to speed of the pattern, the pattern comes to an end also.

Compression of the gas in the shock wave and its transition in more dense phase promotes formation of stars. In spiral galaxies the formation of stars occurs not in all galactic plane where interstellar gas is concentrated, and mainly there, where the amplitude of a shock wave in it is great enough.

## 3. Main assumptions and basic equations

In order to determine the evolutionary model parameters of the Galactic disk (or its selected part) let us consider one element of the disc surface (1 $pc^2$). For this element we can define the surface gas density, surface stars density and the gas metallicity normalized to the yield of primary elements in the approximation of instantaneous recycling of material. Then the system of equations that describe the evolution of this selected area is the following (all the parameters are adopted for the solar neighbourhood):

$\mu_s$, $M_\odot$ $pc^{-2}$ – is the surface density of stars;

Table 1: Various parameters of the models and computed predictions, $t = 15\ Gyr$, $C = 0.15$

| $\tau$ | $k_1$ | $\varepsilon$ | $\mu_g$ | $\mu_s$ | $\frac{z}{y}$ | $k_2$ | $\mu_g$ | $\mu_s$ | $\frac{z}{y}$ |
|---|---|---|---|---|---|---|---|---|---|
| 5.5 | 1 | 0.1 | 14.1 | 68.2 | 1.42 | 1.4 | 4.4 | 77.9 | 1.4 |
| 3.5 | 1 | 0.2 | 6.9 | 75.4 | 2.02 | 1.4 | 2.1 | 80.2 | 1.7 |
| 6.5 | 1 | 0.2 | 11.6 | 70.7 | 1.43 | 1.4 | 4.2 | 78.03 | 1.27 |

$\mu_g$, $M_\odot\ pc^{-2}$ – is the surface density of gas;
$\frac{z}{y}$ – is the gas metallicity normalized to the yield of the primary elements;
$\Psi$, $M_\odot pc^{-2} Gyr^{-1}$ – is the star formation rate;
$f(t)$, $M_\odot\ pc^{-2}\ Gyr^{-1}$ – is the infall rate;
$\alpha$ – is an inverse characteristic distance for the infall rate in the disc,
$\frac{1}{\alpha} = 4300\ pc$ ;
$\tau$, $Gyr$ – is the characteristic time of infall;
$M_p$ – is the present-day mass of the galactic disc,
$6 \cdot 10^{10} M_\odot$; $M_\odot$ – is the mass of Sun;
$(1 - R)\, C$ – is the part of the matter that is created after the $SNe$ explosions, $C$ – const, $(1 - R)\, C = 0.15$;
$t_p$ – is the age of the Galaxy, $t_p = 15\ Gyr$;
$R_G$ – is the galactocentric radius;
$R_\odot = 7.9\ kpc$ – is the radius of Sun, which is adopted.

Let us write the following differential equations for the gas, stars surface densities and metallicity (the system of differential equations was decided by numerical method of $Runge - Kutta\ of\ fourth\ order$).

$$\frac{d\mu_s}{dt} = (1 - R)\,\Psi$$

$$\frac{d\mu_g}{dt} = -(1 - R)\,\Psi + f(t)$$

$$\mu_g \frac{d\frac{z}{y}}{dt} = (1 - R)\,\Psi - f(t)\,\frac{z}{y}$$

As it was showed by *Andrievsky et al.* (2004) some characteristics can be written as follows:

$$\Psi = C\mu_g^k$$

$$f(t) = \frac{\alpha^2 M_p \exp\left(-\alpha R_G - \frac{t}{\tau}\right)}{2\pi\tau\left(1 - \exp\left(-\frac{t_p}{\tau}\right)\right)} \qquad (2)$$

Rather like test was considered in R.Thon, H.Meusinger, 1998.

If we consider the spiral arms, then the function of the star formation rate can be modified:

$$\Psi = C\mu_g^k\,(1 + \Delta)$$

$$\Delta = \varepsilon\theta \frac{\mid \Omega_D - \Omega_P \mid}{C_s} R_G$$

Table 2: Observational data

| | Authors | data |
|---|---|---|
| $\mu_g$ | $Gordon, Burton, 1976$ | 6.5 |
| $\mu_g$ | $Haywood, Robin, 1997$ | 10 |
| $\mu_g$ | $Dickey, 1993$ | 7.5 |
| $\mu_g$ | $Kuijken, Gilmore, 1991$ | 12.7 |
| $\mu_g$ | $Boulares, 1989$ | 14 |
| $\mu_s$ | $Gilmore, 1990$ | $35 \pm 5$ |
| $\mu_s$ | $Andrievsky, 2004$ | 54.8 |
| $\frac{z}{y}$ | $Andrievsky$et.al., 2002$b$ | 1.122 |

$\varepsilon$ – is the factor which define an efficiency of the star formation;
$\theta$ – is the cut-off factor, it is required, because the self-sustained Galactic density waves are known to exist only in so-called wave zone between inner *Lindblad* resonance, and outer *Lindblad* resonance. $\theta = 0$ for $R_G < 3\ kpc$, $\theta = 1$ for $3 < R_G < 13\ kpc$, $\theta = 0$ for $R_G > 13\ kpc$;
$\Omega_D$ – angular speed of rotation of disc of the Galaxy, $\Omega_D = \Omega_D(R_G)$, hence (see *Andrievskyet.al.*, 2004):

$$\Omega_D = -0.069\left(\frac{R}{1000}\right)^3 + 0.447\left(\frac{R}{1000}\right)^2 + 5.601\left(\frac{R}{1000}\right) + 181.844 kms^{-1}$$

$\Omega_P$ – angular speed of the rotation of the spiral pattern, which determines the range of the spiral modes and fixes the location of resonances. Determinations of $\Omega_P$ from observations using different methods have given values of $\Omega_P$ around $20 - 30\ km\ s^{-1}\ kpc^{-1}$. We adopt $\Omega_P = 20\ km\ s^{-1}\ kpc^{-1}$ (recall that the spiral pattern rotates as a solid body, i.e. $\Omega_P = const$, whereas the Galactic disk rotates differentially).
$C_s$ – is the speed of the sound in the interstellar environment, $C_s = 20\ km\ s^{-1}$.

Below we give the set of parameters of our models and computed results of models taking into account the spiral arms (Table 1), and more over then we give the comparative table with observational data (Table 2) (*Dickey*, 1993; *Kuijken&Gilmore*, 1991; *Boulares*, 1989; *Gordon&Burton*, 1976 and so forth).

### 3. Conclusions

It is showed that:

1. the given research comprises construction of the theoretical models describing dynamic evolution of a disk of the Galaxy with different variations of parameters, which are included into the system of differential equations;

2. models consider influence of spiral patterns on surface density of stars, gas and the gas metallicity normalized to the yield of primary elements;

3. comparison of results of numerical modelling with results of observational data shows, that the certain models give good agreement with observational data.

### References

Amaral L.H., Lepine J.R.D.: 1997, *R. Astron. Soc.*, **286**, 885-894.

Andrievsky S.M., Luck R.E., Maciel W., Lepine J.R.D., Beletsky Yu.: 2002, *Astron. Astrophys.*, **384**, 140.

Andrievsky S.M., Luck R.E., Martin P., Lepine J.R.D.: 2004, *Astron. Astrophys*, **413**, 159.

Boulares A.: 1989, *Astron. Astrophys.*, **209**, 21.

Dickey J.M.: 1993, in ASP Conf. Ser., *The Minnesota lectures on clusters of galaxies and large-scale structure*, Ed. Humphreys R.M., San Francisco, p. 93.

Gilmore G., Wyse R., Kuijken K.: 1990, *in Population, Age and Dynamics of the Galaxy*, 172.

Gordon M., Burton W.B.: 1976, *Astrophys. J.*, **208**, 346.

Haywood M., Robin A.C., Greze M.: 1997, *Astron. Astrophys.*, **320**, 440.

Kennicutt R.C.: 1989, *Astrophys. J.*, **344**, 658.

Kuijken & Gilmore: 1991, Mon. Not. *R. Astron. Soc.*, **250**, 320-356.

Quillen A.C.: 2002, *astro-ph/0204040.*

Thon R., Meusinger H.: 1998, *Astron. Astrophys.*, **338**, 413-434.

Vorobyov E.I.: 2002, *astro-ph/0606013.*

# OBSERVATIONS OF CATACLYSMIC VARIABLES AT KOLONICA OBSERVATORY

Š. Parimucha[1], P. Dubovský[2], I. Kudzej[2]

[1] Institute of Physics, Faculty of Natural Sciences, Šafárik University, 04001 Košice, Slovakia *stefan.parimucha@upjs.sk*

[2] Vihorlat Observatory, 06601 Humenné , Slovakia *vihorlatobs1@stonline.sk*

ABSTRACT. We present a small sample of our observations of cataclysmic variable stars obtained at Kolonica Observatory, The presented data for CI UMa, MR UMa and SW UM were obtained in 2006 and 2007. Our observations demonstrate that also the small telescopes with low cost CCD camera could be used for a serious and useful observations.

**Key words**: Stars: binary: cataclysmic; stars: individual: CI UMa, MR UMa, SW UMa.

## 1. Introduction

Observation of cataclysmic variable stars is a part of observing program of Kolonica Observatory, which is a part of the Vihorlat Observatory in Humenné. It is located on the east-north part of Slovakia near borders with Ukraine. The largest telescope at observatory is an 1m Vihorlat National Telescope equipped with 2 channel photoelectric photometer. Another smaller telescopes are used mainly for CCD photometric observations of cataclysmic variable stars and for minima times determinations of the selected eclipsing binaries. All our observations could be found at the web page of observatory: `http://www.astrokolonica.sk/` and data could be obtained from authors by request.

## 2. Used instruments

Our observations of cataclysmic binaries are obtained by two telescopes. The first one, called HUGO, is a Newton type telescope with 265mm diameter of the primary mirror and focus length 1360mm. The second one, called PÚPAVA is also a Newton type 280/1500mm telescope. The both instruments are placed on German equatorial mounts in the areal of the Kolonica Observatory.

The observations were performed by MEADE DSI Pro CCD camera with Sony's ExView HAD Monochrome CCD Image Sensor. The resolution of this camera is 508 x 489 pixels. The observations were obtained with no filters and were not transformed into the international system.

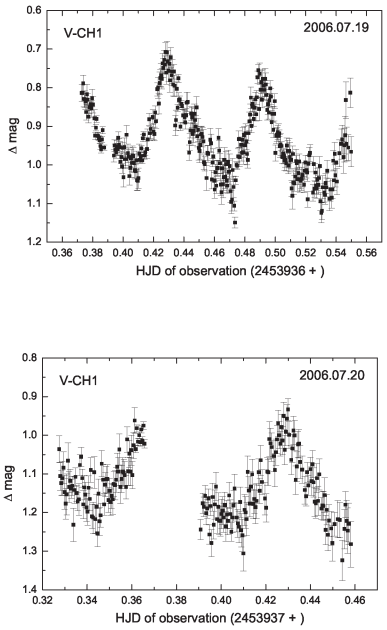


Figure 1: Light curves of CI UMa.

The photometric reduction (dark and bias substraction, flat-field correction) of the obtained CCD images, as well as photometric measurements were performed by C-Munipack package (`http://integral.physics.muni.cz/cmunipack/`) and SPHOTOM package developed by the first author.

## 3. Observed objects

### *3.1. CI UMa*

CI UMa was observed in 3 nights from July 19 to 22, 2006 with HUGO telescope just after alert from

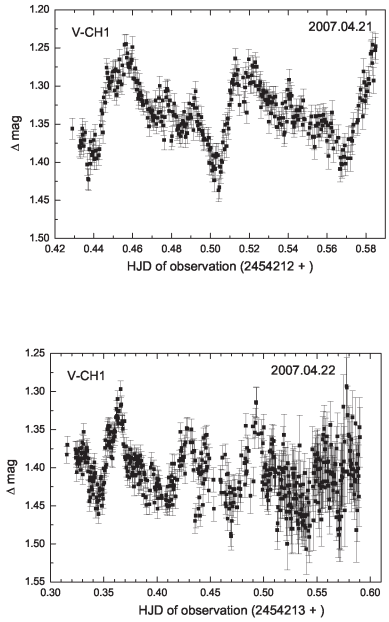


Figure 2: Light curves of MR UMa.

the visual observers. 30s exposure time was used for all observations. Superhumps were detected in two nights, as depicted in Figure 1. Observations from the last night were strongly influenced by clouds and was not usable for another analysis. Analysis of the obtained data was published by Parimucha & Dubovsky (2006).

### *3.2. MR UMa*

MR UMa was observed in 2 nights, April 21 and 22, 2007. HUGO telescope was used for these observations and 30s exposure time was used. Light curves created from our data are shown in Fig. 2. During the first night, nice superhumps with complex structure were detected. The amplitude of light changes was about ∼0.2 mag. The end of the second night was messed by the bad weather conditions.

### *3.3. SW UMa*

Well known cataclysmic variable SW UMa was observed in 3 nights from September 22 to 25, 2006 with HUGO telescope. 30s exposure time was used as well. Light curves from all three nights are shown in Fig. 3. During all nights, superhumps were detected with amplitude about 0.15 mag.

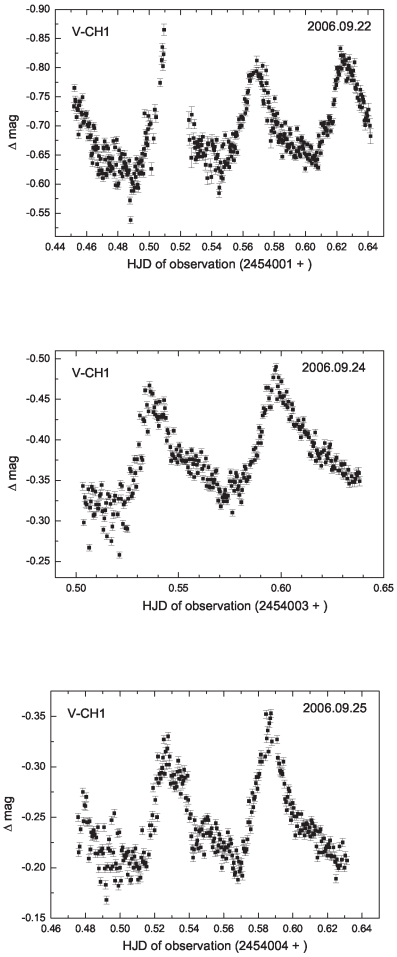


Figure 3: Light curves of SW UMa

## 3. Conclusion

Photometric observations of cataclysmic variables (e.g superhumps detection) are very important for the models of these objects. Our observations can demonstrate that small telescopes with low cost CCD cameras at small observatories could be also used for a serious and useful observations. The greatest advantage of such a instruments could be systematic observations of selected objects.

*Acknowledgements.* This work was supported by VEGA grant No. 7011, internal grant of Šafárik University No. 9/07-08, APVV grant LPP-0049-06 and APVV bilateral grant SK-UK-01006.

## References

Parimucha S., Dubovský P.: 2006, *Open European Journal on Variable Stars,* **50**, 1.

# KOROAPS – SYSTEM FOR A LARGE SCALE MONITORING AND VARIABLE STARS SEARCHING

Š. Parimucha[1], D. Baludanský[2], M. Vadila[3]

[1] Institute of Physics, Faculty of Natural Sciences, Šafárik University, 04001 Košice, Slovakia *stefan.parimucha@upjs.sk*
[2] Roztoky Observatory, Slovakia *bdaniel@pobox.sk*
[3] MiVa, 06601 Humenné , Slovakia *mvadila@centrum.cz*

ABSTRACT. We give an introduction information about the KOROAPS (KOšice ROztoky Automatic Photometry System). It is a system for a large scale automatic multicolor monitoring and variable stars searching. It is in a development at Šafárik University in Košice in cooperation with Roztoky Observatory. The system is now in a test operation at Roztoky Observatory. System consists of Nikkor photolense 2/200 equipped with SBIG ST8 CCD camera and set of the standard VRI photometric filters. It is placed on Celestron's CG-5 Advanced mount. We give description of the basic properties of the instrument, data reduction pipeline and operational modes of the instrument.

**Key words**: Instrumentation: miscellaneous, Methods: data analysis, Techniques: photometric

## 1. Basic Properties of the System

### *1.1 Optics*

The optical part of the system consists of Nikkor photographic photolense 2/200. The diameter of the input aperture is 100mm and focal length is 200mm. The focal plane is optimized for the field with classical dimension of 24 × 36 mm. It gives us a possibility to use a CCD camera with larger chip in the future.

### *1.2 CCD camera*

The Nikkor photolense is at present time equipped by SBIG ST-8 CCD camera. The chip dimension is 1530 × 1020 pixels with 9 $\mu$m pixel. We use set of standard Johnson $VRI$ filters. The field of view of the camera at used optics is 4 × 2.5$^o$ with pixel scale 9.5"/pixel. We use exposure times typically from 30 seconds up to 2 minutes. The limiting magnitude in $V$ filter for 1 minute exposure is ∼16.5 mag.

### *1.3 Mount*

Optics with CCD camera are placed on Celestron CG-5 Advanced Mount with GoTo system. This mount is LX200 compatible mount, which enables us to use an open protocol for its control. Maximum slew speed of the mount is 3$^o$/second. The pointing accuracy is <1', but strongly depends on quality of calibration of the mount (north pole setting and calibration stars selection and alignment). The mount enables to use an autoguiding system using the second camera chip with accuracy better then 10".

### *1.4 Software*

CCD camera and mount control as well as data reduction pipeline are realized by Python scripts, which used corresponding programs depending on operational mode. Data archiving (CCD images, light curves) are performed by MySQL and PHP scripts. We plan to put data on-line on the web page.

## 2. Data Reduction Pipeline

The reduction and analysis of the obtained CCD images can be summarized to the following steps:

1. standart photometric reduction using master bias and dark frame and flat-field. Masters are created every night, if it is permitted by weather conditions.

2. sorting of the CCD images considering to operational mode and used filter.

3. object detection and their photometry. In non-crowded fields we use SEXTRATOR code (Bertin & Arnouts, 1996). For the crowded fields we plan to implement ISIS package (Alard and Lupton, 1998)

Table 1: Operational modes of KOROAPS system and types of observed objects.

| Mode | Description |
|---|---|
| 1 – one region | multicolor photometry of the selected field, typically all night |
| | light curves of eclipsing binaries and CVs |
| 2 – region scan | photometry of 2, 4 or 9 partially overlapping fields |
| | variable stars and/or exoplanets searching, monitoring of variable stars |
| 3 – multiregion | photometry of maximum 16 fields one after another |
| | multicolor monitoring of CVs minima times of eclipsing binaries |

4. cross identification between detected list of objects and catalogs (Tycho2 or USNOA). World Coordinate System (WCS) transformations are calculated and WCS is written to FITS image header.

5. calculation of all necessary corrections (e.g heliocentric correction).

6. calculation of instrumental differential magnitudes with respect to selected comparison stars

7. transformation of magnitudes to international system.

8. final light curves generation and data archiving.

## 3. Operational Modes

KOROAPS can operate in 3 operational modes as listed in Table 1. These modes can be easily changed during night depending on observational conditions as well as types of observed objects.

## 4. Conclusion

KOROAPS is now in a test operation at Roztoky Observatory. We plan to put it to regular work during 2008. We also plan to use new CCD camera with a large chip to maximize field of view. It will be necessary to improve our software and implement other photometric packages.

We have found that KOROAPS could be very useful for the observations of the objects that we want to study, like cataclysmic variables and eclipsing binary stars.

*Acknowledgements.* This project was supported by VEGA grant No.7011 and internal grant of Šafárik University No. 9/07-08 and partially by the private sources.

## References

Alard C., Lupton R.H.: 1998, *Astrophys. J.*, **503**, 325.
Bertin E., Arnouts S.: 1996, *Astron. Astrophys. Suppl. Series*, **117**, 394.

# WZ SGE STARS

E.P. Pavlenko[1,2]

[1] Crimean astrophysical observatory
Nauchny 98409 Crimea, Ukraine, *pavlenko@crao.crimea.ua*
[2] Tavrida national university

ABSTRACT. The WZ Sge type stars is a rare subclass of the cataclysmic variables (CVs). It possesses the properties of both dwarf novae and recurrent novae. The WZ Sge stars have the shortest orbital periods (typically 80 - 90 minutes) known among the dwarf novae, and the long (decades) recurrent time of outbursts never displayed by the dwarf novae but that is typical for the recurrent novae. At the same time the WZ Sge stars show their own unique peculiarities and are the promising objects for search for the brown dwarfs in close binaries. The brief review of the main characters of the known WZ Sge stars is given including the last results of the newly discovered and investigated binaries of this type.

**Key words**: Stars: binary: cataclysmic; stars: individual: WZ Sge, SDSS J0804, V455 And, ASAS J002511+1217.2

## 1. Introduction

The cataclysmic variable stars (CVs) are the close binaries suffering the late stage of their evolution. They consist from the late type star filling its Roshe Lobe and loosing material through the inner Lagrangian point onto the compact primary (white dwarf/neutron star/Black Hole). This class of variables displays the outbursts of different amplitudes and different recurrent time. Basing on the variety of these parameters, the CVs are divided onto several subclass: 1) classical novae: the recurrent time of outbursts presumably is $10^4$ - $10^5$ years, amplitude - more than $6^m$ (in the case of the Nova V1500 Cyg (1975) the amplitude of the outburst was 19 mag!), 2) dwarf novae: The recurrent time of the outbursts is weeks and amplitude is mostly less than 6 magnitudes (Warner, 1995); 3) recurrent novae: time between outbursts is decades of years. The last subclass however covers both close and wide binaries (one could find recurrent novae among symbiotic stars).

WZ Sge stars were extracted into separate subclass last time because of the large ($\sim 8^m$) amplitudes (Bailey, 1979; Downes, Margon, 1981; Patterson et al., 1981; O'Donoghue et al., 1991; Kato et al., 2001a) and specyfic combination of the orbital periods and recurrent time of the outburst: the shortest orbital periods (80 - 90 min.), that is typical to the SU UMa type subclass of the dwarf novae, but contrary to them, the long recurrent time of the outbursts (decades). It is possible to consider the WZ Sge stars as recurrent novae as well. Furthermore, while the symbiotic stars bound the recurrent novae at the longest orbital periods (years or decades) among interacting binaries, the WZ Sge type stars bound this subclass at the shortest orbital periods.

The physics of the classical novae and dwarf novae is principally different. While the nature of the classical nova explosion according to the morden conceptions, is the thermonuclear event in the upper layers of the white dwarf, the nature of the dwarf novae is the thermal-viscous instability that occurs in accretion disc in which the viscosity is given by the alpha-prescription (Warner, 1995; Shakura & Sunyaev, 1973). The outburst in the dwarf novae starts happens when the disc becomes partially ionized and the opacities vary steeply with temperature; this occurs when the disk material reaches temperatures of order of 8000 K (Lasota, 2001). The origin of the WZ Sge type binaries outbursts means also the termal instability of accretion disc.

There is a tendency of growing of the WZ Sge stars number last time not only due to the developed net of the amator monitoring of the outbursts, but, also, due to the possibility to select some candidates aside the outburst on the base of the modern surveys (for example, such as the SDSS, HS, ASAS).

## 2. Types of the outbursts

It is possible to distingwish four types of the outbursts among the WZ Sge type stars.

1. Perhaps the majority of the WZ Sge stars shows single outburst. The examples are: HV Vir(Kato et al., 2001b), WX Cet (Kato et al., 2001a).

2. Outburst with one rebrightening. That is typical to the normal (but not to all!) SU UMa type of the dwarf nova. For example: RZ Leo (Ishioka et al.,

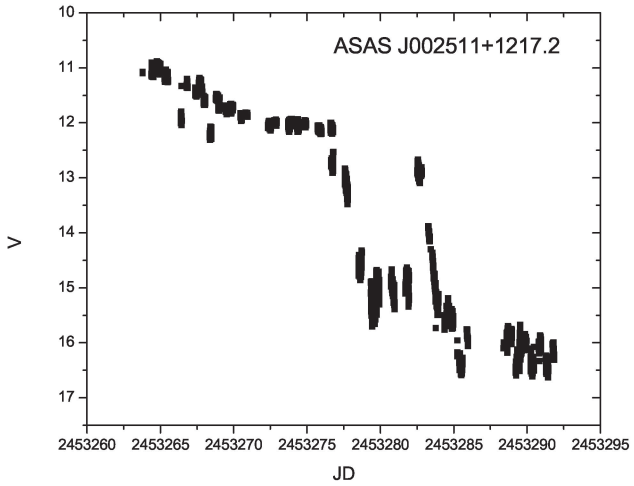


Figure 1: Light curve of the ASAS J002511+1217.2 outburst with single rebrightening (from Golovin et al., 2005).

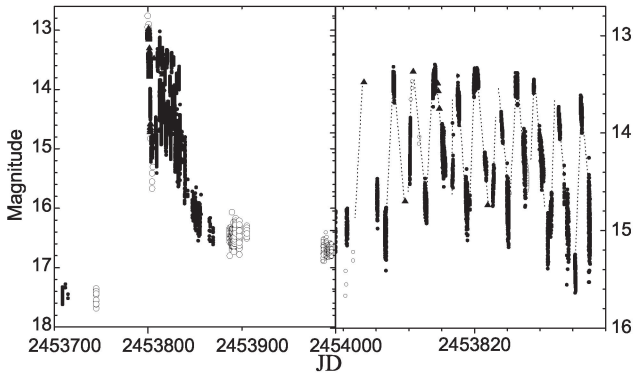


Figure 2: Left: Light curve of the J0804 outburst (from Pavlenko et al., 2007a) with eleven rebrightenings. Right: Detail view of rebrightenings.

2001); ASAS J002511+1217.2 (Golovin et al., 2005). For illustration of such type of the outbursts the light curve of the ASAS J002511+1217.2 is given in Fig.1.

3. The outburst with series of rebrightenings (one could find in literature also another sinonima: reflares, or echo-outbursts). That is a unique fenomena that was observed ONLY in WZ Sge type stars, namely WZ Sge itself -12 rebrightenings (Patterson et al., 2002), SDSS J0804 -11 rebrightenings (Pavlenko et al., 2007), and EG Cnc - 6 rebrightenings (Patterson et al., 1998a). Fig. 2 shows the light curve of SDSS J0804. Several competing points of view try to explain the phenomenon of rebrightenings, for example:

The rebrightenings are triggered while the mass transfer rate is still high after the superoutburst (Buat-Menard and Hameury, 2002).

The heating waves reflected from the cooling waves

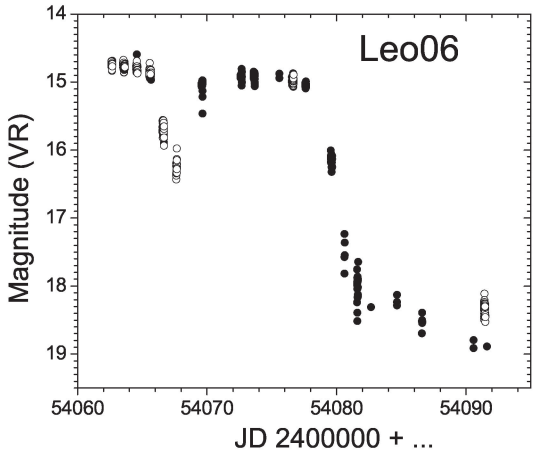


Figure 3: Light curve of the Leo06 = SDSS J102146.44+234926.3 outburst with dip (from Uemura et al., 2007.)

accompanying the decline from the last outburst (Patterson et al., 1998a).

4. Outburst with no rebrightenings but with $1.5^m$ - $2^m$ dip that lasts a few days. Such kind of the outburst could also be called as the outbursts with long-lived plateau (Uemura et al., 2007): AL Com (Nogami et al., 1997), CG CMa (Kato et al., 1999); Leo06 = SDSS J102146.44+234926.3 (Golovin et al., 2007); TSS J0222 (Imada et al., 2006b); V2176 Cyg (Novak et al., 2001). The example of the Leo06 outburst light curve is given in Fig. 3.

### 3. Superhumps and "early" superhumps

Similar to the SU UMa dwarf novae, the WZ Sge binaries also display during the outburst the light variations (superhumps) that a few minutes differ from the orbital period. these variations often appear at the $\sim$ 10th day of the superoutburst (main outburst). The basic origin of the superhump light is the extra heating associated with periodic deformation of the disk shape (Lubow 1992; Murray 1996 etc.): An eccentric instability grows at the 3:1 resonance in the accretion disk, and perturbation by the secondary forces it to precess (Whitehust 1988, Hirose and Osaki 1990, Lubow 1991).

The ordinary superhumps display the one-peaked profile that could be slightly distorted through the course of the outburst. The $q = M_2/M_1$ plays a key role: superhumps produced only below a critical ratio, $q_{crit} \sim 0.3$. During the cource of the main outburst, O-C for the superhumps maxima display the parabolic change that is consistent with period increase for the WZ Sge (Andronov et al., 2002; Patterson et al., 2002), RZ Leo (Ishioka et al., 2001), EG Cnc (Kato et al., 2006), V592 Her (Kato et al., 2007), ASAS J002511+1217.2 (Templeton et al., 2006), AL Com

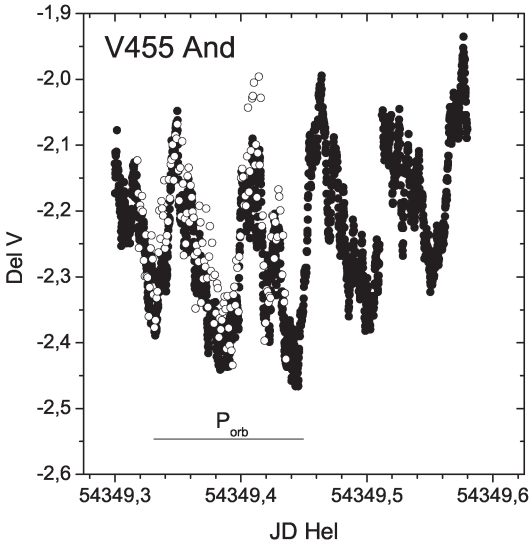


Figure 4: Left: The Early "orbital" humps of the V455 And. Filled circles denotes data obtained with Zeiss-600 telescope (Terskol) while the open circles are the data obtained simultaneously with K-380 telescope (CrAO).

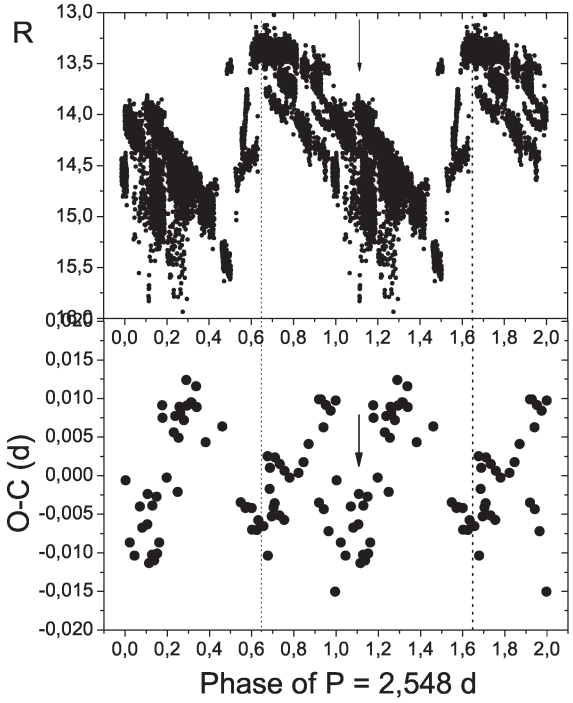


Figure 6: The mean rebrightening profile (upper frame) and superhump maximum O-C for SDSS J0804 folded on the rebrightening cycle (lower frame). The dotted lines plotted through the rebrightenings maxima and O-C minima. Arrow points to the small bump on the rebrightening profile and correspondent O-C minimum. For clarity data are plotted twice.

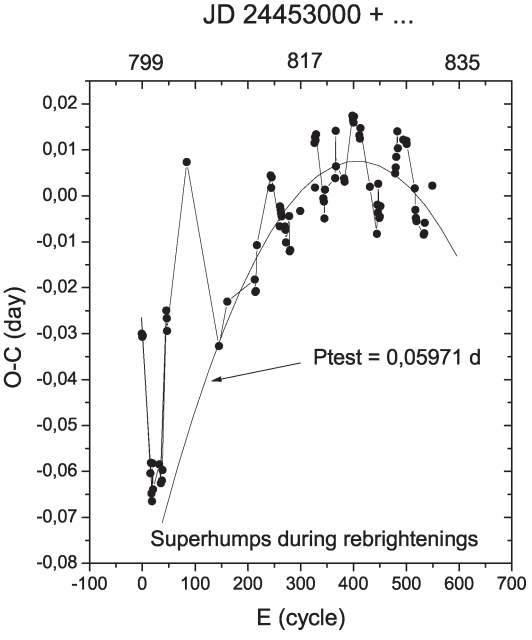


Figure 5: The O-C of superhumps behavior during the rebrightenings for SDSS J0804.

(Nogami et al., 1997), SDSS J0804 (Pavlenko et al., 2006).

Among the WZ Sge stars only 8 binaries show the double-peaked humps ("early superhumps"), that could appear even on the rising branch of the outburst (Andronov et al., 2002). Contrary to the superhumps, the early superhumps profile shows the strong two-picked humps modulated by orbital period.

These binaries are:
ASAS 160048-4846.2 (Imada et al., 2007); AL Com (Patterson etal., 1996); EG Cnc (Patterson et al., 1996); RZ Leo (Ishioka et al., 2001); HV Vir (Ishioka et al., 2003); Var Her 04 (Price 2004); WZ Sge (Andronov et al., 2002; Patterson et al., 2002; Kato et al., 2004); V455 And = HS 2331+3905 (newly discovered in September, 2007 (AAVSO alert, 2007). The nightly light curve that relates to the early part of the outburst is presented in Fig.4. It demonstrates the clear double-peacked humps wich repeat with known orbital periodicity found by Araujo-Betancor et al. (2007) in minimum.

The nature of the two-humped orbital profile is still unclear. Several suggestions connect such profile with:

a) enhanced hot spot caused by a sudden increase of the mass-transfer (Patterson et al., 1981; Patterson et

al., 2002);

b) excitation of the 2:1 tidal resonance in the expanding accretion disc (Osaki and Meyer, 2002; Kato, 2002);

c) geometrical effect with a two-arm spiral wave modifying our view of the inner accretion disc (Wheatley and Mauche, 2004).

### 4. Superhumps during rebrightenings

It was shown that during the rebrightenings (reflares, echo-outbursts) superhumps are still present. The O-C of the superhumps display the parabolic change that is consistent with period decrease for the WZ Sge (Patterson et al., 2002), EG Cnc (Kato et al., 2006), SDSS J0804 (Pavlenko et al., 2006). For the J0804 it was first found the complex O-C variations (Pavlenko et al., 2008). In addition to the parabolic change corresponding to the superhump period decrease, the O-C show more frequent cyclic variations (Fig. 5). These variations strongly correlate with rebrightening phase: The O-C reach the minimal values twice the rebrightening cycle (see Fig. 6). The first O-C minimum coincides with rebrightening maximum, and the second minimum happens at the small and not prominent bump on the ascending branch of the rebrightening profile. The O-C variations reflect the complex precession phenomenon of the accretion disc. Despite of the overall decay of precession, it tends to enhance from one rebrightening to another.

### 5. Orbital humps

While the superhumps are observing during the outburst plateau and rebrightenings, the orbital humps begin to appear already soon after rebrightenings finish during the long-term return to the pre-outburst state. It could be seen in Fig. 7, where the dependence of the photometrical period on time for the SDSS J0804 is shown (Pavlenko et al., 2007). The orbital profile in minimum of some WZ Sge type stars is also two-peaked. For example in Fig. 8 the nightly light curve of the SDSS J0804 obtained approximately in a year after the outburst is presented. Araujo-Betancor et al. (2004) suggested for the case of V455 And as explanation that we are seeing some sort of symmetrical structure, such as two bright spots existence.

### 6. White dwarf

The white dwarfs of some WZ Sge type stars exibit the fast light variability in the range of tens - hundreds seconds that could be connected with white dwarf: either with ZZ Ceti-like pulsations or with

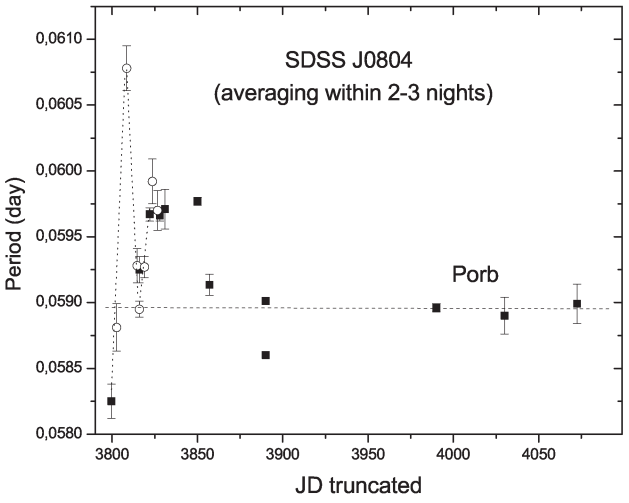


Figure 7: Dependence of photometrical period on time for the SDSS J0804 during the cource of the outburst (Pavlenko et al., 2007b). The dramatical change of the period correspond to the end of the main outburst and rebrightenings era. Later - at least in $\sim$ 150 days after the end of rebrightenings - the photometrical light modulation is close to the orbital period (marked by dotted line) known from spectroscopy of Szcody et al. (2006) in minimum.

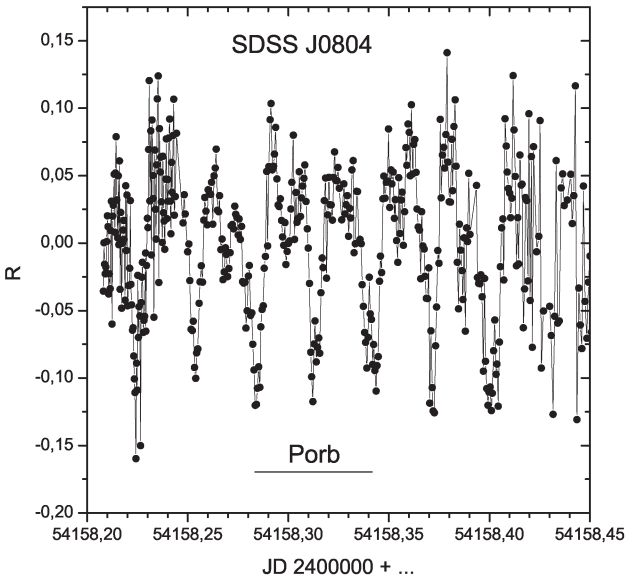


Figure 8: The nightly light curve of the SDSS J0804 obtained with high time resolution with 2.6-m mirrow Shajn telescope of CrAO. The two-peaked structure of the orbital hump with mean amplitude $0.25^m$ is clearly seen. Note the additional splitting of the maxima with less amplitude.

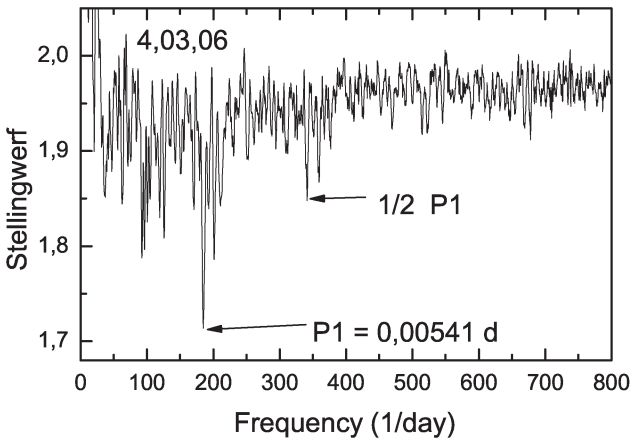


Figure 9: Periodogram for the SDSS J0804 obtained for the data at the main outburst. The most significant peak points to the 0.00541 d light variations (from Pavlenko et al., 2007a).

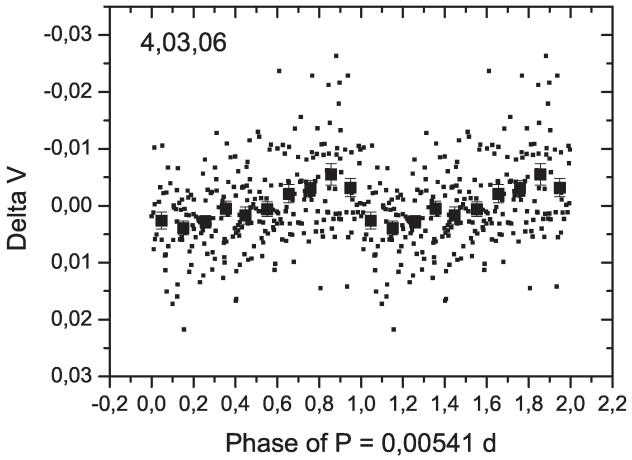


Figure 10: The data of the SDSS J0804 from one night for the main outburst folded on the 0.00541 d period., probably connected with non-radial pulsation of the white dwarf (from Pavlenko et al., 2007a). For clarity data are plotted twice.

white dwarf spin period. The WZ Sge itself displays the 27.9-sec optical and X-ray light variations that believed to be the white dwarf spin period (Patterson, 1998), that, however, is not detecting all the time. The photometric variations with period 72 sec. were recently found by Araujo-Betancor et al.(2007)in V455 And = HS 2331+3905 during its low state and interpreted as its rotational period. This period was not confirmed by Gansicke (2007), instead he found another spin period 67.62 sec. Araujo-Betancor et al. also suggested that there are 5 - 6 min white dwarf nonradial pulsations of V455 And. Gansicke (2007) confirmed the existence of these pulsations. Evidence of probably nonradial pulsations with period 8-9 min. and amplitude $\sim 0.02^m$ were found for SDSS J0804 during one night in the outburst by Pavlenko et al., 2007a (see Fig. 9 and Fig. 10) and were not found by Szkody et al. (2005) in qiiescence. The fast white dwarf rotation could be explain within the model of the magnetic rotator Patterson (1998b). He suggested that a weak magnetic field can allow the very long outburst times by carving out a central cavity in the accretion disc. However this model meets difficulties in specific cases. Also not all quasy-periodical oscillations could be explained as the nonradial pulsations. For example, the white dwarf temperature in V455 And in minimum was 11 000K (Araujo-Betancor et al., 2004) that is well within the instability strip for ZZ Ceti pulsators, so observed 5 - 6 min light oscillations could be the white dwarf pulsations, while the 15-sec light oscillations of WZ Sge during outburst decline could't, because of the current dwarf temperature $\sim$ 25 000K that is far beyond the blue end of the instability strip.

## 7. Red dwarf

According to the current standard model of cataclysmic variable evolution (King 1988) the close binary evolvs to the shorter orbital periods, reach the shortest ($\sim$ 70 min) period and then evolve back to longer orbital periods. These "bouced" systems are these with brown dwarf. Practically the brown dwarf could be found by several ways. The direct way is the radial velocities measure or modeling the spectral-energy distribution. However the white dwarf and accretion disc contribution make the process highly uncertain. The indirect way demands knoledge of the orbital and superhump periods, that could be measured photometrically during the superoutburst (superhump light modulation) and in quiescence (orbital light modulation). The knowledge of these periods leads to the secondary component mass estimation due to the empirical relationship between mass ratio and superhump period excess (Patterson, 1998)

$$\epsilon = 0.23 \times q/(1 + 0.27 \times q)$$

where the superhump period excess

$$\epsilon = (P_{sh} - P_{orb})/P_{orb}$$

Together with assumed (or measured) value of the primary mass, this relationship allows one to calculate the mass of secondary star for eny system with known superhump and orbital period.

As far as WS Sge stars have the orbital period close to the period minimum, they are very promissing candidates to the white dwarf + red dwarf binaries. These binaries with brown dwarfs show the

"bounce" on the "q-Porb" diagramme. While cataclysmic variables approaches the minimum period, the mass of the secondary component - the red dwarf - decreases until it can no longer sustain hydrogen burning. Such secondary becomes increasingly degenerate, entering the browm dwarf regime. Kolb (1993) estimated that 70% of all cataclysmic variables should include such "substellar" secondaries. Despite this theoretical prediction only a few cataclysmic variables (or "stars-bouncers" following the Patterson's terminology) with mass of secondary less than 0.08 of Sollar masses (brown dwarfs) are known. The best candidates are WZ Sge, EG Cnc, EF Eri, DI UMa (Littlefair et al., 2003, Patterson et al., 1998b, Buermann et al., 2000). The first two are the WZ Sge type stars. The descripency of the theory and observations may be caused by both the selection effect (the rarity of the outbursts and faitness of binaries in minimum) or by the incorrectness of theory.

*Acknowledgements.* This work was partially supported by the grant of the Ukrainian Fund of Fundamental Research F 25.2/139 and by the CosmoMicroPhysics program of the National Academy of Sciences and National Space Agancy of Ukraine.

**References**

AAVSO.: 2007, *Alert Notice*, **357**.
Andronov I.L, Yuschenko A.V., Niarcos P.G., Gaseas K.: 2002, *ASP Conference Series*, **261**, 459.
Araujo-Betancor, Gansicke B.T., Hagen H.-J., et al.: 2004 *RevMexAA (Serie de Conferencias)*, **20**, 190.
Araujo-Betancor S., Gansicke, B.T., Hagen H.-J., et al. 2007 : *Astron. Astroph.* in press.
Bailey J.: 1979,*M.N.R.A.S.*, **189p**, 41.
Buermann K., Wheatley P., Ramsay G., et al.: 2000, *Astron.Astroph.*, **354L**, 49.
Buat-Menard V., Hameury J.-M.: 2002, *Astron. Astroph.*, **386**, 891.
O'Donoghue D., Chen A., Marang F.: 1991, *M.N.R.A.S.*, **250**, 363.
Downes R.A., Margon B.: 1981, *M.N.R.A.S.*, **197**, 35.
Gansicke, B. : 2007, *ASP Conference Series*, **372**, 597.
Golovin A., Price, A., Templeton, M., et al.: 2005, *I.B.V.S.*, **5611**, 1
Golovin A., Kazuya A., Pavlenko, E., et al.: 2007, *I.B.V.S.*, **5763**, 1
Hirose M., Osaki Y.: 1990, *P.A.S.J.*, **42**, 135.
Imada A., Kubota K., Kato T., et al.: 2006. *P.A.S.J.*, **58**, L23.
Imada A., Monard B.: 2007, *P.A.S.J.*, in press; arXiv: astro-ph/0511170v1.
Ishioka R., Kato T., Nogami D.: 2001, *P.A.S.J.*, **53**, 905.
Kato T., Matsumoto K., Stubbings R.: 1999, *I.B.V.S.*, **4760**, 1.
Kato T., Sekine Y., Hirata R.: 2001a, *P.A.S.J.*, **53**, 1191.
Kato T., Matsumoto, K., Nogami, D., et al.: 2001b, *P.A.S.J.*, **53**, 893.
Kato T.: 2002, *P.A.S.J.*, **54L**, 11.
Kato T., Nogami D., Matsumoto K., Baba H.: 2004, *P.A.S.J.*, **56**, 109.
Kato T., Uemura M., Matsumoto K. et al.: 2007, *arXiv: astro-ph/0310426v1.*
King A.R.: 1988, *Q.J.R.A.S.*, **29**, 1.
Kolb U.: 1993, *Astron. Astroph.*, **271**, 149.
Lasota J.-P.: 2001, *New Astronomy Reviews*, **45**, 449.
Littlefair S.P., Dhillon V.S., Howell S.B., Ciardi D.R.: 2000, *M.N.R.A.S.*, **313**, 117.
Littlefair S.P., Dhillon V.S., Martin E.L.: 2003, *M.N.R.A.S.*, **340**, 264L.
Lubow S.: 1991, *Ap.J.*, **381**, 268L.
Lubow S.: 1992, *Ap.J.*, **401**, 317L.
Murray J.R.: 1996, *M.N.R.A.S.*, **279**, 402.
Nogami D., Kato T., Baba H., et al.: 1997, *Ap. J.*, **490**, 840.
Novak R., Vanmunster T., Jensen L.T.: 2001, *I.B.V.S.*, **5108**, 1.
Osaki Y., Meyer F.: 2002, *Astron. Astroph.*, **383**, 574.
Patterson J., McGrow J.T., Coleman L., et al.: 1981, *Ap.J.*, **248**, 1067.
Patterson J., Augusteijn T., Harvey D.: 1996, *P.A.S.P.*, **108**, 748.
Patterson J., Hayley R., Kemp J.: 1998b, *P.A.S.P.*, **110**, 403.
Patterson J., Hayley R., Kemp J.: 1998c, *P.A.S.P.*, **110**, 1290.
Patterson J.: 1998, *P.A.S.P.*, **110**, 1132.
Patterson J.: 2001, *P.A.S.P.*, **113**, 736.
Patterson J., Masi G., Richmond M.W., et al.: 2002, *P.A.S.P.*, **114**, 721.
Pavlenko E.P., Shugarov S.Yu., Katysheva N.A., et al.: 2006, *IAU XXVI General Assembly Abstract Book*, 224.
Pavlenko E,P., Shugarov, S.Yu., Katysheva, N.A., et al.: 2007a, *ASP Conference Series*, **372**, 511.
Pavlenko E.P., Shugarov S.Yu., Katysheva N.A., et al.: 2007b, *O.E.J.V.*(in press).
Pavlenko E.P., Shugarov S.Yu., Katysheva N.A., et al.: 2008, in press.
Shakura N.I., Sunyaev R.A.: 1973, *Astron. Astroph.*, **24**, 337.
Szkody P., Henden A., Agueros M., et al.: 2006, *A.J.*, **131**, 973.
Templeton M., Leaman R., Szkody P., et al.: 2006, *P.A.S.P.*, **118**, 236.
Uemura M., Arai A., Krajci T., et al.: 2007, *P.A.S.J.*, in press.
Warner, B.: 1995, *Cataclysmic variable stars*, Cambridge University Press.
Whitehust R.: 1988, *M.N.R.A.S.*, **232**, 35.
Wheatley P.J., Mauche C.W.: 2005, *ASP Conference Series*, **257**.

# V1504 CYG: OUTBURSTS

E.P. Pavlenko[1,2], E. Berezina[3]

[1] Crimean Astrophysical Observatory
*pavlenko@crao.crimea.ua*
[2] Tavrida National University
[3] Kazan State University

ABSTRACT. The behavior of the dwarf nova V1504 Cyg during 2007 superoutburst and during several normal outbursts is considered. The binary during normal outbursts shows loop-like tracks on the V, V-R diagram, where prior the superoutburst the loop is steep and narrow while after the superoutburst the loop is mildly sloping and wider. The loop of the superoutburst resembles those of normal outbursts precedings the superoutburst. V1504 Cyg displays the early superhumps phenomenon during the ricing branch and first few days of the superoutburst.

**Key words**: Stars: binary: cataclysmic; stars: individual: V1504 Cyg

## 1. Introduction

V1504 Cyg is a SU UMa-type dwarf nova. The kind of this subclass of the cataclysmic variables is the presence of two types of outbursts (normal ones and superoutbursts) and orbital periods that are less then 2 h (Warner, 1995). In 1981 V.P. Tsesevich first pointed attention on this non-classified for that time variable star. Later on Raykov & Yuschenko (1988) suggested this star to be the SU UMa type nova, Nogami and Masuda (1997) confirmed this suggestion and found that superhump period is 0.07 day. As the dwarf nova, V1504 Cyg shows two type of the outbursts: the $\sim$ 3-day so-called normal outbursts and $\sim$ 14-day superoutbursts. Pavlenko and Dudka (2002) studied the outburst activity of V1504 Cyg and suggested the two types of the outbursts.

## 2. Observations and results

Observations of V1504 Cyg have been carried out with Cassegrain K-380 telescope in the Crimean astrophysical observatory in VR Johnson photometrical system in 2007, June – September during 31 nights, including superoutburst and two normal outbursts prior and after the superoutburst. The overall light curve is shown in Fig.1. It is seen that the normal outbursts

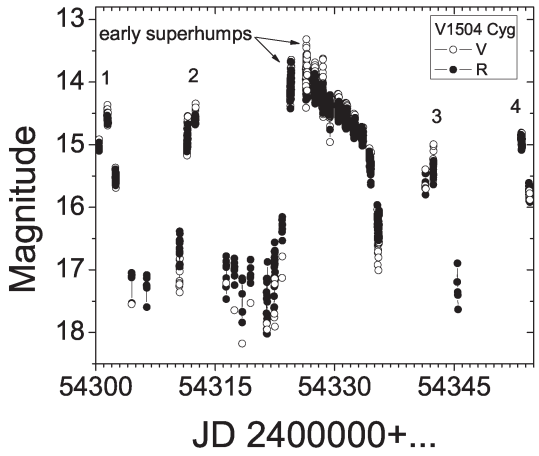


Figure 1: The long-term light curve of the V1504 Cyg. The open circles denote V data and the filled circles – R data. The normal outbursts are numbered.

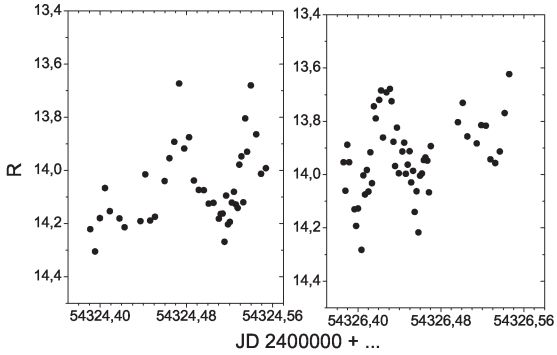


Figure 2: The nightly light curves displaying "early superhumps".

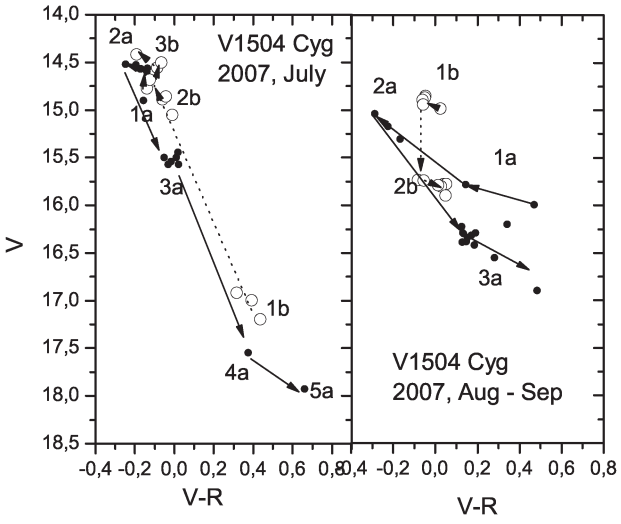


Figure 3: Left: The V, V-R dependence for the 1st (filled circles) and 2nd (open circles) normal outbursts. Right: the same for the 3nd and 4th normal outbursts.

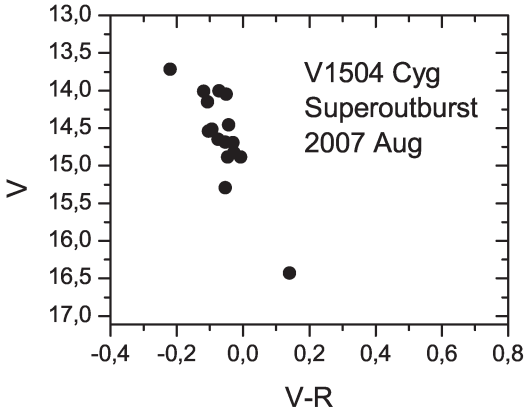


Figure 4: The V, V-R dependence for the superoutburst.

have mean amplitude $3^m$ while the superoutburst – $3.5^m$. The normal outbursts prior the superoutburst are brighter than those after superoutburst. All normal outbursts occured in 11 days. We do not discuss there the superhumps evolution during the course of the superoutburst, but note the appearence of the "early superhumps" on the ricing branch and during the first days of the superoutburst (Fig. 2). The amplitude of this light variations is variable and could reach $0.5^m$, and the profile of the light curve is one-humped.

We constructed the magnitude – color diagrams separately for the normal outbursts before and after superoutburst and for the superoutburst itself (see Fig. 3). To supress the nightly magnitude and color variations, the data within time corresponded to the superhump cycle are averaged. It is seen that binary is bluer when brighter. In the outburst peak it shows the average $V - R \sim -0.2^m$. loop: the star is slightly bluer after passing the outburst peak. Contrary to this behavior, the 3d and 4th outbursts exibit more wide loop. At the same $16^m$ level the width of the first pair of loops is $\sim 0.1^m$, while those for the second pair – $\sim 0.4^m$. Also the first pair behaves steeper then the second one. The behavior of the superoutburst on the magnitude – color diagram resembles those of the 1st and 2nd normal outbursts (Fig. 4).

## 3. Discussion

We have revield that both the normal outbursts and superoutburst have practically the same blue color in maximum. During the outburst the accretion disk or accretion disk + hot belt + boundary layer could be the major contributors to the total light. The observing colors in maximum light correspond to the black-body temperature of order 50 000 K or higher. During the superoutbursts plateau duration the temperature of the hot radiation decreases up to 18 000 K – 19 000 K, and during the phase of rapid brightness decline decreases up to 10 000 K. If this radiation is produced by the accretion disk only, that means the disk is still in the hot stable state (Smak, 1984). In minimum the contributors to the total light are the accretion disk, hot spot on the disk, white dwarf and red dwarf. Just after the end of the superoutburst the mass of the accretion disk is the much smaller than prior the next superoutburst. One could expect that the normal outbursts behavior prior and after the superoutburst also may be different. Indeed, comparing the outbursts 1 and 2 with outbursts 3 and 4, one could see such difference. Before the superoutburst the narrow loop in Fig. 3 (left) corresponds to the "inside-out" propagation of the outburst, while after the superoutburst (Fig. 3, right) the instability is of the "outside – in" type (Smak, 1984).

*Acknowledgements.* This work was partially supported by the grant of the Ukrainian Fund of Fundamental Research F 25.2/139.

## References

Antoniuk O., Pavlenko E.: 2005, *ASP Conf. Ser.*, **330**, 379.

Nogami D., Masuda S.: 1997, *I.B.V.S.*, **4532**, 1.

Pavlenko E.P., Dudka O.I.: 2002, *Astrofizika*, **45**, 1.

Raykov A.A., Yushchenko A.V.: 1988, *Perem.Zvesdy*, **22**, 853.

Smak J.: 1984, *Acta Astronomica*, **34**, 161.

Warner, B.: 1995, *Cataclysmic variable stars*, Cambridge University Press.

# EXTREMELY PECULIAR STARS

Yakiv V. Pavlenko
Main Astronomical Observatory of the National Academy of Sciences,
27 Zabolotnoho, Kyiv-127, 03680, Ukraine

ABSTRACT. The procedure and results of modelling atmospheres, spectral energy distributions and spectra of peculiar stars are discussed. A special attention is drawn to the consideration of the particular problems encountered for peculiar and hydrogen deficient stars on the later stages of evolution. We present some results obtained by fits to observed optical and IR spectra of Sakurai's object, V838 Mon, and RS Oph.

**Key words**: Stars: evolution: cataclysmic; stars: individual: V838 Mon, V4334 Sgr, RS Oph

## 1. Introduction

Life of a star is long. Still sometimes one becomes very bright and evolves in the very short time scales. Stellar spectra demonstrate the drastic changes due to the variation of physical conditions in atmospheres and envelopes. The majority of the observed events occur on the latest stages of evolution. The peculiar stars provide the real challenge for observers and theoreticians.

Abundances of at least light elements, i.e. H, He, Li, C, and N, in the atmospheres of evolved stars of the intermediate mases can significantly differ from the solar abundance ratios. The reason for this is because convection and other mixing processes dredge up the products of the nucleosynthesis from the stellar interior. Naturally, the temperature structure of their model atmospheres and computed spectra response on any change of abundances (see Pavlenko & Yakovina 1994). Strictly speaking we cannot use for analysis of stellar spectra of the evolved stars the model atmospheres from the extended grids computed recently for fixed abundances (see Kurucz (1993, 1999), Hauschildt et al. (1999). Moreover, in most of the computations the solar abundances (Anders & Grevesse 1989) or solar abundances scaled by the metallicity factor [Fe/H] are used which is grude enough approximation of the abundances distribution in the atmospheres of the evolved stars.

Mdelling spectra of the most evolved stars require much more complicate approach. Their atmospheres are hydrogen deficient but helium and carbon rich. The opacity due to $H^-$ absorption is not as important for them. The menagery of opacity sources in their atmospheres differ from the solar case (Asplund et al. 1999).

## 2. Procedure

The plane-parallel model atmospheres of the evolved stars in LTE, with no energy divergence were computed by SAM12 program (Pavlenko 2003). The program is a modification of ATLAS12 (Kurucz 1999). SAM12 uses the standard set of continuum opacities from ATLAS12. The adopted opacity sources account for changes in the opacity as a function of temperature and element abundance. We add some opacities sources which are of importance in the atmospheres of carbon-rich, hydrogen-deficient stars (see Pavlenko 2003 for more details).

Chemical equilibrium is computed for the different sets of molecular species, by assuming LTE. The nomenclatures of molecules accounted for are different in stellar atmospheres atmospheres of $C/O > 1$ and $C/O < 1$.

The opacity sampling approach (Sneden et al. 1976) is used to account for atomic and molecular line absorption. We account mainly for the molecules which are the most abundant or most important sources of opacities. In the case of atmospheres with $C/O < 1$ we account absorption of VO, TiO, $H_2O$ and molecules from the Kurucz (1993) CDs.

In atmospheres with $C/O > 1$ rich models of $T_{\rm eff}<$ 5000 K diatomic molecules contained carbon atoms are main contributors of the opacity. In the atmospheres of $T_{\rm eff}<$ 3000 K HCN, NHC, $C_3$ and other polyatomic carbon molecules contribute to the opacity in the IR part of the spectra (see Harrison at al. 2006 and refs therein).

Synthetic spectra are calculated with the WITA6 program (Pavlenko 1997), using the same approximations and opacities as SAM12.

### *2.1. Fits to observed spectra*

To determine the best fit parameters, we compare

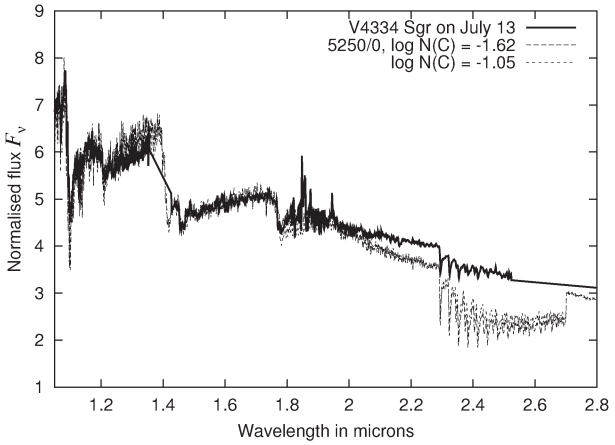


Figure 1: fits to observed spectrum of of Sakurai's Object on 1997 July 13, see Pavlenko et al. (2002) for more details.

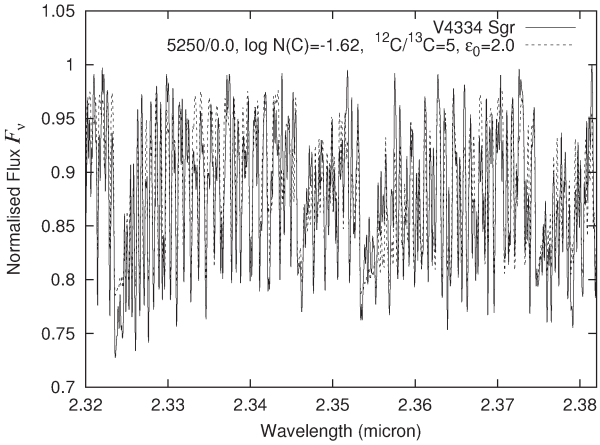


Figure 2: Best fit to 1998 July spectrum found by the minimisation procedure outlined in the text, for $\log N(\mathrm{C}) = -1.05$, see Pavlenko et al. (2005) for more details.

the observed fluxes $F_\nu$ with the computed fluxes following the scheme of Jones et al (2002) and Pavlenko & Jones (2003). We let

$$F_\nu^x = \int F_\nu^y \times G(x-y) * dy,$$

where $r_\nu^y$ and $G(x-y)$ are respectively the fluxes computed by WITA6 and the broadening profile. We adopt a gaussian + rotation profile for the latter. We then find the minima of the 3D function

$$S(f_\mathrm{s}, f_\mathrm{h}, f_\mathrm{g}) = \sum \left(F_{obs} - F^x\right)^2,$$

where $f_\mathrm{s}$, $f_\mathrm{g}$, $f_\mathrm{g}$ are the wavelength shift, the normalisation factor, and the profile broadening parameter, respectively. The parameters $f_\mathrm{s}, f_\mathrm{h}$ and $f_\mathrm{g}$ are determined by the minimisation procedure for every computed spectrum. Then, From the grid of the better solutions for the given abundances and/or other parameters (microrurbulent velocity, effective temperature, isotopic ratios, etc), we choose the best-fitting solution.

## 3. Results

### *3.1. Sakurai's object*

V4334 Sgr (Sakurai's Object) discovered by Y. Sakurai on February 20, 1996 (Nakano et al. 1996) is a very rare example of extremely fast evolution of a star during a very late final helium-burning event (Duerbeck & Benetti 1996).

Theoretical spectral energy distributions computed for a grid of hydrogen-deficient and carbon-rich model atmospheres have been compared with the observed optical (0.35 - 0.97 $\mu$m ) and infrared (1–2.5 $\mu$m) spectra of V4334 Sgr (Sakurai's Object) on 1997 - 1998 (Pablenko et al. 2000, Pavlenko & Duerbeck 2001, Pavlenko & Geballe 2002). We showed that the main features in the observed spectra are strong bands of CN, and $C_2$ in the optical spectra and $C_2$ and CO bands in the IR. Hot dust produces significant excess continuum at the long wavelength ends of the 1997 spectra.

Fits to the IR spectra yield an effective temperature of $T_{\mathrm{eff}} = 5500 \pm 200$ K for the April date and $T_{\mathrm{eff}} = 5250 \pm 200$ K for July.

Fits of our theoretical spectra to the $^{12}$CO and $^{13}$CO bands in Sakurai's spectrum at 2.3 $\mu$m observed in 1997 allows us to determine the $^{12}C/^{13}C$ ratio $^{12}C/^{13}C \simeq 4 \pm 1$ (Pavlenko et al. 2005). It is worth noting that we account here a contribution of some additional flux provided by the hot dust on the wavelengths of the first overtone CO bands. The low ratio of $^{12}C/^{13}C$ is consistent with the interpretation of V4334 Sgr as an object that has undergone a very late thermal pulse.

### *3.2. V838 Mon*

The peculiar variable star V838 Mon was discovered during an outburst in the beginning of 2002 January (Brown 2002). Two further outbursts were then observed in 2002 February (Munari et al. 2002a; Kimeswenger et al. 2002; Crause et al.2003) and in general the optical brightness in V-band of the star increased by 9 mag. Since 2002 March, a gradual fall in V-magnitude began which, by 2003 January, was reduced by 8 mag.

Kaminsky & Pavlenko (2005) obtained $T_{\mathrm{eff}} = 5330 \pm 300$ K, $5540 \pm 270$ K and $4960 \pm 190$ K, for February 25, March 2, and March 26, respectively. The iron abundance $\log N(\mathrm{Fe}) = -4.7$ does not appear to change

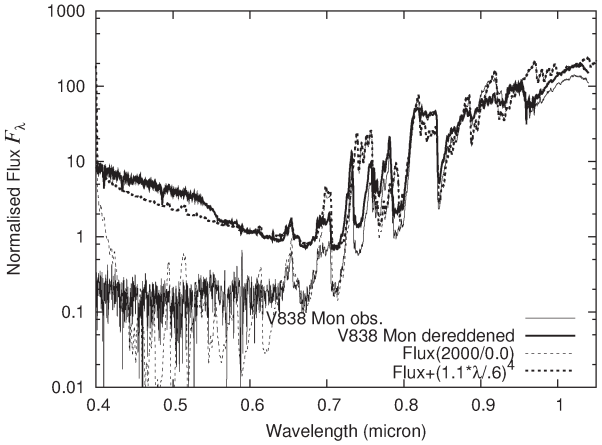


Figure 3: The fit to the observed V838 Mon spectrum on November 6, 2002 , see Pavlenko et al. (2006) for more details.

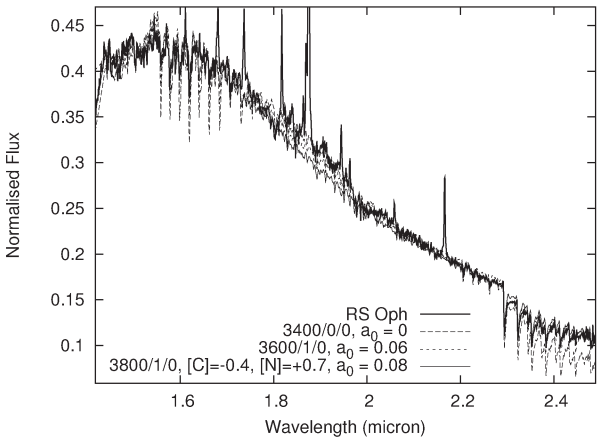


Figure 4: The best fit to the observed spectrum for the cases veiling-free and 'veiled' models, see Pavlenko et al. (2007) for more details.

in the atmosphere of V838 Mon from February 25 to March 26, 2002. Our results agree well with Kipper et al (2005).

Up until November 2002 both effective temperature and luminosity of V838 Mon drop significantly with time (see also Tylenda 2005). Evans et al. (2002) classified one as an L-supergiant (see also Tylenda 2005). The infrared spectrum of V838 Mon shows deep absorption bands of $H_2O$ . In the optical spectra there are strong TiO bands as well as bands of a few diatomic molecules witch can be fitted by theoretical spectrum computed with $T_{eff}$= 2000 K (Pavlenko et al. 2005). Then, at $\lambda < 0.5$ $\mu$m Desidera & Munari (2002) discovered spectroscopically a hot companion later confirmrd by Wagner & Starrfield (2002) and classified as B3V star by Munari et al. (2005). Modelling combined B2 V + M9 III spectrum allows us to determine radius of V838 Mon in November 2002 R $\sim$ 6000 R$\odot$, if both stars form the binary system (Pavlenko et al. 2007).

### *3.3. RS Oph*

Recurrent nova (RNe) provide another class of the extremely evolutionary changes. The best studied recurrent RNe RS Oph forms the binary system (WD +red giant M2 III). RS Oph is known to have undergone at least five eruptions, in 1898, 1933, 1958, 1967 and 1985; eruptions in 1907 and 1945, perhaps, were missed.

Recently Pavlenko et al. (2007) carried out detailed study of the IR spectra of RS Oph to better understand the effect of the giant secondary on the recurrent nova eruption. Both the progress of the eruption, and its aftermath, depend on the poorly known yet composition of the red giant in the RS Oph system.

Synthetic spectra were computed for a grid of M-giant model atmospheres having a range of effective temperatures 4000 < $T_{eff}$ < 3000 K, gravities 0 < log g < 1, and abundances -1 < [Fe/H] < + 0.5, and fitted to infrared spectra of RS Oph as it returned to quiescence after its 2006 eruption. Pavlenko et al (2007) modelled the infrared spectrum in the range $1.4 - 2.5\mu$m to determine metallicity and effective temperature of the red giant. This allows us to refine both parameters from analysis of the best fits of the synthetic spectra to the observed spectrum of RS Oph .

We found, that the slopes of the spectral energy distribution (SED) and the intensity of molecular bands in the modelled spectra depend on both $T_{eff}$ and [Fe/H]. This allows us to determine $T_{eff}$ = 3800 $\pm$ 100 K, $\log g$ = 1.0 $\pm$ 0.5, [Fe/H] = 0.0 $\pm$ 0.5, [C] = $-0.4$, [N] = +0.9 in the atmosphere of the secondary, together with a degree of 'veiling' in the observed spectra; it is not clear at this stage whether the 'veiling' is due to dust in the environment of RS Oph or to inadequate atmospheric cancellation (see Pavlenko et al 2007 for more details).

*Acknowledgements.* This work was supported by an International Joint Project Grant from the UK Royal Society and the "Microcosmos" program of the National Academy of Sciences and Space Agency of Ukraine. I thank Drs. N.Evans (Keele University), G.Duerbeck(Open University), T.Geballe (Gemini), L.Yakovina(MAO NASU), B.Kaminsky(MAO NASU), T.Kerr(JAC, Hilo) for the collaboration and assistance in my investigations.

**Reference**

Anders E., Grevesse N.: 1989, *GeGoAA*, **53**, 197.
Asplund M., Lambert D.L., Kipper T. Pollacco D., Shetrone M.D.: 1999, *A&A*, **343**, 507.
Brown N.J.: 2002, *IAU Circ*, 7785.

Crause L.A., Lawson W.A., Kilkenny D., Van Wyk F., Marang F., Jones A.F.: 2003, *MNRAS*, **341**, 785.
Desidera S., Munari U.: 2002, IAUC7982.
Dürbeck H.W., Benetti S.: 1996, *ApJ*, **307**, L111.
Evans A., Geballe T.R., Rushton M.T., Smalley B., van Loon J.Th., Eyres S.P.S., Tyne V.H.: 2003, *MNRAS*, **343**, 1054.
Hauschildt P.H., Allard F., Baron E.: 1999, *ApJ*, **512**, 377.
Kaminsky B.M., Pavlenko Y.P.: 2005, *MNRAS*, **357**, 38.
Kimeswenger S., Ledercle C., Schmeja S., Armsdorfer B.: 2002, *MNRAS*, **336**, L43.
Kipper T., Klochkova V.G., Annuk K. et al.: 2004, *A&A*, **416**, 1107.
Kurucz: 1993, *CD ROM 9, 18*, Harvard-Smisthonian Observatory.
Kurucz R.L.: 1999, *http://kurucz.harvard.edu.*
Munari U., Henden A., Kiyota S. et al.: 2002, *A&A*, **389**, L51.
Munari U. et al.: 2005, *A&A*, **434**, 1107.
Nakano S., Sakurai Y. et al.: 1996, *IAU Circ.*, 6322.
Pavlenko Y.V., Yakovina L.A.: 1994, *Astron. Rep.*, **38**, 768.
Pavlenko Y.V.: 1997, *Astron. Rep.*, **41**, 537.
Pavlenko Ya.V., Yakovina L.A., Duerbeck H.W.: 2000, *A&A*, **354**, 229.
Pavlenko Ya.V. & Duerbeck H.W.: 2001, *A&A*, **367**, 933.
Pavlenko Ya.V., Geballe T.R.: 2002, *A&A*, **390**, 621.
Pavlenko Ya.V., Jones H.R.A.: 2002, *A&A*, **396**, 967.
Pavlenko Ya.V.: 2003, *Astron. Rep.*, **47**, 59.
Pavlenko Ya.V., Geballe T.R, Evans A., Smalley B., Eyres S.P.S., Tyne V.H., Yakovina L.A.: 2004, *A&A*, **417**, L39.
Pavlenko Ya.V., van Loon J. Th., Evans A., Rushton M.T., Kaminsky B.M., Filippenko A.V., Foley R.J., Li W., Smalley B., Yakovina L.A.: 2006, *A&A*, **460**, 245.
Pavlenko Y., Kaminsky B., Lyubchik Y., Yakovina L.: 2007, *ASPC*, **363**, 225.
Pavlenko Ya.V., Evans A., Kerr T., Yakovina L., Woodward C.E., Lynch D., Rudy R., Pearson R.L.: 2007, *A&A* submitted.
Sneden C., Ivans I.I., Kraft R.P.: 2000, *MmSAI*, **71**, 657.
Rushton M.T., Geballe T.R., Filippenko A.V., Chornock R., Li W., Leonard D.C., Foley R.I., ERvans A., Smalley B., van Loon J., Euras S.P.S.: 2005, *MNRAS*, **360**, 1281.
Tylenda R.: 2005, *A&A*, **436**, 1009.
Wagner R.M., Starrfield S.G.: 2002, *IAUC*, **7992**, 2.
Wallerstein G., Harrison T., Munari U.: 2006, *BAAS*, **38**, 1160.

# SPECTRAL VARIATION OF Be HERBIG STARS

L.A. Pavlova, L.N. Kondratyeva, R.R. Valiullin

Fessenkov Astrophysical Institute,
Observatory, Almaty 050020 Kazakhstan, *lara@aphi.kz lu_kondr@mail.ru*

ABSTRACT. We researched the characteristic time scales and amplitudes of the variability of H$\alpha$ emission and intrinsic polarization of Be Herbig stars: VY Mon, LkH$\alpha$215 and HD 259431. The change of H$\alpha$ profiles as PCyg - PCygIII - single-peaked was revealed in the spectrum of VY Mon. Such transformation is widely accepted to be formed in stellar wind. The double H$\alpha$ profiles of LkH$\alpha$215 and HD 259431 reflect the presence of the rotating disk-like envelope with signs of outflow and infall of matter.

**Key words**: Stars: Be Herbig stars: individual: VY Mon, LkH$\alpha$215 and HD 259431

## 1. Introduction

The high resolution studies of emission line profiles of young AeBe Herbig (HAeBe) stars offer the possibility to understand the structure and the physical conditions in the line-emitting regions. The strongest evidence for a disk-like structure around HAeBe comes from the near-IR and millimeter interferometry. The H$\alpha$ spectropolarimetric observations show traces of dust at the distances of tens of stellar radii (Vinc et al., 2002). Emission line intensities and continuum excesses in the UV may be connected with a level of accretion activity, NIR excesses - with the hot inner disk, millimeter and sub-millimeter excesses - with cold dust in an outer disk. The long-term study of the profile variations can provide a definition of a nature of young stars and the structure of their envelopes.

The emission profiles of H$\alpha$ can be classified as double, single or P Cyg. It is known that in spectra of some stars H$\alpha$ profiles can change from one type to another, but a moment of such transformation is unpredictable because of irregularity of these events.

Variability is mainly revealed in change of the bluer wing and the central peak. A scale of variability is from a few hours up to an year. The presence of P Cyg profile of H$\alpha$ is widely accepted to be the result of the stellar wind. The double profile is explained by the presence of a rotating disk-like envelope with signs of outflow and infall matter of envelope.

We researched the characteristic time scales and amplitudes of H$\alpha$ variability and the intrinsic polarization of the following stars: VY Mon, LkH$\alpha$215 and HD 259431.

## 2. Individual objects

**VY Mon** - the very young star (O9e -B8e) with a large IR excess, ($A_v$=8.7mag, P=10%). It's H$\alpha$ profile changes from PCyg to PCygIII and to single-peaked type. When star is seen as bright, it shows a PCyg profile, when it becomes weaker, an additional blue emission appears, forming a PCygIII profile. And then it turns into a single peak. We received, that PCyg velocity can vary from -62km/s up to -340km/s during 8 months. We have derived the systematic shifts of the main emission centre as: +62km/s, +120km/s, +140km/s for the profiles PCyg, PCygIII and single-peaked, correspondingly. The last observations showed the change of H$\alpha$ profile type from PCygIII (December, 2006) to PCyg (January, 2007). But variations of the central peak intensity relatively to continuum and fluctuations of the red edge of the line were weak.

All three types of the profile can be explained by the models of anisotropic stellar wind with a variable terminal velocity. Cidale and Ringuelet, (1993) showed, that the different velocity gradients at the onset of the wind can result the transformation of an emission profile from single-peaked into PCyg and into double-peaked in order of decreasing velocity gradients.

Polarimetric measurements provided the study of a nature and geometry of the circumstellar matter. Stellar radiation will be affected by an intrinsic polarization only if a distribution of the scattering matter is not spherically symmetric. The existence of circumstellar dust is supported by large values of an intrinsic polarization. We received the polarization data in the B band for 17 stars in Mon RI (Pavlova, Rspaev 1985). Following estimations of the interstellar contribution in this direction were derived: $P_{is}$=0.9%, $\Theta_{is}$=162$^o$. The Stokes parameters U=Psin2$\Theta$ and Q=Pcos2$\Theta$ for the intrinsic polarization were determined as $U_{in}$= U*-$U_{is}$, $Q_{in}$ =Q* - $Q_{is}$. The intrinsic polarization degree $P_{in}$ and position angle $\Theta_{in}$ were evaluated:

$$P_{in} = \sqrt{U_{in}^2 + Q_{in}^2}$$

$$\Theta_{in} = \frac{1}{2} \arctan \frac{U_{in}}{Q_{in}}$$

Then for VY Mon $P_{in}$=10.3% and $\Theta_{in}$=22$^o$. A polarization vector may be parallel or perpendicular relatively to a disk plane. Thus one may expect a correlation between a polarization angle and a direction of jets and outflows or disk orientation.

**LkH$\alpha$215 (B1e-B7e) and HD259431 (B6pe)** have very broad double H$\alpha$ profiles, which reveal a rotating star/disk configuration. The double-peaked H$\alpha$ emissions in spectra of these stars have the constant separations: 173km/s for LkH$\alpha$215 and 96 km/s for HD259431, while the relative intensities of red and blue peaks are variable. We discovered, that in the spectrum of HD259431 the bluer peak became smaller than the red one during 2005, although the earlier observational data have always shown a reverse picture. The relative intensities of the red and blue peaks may change according to an action of the outflow and infall mechanisms in disk/envelope matter.

The velocities of the central absorptions vary from -35km/s to +58km/s for LkH$\alpha$215 and from +18km/s to +32km/s for HD259431. These variations may be connected with a variable thickness of an asymmetric disk-like envelope. The observational data of Fernandez et.al., (1995) show that VV Ser (B5) also has a constant separation of a double-peaked H$\alpha$, about 230 km/s with the variable intensities of the peaks. A deep central absorption testifies that an equatorial tours of obscuring material can be thick and close to the line of sight.

The following estimations of the intrinsic polarization were obtained for LkH$\alpha$215: are $P_{in}$=2.33 - 1.68% $\Theta_{in}$=80 - 78$^o$ and for HD259431: $P_{in}$=2.09% $\Theta_{in}$=93$^o$. An orientation of a polarization vector for an optically thick disk may by parallel to a disk plane, then orientation of a disk of such an object is perpendicular to the Galactic plane ($\Theta_{gal}$ =165$^o$). This situation may be consider as a main attribute of an youth of an object.

### References

Cidale L.S., Ringuelet A.E.: 1993, *Ap.J.,* **411**, 874.
Fernandez M. et. al.: 1995, *A&ASS,* **114**, 439.
Pavlova L., Rspaev F.: 1985, *Astrophysika,* **23**, 521.
Vink J., Drew J.: 2002, *MNRAS,* **337**, 356.

# CIRCUMSTELLAR ACTIVITY OF THE HERBIG AE STAR HD163296

M.A. Pogodin[1], M.M. Guimaraes[2], S.H.P.Alencar[2], W.J.B.Corradi[2], S.L.A.Vieira[3]

[1] Pulkovo Observatory, St.Petersburg 196140, Russia, *pogodin@gao.spb.ru*
[2] UFMG, Belo Horizonte 30123-970, MG, Brazil
[3] Centro Univeritario UNA, Belo Horizonte 30455-590, MG, Brazil

ABSTRACT. We present new results of a high-resolution spectroscopic investigation of the young Ae Herbig star HD 163296. Nineteen spectra of this object had been obtained on May 8 - 10, 2002 at the ESO with the FEROS echelle spectrometer installed at the 1.52m telescope. Striking profile variability has been found in a number of lines originating in the stellar wind. Analysis of the variability revealed manifestation of a layered spatial structure of the wind zone containing layers of preferable generation of local inhomogeneities in the outflowing gas. Correlation between different spectral parameters corresponding to infall and outflow gaseous streams evidence in favour of the physical interdependence between the accretion and the mass loss processes in the circumstellar envelope.

**Key words**: Stars: pre-main sequence: circumstellar matter; stars: individual: HD 163296

## 1. Introduction

The emission line star HD 163296 (B9Ve-A2Ve) was first classified as a young Herbig Ae/Be star by Finkenzeller & Mundt (1984). Afterwards it became a subject of detailed study. The spectrum of the star demonstrates signatures of an intense stellar wind. High-resolution spectroscopic investigations have shown a complex picture of the variability observed in numerous circumstellar (CS) lines. It was interpreted in terms of the long-lived spatial inhomogeneities rotating in the CS envelope (Baade & Stahl 1989, Catala et al. 1989, Pogodin 1994, Beskrovnaya, Pogodin et al. 1998). The study presented here was aimed at further investigation of CS peculiarities of HD 163296 using new data obtained with a high-resolution echelle spectrometer.

## 2. Observations

Nineteen high-resolution (R=48000) spectra of HD 163296 were obtained on May 8-10, 2002 with the FEROS echelle spectrometer installed at the 1.52m telescope of ESO (La Silla, Chile).

Collection of all spectra is presented in the Table. The signal-to noise ratio ($S/N$) at the continuum level for all spectra was from 100 to 200 depending on spectral region.

Table 1: The UT of mid-exposure.

| May 8 | May 9 | May 10 |
|---|---|---|
| $02^h\ 57^m\ 08^s$ | $02^h\ 58^m\ 53^s$ | $02^h\ 30^m\ 58^s$ |
| $04^h\ 33^m\ 08^s$ | $03^h\ 57^m\ 57^s$ | $03^h\ 54^m\ 41^s$ |
| $08^h\ 25^m\ 36^s$ | $05^h\ 08^m\ 17^s$ | $05^h\ 26^m\ 15^s$ |
| $09^h\ 09^m\ 20^s$ | $06^h\ 23^m\ 35^s$ | $06^h\ 40^m\ 46^s$ |
| $10^h\ 31^m\ 51^s$ | $07^h\ 54^m\ 45^s$ | $08^h\ 11^m\ 51^s$ |
| | $09^h\ 09^m\ 08^s$ | $09^h\ 21^m\ 19^s$ |
| | $10^h\ 10^m\ 15^s$ | $10^h\ 20^m\ 00^s$ |

## 3. Results

The results of our investigation are illustrated in Figs.1-6. The radial velocity scale used in the graphs is given in the reference frame connected with the star. The synthetic photospheric profiles calculated with the use of the Piskunov's code SYNTH+ROTATE (Piskunov 1992) are also presented for comparison. The atmospheric model parameters (Teff = $9400^o$K, $\log g = 4.1$, Fe/H = 0.5, $V \sin i = 130$ km/s) were taken from Guimaraes et al. (2006).

The analysis of the obtained results allowed us to draw the following conclusions:

1. During the first observing night (May 8) the Balmer lines display emission profiles with the blue wing overlapped by several local absorptions (Fig.1, *left*). In the following nights these features were decreasing in deepness, and the profiles became double-peaked (Fig1, *right*).

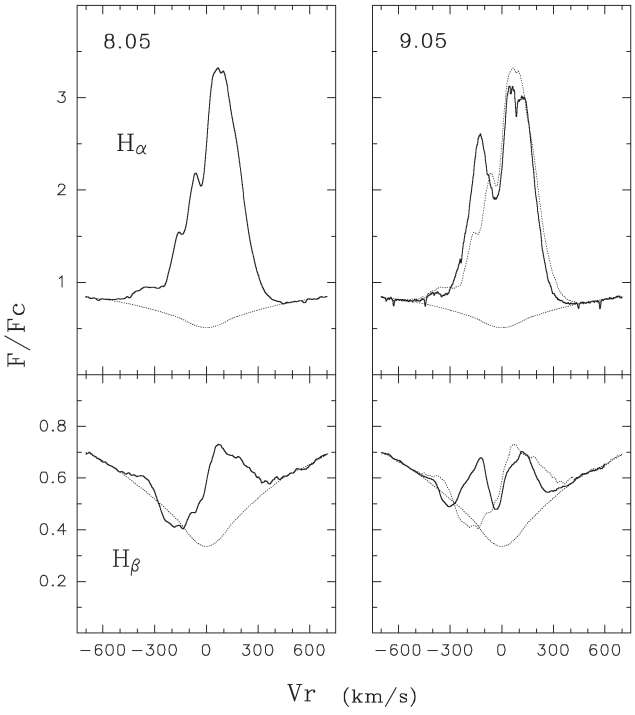


Figure 1: Normalized H$\alpha$ and H$\beta$ profiles obtained at the beginning of night on May 8 and May 9.

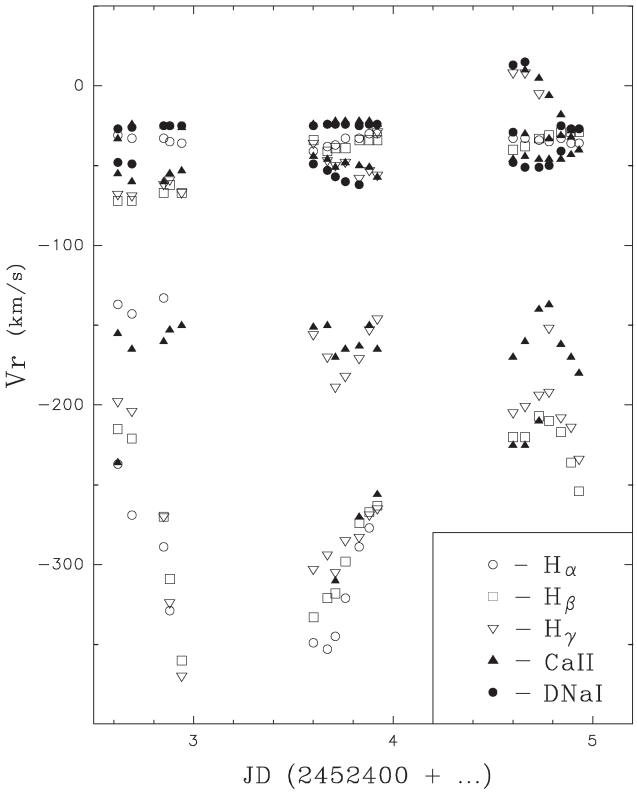


Figure 3: The temporal run of radial velocities of all local absorptions originating in the stellar wind and observed in different lines.

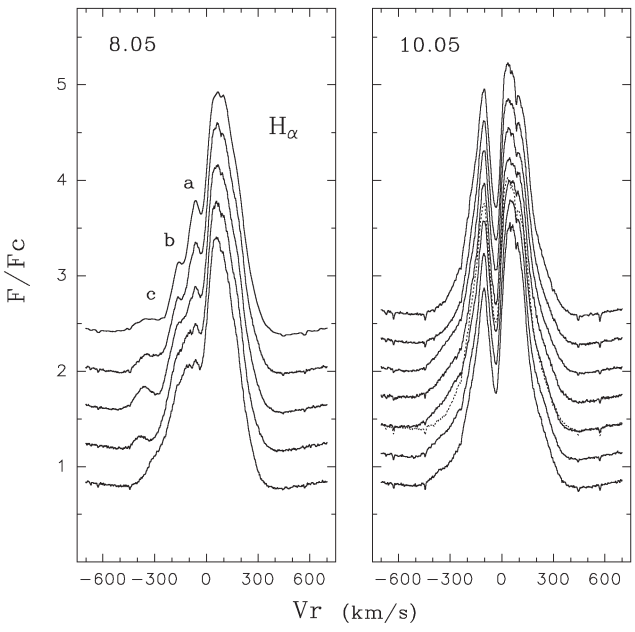


Figure 2: Rapid variability of H$\alpha$ profile observed on May 8 and May 10. Time increases from top to bottom.

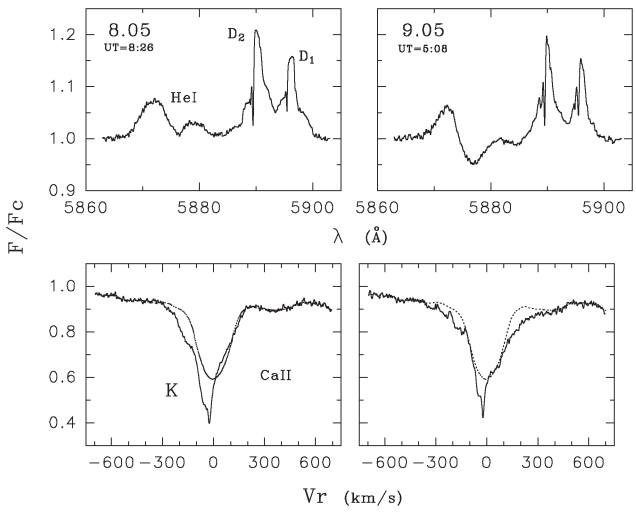


Figure 4: Typical profiles of the HeI, DNaI and CaII K lines in the spectrum of HD 163296.

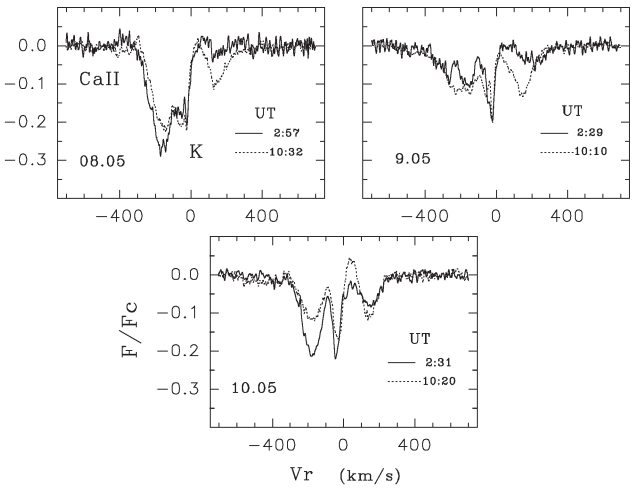


Figure 5: Typical residual profiles of the CaII K line in the spectrum of HD 163296, obtained by subtracting the photospheric component from the entire profile and demonstrating clearly separated CS profile components.

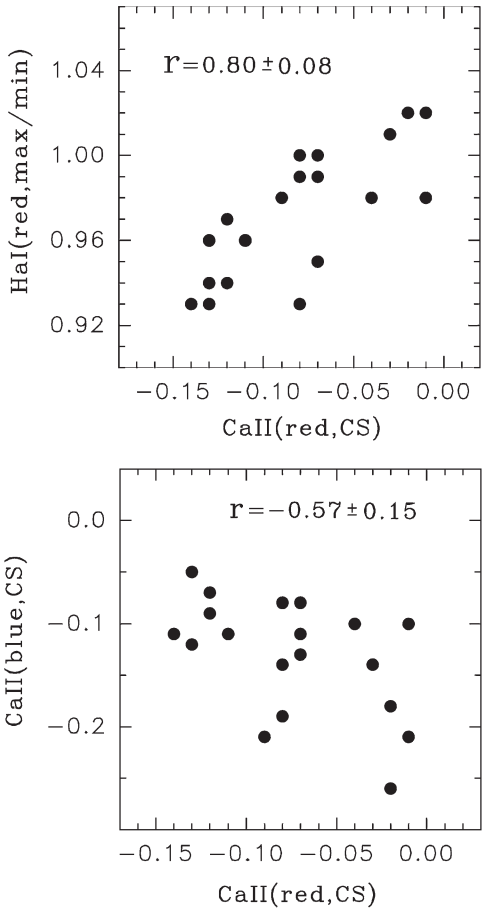


Figure 6: Correlation between the intensity in the visual extremum of the red local feature of the HeI profile and of the red absorption in the residual CaII K profile (*top*). The lower graph illustrates the correlation between the intensity of the blue (at Vr = -140 km/s) and the red (at Vr = +140 km/s) CS absorption in the residual CaII K profiles.

Fig.2 demonstrates the rapid H$\alpha$ variability observed during a night. One can see that the lifetime of separate local features are of several hours. Such character of variations is typical for a stellar wind containing spatial inhomogeneities.

2. The analysis of radial velocity temporal runs of all local absorptions originating in the outflowing matter and observed in different lines shows that at least four variable components can be separated with larger amplitude of variations seen in a component with larger negative velocity (Fig.3). The duration of the observing run was not long enough to conclude with certainty on periodicity. But it is much longer than the expected lifetime of separate local absorptions. Therefore, the observed variability is hardly to be a result of rotational modulation by single long-lived azimuthal inhomogeneities. It is more likely to be a consequence of a layered spatial structure of the stellar wind, which can contain layers of preferential generation of dense outflowing gas. Such structure can be connected with a specific configuration of the global magnetic field in the region of interaction between the star and the accretion disk which must control the mass loss process (Pogodin et al., 2005).

3. The HeI line (at 5876 Å) profile displays a two-component structure with a blue emission peak and the very variable red part which is observed sometimes in absorption and sometimes in emission (Fig.4, *top*). These components are connected with different CS regions: the base of the stellar wind and the accretion flow, correspondingly. The optical depth of the wind is much smaller than one of the infalling gas, and, in contrast to the accreted matter, the wind is transparent in the HeI line.

3. These two CS features are also displayed in the resonance CaII K line (Fig.4, *bottom*). Fig.5 illustrates typical CaII K residual profiles obtained by subtracting the photospheric component from the entire profile. The blue absorption, corresponding to the outflowing gas, and the red local feature, forming in the infalling matter are clearly separated. Additionally, a central narrow absorptions originating in the remote wind is also observed. In contrast to the HeI line, the stellar wind base is not transparent in the CaII K line.

4. Fig.6 (*top*) shows the well-defined correlation (r = 0.85±0.08) between intensities in the red local features in the CaII K and HeI $\lambda$5876 Å profiles, that confirms their common origin in the accretion flow. An appreciable correlation (r = -0.57±0.15) has been also found between the intensity in the blue (Vr = -140 km/s) and the red (Vr = +140

km/s) wings of the CS CaII K line profile. This indicates a possible connection between the accretion process and the mass loss in the envelope of HD 163296.

**References**

Baade D.,Stahl O.: 1989, *A&A* **209**, 268.
Beskrovnaya N.G., Pogodin M.A., Yudin R.V., et al.: 1998, *A&AS* **127**, 243.
Catala C., Simon T., Praderie F., et al.: 1989, *A&A* **221**, 273.
Finkenzeller U., Mundt R.: 1984, *A&AS* **55**, 109.
Guimaraes M.M., Alencar S.H.P., Corradi W.J.B., et al.: 2006, *A&A* **457**, 581.
Piskunov N.E.: 1992, *Stellar Magnetism*, 92.
Pogodin M.A.: 1994, *A&A* **282**, 141.
Pogodin M.A., Franko G.A.P., Lopes D.F.: 2005, *A&A* **438**, 239.

# ON QUASI–PERIODIC INTRINSIC LIGHT VARIABILITY IN A CLOSE SPECTROSCOPIC BINARY CX DRA

I. Pustylnik[1], P. Kalv*[2],V. Harvig[1,2] T. Aas[2]

[1] Tartu Observatory, Estonia
*izold@aai.ee*
[2] Tallinn Observatory, Tallinn University of Technology

ABSTRACT. Quasi–periodic light variations of bright spectroscopic emission-line binary CX Draconis were discovered based on observations at Tallinn Observatory in 1981-1990.

**Key words**: Stars: binary; stars: individual: CX Dra.

## 1. Introduction

CX Draconis is long known as a bright star whose spectra display bright hydrogen lines (Merrill and Burwell 1943).

Lacoarret (1965) found that the star displays variations of the ratio V/R of the emission lines and variations of the ratio E/C of the intensity of this emission to that of the adjacent continuum. The star shows variations of $H_\alpha$ profile with a period of about 7 days, while the E/C variation has been estimated as having a cycle of 3 years.

Merlin (1975) found that this star displays variations in $U$,$B$,$V$ larger than $0\overset{m}{.}1$ but shows no true periodicity. Harmanec et al. (1981) called for systematic observations of the object. Guinan et al. (1984) discovered from observations with HEAO 2 Einstein Observatory, that CX Dra is moderately strong X-ray source. Horn et al. (1992) found the orbit parameters for both components.

Šimon (1996) found parameters for both components: a detached primary (B2.5V, $7.3M_\odot$, $4R_\odot$) and a secondary (F5III, $1.7M_\odot$) probably filling in its Roche lobe. The inclination angle $i$=50°. The equatorial rotational velocity of the primary 210 km/s is highly asynchronous. Emission lines of $H_\alpha$ and HeI 6678Å, were analysed. The V/R ratio of the double peaked emission in the original spectra of $H_\alpha$ smoothly varies with the orbital phase. The difference profiles constructed by subtracting the synthetic spectra of both components from the observed spectra enabled studying the non–photospheric emission (presumably originating in the circumstellar matter). The non–photospheric emission in $H_\alpha$ is interpreted in terms of two distinct components. The broad part following the RV curve of the primary belongs probably to the accretion disk while the other component (narrow peak) cannot be linked with any star. The velocity field of the narrow peak offers a possibility that this feature is connected with the mass stream. The broad double–peaked emission attributed to the accretion disk around the hot primary is visible also in HeI 6678Å. The temperature of the disk must therefore correspond at least to 11000-12000 K and this disk is significantly hotter than in most other Algol–type systems. Conspicuous secular changes of the emission in HeI 6678Å, were revealed. The analysis presented by them led to the conclusion that the Be phenomenon in CX Dra can be explained by the mass transfer in the interacting binary. An extensive collection of spectroscopic observations of CX Dra spanning a 23 year interval have been analyzed by Richards et al. (2000). Their analysis includes a refinement of the orbital solution of CX Dra; equivalent width measurements that show short-, medium-, and long-term behavior of the difference profiles; a calculation of the Balmer decrement; velocity maps based on the velocity curves of the $H_\alpha$ and HeI difference emission peaks; trailed spectrograms of the $H_\alpha$, $H_\beta$, HeI, and SiII lines; and Doppler tomograms at these four wavelengths. The main conclusions by Richards et al. (2000) are:

1. The circumstellar environment in the system changes in cycles of hundreds of days. The length of the cycles is variable. These cycles may be part of a "super" 4000 day cycle.

2. The equivalent widths of the difference $H_\alpha$ and HeI 6678 lines are modulated with the orbital period of $P_{\rm orb} = 6.696$ days.

Berdyugin and Piirola (2002) find from their *UBVRI* polarization measurements that the time scale of several weeks polarization variations clearly correlate with the binary orbital motion and long term changes in polarization are seen in the course of several months. From analysis of the periodic component of polarization they found orbital inclination ($i$∼73°)

*P.Kalv–Author deceased (1934-2002).

which is substantially higher than values previously reported. Their two datasets obtained about 9 months apart reveal significant changes in the distribution of the scattering material of the circumbinary envelope.

## 2. Observations

CX Dra was observed with the Tallinn 50-cm telescope (from 1981, up to 1990 in total 112 nights in *UBVR*). The root–mean–square errors of the normal points, as calculated from the measurements of comparison and the check stars, are less than $0\overset{m}{.}004$ for $V$, $B$-$V$ and $V$-$R$, in $U$ may reach up to $0\overset{m}{.}006$. It took 30-40 minutes to get one normal point, depending on the weather conditions. The data of CX Dra, comparison, check and red standard stars are given in Table 1.

Table 1: CX Dra and standard stars

| Star | | Sp. | $V$ | $B$-$V$ | $U$-$B$ |
|---|---|---|---|---|---|
| CX Dra | HD 174237 | B5 | 5.9 | | |
| comp. | HD 173664 | A2 | 6.19 | 0.08 | 0.13 |
| check | HD 172883 | B9 | 5.99 | -0.07 | -0.23 |
| red std. | HD 175225 | G8 | 5.50 | 0.84 | 0.52 |

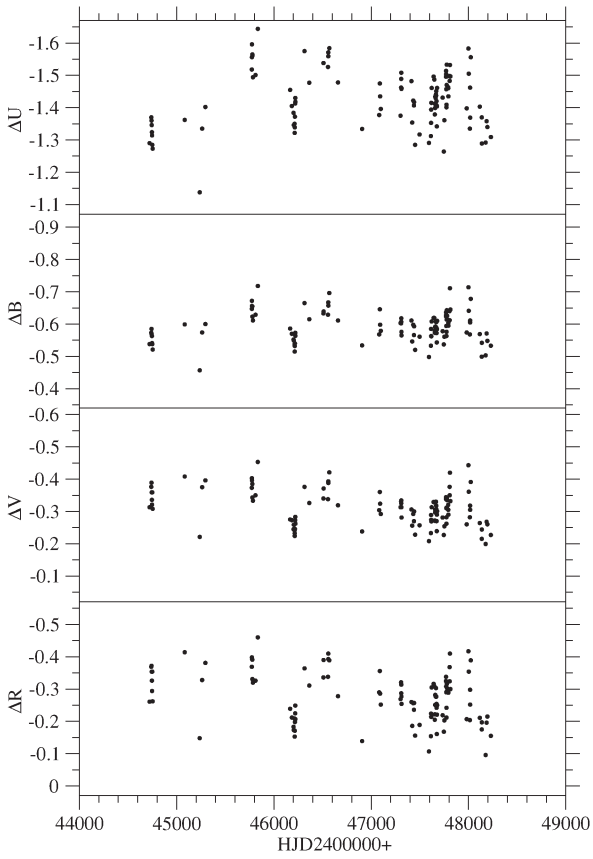


Figure 1: Time diagram for CX Draconis

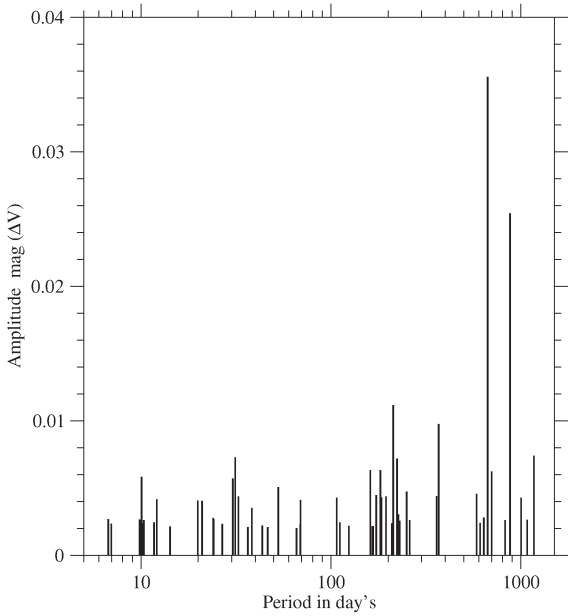


Figure 2: Time–series spectrum of the CX Draconis found by using the CLEAN algorithm (Roberts et al., 1987)

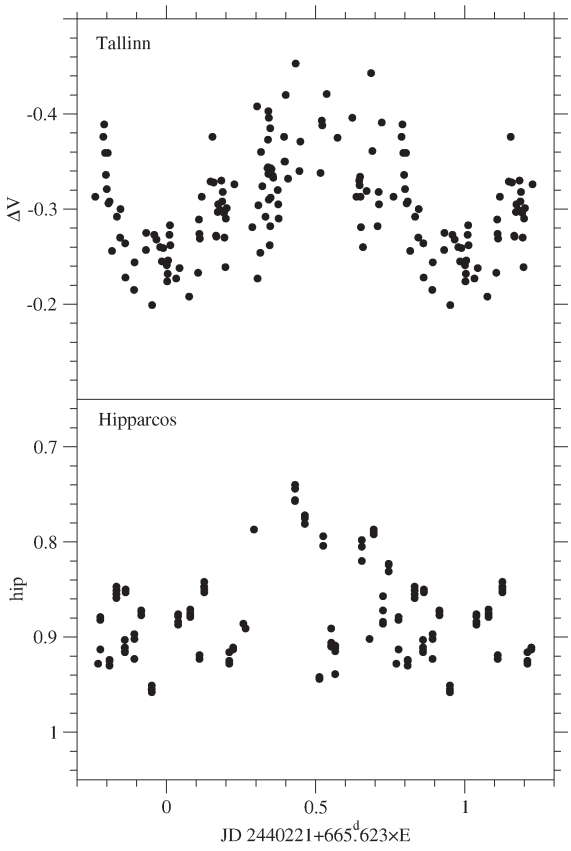


Figure 3: Phase diagram for CX Draconis: upper graph JD 2444721-2448230 and bottom graph JD 2447892-2449050

All measurements have been reduced to the Johnson's system and are available in Kalv et al. (2004) and indicated in Figure 1. The observations were carried out at Tallinn Observatory (former observational station of Tartu Observatory and now is the educational observatory of Tallinn University of Technology). The photoelctric photometers were attached to the Cassegrain focus of the 48 cm reflector AZT-14A (d/f=16).

Photomultiplier Tubes used:

1. EMI 9502B from JD 2439430 to JD 2444000
2. EMI 9502SA
   (a) from JD 2444100 to JD 2444317
   (b) from JD 2445500 to JD 2450220
3. FEU-79 from JD 2444317 to JD 2445000

Filters:

1. B BG–12 + GG–13 (1mm+2mm)
   V GG–11 (2mm)
2. U UG–2 (2mm)
   B BG–12 (1mm)
   V GG–11 (2mm)
   R Photographic
3. U UG–2 + SZS–21 (2mm+3mm (for red leak))
   B BG–12 + SZS–21 (1mm+3mm)
   V GG–11 + SZS–21 (2mm+3mm)
   R Interference Filter $H_\alpha \pm 450$Å
   $H_\alpha$ Interference Filter $H_\alpha \pm 45$Å

As only differential observations of variable stars relative to a comparison stars are made in Tallinn, attention was given to the determination of the mean extinction coefficients. Among several methods of the determination of extinction the differential method (Hardie 1962) is the most suitable for our purposes.

The generic formulae for reductions of observations are:

$$\Delta(U-B) = [\Delta(u-b) - k'_{u-b} \times \Delta X] \times C_1$$
$$\Delta(B-V) = [(1+k''_{b-v} \times \overline{X}) \times \Delta(b-v) - k'_{b-v} \times \Delta X] \times C_2$$
$$\Delta V = \Delta v - k'_v \times \Delta X - C_3 \times \Delta(B-V)$$
$$\Delta(V-R) = [\Delta(v-r) - k'_{v-r} \times \Delta X] \times C_4$$

And the coefficients in formulae above are:

| | JD 2439430–2444000 | JD 2444100–2444317 JD 2445500–2450220 | JD 2444317–2445000 |
|---|---|---|---|
| $k'_{u-b}$ | | 0.26 | 0.32 |
| $k'_{b-v}$ | 0.20 | 0.20 | 0.18 |
| $k'_v$ | 0.36 | 0.36 | 0.24 |
| $k'_{v-r}$ | | 0.11 | 0.11 |
| $k''_{b-v}$ | 0.05 | 0.05 | 0.04 |
| $C_1$ | | 1.19 | 1.12 |
| $C_2$ | 1.19 | 0.94 | 1.00 |
| $C_3$ | 0.07 | 0.09 | 0.11 |
| $C_4$ | | 1.09 | 1.09 |

## 3. Discussion of results

CX Draconis is relatively well observed for tens of years and the spectral observations of different investigators are in rather good agreement. At same time almost every photometric study gives the new significantly different results. To find period of light variations we used Roberts et al. (1987) time–series spectral analysis CLEAN algorithm. In time of our observation the quasi–period of intrinsic variations of light was about 665.6 days.

*Acknowledgements.* Financial support of this investigation by a Grant No. 5760 of the Estonian Science Foundation is acknowledged.

## References

Berdyugin A., Piirola V.: 2002, *A&A*, **394**, 181.
Guinan E.F., Koch R.H., Plavec M.J: 1984, *ApJ*, **282**, 667.
Hardie R.H., 1962, Astronomical Techniques, ed. W.A. Hiltner, University of Chicago Press, p.178
Harmanec P., Horn J., Koubsky P.: 1981, *IBVS*, **1931**, 1.
Hipparcos Catalogue Epoch Photometry Data HIP 92133
Horn J., Hubert A.M., Hubert H., Koubsky P., Bailloux N.: 1992, *A&A*, **259L**, L5.
Kalv P., Aas T., Harvig V.: 2004, *Tallinn Obs.,* **3, 2**, 55.
Lacoarret M.: 1965, *AnAp*, **28**, 321.
Merlin P.: 1975, *A&A*, **39**, 139.
Merrill P.W., Burwell C.G.: 1943, *ApJ*, **98**, 153.
Richards M.T., Koubsky P., Šimon V., Peters G., Hirata R., Škoda P., Masuda S.: 2000, *ApJ*, **531**,1003.
Roberts D.J., Lehar J., Dreher W.: 1987, *AJ*, **93**, 968.
Šimon V.: 1996, *A&A*, **308**, 799.

# ON THE EVOLUTIONARY HISTORY OF PROGENITORS OF EHBS AND RELATED BINARY SYSTEMS BASED ON ANALYSIS OF THEIR OBSERVED PROPERTIES

V.-V. Pustynski[1], I. Pustylnik[2]

[1] Tartu Observatory
Tõravere 61602, Tartumaa, Estonia, *e-mail:vladislav@aai.ee*;
Tallinn University of Technology
Ehitajate tee 5, Tallinn 19086, Estonia

[2] Tartu Observatory
Tõravere 61602, Tartumaa, Estonia, *e-mail:izold@aai.ee*

ABSTRACT. It has been shown quite recently (Morales-Rueda *et al.*, 2003) that dB stars, extreme horisontal branch (EHB) objects in high probability all belong to binary systems. Assuming that the progenitors of EHB objects belong to the binaries with initial separations of a roughly a hundred solar radii and fill in their critical Roche lobes when being close to the tip of red giant branch, we have found in our earlier study that considerable shrinkage of the orbit can be achieved due to a combined effect of angular momentum loss from the red giant and appreciable accretion on its low mass companion on the hydrodynamical timescale of the donor, resulting in formation of helium WD with masses roughly equal to a half solar mass and thus evading the common envelope stage. Far UV upturn phenomenon discovered in elliptical galaxies and spiral galaxy bulges was interpreted in terms of predominant contribution from EHB objects (Dorman, O'Connell, Rood, 1995). This circumstance can provide a reasonable constraint on the initial masses of EHB progenitors and thus the ages of EHB objects.

**Key words**: Stars: binaries: close.

## 1. Introduction

Underluminous sdB stars are thought to be helium burning stars with very low mass hydrogen envelopes. Effective temperatures ($> 25\,000\,K$) and surface gravities ($\log g > 5$) place them on EHB, i.e. they appear in the same region of $T_{\rm eff} - \log g$ plane as evolutionary tracks for core He burning with core masses of about $0.5\,M_\odot$ and extremely thin ($\leq 0.02\,M_\odot$) inert hydrogen envelopes. It is currently accepted that EHBs form due to enhanced mass loss on the RGB when the degenerate helium core loses almost all hydrogen convective envelope close to the RGB tip but the core goes on to ignite helium despite dramatic mass loss and may appear as sdB star. Quite recently it has been discovered that most of EHBs are components of binary systems with orbital periods $P_{\rm orb} \sim 0^{\rm d}.12 \div 27^{\rm d}$ in pair with MS low mass companion. In our earlier study of evolution of the orbit resulting in formation of EHBs when the donor star being close to the tip of RGB fills in its critical Roche lobe and enhanced mass loss and angular momentum loss ensues we restricted our analysis for initial donor masses slightly less than one solar mass (Pustynski & Pustylnik, 2007). Here we extend our treatment assuming that initial mass of progenitor can be somewhat higher, up to $M_1 = 1.25\,M_\odot$. According to (Dorman, O'Connell, Rood, 1995) the ages of globular clusters and elliptical galaxies where EHBs are observed range between 6 and 11 Gyrs. We have found similarly to our earlier findings that with an enhanced mass loss rate (roughly by a factor of 2) compared to a standard rate predicted by Reimers formula during the RGB evolutionary stage. Evolution of the He burning core proceeds smoothly being virtually independent of the properties of an inert low mass hydrogen convective envelope. Below we briefly describe our method of analysis and discuss the implications for the evolutionary history of EHBs.

## 2. Analysis of mass loss, mass transfer and angular momentum loss

To clarify the nature of the EHB progenitors, we have calculated evolution of orbit of a binary assuming that a progenitor of sdB star filled in its critical Roche

lobe when the former during its nuclear evolution was approaching the tip of RGB. We used (Hurley, Pols, Tout, 2000) computer code *sse.f* to follow evolution of the primary until the donor approached its critical Roche lobe. Once the donor fills in its Roche lobe, subsequent evolution depends on the relation between the primary radius $R_1$ and Roche lobe radius $R_L$. If, for instance, the donor reacts to mass loss and mass transfer by further expanding its envelope while the radius of the critical Roche lobe decreases, a considerable shrinkage of the orbit can be expected even on the dynamical timescale $\delta t \sim 10^4\ yrs$. We computed period change caused by mass loss from the system, mass interchange and additional angular moment loss $K = \dot{J}/J$ by matter corotated at the Alfven radius $R_{\rm A}$:

$$K = \frac{2}{3}\, k^2 \left(\frac{R_A}{d}\right)^2 \frac{M}{M_1\, M_2}\, \dot{M}\ , \qquad (1)$$

where $k = R_A/R_1$, $d$ is the semi-major axis of orbit (Tout & Hall, 1991). Mass loss rate by the donor is defined by the Roche lobe overfilling $\Delta R = R_1 - R_L$ as

$$\dot{M}_1 = \frac{M_1}{t_{HD}} \left(\frac{\Delta R}{R_L}\right)^3\ , \qquad (2)$$

$t_{HD} \sim R_1/V_{\rm s}$ being hydrodynamical timescale. To avoid $t_{HD}$ calculation that requires knowledge of temperature-dependent sound velocity $V_{\rm s}$, we introduce free fall timescale $t_{ff} \sim R_1/V_{\rm esc}$ and, using the fact that escape velocity $V_{\rm esc} \gg V_{\rm s}$, we set $t_{HD} \simeq 100 \cdot \sqrt{R_1^3/GM_1}$ avoiding unphysically high mass loss rates; in our case typically $t_{HD} \sim (10^5 - 10^6)\ sec$ which is roughly one order magnitude shorter than donor's thermal timescale. Roche lobe radius $R_L$ is found from the empirical fit of (Eggleton, 1983). Mass accretion rate is set by a predefined value of mass transfer effectiveness parameter $Q = \dot{M}_2/\dot{M}$. The increment of the sellar radius is found from the mass-radius-age relation for a single star as

$$\Delta \log R_1 = \log \frac{M_1}{M_1^o} - t_{KH} \frac{d \log M_1}{dt}\ , \qquad (3)$$

$t_{KH} = GM_1^2/R_1 L_1^o$ being Kelvin-Helmholtz timescale, $M_1^o$ and $L_1^o$ are the primary mass and luminosity at the moment of Roche lobe overfilling. Due to exponential dependence of $\Delta R$ on the mass loss rate, joint application of the Eqs. (2) and (3) may result sometimes in unphysically rapid growth of the donor's radius. Actually, the extent of overfilling is limited by the slit width between the stellar surface and the Roche lobe. We may estimate the effective size of the neck near the first Lagrangian point. The neck cross-section is represented as

$$S \simeq 2\pi \frac{\gamma RT}{\mu} \frac{R_L^3}{GM_1}\ , \qquad (4)$$

$\gamma = C_p/C_v$, $\mu$ molar mass. So linear measure of the neck is $l/R_L \simeq 3V_{\rm s}/V_{\rm esc}$. Considering this diameter as chord to the Roche lobe, one may estimate the relative height scale by simple geometry as $H/R_L \simeq 1 - \sqrt{1 - l^2/4R_L^2}$. Calculus gives $H/R_L \approx 1\%$. So, we should restrict the admissible Roche lobe overfilling rates by several percent.

## 3. Discussion

It was found in our earlier study (Pustynski & Pustylnik, 2007) that the final orbit of the system is quite sensitive to the initial separation of the components, the ratio of mass transfer rate to the mass loss rate and the corotation radius. For larger initial separations the system has time only for moderate orbit shrinkage, when the primary star contracts again and its radius "drops" again below the Roche lobe. Roche lobe contraction follows the contraction of the orbit, but the donor, having lost certain amount of its mass, contracts quicker than the Roche lobe, so its radius becomes again smaller than $R_L$, and the mass transfer disrupts. However, if the stars are initially close enough to each other, the timescale of the donor's contraction is longer than the timescale of the Roche lobe contraction, so the donor overfills its Roche lobe until the orbit shrinks dramatically. Smaller values of the corotation radius do not enable effective orbit shrinkage. With high accretion rates ($\dot{M}_2 \geq 0.3\,\dot{M}$) the system loses the angular momentum much more effectively, and this favors close binary formation. The timescale for formation of a close binary following the Roche lobe filling is several millions of years, which is comparable to the thermal timescale of the low mass companion. For stars with initial mass $M_{1\,\rm init} = 1.25\,M_\odot$ and enhanced mass loss by the margin given above during RGB evolutionary stage we confirm the validity of the basic conclusions concerning the final outcome of evolution of orbit. However for $M_{1\,\rm init} = 1.25\,M_\odot$ EHB object will be formed in roughly 4.8 Gyrs.

The Fig. 1 represents evolution of Roche lobe and the donor's radius at two different initial separation $d_0$. After reaching its Roche lobe, the donor radius follows $R_L$. It is seen that for larger initial separations the system have time only for moderate orbit shrinkage, when the primary star contracts again and its radius "falls" again below the Roche lobe. The initial masses of the components in Figures 1, 3, 4 are $M_{1\,\rm init} = 0.95\,M_\odot$, $M_{2\,\rm init} = 0.23\,M_\odot$ and in Fig. 2 $M_{1\,\rm init} = 1.25\,M_\odot$, $M_{2\,\rm init} = 0.23\,M_\odot$.

The Fig. 2 illustrates influence of the angular momentum loss parameter $k$ on evolution the system. It follows from the figure that effective angular momentum loss is necessary for close binary formation: smaller value of $k$ do not allow the orbit to contract significantly during the stage of mass interchange.

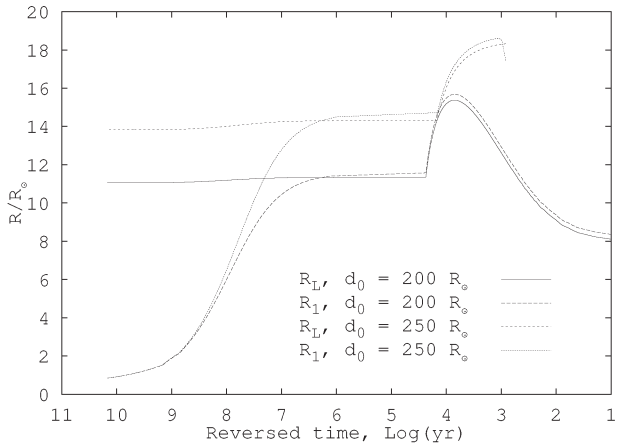


Figure 1: $R_L$ and $R_1$ evolution for different initial semi-major axis values $d_0$. $Q = 0.3$, $k = 6$. The time on the x-axis is counted backwards, so that the zero point is the final point of the model computation.

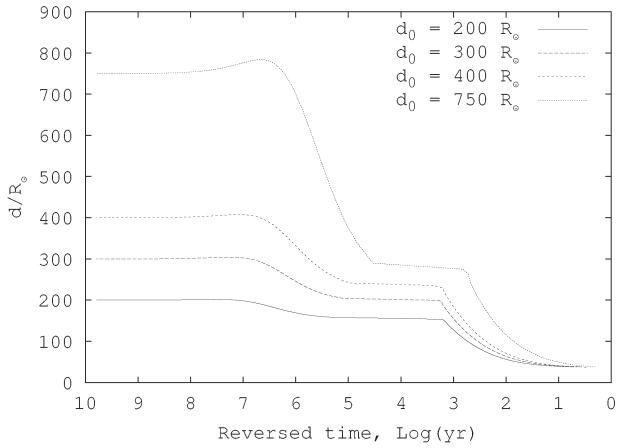


Figure 2: Separation evolution for different initial values of semi-major axis of orbit and mass of the donor $M_1 = 1.25 M_\odot$.

The Fig. 3 demonstrates semi-major axis evolution for different initial separations. The biggest value of $d_0 = 1500\,R_\odot$ corresponds to the case when the donor does not reach its Roche lobe during the time of nuclear evolution. With $d_0 = 1200\,R_\odot$, the overfilling occurs at the top of the donor's evolution as red giant, so the separation only experiences slight growth due to mass loss. Only with small initial separations effective orbital shrinkage may occur.

The Fig. 4 represents thermal mass radius exponent $\zeta_{\rm th} = (\partial R_2/\partial M_2)_{\rm th}$, adiabatic mass radius exponent $\zeta_{\rm ad} = (\partial R_2/\partial M_2)_{\rm ad}$ and Roche lobe mass radius exponent $\zeta_{\rm R_L} = (\partial R_L/\partial M_2)_*$ computed for different momentum loss parameters $k$ and mass transfer effectiveness parameters $Q$. We followed (Ritter, 1999) to adopt a constant value for thermal mass exponent, so on the Fig. 4 $\zeta_{\rm th} \equiv -0.3$. The expression for $\zeta_{\rm R_L}$

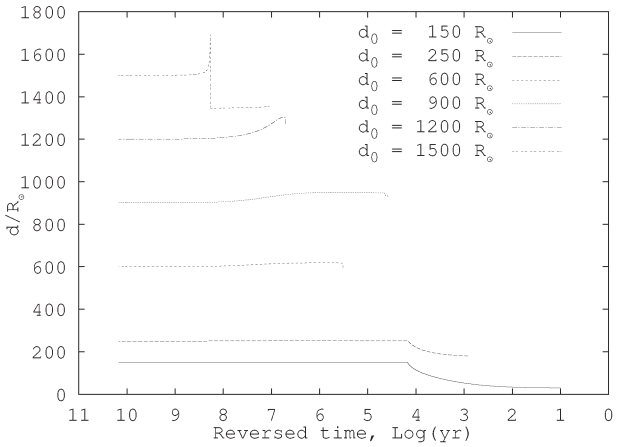


Figure 3: Separation $d$ evolution for different initial semi-major axis values.

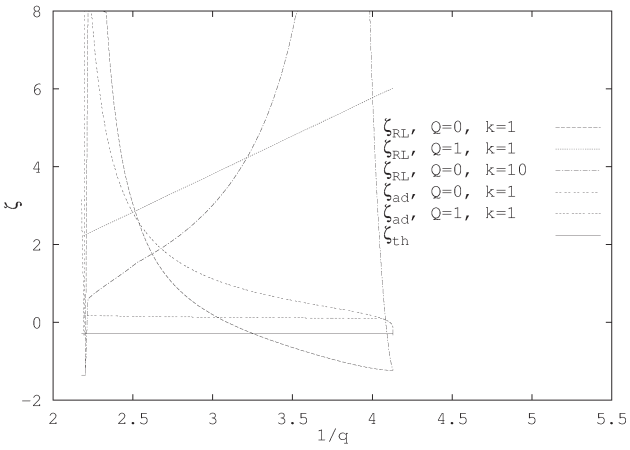


Figure 4: Thermal mass radius exponent $\zeta_{\rm th}$, adiabatic exponent $\zeta_{\rm ad}$ and Roche lobe mass radius exponent $\zeta_{\rm R_L}$ as functions of mass ratio, for different $k$ and $Q$.

was also taken from (Ritter, 1999), $\zeta_{\rm ad}$ was calculated following (Soberman, Phinney, van den Heuvel, 1997).

## 4. Conclusions

Our approach enabled us to determine the ranges of initial parameters of a binary for which effective mass transfer and angular momentum loss result in formation of a close binary with properties characteristic for EHBs. The most important role plays initial separation, the angular momentum loss parameter and the mass transfer rate parameter. We conclude that binarity indeed favors EHB formation. Assuming that the EHB progenitors belong to the binaries with initial separations of $100 - 150\,R_\odot$ and fill in their Roche lobe while being close to the RGB tip, we have found that considerable shrinkage of the orbit can be achieved due to the combined effect of angular

momentum loss and appreciable accretion on its low mass companion on the hydrodynamical timescale of the donor, resulting in formation of HeWD with masses about $0.5\,M_{\odot}$.

*Acknowledgements.* This investigation has been supported by Grant 5760 of Estonian Science Foundation. The authors are thankful to J. R. Hurley for providing their *sse.f* code.

**References**

Dorman B., O'Connell R.W., Rood R.T.: 1995, *ApJ*, **442**, 105.

Eggleton P.P.: 1983, *ApJ*, **268**, 368.

Hurley J.R., Pols O.R. & Tout C.A.: 2000, *MNRAS*, **315**, 543.

Morales-Rueda L., Maxted P.F.L., Marsh T.R., North R.C. & Heber U.: 2003, *MNRAS*, **338**, 752.

Pustylnik I.B., Pustynski V.-V.: 2007, *in: Binary Stars as critical tools and tests in contemporary astrophysics, Proc. IAU Symp. No. 240, Eds. W.I.Hartkopf, E.F.Guinan, P.Harmanec, Cambridge University Press*, **S240**, 389.

Ritter H.: 1999, *MNRAS*, **309**, 360.

Soberman G.E., Phinney E.S., van den Heuvel E.P.J.: 1997, *A&A*, **327**, 620.

Tout C.A., Hall, D. S.: 1991, *MNRAS*, **253**, 9.

# V.P. TSESEVICH AND MOSCOW VARIABLE-STAR ASTRONOMERS

N.N. Samus[1,2,3]

[1] Institute of Astronomy, Russian Acad. Sci.
48, Pyatnitskaya Str., Moscow 119017 Russia, *samus@sai.msu.ru*
[2] Sternberg Astronomical Institute, Moscow University
13, University Ave., Moscow 119992 Russia
[3] Euro-Asian Astronomical Society
13, University Ave., Moscow 119992 Russia

ABSTRACT. This paper is a brief account of the variety of ties between V.P. Tsesevich and the Moscow variable-star team: publications in co-authorship (mainly in the form of collective monographs), Tsesevich's work in the Moscow plate stacks, conferences, Tsesevich's contribution to the General Catalogue of Variable Stars, etc.

**Key words**: Astronomy: history, stars: variable.

## 1. Introduction. My personal contacts with Tsesevich

For the Moscow variable-star team, Prof. V.P. Tsesevich is a brilliant example of a science enthusiast, a really independent scientist who respected his well-known colleagues but was critical and never simply followed them and thus was able to create a world-recognized scientific school of his own. Moreover, being not born in Odessa, he is an excellent example of the real Odessa spirit in every aspect of his life.

Like many astronomers of my generation, who entered astronomy in the 1960s or 1970s, my first acquaintance with Tsesevich was through his famous book "What and How to Observe on the Sky", which I had first read still being a schoolboy. For me, it was my first really serious popular-science book on astronomy, not only telling its readers about scientific achievements but also explaining what they can see themselves and how they can contribute to astronomy. With P.G. Kulikovsky's "Handbook of an Amateur Astronomer", it became my favorite reference book for many years.

I believe that the first time I saw Tsesevich was over black-and-white TV, in a live program from Odessa featuring a local KVN game[1], still of the period before the KVN program was closed. Tsesevich was in the KVN jury, thus officially recognized by Odessa people as an expert in the most Odessa-like field of activity, humor.

Then, about 1969, at Sternberg Institute, in the study of Prof. P.N. Kholopov, my scientific advisor at that time, I was discussing some problems of my student variable-star research when a scientist, a stranger for me, had appeared, asked Kholopov a question, and left. I remember quite vividly Kholopov's very respectful tone: "Do you know who is this? The famous Tsesevich!" and my deep impression of the first encounter with a great scientist.

In 1974, during the Moscow IAU Symposium on variable stars and stellar evolution, Tsesevich was very actively helping the organizers, and I, still a post-graduate student, had a mission, rather important for a young person, as the head of a team of astronomers who helped with translation and interpreting during the conference. My contacts with Tsesevich at the conference were, for the first time, very close. It has been a surprise for me when, preparing this paper, I found that Tsesevich was not in the official list of the organizing committee. However, he participated in the inofficial party of the organizers after the symposium, and it was on that day when I heard my first joke told by Tsesevich — and, as I learned later, he was famous for knowing hundreds of jokes and telling them in a brilliant manner. The joke told in 1974 shows, among other things, the outstanding Tsesevich's capability of self-irony: the joke told of a man who married for the second time, after divorce, and was punished by God for foolishness, and Tsesevich, as far as I remember, was in his third divorce at that time. Since then, I had many possibilities to see Tsesevich not only in Moscow

[1] KVN is a very popular program, still existing, a TV club featuring young people competing in jokes, songs, funny performances. It was founded more than 40 years ago but was closed for two decades during the late Soviet era.

but, luckily, also in Odessa, where his individuality was best felt by everyone.

## 2. Tsesevich in Publications with Moscow Co-authors

After Tsesevich's death in 1983, I was asked by Dr. N.B. Grigoryeva to write a paper about Tsesevich for "Istoriko-Astronomicheskiye Issledovaniya"[2]. My paper "V.P. Tsesevich, Never to Be Forgotten" was published several years later (Samus, 1988). Reading this paper now, I find it quite incomplete and not free of mistakes, but I am very proud to be the first author of a biographic publication about Tsesevich (and, frankly, feel that I did not deserve the honor at that time). I mention in the paper that I had an experience of being Tsesevich's coauthor only once (Tsesevich et al., 1979), I was somewhat ashamed of the fact of only a single co-authorship paper when writing about it. Now I know that Tsesevich was never active in publishing journal papers in co-authorship, and a single paper with Tsesevich, as in my case, is quite a good result for a Moscow astronomer. Actually, using ADS[3] and Russian bibliographic journals, I have not been able to find any other Tsesevich's journal paper in co-authorship with Moscow variable-star scientists. His paper with the brilliant Moscow variable-star researcher who perished in the Moscow battle of the World War II, Nikolai Florya, on brightness variations of the minor planet Eros (Zessewitch and Florja, 1931) is no exception: Florya worked in Leningrad, not in Moscow, at that time. Even journal papers with Odessa co-authors are not numerous. Odessa colleagues tell me that Tsesevich often refused to become a co-author considering (often too modestly) his personal contribution minor and used to recommend his collaborators to publish their results in single-author papers.

However, searching outside the ADS, we easily find several major Tsesevich's publications with Moscow co-authors. These are very serious *books* on variable stars written by Tsesevich together with his Moscow friends. In such books, each author would write his own chapter, with minimal interaction with the other authors. An excellent example is Zverev et al. (1947), a multi-author monograph where Tsesevich was the author of five chapters (157 book pages, with numerous formulas and tables) on techniques of studies of eclipsing variable stars. Actually, this is Volume III (the last one) of the series of books on variable stars, started before the World War II but finished only after its end. We do not find Tsesevich's name among the authors of the first two volumes.

Some 20 years later, a new, five-volume series of books on variable stars was initiated, mainly by Moscow astronomers but with participation of several well-known Soviet scientists from other cities. The editorial board of the series, its first volume published in 1969, contains many famous names (such as the Moscow scientists B.V. Kukarkin, D.Ya. Martynov, P.N. Kholopov, and also such prominent figures of our astronomy as V.A. Ambartsumian, A.A. Boyarchuk — a Crimean astronomer at that time, and others), and Tsesevich is one of them. He published several chapters in different volumes of the series (I would like to mention a very informative chapter on RR Lyrae variables in the volume devoted to pulsating stars) and, most important, was the sole editor of the volume on eclipsing variable stars (Tsesevich, 1974).

## 3. Tsesevich and the Moscow Plate Stacks

During the whole period of my personal acquaintance with Tsesevich, he would appear in Moscow from time to time and make many eye estimates of sky photographs of the Sternberg Institute's rich plate collection. Like all of us, he strongly preferred high-quality plates taken at the "Hoffmeister" 40-cm astrograph. These plates, 30 by 30 cm in size, cover a $10^\circ \times 10^\circ$ field and have a typical plate limit of $17^m - 18^m B$. The telescope was made in the 1930s for the Sonneberg Observatory (Germany), C. Hoffmeister started his deep-sky studies with it, and eventually became the world's most successful variable-star discoverer of the classical photographic era. After World War II, the astrograph was taken from Germany (on B.V. Kukarkin's initiative) as a part of Soviet reparations, first installed in Simeiz (Crimea), then moved to the Sternberg Institute's station in Kuchino near Moscow, and finally, to the same Institute's Crimean Laboratory in Nauchny; it is still in a good working condition. Along with many plates from different observatories he studied, Tsesevich made several thousand estimates of variable stars on Moscow plates. Many of his estimates can be found published in Tsesevich's books on different types of variable stars or on variable stars in different selected fields of the sky.

The leaders of the Moscow variable-star team of that time, B.V. Kukarkin and P.N. Kholopov, were always glad to greet Tsesevich during such visits to Moscow. Quite often, he spent days and nights in the plate collection and slept on a sofa in Kukarkin's study at Sternberg Institute. He was the only person whom Kukarkin permitted to smoke in the rooms of the variable star department. I personally witnessed occasions when Kukarkin had guessed Tsessevich's arrival by the smell of tobacco smoke in the offices.

Not only did Tsesevich use Moscow archival plates to study stars of his interest. He suggested fields to be

[2] "Studies in the History of Astronomy", a Russian edition.

[3] It is not easy to use ADS looking for Tsesevich's publications because of numerous versions of Latin-alphabet spelling of his name (Tsesevich, Tsessevich, Zessevich, Zessewitsch...); some references can be easily overlooked.

photographed using different telescopes of the Sternberg Institute. The above-cited paper, Tsesevich et al. (1979), is a result of Tsesevich's suggestion to use the Cassegrain focus of the Moscow 70-cm reflector to take photographs of the dwarf nova EF Peg, with the result that an outburst was observed at a good angular resolution, proving that a faint star rather than its brighter close neighbor experienced outbursts.

Rather unusual for active plate users, Tsesevich was not very interested in variable-star search on photographic plates. He did make several discoveries by chance but, as far as I know, never worked on discoveries of variable stars systematically. I remember that, on an occasion when he wanted to use the Sternberg Institute's Karl Zeiss blink comparator, of the design most common at Soviet observatories of that time, Tsesevich asked help from local staff — and found that the "additional" star he had noticed was a minor planet. It seems like he felt he already had enough interesting variable stars to study, a feeling quite common among astronomers today.

Figure 1: V. Tsesevich, B. Firmanyuk, Yu. Romanov, M. Skulsky, V. Oskanyan at the Odessa conference of 1980.

## 4. Tsesevich and Moscow: Conferences and Dissertations

In my opinion, one of the most important Tsesevich's contributions to the current style of variable-star research in the countries of the former Soviet Union is his initiative to organize regular conferences on variable stars in Odessa. The group photograph from the All-Union Variable-Star conference in Chernomorka (the southern suburb of Odessa) in 1980 is well known. It should be reminded that 1980 was the year of the Moscow Summer Olympics, with much tumult at that time and immediately after it, and probably some people had different thoughts in September, 1980 than visiting conferences. Nevertheless, I found more than 20 Moscow astronomers on that photograph; the number of participants from Moscow at our conference in 2007, though considerable, is much lower. The conference of 1980 was very large, it lasted for almost two weeks. After that, our meeting in Odessa became very regular, and this tradition is still quite alive and useful.

I already mentioned Tsesevich's great contribution to the success of the Moscow IAU Symposium of 1974. My knowledge of his activity at other meetings together with Moscow variable-star astronomers is too limited for presenting any additional details here, but I am sure this was always an important field of contacts and cooperation.

It was also a tradition that Tsesevich had often been invited as a reviewer of variable-star dissertations by Moscow researchers — and the famous Moscow variable-star experts had been invited to review dissertations written by Tsesevich's disciples. In this field, Tsesevich was always a very responsible and attentive reviewer. If he did not like a dissertation, the well-known name of its supervisor was no help.

## 5. Tsesevich and the GCVS

It is well known that the most important project of the Moscow team of variable-star researchers after the World War II is the General Catalogue of Variable Stars (GCVS), regularly prepared and published by astronomers of Moscow University and the Russian Academy of Science on behalf of the IAU. Tsesevich's name is one of those most frequently cited in the GCVS list of references — the GCVS (fourth edition, 1985–1995) contains about 150 references to different papers by Tsesevich. Moreover, one of these references belongs to those used for the largest numbers of stars: this is the atlas of finding charts by Tsesevich and Kazanasmas (1971). The atlas consists of hand-plotted charts of different scale and different quality; it is now very easy to prepare a better chart if you know your star's correct coordinates. The main importance of the atlas follows from the fact that it was, by the time of its publication, the only reliable source of identification for many variable stars discovered in the beginning of the 20th century at Harvard Observatory and announced with rough coordinates and no finding charts provided by the discoverers. Tsesevich spent a long time at Harvard Observatory studying discoverers' notebooks, original plates with discoverers' ink marks and was able to find a large number of old Harvard variables. This line of study was much later, in 1999–2005, continued by Martha Hazen (1931–2006) who prepared several thousand new finding charts for Harvard variables upon request from the GCVS team.

Tsesevich's knowledge of variable stars was vast and impressive. My friend and colleague M.S. Frolov

(1937–2006) used to tell me stories about Tsesevich's memory concerning his favorite RR Lyrae stars. Tsesevich was able, from his memory, to answer questions on period variations (the year and amount of the abrupt period change) for almost any star. Of course, the GCVS team used to address Tsesevich for information in difficult cases. The story of the eclipsing star YY Dra[4] was described in detail in Samus (1988): Tsesevich remembered the field of the variable nearly 50 years after he had studied it but died before he could mark the correct star on a good plate sent him from Moscow.

## 6. Concluding remarks


Figure 2: The grave of the singer Platon Tsesevich in Moscow.

I think I have been able to give you an impression, though definitely incomplete, of the many-sided contacts, cooperation, and friendship (despite unavoidable conflicts of brilliant personalities that also happened and were described by Tsesevich in his reminiscences) between V.P. Tsesevich and the Moscow team of variable-star researchers.

Moscow is also related to Tsesevich's memory in another important aspect. The grave of Tsesevich's father, the outstanding opera basso, is in Moscow, at the Novodevichye Cemetery, among graves of the most well-known actors, writers, artists, politicians. Another famous Moscow cemetery, Vagankovskoe, keeps graves of several other Tsesevich's close relatives.

[4]YY Dra was never observed by anyone else after Tsesevich's discovery in 1934, no finding chart is available. Almost half a century later, a much fainter dwarf nova was discovered in the field, and some authors use to call the dwarf nova YY Dra. The GCVS uses the name DO Dra for the dwarf nova instead.

*Acknowledgements.* I would like to thank the organizers for the possibility to present this talk at the Tsesevich's memorial conference. The works of the Moscow variable-star team are financially supported by grants from the Russian Foundation for Basic Research and from the Program of Support to Leading Scientific Schools of Russia.

## References

Samus N.N.: 1988, *Istoriko-Astronomicheskiye Issledovaniya*, **20**, 216.

Tsesevich V.P. (editor): 1974, *Eclipsing Variable Stars*, M.: Nauka.

Tsesevich V.P., Goranskij V.P., Samus N.N., Shugarov S.Yu.: 1979,*Astron. Tsirk.*, No. 1043, 3.

Tsesevich V.P., Kazanasmas M.S.: 1971, *An Atlas of Finding Charts for Variable Stars*, M.: Nauka.

Zessewitsch W., Florja N.: 1931, *AN*, **243**, 97.

Zverev M.S., Kukarkin, B.V., Martynov D.Ya., Parenago P.P., Florya N.F., Tsesevich V.P.: 1947, *Methods of Observing and Investigating Variable Stars* (in Russian), Moscow and Leningrad: Gostekhizdat.

# STUDIES OF GALACTIC CEPHEIDS: THE INASAN/SAI INTEGRATED PROGRAM

N.N. Samus[1,2,3], S.V. Antipin[2,1], L.N. Berdnikov[2], A.K. Dambis[2], N.A. Gorynya[1], A.S. Rastorguev[2]

[1] Institute of Astronomy, Russian Acad. Sci.
48, Pyatnitskaya Str., Moscow 119017 Russia, *samus@sai.msu.ru*
[2] Sternberg Astronomical Institute, Moscow University
13, University Ave., Moscow 119992 Russia
[3] Euro-Asian Astronomical Society
13, University Ave., Moscow 119992 Russia

ABSTRACT. We present the review of the main results of more than two decades of the Moscow program of Cepheid studies, carried out at the Institute of Astronomy (INASAN) and Sternberg Astronomical Institute (SAI). This program consists of extensive photometry and radial velocity measurements (the contribution from our team being the largest among observations of comparable precision), studies of period variations (permitting identification of the number of a particular star's current instability-strip crossing), detection of spectroscopic binaries among Cepheids, determinations of Cepheid radii, discoveries of double-mode Cepheids, studies of galactic structure, kinematics, and dynamics, etc.

**Key words**: Stars: variable: Cepheids.

## 1. Introduction

Our program of Cepheid studies, a joint project of the Sternberg Astronomical Institute of Moscow University (SAI) and the Institute of Astronomy of Russian Academy of Sciences (INASAN), is mainly devoted to classical Cepheids (DCEP and subtypes in the GCVS), though some of our results deal with Population II Cepheids (W Vir and BL Her stars, or CWA and CWB in the GCVS). Classical Cepheids are comparatively young stars in the Galaxy's thin disk, whereas Population II Cepheids are members of the thick disk and halo populations. Our team is engaged in Cepheid studies since the 1970s, the most active period of the program started in 1980s and is still under way. It is now time to summarize the most important results of the program.

Classical Cepheids remain very important in many fields of astrophysics and galactic research. The primary reason for their importance is that, thanks to the famous period–luminosity relation, Cepheids are objects with the most reliable distance scale. They are supergiants traceable at large distances and thus present a link between close objects, with trigonometric parallaxes, and distant parts of our Galaxy as well as extragalactic objects. An important period–age relation allows astronomers to estimate ages of stellar aggregates containing Cepheids in a very simple way. Cepheid period variations give insight into stellar evolution and permit identification of the number of a Cepheid's current crossing of the instability strip. Additional information on stellar evolution comes from double-mode Cepheids thanks to co-existence of two pulsation modes, with periods differently dependent on stellar parameters. Being radially pulsating stars, Cepheids permit application of the well-known Baade–Wesselink technique to their photometry and radial velocity measurements, so that we are able to determine their radii and to study the period–radius relation. Many Cepheids are members of binary systems with long periods (months or years), so it is possible to derive limits on the masses of their companions. As typical representatives of Population I, classical Cepheids are a good tool for studies of structure, kinematics, and dynamics of our Galaxy's thin disk.

## 2. Photometry and Spectroscopy

Twenty-five years ago L.N. Berdnikov initiated our program of high-precision Cepheid photometry, which is being continued till now. Initially, Cepheids were observed photoelectically, mainly using telescopes at the excellent conditions of Mt. Maidanak (Uzbekistan). Later on, our observations were continued at many other observatories in different countries (Russia, Uzbekistan, Australia, South Africa, Chile). Currently, we use both principal techniques of accurate

photometric observations (photoelectric and CCD photometry).

The total number of our accurate $UBVRI$ measurements collected by now is approximately 75 000, for about 650 Cepheids. Many of these measurements can be found in numerous publications by our team. A recent version of the catalogue of our measurements is available in Internet (Berdnikov, 2006). Photoelectric and CCD measurements were supplemented by a large number of brightness estimates made in photographic plate stacks of different observatories, in particular, in the Sternberg Institute's and Harvard Observatory's plate archives. We collected published information on visual photometry, including that acquired during time intervals not covered with our observations. For some stars, the time span of available observations is up to 150 years or even more. Our photometric observations and data collected from the literature permitted us to compile the world's most complete data bank of Cepheid photometry.

About 20 years ago, we got access to the excellent instrument for radial velocity measurements, the CORAVEL-type correlation spectrometer designed and built by A.A. Tokovinin, and started regular observations of Cepheids in Moscow, Crimea (Simeiz and Nauchny), and at other observatories. Currently, the instrument is used in Simeiz, almost exclusively for our Cepheid program. It permits us to measure radial velocities for stars brighter than $12^m - 13^m$ with a good productivity, the characteristic accuracy (in the sense of external agreement) for tenth-magnitude stars is about 0.3 km $s^{-1}$. Three catalogues of our measurements, with the total number of observations about 6000, were published (cf. Gorynya et al., 1998a, and references therein), the observations from these publications are available in the electronic catalogue III/229 in VizieR (Gorynya et al., 1998b). Currently, the number of our radial velocity measurements for 165 Cepheids is about 10 000.

Our photometry as well as our radial velocities comprise a total of about 60% of all measurements of comparable precision available in the world.

## 3. Period Variations

The data bank on Cepheid photometry permits us to study period variations of Cepheids. The sample we used for period–variation studies contains about 230 Cepheids with observations covering 100–150 years. For the oldest known Cepheids, $\eta$ Aql and $\delta$ Cep, epochs of maxima usable for period-change studies span 230 years.

Most Cepheids are rather stable pulsators. However, small variations of their periods were already noticed decades ago. The theory predicts quite detectable period variations due to stellar evolution. Such variations are progressive and can be described with a more or less stable rate of period change. Thus, the $O - C$ diagram for evolutionary period variations should be a parabola, and the parabola's orientation (branches upwards or downwards) will be different for odd and even numbers of the star's instability-strip crossing. For different precursor main-sequence luminosities, the theory permits us to expect from 1 to 5 crossings of the instability strip during the life of a Cepheid. If the period-variation rate is precisely determined from observations, we can even hope to specify the particular number of the odd or even crossing (cf. Turner et al., 2006). Our analysis of Cepheid period variations is based on very accurate timings of maxima determined using a uniform technique, the computer version of the Hertzsprung method that takes into account the complete light curve, not only the data points immediately around the maximum (Berdnikov, 1992). This makes our findings concerning period variations especially reliable.

It was, however, noticed quite long ago that the character of period variations for many Cepheids was much more complex than the simple pattern of evolutionary variations outlined above. Many Cepheids demonstrate abrupt period changes or more or less irregular period variations, period increases can be followed by period decreases and *vice versa*, so that the overall period-variation picture is clearly determined not only by evolution. The causes of observed non-evolutionary period changes are still not completely understood, several mechanisms were suggested. Nevertheless, we find from our data that the evolutionary period variations, masked with those of different nature, can be detected for 90% of all Cepheids with observations covering 100 years or more. Figure 1 shows a typical example of the $O - C$ diagram revealing an evolutionary period increase (an odd crossing of the instability strip), while the $O - C$ diagram in Fig. 2 apparently permits us to identify the period increase (an odd crossing) also reliably, despite strong overlapping non-evolutionary period variations.

If the number of the particular instability-strip crossing is known, it should be taken into account when determining the Cepheid's distance. Equal periods can be met for Cepheids of different masses, at different instability-strip crossings. The period–luminosity relations for different crossings can differ by several tenths of a magnitude. Thus, detailed studies of Cepheid period variations are a tool for considerable improvement of the distance scale in the Universe.

## 4. Binary Cepheids

Cepheids can be members of binary star systems. Being supergiants, they have characteristic orbital periods in excess of a year. Though binarity of several

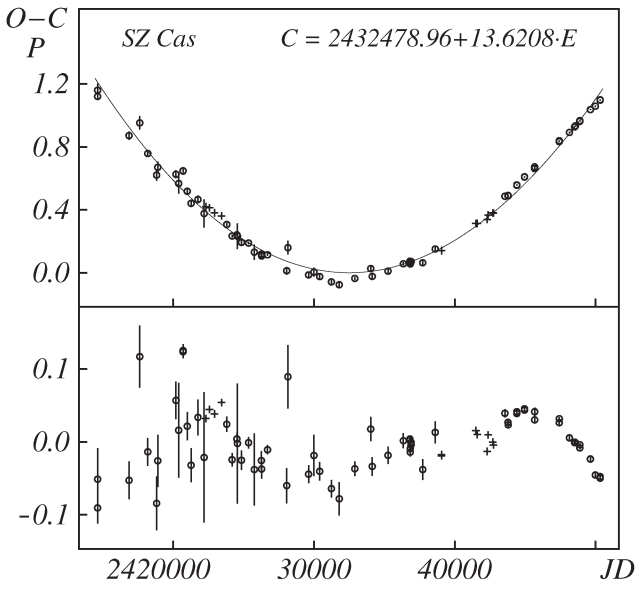


Figure 1: The $O-C$ diagram for SZ Cas showing an obvious period increase, corresponding to an odd crossing of the instability strip. The bottom panel shows residuals after fitting a parabola to the $O-C$ curve.

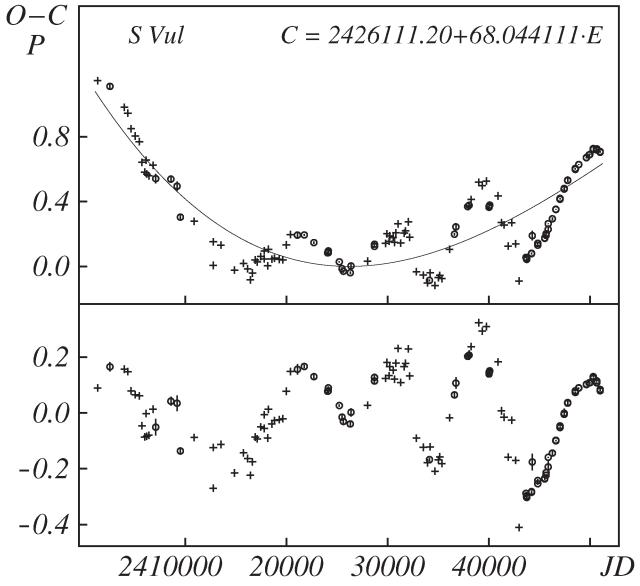


Figure 2: The $O-C$ diagram for S Vul showing a period increase, corresponding to an odd crossing of the instability strip, masked with non-evolutionary period variations.

Cepheids was suspected from possible light-time effect in their $O-C$ diagrams, the complex character of such diagrams (Section 3) makes this technique not very reliable. According to Szabados (2003), who strongly relies on the $O-C$ diagrams, the fraction of binaries among bright Cepheids approaches 90%. We are afraid that this is an overestimate, including wrong detections from $O-C$ diagrams and physically unrelated neighbors on the sky. In our opinion, to reliably discover a binary Cepheid, it is necessary to detect its orbital radial-velocity variations, to separate the star's orbital and pulsational velocity curves, and, if possible, to derive the parameters of the binary's components. The latter task is simplified thanks to the mass of the Cepheid component known from the pulsation theory. Of course we will be unable to detect some really binary Cepheids in a case of an unfavorable inclination of their orbits, but the same is true for the $O-C$ techniques.

Our team has excellent possibilities for studies of binary Cepheids thanks to our high-quality original radial velocities. We discovered (or suspected with good reason) five new spectroscopic-binary Cepheids (Gorynya et al., 1992, 1994; Samus et al., 1993; Gorynya et al., 1996) and were able to confirm many previously known ones. From our data, we estimate the lower limit on the incidence of spectroscopic binaries among classical Cepheids as 22% (Gorynya et al., 1996). For 20 Cepheids, including the new binaries, we were able to determine orbital elements and to estimate companions' masses.

During the recent years, several eclipsing Cepheids were discovered in external galaxies, primarily in the Magellanic Clouds. However, there were no known eclipsing Cepheids in our Galaxy. Very recently, Antipin et al. (2007) found the first Galaxy's eclipsing Cepheid, TYC 1031 01262 1. It should be noted that the star's position with respect of the Milky Way and its orbital period, 51 days, which is too short for sizes of supergiant classical Cepheids, suggest that TYC 1031 01262 1 is a Population II star. Interesting enough, the star shows strong brightness variations outside eclipses, also satisfying the orbital period (Fig. 2). It may indicate that the components of the binary are non-spherical, which is, however, unfavorable for stability of pulsations. Further observations of the star are evidently needed. The new binary resembles the three short-period Population II spectroscopic binaries without eclipses discussed by Harris and Welch (1989): IX Cas ($P = 110^d$), TX Del ($P = 133^d$), and AU Peg ($P = 53^d$), but TYC 1031 01262 1 has the shortest period of them all. TX Del and AU Peg were also in our program of binary-Cepheid studies from radial velocities, we detected the spectroscopic binarity of TX Del before learning about its discovery by Harris and Welsh. The existence of sufficiently close binaries among evolved Population II stars is not widely

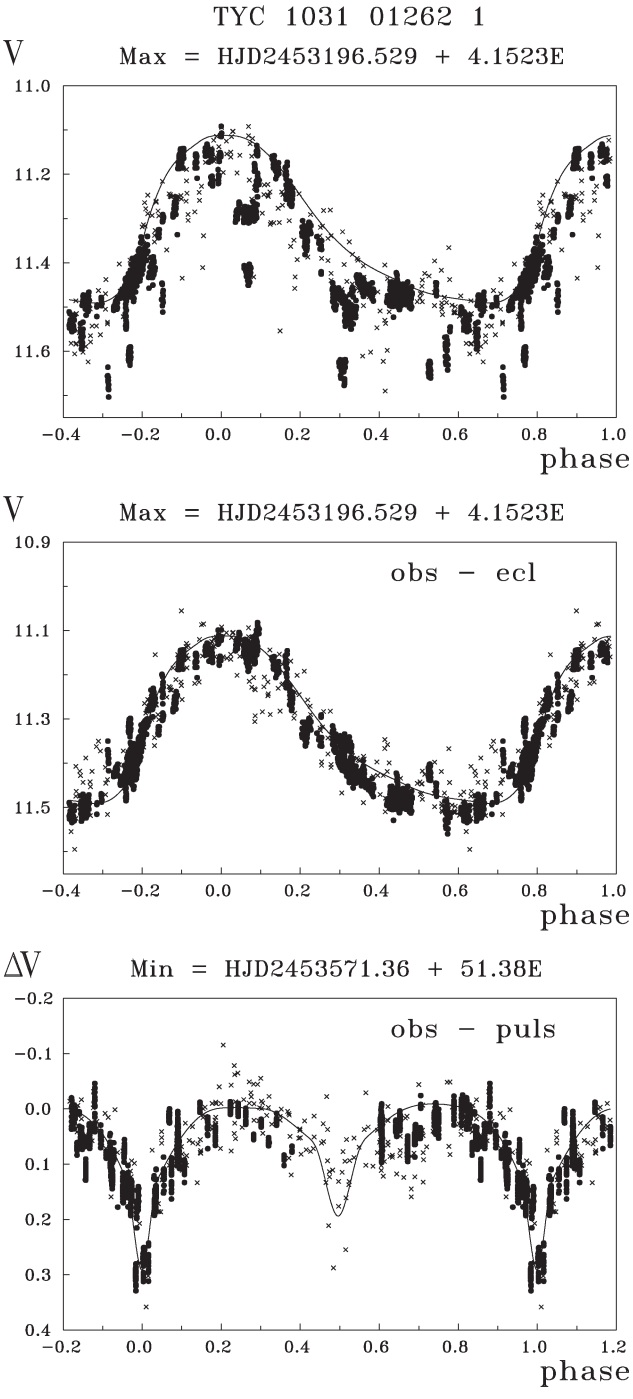


Figure 3: The light curves of TYC 1031 01262 1. Top: observations folded with the pulsation period. Middle: same, with orbital variations removed. Bottom: observations with the pulsational variations removed, folded with the orbital period.

recognized and quite interesting for understanding the Galaxy's old populations.

## 5. The Baade–Wesselink Analysis. Identification of Cepheid Pulsation Modes.

It is well known that radial velocities of radially pulsating variable stars combined with their multicolor photometry can be used to determine their physical characteristics, in particular radii, using the Baade–Wesselink technique. In essence, the color information gives insight into variations of the effective temperature, the magnitude difference at different phases reflects the radius ratio, and the integral of the radial velocity curve is the difference of the radii at corresponding phases multiplied by a known correction factor. The particular version of the method we use is the technique described by Balona (1977) and somewhat improved by us. The result of the method's application to a particular pulsating star is its mean radius as well as the curve of the radius variations during the pulsation cycle. We are now working on new modifications of the method taking into account the most current understanding of the physics of stellar pulsations.

The results of our Baade–Wesselink studies of classical Cepheids using our original photometry and radial velocities were summarized in Sachkov et al. (1998). From 62 Cepheids, a period–radius relation for the fundamental mode was determined. Some Cepheids clearly deviate from the relation, they should probably be identified with first-overtone pulsators.

Note that mode identification for our Galaxy's classical Cepheids is not straightforward, whereas the data for different galaxies (like OGLE data for the LMC) show two different period–luminosity relations, for the fundamental and first-overtone modes, separated by about 0.15 in $\log P$ (according to the pulsation theory, $P_1/P_0 \approx 0.71$, where $P_0$ is the fundamental-mode period and $P_1$, that of the first overtone). The mode ambiguity is an important uncertainty source for Cepheid distances. If a star is wrongly classified as a first-overtone pulsator, a lumunosity error of about $0.65^m$ will be introduced.

Besides the period–radius relation, an important tool of mode diagnostics is the Fourier analysis of light curves. We attempted to apply the neural network technique to $V$-band light curves of more than 400 galactic Cepheids using OGLE data on LMC Cepheids as a training sample (Zabolotskikh et al., 2005). As expected, most Cepheids classified as DCEPS (small amplitudes, rather symmetric light curves) in the 4th edition of the General Catalogue of Variable Stars (GCVS; Kholopov, 1985–1987) turned out to be first-overtone pulsators, but we detected 9 stars with GCVS classification leading to a wrong mode identification. Zabolot-

skikh et al. (2005) suggested new Cepheid period–radius relations, separately for the fundamental-mode pulsators,

$$\log R = 1.08(\pm 1.01) + 0.74(\pm 0.01) \log P,$$

and for the first-overtone pulsators,

$$\log R = 1.19(\pm 1.01) + 0.74(\pm 0.01) \log P.$$

They have the same slope but differ in the zero point.

A Fourier analysis of radial velocity curves is also of interest, the results are easier to interpret from the point of view of the pulsation theory. Such studies are also under way in our team (N.A. Gorynya in cooperation with P. Moskalik, Warsaw). New radial-velocity observations are arranged to ensure complete phase coverage of velocity curves, which was already successfully achieved for most program stars.

## 6. Double-Mode Cepheids

Double-mode Cepheids are met not very frequently in our Galaxy and only among Cepheids with comparatively short pulsation periods. Most of them exhibit simultaneously excited pulsations in the fundamental mode and the first overtone, with rare cases of the co-excited first and second overtones (the particular modes are identified by comparison of the observed period ratios to theoretical predictions). Triple-mode stars (Antipin, 1997) are extremely rare, it is not clear if they should be analyzed with Cepheids or with RR Lyrae stars. Studying simultaneous pulsations in two modes, it is possible to derive masses and radii and get additional insight into evolution of Cepheids.

Currently, 23 double-mode Cepheids are known in our Galaxy; five of them were discovered at the SAI. Whereas the first stars were found photographically (the first SAI discovery was V367 Sct; Efremov and Kholopov, 1975), our most recent discovery (ASAS 062726+0111.6; Antipin, 2006) was made in the data publicly available from the ASAS-3 automatic survey (Pojmanski, 2002).

## 7. The Period–Luminosity Relation

It is widely known that the period–luminosity relation is the most important relation for Cepheids, it is this relation that makes Cepheids so important for galactic and extragalactic studies. Small revisions of the period–luminosity relation can have serious consequences for our understanding of many "hot" problems of astrophysics and even cosmology.

Berdnikov et al. (1996) revised the period–luminosity relation using the best modern data for 9 Cepheids in 7 open star clusters. The distances to the open clusters were accurately determined by main-sequence fitting. They were able to derive the parameters (both the zero point and slope) of the consistent period–luminosity relations in the Johnson $BVRI$, Cousins $(RI)_C$, and CIT $JHK$ bands. As an example, the $V$-band period–luminosity relation is:

$$< M_V >= -3.88 - 2.87(\log P - 1).$$

The near-infrared relations are particularly useful because of much lower influence of interstellar extinction at large wavelengths.

The period–luminosity relations from Berdnikov et al. (1996) agree with our findings from statistical parallaxes (see next Section).

## 8. Cepheids and the Structure and Kinematics of our Galaxy

Being objects with the most accurate distance scale (in the sense of random errors), Cepheids are very suitable objects for studies of the structure and dynamics of the Galaxy's disk. These stars are relatively young, they outline star formation regions and local spiral arms. By means of cluster analysis in a 5 pc×5 pc region around the Sun, more than 60 Cepheid complexes, with sizes from 600 pc to 1.4 kpc, have been revealed (Berdnikov et al., 2006).

It is known that studies in the optical domain are seriously hindered with large and irregular interstellar extinction of light, causing observational selection effects that are strong and difficult to correct for. Selection effects are not that important if we use kinematics instead of magnitudes and local densities. For this reason, kinematical effects due to spiral density waves are often used to study the local spiral pattern. Photometric parallaxes of Cepheids, combined with their precise radial velocities, Hipparcos and Tycho-2 proper motions are quite usable to analyze such kinematical effects. We detected a radial periodicity in residual velocities of Cepheids and other young objects, it permitted us to independently estimate the distance between the spiral arms of our Galaxy as 2 kpc (Mel'nik et al., 1999).

Using a technique based on the maximum likelihood principle, it is possible to analyze the field of Cepheid spatial velocities (Zabolotskikh et al., 2002). The resulting complete set of kinematical characteristics (mainly based on the cited paper) contains the rotation curve parameters for the Cepheid subsystem (the local disk rotation velocity of $206 \pm 10$ km s$^{-1}$, the Oort's constant $A = 17.5$ km s$^{-1}$kpc$^{-1}$), the axes of the residual velocity ellipsoid ($14 \pm 1$, $9 \pm 0.5$, $7 \pm 1$ km s$^{-1}$), the perturbation amplitudes ($7 \pm 2$ and $2 \pm 0.5$ km s$^{-1}$), the pitch angle of the spiral pattern ($7° \pm 1°$), and the phase angle of the Sun ($85° \pm 15°$). The statistical parallax method applied to

the 3D velocity field confirms the short distance scale of Cepheids, corresponding to the distance modulus of the Large Magellanic Cloud close to $18.3^m$.

*Acknowledgements.* It is a pleasure to acknowledge the financial support of our Cepheid studies from the Russian Foundation for Basic Research and the Program of Support for Leading Scientific Schools of Russia.

**References**

Antipin S.V.: 1997, *Astron. and Astrophys.*, **326**, L1.
Antipin S.V.: 2006, *Perem. Zvesdy Prilozh.*, **6**, No. 9.
Antipin S.V., Sokolovsky K.V., Ignatieva T.I.: 2007, *Mon. Not. R. Astron. Soc.*, **379**, L60.
Balona L.A.: 1977, *Mon. Not. R. Astron. Soc.*, **178**, 231.
Berdnikov L.N.: 1992, *Sov. Astron. Lett.*, **18**, 207.
Berdnikov L.N.: 2006, *A Catalogue of Cepheid Observations* (http://www.sai.msu.su/groups/cluster/CEP/ PHE/cepheids-16-03-2006.zip).
Berdnikov L.N., Efremov Yu.N., Glushkova E.N., Turner D.G.: 2006, *Odessa Astron. Publ.*, **18**, 26.
Berdnikov L.N., Vozyakova O.V., Dambis A.K.: 1996, *Astron. Letters*, **22**, 839.
Efremov Yu.N., Kholopov P.N.: 1975, *Inform. Bull. Var. Stars*, No. 1073.
Gorynya N.A., Rastorguev A.S., Samus N.N.: 1996, *Astron. Letters*, **22**, 175.
Gorynya N.A., Samus N.N., Rastorguev A.S.: 1992, *Inform. Bull. Var. Stars*, No. 3776.
Gorynya N.A., Samus N.N., Rastorguev A.S.: 1994, *Inform. Bull. Var. Stars*, No. 4130.
Gorynya N.A., Samus N.N., Rastorguev A.S. et al.: 1998a, Astron. Letters, **24**, 815.
Gorynya N.A., Samus N.N., Sachkov M.E. et al.: 1998b, VizieR III/229 (http://cdsarc.u-strasbg.fr/viz-bin/Cat?III/229).
Harris H.C., Welch D.L.: 1989, *Astron. J.*, **98**, 981.
Kholopov P.N. (ed.): 1985–1987, *General Catalogue of Variable Stars*, Vols. I–III, Moscow: Nauka.
Mel'nik A.M., Dambis A.K., Rastorguev A.S.: 1999, *Astron. Letters*, **25**, 518.
Pojmanski, G.: 2002, *Acta Astron.*, **52**, 397.
Sachkov M.E., Rastorguev A.S., Samus N.N., Gorynya N.A.: 1998, *Astron. Letters*, **24**, 377.
Samus N.N., Gorynya N.A., Kulagin Yu.V., Rastorguev A.S.: 1993, *Inform. Bull. Var. Stars*, No. 3934.
Szabados L.: 2003, *Inform.Bull.Var.Stars*, No.5394.
Turner D.G., Abdel-Latif M.A.-S., Berdnikov L.N.: 2006, *Publ. Astron. Soc. Pacific*, **118**, 410.
Zabolotskikh M.V., Rastorguev A.S., Dambis A.K.: 2002, *Astron. Letters*, **28**, 454.
Zabolotskikh M.V., Sachkov M.E., Berdnikov L.N. et al.: 2005, in: *The Three-dimensional Universe with GAIA*, ESA Publ. SP-576, 707.

# THE OBSERVATION OF TOTAL SOLAR ECLIPSE ON MARCH 29,2006 IN KAZAKHSTAN

L.I. Shestakova[1], F.K. Rspaev[1], G.S. Minasyants[1], A.I. Dubovitskiy[1], A. Chalabaev[2]

[1] Fesenkov Astrophysical Institute
Almaty 050020 Kazakhstan *shest@aphi.kz*

[2] Laboratoire DAstrophysique,Observatoire de Grenoble
Universite Joseph Fourier CNRS, France

ABSTRACT. The observations of total solar eclipse on March 29, 2006 were carried out by forces of united expedition of Fesenkov Astrophysical institute in Kazakhstan (settlement Mugalghar, Actobe region). The main problem was the interferometric observations of the outer solar corona at distances from 3 to 10 solar radii. The field of radial velocities of dust was obtained by Doppler shifts of absorption lines.

**Key words**: Sun: solar eclipse, F-corona; radial velocity.

## 1. Introduction

The problem of observation of field of dust radial velocities in the outer solar corona in first was set and realized during total solar eclipse July 31, 1981 (Shcheglov et al., 1987; Shestakova, 1987). At this moment it was seemed that the performance of such tasks is principally impossible, insofar as on elongation, exceeded 4 solar radii, the brightness of atmosphere background exceeds the corona brightness.

## 2. Observations

The coronograph with artificial moon, shutting the inner corona up to $2.5R_S$, where $R_S$ - radius of the Sun, the interference filter with half-width $10\mathring{A}$ on region of line MgI $\lambda$ 5173Å, Fabry-Perot etalon and CCD matrix Apogee Alta-10 were used under making of observations. The field of view of telescope exceeds $5^o$, what allowed to receive the information about radial velocities of dust in outer solar corona for distances from $3R_S$ to $10R_S$.

The duration of the eclipse totality was 170 seconds at the Sun altitude above horizon $27^o.5$. The non-winder weather and completely clear sky with the low brightness were in the day of eclipse. The two working images were taken during total phase. The first image(exposition 130 seconds)contains the information about radial velocities of dust in the F-corona. The emission rings of scattered in optics light of green coronal line $\lambda$ 5303Å are seen on second image (exposition 20 seconds. The two images of daily sky, received before and after totality, are used as reference images. The results of both treatments are coincided in limits $\pm 10 km/s$.

The twenty absorption lines distributed at distances from 3 to 11 solar radii are taken for processing. Among them there are all three lines of green triplet Mg I: $\lambda$ 5184Å, $\lambda$ 5173Å and $\lambda$ 5167Å, and also some weak lines. The spectral resolution $\delta\lambda_{1/2} = 1\mathring{A} \pm 0.1\mathring{A}$ was derived on emission lines $\lambda 5303\mathring{A}$. It was carried on the 18 diameter scans with interval of $10^o$. The reference point of positional angles is began from ecliptic north pole counter-clockwise. The east direction is $90^o$, and west is $270^o$. Thus, the total volume of measurements is 20 lines on 36 directions.

## 3. Results

The average values of measured radial velocities versus the distance from the Sun (averaged on all 36 directions) are represented on Fig.1. In such average method the all velocities corresponding to orbital motion of dust around the Sun must be compensated. Thus, Fig.1 mainly reflects the radial motion of dust relatively the Sun.

On Fig.2 the averaged radial velocities versus the positional angles are represented. Such average method allows to allot the influence of orbital motion of dust. If the orbital motion of dust is like circular, the Doppler negative velocities must be observed near $P = 90^o$, and the Doppler positive ones near $P = 270^o$. In first it was obtained on results of 1981 year observations (Shcheglov et al.,1987.

Thus, the results of 2006 year observations confirm the predomination of negative velocities (Fig.1) at near distances from Sun ($r < 4R_S$). The averaged radial velocities on all distances (Fig.2) does not show the presence of regulate orbital motion of dust as it was observed at 1981 year (Fig.3).

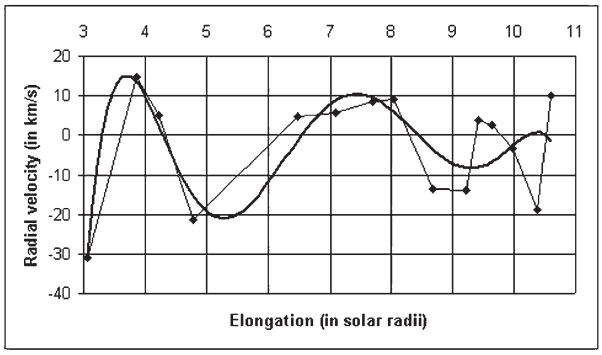


Figure 1: The average on all positional angles radial velocities versus the distance from the Sun. The solid line - the observation approximation by polynomial of 6-th order.

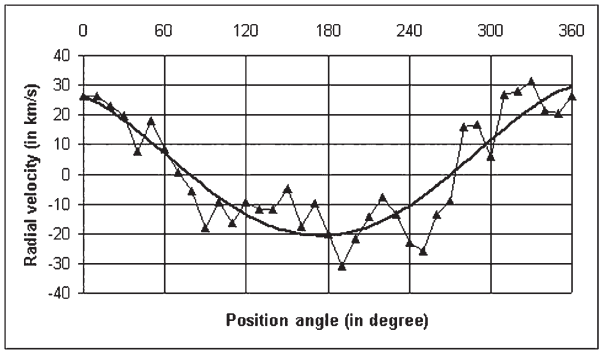


Figure 2: The averaged on all distances radial velocities versus positional angle. The reference point - the ecliptic north pole. $90^o$ - east, $180^o$- south,$270^o$ - west. The solid line - the observation approximation by polynomial of 4-th order.

## 4. Discussion

Evidence of fast disturbing action of non-gravitational forces on dust particles is the absence of clearly seeing orbital motion of dust at near-by distances from the Sun. Really magnetic field of the Sun can act on dust grains of small dimension $< 1mkm$. It seems to be natural the conclusion about predomination of grains of comet origin rather than asteroid one, insofar as the sizes of comet particles are small and the orbits are no practically connected with ecliptic plane.

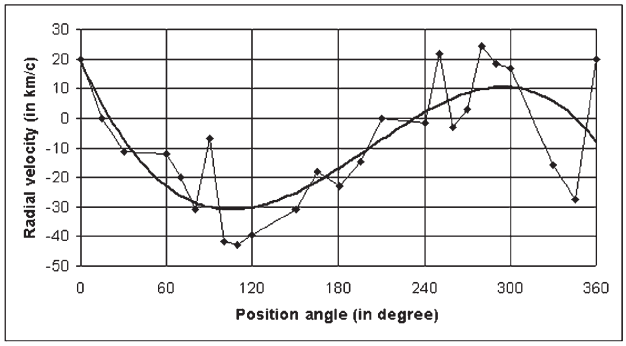


Figure 3: The averaged radial velocities in the F-corona on July 31, 1981. The solid line - the observation approximation by polynomial of 4-th order.

Perhaps, in investigated region the composition of dust grains is changed with time. The results of action of the Sun magnetic field on these particles might also be changed in connection with variations of solar activity (1981-year of maximum, and 2006-year of solar activity minimum). The new theoretical approaches should be needed for more careful analysis of 2006 year observations.

*Acknowledgements.* The authors are thankful to all participant of our expedition.

### References

Shcheglov, P.V., Shestakova, L.I., Ajmanov, A.K.: 1987, *Astron. & Astrophys.,* **173**, 383.

Shestakova, L.I..: 1987, *Astron.& Astrophys.,* **175**, 289.

# THE CBS SPECTRA INVESTIGATION AS METHOD OF THE PN CHEMICAL COMPOSITION ANALYSIS

N.N. Shimanskaya, V.V. Shimansky, I.F. Bikmaev, N.A. Sakhibullin, R.Ya. Zhuchkov

Astronomy Department, Kazan State University
str. Kremlevskaya, 18, Kazan, 420008 Russia
*Nelli.Shimanskaya@ksu.ru*

ABSTRACT. We report the results of the investigations of chemical composition of close binaries which had gone through the stage of common envelope and which are the remnants of planetary nebular cores. High resolution spectra for different phases of orbital period of V471 Tau were taken by RTT-150 telescope and were investigated by the modified SYNTH-K program. It was found that the spectra show noticeable variability with appearance of emission components depended on the orbital period phase. For chemical composition determination the "solar" oscillator strengths for 700 lines were taken. It was found that the chemical content of V471 Tau is composite one and characterized by excess of ?-process elements in the contrast to small underabundance of iron-peak elements. The estimation of different elements excesses allows to determine their contents in planetary nebular phase.

**Key words**: Stars: binary: cataclysmic; stars: individual: Sun, V471 Tau

## 1. Introduction

Modern theory of chemical evolution of our Galaxy considers several sources of changing of the matter composition:

1) supernovae SNI and SNII explosions,
2) formation of planetary nebulae (PN),
3) Novae explosions,
4) WR-stars,
5) natural radioactivity,
6) the interaction with cosmic particles.

To check the correctness and the accuracy of this theory two types of observational criteria may be used.

1) Global - the determination of chemical composition of the gas and stars of different ages and comparison with theoretical predictions. These criteria allow to check the theory as whole, but do net give a possibility to improve the models of different objects.

2) Particular - the determination of the nuclear synthesis efficiency for some objects using direct observations.

Unfortunately the complication of the theory for the SN and PN radiation formation put a limit on the accuracy 0.5-1.0 dex for chemical determinations. The chemical content of stellar remnants ( white dwarfs and blue subdwarfs) is influenced by stratification effects. As a result we have no reliable direct observational data of nuclear synthesis at the final stages of stellar evolution.

In this work we investigate the possibility to get such data by alternative method of the probe. It is assumed that this probe should be in deep layers of evolving star. Then the chemical composition of a matter enriched by the probe may be investigated by traditional stellar atmospheres modeling. The natural realization of such a probe is close binary systems. These systems are forming from broad stellar pairs with the main component which after evolution on the main sequence stage is expanding up to the supergaint size. The orbital velocity of both components is 10 times larger then the rotational velocity of the envelope. As a result the system begins to loose the angular momentum, to decrease the large semiaxis and to mix a matter. Finally after the supergaint envelope loss secondary component (enriched by nuclear synthesis products) may be observed.

The accuracy of abundance determination of this component depends on the conditions of observations. In cataclysmic variables with bright accretion disc the radiation input of the secondary component is small, so the possibilities of investigation are limited. In massive X-ray binaries the disc luminosity is small, so there are good conditions to investigate the abundance of the matter produced by SNII. Precataclysmic variables gives an optimum possibility for the analysis of the nuclear synthesis efficiency during PN formation because there are no accretion effects. In our work we pot our attention on the old PN - V471 Tau.

V471Tau was discovered by Nelson and Yuong (1970) as eclipsing binary system with the orbital period $P = 0.^d52118$. The brightness of this object ($m_b = 10.24^m$, $m_V = 9.48^m$) permits to get high resolution spectra which show that red dwarf dominates in optical radiation. This objects has a variability with

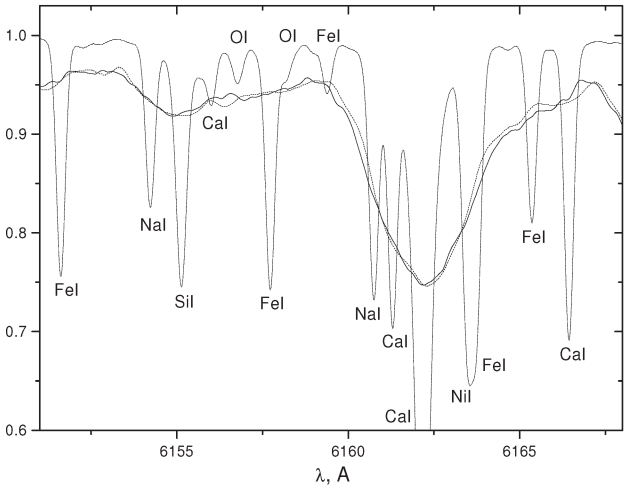


Figure 1: Theoretical (not broadened) profiles for l forming blends and theoretical and observed blend

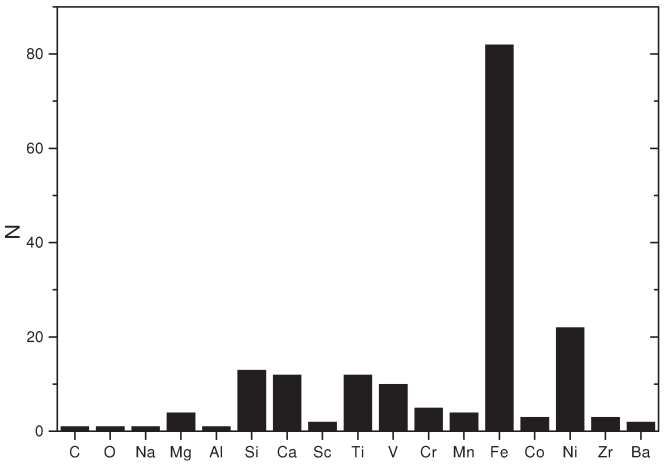


Figure 2: The distribution of numbers of abundance determinations for different elements.

unstable amplitude coursed by interaction of magn fields of both components. The full list of fundame stellar parameters was taken from the paper by O'B at al. (2001). Chemical abundance of the secondary component was analyzed by using moderate resolution spectra (Martin et al., 2001) and X-ray fluxes (Still et. al, 2003). The accuracy of abundance determinations for 4-5 elements is about 0.4 dex and shows considerable differences. So we decided to perform the abundance determination of this object with higher accuracy.

## 2. Observations and spectra modeling for V471Tau

Eleven spectra of high resolution ($\frac{\lambda}{\Delta\lambda} = 40000$, $S/N = 70-90$, $\Delta\lambda = 3900-8800\mathring{A}$) were observed by the RTT telescope during the nights 12/13, 13/14, December, 2004. Coude–eshelle spectrometer CES and CDC detector with nitrogen cooling was used. The data reduction was performed by DECH computer complex. The comparison of spectra in different phases showed the emission components in the Balmer lines which caused by reflection effects. Line profiles for heavy elements are not changing and may by used for abundance determination by stellar atmospheres models.

Spectra modeling was performed by using the SYNTH program and model atmospheres by Kurucz (1994). We include in calculations instrumental profile, macroturbulence ($V_{macro} = 1.8km/sec$) and microturbulence ($\xi_{turb} = 1.0km/sec$) broadening and stellar rotation. The velocity of the red dwarf rotation (Vsini=83 km/sec) was estimated from the analysis of the spectra. For stellar abundance analysis we redetermined line parameters by comparison of calculated solar spectrum with the flux Atlas for the Sun (Kurucz et al., 1984). In result we determined more than 600 solar oscillator strengths and van der Waals damping constants. The comparison of solar oscillator strengths $\log gf$ with Kurucz data (Kurucz,1994) showed that the last data in general are overestimated by the factor 0.14 dex independently on the ionization stage, excitation energy and wave lengths. Empirical van der Waals damping constants overestimate classical Unsold values by the factor 6. Moreover, there are two groups of lines with completely different (in 2.5 times) scaled factors for damping.

## 3. The analysis of results

The abundance determinations for V471Tau was performed by their variations to achieve the best agreement of observed and calculated blends as shown on fig.1. In result we have investigated 113 line blends, 104 blends gave us abundances for 16 Chemical elements. The iron abundance was based on 83 blends with the accuracy 0.02 dex. For 5 elements (Si, Ca, Ti, V, Ni) we had about 10 estimations with average accuracy 0.08 dex. For Mg, Cr, Mn, Co and Zr there were 3-5 estimations only. Abundances of other elements we found using 1-2 estimations and should be improved.

Chemical abundances relative to the solar ones are shown in fig 3. The analysis of these data allows to make the next conclusions.

1) The metalicity of V471Tau ([Fe/H])=- 0.2 dex) indicates that this star belongs to the thin galactic disc. At the same time it is less (0.3 dex) than the average stellar metalicity in the Hyada cluster. It is in a good agreement with suggestion of O'Brien et al. (2001) that V472Tau does not belong to the cluster.

2) The abundances of odd and iron group elements (Na, Al, Ca, Ti, Cr, Mn, Co, Ba) corresponds to the value of the metalicity. According to theoretical predictions these elements are not producing in stars with

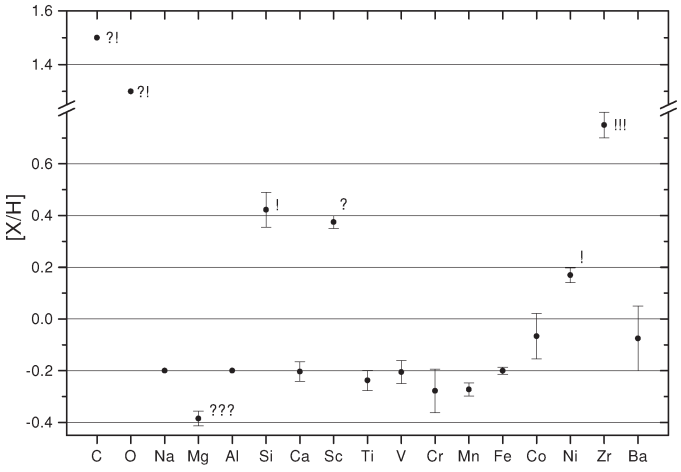


Figure 3: V471 Tau abundance [X/H] elements relative to the solar ones.

masses 5-7 $M_{\odot}$.

3) Large excesses for carbon ([C/H]=1.8 dex) and oxygen ([O/H]=1.3) are producing by $\alpha$- process acting in the final stage of supergaint life. For white dwarfs with the mass 0.83 $M_{\odot}$ $\alpha$- process must be ended by the synthesis of neon and magnesium. So we assume that these elements must be overabundant.

4) The circonium excess ([Zr/H]=0.73 dex) is explained by s-process acting simultaneously with $\alpha$-process. The same excesses were found by Thevenin et al. (1997) for others elements of s-process ([Y/H]=0.40, [Sr/H]=0.80 dex) in the nuclei of PN Abell 35.

5) The deficiency of Mg ([Mg/H]=-0.38 dex) and the excess for Si ([Si/H]=0.42 dex) contradict to theoretical predictions mentioned above. We suppose that at the supergaint stage there were important transformation of Mg to Si in a process similar to $\alpha$-process. The reasonsof such process should be investigated in details.

6) The excess of Sc ([Sc/H]=0.38 is probably coursed by measurement errors and needs additional analysis.

7) The excess for Ni ([Ni/H]=0.17) is in a serious contradictions with modern ideas about nuclear synthesis. This element is producing together with iron in SNI only. Therefore this result should be checked by observations and the theory.

Finally we conclude that abundance investigations of close binaries provide important information about the efficiency of nuclear synthesis on last stages of stellar evolution.

*Acknowledgements.* This work was supported by the RFFI foundation (grant 05-02-17744) and the President Program. (grant NSh -784.2006.2).

**References**

Nelson B. and Young A.: 1970, *PASP,* **82**, 699.

O'Brien M.S., Bond H.E., Sion E.H.: 2001, *A. J.*, **563**, 971.

Martin L., Pavlenko J., Rebolo R.: 1997, *A. J.*, **326**, 731.

Still M. and Hussain G.: 2003, *A. J.*, **597**, 1059.

Kurucz R.L.: 1994, *SAO CD-ROMs. Cambridge, MA02138, USA.*

Kurucz R.L., Furenlid I., Brault J., Testerman L.: 1984, *Solar Flux Atlas from 296 to 1300nm.* Nat. Solar Obs., Sunspot, New Mexico.

Thevenin F. and Jasniewicz G.: 1997, *A&A.*, **320**, 913.

# SIMULATION OF COLOR VARIATIONS IN GRAVITATIONALLY LENSED QUASAR Q2237+0305 (THE EINSTEIN CROSS)

G.V. Smirnov[1], V.G. Vakulik[1,3], R.E. Schild[2], V.S. Tsvetkova[3]

[1] Institute of Astronomy, V.N.Karasin Kharkiv National University
35 Sumska Str., Kharkiv 61022 Ukraine, *vakulik@astron.kharkov.ua*
[2] Center for Astrophysics
60 Garden Str., Cambridge, MA 02138, U.S.A., *rschild@cfa.harvard.edu*
[3] Institute of Radio Astronomy of Nat.Ac.Sci. of Ukraine
4 Chervonopraporna Str., Kharkiv 61002 Ukraine, *tsvetkova@astron.kharkov.ua*

ABSTRACT. A mechanism of colorized phenomena in gravitationally lensed quasar Q2237+0305 due to microlensing is analysed in computer simulation. A two-component quasar spatial structure model consisting of a hot central source surrounded by an extended outer structure with a more low-temperature radiation was proposed. The model was shown to provide relationship between variations of the $(V-I)$ color indices and $R$ magnitudes, which is consistent to the observed one presented in our recent publication.

**Key words**: gravitational lensing: quasars: individual: Q2237+0305.

## 1. Introduction

The study of microlensing events is known to provide a unique possibility for the quasar spatial structure to be resolved with the unprecedented angular resolution. A regular and highly accurate photometric monitoring of variability is the basis for solving this problem. The programs of such monitoring for Q2237+0305 were undertaken repeatedly, (Corrigan et al. 1991, Ostensen et al. 1996, Alcalde et al. 2002), with the most well-sampled and accurate monitoring data in the $V$ filter obtained by OGLE (Optical Gravitational Lensing Experiment) program, (Wozniak et al. 2000, Udalski et al. 2006). Also, monitoring of the Einstein Cross Q2237+0305 in the $V$, $R$ and $I$ filters is being carried out with the Maidanak 1.5-m telescope since 1997 (Vakulik et al. 1997, Dudinov et al. 2000, Vakulik et al. 2004, Vakulik et al. 2006).

The importance of multicolor photometry for this object was demonstrated in the first observations of Q2237+0305 by Yee (1988) where the difference in color indices of the components was explained by differential extinction. However, a suspicion arose a bit later (Corrigan et al. 1991, Rix et al. 1992), that the color indices of the components might have changed since the first three-color observations by Yee (1988). As far back as 1986, Kayser, Refsdal & Stabell suggested that colorized phenomena in gravitationally lensed quasars can be expected in microlensing of a source with a radial temperature gradient. This was later confirmed in simulations by Wambsganss & Paczyński (1991). Recently, Vakulik et al. (2004) have shown that a significant correlation between the brightness changes and color changes of the Q2237+0305 components exists, which should be attributed to microlensing events rather than to the variable extinction in the lensing galaxy.

In the present work, we proceed from the assumption that the effective sizes of the quasar emitting regions may be wavelength-dependent, and consider a photometric model of the Q2237 quasar, consisting of a compact central source at some brightness pedestal, as used in our recent work (Vakulik et al. 2006). In the present study, we use the same model to simulate the observed variations of colors in Q2237 reported in the work by Vakulik et al. (2004). Our simulations permitted to obtain the estimates of the compact central part dimension and the energy contributions of the extended outer structure at the spectral intervals corresponding to the $V$, $R$ and $I$ bands.

## 2. Simulation of microlensed light curves

Using a method of the inverse ray tracing, (Schneider et al. 1992), it is possible to calculate the distribution of magnification rate $M(y_1, y_2)$ for a small (quasi-point) source for all possible locations $(y_1, y_2)$ – the so-called magnification map. In microlensing of a finite-size source, which is situated at the point $(y_1', y_2')$ of the magnification map and is characterized by a surface brightness distribution $B(y_1, y_2)$, the magnifica-

tion rate is determined by the formula:

$$\mu(y_1', y_2') = \frac{\int\int B(y_1, y_2) M(y_1 - y_1', y_2 - y_2') dy_1 dy_2}{\int\int B(y_1, y_2) dy_1 dy_2}, \quad (1)$$

where the integrals are calculated within a region where the surface brightness $B(y_1, y_2)$ is non-zero.

The inner compact feature of our two-component source model describes the central part of the accretion disc and is characterized by a surface brightness distribution $B_1(y_1, y_2)$. The other, outer feature is associated with larger structural elements – a shell, a torus, Elvis's biconics (Elvis 2000), – which are of a substantially lower surface brightness $B_2(y_1, y_2)$. For such a two-component source, situated at a point $(y_1', y_2')$, the values of the magnification rate $\mu_{12}$ can be calculated from expression:

$$\mu_{12}(y_1', y_2') = \frac{\mu_1(y_1', y_2') + \varepsilon \mu_2(y_1', y_2')}{1 + \varepsilon}. \quad (2)$$

The magnification rates $\mu_1$ and $\mu_2$ are calculated according to (1) for the surface brightness distributions $B_1$ and $B_2$, while $\varepsilon$ is determined as a ratio of the integral luminosities of these structures.

The characteristic time-scale of the observed Q2237 microlensing brightness fluctuations is known to be almost a year. We regard that such a scale is due to microlensing of the compact inner quasar structure. Since the expected spatial scale of the outer structure may be more than an order of magnitude larger as compared to the inner part, (Elvis 2000, Schild & Vakulik 2003), the expected time scale of its microlensing brightness variations will exceed ten years. In addition, because of the large dimensions of the outer structure, the amplitudes of microlensing magnification must be noticeably less, as compared to microlensing of the compact structure. Thus we suggest as well, that on time-scales of about 4 years, the magnification rate $\mu_2(y_1, y_2)$ is almost invariable and does not differ noticeably from the average magnification rate of the $j$-th component $\mu_j$ resulting from microlensing, that is, $\mu_2(y_1, y_2) \approx \langle \mu_2(y_1, y_2) \rangle \approx \mu_j$ in expression (2).

It is clear that, at the short time intervals, microlensing of the extended structure reveals itself in reducing, by a factor of $1/(1 + \varepsilon)$, the amplitudes of brightness variations resulted from microlensing of the compact structure. Therefore, in analysing the light curves at the time interval of 4 years, we did not seek estimation the effective size of the outer structure, and the value of $\varepsilon$ was its only characteristics. The inner compact structure, which imitates a central part of the accretion disc, was modeled by a disc with the Gaussian brightness profile, and its effective size $r/r_E$ at the half-intensity level was the sought-for parameter, ($r_E$ is the Einstein radius of a microlens).

## 3. Results of simulation

Since multicolor observations of Q2237+0305 have been carried out only episodically, there was no possibility to analyse a behavior of color variations of the components in time. Therefore, in the present work, we focused at simulation of statistical relations between the color indices and magnitudes, which have been recently discovered and analysed in (Vakulik et al. 2004). And it was only for the C component, for which, in addition to the detailed $V$ light curve (Woźnyak et al. 2000), the brightness estimates near the 1999 microlensing brightness peak were also available in $R$ and $I$, that an attempt to simulate the light curves had been undertaken.

From the magnification map for the C component, using the method of a random search, we found the light curves which fitted qualitatively to its light curve obtained by the OGLE collaboration in the $V$ filter during 1997-2000 (Woźnyak et al. 2000). Varying the source model parameters – the effective size of the central compact feature $r$ and the relative intensity of the outer extended structure $\varepsilon$, – we reached the best fit of the simulated light curve to the observed one. For the same source trajectory, the source model parameters $r$ and $\varepsilon$ were estimated similarly for the $R$ and $I$ light curves by fitting the simulated light curves to those obtained from observations at the Maidanak Observatory (Vakulik et al. 2004). For one of successful trials, the parameters estimates were obtained to be $r = 0.36 r_E$, $0.53 r_E$, $0.71 r_E$, and $\varepsilon$= 3.3, 5.0, 6.2 for the $V$, $R$ and $I$ filters, respectively. Since our observations in the $R$ and $I$ filters were not regular enough, the obtained differences between the central source size estimates in different filters can not be regarded as significant. However, the relative energy contribution of the extended outer structure definitely tends to increase towards the longer wavelengths. This may be explained as due to the more low-temperature radiation from the extended structure. This result is an expected one, since in our model, radiation from the central source is associated with a high-temperature emission of the inner edge of the accretion disc, while the outer structure most probably re-emits the hard short-wave radiation of the accretion disc.

For the source model described above, a statistical analysis of variations of colors and brightness was carried out as well. To analyse the effects of differences of both the central source dimensions and energy contributions from the outer structure on variations of colors, we simulated microlensing events for three sets of the source parameters $r$ and $\varepsilon$. In one case, the values of the source parameters obtained in fitting of the simulated light curve to that observed in filter $V$ for image C were accepted. In the second case, the central compact source size was regarded to be the same for all

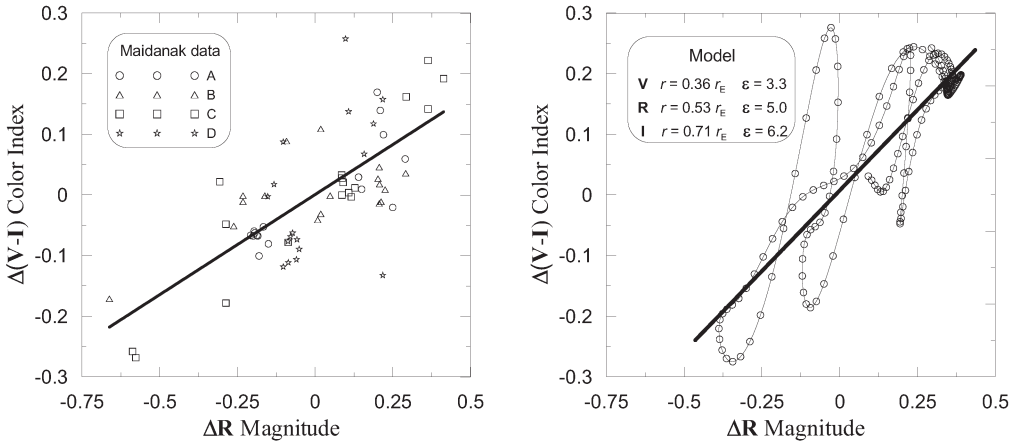


Figure 1: – (a)(left panel): variations of the color indices $\Delta(V-I)$ vs variations of brightness $\Delta R$, built from the observations of 1997-2000 at the Maidanak Observatory; (b)(right panel): a similar dependence built from the simulated light curves for the two-component source model with the compact feature dimensions $r/r_E$ and with the time-dependent relative energy contribution of the extended structure $\varepsilon$.

Table 1: The maximal variations of color indices and $R$ magnitudes, as well as regression line slopes $a$ and correlation indices $k$ for dependencies $(V-I)$ vs $R$ as was obtained from the Maidanak data (the first line), and calculated for various parameters of the two-component source model in simulations (the last three lines).

| | $V$ | $R$ | $I$ | $\Delta(V-R)$ | $\Delta(R-I)$ | $\Delta(V-I)$ | $\Delta R$ | $(V-I)$ vs $R$ $a$ | $k$ |
|---|---|---|---|---|---|---|---|---|---|
| Observational data | | | | $0.32 \pm 0.09$ | $0.31 \pm 0.09$ | $0.49 \pm 0.14$ | $0.71 \pm 0.27$ | $0.31 \pm 0.08$ | $0.75 \pm 0.08$ |
| $r/r_E$ | 0.36 | 0.53 | 0.71 | $0.41 \pm 0.09$ | $0.20 \pm 0.05$ | $0.55 \pm 0.13$ | $0.78 \pm 0.23$ | $0.53 \pm 0.06$ | $0.86 \pm 0.03$ |
| $\varepsilon$ | 3.3 | 5.0 | 6.2 | | | | | | |
| $r/r_E$ | 0.53 | 0.53 | 0.53 | $0.23 \pm 0.07$ | $0.11 \pm 0.03$ | $0.33 \pm 0.10$ | $0.77 \pm 0.22$ | $0.44 \pm 0.03$ | $0.99 \pm 0.00$ |
| $\varepsilon$ | 3.3 | 5.0 | 6.2 | | | | | | |
| $r/r_E$ | 0.36 | 0.53 | 0.71 | $0.87 \pm 0.16$ | $0.52 \pm 0.11$ | $1.20 \pm 0.26$ | $2.87 \pm 0.87$ | $0.08 \pm 0.21$ | $0.28 \pm 0.15$ |
| $\varepsilon$ | 0 | 0 | 0 | | | | | | |

filters, and only energy contribution of the outer structure was varied. In the third case, the outer structure was absent, and the values $r = 0.36r_E$, $0.53r_E$, $0.71r_E$ were adopted for the $V$, $R$ and $I$ filters, respectively. Since statistical characteristics of microlensed light curves have been shown to depend on the effective size of the source rather than on the brightness distribution over the source (Mortonson et al. 2005), we used the effective source radii in our analysis.

For each of these cases, 10 trajectories of the source were randomly selected at the magnification maps and the light curves were calculated corresponding to observations in filters $VRI$. The estimates of variations of color indices and magnitudes were obtained from these data, correlation coefficients and regression line slopes were determined, and a comparison with the corresponding data of observations presented in (Vakulik at al. 2004) was made. The results are presented in Table 1. For the source model with the parameters obtained in fitting the image C light curves, a regression line slope for the $(V-I)$ color – $R$ magnitude dependence is $a = 0.53$, and a correlation index is $k = 0.86$ (Fig. 1b). It is a bit larger values than those obtained by (Vakulik et al. 2004) from the data of observations, ($a = 0.31$, $k = 0.75$, Fig. 1a). However, taking into account the random errors inherent in the photometry data, which decrease both a correlation index and a regression line slope, we regard the modeled and observed color-magnitude dependencies to be consistent.

In the second case, when the effective size of the inner compact source component is not wavelength-dependent, the regression line slope decreases ($k = 0.4$), and becomes closer to the value obtained from observations (Vakulik et al. 2004), but extremely high correlation index of $k = 0.99$ is observed. This is a consequence of virtually unambiguous relationship between the color and brightness variations in this case: in microlensing of such a source, the increase of brightness always is accompanied by the shift of the color indices towards the bluer ones.

Finally, noticeable color variations can be obtained in the third case, when the effective source size is sub-

stantially wavelength-dependent, much more dependent than the classical blackbody-radiating accretion disc. However, since there is no unique dependence between the color and brightness variations in this case, the color-brightness correlation index is low ($k = 0.28$), and consequently, the regression line slope is low too ($a = 0.08$), that is much less than those obtained for the data of observations.

It was interesting to estimate the linear dimensions of the central compact feature of the source from the results of fitting the $VRI$ light curves for image C. If the effective velocity of the source is accepted to equal $V_e = 5000$ km·s$^{-1}$, then the estimate of the linear radius in filter $R$ will be $r = 3.3 \cdot 10^{15}$cm, while a typical microlens mass is $\langle m_* \rangle = 1.6 \cdot 10^{-3} h^2 M_\odot$. This is consistent with the estimates obtained by other authors.

It should be noted in conclusion that the solution found in simulation for the image C light curve is not a unique one. Other solutions are possible, which may provide somewhat different values for the source model parameters. Therefore, the analysis presented here should be regarded as a qualitative one, and therefore, we do not indicate the errors for the obtained estimates of the source model parameters. Nevertheless, we have managed to follow the principal peculiarities qualitatively, and to understand possible reasons for color variations emerging in microlensing events of the source with a complicated structure, as is formulated below.

## 4. Conclusions

To explain possible reasons for color variations observed in the Q2237+0305 gravitationally lensed quasar, microlensing of a source consisting of a compact inner feature and an extended outer structure has been simulated. By fitting the simulated and observed light curves of the C component, the inner feature dimensions have been estimated to be $r = 0.36 r_E$, $0.53 r_E$, and $0.71 r_E$ for filters $V$, $R$ and $I$, respectively, with the corresponding estimates for the relative energy contributions from the extended structure of $\varepsilon = 3.3$, 5.0 and 6.2. Simulation and statistical analysis of microlensing of such a source demonstrates a satisfactory consistency of the simulated relationships between the color and brightness variations to those obtained from the data of observations for Q2237+0305.

Also, the cases have been analysed, when the size of the compact feature does not depend on the wavelength, or when the energy contribution from the outer structure is $\varepsilon = 0$, which is equivalent to a particular case of a simple (Gaussian) source with the wavelength-dependent effective size. Noticeable color variations were shown to appear in this case as well, but however, the correlation index for the color-magnitude dependence is low and, as a consequence, the regression line slope is inconsistent to that obtained from observations. Therefore, a suggestion that variations of colors in gravitationally lensed quasars are due to microlensing of the accretion disc, does not seem to be convincing enough. A model consisting of a hot central source surrounded by an extended outer structure with a more low-temperature radiation seems to be preferable.

*Acknowledgements.* This work has become possible thanks to the support from the STCU grant U127, and from the target program of the Nat.Ac.Sci. and Nat. Space Agency of Ukraine "Investigation of the Universe structure and composition; search for the hidden mass and dark energy", ("Cosmomicrophysics").

### References

Alcalde D., Mediavilla E., Moreau O., et al.: 2002, *ApJ*, **572**, 729.
Corrigan R.T., Irwin M.J., Arnaud J.: 1991, *AJ*, **102**, 34.
Dudinov V.N., Vakulik V.G., Zheleznyak A.P. et. al.: 2000, *Kinem. i Fiz. Neb. Tel.*, **16**, 346.
Elvis M.: 2000, *ApJ*, **545**, 63.
Huchra J., Gorenstein M., Kent S., et. al.: 1985, *AJ*, **90**, 691.
Kayser R., Refsdal S., Stabell R.: 1986, *A&A*, **166**, 36.
Mortonson M.J., Schechter P.L., Wambsganss J.: 2005, *ApJ*, **628**, 594.
Ostensen R., Refsdal S., Stabell R., et al.: 1996, *A&A*, **309**, 59.
Racine R.: 1992, *ApJ*, **395**, L65.
Rix, H.-W.; Schneider, D.P.; Bahcall, J.N.: 1992, *AJ*, **104**, 967.
Schild R., Vakulik V.: 2003, *AJ*, **126**, 689.
Schneider P., Ehlers J., Falco E.E.: 1992, *Gravitational Lenses*, Springer-Verlag.
Udalski A., Szymanski M. K., Kubiak, M., et al.: 2006, *Acta Astronomica*, **56**, 293.
Vakulik V.G., Dudinov V.N., Zheleznyak A.P., et al.: 1997, *Astron. Nachr.*, **318**, 73.
Vakulik V.G., Schild R.E, Dudinov V.N., et al.: 2004, *A&A*, **420**, 447.
Vakulik V.G., Schild R.E., Dudinov V.N., et al.: 2006, *A&A*, **447**, 905.
Vakulik V.G., Schild R.E., Smirnov G.V., et al.: 2007, *arXiv:0708.1082*
Wambsganss J., Paczyński B.: 1991, *AJ*, **102**, 864.
Wozniak P.R., Alard C., Udalski A., et al.: 2000, *ApJ*, **529**, 529.
Yee, H.K.C.: 1988, *AJ,* **95**, 1331.

# THE DETERMINATION OF METEOROIDS' LIFE TIME UNDER ACTION OF PHOTONS AND PROTONS

E.N. Tikhomirova

Astronomical Observatory, State Pedagogical University
108 Respublikanskaya Str., Yaroslavl 150000 Russian Federation, *en_ tihomirova@mail.ru*

ABSTRACT. The life time of meteor streams under action of photons and protons is estimated. The interval of time after which the particles of the comet 9P (1867 G1)/ Tempel 1 (after bombarding the comet during the mission "Deep Impact") reach the Earth is estimated (the meteor stream is observed). The account of the action of photons only and the corpuscular analogue of Poynting-Robertson effect is made at the calculations. According to the results the intervals of time after which the particles reach the Earth can differ by 1.5 times.

**Key words**: Comets; meteors: Poynting-Robertson effect: life-time

## 1. Introduction

In works (Wyatt et al., 1950) and (Ryabova, 2005) in semi analytical form the influence of photons and the Solar Wind on motion of meteoroids is taken into account separately. Here we determine meteor shower's life time analytically in view of simultaneous action of photons and protons.

## 2. The Fundamental Equation of Motion of the Meteoroids under Action of Photons

The differential equation of motion submitted in the vector form, absolutely black spherical body, isotropic re-radiating a solar energy and moving with velocity $\nu$, making an angle $u$ with a direction of a heliocentric radius - vector $\vec{r}$ (Radzievskii, 2003) looks like :

$$\ddot{\vec{r}} = -\frac{GM'\vec{r}}{r^3} - \frac{2\pi R^2 q r^2_{S-E}}{Mc^2}\nu\cos u\frac{\vec{r}}{r^3} - \frac{\pi R^2 q r^2_{S-E}}{Mc^2 r^2}\nu\sin u\vec{e_t} \quad (1)$$

M′ is the reduced mass of the Sun connected to mass of the Sun $M_S$ and mass of (spherical) particle M, by the ratio:

$$M' = M_S - \frac{\pi R^2 q r^2_{S-E}}{GMc} \quad (2)$$

The equation (1) is applicable in case R>λ. The effect of Poynting - Robertson is characteristic for the particles with radii from 1m up to 1cm.

To apply methods of theory of perturbed motion let's suppose that in right part of the equation (1) the first term ("photogravitational"acceleration - $f_0$) exceeds for more than tens and hundreds times the second and the third ones ($f_r$ and $f_t$ - perturbating accelerations).

For a case of small perturbations from the equation (1), after averaging for one orbital evolution of a meteoric particle and the subsequent integration, according to (Wyatt et al., 1950):

$$\frac{a}{a_0} - \frac{e^{4/5}(1-e_0^2)}{e_0^{4/5}(1-e^2)} = 0 \quad (3)$$

and also a quadrature :

$$I(e,e_0) = \int_{e_0}^{e}\frac{e^{3/5}}{(1-e^2)^{3/2}}de =$$

$$= -\frac{5\pi^2 R^2 q_{S-E} r^2_{S-E} e_0^{8/5}}{\sqrt{GM'}Mc^2 T_0 a_0^{1/2}(1-e_0^2)^2}(t-t_0) \quad (4)$$

Let's assume, that after disintegration of the cometary's nucleus large fragments stay in the initial cometary's orbit (its parameters are $a_0$, $e_0$, $i_0$). The values of parameters of cometary's orbit (semimajor axis $a_c$, eccentricity $e_c$ and inclination $i_c$) vary insignificantly ($a_c \approx a_0$, $e_c \approx e_0$, $i_c \approx i_0$) during the intervals of time corresponding the tens and hundreds orbital periods. In this model of the cometary and meteoroidal motion the longitude of the ascending node ($\Omega_c$) of the plane of cometary orbit (meteoroid) and the argument of perihelion ($\omega_c$) can vary significantly.

W t k i t t th t th b di f ll i are under action of light pressure and the Poynting - Robertson effect ($a = a(t)$, $e = e(t)$), we also assume $i = i_0$.

### *2.1. The Examples*

Let's estimate the time of life of meteor stream with the help of the integral 4. For example, after the

artificial explosion made July, 4, 2005 during the space mission "Deep Impact"(comet 9P (1867 G1)/ Tempel 1), at density of meteoroids' substance $\rho = 1$ g/cm$^3$, we shall come to the following estimations of a required interval of time $\tau_{LT}$ at various values of meteoroids' radii R (see Table ).

| Radius of meteoroids $\mu$m | 100 | 10 | 1 |
|---|---|---|---|
| $\tau_{LT} = t - t_0$, (years) | 337400 | 32800 | 2200 |

Таблица 1: The calculation of the life time of meteoroids of various radii, with account of the action of photons; the initial parameters of the meteoroids' orbit coincide with the parameters of the cometary's orbit (comet 9P (1867 G1)/ Tempel 1).

Here $\tau_{LT}$ is the interval of time (since the disintegration of the cometary's nucleus), after which it is possible to observe the meteor stream.

## 3. The Account of Simultaneous Action of Photons and Protons on the Meteoroids

In (Ryabova, 2005) in semianalytical form the influence of a solar wind on motion of meteoroids is taken into account. Mean value of velocity of the Solar Wind (in the radial direction) is w=400 km/s (for distances $0.3AU < r < 10AU$). The concentration of protons $n_p$ in the Solar Wind varies as $n_p = 8.1(r_{S-E}/r)^2(400/w)$ cm$^{-3}$. We also use ratios: $U = w - v$, $n_\alpha/n_p = 0.05$. The action of electrons and heavy ions at meteoroids is not taken into account. The parameter of the model is $\psi$, which takes on values: 1.6 (water ice), 1.4 (magnetite), 1.1 (obsidian).

Summarizing the results of the works (Wyatt et al., 1950) and (Ryabova, 2005), for the averaging equations of motion we shall find the integral of motion 5:

$$\frac{a}{a_0} - \frac{(1-e_0^2)e^{\frac{4+2k}{5+2k}}}{(1-e_0^2)e_0^{\frac{4+2k}{5+2k}}}, \tag{5}$$

$$k = k_w/k_p, \tag{6}$$

$$k_w = 3.65 \cdot 10^3 \Psi \bar{U}, \tag{7}$$

$$k_p = \frac{\pi q_{S-E} r^2_{S-E} a_0^{3/2}}{\sqrt{GM'}c^2 T_0}, \tag{8}$$

$a_0$ and $e_0$ are the origin values of semimajor axes and eccentricity of the meteoroid's orbit, $\bar{U}$ is the averaging value of |U| at the period of time of the meteoroid's moving.

Here $k_w$ and $k_p$ are the values proportional to the action of protons (of the Solar Wind) and photons, correspondingly; $a_0$ and $e_0$ are the initial values of the semimajor axis and the eccentricity of the meteoroid's orbit.

Let's pay attention, that for possible maximal value of $k_w$ ($\bar{U} = 400 \cdot 10^5 cm/s, \psi = 1.6$) and possible minimal value of $k_p$ ($M' = M_S$, $a_0^{3/2}/T_0 = \frac{\sqrt{GM_S}}{2\pi}$) their ratio is not greater than 1.5. Therefore it is possible to put:

$$0 < k < 1.5 \tag{9}$$

Let's find $k$ from (5):

$$k = \frac{(5 \ln \frac{a(1-e^2)}{a_0(1-e_0^2)} - 4 \ln \frac{e}{e_0})}{(\ln \frac{e}{e_0} - \ln \frac{a(1-e^2)}{a_0(1-e_0^2)})} \tag{10}$$

Averaging the equation (1) and taking into account the action of the Solar Wind, we shall find the quadrature (11), analogous the quadrature (4):

$$I(e, e_0) = -\frac{\pi q r^2_{S-E} a_0^{3/2} R^2}{\sqrt{GM'}c^2 T_0 M}(t - t_0) \tag{11}$$

### *3.1. The Examples*

The obtained results also can be used for estimation of the life time of meteor stream associated with the comet Tempel 1. At calculations: $e_0 = 0.519$, $a_0 = 3.118$ AU, $e = 0.243$, $a = 1.322$ AU, where $a$ and $e$ are the semimajor axis and the eccentricity of the meteor stream's orbit, $a_0$ and $e_0$ are the semimajor axis and the eccentricity of the orbit of Tempel 1.

| $k$ | $\tau_{LT} = t - t_0$ (years) |
|---|---|
| 0 | 2200 |
| 0.5 | 1800 |
| 0.918 | 1562 |
| 1 | 1522 |
| 1.5 | 1319 |

Таблица 2: The calculation of the life time of meteoroids (radius $R = 1\mu$m) with account of the action of photons and protons ($k$ varies from 0 up to 1.5); the initial parameters of the meteoroids' orbit coincide with the parameters of the cometary's orbit (comet 9P (1867 G1)/ Tempel 1).

Then, the particles with radius $R = 1\mu$m reach the Earth past 1522 years after bombarding of the comet by the "Deep Impact"(if perturbating forces of photons and protons are equal) and a new meteor stream should appear.

The suggested equations can be used for the identification of meteor streams and their parent bodies.

## 4. Conclusion

According to the calculations particles of the comet 9P (1867 G1)/ Tempel 1 reach the orbit of the Earth past 1522 years (after disintegration of the cometary's nucleus) and a new meteor stream should appear. The problem of determination of the meteoroids' life time is not solved finally, so as for the problem of the discovery of meteor streams' parent bodies. The results of this work approach the solution of indicated problems.

*Acknowledgements* The author gives the acknowledgments the professors A. V. Bagrov and N. I. Perov for the attention to the work.

## References

Radzievskii V.V.: 2003, *Photogravitational celestial mechanics, Eds. Nickolaev Yu.A. Nizhniy Novgorod*, 196.

Ryabova G.O.: 2005, in *Proc. of the 197th Coll. of the IAU*, 49.

Wyatt S.P., Jr., Whipple F.L.: 1950, *ApJ*, **111**, 134.

# EXPANSION OF COCOONS AND PHYSICAL FEATURES OF THE FRI-FRII MORPHOLOGY OF EXTRAGALACTIC RADIO SOURCES

N.O. Tsvyk

Institute of Radio Astronomy of NASU
4, Chervonopraporna, Kharkiv 61002, Ukraine, *tsvyk@ira.kharkov.ua*

ABSTRACT. It is shown that the morphological different FRI-FRII structures arise in depending on the type of interaction of the relativistic electrons with MHD cocoon turbulence, on velocity of turbulence dissipation, and on the power of extragalactic radio sources. FRII cocoon is filled with the Alfven solitary wave train which keeps the relativistic electrons within the slow cocoon flow and moves the same as the cocoon boundary. FRI cocoon (galo) arises due to anomalous diffusion of the relativistic electrons through the turbulence with stochastic week waves. It forms the halo which size is increasing with reduce of observation frequency, as is really observed.

**Key words**: radio galaxies: cocoon; MHD waves; diffusion; individual: 3C405 (Cygnus A), M87, 3C216.

## 1. Introduction

The usual assumption is the morphologically difference of FRI-FRII extragalactic radio sources appear in depending on how great jet power is to form the shock wave in the cocoon (De Young 2002). On the other way, the type of the source is determined by the character of interaction between the broadening of relativistic electrons in the cocoon and the form of cocoon turbulence.

The accent should be made on the question what type of waves fills the cocoon. The relativistic electrons interact differently with a single wave of various type.

There are many types of waves which can arise in the cocoon plasma. Here are: simple waves, shock waves, solitary waves (solitons).

The turbulence ordinary corresponds to the stochastic waves, arising and broken in the medium with strong dissipation processes. So, in condition with not strong dissipation, the cocoon turbulence can be described not only as stochastic simple waves, but as the solitary waves, or the weak shock waves.

The cocoon turbulence provides transportation of hot plasma flowing from the jet into the source galo, that is a cocoon periphery, through the inter cluster medium (ICM). The relativistic electrons flowing from the jet is transported through it.

It is assumed that FRII extragalactic sources are connected with the solitary wave train, contained into the cocoon bounded by strong shock wave. It keeps a cocoon as compact structure that expands with a slow velocity. An example is Cygnus A (Kaiser 2000, Wilson et al 2006).

FRI extragalactic sources are connected with weak shock waves or with week stochastic waves, forming "diffuse" cocoon - galo of large size (like M87 (Owen et al 2000) or 3C216 (Meng et al 2001)), changing with observation frequency.

## 2. FRII: the keeping of the relativistic electrons by MHD solitons

FRII extragalactic sources are power sources which is bounded by hydrodynamical shock wave. The observations show that FRII cocoons answer the spectral aging model (Kaiser 2000) in which relativistic electrons aging as far as they move off the hotspot. In this model the diffusion of relativistic electrons is absent; and the relativistic electrons lose energy only due to synchrotron and inverse Compton emissions and to the adiabatic expansion of the cocoon.

The problem arised: how are cocoon relativistic electrons kept within the flow that runs with a small velocity, $u_c < 0.1c$?

In this work this problem is solved in the assumption that the turbulence of FRII cocoon is built in the MHD solitary wave train. These waves naturally arise in the sources of great power. They may be exited in the processes when the jet shock wave goes round compact regions like clouds near the hotspot.

The relativistic particles (relativistic electrons) move

nearly along the magnetic field lines. On that reason they mainly interact with MHD and Alfven solitary waves, that easily can be formed in FRII cocoons.

A dissipation of Alfven solitary wave is minimum when Mach number is $M_a = 3$ (Sagdeev 1964).

The solitary wave profile comes back to the initially state, so that it gives us the conditions for good reflection of relativistic electrons without change in its energetic spectra. So, the relativistic electrons flow with the same velocity as the solitary wave train.

This model has a good consideration with the data for the extragalactic radio source of Cygnus A. There are such cocoon parameters of Cygnus A (Wilson et al 2006) (received from the analysis of X-ray data by *Chandra*): $n_c \sim 0.065$ cm$^{-3}$ - cocoon particle density, $T_c \sim 7 \cdot 10^7$ K - the temperature, $B_c \sim 6 \cdot 10^{-5}$ G - the average magnetic field (from the radio emission data), $u_s \sim 1100$ km/s - the cocoon sound velocity, $u_c \sim 0.05c$ (1000 km/s$< u_c <$ 2150 km/s) - the velocity of cocoon boundary hydrodynamical shock wave, $u_c/u_s \sim (1 \div 2)$.

It means: $u_a \approx 500$ km/s, $3u_a \approx 0.05c$. That coincides exactly with the model when Alfven solitary waves with $M_a \approx 3$ move with the same velocity as the cocoon boundary velocity ($u_c$).

### 3. FRI: anomalous diffusion of the relativistic electrons throughout the turbulent plasma

FRI cocoons are formed by the turbulence, and they are bounded by the weak shock wave train of broken type, dissipating in interaction with ICM. This gives us the condition when the relativistic electrons are anomaly diffused into the galo of extragalactic radio sources (Chuvilgin, Ptuskin 1993).

Diffusion process of the relativistic electrons is determined by those parameters:

$\gamma \simeq c \cdot p/$ 1 MeV - electron energy (relativistic $\gamma$-factor), $p$ is an electron momentum;

$\lambda \simeq 10^{18}(\gamma \cdot 10^{-3})^{0.3}$ cm - free path of the relativistic electron; $\lambda/c \simeq 3 \cdot 10^7(\gamma \cdot 10^{-3})^{0.3}$ s;

$v_a$ - Alfven velocity; for the cocoon concentration of $n_c = 0.03$ cm$^{-3}$ and the average magnetic field of $B_c \sim 3 \cdot 10^{-6}$G, it is $v_a \simeq 30$ km/s;

$L_1 \sim 1$ pc $= 3 \cdot 10^{18}$ cm - characteristic length scale of the small-scale random magnetic field;

$\tau \simeq L_1/c$ - characteristic scattering time of the relativistic electron on small-scale inhomogeneity;

$L_2 \sim 100$ pc $= 3 \cdot 10^{20}$ cm, $\tau_2 = L_2/v_a$ - characteristic spatial and time scales of the large-scale random field;

$\kappa_\parallel$, $\kappa_\perp$ - longitudinal and perpendicular components of the diffusion tensor in the normal diffusion process (in a state medium); $\kappa_\parallel = \lambda c/3$, $\kappa_\perp = \kappa_\parallel/(1 + \omega_B^2\tau^2) << \kappa_\parallel$;

$\tau_d \simeq L_2^2/\kappa_\parallel \sim 3 \cdot 10^{12}$s - characteristic diffusion time.

Diffusion process for relativistic electrons in the cocoon is an anomalous diffusion because the electrons are transported in the medium with turbulence (Chuvilgin, Ptuskin 1993). The values of $L_2$ and $L_1$ are the characteristic spatial scales of that turbulence spectrum.

In FRI cocoons: $\tau_2 > \tau_d >> \tau$. It gives us the coefficient of anomalous diffusion (Chuvilgin, Ptuskin 1993):

$$D(\gamma) = A^2\sqrt{\kappa_\perp \kappa_\parallel} + A^2(u_a L_2) + 0.5A^4\kappa_\parallel, \quad (1)$$

where $A = B_2/B_0$ is an amplitude of the large scale fluctuation of the magnetic field.

The velocity of the anomalous diffusion flow is

$$u_{diff} = \sqrt{D(\gamma)c/\lambda(\gamma)}, \quad (2)$$

$$u_{diff} \approx (0.1A(\gamma \cdot 10^{-3})^{-0.15} + 0.2A^2)c. \quad (3)$$

It is about $u_{diff} \sim 0.1c$. So, FRI age in this model is about $t_{age} = R_c/u_{diff} \simeq 10R_c/c$, where $R_c$ is the cocoon radius.

When relativistic electrons interact with the galo turbulence, there change of its energy distribution. This interaction changes the galo size (that is FRI cocoon size) increasing it when observational frequency is reduced. This fact is really observed (Meng et al 2001).

Thus, FRI extragalactic sources with great galo are explained by the mechanism of anomalous diffusion of the relativistic electrons. For example, the extragalactic source of 3C216 has $R_c \sim 200$ kpc (Meng et al 2001)(the angular size is $20''$, the source distance is 2700 Mpc), and this model gives us its age, $t_{age} \simeq 6 \cdot 10^7$ yr. For M87: $R_c \sim 60$ kpc (Owen et al 2000), and it gives us the age $t_{age} \simeq 2 \cdot 10^7$ yr.

### References

Chuvilgin L.G., Ptuskin V.S.: 1993, *Astron.Astroph.*, **279**, 278.

De Young D.S.: 2002, *The physics of extragalactic radio sources*, the University of Chicago Press.

Kaiser C.R.: 2000, *Astron.Astroph.*, **362**, 447.

Meng A.V., Braude S.Ya., et al.: 2001, *Kinemat. Fiz.Neb.Tel (Ukraine)*, **17**, 195.

Owen F.N., Eilek J.A., Kassim N.E.: 2000, *Astron.Astroph.*, **543**, 611.

Sagdeev R.Z.: 1964, *in The Questions of Plasma Theory*, eds. Leontovich M.A, **v.4**, 20, Moscow.

Wilson A.S., D.A. Smith, A.J. Young: 2006, *ApJ L*, **644**, L9.

# PHOTOMETRIC OBSERVATIONS AND PERIOD CHANGES FOR THE THREE RR LYRAE TYPE STARS: DM CYG, V341 AQL and AV PEG

S.N.Udovichenko

Astronomical Observatory, Odessa National University
T.G.Shevchenko Park, Odessa 65014, Ukraine
*udovich@farlep.net*

ABSTRACT. During observational period 2006-2007 the CCD photometric observation with V system for three RR Lyr type stars: DM Cyg, V341 Aql and AV Peg have been carried out. It was the light curves obtained and the maxima moments were determined. For the purpose of periods changes variation the graphics of O - C was plotted for long term intervals of time, containing several dozen of years, having applied the early published moments of light variations maxima. From these data the new elements for determine of light variations maxima was calculated.

**Key words:** RR Lyrae – stars: individual (DM Cyg, AV Peg, V341 Aql).

## 1. Introduction

This photometric study for three RR Lyr stars was undertaken to continue the numerous investigation of RR Lyr stars, which in Astronomical Observatory of Odessa National University were made.

The photometric observation of stars were carried out using the 48 cm reflector AZT-3 with the f/4.5 Newtonian focus and CCD photometer with V filter of UBV system. The CCD photometer was created using CCD chip Sony ICX429ALL, hermetic housing and thermoelectric (Peltier) cooler, which provide a temperature difference between the crystal and the environment of about -30$^o$C – -40$^o$C. The exposure time for variable and comparison stars for the most part were choosed for more brightest comparison stars to except a saturation of frame and consist 10 - 15 sec. Evening and morning twilight flat-field frames were obtained for each night to flatten the raw CCD frames. For CCD differential photometry a program was used that performed CCD control, image processing, and aperture photometry. The procedures for the aperture photometry are composed of the dark-level and flat-field corrections and determination of the instrumental magnitude and precision. The mean measurement error was about 0.01 - 0.02 mag.

## 2. DM CYG

DM Cyg is known as RR Lyr-star type (RRAB) with amplitude $10.^m93 - 11.^m99$ (V), has spectrum A9-F6 and period $0.^d41986$, Kholopov et al. (1985).

The variability was found by L.P.Tserasskaya (1928). The star thoroughly was investigated by D.Ya.Martynov, which determined the primery elements of period. V.P.Tsessevich referred this star to type the stars with suddenly variations of period.

From 500 CCD images of variable DM Cyg were determined the magnitudes comparatively of comparison stars Tycho 2707-01803-1. The phase curves were computed from elements:
Max HJD=2442582.406 + 0.4198600 * E, Kholopov et al. (1985). The light curves of DM Cyg are shown on fig. 1. Dots are data JD2453993, triangles are JD2453995, squares are JD2453985, asterisks are 2454391. The moments of light maxima are shown in table 1. The different amplitudes of light variation on figure is a result of the Blazhko effect.

It is interesting to observe a secular variation of period. To construct the updated O-C diagram, all available data from literature have been collected: (Tsesevich, 1966; Lysova et al., 1980; Braune et al., 1967; Batyrev, 1962; Born et al., 1955; Fitch et al., 1966; Agerer, 2003; Hubscher et al., 2005; Le Borgne et al., 2005). The resulting diagram is plotted in Fig. 2. A least-squares linear fit of O-C diagram have been obtained by new formula for light elements:
Max HJD=2425887.5376 + 0.4198596 x E
A greater accuracy gives parabolic formula:
Max HJD=2425887.561 + 0.4198569 * E+
$+(4.5*10^{-11})*E^2$.

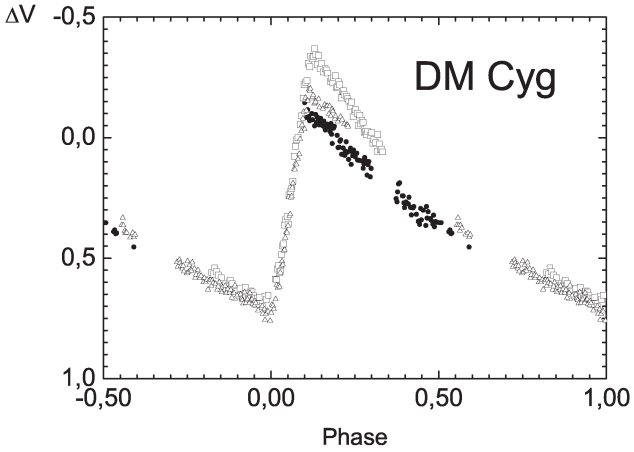


Figure 1: Light curves of DM Cyg. Dots are JD2453993, triangles are JD2453995, squares are JD2453985, asterisks are JD2454391

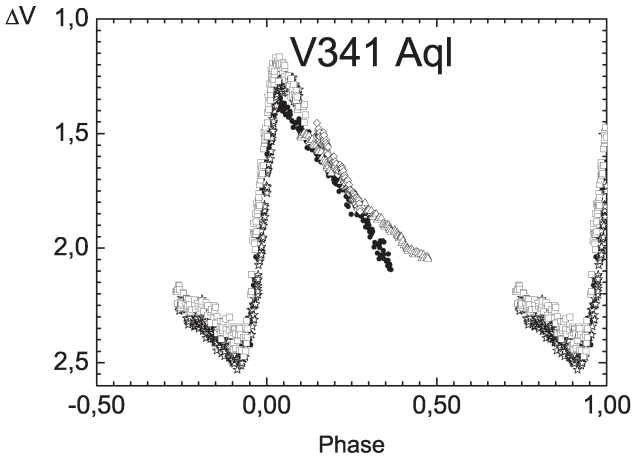


Figure 2: Light curves of V341 Aql. Dots are data JD2453965, triangles are JD2453935, squares are JD2453966, asterisks are 2454362, rhombs are JD2454361

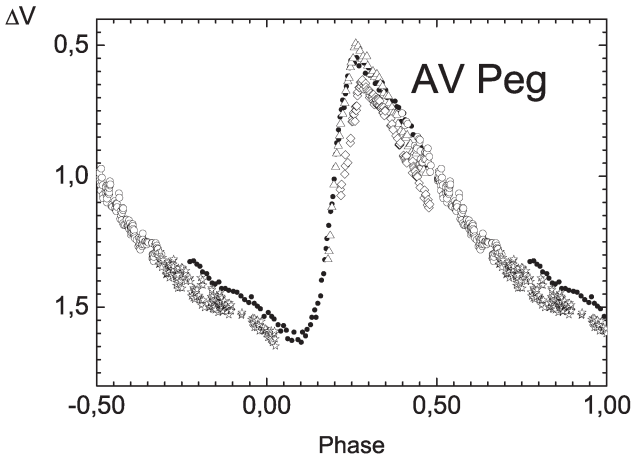


Figure 3: Light curves of AV Peg. Dots are data JD2454028, triangles are JD2454036, open circles are JD2454376, asterisks are JD54378, rhombs are JD2454377

### 3. V341 Aql

V341 Aql is known as RR Lyr-star type (RRAB) with amplitude $10.^m13-11.^m39$ (V), has spectrum A6-F5 and period $0^d.57802054$, (Kholopov et al., 1985).

The variability was found by K.Hoffmeister (1934). The star was investigated by S.M.Selivanov, which determined the primary elements of period. V.P.Tsessevich referred this star to type the stars with light variations proportionally of time.

From 970 CCD images of variable V341 Aql were determined the magnitudes comparatively of comparison stars Tycho 0510-01216-1. The phase curves were computed from elements:
Max HJD=2441196.251 + 0.57802054 * E, Kholopov et al. (1985). The light curves of V341 Aql are shown on fig. 3. Dots are data JD2453965, triangles are JD2453935, squares are JD2453966, asterisks are JD2454362, rhombs are JD2454361. The moments of light maxima are shown in table 1.

Table 1: The moments of light maxima from CCD observations 2006-2007

| | |
|---|---|
| DM Cyg | 2453993.413 |
| | 2453995.460 |
| | 2453985.380 |
| | 2454391.446 |
| V341 Aql | 2453965.322 |
| | 2453966.480 |
| | 2454362.428 |
| AV Peg | 2454028.382 |
| | 2454036.193 |
| | 2454377.386 |

To construct the updated O-C diagram, all available data from literature have been collected: (Tsessevich, 1966; Stepien, 1972; Fitch et al., 1966; Pojmanski, 2002; Agerer, 2003; Hubscher et al., 2005).

The resulting diagram is plotted in Fig. 4. A least-squares linear fit of O-C diagram have been obtained by new formula for light elements:
Max HJD=2434244.4168 + 0.57902016 x E
A greater accuracy gives parabolic formula:
Max HJD=2434244.401 + 0.578019 * E+ $+(7.2{*}10^{-11}){*}E^2$.

### 4. AV Peg

AV Peg is known as RR Lyr-star type (RRAB) with amplitude $9.^m88 - 10.^m92$ (V), has spectrum A7-F6 and period $0^d.3903747$, (Kholopov et al., 1985).

The variability was found by K.Hoffmeister (1931). After two years H.Shapley and E.Use independently

discovered it on Observatory in Harvard. C.Pain-Gaposhkin and S.Gaposhkin found the variability of light from Harvard photo plates.

V.P.Tsessevich referred this star to type the stars with light variations proportionally of time.

From 820 CCD images of variable AV Peg Aql were determined the magnitudes comparatively of comparison stars Tycho 2202-00987-1. The phase curves were computed from elements:
Max HJD=2443790.316 + 0.3903747 * E, Kholopov et al. (1985). The light curves of AV Peg are shown on fig. 5. Dots are data JD2454028, triangles are JD2454036, open circles are JD2454376, asterisks are JD54378, rhombs are JD2454377. The moments of light maxima are shown in table 1.

To construct the updated O-C diagram, all available data from literature have been collected: (Tsessevich, 1966; Lysova, 1980; Firmanyuk, 1976; Ahnert, 1960; Braune et al., 1967; Fitch et al., 1966; Szeidl et al., 1986; Agerer, 2003; Hubscher et al., 2005; Le Borgne et al., 2005).

The resulting diagram is plotted in Fig. 6. A least-squares linear fit of O-C diagram have been obtained by new formula for light elements:
Max HJD=2418950.0788 + 0.3903732 x E
A greater accuracy gives parabolic formula:
Max HJD=2418950.257 + 0.3903646 * E+ $+(9.0*10^{-11})*E^2$.

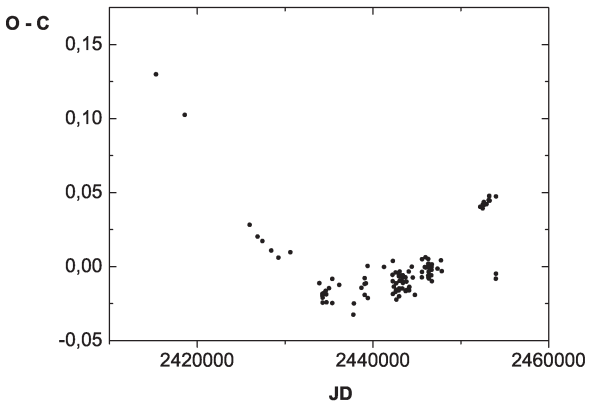


Figure 4: The mean O - C diagram of DM Cyg from 1929 to 2007

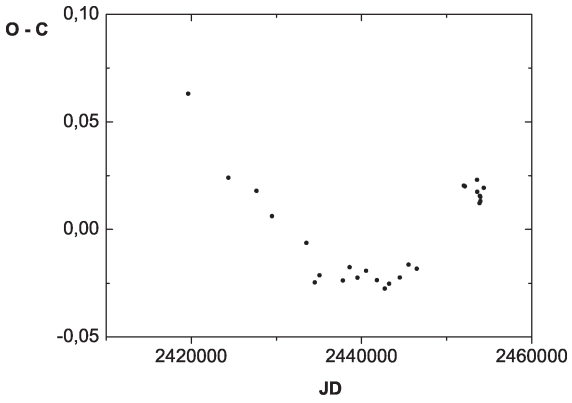


Figure 5: The mean O - C diagram of V341 Aql from 1934 to 2007

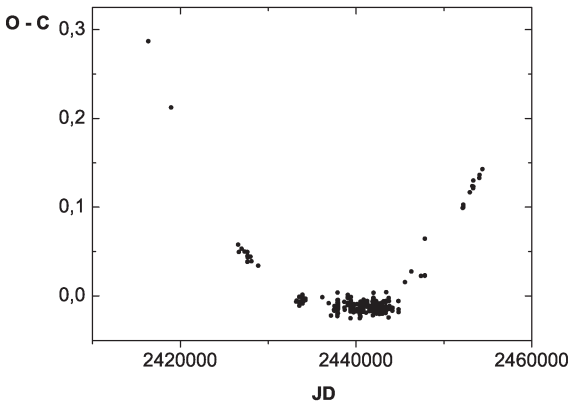


Figure 6: The mean O - C diagram of AV Peg from 1904 to 2007

## References

Agerer F.: 2003, *IBVS*, N 5485.
Ahnert P.: 1960, *AV Pegasi. N.V.S.*, N 438.
Batyrev A.A.: 1975, *Peremennye Zvezdy. Suppl.*, **2**, N10.
Born F., Sofronievitsch H., Pohl E.: 1955, *Astron. Nachr.*, 282 H.5.
Braune W., Hubscher J.: 1967, *Astron.Nachr.*, 290, H.3.
Firmanyuk B.N.: 1976, *IBVS*, N 1152.
Fitch W.S., Wisniewski W.Z., Johnson H.L.: 1966, *Comm. of the Lunar and Planetary Lab.*, The Univer. of Arizona, 1966, **5**, N 71.
Hubscher J., Paschke A., Walter F.: 2005, *IBVS*, N5657.
Kholopov P.N., Samus N.N., Frolov M.C., Goransky V.P., Gorynya N.A., Kireeva N.N., Kukarkina N.P., Kurochkin N.E., Medvedeva G.I., Perova N.B., Shugarov S.Yu.: 1985, *General catalogue of variable stars* **1-3**.
Le Borgne J.F., Klotz A.3, Boer M.: 2005, *IBVS*, N 5622.
Lysova L.E., Firmanyuk B.N.: 1980, *Astron. Cyr.*, N 1122.
Pojmanski G.: 2002, *Acta Astron.*, **52**, 397.
Stepien K.: 1972, *Acta Astron.*, **22**, N 3.
Szeidl B., Olah K., Mizser A.: 1986, *Comm. Konkoly Obs.*, N 89 (Vol.X, 3).
Tsessevich V.P.: 1966, *RR Lyrae-type variable stars*, Naukova Dumka, Kiev.

# POLARIS ($\alpha$ *UMi*),- MULTISTELLAR SYSTEM IN THE OPEN CLUSTER

I.A. Usenko,[1], A.S. Miroshnichenko,[2], V.G. Klochkova,[3], V.E. Panchuk[3]

[1] Department of Astronomy, Odessa National University
T.G.Shevchenko Park, Odessa 65014 Ukraine, *igus@deneb1.odessa.ua*
[2] Dpt of Physics and Astronomy, University of North Carolina at Greensboro
Greensboroo, NC 27402-6170, USA, *amirosh@uncq.edu*
[3] Special Astrophysical Observatory, Russian Academy of Sciences
Nizhnij Arkhyz, Karachaevo-Cherkessia, 369167 Russia *valenta@sao.ru; panch@sao.ru*

ABSTRACT. We present the results of our analysis of high-resolution spectroscopic observations of Cepheid $\alpha$ UMi (Polaris A) and main-sequence type stars Polaris B and HD 5914, - optical companion and a member of Polaris open cluster. The last ones are objects with high projected rotational velocities v $\sin i$ = 110 km s$^{-1}$ and 100 km s$^{-1}$, respectively. The derived atmosphere parameters are: Polaris A: T$_{eff}$=6022 K; $\log g$=2.2; V$_t$=4.3 km s$^{-1}$; Polaris B: T$_{eff}$=6900 K; $\log g$=4.3; V$_t$=2.5 km s$^{-1}$; HD 5914: T$_{eff}$=8800 K; $\log g$=4.0; V$_t$=2.0 km s$^{-1}$. C, Na and Mg content in last two stars is close to solar, whereas Polaris A demonstrates its that is typical for Cepheid after the first dredge-up stage. The distances to Polaris B and HD 5914 are 109.5 and 108 pc, respectively. The *RV* pulsational amplitude of Polaris A decreased to 0.6 s$^{-1}$ in 2005 and increased to 7.5 km s$^{-1}$ in 2003

**Key words**: Stars: abundances - Stars: distances - Stars: Cepheids - Stars: main-sequence stars - Stars: individual - $\alpha$ UMi (Polaris A), Polaris B, HD 5914

## 1. Introduction

S-Cepheid (DCEPS) $\alpha$ UMi named Polaris is an unique object for astrophysical research due to the following:

1. It is the nearest ($d$ = 99 (Turner, 2005) - 132 pc (ESA 1997)) yellow supergiant and Cepheid in the Galaxy.
2. Polaris is a well-known multiple system with three visual components (Polaris B (BD+88°9, C and D) that are main-sequence stars (Fernie 1966), and the spectroscopic one (Polaris Ab with an orbital period 29.71 yrs (Turner et al. 2006).
3. Polaris is a member of an anonymous open cluster, which contains late A-type and early F-type main sequence stars.
4. Polaris, - one from four nearest Cepheid with the radius, 46±3 $R_\odot$, determined by means of optical interferometry (Nordgren et al. 1999).
5. CNO-abundances analysis data for Cepheid agree well with theoretically predicted ones for 3rd (or 5th) crossing of the Cepheids instability strip.

Thus, the main task consist in:

1. To obtain the high-resolutioned spectra of Polaris ($F6 - F8I$), its the nearest visual companion Polaris B ($F3V$), and the brightest main-sequence member of Polaris cluster HR 5914 ($A3V$) to determine its atmospheric parameters, chemical composition, absolute magnitudes, masses and distances, respectively.
2. To measure the radial velocities of Polaris A during the lond observational period (1999-2006) to determine its pulsational amplitude changes.

## 2. Observations

Observations of these objects have been realized using:

1. 1m telescope - Ritter Observatory, University of Toledo (Toledo, OH, USA) - fiberfed echelle spectrograph 1150×1150 pixel CCD ($\lambda\lambda$ 5800-6800 Å).
2. 2.1m Otto Struve telescope -McDonald Observatory (Texas, USA) - SANDIFORD spectrograph (McCarthy et al. 1993) 1200×400 pixel CCD ($\lambda\lambda$ 5500-7000 Å).

Table 1: Observational data of Polaris cluster's objects

| Object | HJD | NS | $T_{eff}$ | $\log g$ | $V_t$ |
|---|---|---|---|---|---|
| $\alpha$ UMi | 2449513-9649 (1994) | | 5968±29 | 2.2 | 4.35 |
| | 2451240-2192 (1999) | 4 | 5973±15 | 2.1 | 4.30 |
| | 2452416-2515 (2002) | 9 | 6011±25 | 2.2 | 4.60 |
| | 2452782-2986 (2003) | 11 | 6018±25 | 2.2 | 4.30 |
| | 2453005-3367 (2004) | 10 | 6027±15 | 2.2 | 4.30 |
| | 2453686-3693 (2005) | 6 | 6063±10 | 2.3 | 4.00 |
| | 2453751-4169 (2006) | 7 | 6055±30 | 2.2 | 4.00 |
| | Mean | 53 | 6022±21 | 2.2 | 4.30 |
| Polaris B | | 1 | 6900±50 | 4.3 | 2.50 |
| HD 5914 | | 1 | 8800±50 | 4.0 | 2.00 |

Table 2: Radial velocity data of $\alpha$ UMi during 2005-2006

| HJD 2400000+ | Number of orders | $RV$ (km s$^{-1}$) | $\sigma$ | NL |
|---|---|---|---|---|
| 53686.615 | 20 | -17.68 | 1.05 | 198 |
| 53687.614 | 27 | -17.82 | 1.00 | 616 |
| 53689.647 | 27 | -18.24 | 1.20 | 589 |
| 53690.109 | 27 | -17.80 | 1.13 | 566 |
| 53691.633 | 27 | -17.82 | 1.06 | 550 |
| 53693.124 | 27 | -17.93 | 1.06 | 549 |
| 53751.121 | 27 | -16.83 | 1.21 | 581 |
| 53808.277 | 27 | -18.78 | 1.55 | 933 |
| 53904.350 | 27 | -17.87 | 1.09 | 506 |
| 53980.589 | 27 | -17.40 | 1.29 | 569 |
| 54073.589 | 27 | -18.43 | 1.15 | 579 |
| 54077.651 | 27 | -17.58 | 1.21 | 406 |

3. 6m telescope BTA - SAO RAS(Russia) - LYNX(Panchuk et al. 1999), PFES(Panchuk et al. 1998), NES(Panchuk et al. 2002) spectrometers ($\lambda\lambda$ 5050 - 7100 Å.)

The reduction was made using IRAF software, MIDAS software, DECH20 software (Galazutdinov, 1992). The observational log is given in Table 1. In Table 2 we present new radial velocity data of Polaris A, obtained during 2005-2006. Our preceding $RV$ data are given in Table 1 of Usenko et al. (2005a) paper

## 2. Atmosphere parameters and chemical composition

Atmosphere parametrs were determined:

1) $T_{eff}$: line deph ratio (Kovtyukh & Gorlova, 2000) for Polaris (accuracy: 15 - 70 K); $(B-V)$-$T_{eff}$, $\log g$ and SYNTH for Polaris B and HD 5914 (accuracy: 50 K);

2) $\log g$: by adopting the same iron abundance for Fe I and Fe II lines. (accuracy: 0.15 dex) for Polaris; $(B-V)$-$T_{eff}$, $\log g$ and SYNTH for Polaris B ($H_\beta$); see Figure 1) and HD 5914 ($H_\alpha$; see Figure 2)(accuracy: 0.15 dex );

3) $V_t$ - by assuming abundances of the Fe II lines independent of the $W_\lambda$ for Polaris (accuracy: 0.25 km/s). For Polaris B and HD 5914 these $V_t$ data were selected using SYNTH.

The mean atmosphere parametrs are given in Table

Table 3: Average abundances for Polaris cluster's objects

| Elements | Polaris | Polaris B | HD 5914 |
|---|---|---|---|
| [C/H] | -0.17±0.10 | -0.00±0.05 | -0.01 |
| [N/H] | +0.42±0.00 | +0.00 | +0.00 |
| [O/H] | -0.00±0.15 | -0.00 | -0.02±0.09 |
| [Na/H] | +0.09±0.11 | +0.03 | -0.02 |
| [Mg/H] | -0.21±0.12 | +0.04±0.12 | - |
| [Fe/H] | +0.07±0.10 | +0.07±0.15 | +0.05±0.15 |

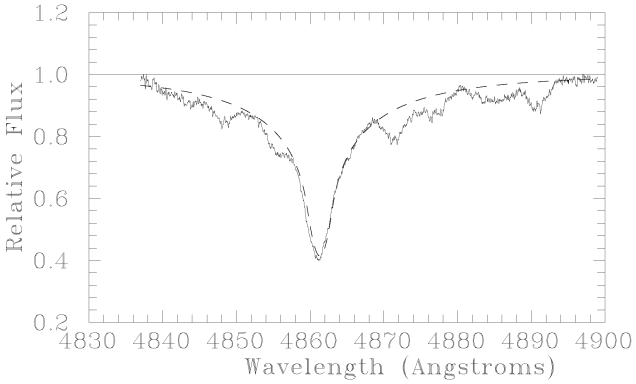


Figure 1: Fragment of Polaris B spectrum in the range 4930-4943 ÅÅwith synthetic spectrum (dashed line) for $T_{eff}$ = 6900 K; $\log g$ = 4.3; $V_t$ = 4.30 km s$^{-1}$ and v $\sin i$ = 110 km s$^{-1}$ is shown for comparison.

1. It is necessary to note that Polaris B and HD 5914 are high-rotating objects with v $\sin i$ = 110 km s$^{-1}$ and 100 km s$^{-1}$, respectively (see Figures 1 and 2).

As seen from Table 3, a comparison of chemical abundances (CNO-elements, sodium, magnesium and iron) for Cepheid, its visual companion and main-sequence star from open cluster reveals some interesting features. All three stars display essentially identical abundances of iron, thereas Polaris B and HD 5914 appears to have a solar carbon content. The same fact noticeable for sodium and manganise content for these stars. On the other hand Cepheid Polaris A exhibits an obvious deficit of carbon, overabundance of nitrogen, small overabundance of sodium and noticeable deficit of manganese. These features agrees well with theoretically predicted abundances for 5 $M_\odot$ star after 3rd or 5th crossing of the Cepheid instability strip (Usenko et al. 2005).

## 3. Colour-Excess and Reddening

The use of the line depth ratio method for the $T_{eff}$ determination allows us to obtain the accurate $E_{B-V}$ colour-excesses. Knowning the average $T_{eff}$ and $(B-V)$ for the Cepheid and using the Gray's (1992) $(B-V)$ vs. $T_{eff}$ relationship, we can calculate

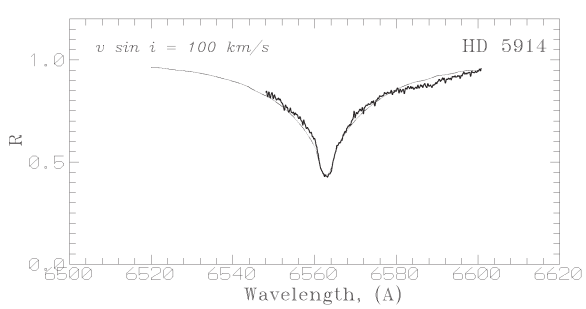


Figure 2: Fragment of HD 5914 spectrum in the range 6500-6620 ÅÅwith synthetic spectrum (dashed line) for $T_{eff}$ = 8800 K; $\log g$ = 4.0; $V_t$ = 2.00 km s$^{-1}$ and v $\sin i$ = 100 km s$^{-1}$ is shown for comparison.

the intrinsic colour $(B-V)_0$, colour-excess $E_{B-V}$, and reddening $A_V$. For the mean $T_{eff}$ = 6021 K we have $E_{B-V}$ = 0.034 mag; $A_V$ = 0.102 mag, R = 3.0 (Arellano Ferro, 1984) BC=0.01 mag (Bessell, Castelli, & Plez 1998).

### 4. Distances, Luminocities, Radii and Masses

As known (Usenko et al. 2005) the distance determination for Polaris system is problematical, - different methods give unequal estimates, - from 99 pc (Turner, 2005) to 132 pc (ESA 1997, Norgren et al. 1999). Known that Polaris B is $F3V$ main-sequence star, then its radius is near 1.38 $R_\odot$ (Straižys, 1982). Using our $T_{eff}$ we can obtain its luminosity of 3.868 $L_\odot$, equivalent to an absolute magnitude $M_V$ = +3.30 mag. Using our $A_V$ = 0.102 mag we have obtained a distance $d$ = 109.5 pc. This result coincide with Kamper's (1996) one of 110 pc, determined by astrometrical methods.

As known, for main-sequence stars $\log(L/L_\odot) = 4\log(M/M_\odot)$. Using our gravity and radius values for Polaris B, we can obtain its mass of 1.39 $M_\odot$, that agrees well with Polaris Ab $F4V$ type spectroscopic companion, - 1.38±0.61 $M_\odot$ (Evans et al. 2007).

In the case of HD 5914 we have obtained its radius of 2.14 $R_\odot$, $M_V$ = +1.3 mag, $d$ = 108 pc, and $M$ = 1.66 $M_\odot$, respectively. Therefore, for Polaris A, in the case of distance $d$ = 109.5 pc and $T_{eff}$ = 6021 K, we have: $M_V$ = -3.31 mag, $\log(L/L_\odot)$ = 3.232, $R$ = 38 $R_\odot$, and $M$ = 5 $M_\odot$, respectively.

### 5. RV Pulsational Amplitude Changes

As seen from Figures 3-7 $RV$ pulsational amplitude of Polaris during 2002-2006 undergoes the changes. It is interesting that it increased from 3 to 7.5 km s$^{-1}$ during 2002-2003, after that we can see a decreasing from 2 to 0.6 km s$^{-1}$ during 2004-2005, and new

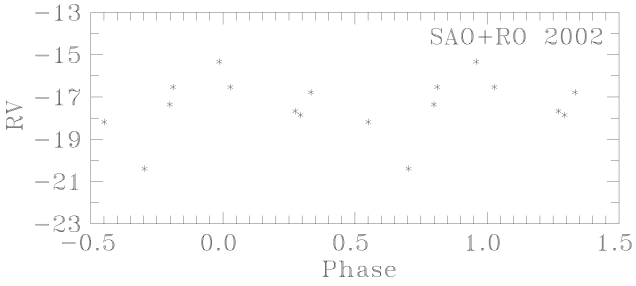


Figure 3: Radial velocity curve for Polaris A in 2002

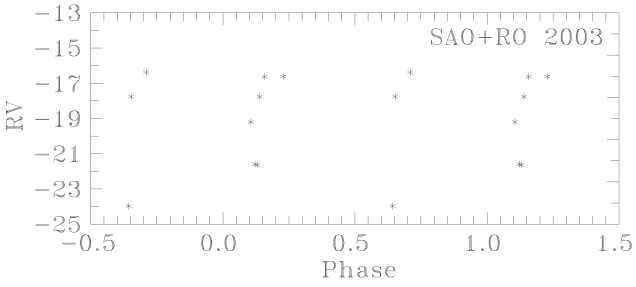


Figure 4: Radial velocity curve for Polaris A in 2003

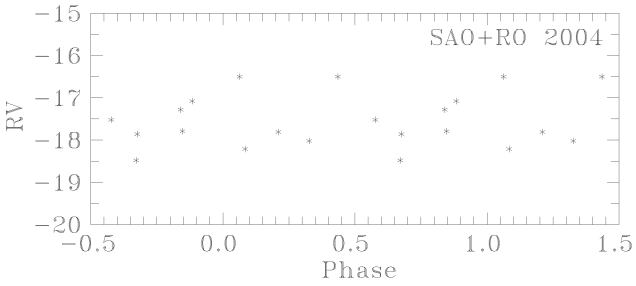


Figure 5: Radial velocity curve for Polaris A in 2004

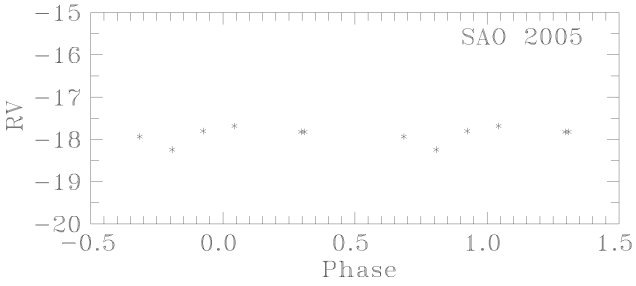


Figure 6: Radial velocity curve for Polaris A in 2005

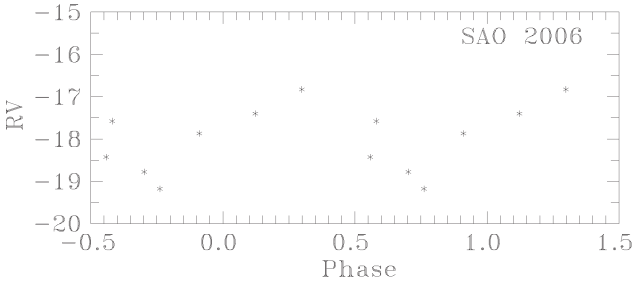


Figure 7: Radial velocity curve for Polaris A in 2006

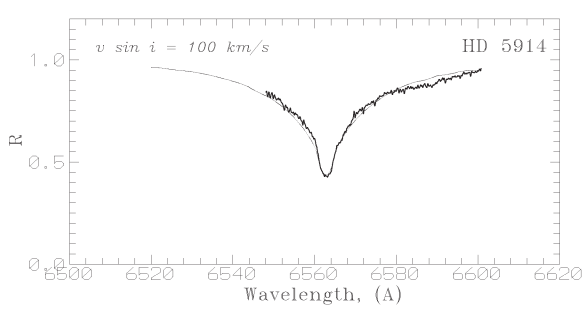


Figure 2: Fragment of HD 5914 spectrum in the range 6500-6620 ÅÅwith synthetic spectrum (dashed line) for $T_{eff}$ = 8800 K; $\log g$ = 4.0; $V_t$ = 2.00 km s$^{-1}$ and v $\sin i$ = 100 km s$^{-1}$ is shown for comparison.

the intrinsic colour $(B-V)_0$, colour-excess $E_{B-V}$, and reddening $A_V$. For the mean $T_{eff}$ = 6021 K we have $E_{B-V}$ = 0.034 mag; $A_V$ = 0.102 mag, R = 3.0 (Arellano Ferro, 1984) BC=0.01 mag (Bessell, Castelli, & Plez 1998).

### 4. Distances, Luminocities, Radii and Masses

As known (Usenko et al. 2005) the distance determination for Polaris system is problematical, - different methods give unequal estimates, - from 99 pc (Turner, 2005) to 132 pc (ESA 1997, Norgren et al. 1999). Known that Polaris B is $F3V$ main-sequence star, then its radius is near 1.38 $R_\odot$ (Straižys, 1982). Using our $T_{eff}$ we can obtain its luminosity of 3.868 $L_\odot$, equivalent to an absolute magnitude $M_V$ = +3.30 mag. Using our $A_V$ = 0.102 mag we have obtained a distance $d$ = 109.5 pc. This result coincide with Kamper's (1996) one of 110 pc, determined by astrometrical methods.

As known, for main-sequence stars $\log(L/L_\odot) = 4\log(M/M_\odot)$. Using our gravity and radius values for Polaris B, we can obtain its mass of 1.39 $M_\odot$, that agrees well with Polaris Ab $F4V$ type spectroscopic companion, - 1.38±0.61 $M_\odot$ (Evans et al. 2007).

In the case of HD 5914 we have obtained its radius of 2.14 $R_\odot$, $M_V$ = +1.3 mag, $d$ = 108 pc, and $M$ = 1.66 $M_\odot$, respectively. Therefore, for Polaris A, in the case of distance $d$ = 109.5 pc and $T_{eff}$ = 6021 K, we have: $M_V$ = -3.31 mag, $\log(L/L_\odot)$ = 3.232, $R$ = 38 $R_\odot$, and $M$ = 5 $M_\odot$, respectively.

### 5. RV Pulsational Amplitude Changes

As seen from Figures 3-7 $RV$ pulsational amplitude of Polaris during 2002-2006 undergoes the changes. It is interesting that it increased from 3 to 7.5 km s$^{-1}$ during 2002-2003, after that we can see a decreasing from 2 to 0.6 km s$^{-1}$ during 2004-2005, and new

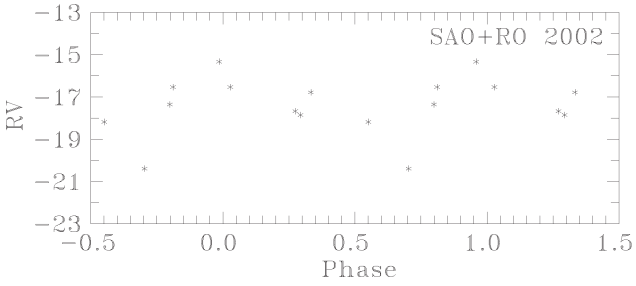


Figure 3: Radial velocity curve for Polaris A in 2002

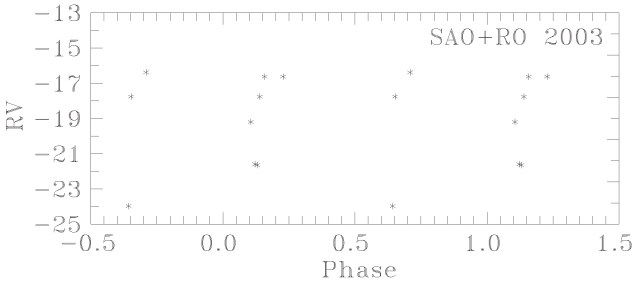


Figure 4: Radial velocity curve for Polaris A in 2003

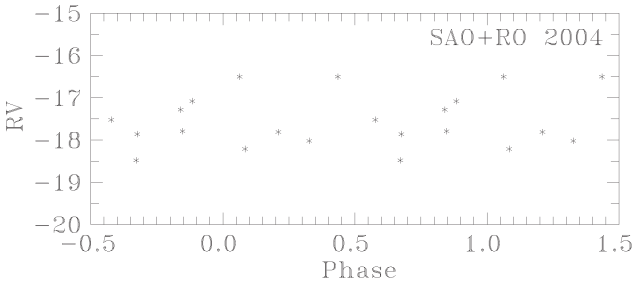


Figure 5: Radial velocity curve for Polaris A in 2004

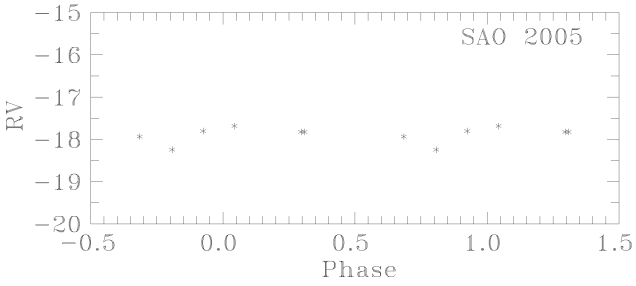


Figure 6: Radial velocity curve for Polaris A in 2005

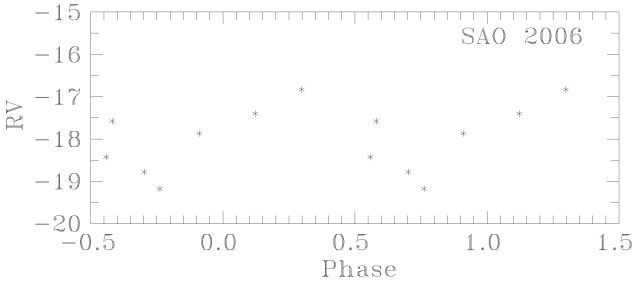


Figure 7: Radial velocity curve for Polaris A in 2006

increasing to 2 km $s^{-1}$ in 2006.

## 6. Conclusions

We can summarize the results of our investigations as follows.

1. A large projected rotational velocity v $\sin i$ = 110 km $s^{-1}$ for Polaris B is an evidence that Polaris system is young and Polaris B is likely to be single, since most binaries of $A - F$ types have slow rotation, the angular momentum being tied up in orbital motion. Moreover, the rapid rotation's observation could be mean that we see the star nearly equator-on. Atmosphere parametres, obtaines for Polaris B are typical for $F3V$ star.

2. The same conclusions we can sum up for HD 5914 with its projected rotational velocity v $\sin i$ = 100 km $s^{-1}$ and typical $A3V$ spectral type.

3. The majority of Polaris B and HD 5914 chemical elements shows abundances, equal to Polaris A and close to solar one. But carbon, sodium and magnesium in these stars close to solar content, therefore Polaris A demonstrates a typical for the first dredge-up yellow supergiants deficit of C and Mg and overabundance of N and Na (Usenko et al. 2005). Therefore we are eye-witnesses of evolutional history of three stars with different masses in the same stellar system.

4. Absolute magnitude +3.30 mag for Polaris B is equal to one from Fernie (1966). Spectroscopically determined $T_{eff}$ = 6900 K combinating with radius of 1.38 $R_\odot$ give the distance near 109.5 pc, - a fine agreement with Kamper's (1996) one near 110 pc. This result is quite unexpected, because Turner (2005) denoted 101±3 pc to this object and Polaris system as a whole. Whereas HIPPARCOS parallax (ESA 1997) and optical interferometry (Nordgren et al. 1999) results give 132±9 pc to the Polaris A.

5. For HD 5914 we have the absolute magnitude +1.30 mag and for spectroscopically determined $T_{eff}$ = 8800 K and radius of 2.14 $R_\odot$ the desired value of distance come to 108 pc. It is a real confirmation that this star is a member of Polaris open cluster.

6. The obtained mass of Polaris B near 1.39 $M_\odot$ has been founded as unexpected close to one of Polaris Ab spectroscopic companion, - 1.38±0.61 $M_\odot$ (Evans et al. 2007), which is a main-sequence star of earlier than $F4V$ spectral type (Evans et al. 2002). The mass of HD 5914 near 1.66 $M_\odot$ is a typical for main-sequence early $A-$ type stars.

7. If the distance to Polaris A of 109.5 pc is true, then in case of mean $T_{eff}$ = 6021 K its absolute magnitude is -3.31 mag, radius is near 38 $R_\odot$ and mass is equal to 5 $M_\odot$, respectively.

8. *RV* pulsational amplitude of Polaris A during last years undergoes sporadical changes minimized to 0.6 km $s^{-1}$ in 2005 and culminated to 7.5 km $s^{-1}$ (like before 1950 (Roemer, 1965)) in 2003. In last year we can see its new increasing.

## References


Arellano Ferro A.: 1984, *MNRAS,* **209**, 481.

Bessel M.S., Castelli F., Pfelz B.: 1998, *A&A,* **333**, 231.

ESA, 1997: *The Hipparcos and Tycho catalogues*, ESA-SP 1200.

Evans N.R., Sasselov D.D., Short C.I.: 2002, *ApJ,* **567**, 1121.

Evans N.R., Schaefer G., Bond H.E. et al.: 2007, *Proceed. IAU Symp.* **No. 240** (in press).

Fernie J.D.: 1966, *AJ,* **71**, 731.

Galazutdinov G.A.: 1992, *Preprint SAO RAS* **No.92**.

Gray D.: 1992, *Observation and Analysis of Stellar Atmospheres, (Cambrige Univ. Press, 2nd edition).*

Kamper K.W.: 1996, *JRASC,* **90**, 140.

Kovtyukh V.V., Gorlova N.I: 2000, *A&A* **358**, 587.

Nordgren T.E. et al.: 1999, *AJ*, **118**, 3032.

Panchuk V.E., Najdenov I.D., Klochkova V.G. et al.: 1998, *Bull. SAO RAS* **44**, 127.

Panchuk V.E., Klochkova V.G., Najdenov I.D. et al.: 1999, *Preprint SAO RAS*, **No. 139**.

Panchuk V.E., Piskunov N.E., Klochkova V.G., Yushkin M.V., Ermakov S.V.: 2002, *Preprint SAO RAS*, **No. 169**.

Roemer E.: 1965, *ApJ,* **141**, 1415.

Straižys V.: 1982, *"Metal-Deficient Stars", Vilnius, "Mosklas"*, 300.

Turner D.G.: 2005, *OAP*, **18**, 115.

Turner D.G., Usenko I.A., Miroshnichenko A.S., Klochkova V.G., Panchuk V.E., Yang S.L.S, Gregory P.C.: 2006, *BAAS*, **38**, 118.

Usenko I.A., Miroshnichemnko A.S., Klochkova V.G., Yushkin M.V.: 2005, *MNRAS,* **362**, 1219.

Usenko I.A., Miroshnichemnko A.S., Klochkova V.G., Panchuk V.E.: 2005a, *OAP,* **18**, 130.

# PULSATIONAL AND ORBITAL PERIODS OF SMALL-AMPLITUDE CEPHEID SU CAS

I.A. Usenko[1], V.G. Klochkova[2], N.S. Tavolzhanskaya[2]

[1] Department of Astronomy, Odessa National University
T.G.Shevchenko Park, Odessa 65014 Ukraine, *igus@deneb1.odessa.ua*
[2] Special Astrophysical Observatory, Russian Academy of Sciences
Nizhnij Arkhyz, Karachaevo-Cherkessia, 369167 Russia *valenta@sao.ru; nonna@sao.ru*

ABSTRACT. New seven high-resolutional spectra of small-amplitude Cepheid SU Cas have been obtained to determine its atmosphere parameters ($T_{eff}$=6384 K; $\log g$=2.4; $V_t$=3.3 km $s^{-1}$) and to measure its radial velocities. The last ones were added to the total list (360 values) and using the frequency analysis we can specify the pulsational and orbital periods of this Cepheid. With the well-known main pulsational period of 1.949329 days, classified as fundamental tone, we can detect the presence of two equidistant periods at a distance of ±0.003 c/d from it, and the secondary (possible first overtone) one of 2.040461 day. Their ratio $P_1/P_0 = 0.96$ supposed about an an existence of non-radial pulsations in the Cepheid's atmosphere. Changes of the mean colour-index, effective temperature and $\gamma$-velocity confirmed the presence of one or more companions with possible periods of 463.7 – 483.8, 1738.8 and 7490.3 days.

**Key words**: Stars: Pulsational periods – Stars: Orbital periods - Stars: Cepheids – Stars: individual – SU Cas

## 1. Introduction

S-Cepheid (DCEPS) SU Cas is an interest object for astrophysical research due to the following aspects:

1. It is one of the nearest ($d$ = 258 pc (Turner & Evans 1984) Cepheid in the Galaxy.
2. SU Cas is a member of Cas OB2 association (Racine 1968).
3. CNO-abundances analysis data for Cepheid agree well with theoretically predicted ones for 3rd crossing of the Cepheids instability strip in case if it mass is close to 3.7 $M_\odot$ (Usenko et al. 2001).
4. SU Cas has a close companion $B9.5 - -A5V$ (Turner & Evans 1984, Usenko 1990, Evans 1991) with possible orbital periods of 462.5, 928, 1375 and 1682 days, respectively (Szabados 1991).

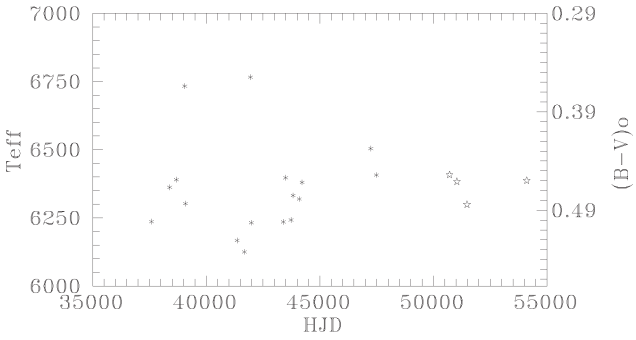


Figure 1: Variations of the mean effective temperature and colour-index during the last fourty years. Six-point stars, – the photometrical data from Mitchell et al. (1964), Wisniewski & Johnson (1968), Milone (1970), Sudzius (1969), Feltz & McNamara (1980), Szabados (1977), Niva & Schmidt (1979), Moffett & Barnes (1984); five-point stars, – the data obtained from spectroscopy (Usenko et al. 2001, Luck 2001, and this work).

Nevertheless there are some problems connected with unusual character of this Cepheid, namely:

1. Identification of its pulsational mode:
   a) Fundamental mode: $R$ = 18.2 $R_\odot$; $T_{eff}$ = 6328 K; $d$ = 258 pc (Turner & Evans 1984); $\log g$ = 2.35 (Usenko et al. 2001);
   b) First overtone: $R$ = 29 $R_\odot$; $T_{eff}$ = 6600 K; $d$ = 407 pc; $M_{ev}$ = 4.3 $M_\odot$ (Gieren 1976);
   c) Second overtone: $R$ = 33.8 $R_\odot$; $T_{eff}$ = 6300 K; $d$ = 433 pc; (ESA 1997; Evans 1991).
2. Noticeable variations of the mean $(B-V)_0$ duling last decades (see Figure 1).
3. Relatively small number of radial velocity measurements (353 estimates from 1918 to 1999 in 20 observational sets).

Thus, the main task consist in:

Table 1: Observations and radial velocities of SU Cas

| Spectrum | HJD 2400000+ | $RV$ ($\mathrm{km\,s^{-1}}$) | $\sigma$ ($\mathrm{km\,s^{-1}}$) | NL |
|---|---|---|---|---|
| s482013 | 54074.392 | 1.52 | 1.3 | 512 |
| s484026 | 54076.583 | -7.41 | 1.3 | 463 |
| s485017 | 54077.315 | -8.72 | 1.2 | 559 |
| s490017 | 54137.430 | -13.79 | 1.4 | 599 |
| s492002 | 54139.142 | -14.76 | 1.6 | 471 |
| s493012 | 54139.595 | -15.91 | 1.2 | 472 |
| s494020 | 54169.542 | 0.43 | 1.3 | 594 |

1. To obtain the high-resolutioned spectra set of SU Cas ($F6IIb - -F8IIb$), to determine its atmospheric parameters and to compare its with the same from other authors.

2. To measure the radial velocities of SU Cas from this set.

3. To add these radial velocity's data to the tolal list, obtained during the lond observational period (1918-2007).

4. To make more exact of SU Cas pulsational and possible orbital periods using Fourier analysis.

## 2. Observations

Observations of these objects have been realized using 6m telescope BTA - SAO RAS(Russia) equiped by LYNX(Panchuk et al. 1999), PFES(Panchuk et al. 1998), NES(Panchuk et al. 2002) spectrometers ($\lambda\lambda$ 4800 – 6600 Å.)

The reduction was made using IRAF software, the MIDAS context ECHELLE modified for extraction of echelle spectra obtained with an image slicer (Yushkin & Klochkova 2005) , DECH20 software (Galazutdinov, 1992). The observational log is given in Table 1.

## 3. Atmosphere parameters and chemical composition

Atmosphere parametrs were determined:

1) $\mathrm{T}_{eff}$ : line deph ratio (Kovtyukh & Gorlova, 2000).

2) $\log g$: by adopting the same iron abundance for Fe I and Fe II lines. (accuracy: 0.15 dex)

3) $\mathrm{V}_t$ – by assuming abundances of the Fe II lines independent of the $\mathrm{W}_\lambda$ for Polaris (accuracy: 0.25 km/s).

The mean atmosphere parametrs are given in Table 2.

Table 2: Atmosphere parameters of SU Cas

| Spectrum | $\mathrm{T}_{eff}$ (K) | $\log g$ | $\mathrm{V}_t$ ($\mathrm{km\,s^{-1}}$) |
|---|---|---|---|
| s482013 | 6298±11 | 2.30 | 3.00 |
| s484026 | 6485±65 | 2.50 | 3.30 |
| s485017 | 6256±38 | 2.25 | 2.70 |
| s490017 | 6514±13 | 2.40 | 3.15 |
| s492002 | 6548±38 | 2.55 | 4.30 |
| s493012 | 6427±62 | 2.55 | 4.00 |
| s494020 | 6162±17 | 2.30 | 2.85 |
| Mean | 6384±35 | 2.40 | 3.30 |

## 4. Frequency analysis

Frequency analysis have been completed for SU Cas radial velocity data using **PERIOD 98** software (Sperl 1998). **PERIOD 98** allows to search for and to fit sinusoidal patterns within the time series of data containing huge gaps. It used techniques of Fourier and Fast Fourier analysis with residuals minimization of sinusoidal fits to the data.

For calculations we have 360 radial velocities totally, obtained during the period of 1918-2007 (357 values from other authors and 7 our ones). The Fourier amplitude spectra were obtained over the frequency range 0 – 1 c/d at a resolution of 0.00002 c/d. These calculations were based on the original data (pulsational periods search), and the residuals at original (orbital periods search).

### *4.1. Pulsational periods*

As seen from Figure 2, we can observe the main pulsational period of 1.949329 days with two equidistant ones ±0.003 c/d (1.939059 days and 1.959787 days, respectively). And, the presence of secondary pulsational period is visible well too, – 2.040461 days. Their ratio consists 0.96 what is typical for non-radial pulsations. It is interesting that Stobie's model 9e for 5 $M_\odot$ star gives the period of 2.07 days in case of *first* harmonic (Stobie 1969).

### *4.2. Orbital periods*

An existence of SU Cas hot companion is a notorious fact. Turner & Evans (1984), Usenko (1990) and Evans (1991) have predicted its spectral type within the limits of *B9.5 – A5 V*. Szabados (1991) has estimated its orbital period of 462.5, 928, 1375 and 1682 days, at that he has gave preference to the first value. In Table 3 we represented the $\gamma$ - velocities, estimated for different observational sets. As seen from Figure 3, these changes show an evidence of SU Cas system

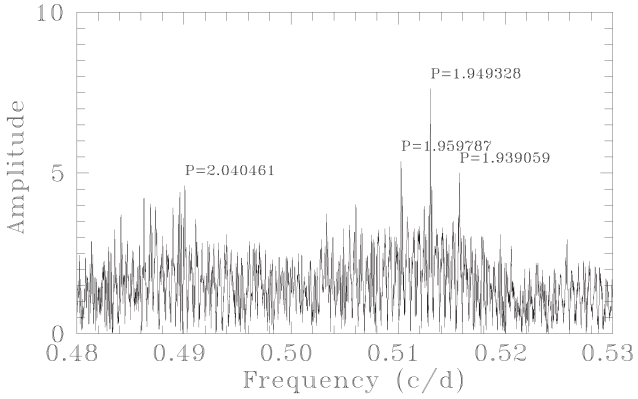


Figure 2: Fragment of Fourier amplitude spectrum of SU Cas over a narrow frequency range corresponding to pulsational periods with calculations based on the original data.

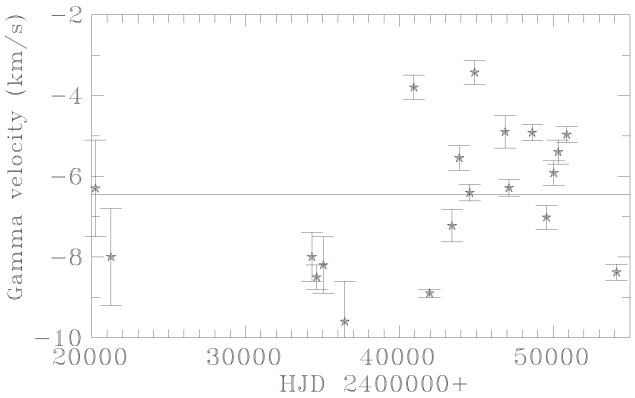


Figure 3: $\gamma$ – velocity values of SU Cas during 1918 - 2007.

Table 3: $\gamma$-velocities of SU Cas

| HJD 2400000+ | $\gamma$ (km s$^{-1}$) | $\sigma$ (km s$^{-1}$) | N | Reference |
|---|---|---|---|---|
| 20229 | -6.3 | 1.2 | 4 | Adams & Shapley (1918) |
| 21252 | -8.0 | 1.2 | 4 | Adams & Shapley (1918) |
| 34307 | -8.0 | 0.6 | 4 | Abt (1959) |
| 34621 | -8.5 | 0.3 | 14 | Abt (1959) |
| 35051 | -8.2 | 0.7 | 3 | Abt (1959) |
| 36451 | -9.6 | 1.0 | 1 | Abt (1959) |
| 40943 | -3.8 | 0.3 | 7 | Niva & Schmidt (1979) |
| 41962 | -8.9 | 0.1 | 63 | Gieren (1976) |
| 43421 | -7.2 | 0.4 | 39 | Niva & Schmidt (1979)+ +Wilson et al. (1989) |
| 43889 | -5.6 | 0.3 | 72 | Beawers & Eitter (1986)+ +Barnes et al. (1987) |
| 44570 | -6.4 | 0.2 | 15 | Häupl (1988)+ +Barnes et al. (1987) |
| 44895 | -3.4 | 0.3 | 12 | Häupl (1988)+ +Barnes et al. (1987) |
| 46866 | -4.9 | 0.4 | 2 | Gorynya et al. (1992) |
| 47126 | -6.3 | 0.2 | 19 | Bersier et al. (1994) |
| 48630 | -4.9 | 0.2 | 18 | Gorynya et al. (1992, 1996) |
| 49563 | -7.0 | 0.3 | 14 | Gorynya et al. (1996) |
| 50035 | -5.9 | 0.2 | 16 | Sachkov et al. (1998) |
| 50318 | -5.4 | 0.3 | 9 | Sachkov et al. (1998) |
| 50741 | -5.0 | 0.3 | 27 | Sachkov et al. (1998) + Luck (2001)+SAO (2001) |
| 54116 | -8.4 | 0.3 | 7 | This work |

Reference: SAO (2001) – two spectra from Usenko et al. (2001) with radial velocities, measured by author.

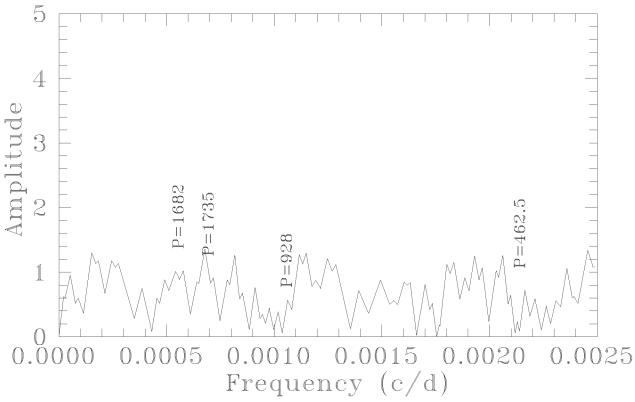


Figure 4: Fragment of Fourier amplitude spectrum of SU Cas over a narrow frequency range corresponding to orbital periods with calculations based on the original data. Periods values from Szabados (1991)

orbital motion, at that the mean $\gamma$ velocity is equal to -6.46 km s$^{-1}$.

To confirm Szabados' conclusions, we have began a search of peaks on the Fourier amplitude spectrum, which could be correspond to his orbital periods, mentioned above (see Figure 4). Evidently, these peaks are very slight and insignificant in case of calculations based on the original data. To improve this situation we calculated the Fourier amplitude spectrum based on the residuals at original ones (see Figure 5). As seen from this figure, the highest amplitude corresponds to 7490.3, 1738.8, 483.8 and 463.7 days, at that last two values are very close to Szabados' (1991) data.

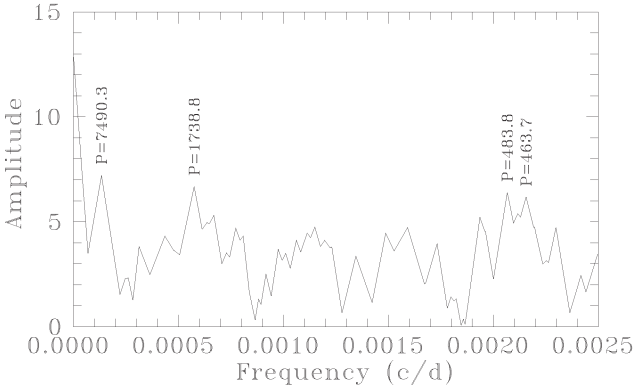


Figure 5: Fragment of Fourier amplitude spectrum of SU Cas over a narrow frequency range corresponding to orbital periods with calculations based on the residuals at original data.

## 5. Conclusions

1. According to our determination of $T_{eff}$ and $(B-V)_0$ data, SU Cas demonstrates their sporadic changes with unestablished period.

2. In case of mean gravity value 2.35 – 2.40 we can consider SU Cas as *fundamental mode* pulsator with period of 1.949329 days.

3. The presence of two equidistant periods at a distance of ±0.003 c/d from the main pulsational period and possible *first overtone* period of 2.040461 days, and $P_1/P_0 = 0.96$ suggest an idea to an existence of non-radial pulsations in the Cepheid's atmosphere.

4. Szabados'(1991) 462.5 days orbital period need to be improved. Its value could be consist with in the limits of 463.7 – 483.8 days. We need as much as possible new radial velocity data to make it.

5. It is possible that SU Cas has one more companion(s) with long orbital periods near 7490.3 and 1738.8 days.

## References


Abt H.A.: 1959, *ApJ*, **130**, 1021.
Adams W.S. & Shapley H.: 1918, *ApJ*, **47**, 46.
Barnes T.G. III, Moffet T.J., Slovak M.H.: 1987, *ApJS*, **65**, 307.
Beavers W.I. & Eitter J.J.: 1986, *ApJS*, *62*, 147.
Bersier D., Burki G., Mayor M., Duquennoy A.: 1994, *A&AS*, **108**, 25.
ESA, 1997: *The Hipparcos and Tycho catalogue*, ESA-SP 1200.
Evans N.R.: 1991, *ApJ*, **372**, 597.
Feltz K.A. & McNamara D.H.: 1980, *PASP*, **92**, 609.
Galazutdinov G.A.: 1992, *Prep. SAO RAS*, **No. 92**.
Gieren W.: 1976, *A&A*, **47**, 211.
Gorynya N.A., Irsmambetova T.R., Rastorguev A.S., Samus N.N.: 1992, *SvA Lett.*, **18**, 777.
Gorynya N.A., Samus N.N., Rastorguev A.S., Sachkov M.E.: 1996, *SvA Lett.*, **22**, 198.
Gray D.: 1992, *Observation and Analysis of Stellar Atmospheres, (Cambrige Univ. Press, 2nd ed.).*
Häupl W.: 1988, *Astr. Nachr.*, **309**, 327.
Kovtyukh V.V., Gorlova N.I: 2000, *A&A*, **358**, 587.
Luck R.E.: 2001, *priv. comm.*
Milone E.F.: 1970, *IBVS*, **No. 482**.
Mitchell R.I., Iriarte B., Steinmetz D., Johnson H.L.: 1964, *Bol. Obs. Tonantzintla y Tacubaya*, **3**, No. 24.
Niva G.D. & Schmidt E.G.: 1979, *ApJ*, **234**, 245.
Panchuk V.E., Najdenov I.D., Klochkova V.G. et al.: 1998, *Bull. SAO RAS*, **44**, 127.
Panchuk V.E., Klochkova V.G., Najdenov I.D. et al.: 1999, *Prep. SAO RAS*,**No. 139**.
Panchuk V.E., Piskunov N.E., Klochkova V.G., Yushkin M.V., Ermakov S.V.: 2002, *Prep. SAO RAS*, **No. 169**.
Racine R.: 1968, *AJ*, **73**, 588.
Sachkov M.E., Rastorguev A.S., Samus N.N., Gorynya N.A.: 1998, *SvA Lett.*, **24**, 443.
Sperl M.: 1998, *PERIOD 98,* program.
Stobie R.S.: 1969, *MNRAS*, **144**, 511.
Sudzius J.: 1969, *Vilnius Observ. Bull.*, **No. 26**.
Szabados L.: 1977, *Bud. Mitt.*, **No. 70**.
Szabados L.: 1991, *Bud. Mitt.*, **11, No. 9**, 125.
Turner D.G. & Evans N.R.: 1984, *ApJ*, **83**, 254.
Usenko I.A.: 1990, *Kinem. i Fiz. Neb. Tel*, **6, No. 3**, 91.
Usenko I.A., Kovtyukh V.V., Klochkova V.G., Panchuk V.V., Yermakov S.V.: 2001, *A&A*, **367**, 831.
Wilson T.D., Carter M.W., Barnes T.G. III, van Citters G.W., Moffett T.J.: 1989, *ApJS*, **69**, 951.
Wisniewski W.Z. & Johnson H.L.: 1968, *Commun. Lunar Planet. Lab.*, **7** , No. 112.
Yushkin M.V. & Klochkova V.G.: 2005, *Prep. SAO RAS*, **No. 206**.

# THE DISTRIBUTION OF THE GALAXY NONTHERMAL RADIO EMISSION SPECTRAL INDEX AT DECAMETER WAVELENGTHS

N.M. Vasilenko

Institute of Radio Astronomy of National Academy of Sciences of Ukraine
4,Chervonopraporna St., Kharkov 61002 Ukraine, *vasnat@ira.kharkov.ua*

ABSTRACT. A spatial distribution map for the background spectral index of the decameter radio-wave emission from the Northern sky is presented. The spectral index was determined by using radio surveys obtained with the UTR-2 radio telescope for 14.7, 16.7, 20, and 25 MHz. The temperature spectral index $\beta\left(T_\nu \sim \nu^{-\beta}\right)$ was calculated for all pairs of the above frequencies and then averaged. The contributions from the point and extended Galactic sources were removed from $\beta$ with the a low-pass FIR filter. The spectral index distribution includes the continuous galactic and the isotropic extragalactic components. The spectral index averaged over the entire investigated part of the sky is $\sim$ 2.43. For a rather large region with high galactic latitudes ($b > 30°$), the spectral index flattens to become $\sim$ 2.24. The map clearly reveals regions with increased values of the spectral index ($\beta \sim 2,6 - 2.8$); they correspond to parts of Loop I and Loop III.

**Key words**: Galaxy: structure - Galactic radio spectral index - radio continuous: general; ISM.

## 1. Introduction

Obtaining maps of the Galactic radio emission at different frequencies is one of the major tasks of radioastronomy. Such maps allow us to determine the structure of the Galaxy and that of its individual emission sources in different wavebands. By comparing radio surveys for several frequencies, we can establish significant properties of the Galaxy emission. It is this way that enables us to separate the thermal and the nonthermal Galaxy emissions, find the spectral index distribution for the radio emission, and obtain direct information of the electron energy spectrum and the magnetic field in the Galaxy.

The temperature spectral index $\beta_{i-j}$ is calculated between two frequencies $\nu_i$ and $\nu_j$ as

$$\beta_{i-j} = log(T_i/T_j)/log(\nu_j/\nu_i),$$

where $T_i$ and $T_j$ are the Galactic brightness temperatures corresponding to $\nu_i$, $\nu_j$. The distribution of the spectral index of the Galactic radio emission over the sky depends on the frequency and direction of observations. The spectral index varies over the entire sky. The variations of the spectral index for continuous emission of low frequency may be indicative of peculiarities of the interstellar magnetic field, or a mechanism of propagation of cosmic rays in the Galaxy. Those for high radio frequencies may suggest a non-uniformity of the density distribution of sources of cosmic rays.

Early investigations of the distribution of $\beta$ were carried out with a low angular resolution ($> 10°$). Detailed maps of the temperature spectral index for radio emission from of the northern sky $\beta_{408-1420MHz}$ (Reich and Reich 1988) and the map $\beta_{22-408MHz}$ (Roger et al. 1999) for a greater part of the sky were obtained with an angular resolution of $\sim 2°$. Recently published 5°-angular-resolution maps of the spectral index for the entire sky were calculated between the pairs of frequencies 408 MHz –1420 MHz and 1420 MHz –22.8 GHz (Reich et al. 2003).

It follows from the above papers that the spectral index variations for radio emission are in the range from 2.3 to 3.0. It was noticed that the low-frequency part of the spectrum is rather flat: $\beta = 2.3 - 2.6$. At frequencies $\nu > 100$ MHz, the spectral index increases to 2.8–3.0. The structure of the spectral index maps changes according to the ratio of the thermal and the nonthermal contributions to the total Galaxy emission. For example, the spectral index maps for low frequencies, where nonthermal emission is dominant, reveal high-latitude regions with steep spectra, called Loop I and Loop II. The high-frequency maps demonstrate rather flat spectra of the Galaxy plane, where the thermal emission is prevailing. The separation of these components introduces some uncertainty. After the separation of the thermal component with spectral index $\beta_{th} = 2.1$ from the galactic emission, a mean nonthermal spectral

index $\beta_{non}$ for different frequencies was determined to range from 2.6 to 3.1 (see Reich and Reich 1988b). It should be noted that the spectral index for very low radio frequencies (decameter wavelengths), the spectral index the Galaxy radio emission characterizes basically the nonthermal radiation.

## 2. Results of measurements and discussion.

In the present work, the calculations of the spatial distribution of the spectral index are based upon radio survey maps of part of the Northern sky (Vasilenko et al. 2006), which were obtained with the world-biggest low-frequency radio telescope UTR-2 (Vasilenko et al. 2006). The brightness temperature maps were obtained for frequencies of 12.6, 14.7, 16.7, 20 and 25 MHz with an angular resolution of 65° to 28° near the zenith direction. The survey covers the Northern sky region with $0^h < R.A. < 20^h, +29° < Dec. < +55°$. The fluctuation sensitivities of the survey on the Galaxy plane and away from the Galaxy plane are given in Table 1. To analyze the spectral parameters of the continuum nonthermal emission, we used a low-pass FIR filter to remove the contributions from both point sources and extended Galactic sources.

Table 1: Survey fluctuation sensitivity.

| Frequency | FLUCTUATION On the Galaxy plane | SENSITIVITY Away from Galaxy plane |
|---|---|---|
| 12.6MHz | 5.58 kK | 7.27 kK |
| 14.7MHz | 3.38 kK | 3.83kK |
| 16.7 MHz | 2.45 kK | 3.11 kK |
| 20 MHz | 1.250 kK | 1.77 kK |
| 25 MHz | 0.94 kK | 1.36 kK |

The background emission temperature $T_b$ includes the isotropic extragalactic component, which is the contribution from unresolved extragalactic sources. The estimate of this contribution for the decameter waveband reveals some peculiarity and requires special consideration. A frequency of 12.6 MHz was excluded from the analysis due to a poor statistic and a large number of missing figures in the data arrays, as compared to our other frequencies. For the same reason, we restricted our consideration to $0^h30^m < R.A. < 19^h00^m$. The temperature spectral index $\beta_{14.7-25MHz}$ was calculated for all pairs of the above frequencies and then averaged.

The resulting map shows small-scale and large-scale variations of the spectral index over the sky. The variations of the temperature spectral index lie in the range from 2 to 2.8, the root-mean-square error being 0.2. With the survey fluctuation sensitivity being good, this error, rather large, is a result of the closeness of the frequencies used in the study. The spectral index averaged over the entire investigated part of the sky is $\sim 2.43$. A rather large region of the sky ($8^h < R.A. > 12^h$), corresponding to high galactic latitudes ($b > 30°$), shows a flatter spectral index, with its average value being 2.24. The maps of the spectral index for the galactic radio emission clearly reveal regions of increased values of the spectral index ($\beta \sim 2,6 - 2.8$). These regions extend to high galactic longitudes and correspond to parts of North Polar Spur (LoopI) and Loop III, the southern and northern edges of these loops respectively.

Fig.1 represents the map of the spectral index $\beta_{14.7-25MHz}$ in the equatorial coordinates in shade of gray. The grid of the galactic coordinates is superposed in steps of 30° in l and b. The spectral index values change within the range from 2 up to 2.8.

The spectral index map obtained in the present work was compared with the $\beta_{22-408MHz}$ map presented by Roger et al (1999). It should be noted that in determining the spectral index, the surveys (Roger et al. 1999)were used, which were carried out for a frequency of 22 MHz, belonging to our frequency range, and a frequency of 408 MHz (Haslam et al. 1982). In addition, the contribution from the isotropic extragalactic components was not removed from the total emission. We observe a good visual agreement between our map (see fig. 1) and the map (fig. 5 in work Roger et al. 1999). A numerical comparison for three regions of the sky is given in Tab. 2. The greatest difference between the spectral index values for these regions corresponds to the region of lowest radio emission $(10^h, 40°)$. This fact may be related to a large root-mean-square error in determining the spectral index for our frequencies, as compared to that of Roger et al.(1999), where the frequency spacing in determining the spectral index was considerably greater. Besides, some discrepancy are due to the following factors. First, the continuous radiation of the Galaxy at 408 MHz includes 11-16% of the thermal radiation (Reich and Reich 1988b). Second, the spectral index of the nonthermal emission becomes steeper at frequencies > 100 MHz. Finally, a small scale of the presented map hinders a detailed comparison of the results.

Table 2: Spectral index for three regions of sky such as the outside of Galactic plane, the minimum radio emission and Loop I, Loop III.

| spectral index | $b > 10°$ | min fon | Loop I, III |
|---|---|---|---|
| $\beta_{22-408MHz}$ | 2.47 | 2.41 | 2.51-2.54 |
| $\beta_{14.7-25MHz}$ | 2.4 | 2.2 | 2.6-2.8 |

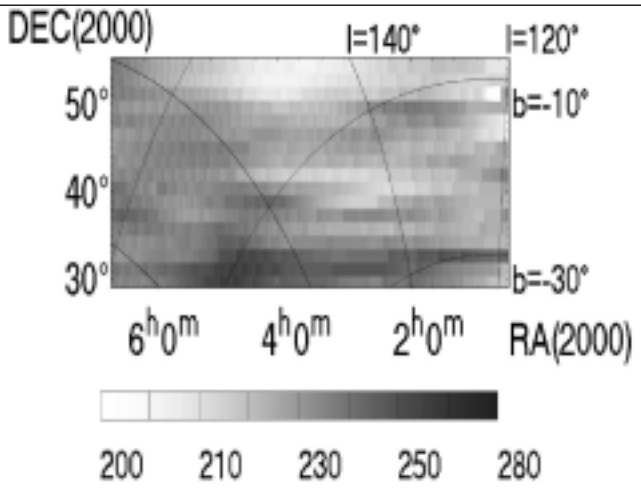


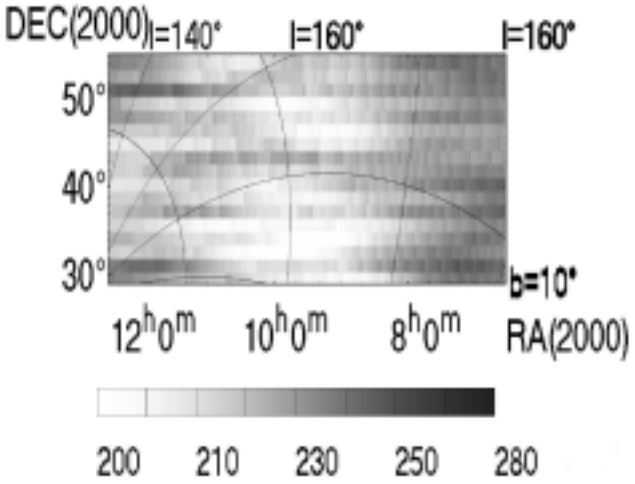


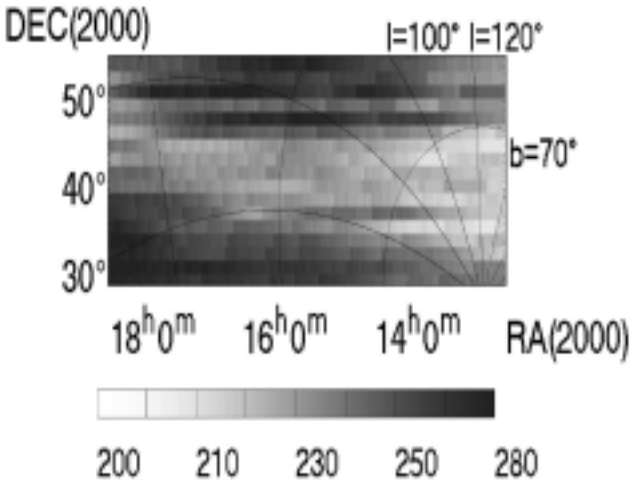


Figure 1: A map of the spectral index sky region with $+29° < Dec. < +55°$ and R.A.: $0^h30^m - 6^h30^m$; $6^h30^- 12^h30^m$; $12^h30^m - 18^30^m$ at decameter in shaded grey levels as indicated by the bar scale.Index values are $\times 10^{-2}$

### 3. Conclusion.

For the first time, a Galaxy radio emission map with high resolution and fluctuation sensitivity at ultralow frequency has been obtained for five frequencies together. These data made it possible to calculate the spectral index for frequencies where the radiation is practically completely nonthermal. Even though the close spacing of the frequencies used leads to a larger mean-square-root error, there is no difference in the radiation mechanism for such a a not large frequency spacing. Some uncertainty is introduced by the contribution from the isotropic extragalactic component, whose spectrum is steeper, $\sim 2.75$ (Bridle 1967), $\sim 2.9$ (in Reich et al 2003), than that of the galactic component. The correct account of this component will allow one to speak of a purely spectral index of the Galaxy radiation.

*Acknowledgements.* My thanks to my colleagues, Sidorchuk M.A.for the proofreading and discussion, Mukha D.V. for assistance with the computer and also Sushko M.S for proofreading.

### References

Bridle A.H.: 1967, *M.N.R.A.S.,* **136**, 219.
Haslam C.G.T., Salter C.J., Stoffel H., Wilson W.E.: 1982, *A.A.S.S.,* **47**, 1.
Reich P., Reich W.: 1988 *A.A.S.S.,* **74**, 7.
Reich P., Reich W.: 1988b *A.A.,* **196**, 211.
Reich P., Reich W. and Testori J.C.: 2004, *in Magnetized Interstellar Medium, Turkey,* 63.
Roger R.S., Costain C.H., Landecker T.L., Swerdlyk C.M.: 1999, *A.A.S.S.* **137**, 7.
Vasilenko N.M., Sidorchuk M.A., Mukha D.V., Zakharenko S.M.: 2006, *XXVI General Assembly, Prague, Abstract,* **JD12-45**, 370.

# SEARCH OF TRACES OF GEOPHYSICAL PHENOMENA IN SERIES OF LATITUDE DETERMINATIONS ON PRISMATIC ASTROLABE IN POLTAVA

N.M. Zalivadnyi, L.Ya. Khalyavina, T.Ye. Borisyuk

Poltava Gravimetrical observatory NAS of Ukraine
Myasoyedova Str. 27/29, Poltava 36029 Ukraine, *pgohal@mail.ru*

ABSTRACT. The influences of some geophysical phenomena on the long-term observation results which are obtained in Poltava with prismatic astolabe, are have been studied. It is established: 1) the non-polar variations of latitude reveals global cycles, typical for uniform system the Ears - the ocean - the atmosphere; 2) the correlation degree between non-polar zenith shifts and Solar activity index in media-term region (6-12 years) of spectrum is very high.

**Key words**: Astrometry: Earth orientation parameters(EOP), Chandler wobble, non-polar variations of coordinates; geophysics: the Earth- the atmosphere-the ocean oscillations, Solar activity index (SAI).

## 1. Introduction

Astronomical observations of point coordinate changes were conducted with the purpose of determination of the EOP. The results of these observations have been influenced by many factors, geophysical ones in particular, that become apparent in non-polar components of coordinates variations. In the preceding period the non-polar variations were considered as interferences in the study of EOP. After the scientific and technological breakthroughs that substantially improved accuracy of EOP, the geophysical influences themselves became the object of researches (Gorshkov *et al.*, 2005; Chapanov, 2005; Hui hu *et al.*, 1989).

45-year series of observations on prismatic astrolabe on coordinate variations have been accumulated in Poltava observatory. The astrolabe observations give an accurate account of movement of the observatory zenith. Data collection and processing automatization allowed to improve the theory of instrument that was taken into account in the process of series revisions (Khalyavina, 1999; Khalyavina, Kislitsa, Borisyuk *et al.*, 2001; Khalyavina, 2005). The astrolabe observation sets is reprocessed in reference to the ICRS catalogues (HC, ARIHIP, Tycho-2) and with use of the IAU2000 precession-nutation model (D.McCarthy, N.Capitane, 2002).

## 2. Series analysis.

Analysis of latitude series of astrolabe observations on basis of additive-multiplicative model of the process has been conducted (Zalivadnyi *et al.*, 2005). The proposed algorithm allows to determine parameters of the components of the series under study more precisely as compared to the traditional analysis methods. Effectiveness of this method is confirmed by the resulted assessment of the parameters of the polar components of latitude series of Poltava astrolabe. The following values of component periods (T) and amplitudes (A) have been received: Chandler term: T=$432.13^d\pm0.26$ (days) and A=$0.136''\pm0.005$; annual: T=$365.06^d\pm0.19$ and A=$0.086''\pm0.004$. These results are in good agreement with the characteristics of polar oscillations, received as the result of analysis of many series (Vicente, Wilson, 1997).

The significant cyclicity with periods of 14.00; 7.00; 4.67; 3.23; 2.80; 2.33; 2.00; 1.83 years have been revealed as the result of analysis. It should be noted that some of the cyclicities are multiple of Chandler term $T_C\approx1.18$y. Thus $6\times T_C\approx7.00$; $4\times T_C\approx4.67$; $2\times T_C\approx2.33$ years, i.e. they are sub-harmonics of Chandler term. Existence of such periodicals in series that determine global meteorological conditions and their connection with polar motion are specified in Sidorenkovs works (Sidorenkov, 2002). In the authors opinion, existence of such sub-harmonics is an evidence of close connection of processes in the atmosphere and in the ocean and luni-solar nutation and Earths polar motion. The cyclicities close to 2 years are probably related to quasi-biennial variations appearing in many processes on the Sun and the Earth. They are discovered in heliomagnetic activity indexes, in changes of terrestrial and solar magnetic fields, in low-latitude stratospheric wind, in Earths rotational velocity, and it is determined that quasi-biennial variations on the Sun and the Earth are interrelated (Ivanov-Kholodnyi, Chertoprud, 2005).

Therefore there is quite real significanc harmonics discovered in the series of non-pola nents. These harmonics may reflect long-run in the atmosphere caused by the mentioned It is the custom to call the Sun the most i influence on atmospheric processes.

### 3. Influence of solar activity

Influence of solar activity on results of diffe physical observations, including astronomical been the subject of intensive study for m half a century. The references about the r are given, for example, in (Turenko, 1992). ries comparison the series of average monthl of solar activity(SAI) were used (RI - Wolf (*ftp* : *//ftp.ngdc.noaa.gov/STP/SOLAR* – *SUNSPOOT* – *NUMBERS*). It was found components with periods: 7.0; 5.25; 3.23; 2 years are revealed for the series under consi The components with the same periods or clos are revealed in the latitude series as well.

Study of slow variations of non-polar components (T≥6 years) and medium-term v SAI (T≥11 years) points to their statistical nection. The changes of meridional comp that are in anti-phase to the mentioned v

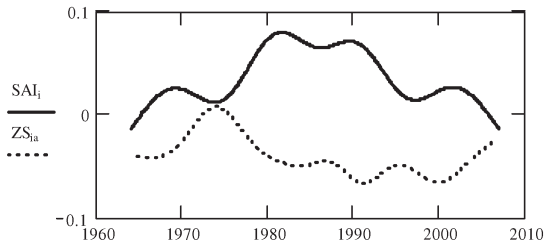


Figure 1: Long-period modulation of SAI non-polar latitude variations.

The similar comparison of non-polar vari longitude direction (WS) and modulations I period of 1988-2006 points to synchronism changes (Fig.2). (The cause of reduced size series is inaccuracy of assessment of instrumental errors in longitude before 1988). After excluding of linear trends on the given segments SAI and WS correlation coefficient of the mentioned components reaches +0.91.

The findings should be considered as exploration ones. They should be thoroughly checked and substantiation of specific mechanism of influence of solar

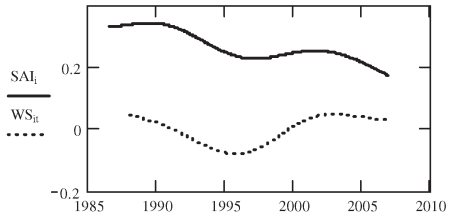


Figure 2: Long-period modulation of SAI and slow non-polar longitude variations.

activity on atmosphere parameters should be given. Perhaps use of SAI, as the one of main parameters, will allow to develop a real model of accounting of long-term atmospheric influences on astrometrical observations.

### References

Gorshcov V.L., Miller N.O., Prudnikova Ye.Ya.: 2005, *Trudy GAIS.,* **78**, 23.

Chapanov Ya.: 2005, *Kinemat. and Physik of celest. bodies Supp.,* **5**, 347.

Hui hu, Rongia Kan, Rui Wang *et al.*: 1989, *Astron. Astrophys.*, **224**, 321.

Khalyavina L.Ya.: 1999, *Kinemat. and Phys. of celest. bodies,* **15**, 177.

Khalyavina L.Ya., Kislitsa Ye.N., Borisyuk T.Ye. *et al.*: 2001, *Kinemat. and Phys. of celest. bodies,* **17**, 372.

Khalyavina L.Ya.: 2005, *Kinemat. and Phys. of celest. bodies,* **21**, 66.

McCarthy D., Capitane N.: 2002, *IERS Tech. Note,* **29**, 9.

Zalivadnyi N.M., Nekrasov V.V., Schliahovoi V.V.: 2005, *Kinemat. and Phys. of celest. bodies Supp.* **5**, 365.

Vicente R.O., Wilson C.R.: 1997, *J.Geoph.Res.* **102**,(B9) 20439

Sidorenkov N.S.: 1999, *Kinemat. and Phys. of celest. bodies Supp.***1**, 55

Ivanov-Kholodnyi G.S., Chertoprud V.Ye.: 2005, *Trudy GAIS.,* **78**, 33.

Turenko V.I.: 1992, *in Vrashchenie i deformatsii Zemli, Kiev*, 23. (in russian)

# OSCILLATIONS IN TW DRACONIS

M. Zejda[1], Z. Mikulášek[1,2]

[1] Institute of Theoretical Physics and Astrophysics, Masaryk University, Kotlářská 2, CZ-611 37 Brno, Czech Republic, *(zejda,mikulas)@physics.muni.cz*

[2] Observatory and Planetarium of J. Palisa, VŠB – Technical University, Ostrava, Czech Republic

ABSTRACT. TW Draconis is one of the well-know known and studied Algol-like eclipsing binaries. The light variations of TW Dra are caused predominantly by eclipses of the hot main sequence star A8 V by the cooler and fainter giant component K0 III. The total primary minimum deep 2.3 mag in B takes 11.5 hours and repeats with the orbital period about 2.807 days. We target our analysis to the study of oscillations in the system of all kind. Combining all available timings of minima we found oscillations of orbital period manifesting in O-C values variations. We speculate they are caused by the mass and angular momentum transfer and the presence of the third body in the system. Our photometric observations confirm also previously revealed oscillations in the light curve. Delta Scuti-like oscillations of the primary component cannot be the only explanation of them, as we found these small light variations also in the bottom of the totality. The complete paper is to be published elsewhere.

**Key words**: Stars: binary: eclipsing; stars: individual: TW Dra.

## 1. Introduction

TW Draconis (also HD 139319, BD+64 1077, HIP 76196, $\alpha = 15^{\rm h}33^{\rm m}51\overset{\rm s}{.}1$, $\delta = 63°54'26''$, J2000.0). Eclipsing pair is also A-component of visual binary OΣ 299 = ADS 9706. The B-component is the 9.987 mag (VT) star HD 140512=TYC 4184 61 2 only 3.3" away from TW Dra. The eclipsing variability was discovered by Annie Cannon in 1910, however the older observations are noted in 1858. The star was studied both photometrically and spectroscopically in several campaigns, which revealed also some small changes of the light curve – small oscillations, irregularities, deformations. Furthermore it was also included in several surveys. Singh et al. (1995) obtained its first X-ray spectrum using the ASCA and ROSAT satellites and confirmed the results of White & Marshall (1983) revealing TW Dra as an X-ray source. Umana et al.(1991) found that radio-fluxes of Algols are generally comparable to those emitted from the RS CVn stars and that they are changing.

## 2. Time scales in TW Dra

It seems TW Dra is very complex system with large variety of phenomena found there. These physical phenomena caused variations of parameters on different time scales. However only some of them are well confirmed by observations and only a part of well observed variations are clearly explainable. The table 1 shows different time scales on which we can study different phenomena in TW Dra.

Table 1: Time scales found in TW Dra.

| period | event(s) |
|---|---|
| 0.01 d | small quasi-periodic oscillat. on LC |
| 0.47 d | eclipse duration, |
| 1.66 d | rotational period of the prim. star |
| 2.81 d | orbital period P/period of the main light changes, |
| 6.5 y | orbital period $P_3$ of the third body, |
| 21.6 y | change of orbital period P/oscillations in O–C, |
| decades of years | (ir)regular small deformations of LC, |
| > 100 years | orb. period $P_4$ of visual companion |

Although TW Dra is really a unique close binary system the photometric observations was done only several times in the history. Only Baglow (1952), Walter (1978), Papoušek et al. (1984) covered the whole light curve and built model of the system based on their own observations. So we decided in 2004 to start new campaign to obtain new photometric measurements of the system (see Tab. 2). In 83 nights (2001–2007) we collected 48 723 CCD or photoelectric measurements in *UBVRI* filters. The light curve is shown in Fig. 1.

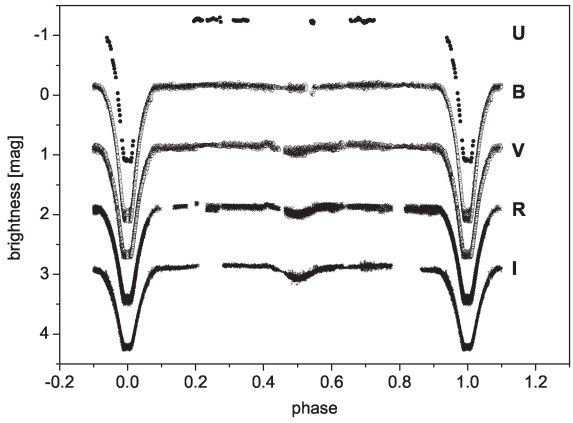


Figure 1: UBVRI light curves of TW Draconis .

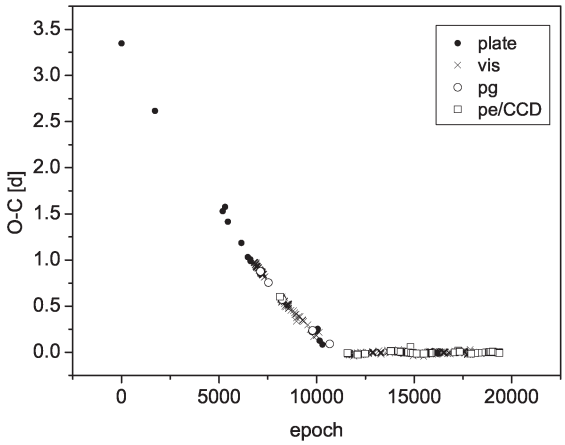


Figure 2: O–C diagram of TW Dra in 1858–2007.

Table 2: Review of photometric observations.

| year(s) | observer(s) |
|---|---|
| 1950–1 | Baglow, Baker (DDO, Steward Observ.) |
| 1964–5 | Walter (Osserv. Astrofisico di Catania) |
| 1969–72 | Walter (University of Tübingen) |
| 1976–9 | Tremko (Tatranska Lomnica) |
| 1967–80 | Papoušek, Vetešník (Masaryk Univ., Brno) |
| 2001 | Kusakin et al. (Tien-Shan Astr. Obs.) |
| 2001–2 | Kim et al. (Sobaeksan Optical Astr. Observatory) |
| 2004–6 | Zejda (N. Copernicus Observatory and Planetarium Brno – CCD) |
| 2005 | Zejda, Janík, Božić (Hvar Observ.) |
| 2005–7 | Svoboda, Szász, Chrastina, Hroch, Brát (different observatories – CCD) |
| 2006 | Zejda, Janík (Mt. Suhora Observatory) |

## 3. O–C oscillations

Studying the binary stars one can have a different views of the system:

**macro-view** – we can understand as a study of long-term global characteristics e.g. O–C diagram;

**simple/basic-view** – means a finding of basic characteristics during a campaign, e.g. determination of inclinations, radii, luminosities...;

**micro-view** – detailed study of the second order characteristics e.g. small variations on the light curve during a campaign or several observational runs.

This paper is only the first parts of the detailed study of TW Dra. It is necessary to start with a macro-view of the system. The basic time–scale in eclipsing binaries is that determined by orbital period. However one must know if this period is stable or changing and if it is changing it is necessary to describe all this changes. Only then one can for example construct the phased light curve! We concentrated in this paper on the change or let say oscillations in orbital period of the system. Summary of used observational data is given in the Tab. 3. There are only 8 secondary minima observed and furthermore the first one is wrong. We decided to use only primary minima for the study of O–C diagram.

Table 3: Review of timings of minima.

| since | type | subtype | number |
|---|---|---|---|
| 1858 | photographic | plates | 12 |
| 1913 | | series | 6 |
| 1910 | visual | | 419 |
| 1947 | photometry | photoelectric | 58 |
| 1996 | | CCD | 66 |
| 1858 | primary | | 553 |
| 1972 | secondary | | 8 |
| 1858 | totally | | 561 |

There are two gaps in the O–C data (see Fig. 2), which correspond the World War I and II, respectively. Unfortunately, especially during the 40's years of the last century the great change of orbital period happened. Thus we divided all data in two intervals splitting them in 1942.

The first interval contain 141 observations (9 plate faintenings, 125 visual timings, 7 pep/pg minima). Till the discovery in 1905 there are only 9 the less precise plate faintenings. For this part we used the simplest model - linear function sharing one point with the quadratic function which is suitable for the second

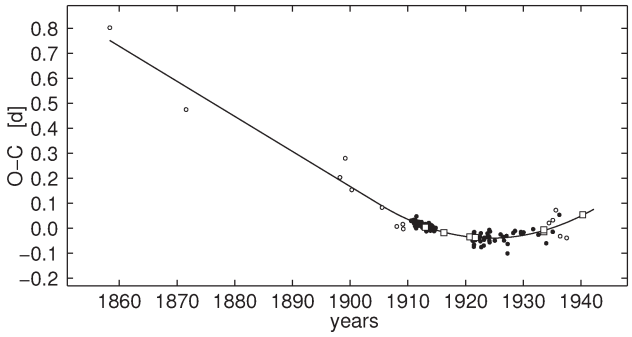


Figure 3: O–C diagram of TW Dra in 1858–1942. Plate faintening are drawn by small dots, visual observations by circles and sets of photographic or photoelectric measurements by squares.

part of the data in 1905-1942 (see Fig. 3). Then the relevant light ephemeris in 1858–1905 are

$$\begin{aligned}\text{Pri.Min.} &= M_0 + P_1\,(E - E_1)\\ &= 24\,17065.3683(29) + 2\overset{\text{d}}{.}806513(9)\cdot(E - 6140)\end{aligned} \quad (1)$$

where $E = 0$ corresponds to the time of the first faintening in our data in 1858.
The proper light ephemeris in 1905–1942 are given by following quadratic orthogonal form (see Mikulášek, these proceedings)

$$\text{Pri.Min.} = M_0 + \overline{P}\,E' + \frac{\dot{P}\,\overline{P}}{2}\left(E'^2 - \frac{\overline{E'^3}}{\overline{E'^2}}\,E' - \overline{E'^2}\right), \quad (2)$$

where basic minimum for the centre of gravity of data is $M_0 = 2\,422\,032.9979(7)$, the mean period $\overline{P} = 2\overset{\text{d}}{.}8066209(6)$ d, time derivation of the period $\dot{P} = 1.53(5)\times10^{-8} = 5.69\times10^{-8}$ d/year, where numbers in brackets here and hereafter mean standard error of found values of parameters. Furthermore epoch $E' = E - \overline{E}$, where $\overline{E} = 7910$, $\overline{E'^3}/\overline{E'^2} = 1360$ and $\overline{E'^2} = 1.39\times10^6$. The entering data had different quality, so we calculate for then the correct weights as $s^{-2}$, where $s$ is standard error for the group of data in the model used. After several iterations we found following weights:

- plate faintening $w_1 = 1$,
- visual data 1920-1942 $w_2 = 4$,
- visual data 1905-1920 $w_3 = 28$,
- photoel./photogr. series $w_4 = 266$(!).

The period increased by $1.94\times10^{-4}$ day during whole epoch 1858–1942. Using the well–known formula (Kwee & van Woerden, 1958)

$$\frac{1}{M}\frac{\mathrm{d}M}{\mathrm{d}t} = \frac{q}{3P(q^2-1)}\frac{\mathrm{d}P}{\mathrm{d}t}, \quad (3)$$

where $M = M_1 + M_2$ is a mass of the binary system (in $\mathrm{M}_\odot$) and $q = M_2/M_1$, we can estimate the rate of mass exchange in the system by prediction of conservative mass transfer and no exchange between rotational and orbital angular momentum. Assuming component masses $M_1 = 1.9\ \mathrm{M}_\odot$ and $M_2 = 0.82\ \mathrm{M}_\odot$ (Al-Naimiy & Al-Sikab, 1984) we found mass exchange rate of $3.9\times10^{-7}\ \mathrm{M}_\odot$/year. This short epoch of very high mass transfer was followed by the period supposedly called "relaxation epoch".

The second time interval 1942–2007 is better covered by the data and the data are in majority better quality than in the previous interval. The O–C diagram (see Fig. 4) shows cyclic variations of O–C values. However it is also seen from this figure that the amplitude as well as the period of the cycle is diminishing. To describe such run of the O–C values we built the following mathematical model. The periodicity of the O–C values variations can be described simply by a function $\cos(2\pi\vartheta)$, where $\vartheta$ is time expressed by the number of passed cycles and phase in the actual cycle. The duration $\Theta$ of each further cycle is shortened by the same relative part

$$\dot{\Theta} = \frac{\mathrm{d}\,\Theta}{\mathrm{d}\,\vartheta}\frac{1}{\Theta} = \text{const.} \quad (4)$$

For the chosen reference timing $T_0$ of the O–C curve extremum is $\Theta = \Theta_0$ and $\dot{\Theta} = \dot{\Theta}_0$ and then

$$\Theta = \frac{\mathrm{d}t}{\mathrm{d}\vartheta} = \Theta_0 e^{\dot{\Theta}_0\vartheta}, \quad (5)$$

where $t$ is flowing time. Solving the equation (5) we obtain

$$\vartheta = \frac{1}{\dot{\Theta}_0}\ln\left[1 + \frac{\dot{\Theta}_0}{\Theta_0}\,(t - T_0)\right], \quad (6)$$

The decreasing amplitude of the change of O–C values in time could be expressed by a multiplicative term $B\left(\frac{\Theta}{\Theta_0}\right)^2$, where $B$ is semi-amplitude of O–C value change in time $T_0$. Then we are able describe the O–C value variations by the following wavy quadratic function

$$\begin{aligned}\text{Pri.Min.} = M_0 + \overline{P}\,E' + \frac{\overline{P}\dot{P}}{2}\left(E'^2 - \frac{\overline{E'^3}}{\overline{E'^2}}\,E' - \overline{E'^2}\right)\\ + B\left(\frac{\Theta}{\Theta_0}\right)^2\cos(2\pi\vartheta),\end{aligned} \quad (7)$$

where $E'$ means centre of gravity of the data in selected period as mentioned above ($E' = E - \overline{E} = E - 16634$). After some modifications

$$\text{Pri.Min.} = M_0 + \overline{P}\,E' + \frac{\dot{P}\,\overline{P}}{2}\left(E'^2 - \frac{\overline{E'^3}}{\overline{E'^2}}\,E' - \overline{E'^2}\right) \tag{8}$$
$$+B\left[1+\dot{\Theta}_0\frac{E'-E_0}{\Theta_0}\right]^2\cos\left[\frac{2\pi}{\dot{\Theta}_0}\ln\left(1+\dot{\Theta}_0\frac{E'-E_0}{\Theta_0}\right)\right],$$

where $E_0$ is the epoch of a basic extremum, $\Theta$ is expressed in orbital periods.

Applying the robust nonlinear regression we found out that we can neglect the quadratic for this epoch. However, the O–C residual diagram is showing another periodic term (see Fig. 5). Thus, finally we excluded the quadratic term and included the new term as well, yielding the following equation

$$\text{Pri.Min.} = M_0 + \overline{P}\,E' \tag{9}$$
$$+B_1\left[1+\dot{\Theta}_0\frac{E'-E_{01}}{\Theta_0}\right]^2\cos\left[\frac{2\pi}{\dot{\Theta}_0}\ln\left(1+\dot{\Theta}_0\frac{E'-E_{01}}{\Theta_0}\right)\right]$$
$$+B_2\cos\left[\frac{2\pi\,(E'-E_{02})}{P_2}\right]$$
$$+B_2\,b_2\left\{\sin\left[\frac{2\pi\,(E'-E_{02})}{P_2}\right]-\frac{1}{2}\sin\left[\frac{4\pi\,(E'-E_{02})}{P_2}\right]\right\}.$$

Applying the robust nonlinear regression we found following basic light ephemeris:

$M_0 = 2\,446\,519.31969(18)$, $\overline{P} = 2\overset{\text{d}}{.}80685567(9)$

and the values of the coefficients

$B_1 = -0.01135(24)$ days,
$\dot{\Theta}_0 = -0.257(7)$,
$\Theta_0 = 2816(16)\overline{P} = 21.64(12)$ years,
$E_{01} = -1247(13)$; $T_{01} = 2\,443\,019(33) \sim 1976.7$,
$B_2 = 0.00279(24)$ days,
$b_2 = 0.51(13)$,
$P_2 = 847(4)\overline{P} = 2377$ days $= 6.51(3)$ years,
$E_{02} = -162(15)$; $T_{02} = 2\,446\,065(42) \sim 1985.0$,

where indices 1 and 2 indicate the parameters of the major oscillation and the small oscillations caused probably by the third body, respectively. Also in the second interval we calculated the weight of the used data according to the chosen mathematical model. There are only two group of data - less precise visual timings of minima with the weight $w_1 = 1$ and photoelectric or CCD minima with the weight $w_2 = 35$.

Regarding to the resulting coefficients, we conclude that the major oscillations in O–C diagram will disappear in $2051 \pm 9$. We predict the closest extrema in $2010.5 \pm 1.5$ and $2021.9 \pm 2.2$, respectively. The hypothetic third body causes more or less cyclic undulation of main O–C course with the period of 6.51 years and an amplitude of 0.0065 days. The final fit according to eq. (9) is shown in Fig. 4.

The cyclic O–C variations could be explained by several ways. Apsidal motion is generally an inviable explanation for such period changes because the orbital

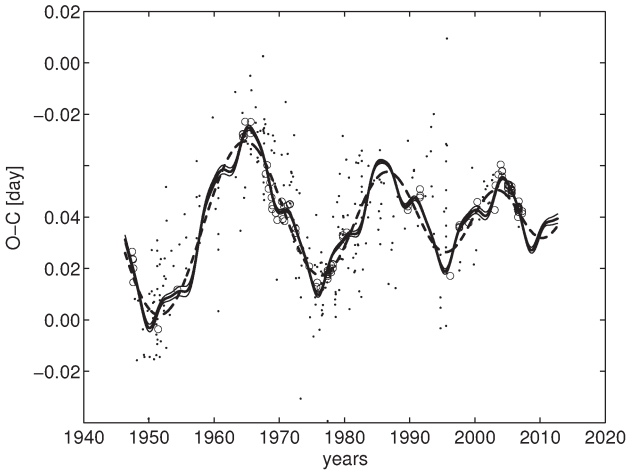


Figure 4: The O–C diagram of TW Dra in 1942–2007. Visual observations are drawn by points and CCD or photoelectric ones by empty circles. The dashed line shows the fit of the major period changes according to eq. (8) without quadratic term and the full line shows the fit including changes caused by the third body.

eccentricity for active close binaries is negligible. The orbit of TW Dra is circular. Light–time effect (hereafter LITE) needs strictly periodic variations of O–C residuals and it is fulfilled only in small oscillations in residuals after subtracting the large oscillations (see Fig. 5). So these small oscillations could be explained by the presence of the third body with estimated minimum mass $M_{3,min} = 0.3$ M$_\odot$ with the assumption of a coplanar orbit and masses $M_1 = 1.9$ M$_\odot$ and $M_2 = 0.82$ M$_\odot$ (Al-Naimiy & Al-Sikab, 1984). We can also interpret the cyclic O–C variations by interrupted mass transfer when secondary component is close to the Roche limit or by the (ex)change of angular momentum of the system. However influence of magnetic field offers the most probably explanation of such O–C changes. If the secondary companion is spectral type F5 or later (here K0III), there is sizeable convective envelope, which together with rapid rotation provide conditions for development of strong dynamo action in star. Matese &Whitmire (1983), Applegate (1992), Lanza et al. (1998) showed that magnetic activity could lead to a cyclic change of gravitational quadrupole moment of active stars and as a result of it to cyclic change of period. This dependence is possible to express according to Applegate & Patterson (1987) as follows

$$\frac{\Delta P}{P} = -9\left(\frac{R_2}{a}\right)^2\frac{\Delta Q}{M_2 R_2^2}, \tag{10}$$

where $\Delta P$ is a period change, $\Delta Q$ a change in the quadrupole moment, $M_2$ and $R_2$ are mass and radius of the secondary star and $a$ is orbital separation of components. We calculated $\Delta Q$ for six in-

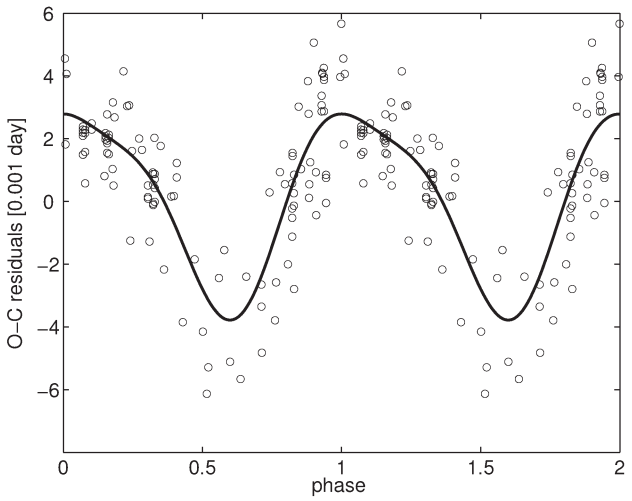


Figure 5: Residuals of O–C after subtracting the major oscillations phased with the period 6.51 year.

tervals with a good coverage of the period change.

| Interval years | $\lvert\Delta P\rvert$ [$10^{-5}$ day] | $\lvert\Delta Q\rvert$ [$10^{50}$ g cm$^2$] |
|---|---|---|
| until 1942 | 19.4 | 88.6 |
| 1952-1965 | 1.98 | 9.0 |
| 1965-1976 | 1.75 | 8.0 |
| 1976-1987 | 1.52 | 6.9 |
| 1987-1996 | 1.34 | 6.1 |
| 1996-2003 | 1.18 | 5.4 |

These values corresponds to the typical values of the quadrupole moment in Algols and RS Canum Venaticorum systems (Lanza, 2006).

## 4. Conclusion

We made the detailed analysis of O–C values using different mathematical models for two parts of O–C diagram. The major oscillations found in more precise O–C values after 1942 are probably caused by the change of quadrupole moment as a result of the presence of magnetic field in the system. Subtracting this O–C changes we found also small oscillations. We suppose they are caused by the presence of the third body in the system with estimated mass 0.3 $M_\odot$. According to the used mathematical model we were able to predict the next development of the oscillations in the system. The further observations are desirable to confirm our prediction.

*Acknowledgements.* This investigation was supported by the Grant Agency of the Czech Republic, grant No. 205/06/0217. This research has made use of the SIMBAD database, operated at CDS, Strasbourg, France, and of NASA's Astrophysics Data System Bibliographic Services.

## References

Al-Naimiy, H. M. K., Al-Sikab, A. O., 1984, *Astroph. Space Sci*, **103**, pp. 115-124

Applegate, J. H., 1992, *ApJ*, **385**, p. 621-629

Applegate, J. H., Patterson, J., 1987, *ApJ*, **322**, L99-L102

Baglow, R.L., 1952, *Publ. David Dunlap Obs.*, **2**, No. 1

Kwee, K. K., van Woerden, H., 1958, *BAN*,**12**, 357

Lanza, A. F., Rodono, M., Rosner, R., 1998, *MNRAS*, **296**, pp. 893-902

Lanza, A. F. 2006, *MNRAS*, **369**, pp. 1773-1779

Matese, J. J., Whitmire, D. P., 1983, *A&A*, **117**, L7-L9

Papoušek, J., Tremko, J., Vetešník, M., 1984, *Folia Facultatis scientiarum naturalium Universitatis Purkynianae Brunensis*; tomus 25, opus 4. Physica 42

Singh, K. P., Drake, S. A., White, N. E., 1995, *Astroph. J.*, **445**, pp. 840-854

Umana, G., Catalano, S., Rodono, M., 1991, *A&A*, **249**, 217

Walter, K., 1978, *A&AS*, **32**, 57

White, N. E., Marshall, F. E., 1983, *ApJ*, **268**, L117

*Наукове видання*

**Вісті Одеської астрономічної обсерваторії**
том 20 часть 1 (2007)

***Англійською мовою***

Технічний редактор М. І. Кошкін

---

Підписано до друку 04.02.08. Формат 60x84/8.
Ум. друк. арк. 27.90. Друк офсетний. Папір офсетний. Тираж 300 прим. Зам. .

**Видавництво «АстроПринт»**
65026, м. Одеса, вул. Преображенська, 24.
Тел.: +38 (048) 726-96-82, 726-98-82, 37-14-25.